



HAL
open science

Characterization of trace compounds in biogas and biomethane: development of a sampling-, in situ preconcentration- and analysis method

Aurore Lecharlier

► To cite this version:

Aurore Lecharlier. Characterization of trace compounds in biogas and biomethane: development of a sampling-, in situ preconcentration- and analysis method. Analytical chemistry. Université de Pau et des Pays de l'Adour, 2022. English. NNT: 2022PAUU3008 . tel-04095208

HAL Id: tel-04095208

<https://theses.hal.science/tel-04095208>

Submitted on 11 May 2023

HAL is a multi-disciplinary open access archive for the deposit and dissemination of scientific research documents, whether they are published or not. The documents may come from teaching and research institutions in France or abroad, or from public or private research centers.

L'archive ouverte pluridisciplinaire **HAL**, est destinée au dépôt et à la diffusion de documents scientifiques de niveau recherche, publiés ou non, émanant des établissements d'enseignement et de recherche français ou étrangers, des laboratoires publics ou privés.

THÈSE

UNIVERSITÉ DE PAU ET DES PAYS DE L'ADOUR

École doctorale des sciences exactes et leurs applications (ED 211 SEA)

Présentée et soutenue le 8 avril 2022

par **Aurore LECHARLIER**

pour obtenir le grade de docteur
de l'Université de Pau et des Pays de l'Adour
Spécialité : Chimie analytique et environnement

CARACTÉRISATION DES COMPOSÉS TRACES DANS LE BIOGAZ ET BIOMÉTHANE : DÉVELOPPEMENT D'UNE MÉTHODE D'ÉCHANTILLONNAGE, DE PRÉCONCENTRATION *IN SITU* ET D'ANALYSE

MEMBRES DU JURY

RAPPORTEURS

- Chrystelle MONTIGNY
- Pierre GIUSTI

Maître de conférences HDR / Université de Montpellier, France
Directeur de recherche CNRS / Université de Rouen Normandie, France

EXAMINATEURS

- Jörg FELDMANN
- Guillaume GALLIERO

Professeur des Universités / Université de Graz, Autriche
Professeur des Universités / Université de Pau et des pays de l'Adour, France

DIRECTEURS

- Isabelle LE HÉCHO
- Hervé CARRIER

Maître de conférences HDR / Université de Pau et des pays de l'Adour, France
Professeur des Universités / Université de Pau et des pays de l'Adour, France

MEMBRES INVITÉS

- Brice BOUYSSIERE
- Guilhem CAUMETTE
- Pierre CHIQUET

Professeur des Universités / Université de Pau et des pays de l'Adour, France
Ingénieur environnement, recherche et énergie / Teréga
Responsable du service géosciences – Direction opérations / Teréga



Université de Pau et des Pays de l'Adour (UPPA)

Laboratoires

- IPREM (Institut des Sciences Analytiques et de Physico-Chimie pour l'Environnement et les Matériaux)
- LFCR (Laboratoire des Fluides Complexes et leurs Réservoirs)

École Doctorale des Sciences Exactes et leurs Applications (ED 211 SEA)

Doctoral thesis

**CHARACTERIZATION OF TRACE COMPOUNDS IN BIOGAS AND BIOMETHANE:
DEVELOPMENT OF A SAMPLING-, *IN SITU* PRECONCENTRATION- AND ANALYSIS METHOD**

~

Thèse de doctorat

**CARACTÉRISATION DES COMPOSÉS TRACES DANS LE BIOGAZ ET BIOMÉTHANE:
DÉVELOPPEMENT D'UNE MÉTHODE D'ÉCHANTILLONNAGE, DE PRÉCONCENTRATION *IN SITU* ET D'ANALYSE**

Prepared by ~ Préparée par
Aurore LECHARLIER

Under supervision of ~ Sous la direction de
Isabelle LE HÉCHO
Hervé CARRIER

Industrial coordinators ~ Encadrants industriels
Guilhem CAUMETTE
Pierre CHIQUET

November/Novembre 2018 – March/Mars 2022

REMERCIEMENTS

Je souhaite tout d'abord remercier les membres du jury de cette thèse.

Isabelle Le Hécho et Hervé Carrier ont été des directeurs de thèse on ne peut plus bienveillants malgré leurs emplois du temps chargés. Dès le début de la thèse, la confiance et l'amitié ont été réciproques, sentiments indispensables pour le déroulement serein d'un travail de plusieurs années en équipe. Je les remercie pour leur sang-froid et leur humour, bienvenus durant tous les obstacles absurdes rencontrés durant la thèse. Je les remercie pour leur humanisme, leur écoute et leur professionnalisme. Et pour tous les agréables moments passés ensemble.

Je remercie les rapporteurs, Mme Chrystelle Montigny, maître de conférences HDR à l'université de Montpellier, et M. Pierre Giusti, directeur de recherche CNRS à l'université de Rouen Normandie, qui ont évalué mon travail en amont de la soutenance de thèse. Je remercie également Jörg Feldmann et Guillaume Galliero, professeurs des universités respectivement à l'université de Graz en Autriche, et à l'université de Pau et des pays de l'Adour, qui ont chacun assumé le rôle d'examineur de cette thèse.

Je remercie aussi la société *Teréga* pour le financement des travaux de cette thèse, et en particulier messieurs Guilhem Caumette et Pierre Chiquet pour leurs conseils et leur aide à la définition et l'orientation du sujet de recherche.

Je remercie enfin la société *nCx Instrumentation* pour le prêt du prototype de thermodésorption de tubes adsorbants, qui a été utilisé tout au long de cette thèse.

Ensuite, j'adresse un grand merci aux nombreux chercheurs et ingénieurs des laboratoires de l'IPREM et du LFCR qui m'ont consacré du temps et conseillé sur des questions tant pratiques, matérielles que théoriques.

Emmanuel Tessier, un personnage extraordinaire, requiert un paragraphe de remerciements à lui seul. Quincaillier hors-pair, plombier à toute heure, ingénieur des matériaux et de l'échantillonnage, mais surtout doté d'une rare intelligence, d'un goût de la transmission du savoir et d'une grande générosité, il a aidé des générations de doctorants à se dépatouiller des dilemmes des plus rudimentaires aux plus complexes de la pratique de la chimie analytique. Je le remercie surtout pour tous ses conseils et explications, sa disponibilité, son humour, et pour tous les outils et matériels prêtés.

Je remercie ensuite Brice Bouyssié pour sa disponibilité, sa bonne humeur et sa contribution considérable à la mise en œuvre analytique des manipulations de cette thèse, à l'interprétation et à la valorisation des résultats.

Sont aussi remerciés : Mickael Le Béhec, Stéphane Labat, Marie Larregieu, Eric Normandin et Eddy Lasseur de l'IPREM, Jean-Patrick Bazile et Djamel Nasri du LFCR, et Stéphane Ducos du département de Chimie. Je remercie de tout cœur Jean-Patrick Bazile et Djamel Nasri dont j'ai particulièrement apprécié les compétences, la patience et la disponibilité. Je remercie aussi Hervé Pinaly (IPREM) qui, bien que bourru et refusant d'adresser la parole aux "étudiants", a de temps à autres accepté de me prêter des outils et de répondre à quelques questions.

Par ailleurs, plusieurs dispositifs instrumentaux nécessaires aux travaux de cette thèse ont été réalisés par les soins de l'atelier de physique de l'UPPA, tenu par les rennes par l'équipe très amicale de Laurent Marlin, et je les en remercie chaleureusement.

Je remercie également le service de gestion des produits chimiques de l'UPPA, et notamment Isabel Boisard, Vincent Rey-Trichot et Jean-Yves Deluze, qui ont été d'une grande aide, et d'une sympathie bienvenue, pour la manipulation quotidienne et le stockage des cylindres de gaz synthétiques pressurisés utilisés durant les travaux de cette thèse.

Ensuite, je ne peux omettre de remercier Monsieur Benoît Sourigues, ex-ingénieur d'Agilent, qui, armé d'un sourire ineffaçable, a résolu de nombreux problèmes analytiques et techniques aux divers instruments utilisés (notamment GC-MS, passeurs automatiques).

Je remercie également et vivement tous les producteurs professionnels de biogaz et de biométhane qui ont accueilli notre équipe sur leurs sites de production et qui, outre la transmission abondante d'informations techniques sur leurs technologies de production, nous ont permis d'échantillonner leurs gaz. Sans de tels échantillons réels, les travaux menés dans cette thèse n'auraient pas eu l'envergure qu'ils ont.

Le personnel d'accueil administratif du laboratoire de l'IPREM, en particulier Maria Lidia Ventura et Danielle Bergès, fut également d'un soutien incontournable pour la logistique de la réception des nombreux colis de matériel commandés pour la thèse. De surcroît, leur bienveillance et bonne humeur permanente ont agrémenté quotidiennement le travail. Je remercie aussi ma gestionnaire financière Pascale Guillaume pour sa disponibilité et la rapidité avec laquelle elle a systématiquement traité les commandes et les réservations liées à des déplacements et des missions de prélèvements.

Concernant les remerciements plus personnels, je remercie chaleureusement mes collègues de bureau Lucile Marigliano et Khouloud El Hanafi pour tous les bons moments passés ensemble. Je remercie également de tout cœur Aurore Méré pour son amitié et pour les nombreux moments d'entraide au laboratoire, et Audrey Capber pour sa joie, sa bonne humeur, son efficacité et son aide précieuse au laboratoire et à distance.

Enfin, je remercie mon conjoint Gilles pour son soutien quotidien indispensable et assidu durant ces trois ans et demi de thèse et pour son intérêt envers la recherche menée. Je remercie également mes parents et tous les proches qui ont manifesté de l'intérêt pour le sujet de recherche et, accessoirement, pour mon état durant ces années.

ABSTRACT (ENGLISH)

In pursuance of enhancing knowledge on biogas and biomethane's trace compounds to help guarantee their sustainable integration in today's European energy mix, a field sampling set-up enabling direct *in situ* preconcentration of non-metallic trace compounds in such gas samples at their pipe working pressure (up to 200 bar_a) was developed. Non-metallic trace compounds targeted in this work included alkanes (linear, cyclic, polycyclic), aromatics, terpenes, alkenes, halogenated organic species, oxygenated organic species (alcohols, aldehydes, esters, furans and ethers, ketones), siloxanes, organic and inorganic Sulphur-compounds.

Firstly, state-of-the-art gas sampling and preconcentration techniques for the determination of trace compounds in gaseous matrices were reviewed. Based on this review, preconcentration was chosen to be performed on self-assembled multibed adsorbent tubes (MAT). The preconcentration system was elaborated and optimized in the laboratory: convenient commercial adsorbents were selected; procedures for the assembly and conditioning of new MAT were established; four MAT configurations were tested on their efficiency in adsorbing and releasing targeted trace compounds using certified synthetic gas mixtures containing targeted species at trace concentrations (1 ppm_{mol}) in CH₄ or N₂ matrices. Analytes preconcentrated on MAT were recovered for analysis by thermal desorption (TD) of the tubes using a new TD prototype followed by gas chromatography (GC) hyphenated with mass spectrometry (MS) (TD-GC-MS).

Secondly, the analytical method, and in particular the new TD prototype, was validated. The chromatographic resolution power of the new TD prototype was proved to be higher than that obtained from other well established preconcentration or GC-injection methods such as solid phase microextraction or direct headspace gas injection. Besides, GC-MS parameters were optimized to detect the broad range of trace compounds potentially found in biogas and biomethane.

Thirdly, the use of a novel high-pressure tube sampling (HPTS) prototype was evaluated for the circulation of pressurized gases (up to 200 bar_a) through MAT for the direct high-pressure preconcentration of trace compounds from such gases. The HPTS was first validated in the laboratory using pressurized certified synthetic gas mixtures, and then used on field to sample compressed biomethane at a natural gas grid injection station at 40 bar_a.

Subsequently, the field sampling chain was set-up and 6 field sampling campaigns were conducted where 6 different streams of landfill gas, biogas and biomethane were collected at a landfill plant and two anaerobic digestion plants treating diverse feedstocks. Trace compounds were qualitatively determined in all gas samples via the developed TD-GC-MS method. In a single sampling run and using limited gas volumes ranging 0.5 – 2 L_N, a wide range of trace compounds in a variety of chemical families (alcohols, aldehydes, alkenes, aromatics, alkanes (linear, cyclic and polycyclic), esters, furans and ethers, halogenated species, ketones, Sulphur-compounds, siloxanes and terpenes) were identified. Variations in trace compounds composition were observed in the different gases sampled and potential correlations between feedstocks nature, implemented gas treatment processes and trace compounds determined were discussed. In particular, the substantial generation of the mono-terpene *p*-cymene and of other terpenes was evidenced for anaerobic digestion plants treating principally food-wastes.

It is believed the shortened and high-pressure-proof field preconcentration procedure developed in this work can contribute facilitating field sampling operations for the determination of trace compounds in complex gas matrices such as biogas and biomethane.

RESUME (FRANÇAIS)

Afin d'accroître les connaissances sur les composés traces présents dans les biogaz et biométhane et de garantir l'intégration durable de ces gaz dans le mix énergétique européen, une chaîne analytique complète a été développée dont un élément central est un dispositif d'échantillonnage de terrain permettant la préconcentration directe *in situ* des composés traces en prélevant ces gaz à leur pression actuelle ($\leq 200 \text{ bar}_a$). Les composés traces ciblés dans ce travail incluent : alcanes (linéaires, cycliques, polycycliques), aromatiques, terpènes, alcènes, espèces organiques halogénées, espèces organiques oxygénées (alcools, aldéhydes, esters, éthers, cétones), siloxanes, composés soufrés organiques et inorganiques.

L'état de l'art des techniques de prélèvement de gaz et de préconcentration pour la détermination de composés traces dans des matrices gazeuses a premièrement été réalisé. Sur base de cette étude, il fut choisi d'effectuer la préconcentration sur des tubes d'adsorbants multi-lits (TAM) assemblés manuellement. Le système de préconcentration fut élaboré et optimisé au laboratoire en sélectionnant des adsorbants commerciaux; les procédures d'assemblage et de conditionnement des nouveaux TAM furent établies; l'efficacité de quatre configurations de TAM à adsorber et libérer des composés traces ciblés fut testée en utilisant des mélanges de gaz synthétiques certifiés contenant des composés à l'état de traces ($1 \text{ ppm}_{\text{mol}}$) dans une matrice N_2 ou CH_4 . Les analytes préconcentrés sur les TAM sont récupérés par désorption thermique (DT) des tubes au moyen d'un nouveau prototype de DT pour être analysés par chromatographie en phase gazeuse (CG) couplée à la spectrométrie de masse (SM).

Deuxièmement, la méthode analytique et le prototype de DT ont été validés. Il fut démontré que le pouvoir résolutif du prototype de DT était plus élevé que celui obtenu par d'autres techniques de préconcentration ou d'autres méthodes d'injection en CG, telles que la microextraction en phase solide ou l'injection directe de gaz. Par ailleurs, les paramètres de CG-SM furent optimisés pour détecter le large spectre de composés traces potentiellement présents dans le biogaz et biométhane.

Troisièmement, un prototype haute-pression innovant fut évalué, permettant le prélèvement de gaz pressurisés ($\leq 200 \text{ bar}_a$) à travers les TAM pour la préconcentration directe et sous haute-pression des composés traces présents dans ces gaz. Ce prototype fut validé au laboratoire au moyen de mélanges de gaz synthétiques pressurisés avant d'être utilisé sur le terrain pour prélever du biométhane à 40 bar_a au niveau d'un poste d'injection dans le réseau de gaz naturel.

Ensuite, la chaîne d'échantillonnage fut assemblée pour mener 6 campagnes de prélèvement durant lesquelles 6 flux différents de biogaz et biométhane furent prélevés sur une installation de stockage de déchets non dangereux et deux sites de méthanisation valorisant divers intrants. Les composés traces de ces gaz furent qualitativement déterminés via la méthode de DT-CG-SM élaborée. En un unique prélèvement et utilisant des volumes de gaz réduits ($0.5 - 2 \text{ L}_N$), un large spectre de composés traces issus de diverses familles chimiques (alcools, aldéhydes, alcènes, aromatiques, alcanes, esters, éthers, halogénés, cétones, soufrés, siloxanes et terpènes) furent identifiés. Des variations de composition en composés traces furent observées dans les différents gaz et les corrélations potentielles entre intrants, procédés de traitement des gaz et composés traces identifiés, furent discutées. La génération du monoterpène *p*-cymène et d'autres terpènes dans les méthaniseurs digérant surtout des résidus alimentaires, a notamment été mise en évidence.

La procédure de préconcentration haute-pression et *in situ* développée dans ce travail peut certainement contribuer à faciliter les opérations de prélèvements de gaz sur le terrain pour déterminer les composés traces dans des matrices gazeuses telles que le biogaz et le biométhane.

KEYWORDS

Field gas sampling

Trace compounds

(Halogenated) volatile organic compounds, siloxanes, volatile Sulphur compounds

Biogas

Biomethane

Landfill gas

Direct *in situ* high-pressure preconcentration

Multibed adsorbent tubes

Thermal desorption

Gas chromatography – mass spectrometry

ABBREVIATIONS

AD	Anaerobic digestion
AES	Atomic emission spectrometry
b.p.	Boiling point
BTEX	Benzene; Toluene; Ethylbenzene; <i>o</i> -, <i>m</i> -, <i>p</i> -Xylene
BV	Breakthrough volume
CAR	Carboxen
CH ₄	Methane
CHP	Combined heat and power
CO ₂	Carbon dioxide
CO ₂ -eq	Carbon dioxide equivalent
CpX	Carbopack™X
CT	Cryotrapping
CX	Carboxen®1000
D3	Hexamethylcyclotrisiloxane
D4	Octamethylcyclotetrasiloxane
D5	Decamethylcyclopentasiloxane
D6	Dodecamethylcyclohexasiloxane
DMDS	Dimethyldisulfide ((CH ₃) ₂ S ₂)
DMS	Dimethylsulfide ((CH ₃) ₂ S)
E.U.	European Union
ECD	Electron capture detector
FID	Flame ionization detector
GC	Gas chromatography
GHG	Greenhouse gas(es)
GWh	Giga (10 ⁹) watt hours
HPLC	High pressure liquid chromatography
HPTS	High-pressure tube sampling prototype
HS	Headspace sampler
HVOC	Halogenated volatile organic compound
ICP	Inductively coupled plasma
ID	Internal diameter
L	Length

L2	Hexamethyldisiloxane
L3	Octamethyltrisiloxane
L4	Decamethyltetrasiloxane
L5	Dodecamethylpentasiloxane
LCV	Lower calorific value
LOD	Limit of detection
MAT	Multibed adsorbent tube
MF	Molecular formula
MS	Mass spectrometry
MSW	Municipal solid waste
MWh	Mega (10 ⁶) watt hours
N ₂	Dinitrogen gas
nCx-TD	New thermal desorber prototype by <i>nCx Instrumentation</i>
Nm ³	Normal cubic meter: measured at 0°C and 1013 mbar (1 atm)
OD	Outer diameter
OES	Optical emission spectrometry
PBR	Photobioreactor
PDMS	Polydimethylsiloxane
PRS	Pressure regulating system
PTFE	Polytetrafluoroethylene
RA	Relative abundance
RA _F	Per-family relative abundance
RA _G	Global relative abundance
RH	Relative humidity
SGM	Synthetic gas mixture
Sm ³	Standard cubic meter: measured at 15°C and 1013 mbar (1 atm)
SNG	Synthetic natural Gas
SPME	Solid phase microextraction
SSV	Safe sampling volume
TA	Tenax®TA
TA15	Self-assembled 15 mg Tenax TA adsorbent tube
TC	Trace compound(s)
TD	Thermal desorption
TD-GC-MS	Thermodesorption – gas chromatography – mass spectrometry

THT	Tetrahydrothiophene
TIC	Total ion current chromatogram
TJ	Tera joule (10^{12} Joules)
TMA	Trimethylarsine
TWh	Tera (10^{12}) watt hours
VMS	Volatile methyl siloxane
VOC	Volatile organic compound(s)
VSC	Volatile Sulphur compound
WWTP	Wastewater treatment plant

TABLE OF CONTENTS

Remerciements.....	3
Abstract (English)	5
Résumé (Français)	6
Keywords	7
Abbreviations.....	8
Table of Contents.....	11
List of Figures.....	16
List of Tables.....	22
PART 1 – INTRODUCTION	25
Abbreviations Part 1	26
I. Context	27
I.1. Energy transition and circular economy	27
I.2. Biogas and biomethane world trends	30
II. Birth and Definition of the Research Problem	33
III. Doctoral Thesis Objectives.....	36
IV. General Structure of the Manuscript.....	39
V. References Part 1	40
PART 2 – STATE OF THE ART	49
Chapter 1 – Biogas and Biomethane Production.....	51
Abbreviations Chapter 1	51
I. Biogas Definition.....	51
II. Biomethane Definition.....	53
III. Overview of Bio-methane Production Processes.....	53
III.1. Methanization of humid biomass.....	53
III.2. Landfill gas extraction.....	54
III.3. Pyrogasification and methanation of dry biomass.....	58
III.4. Micro- and macro-algae methanization	66
IV. References Chapter 1	70
Chapter 2 – Review of Gas Sampling and Preconcentration Techniques for the Determination of Trace Compounds in Methane-like Field Gas Samples	79
Abstract.....	79
Keywords	80
Abbreviations Chapter 2	81
I. Introduction	83
II. Gas Sampling Without Enrichment (whole gas sampling)	85

II.1.	Gas sampling bags.....	85
II.2.	Gas cylinders	93
II.3.	Canisters	96
III.	Gas Sampling With Enrichment (preconcentration).....	102
III.1.	Trapping on solid media	103
III.1.1.	Adsorbent tubes	103
Sorbent tube self-assembly and adsorbent conditioning.....		104
Sorbent tube desorption methods.....		111
Adsorbent material choice		117
Sorbent tube field considerations for biogas and biomethane sampling.....		127
Advantages and disadvantages of sorbent tube sampling.....		128
Landfill gas, biogas and biomethane trace compounds sampling via adsorbent tubes		128
Special cases of adsorbent sampling of volatile metal(loid) compounds.....		149
III.1.2.	Chemisorption (chemotrapping) and on-tube derivatization	152
III.1.3.	Amalgamation: trapping of volatile Mercury species	156
III.1.4.	Solid Phase Microextraction	159
III.2.	Trapping in liquid media: absorption in bubbling traps (impingers).....	161
III.3.	Cryogenic preconcentration (cryotrapping).....	169
IV.	Conclusions and Recommendations.....	174
V.	References Chapter 2	178
	PART 3 – EXPERIMENTAL SECTION.....	201
	Chapter 3 – Elaboration and Preliminary Laboratory Optimization of Multibed Adsorbent Tubes	203
	Abbreviations Chapter 3	203
	I. Introduction	203
	II. Adsorbent Material Choice	205
	III. Evaluation of Different Multibed Adsorbent Tube Configurations Using Synthetic Gas Mixtures	207
	III.1. Materials and methods	207
	III.1.1. Adsorbent tube assembly and conditioning	207
	III.1.2. Reagents: multibed adsorbent tube configurations and synthetic gas mixtures	209
	III.1.3. Synthetic gas sampling.....	211
	III.1.4. Analysis	212
	III.2. Results.....	213
	III.2.1. Multibed adsorbent tube blanks	213
	III.2.2. Efficiency of multibed adsorbent tubes	214

III.3. Discussion	219
IV. Conclusions.....	221
V. References Chapter 3	222
Transition Chapter 3 – 4.....	223
Chapter 4 – Promises of a New Versatile Field-deployable Sorbent Tube Thermodesorber by Application to BTEX Analysis in CH ₄	225
Abstract.....	225
Keywords	226
Abbreviations Chapter 4	226
I. Introduction	227
II. Materials and Methods.....	229
II.1. Thermodesorber prototype.....	229
II.2. Tenax TA adsorbent tube self-assembly.....	231
II.3. Gas samples	231
II.4. Analysis	232
II.5. Calculations	234
Chromatographic peak resolution.....	234
Instrument detection limit.....	234
Statistical tests	235
III. Results and Discussion	235
III.1. Chromatographic peak resolutions.....	235
III.2. Preconcentration of natural gas trace compounds	238
III.3. Instrument detection limits.....	242
III.4. A first step towards semi-quantification	244
IV. Conclusions and Perspectives	247
V. Supplemental Information Chapter 4	249
VI. References Chapter 4	255
Transition Chapter 4–5.....	261
Chapter 5 – Novel Field-portable High-pressure Adsorbent Tube Sampler Prototype for the Direct <i>In Situ</i> Preconcentration of Trace Compounds in Gases at their Working Pressures: Application to Biomethane.....	263
Abstract.....	263
Keywords	264
Abbreviations Chapter 5	264
I. Introduction	265
II. Materials and Methods.....	267
II.1. Multibed adsorbent tubes	267
II.2. High-pressure sampling prototype.....	268

II.3.	Sampling	268
II.3.1.	Synthetic gas sampling.....	269
II.3.2.	<i>In situ</i> biomethane sampling	271
II.4.	Analysis	271
II.5.	Calculations	272
III.	Results and Discussion	273
III.1.	High-pressure sampling prototype validation	273
III.2.	Multibed adsorbent tubes adequacy	273
III.3.	Influence of the gas pressure on the preconcentration.....	274
III.4.	High-pressure sampling prototype application to biomethane's trace compounds characterization	280
IV.	Conclusions and Perspectives	286
V.	Supplemental Information Chapter 5	288
	Theoretical note on multibed adsorbent tubes	288
	Supplemental Tables	290
	Supplemental Figures	291
VI.	References Chapter 5	303
	Transition Chapter 5 – 6.....	309
	Chapter 6 – Trace Compounds Determination in Landfill Gas, Biogas and Biomethane by Direct <i>In Situ</i> Preconcentration at the Prevailing Gas Production Pressure	311
	Abstract.....	311
	Keywords	312
	Abbreviations Chapter 6	312
I.	Introduction	313
II.	Materials and Methods	314
II.1.	Multibed adsorbent tubes	314
II.2.	Sampling	315
II.3.	Analysis	319
II.4.	Calculations	320
III.	Results and Discussion	320
III.1.	Multibed adsorbent tube blanks.....	320
III.2.	Sampled volumes	321
III.3.	Multibed adsorbent tube configuration appropriateness	322
III.4.	Fluctuations of trace compounds in sampled gases	328
III.4.1.	Plant A.....	328
III.4.2.	Plant B.....	331
III.4.3.	Plant C.....	336

III.5. Potential influences of feedstock’s nature on trace compounds in raw biogas and landfill gas	339
III.6. A first step towards semi-quantification	341
IV. Conclusions.....	344
V. Supplemental Information Chapter 6	345
VI. References Chapter 6	353
PART 4 – CONCLUSIONS AND PERSPECTIVES.....	359
Conclusions and Perspectives.....	361
Operational Achievements	361
Strategical Achievements.....	363
Operational Perspectives	364
Strategical Perspectives.....	365

LIST OF FIGURES

Figure I.1: Achieving doctoral thesis objectives 2 and 3: stepwise approach for the laboratory development and validation part. TC: trace compounds.	37
Figure I.2: Achieving doctoral thesis objective 4: stepwise approach for the field validation part. HPTS: high-pressure tube sampling support prototype. TC: trace compounds. TD-GC-MS: thermodesorption – gas chromatography – mass spectrometry.	38
Figure 1.1: Sanitary landfills are equipped with underground protective liners and leachate- and gas collection systems.	54
.....	55
Figure 1.2: Progressive filling of a sanitary landfill, equipped with underground protective liners and leachate- and gas collection systems.	55
Figure 1.3: Landfill gas composition evolution over time (time scale being different for each single landfill)	56
Figure 1.4: Zonal location of the thermochemical reaction processes occurring in updraft (left) and downdraft (right) fixed-bed dry biomass gasification reactors. From [83].....	61
Figure 1.5: Updraft (left) and downdraft (right) fixed-bed dry biomass gasification reactors. Air represents the gasifying agent. From [84].....	61
Figure 1.6: Overview of different pathways to produce SNG. Adapted from [79].	65
Figure 1.7: Simplified closed-loop example of biomethane production based on the anaerobic digestion of algae grown on the digestate and CO ₂ of the produced biogas.....	67
Figure 2.1: Whole gas sampling vessels: a) Polymer bag. b) Cylinder. c) Canister.....	91
Figure 2.2: Adsorption and desorption results of D5 siloxane in a Summa canister according to the Eichler et al. [72] experiment (figure from [72]).	101
Figure 2.3: Sorption mechanisms. Adapted from [81].	104
Figure 2.4: Schematic of a multibed sorbent tube. 100 mesh stainless-steel gauzes and tension springs are typically used together in stainless-steel tubes whereas unsilanized glass or quartz wool plugs are used in glass tubes to secure adsorbent beds [107]. Constriction of the tube internal diameter at the tube extremities can additionally help securing the sorbent beds. The desorption direction is always the reverse of the sampling direction even for single bed tubes [110].	105
Figure 2.5: Chemical structure of two commonly used adsorbents: a) Tenax TA (poly-2,6-diphenyl-p-phenylene oxide). b) Carbotrap B (graphitized carbon black). Adapted from [153].	125
Figure 3.1: Purpose-built 20-positions adsorbent tube conditioning support	208

Figure 3.2: Gas pressure regulating system for the sampling of pressurized synthetic gas mixtures on multibed adsorbent tubes (MAT). Following gas flow: 1: pressurized synthetic gas cylinder, 2: manual high-pressure valve, 3: manometer-gas pressure regulator, 4: manometer, 5: manual micrometric valve, 6: manual valve, 7: gas needle, 8: vacuum pump. All tubing is of stainless-steel 1/8" outer diameter212

Figure 3.3: TIC of new blank MAT for the four MAT configurations evaluated with indication of inherent background contamination (benzene and septum-released siloxanes)214

Figure 3.4: TIC of the 41 HVOC synthetic gas mixture sampled on TA14-CX26 and on TA14-CpX29 multibed adsorbent tubes (TIC of the front tubes of the sampling series). Detail of the detected compounds and their retention times is given in Table 3.6.217

Figure 4.1: Schematic of the nCx-TD. (A) 1= injection head, 2= heating core, 3= injection needle, 4= adaptable GC-fixation nut, 5= monitor casing, 6= carrier gas inlet, 7= compressed air inlet (pneumatic line), 8= USB connection to computer, 9= electrical alimentation, 10= monitor connection to the heating core, 11= monitor connection to the injection head with distribution of the compressed air (12) and carrier gas (13), 14= monitor connection to the GC for synchronization. (B) Detail of the heating core with dismantlement of the injection needle. Same numbering as in (A). 15= adsorbent tube location.....230

Figure 4.2: Custom-built glass tube intended for packing with adsorbents and thermal desorption in the nCx-TD. ID = internal diameter, L = length.....230

Figure 4.3: Total ion current chromatograms for the determination of the peak resolution between B,T,E,X chromatographic signals obtained from the different injection techniques tested for the 10 ppm_v BTEX-CH₄ synthetic gas.....236

Figure 4.4: Peak resolution R, Gaussian peak resolution R_G and peak separation factor α of 10 ppm_v BTEX-CH₄ synthetic gas injected via the nCx-TD (n=7 successful injections on 10 performed), SPME (n=3) and Headspace (n=14). T - B: resolution between benzene and toluene. E - T: resolution between toluene and ethylbenzene. m,p-X - E: resolution between ethylbenzene and m- and p-xylene. o-X - m,p-X: resolution between m- and p-xylene and o-xylene. Error bars indicate the standard deviation.....237

Figure 4.5: A and B: Total ion current chromatograms of the building grid natural gas (NG-A) sampled on TA15 tubes (nCx-TD injection), on the CAR/PDMS 75 μ m SPME fiber and in vials (Headspace injection) on the same day. C: the nCx-TD-GC-MS output of a new blank TA15 tube is contrasted to a NG-A sampled TA15 tube, analyzed with the same parameters. Note a tiny benzene (2.62 min) contamination inherent to new blank TA15 tubes (see section III.3) and hexamethylcyclotrisiloxane (6.61 min) released from the silicone layer of the TA15 tube capping-septum.....240

Figure 4.6: Total ion current chromatograms of a blank TA15 tube, a blank of the CAR/PDMS 75 μ m SPME fiber and a pure CH₄-filled vial.243

Figure 4.7: Instrument detection limits (peak height signal abundance) of trace compounds determined in the NG-A building grid natural gas sample on TA15 tubes and on the CAR/PDMS 75 μ m SPME fiber. Numerical values are available in Table 4.S3.....	244
Figure 4.S1: Purpose-built 20-positions adsorbent tube conditioning support.....	251
Figure 4.S2: Gas pressure regulating system for the sampling of pressurized gases. 1=pressurized synthetic gas bottle, 2>manual high pressure valve, 3=manometer-gas pressure regulator, 4=manometer, 5>manual micrometric valve, 6>manual valve, 7=gas needle "n", 8=vacuum pump. A=sampling through an adsorbent tube. B=sampling in a vacuumed glass vial.....	252
Figure 4.S3: Sampling of gas concentrations C_i from a Tedlar bag (A) through an adsorbent tube or (B) in a vacuumed glass vial.....	252
Figure 4.S4: Calibration curves (average chromatographic peak area) for benzene, toluene, ethylbenzene, m- and p-xylene and o-xylene acquired for six concentrations (0, 1, 2.5, 5, 7.5, 10 ppm _v) by different injection techniques (nC _x -TD, SPME and headspace). Vertical bars at each concentration indicate the standard deviation (3 replicates at each concentration)...	253
Figure 4.S5: Least squares linear regression model fitted on the average Gaussian peak resolution R_G between ethylbenzene and m-, p-xylene acquired for six concentrations (0, 1, 2.5, 5, 7.5, 10 ppm _v) by different injection techniques (nC _x -TD, SPME and headspace). Vertical bars at each concentration indicate the standard deviation (3 replicates at each concentration).....	254
Figure 5.1: The high-pressure tube sampling prototype. Gas sampling direction is from A to C.	268
Figure 5.2: High-pressure preconcentration sampling chain.	269
Figure 5.3: TIC of a new blank TA14-CpX29 MAT with indication of septum-released siloxane background contaminants.....	274
Figure 5.4: TIC of the 41 HVOC SGM sampled (2L _N) at 100 bar _a on TA14-CpX29 MAT in the HPTS. Retention times are given in Table 5.SI-1.	275
Figure 5.5: High-pressure adsorption isotherms of 10 randomly selected HVOC (out of the 41) for test-condition A (2 L _N of the SGM sampled at 5, 40 and 100 bar _a on TA14-CpX29 MAT). Average peak area with indication of the standard deviation. The remaining HVOC are plotted in the Supplemental Information (SI): Fig.5.SI-1.....	276
Figure 5.6: High-pressure adsorption isotherms of 10 randomly selected HVOC (out of the 41) for test-condition B (5 L _N of the SGM sampled at 5, 40, 68 and 74 bar _a on TA14-CpX29 MAT). Average peak area with indication of the standard deviation. The remaining HVOC are plotted in Fig.5.SI-2.....	277
Figure 5.7: Partial breakthrough curves for 10 randomly selected HVOC (out of the 41) for test-condition C (1, 2 and 5 L _N of the SGM sampled at 40 bar _a on TA14-CpX29 MAT). Average	

peak area with indication of the standard deviation. The remaining HVOC are plotted in Fig.5.SI-3.....278

Figure 5.8: Partial breakthrough curves for 10 randomly selected HVOC (out of the 41) for test-condition D (2, 5 and 6 L_N of the SGM sampled at 5 bar_a on TA14-CpX29 MAT). Average peak area with indication of the standard deviation. The remaining HVOC are plotted in Fig.5.SI-4.....279

Figure 5.9: TIC of two biomethane samples: 2 L_N collected on TA14-CpX29 MAT at 1 L_N·min⁻¹ at 1.45 bar_a after depressurization versus directly at 40 bar_a in the HPTS.....281

Figure 5.10: Average chromatographic peak area, with indication of the standard deviation, of 10 TC identified in the TIC of both biomethane sample types: 2 L_N collected on TA14-CpX29 MAT at 1 L_N·min⁻¹ at 1.45 bar_a after depressurization (n=5 successful replicates) versus directly at 40 bar_a in the HPTS (n=6 successful replicates)).....282

Figure 5.11: Per-chemical family and global relative abundances (RA, %) of molecular formulas, with indication of the potential corresponding TC, identified in both biomethane sample types: 2 L_N collected on TA14-CpX29 MAT at 1 L_N·min⁻¹ at 1.45 bar_a after depressurization (n=5 successful replicates) versus directly at 40 bar_a in the HPTS (n=6 successful replicates)). Compounds marked with a "*" are unequivocally identified.....284

Figure 5.12: TIC of two biomethane replicates preconcentrated directly at 40 bar_a compared to the TIC of two 41 HVOC SGM replicates sampled and analyzed under the same conditions: 2 L_N collected at 40 bar_a on TA14-CpX29 MAT at 1 L_N·min⁻¹ in the HPTS.285

Figure 5.SI-1: High-pressure adsorption isotherms of the HVOC not shown in Fig.5.4 of the core paper for test-condition A (2 L_N of the SGM sampled at 5, 40 and 100 bar_a on TA14-CpX29 MAT). Average peak area with indication of the standard deviation.....291

Figure 5.SI-2: High-pressure adsorption isotherms of the HVOC not shown in Fig.5.5 of the core paper for test-condition B (5 L_N of the SGM sampled at 5, 40, 68 and 74 bar_a on TA14-CpX29 MAT). Average peak area with indication of the standard deviation.294

Figure 5.SI-3: Partial breakthrough curves for the HVOC not shown in Fig.5.6 of the core paper for test-condition C (1, 2 and 5 L_N of the SGM sampled at 40 bar_a on TA14-CpX29 MAT). Average peak area with indication of the standard deviation.....297

Figure 5.SI-4: Partial breakthrough curves for the HVOC not shown in Fig.5.7 of the core paper for test-condition D (2, 5 and 6 L_N of the SGM sampled at 5 bar_a on TA14-CpX29 MAT). Average peak area with indication of the standard deviation.....300

Figure 6.1: TIC of a new blank TA14-CX26 and a new blank TA14-CpX29 MAT with indication of septum-released siloxane background contaminants.320

Figure 6.2: TIC of 0.5 versus 1 L_N dried raw biogas of plant C sampled on individual TA14-CpX29 MAT.....322

Figure 6.3: TIC of landfill gas (plant A, November 2021), raw biogas (plant B, March 2021) and dried biomethane (plant B, March 2021) sampled on TA14-CX26 or on TA14-CpX29 MAT as described in Table 6.3.324

Figure 6.4: Per-family relative abundance (%) of trace compounds identified in the landfill gas of plant A sampled on TA14-CX26 versus on TA14-CpX29 MAT. Compounds marked with a “*” are unequivocally identified.....325

Figure 6.5: Per-family relative abundance (%) of trace compounds identified in the raw biogas of plant B sampled on TA14-CX26 versus on TA14-CpX29 MAT. Compounds marked with a “*” are unequivocally identified.326

Figure 6.6: Per-family relative abundance (%) of trace compounds identified in the dried biomethane of plant B sampled on TA14-CX26 versus on TA14-CpX29 MAT. Compounds marked with a “*” are unequivocally identified.327

Figure 6.7: TIC of landfill gas (plant A) sampled on TA14-CX26 in March versus in November 2021.329

Figure 6.8: Per-family relative abundance (%) of trace compounds identified in the landfill gas (plant A) sampled on TA14-CX26 in March versus in November 2021. Compounds marked with a “*” are unequivocally identified.330

Figure 6.9: TIC of raw biogas and dried biomethane of plant B sampled on TA14-CpX29 in March 2021.332

Figure 6.10: Per-family relative abundance (%) of trace compounds identified in the raw biogas and dried biomethane of plant B sampled on TA14-CpX29 in March 2021. Compounds marked with a “*” are unequivocally identified.333

Figure 6.11: TIC of the grid-biomethane of plant B sampled on TA14-CpX29 in April, May and December 2021.334

Figure 6.12: Per-family relative abundance (%) of trace compounds identified in the grid-biomethane of plant B sampled on TA14-CpX29 in April, May and December 2021. Compounds marked with a “*” are unequivocally identified.335

Figure 6.13: TIC of the dried raw biogas and pre-treated biogas of plant C sampled on TA14-CpX29 in March 2021337

Figure 6.14: Per-family relative abundance (%) of trace compounds identified in the dried raw biogas and pre-treated biogas of plant C sampled on TA14-CpX29 in March 2021. Compounds marked with a “*” are unequivocally identified.338

Figure 6.15: TIC of 0.5 L_N landfill gas of plant A sampled in March and November 2021 on TA14-CX26 and of the synthetic gas mixture (SGM) sampled and analyzed identically.342

Figure 6.16: TIC of 0.5 L_N raw biogas of plant B sampled in March 2021 on TA14-CpX29 and of the synthetic gas mixture (SGM) sampled and analyzed identically.342

Figure 6.17: TIC of 2.3 L_N grid-biomethane of plant B sampled in December 2021 at 40 bar_a on TA14-CpX29 and of the synthetic gas mixture (SGM) sampled and analyzed identically.343

Figure 6.18: TIC of 0.5 L_N dried raw biogas of plant C sampled in March 2021 on TA14-CpX29 and of the synthetic gas mixture (SGM) sampled and analyzed identically.343

Figure 6.SI-1: 0.5 L_N raw biogas from plant B sampled at 75 ± 0.5 mL_N·min⁻¹ on 3 TA14-CX26 MAT in series (front, mid and back MAT): overlay of the TIC of each tube in the series.....345

Figure 6.SI-2: 0.5 L_N raw biogas from plant B sampled at 75 ± 0.5 mL_N·min⁻¹ on 3 TA14-CpX29 MAT in series (front, mid and back MAT): overlay of the TIC of each tube in the series.....345

Figure 6.SI-3: 1L_N raw biogas from plant C sampled at 60 ± 0.5 mL_N·min⁻¹ on 3 TA14-CX26 MAT in series (front, mid and back MAT): overlay of the TIC of each tube in the series.....346

Figure 6.SI-4: 1L_N raw biogas from plant C sampled at 60 ± 0.5 mL_N·min⁻¹ on 3 TA14-CpX29 MAT in series (front, mid and back MAT): overlay of the TIC of each tube in the series.....346

Figure 6.SI-5: 1L_N pre-treated biogas from plant C sampled at 65 ± 0.5 mL_N·min⁻¹ on 3 TA14-CX26 MAT in series (front, mid and back MAT): overlay of the TIC of each tube in the series.347

Figure 6.SI-6: 1L_N pre-treated biogas from plant C sampled at 65 ± 0.5 mL_N·min⁻¹ on 3 TA14-CpX29 MAT in series (front, mid and back MAT): overlay of the TIC of each tube in the series.347

Figure 6.SI-7: Global relative abundance (%) of trace compounds identified in the landfill gas (plant A) sampled on TA14-CX26 in March versus in November 2021. Compounds marked with a “*” are unequivocally identified.348

Figure 6.SI-8: Global relative abundance (%) of trace compounds identified in the raw biogas and dried biomethane of plant B sampled on TA14-CpX29 in March 2021. Compounds marked with a “*” are unequivocally identified.349

Figure 6.SI-9: Global relative abundance (%) of trace compounds identified in the grid-biomethane of plant B sampled on TA14-CpX29 in April, May and December 2021. Compounds marked with a “*” are unequivocally identified.350

Figure 6.SI-10: Global relative abundance (%) of trace compounds identified in the dried raw biogas and pre-treated biogas of plant C sampled on TA14-CpX29 in March 2021. Compounds marked with a “*” are unequivocally identified.351

LIST OF TABLES

Table I.1: Biogas production and biogas share in the natural gas consumption in European countries in 2015. “-“ = no available data. Adapted from [46].	32
Table I.2: Amount and type of biogas plants in several Asian countries in 2014. “-“ = no available data. Adapted from [45].	32
Table 1.1: Known thermochemical reactions taking place during dry biomass gasification using steam as gasifying agent in fixed-bed reactors. From [77].	62
Table 2.1: Physico-chemical features of some common gas sampling bags according to manufacturer’s informations. Bags with stainless-steel valves usually have a higher maximal working temperature due to the higher thermal resistance of the o-ring in those valves compared to the polypropylene valves with integrated septum.	92
Table 2.2: Properties of common commercial adsorbents used in thermodesorption applications.	109
Table 2.3: Examples of sorbent tube conditioning parameters	111
Table 2.4: Examples of second cold focusing sorbent traps used for the thermal desorption analysis of air or biogas trace compounds sampled on adsorbent tubes. (H)VOC: halogenated volatile organic compounds.	115
Table 2.5: Review of studies using adsorbent tubes to sample and preconcentrate trace compounds in landfill gas, biogas and biomethane. All gas samples were taken at near atmospheric pressure.	143
Table 2.6: Review of the applications of SPME for the determination of trace compounds in biogas, biomethane and landfill gas.	160
Table 2.7: Review of the applications of impingers for the determination of trace compounds in biogas, biomethane and landfill gas.	165
Table 2.8: Review of the applications of cryotrapping – gas chromatography – inductively coupled plasma – mass spectrometry (CT-GC-ICP-MS) for the determination of traces of (in)organic volatile metals and metalloids in biogas, landfill gas and natural gas.	172
Table 2.9: Global features of gas sampling techniques: whole gas sampling and gas sampling with enrichment.	176
Table 3.1: Multibed adsorbent tube (MAT) configurations evaluated.	209
Table 3.2: Certified synthetic gas mixtures (SGM) used. TC: trace compound.	210
Table 3.3: Sampling experiments of the synthetic gas mixtures on the multibed adsorbent tubes (MAT)	211
Table 3.4: TD-GC-MS operational parameters	213

Table 3.5: Results of the sampling experiments of the synthetic gas mixtures (SGM) on the multibed adsorbent tubes (MAT). TC: trace compound.....	216
Table 3.6: Chromatographic retention times of the trace compounds in the 41 HVOC synthetic gas mixture (SGM) sampled on TA14-CX26 and on TA14-CpX29 multibed adsorbent tubes (retention times on the front tubes of the sampling series).....	218
Table 4.1: Operational parameters for the GC-MS, nCx-TD and Network Headspace Sampler	233
Table 4.2: Main qualifying ions for the IDL determination of compounds determined in NG-A	234
Table 4.3: Main trace compounds identified via the NIST-library from the building grid natural gas (NG-A) chromatograms (Fig.4.5) obtained by sampling on TA15 tubes, CAR/PDMS 75 μ m SPME fiber and in headspace vials.....	241
Table 4.4: Standard deviation (Std dev), relative standard deviation (RSD% = 100 Std dev/average) and instrument detection limit (IDL = 3 Std dev) (signal abundance) of the BTEX background noise (peak height) in 10 blanks of the CAR/PDMS 75 μ m SPME fiber, in the blanks of 10 new Tenax TA15 tubes and in 10 vials of pure CH ₄ for HS injections.....	242
Table 4.5: Linear regression output (Peak Area = slope a x Concentration) and analysis of variance (F-statistical test) between average peak area of BTEX compounds and concentration, at a significance level $\alpha = 0.05$. The critical F-value $F_{(1,5)}$ at $\alpha = 0.05$ is 6.6079.	246
Table 4.6: Semi-quantification (ppb _v) of the BTEX contamination background in new TA15 blank tubes, a blank SPME fiber and 'blank' (pure CH ₄) vials based on the BTEX peak areas in 10 ppm _v BTEX-CH ₄ samples.	246
Table 4.S1: nCx-TD operational parameters	249
Table 4.S2: Chromatographic peak areas of 10 ppm _v benzene, toluene, ethylbenzene, m-,p-xylene and o-xylene and chromatographic peak resolutions between toluene and benzene, ethylbenzene and toluene, m-,p-xylene and ethylbenzene, o-xylene and m-,p-xylene acquired at 10 ppm _v from the three injection systems studied (nCx-TD, SPME and Headspace). Std dev: standard deviation. RSD%: relative standard deviation = 100 · Std dev / average. n = number of injections.....	249
Table 4.S3: Instrument detection limits (IDL = 3 Std dev) (peak height signal abundance) of trace compounds determined in the NG-A building grid natural gas sample on TA15 tubes and on the CAR/PDMS 75 μ m SPME fiber (Fig.4.7 in paper).....	250
Table 4.S4: Relative standard deviations (% ; n=3) of the peak areas obtained for each BTEX compound at the 6 concentrations tested for each injection technique.	250
Table 4.S5: Linear regression output and analysis of variance (F-statistical test) between concentration (1, 2.5, 5, 7.5, 10 ppm _v) and average Gaussian peak resolution between	

ethylbenzene and m-, p-xylene, at a significance level $\alpha = 0.05$. The critical F-value $F(1,3)=10.13$ at $\alpha = 0.05$251

Table 5.1: Properties of commercial adsorbents used in the MAT.....267

Table 5.2: The 41 HVOC present in the SGM used, listed in order of increasing boiling points. Note 1,2-dichloropropane was never detected on the TA14-CpX29 MAT despite both adsorbents should enable fair adsorption and recovery (>80%) of this compound [44].....270

Table 5.3: Experimental conditions for the HPTS lab validation. n= amount of successful replicates.....271

Table 5.4: TD-GC-MS instrument parameters.....272

Table 5.SI-1: Chromatographic retention times (min) of compounds identified from the TD-GC-MS analysis of the SGM sampled at different test-pressures and different volumes at $1 \text{ L}_N \cdot \text{min}^{-1}$ on the TA14-CpX29 MAT in the HPTS prototype. STDEV : standard deviation. * : absent. \diamond : co-elution of tetrachloromethane, acrylonitrile and benzene290

Table 6.1: Composition and properties of multibed adsorbent tubes (MAT) configurations.315

Table 6.2: Gas production plants where landfill gas, biogas and biomethane samples were collected. THT= tetrahydrothiophene.....317

Table 6.3: Operational sampling parameters. P= pressure. MAT= multibed adsorbent tube. V= volume. n= number of MAT replicates taken. Q= flowrate. T= temperature. L= length. THT= tetrahydrothiophene. PTFE=polytetrafluoroethylene. PFA= Perfluoroalkoxy-alkane. SS= stainless-steel.....318

Table 6.4: TD-GC-MS instrument parameters.....319

Table 6.SI-1: The 41 halogenated volatile organic compounds present in the synthetic gas mixture, listed in order of increasing boiling points.....352

PART 1 - INTRODUCTION

ABBREVIATIONS PART 1

CH ₄	Methane
CO ₂	Carbon dioxide
CO ₂ -eq	Carbon dioxide equivalent
E.U.	European Union
GC	Gas chromatography
GWh	Giga (10 ⁹) watt hours
MS	Mass spectrometry
MWh	Mega (10 ⁶) watt hours
Nm ³	Normal cubic meter: measured at 0°C and 1013 mbar (1 atm)
Sm ³	Standard cubic meter: measured at 15°C and 1013 mbar (1 atm)
TC	Trace compound(s)
TD	Thermal desorption
TJ	Tera joule (10 ¹² Joules)
TWh	Tera (10 ¹²) watt hours

I. CONTEXT

I.1. Energy transition and circular economy

Driven by its tremendous eagerness for economic growth and social prosperity, mankind has been the only living being capable of irremediably spoiling its life environment by over-consuming natural resources, transforming them into long-lasting, difficultly degradable materials, as such generating permanent and potentially dangerous waste.

Climate change is a daily ominous happening. Environmental concerns and the concepts of energy transition and circular economy benefit from a rising worldwide attention the last years in view of the increasingly threatening depletion of fossil and finite energy sources and of the consequences of their use on the environment. If our society is doomed to continuously procreate, progress in medicine and technologies, produce and build, other material and energy sources than mineral ores, primary resources and fossil fuels must be thought of to sustain the long term.

In 2020, the world total energy consumption (oil, natural gas, coal, nuclear energy, hydroelectricity, renewable energies) was 557.10 Exajoules with renewable energies (solar thermal and photovoltaic, geothermal, wind and biomass energy) accounting for 5.7% of this global energy consumption (against 5.0 % in 2019) while oil, natural gas and coal respectively accounted for 31.3%, 24.7% and 27.2% [1]. After oil and coal, natural gas is the third most exploited energy source. In spite of its greener label owing to the lesser amounts of greenhouse gases and other air polluting compounds (SO_2 , NO_x) or particles emitted during its combustion per joule of energy produced compared to the combustion of oil and coal [2–9], natural gas is also a finite fossil fuel and therefore not a sustainable energy source. The world proved reserves-to-production ratio of natural gas, indicating known reserves will be exhausted in x years if the production and consumption rates remain the same as in a given year, keep on decreasing as they amounted respectively 52.6; 50.9 and 48.8 years at the end of 2017, 2018 and 2020 [1,10,11]. Henceforth, not only reducing global energy consumption but also using alternative more sustainable energy sources is crucial to sustain the ‘welfare’ of future generations.

The consumption rate of natural gas is nevertheless expected to further strongly increase: the attractive relatively greener combustion of natural gas brings hope in many large fast growing cities of emerging economies such as China [4,6,10,12–14], Japan [4,6,7,10], India [4,6,13] and Brazil [4,8] facing major atmospheric pollution issues [6,7,12,15] due to urbanization, traffic and old remaining coal or fuel fired power plants [13]. The use of natural gas is especially strongly being promoted in Asia and India to replace lower grade coal (the so-called “coal-to-gas switching” [12]) whose combustion not only results in the emission of large volumes of greenhouse gases and SO_2 provoking acid rains and ozone layer degradation, but also emits carbon monoxide and particulate matter (notably PM 2.5: particles having a mean diameter $< 2.5 \mu\text{m}$) causing severe air pollution [6,7,12,16] and associated respiratory diseases. In those fast growing economies and elsewhere, natural gas is especially going to be more and more used for electric and thermal power generation, natural gas vehicles, industrial (plastic, pharmaceuticals, glass manufacturing [6]) and residential (cooking, warming, water heating) purposes [6,12,16].

To preclude the day fossil natural gas will be depleted, promising, efficient, abundant and renewable energy alternatives are needed. These alternative fuels are all the more urgently required that the risk exists that emerging economies get back to coal in the short term in case natural gas would become unappealing due to price rises, supply failures or deficits [6], with all the environmental consequences this retrogression would entail. In France, in an attempt to meet the Paris Agreement target of maximum 1.5°C global temperature rise, the goal is to bring the share of renewable gases to 7 to 10% of the total gas consumption by 2030 depending on costs cuts [17,18]. Those renewable gases include [19–21]:

- biomethane from the anaerobic digestion of humid organic wastes,
- synthetic natural gas from the pyrogasification of dry ligneous biomass waste or refuse-derived fuel,
- synthetic natural gas from the methanation of hydrogen with carbon dioxide or carbon monoxide where the hydrogen can come from the hydrolysis of water by (green) electricity surpluses (power-to-gas technology),
- hydrogen gas generated by power-to-gas technology.

The feasibility of the even more optimistic scenario of 100% renewable gas by 2050 in France, with an estimated gas consumption of 300 TWh by then compared to 460 TWh in 2017, was evaluated as positive if the production and use of the four mentioned sources of renewable gases are optimized [19,21].

The optimal substitute for natural gas must have virtually the same composition while being renewable at a human time scale. Natural gas is composed for ~90 mol% of methane (CH₄), ~7 mol% of paraffins and aromatic compounds, ~3 to 15 mol% of inorganic compounds (CO₂, CO, H₂S, N₂, H₂O, He, Ar and other noble gases) [3,22–24] and trace levels of Hg, As, Zn, Ni, Sn, Cu, V, Rn [22–25] and organic Sulphur compounds [25]. Biomethane, a pure renewable methane gas stream resulting from the upgrading of the so-called biogas produced during the microbially driven anaerobic digestion of humid organic matter in controlled digester reactors, has almost the same calorific value as fossil methane (natural gas) with CO₂ levels lower than 3 %_{vol} [26–28]. Yet the trace element composition of biomethane may differ from that of natural gas [22,29] and varies depending on the organic matter type digested, on the physico-chemical operational digester parameters (temperature, pH, humidity retention times, process materials...) [30–33] and on the implemented biogas upgrading process [28,34], this gas has gained interest in the energy sector as it satisfies the criteria for an ideal natural gas substitute. Provided its stringent compliance to natural gas quality standards stipulating maximal levels of several chemical compounds (e.g. total Sulphur <30 mgS·Nm³, H₂S and COS <5 mgS·Nm³, CO₂ <2.5 %_{mol}, CO <2%_{mol}, O₂ <0.001%_{mol}, H₂ <6%_{mol}, NH₃ <3 mg·Nm³, Hg <1 µg·Nm³, chlorinated species <1 mg·Nm³, fluorinated species <10 mg·Nm³, siloxanes <5 mg·Nm³) [35], biomethane is intended for injection in the existing natural gas transport grid [36] to gradually substitute natural gas in any of its applications and in particular as transport fuel [37–39]. Biogas itself, either produced in controlled digesters or spontaneously in landfills, is mainly composed of CH₄ (≥50 %_{vol}) and CO₂ (<50%_{vol}) [28,30] and has also direct heat and power generation applications by its combustion in boilers, cookers [16], internal combustion engines [40,41], (solid oxide) fuel cells [42–44] and combined heat and power generation engines [41,45–47]. Ideally generated out of

anthropogenic organic wastes (agricultural residues, manure, food-processing and catering residues, organic and green municipal and household wastes, sewage sludge), biogas and biomethane concomitantly fit in the circular economy and energy transition.

Generating biomethane out of organic wastes has economic, social and environmental advantages [48,49]. Local circular economies are created [20,49] since anaerobic digesters are fed with organic wastes from various society sectors. Valorizing organic wastes this way moreover avoids the costs of their otherwise conventional treatment and the side-products of anaerobic digestion are also valuable (digestates [50], CO₂ [51,52]). Next, biomethane is a flexible energy carrier since it is storable, just as natural gas, allowing to balance the loads in energy networks between winter and summer [46]. The existing gas transport, distribution and storage infrastructures can moreover be directly exploited and perpetuated in the long-term [20,47]. Also, as opposed to wind and solar renewable energies having an intermittent character, biomethane can be produced continuously due to the uninterrupted supply of organic wastes and the independency to weather variables [47,53]. Lastly, while most countries depend on suppliers and imports for oil, natural gas or coal, nationally producing biomethane from organic wastes, available in all countries in contrast to fossil fuels, strengthens the economic and energetic self-sufficiency of a country [18,54]. Socially, the growing biogas-biomethane sector is an opportunity for employment creation, with averagely 3-4 local fixed employs per anaerobic digestion plant [20,55]. For farmers producing and injecting biomethane in the gas grid and selling the digestates, such projects signify also additional incomes following returns on investments [47,56,57]. Biomethane, when produced from organic wastes, is furthermore ethical in contrary to food- or energy-crop based biofuels [46,58]. Environmentally, biomethane is greener than natural gas. Natural gas consumption still induces atmospheric pollution (500 t SO₂, 6400 t NO_x, 35000 t CO emitted in 2016 in France) and the release of greenhouse gases (73 Mt CO₂-equivalent in 2016 in France) [18]. On the contrary, when burning a renewable gas like biomethane, greenhouse gases emissions are approximately compensated by the carbon uptake required for the synthesis of the gas. If naturally allowed to rot in piles, the huge quantities fermentable wastes our society produces would emit proportionally large methane volumes to the atmosphere [16,46,59] while the global warming potential of methane amounts ~25 for a 100 years time span, rendering it 25 times more injurious than CO₂ regarding global warming [16,60,61]. Controlling the degradation of such organic wastes in anaerobic digesters avoids such emissions insofar as the produced methane is collected for energy purposes. Subsequent combustion of biomethane releases CO₂ to the atmosphere (0.8 kg CO₂/kg biogas [18]) albeit this contributes to less global warming than the direct emission of methane [16]. Moreover, this emitted CO₂ is later again taken up by growing vegetation that eventually will die, releasing the metabolized CO₂ as methane if used as feedstock in digesters [18]. A Life Cycle Analysis (LCA) of biomethane reports the production and combustion of biomethane for heat purposes results in emission savings of 218 kg CO₂-eq/MWh compared to natural gas [55,62]. This allowed already a 90 000 tons CO₂-eq saving in 2017 in France and the biomethane sector should enable a saving of 1.7 million tons CO₂-eq in 2023 in France when considering the French objective to inject 8 TWh biomethane in the existing gas grid infrastructures by 2023 [55,62]. Besides, biomethane used as vehicle fuel emits 80% less greenhouse gases than diesel [55].

I.2. Biogas and biomethane world trends

Biogas is the third fastest growing renewable electricity source after solar and wind derived electricity, with an annual growth rate of 12% since 1990 [63]. The global biogas production was more than quadrupled (from 78 to 364 TWh) between 2000 and 2017 [58]. Throughout the world, Europe dominates the biogas and biomethane production market followed by China and the United States of America. While Europe mostly produces biogas in anaerobic digesters from energy-crops and organic wastes, landfill biogas accounts for 90% of the biogas production in the USA. In China, household-scale anaerobic digesters have been promoted in rural areas and account for up to 70% of the current installed biogas capacity [37].

Applications of biogas or biomethane vary across world regions. High-income countries rather convert biogas into electricity and heat and biomethane into vehicle fuel [16,46,58]. Leading vehicle fuel consumers are public and private transport companies motivated to curtail their greenhouse gases emissions while leading biogas-derived heat consumers are local authorities' public buildings [20]. Low income countries rather use biogas for cooking and lighting, which advantageously reduces deforestation (wood is the main heat source for cooking and heating) and improves indoor air quality (wood or coal cooking releases greenhouse gases and fine particles able to enter lungs, causing respiratory diseases) [16,46].

The most recent *and* comprehensive review on biogas developments in Europe [46] pinpointed biogas consumption accounted for averagely 4% of the natural gas consumption in 2015, with Germany using the most biogas, namely 12% of its yearly natural gas consumption. The dominant biogas producers in the European Union (EU) were Germany, generating 50% of the total European biogas production, the United Kingdom, Italy, Czech Republic and France (Table I.1) [46]. According to the European Biogas Association, 18943 biogas production plants and 725 biomethane production plants were in service across Europe by the end of 2019 [64] with ~10% of the biogas production upgraded to biomethane. By 2030, up to 20% of the biogas production could be upgraded to biomethane [37,65]. While in 2015 the EU counted over 300 plants injecting biomethane in the natural gas grids [46], end 2020 635 out of the almost 730 biomethane plants were injecting a total of 25 TWh biomethane in the natural gas grids [19]. The number of EU countries injecting biomethane in the grids rose from 10 in 2015 (mainly Germany 165 injection plants, the United Kingdom 80 injection plants, Switzerland 35 injection plants)[46] to 18 in 2020 (numbers of plants connected to the grids: Ireland 1; UK 80; Iceland 2; Norway 3; Sweden 16; Finland 5; Estonia 2; Denmark 45; The Netherlands 48; Belgium 4; Luxembourg 3; Germany 230; Hungary 1; Austria 14; Switzerland 36; Italy 17; France 214; Spain 2)[19]. In France, biomethane grid injection is authorized since July 2011 and the sector has substantially expanded since then with the introduction of feed-in tariffs in 2011 [20]. Biomethane quantities injected in the grid rose by 90% in one year, going from 215 GWh in 2016 to 406 GWh in 2017 [55] and by 80% in 2020, reaching 2207 GWh injected end 2020 [19]. End 2020, a total of 1075 biogas plants were operating in France, of which 20% (214 plants) upgrade biogas in biomethane for grid injection and the remaining 80% (861 plants) valorize biogas via combined heat and power generation. After Germany (232 biomethane production plants), France counted the most biomethane plants in the EU, and French biomethane as such covered 0.5% of the French natural gas consumption in 2020 [19]. Besides, Europe supplied 160 million

Sm³ biomethane for transport fuel purposes in 2015, distributed by almost 700 biomethane filling stations especially across Sweden (205 stations), Germany (288 stations), Switzerland (140 stations), Norway (24 stations), Iceland, Finland and Italy [46]. In France, biomethane as vehicle fuel accounts for the largest market part [20] and the ambition is to foresee up to 360 biomethane filling stations by 2023 and up to 840 stations by 2028 [17]. The use of biomethane as vehicle fuel is still in its infancy but is expected to rise depending on subsidies or promotion programs. Its share in the transport biofuel market will also increase as the share of food-based biofuels is about to be abated to 3.8% in 2030 [46]. By 2030, biomethane production for grid injection and vehicle fuel could potentially reach ~50 billion Nm³/year across the E.U. from anaerobic digestion and from the pyrogasification of dry ligneous biomass [46]. These positive development trends in the EU biomethane sector were initially enabled by favorable energy policies, EU directives and grant or incentives programs such as tariff rebates on the gas distribution grid connection costs or state/European/regional financial support to promote biogas production [46,48,62]. Brémond et al. [58] nevertheless reviewed future trend perspectives and challenges for this sector towards 2030 as it nowadays faces development paradigm shifts with notably a decline in subsidy schemes and a transition to feedstocks from the wastes sectors only, encouraging the gradual abandonment of high methane potential energy-crops as feedstocks in anaerobic digesters.

In the USA, more than 2100 biogas plants were recorded in 2017: 250 farm plants fed with animal manure, 654 landfill gas production plants, 1240 sludge-fed waste water treatments plants, altogether producing 18.5 billion Sm³ biogas/year [46].

All over Asia the amount of small and large scale anaerobic digesters for biogas generation increases [46] and in 2020, next to China, Thailand and India contributed the most [37]. In China 15 billion Sm³ biogas were produced in 2014 by ~100 000 modern and ~40 million residential-scale biogas plants. India had the ambition to build more than 100 000 biogas plants between 2014 and 2019, encouraging the installation of residential- and farm-scale plants [46]. In Malaysia, 90 biogas plants were operating in 2017, 6 were under construction and 145 were planned [66]. Some information on the situation in other Asian countries issued from the most recent *and* comprehensive review on biogas developments is summed up in Table I.2.

In Africa biogas production is not well developed yet and data is missing. Benin, Burkina Faso and Ethiopia nonetheless started providing subsidies to cover investments and non-governmental organisations are also getting involved [37].

In Latin America, Bolivia created at least 1000 household biogas plants and in Columbia, Honduras and Argentina, large-scale plants were built with effluents from palm oil mills and farms as feedstock. Brazil has also 127 biogas plants fed with industrial and agricultural waste, sewage sludge and landfill waste, altogether producing ~584 billion Nm³ biogas/year what contributed to generate 3835 GWh energy in 2015 [46].

Table I.1: Biogas production and biogas share in the natural gas consumption in European countries in 2015. "-" = no available data. Adapted from [46].

Country	Biogas Production (TJ)	Biogas share (%) in the natural gas consumption
Belgium	9 492	1.6
Bulgaria	820	0.8
Czech Republic	25 681	9.5
Denmark	6 347	5.3
Germany	328 840	12.1
Estonia	550	3.4
Ireland	2 287	1.5
Greece	3 826	3.4
Spain	10 954	1.1
France	22 549	1.5
Croatia	1 507	1.7
Italy	78 355	3.4
Cyprus	471	-
Latvia	3 674	8.0
Lithuania	981	1.1
Luxembourg	739	2.3
Hungary	3 335	1.1
Malta	69	-
The Netherlands	13 693	1.1
Austria	12 563	4.4
Poland	9 581	1.7
Portugal	3 457	2.0
Romania	767	0.2
Slovenia	1 242	4.5
Slovakia	6 223	3.8
Finland	4 321	4.6
Sweden	7 009	23.2
United Kingdom	94 303	3.7
Switzerland	4 591	3.8
Iceland	69	-
Norway	1 866	0.8
Former Yugoslav Republic of Macedonia	206	4.4
Serbia	242	0.3
Moldova	401	1.3
Ukraine	600	0.1
European Union (mean values)	653 636	4.4
European continent (mean values)	661 611	4.0

Table I.2: Amount and type of biogas plants in several Asian countries in 2014. "-" = no available data. Adapted from [45].

Country	Residential-scale plants	Commercial-scale plants
Bangladesh	36 000 (100 000 more expected by 2020)	500 – 600 (130 more expected in 2017)
Nepal	330 000	-
Sri Lanka	6000	-
Pakistan	4000	-
Vietnam	-	183 000

II. BIRTH AND DEFINITION OF THE RESEARCH PROBLEM

Previous sections highlighted the biogas and biomethane sector are getting momentum worldwide as nations tend to increase the share of renewable gases in their global energy consumption to trigger energy transition and circular economies. Biogas is predominantly converted in heat and electricity for injection on local grids whereas biomethane is meant to supplant natural gas in any of its applications.

It has nevertheless been acknowledged biogas generated in landfills or in anaerobic digesters contains, next to its two major constituents CH_4 ($\geq 50\%$ vol) and CO_2 ($< 50\%$ vol), minor constituents like N_2 , H_2O , H_2S , NH_3 , H_2 , CO , O_2 and traces of volatile compounds ('trace compounds', TC) from various families: alkanes (linear, cyclic, polycyclic), aromatics, terpenes, alkenes, halogenated organic species, oxygenated organic species (alcohols, aldehydes, esters, furans and ethers, ketones), Silicon-compounds including siloxanes and silanes, organic and inorganic Sulphur-compounds [28,30,31,67–75] and (in)organic metal(loid) species [22,70,76–79]. This biogas composition is strongly dependent on the organic matter being digested and on the physicochemical parameters driving the anaerobic digestion (hydraulic retention time, temperature, humidity, pH...) [30–33]. Observed concentrations range $30 - 35000 \mu\text{g}\cdot\text{m}^{-3}$ [80] and $< 10 - 700 \text{ mg}\cdot\text{m}^{-3}$ [81] for total volatile organic compounds; $< 100 \mu\text{gSi}\cdot\text{m}^{-3}$ for total siloxanes [81] and $< 300 \mu\text{gSi}\cdot\text{m}^{-3}$ for total volatile methyl siloxanes [71]; and $0.1 - 100 \text{ ng}\cdot\text{Nm}^{-3}$ for metallic TC [22]. In function of the handled technology to upgrade the CH_4 fraction (biomethane) of biogas by separation from the CO_2 fraction, a variety of those TC are also found lurking in biomethane [22,27,28,34,71,72,80]. Natural gas also contains TC originating from geological processes (metals, volatile organic compounds, Sulphur-compounds, NOx particles...)[3,23–25,82–84], but the nature and diversity of TC in biogas and biomethane may differ owing to the anthropogenic or vegetal origin of the feedstocks used in landfills and anaerobic digesters.

Depending on the intended energy application, removal of minor- and TC in biogas and biomethane is crucial inasmuch as compounds such as H_2S , NH_3 , COS , CS_2 , thiols, halogenated compounds, siloxanes, aliphatic or aromatic hydrocarbons can have deleterious effects (acid corrosion, abrasion, fouling, depositions, catalyst deactivation...) on gas transport infrastructures and in boilers, engines and fuel cells upon combustion of the gas [32,33,43,68,73,85–87]. Odorous compounds like terpenes are also known to attack rubber seals in gas infrastructures, to engender air quality issues and to mask the tetrahydrothiophene artificial odor of grid-injected biomethane [34]. Determining suitable abatement techniques requires the preliminary qualitative and quantitative characterization of TC and field- or *in situ* gas sampling is the first and most critical step of the analytical chain leading to this characterization.

Field sampling, identification and quantification of TC in gaseous matrices such as biogas, biomethane or natural gas is challenging owing to their low concentrations and the intricate interactions between compounds and gas matrices present. The low concentrations not only imply high risks for TC masking by contamination and for TC loss by sorption to tubing, connectors and vessels in the sampling and analytical chains [69,81,88,89], but they often lie

below the detection limits of analytical instruments, meaning a 'preconcentration' step is essential (the gas flows through a dedicated small-volume support with specific retention affinity for only given TC. Since the very volatile gas matrix itself (CH₄) is not retained, TC are preconcentrated). *In situ*, gas can either be bulk-sampled in a whole gas sampling vessel (bag, canister, cylinder) subsequently transported to a laboratory where the gas is transferred to a preconcentration unit, or gas can be directly circulated through a preconcentration unit (e.g. adsorbent tubes, bubbling absorption solutions, cryogenic traps) enriching desired TC only [81,90–92]. However, because TC lurk in complex mixtures of inorganic, organic, metallic and metalloid species potentially reacting with each other, not any sampling nor preconcentration system is able to quantitatively trap all families of TC in one run in view of the complexity and diversity in physicochemical properties of TC present (volatility, polarity, water solubility, reactivity...). This results in different affinities and stabilities in the preconcentration and sampling devices used, complicating the choice of an appropriate sampling methodology as furthermore the TC composition of a biogas or a biomethane is unknown until the first sampling and analysis campaigns [69,75,80,81,88,93]. For instance, whole gas sampling with ensuing transport of the whole gas sampling vessel and delayed transfer to a preconcentration unit entails risks of TC losses during transport and storage by sorption to or permeation through the whole gas sampling vessel walls, risks of chemical conversion reactions inside vessels as well as loss and contamination risks during transfer to the preconcentration unit, endangering sample stability and TC recovery [67,75,81,83,91,93–96]. Moreover, collected samples must be representative of the effective gas composition at a given time and under the prevailing gas pressure and temperature. In particular, monitoring TC in biomethane may imply it has already been compressed to the grid pressure (French distribution network: 4-6 bar_a, transportation network: 8-80 bar_a). So far, biomethane has only been *in situ* sampled directly on the pipelines at 40 bar_a by Cachia et al. using a high-pressure acid bubbling sampler for the direct preconcentration of metallic TC [22,23]. Other determinations of TC in high-pressure gases (typically natural gas) have mostly been carried out by high-pressure cylinder sampling of a whole gas sample followed by cylinder transport to the lab, depressurization of the gas and preconcentration at atmospheric pressure [69,82,83,95].

In pursuance of enhancing knowledge on biogas and biomethane's trace compounds to help guarantee their sustainable integration in today's European energy mix, the TERÉGA company (Pau, France), a major actor in gas transport and -storage infrastructures in France and Europe to make gas an accelerator of the energy transition, took up the above-mentioned issues and took the lead to finance this doctoral thesis to further investigate and bring answers to the challenges of gas sampling for trace compounds determination. Hence, this doctoral thesis entitled '*Characterization of trace compounds in biogas and biomethane: development of a sampling-, in situ preconcentration- and analysis method*' aimed first at reviewing existing state-of-the-art field gas sampling and preconcentration methods to eventually develop and optimize an improved though simplified field gas sampling method preconcentrating TC directly *in situ* at the actual gas pressure with a shortened sampling chain minimizing contaminations and TC losses and ensuring the stability of sampled compounds (no loss, no degradation, no contamination) between sampling and analysis. The developed method would seek to connect preconcentration units as straightly as possible to the gas pipes without gas depressurization

and to reduce required sampling volumes to limit sampling campaigns duration and to limit discharges of sampled CH₄ volumes to the atmosphere. In that respect, the development of a direct high-pressure preconcentration device freeing the sampling protocol from depressurization operations was soon considered. Indeed, when dealing with pressurized gases and assuming the ideal gas law $PV=nRT$, a dilution factor equal to the ratio of the high pressure to the pressure after depressurization leads to a concentration decrease of TC upon depressurization, implying larger gas volumes have to be sampled at atmospheric pressure than at high pressure to trap a given amount of TC. The preconcentration would finally enable to trap, in a single sampling run, a wide range of unknown TC in a variety of chemical families and would enable, in collaboration with an appropriate analytical set-up, to lower the detection limit of that wide range of TC to obtain a detailed screening of the TC composition of a given gas.

Overall, the developed sampling protocol should contribute making field sampling campaigns more efficient and easier for routine operators and above all contribute to enrich the database of TC in biogas and biomethane and to establish correlations between gas production conditions (feedstocks nature, anaerobic digestion operational parameters, treatment and upgrading technologies implemented...) and TC present.

In the following section, main and detailed doctoral thesis objectives are delineated.

III. DOCTORAL THESIS OBJECTIVES

The pragmatic objectives of this doctoral thesis are:

Objective 1: reviewing state-of-the art gas sampling and preconcentration techniques for the determination of trace compounds in methane-like gas samples.

Objective 2: based on learnings from the review, developing and optimizing a field gas sampling method for the direct *in situ* preconcentration of non-metallic trace compounds (TC) in gas samples such as biogas and biomethane, at the gas working pressure, where preconcentration occurs by adsorption onto self-assembled multibed adsorbent tubes (MAT) enabling to trap, in a single sampling run, a wide range of unknown TC in a variety of chemical families as it was evidenced from the review this preconcentration method answered the best these requirements.

Objective 3: validating and optimizing the ensuing qualitative and quantitative analytical method where analytes preconcentrated on adsorbent tubes are recovered by thermal desorption of the tubes followed by gas chromatography – mass spectrometry analysis (TD-GC-MS).

Objective 4: applying the developed direct *in situ* preconcentration and analysis method to sample and determine TC in real biogas and biomethane samples generated at different production plants and from various feedstocks in France.

Non-metallic TC targeted in this work include alkanes (linear, cyclic, polycyclic), aromatics, terpenes, alkenes, halogenated organic species, oxygenated organic species (alcohols, aldehydes, esters, furans and ethers, ketones), siloxanes, organic and inorganic Sulphur-compounds.

To achieve objectives 2 – 4, a stepwise approach has been followed with a first laboratory development and validation part (Fig.I.1) and a second field validation part (Fig.I.2).

LABORATORY DEVELOPMENT AND VALIDATION WORK (objectives n°2 – 3)

- A -

Development of the preconcentration unit: adsorbent tubes

Selection of commercial adsorbents based on a preliminary literature review

- Tenax®TA 60-80 mesh
- Carbo-pack™TX 40-60 mesh
- Carbo-pack™MB 60-80 mesh
- Carboxen®1000 60-80 mesh

Design of the adsorbent tube assembly and conditioning procedure

- Untreated quartz wool plugs secure adsorbent beds in the tubes
- Fixed bed volume 0.05 cm³ for each adsorbent in the tube
- Fabrication of a 20-position tube conditioning support for installation in conditioning oven under N₂ flow

Preliminary validation tests of adsorbent tubes using certified synthetic gas mixtures containing targeted compounds (simulating biogas or biomethane TC) at trace concentrations (1 ppm_{mol}) in CH₄ or N₂ matrices

Evaluation of preconcentration on and recovery from single bed adsorbent tubes

Evaluation of preconcentration on and recovery from multibed adsorbent tubes (MAT)

Different MAT configurations tested:

- Tenax®TA - Carboxen®1000
- Tenax®TA - Carbo-pack™TX
- Carbo-pack™MB - Carboxen®1000
- Tenax®TA - Carbo-pack™MB - Carboxen®1000

- B -

Study of preconcentration under high pressure

Presentation of a high-pressure adsorbent tube sampling support (HPTS) prototype (0 - 200 bar_a)

Physicomechanical validation of the HPTS by sampling pressurized certified synthetic gas mixtures on the developed MAT

Investigation of the effect of pressure on adsorption and recovery of trace compounds from certified synthetic gas mixtures sampled on developed MAT

- C -

Validation of the analysis method: TD-GC-MS

Thermal desorption of adsorbent tubes using a thermodesorber (TD) prototype

- Attempt to validate the TD-prototype by comparison to SPME preconcentration and direct headspace gas injection

Gas chromatography - mass spectrometry (GC-MS): optimization of apparatus parameters for the detection of a wide range TC

Figure I.1: Achieving doctoral thesis objectives 2 and 3: stepwise approach for the laboratory development and validation part. TC: trace compounds.

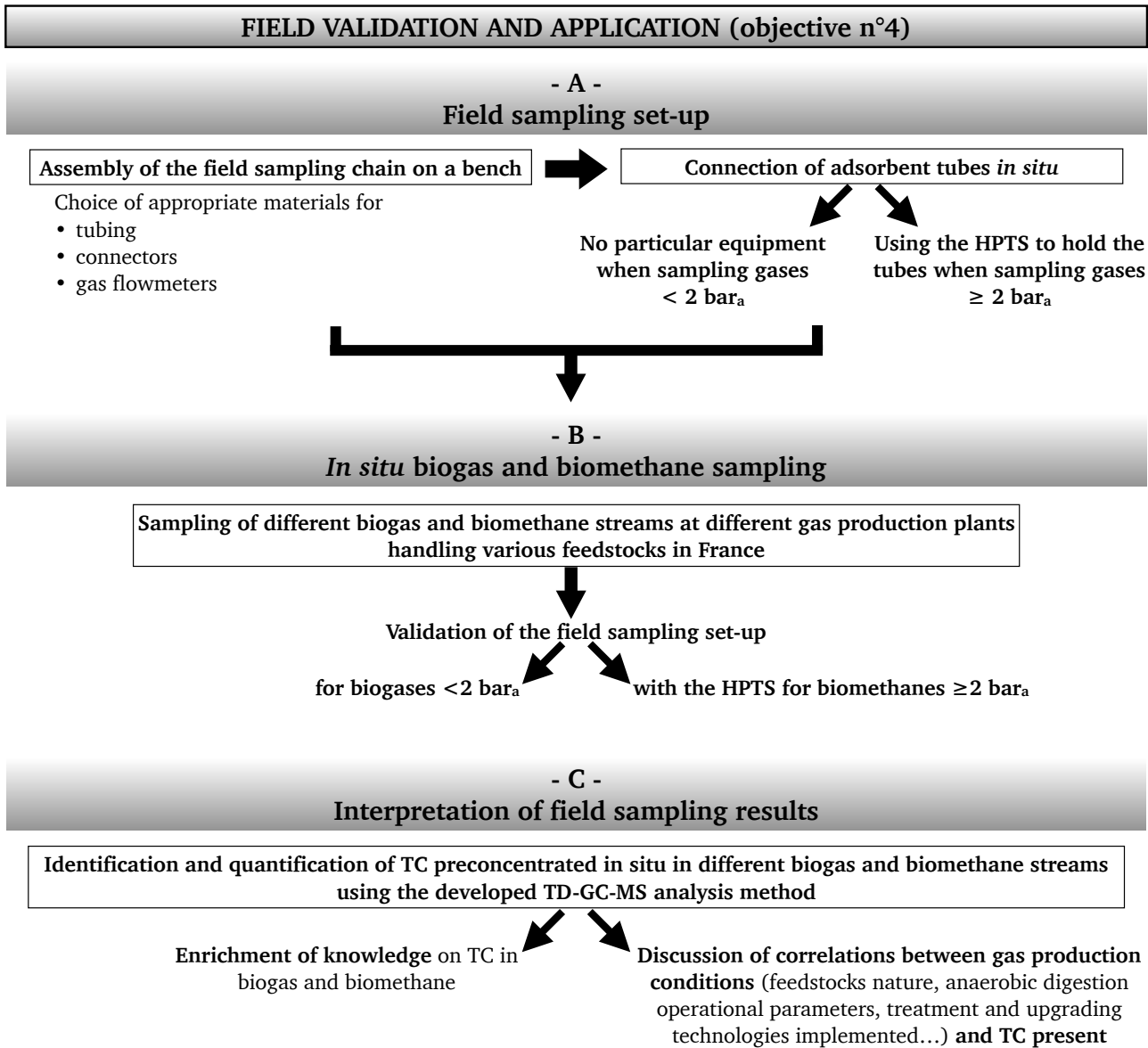


Figure I.2: Achieving doctoral thesis objective 4: stepwise approach for the field validation part. HPTS: high-pressure tube sampling support prototype. TC: trace compounds. TD-GC-MS: thermodesorption – gas chromatography – mass spectrometry.

IV. GENERAL STRUCTURE OF THE MANUSCRIPT

Part 1 of this manuscript presented the global and scientific context having led to the research problem of this doctoral thesis, and related objectives have been described.

In Part 2, following **Chapter 1** which defines biogas, landfill gas and biomethane and revises their main production processes, the state-of-the-art gas sampling and preconcentration techniques for the determination of trace compounds in methane-like gas samples are extensively reviewed and discussed (**Chapter 2**) to address Objective 1 of this thesis.

Part 3 then presents the experimental work conducted during this doctoral thesis to achieve Objectives 2 – 4.

Chapter 3 partly deals with Objective 2 by developing and optimizing multibed adsorbent tubes. The choice of adsorbent materials is motivated, the adsorbent tube assembly- and conditioning-procedures are presented and the efficiency of different multibed adsorbent tube configurations for the adsorption and thermal desorption of compounds present at trace concentrations in synthetic gas mixtures, is assessed to eventually design the most suitable multibed adsorbent tubes.

Addressing Objective 3, **Chapter 4** then presents the new thermal desorber prototype used throughout the work to thermally desorb all laboratory- and field-sampled multibed adsorbent tubes and as such recover and analyze preconcentrated analytes via gas chromatography – mass spectrometry. In particular, the chromatographic performance of this new thermal desorption prototype is compared to other chromatography injection techniques such as solid-phase microextraction and direct gas injection. The potential and strength of the combination of adsorbent tubes with the thermal desorption prototype are then demonstrated on real natural gas samples.

Chapter 5 further addresses Objective 2 by presenting and validating a novel high-pressure adsorbent tube sampling prototype enabling to sample pressurized gases ($\leq 200 \text{ bar}_a$) such as grid-injected biomethane, through the multibed adsorbent tubes by a direct connection to the field gas pipes. The effect of the gas pressure on the adsorption and desorption of trace compounds onto and from the multibed adsorbent tubes is also investigated.

Lastly, **Chapter 6** is devoted to the achievement of Objective 4: the developed direct *in situ* high-pressure preconcentration method is implemented to sample non-metallic trace compounds in landfill gas, biogas and biomethane from a landfill and two anaerobic digestion plants treating diverse feedstocks, and to qualitatively determine them by the established thermal desorption – gas chromatography – mass spectrometry analytical chain. Variations in trace compounds compositions observed between the gases are discussed.

Part 4 ultimately closes the manuscript with general conclusions and perspectives on the conducted doctoral thesis work and achievements reached.

V. REFERENCES PART 1

- [1] BP p.l.c, BP Statistical Review of World Energy 2021 - 70th edition, London, 2021.
- [2] S. Mokhatab, W.A. Poe, J.Y. Mak, Chapter 1 - Natural Gas Fundamentals, in: S. Mokhatab, W.A. Poe, J.Y. Mak (Eds.), *Handb. Nat. Gas Transm. Process. Fourth Ed.*, Gulf Professional Publishing, 2019: pp. 1–35. <https://doi.org/10.1016/B978-0-12-815817-3.00001-0> .
- [3] S. Faramawy, T. Zaki, A.A.-E. Sakr, Natural Gas Origin, Composition, and Processing: A Review, *J. Nat. Gas Sci. Eng.* 34 (2016) 34–54. <https://doi.org/10.1016/j.jngse.2016.06.030> .
- [4] W. Mazyan, A. Ahmadi, H. Ahmed, M. Hoorfar, Market and technology assessment of natural gas processing: A review, *J. Nat. Gas Sci. Eng.* 30 (2016) 487–514. <https://doi.org/10.1016/j.jngse.2016.02.010> .
- [5] T. Keipi, V. Hankalin, J. Nummelin, R. Raiko, Techno-Economic Analysis of Four Concepts for Thermal Decomposition of Methane: Reduction of CO₂ Emissions in Natural Gas Combustion, *Energy Convers. Manag.* 110 (2016) 1–12. <https://doi.org/10.1016/j.enconman.2015.11.057> .
- [6] I. Cronshaw, Q. Grafton, L. Hughes, Increasing the Use of Natural Gas in the Asia-Pacific Region, *Counc. Foreign Relat. - Maurice R Greenberg Cent. Geoeconomic Stud.* (2017) 28.
- [7] U.S. Energy Information Administration. Independent Statistics and Analysis, *International Energy Outlook 2016*, (2016) 290. [https://doi.org/DOE/EIA-0484\(2016\)](https://doi.org/DOE/EIA-0484(2016)) .
- [8] F.P. Vahl, N.C. Filho, Energy Transition and Path Creation for Natural Gas in the Brazilian Electricity Mix, *J. Clean. Prod.* 86 (2015) 221–229. <https://doi.org/10.1016/j.jclepro.2014.08.033> .
- [9] SNAM (Società nazionale Metanodotti), IGU (International Gas Union), BCG (The Boston Consulting Group), *Global Gas Report 2018. 27-th World Gas Conference. Special Edition*, (n.d.). http://www.snam.it/export/sites/snam-rp/repository/file/gas_naturale/global-gas-report/global_gas_report_2018.pdf (accessed January 15, 2019).
- [10] BP p.l.c, BP Statistical Review of World Energy 2018 - 67th edition, London, 2018.
- [11] BP p.l.c, BP Statistical Review of World Energy 2019 - 68th edition, London, 2019.
- [12] A. Miyamoto, C. Ishiguro, *The Outlook for Natural Gas and LNG in China in the War Against Air Pollution*, Oxford Institute for Energy Studies, 2018. <https://doi.org/10.26889/9781784671242> .
- [13] B. Raj Singh, O. Singh, Chapter 8 - Global Trends of Fossil Fuel Reserves and Climate Change in the 21st Century, in: S. Khan (Ed.), *Foss. Fuel Environ., InTech*, 2012. <https://doi.org/10.5772/38655> .
- [14] V. Esen, B. Oral, Natural Gas Reserve/Production Ratio in Russia, Iran, Qatar and Turkmenistan: A Political and Economic Perspective, *Energy Policy.* 93 (2016) 101–109. <https://doi.org/10.1016/j.enpol.2016.02.037> .
- [15] Economic Research Institute for ASEAN and East Asia, *ERIA Research Project Report 2016, n°07a. Formulating Policy Options for Promoting Natural Gas Utilization in the East Asia Summit Region. Volume 1: Demand Side Analysis*, (2018).

- [29] D.L. Saber, S.F. Takach, Pipeline Quality Biomethane: North American Guidance Document for Introduction of Dairy Waste Derived Biomethane into Existing Natural Gas Networks. Technology Investigation, Assessment and Analysis. Task 1 Final Report, GTI Project Number 20614, (2009). <http://www.agriwasteenergy.com/pdf/FINALTASK1FINALREPORT-REFORMATTED.pdf> (accessed December 12, 2019).
- [30] S. Rasi, A. Veijanen, J. Rintala, Trace Compounds of Biogas from Different Biogas Production Plants, *Energy*. 32 (2007) 1375–1380.
<https://doi.org/10.1016/j.energy.2006.10.018> .
- [31] J.I.S. Gómez, H. Lohmann, J. Krassowski, Determination of Volatile Organic Compounds from Biowaste and Co-Fermentation Biogas Plants by Single-Sorbent Adsorption, *Chemosphere*. 153 (2016) 48–57. <https://doi.org/10.1016/j.chemosphere.2016.02.128> .
- [32] S. Rasi, J. Läntelä, J. Rintala, Trace Compounds Affecting Biogas Energy Utilisation – A Review, *Energy Convers. Manag.* 52 (2011) 3369–3375.
<https://doi.org/10.1016/j.enconman.2011.07.005> .
- [33] M. Arnold, T. Kajolinna, Development of on-Line Measurement Techniques for Siloxanes and Other Trace Compounds in Biogas, *Waste Manag.* 30 (2010) 1011–1017.
<https://doi.org/10.1016/j.wasman.2009.11.030> .
- [34] K. Arrhenius, A. Holmqvist, M. Carlsson, J. Engelbrektsson, A. Jansson, L. Rosell, H. Yaghooby, A. Fischer, Terpenes in Biogas Plants Digesting Food Wastes. Study to Gain Insight into the Role of Terpenes. Energiforsk AB. ISBN 978-91-7673-350-9, (2017).
- [35] Teréga, Prescriptions Techniques Applicables Au Raccordement D'un Ouvrage Tiers Au Réseau De Transport De Gaz Naturel De Teréga, (2017).
- [36] European Committee for Standardization, EN 16723-1 Natural Gas and Biomethane for Use in Transport and Biomethane for Injection in Natural Gas Network - Part 1: Specifications for Biomethane for Injection in the Natural Gas Network, (2016).
- [37] International Energy Agency (IEA), Outlook for Biogas and Biomethane. Prospects for Organic Growth. World Energy Outlook Special Report, (2020).
- [38] European Committee for Standardization, EN 16723-2 Natural Gas and Biomethane for Use in Transport and Biomethane for Injection in the Natural Gas Network - Part 2: Automotive Fuels Specification, (2017).
- [39] M. Prussi, M. Padella, M. Conton, E.D. Postma, L. Lonza, Review of Technologies for Biomethane Production and Assessment of Eu Transport Share in 2030, *J. Clean. Prod.* 222 (2019) 565–572. <https://doi.org/10.1016/j.jclepro.2019.02.271> .
- [40] P. Jaramillo, H.S. Matthews, Landfill-Gas-to-Energy Projects: Analysis of Net Private and Social Benefits, *Environ. Sci. Technol.* 39 (2005) 7365–7373.
<https://doi.org/10.1021/es050633j> .
- [41] L. Pizzuti, C.A. Martins, P.T. Lacava, Laminar Burning Velocity and Flammability Limits in Biogas: A Literature Review, *Renew. Sustain. Energy Rev.* 62 (2016) 856–865.
<https://doi.org/10.1016/j.rser.2016.05.011> .
- [42] Y. Shiratori, T. Oshima, K. Sasaki, Feasibility of Direct-Biogas SOFC, *Int. J. Hydrog.*

- Energy. 33 (2008) 6316–6321. <https://doi.org/10.1016/j.ijhydene.2008.07.101> .
- [43] N. de Arespacochaga, C. Valderrama, C. Mesa, L. Bouchy, J.L. Cortina, Biogas Deep Clean-up Based on Adsorption Technologies for Solid Oxide Fuel Cell Applications, *Chem. Eng. J.* 255 (2014) 593–603. <https://doi.org/10.1016/j.cej.2014.06.072> .
- [44] L. Lombardi, E. Carnevale, A. Corti, Greenhouse Effect Reduction and Energy Recovery from Waste Landfill, *Energy*. 31 (2006) 3208–3219. <https://doi.org/10.1016/j.energy.2006.03.034> .
- [45] F. Teymoori Hamzehkolaei, N. Amjady, A Techno-Economic Assessment for Replacement of Conventional Fossil Fuel Based Technologies in Animal Farms with Biogas Fueled Chp Units, *Renew. Energy*. 118 (2018) 602–614. <https://doi.org/10.1016/j.renene.2017.11.054> .
- [46] N. Scarlat, J.-F. Dallemand, F. Fahl, Biogas: Developments and perspectives in Europe, *Renew. Energy*. 129 (2018) 457–472. <https://doi.org/10.1016/j.renene.2018.03.006> .
- [47] W.M. Budzianowski, D.A. Budzianowska, Economic Analysis of Biomethane and Bioelectricity Generation from Biogas Using Different Support Schemes and Plant Configurations, *Energy*. 88 (2015) 658–666. <https://doi.org/10.1016/j.energy.2015.05.104> .
- [48] B. Stephan, Chapter 19 - Market Development and Certification Schemes for Biomethane, in: A. Wellinger, J. Murphy, D. Baxter (Eds.), *Biogas Handb.*, Woodhead Publishing, 2013: pp. 444–462. <https://doi.org/10.1533/9780857097415.3.444> .
- [49] F. Cucchiella, I. D’Adamo, Technical and Economic Analysis of Biomethane: A Focus on the Role of Subsidies, *Energy Convers. Manag.* 119 (2016) 338–351 . <https://doi.org/10.1016/j.enconman.2016.04.058> .
- [50] B. Stürmer, E. Pfundtner, F. Kirchmeyr, S. Uschnig, Legal Requirements for Digestate as Fertilizer in Austria and the European Union Compared to Actual Technical Parameters, *J. Environ. Manage.* 253 (2020) 109756. <https://doi.org/10.1016/j.jenvman.2019.109756> .
- [51] P. Collet, A. Hélias, L. Lardon, M. Ras, R.-A. Goy, J.-P. Steyer, Life-Cycle Assessment of Microalgae Culture Coupled to Biogas Production, *Bioresour. Technol.* 102 (2011) 207–214. <https://doi.org/10.1016/j.biortech.2010.06.154> .
- [52] D. Nagarajan, D.-J. Lee, J.-S. Chang, Integration of Anaerobic Digestion and Microalgal Cultivation for Digestate Bioremediation and Biogas Upgrading, *Bioresour. Technol.* 290 (2019) 121804. <https://doi.org/10.1016/j.biortech.2019.121804> .
- [53] W.M. Budzianowski, M. Brodacka, Biomethane Storage: Evaluation of Technologies, End Uses, Business Models, and Sustainability, *Energy Convers. Manag.* 141 (2017) 254–273. <https://doi.org/10.1016/j.enconman.2016.08.071> .
- [54] J. Speirs, C. McGlade, R. Slade, Uncertainty in the Availability of Natural Resources: Fossil Fuels, Critical Metals and Biomass, *Energy Policy*. 87 (2015) 654–664. <https://doi.org/10.1016/j.enpol.2015.02.031> .
- [55] GRDF, GRTGaz, SPEGNN, SER, Teréga, *Panorama Du Gaz Renouvelable En 2017*, (2017). <http://www.grtgaz.com/fileadmin/plaquettes/fr/2018/Panorama-du-gaz-renouvelable-2017.pdf> (accessed January 21, 2019).

- [56] Ministère de la Transition Ecologique et Solidaire, République Française, Synthèse Stratégie Française pour l’Energie et le Climat - Programmation Pluriannuelle de l’Energie 2019-2023 & 2024-2028, (2018).
- [57] L. Lavocat, La Méthanisation, Une Bonne Solution Menacée Par Le Gigantisme, Reporterre Quotid. Lécologie. (2014). <https://reporterre.net/La-methanisation-une-bonne-solution-menacee-par-le-gigantisme> (accessed July 26, 2019).
- [58] U. Brémond, A. Bertrandias, J.-P. Steyer, N. Bernet, H. Carrere, A Vision of European Biogas Sector Development Towards 2030: Trends and Challenges, J. Clean. Prod. 287 (2021) 125065. <https://doi.org/10.1016/j.jclepro.2020.125065> .
- [59] Carburants Et Combustibles Liquides Ou Gazeux, Ministère Transit. Écologique Solidaire. (n.d.). <http://www.ecologique-solidaire.gouv.fr/carburants-et-combustibles-liquides-ou-gazeux> (accessed January 21, 2019).
- [60] UNFCCC, Climate Change 1995, The Science of Climate Change: Summary for Policymakers and Technical Summary of the Working Group I Report, p.22, Glob. Warm. Potentials. (n.d.). <https://unfccc.int/process/transparency-and-reporting/greenhouse-gas-data/greenhouse-gas-data-unfccc/global-warming-potentials> (accessed January 22, 2019).
- [61] O. Boucher, P. Friedlingstein, B. Collins, K.P. Shine, The Indirect Global Warming Potential and Global Temperature Change Potential Due to Methane Oxidation, Environ. Res. Lett. 4 (2009) 044007. <https://doi.org/10.1088/1748-9326/4/4/044007> .
- [62] Association française du gaz, Gaz Renouvelables: les Leviers de Développement, (2018). https://www.afgaz.fr/sites/default/files/u200/afg_livret_gaz_renouvelables_200x280_def110918.pdf (accessed January 22, 2019).
- [63] International Energy Agency (IEA), Renewables Information: Overview. Statistics, (2018). https://webstore.iea.org/download/direct/2260?fileName=Renewables_Information_2018_Overview.pdf (accessed May 6, 2019).
- [64] European Biogas Association, EBA Statistical Report 2020, (2020). https://www.europeanbiogas.eu/wp-content/uploads/2021/01/EBA_StatisticalReport2020_abridged.pdf (accessed January 5, 2022).
- [65] International Energy Agency (IEA), IEA World Energy Outlook 2021, (2021). www.iea.org/weo (accessed January 5, 2022).
- [66] P.Y. Hoo, H. Hashim, W.S. Ho, Opportunities and Challenges: Landfill Gas to Biomethane Injection into Natural Gas Distribution Grid Through Pipeline, J. Clean. Prod. 175 (2018) 409–419. <https://doi.org/10.1016/j.jclepro.2017.11.193> .
- [67] M. Schweigkofler, R. Niessner, Determination of Siloxanes and VOC in Landfill Gas and Sewage Gas by Canister Sampling and GC-MS/AES Analysis, Environ. Sci. Technol. 33 (1999) 3680–3685. <https://doi.org/10.1021/es9902569> .
- [68] M.R. Allen, A. Braithwaite, C.C. Hills, Trace Organic Compounds in Landfill Gas at Seven U.K. Waste Disposal Sites, Environ. Sci. Technol. 31 (1997) 1054–1061.

<https://doi.org/10.1021/es9605634> .

- [69] A.S. Brown, A.M.H. Van Der Veen, K. Arrhenius, A. Murugan, L.P. Culleton, P.R. Ziel, J. Li, Sampling of Gaseous Sulfur-Containing Compounds at Low Concentrations with a Review of Best-Practice Methods for Biogas and Natural Gas Applications, *TrAC Trends Anal. Chem.* 64 (2015) 42–52. <https://doi.org/10.1016/j.trac.2014.08.012> .
- [70] K.F. Chin, C. Wan, Y. Li, C.P. Alaimo, P.G. Green, T.M. Young, M.J. Kleeman, Statistical Analysis of Trace Contaminants Measured in Biogas, *Sci. Total Environ.* 729 (2020). <https://doi.org/10.1016/j.scitotenv.2020.138702> .
- [71] M. Ghidotti, D. Fabbri, C. Torri, Determination of Linear and Cyclic Volatile Methyl Siloxanes in Biogas and Biomethane by Solid-Phase Microextraction and Gas Chromatography–Mass Spectrometry, *Talanta.* 195 (2019) 258–264. <https://doi.org/10.1016/j.talanta.2018.11.032> .
- [72] F. Hilaire, E. Basset, R. Bayard, M. Gallardo, D. Thiebaut, J. Vial, Comprehensive Two-Dimensional Gas Chromatography for Biogas and Biomethane Analysis, *J. Chromatogr. A.* 1524 (2017) 222–232. <https://doi.org/10.1016/j.chroma.2017.09.071> .
- [73] S. Rasi, J. Lehtinen, J. Rintala, Determination of Organic Silicon Compounds in Biogas from Wastewater Treatments Plants, Landfills, and Co-Digestion Plants, *Renew. Energy.* 35 (2010) 2666–2673. <https://doi.org/10.1016/j.renene.2010.04.012> .
- [74] F.A.T. Andersson, A. Karlsson, B.H. Svensson, J. Ejlertsson, Occurrence and Abatement of Volatile Sulfur Compounds during Biogas Production, *J. Air Waste Manag. Assoc.* 54 (2004) 855–861. <https://doi.org/10.1080/10473289.2004.10470953> .
- [75] K. Arrhenius, H. Yaghooby, L. Rosell, O. Büker, L. Culleton, S. Bartlett, A. Murugan, P. Brewer, J. Li, A.M.H. van der Veen, I. Krom, F. Lestremau, J. Beranek, Suitability of Vessels and Adsorbents for the Short-Term Storage of Biogas/Biomethane for the Determination of Impurities – Siloxanes, Sulfur Compounds, Halogenated Hydrocarbons, BTEX, Biomass Bioenergy. 105 (2017) 127–135. <https://doi.org/10.1016/j.biombioe.2017.06.025> .
- [76] J. Feldmann, I. Koch, W.R. Cullen, Complementary Use of Capillary Gas Chromatography–Mass Spectrometry (ion Trap) and Gas Chromatography–Inductively Coupled Plasma Mass Spectrometry for the Speciation of Volatile Antimony, Tin and Bismuth Compounds in Landfill and Fermentation Gases, *The Analyst.* 123 (1998) 815–820. <https://doi.org/10.1039/a707478f> .
- [77] J. Feldmann, Determination of Ni(CO)₄, Fe(CO)₅, Mo(CO)₆, and W(CO)₆ in Sewage Gas by Using Cryotrapping Gas Chromatography Inductively Coupled Plasma Mass Spectrometry, *J. Environ. Monit.* 1 (1999) 33–37. <https://doi.org/10.1039/A807277I> .
- [78] J. Feldmann, W.R. Cullen, Occurrence of Volatile Transition Metal Compounds in Landfill Gas: Synthesis of Molybdenum and Tungsten Carbonyls in the Environment, *Environ. Sci. Technol.* 31 (1997) 2125–2129. <https://doi.org/10.1021/es960952y> .
- [79] J. Feldmann, A.V. Hirner, Occurrence of Volatile Metal and Metalloid Species in Landfill and Sewage Gases, *Int. J. Environ. Anal. Chem.* 60 (1995) 339–359. <https://doi.org/10.1080/03067319508042888> .

- [80] K. Arrhenius, A. Fischer, O. Bükler, Methods for Sampling Biogas and Biomethane on Adsorbent Tubes After Collection in Gas Bags, *Appl. Sci.* 9 (2019) 1171. <https://doi.org/10.3390/app9061171>.
- [81] K. Arrhenius, A.S. Brown, A.M.H. van der Veen, Suitability of Different Containers for the Sampling and Storage of Biogas and Biomethane for the Determination of the Trace-Level Impurities – A Review, *Anal. Chim. Acta.* 902 (2016) 22–32. <https://doi.org/10.1016/j.aca.2015.10.039>.
- [82] E.M. Krupp, C. Johnson, C. Rechsteiner, M. Moir, D. Leong, J. Feldmann, Investigation into the Determination of Trimethylarsine in Natural Gas and Its Partitioning into Gas and Condensate Phases Using (cryotrapping)/Gas Chromatography Coupled to Inductively Coupled Plasma Mass Spectrometry and Liquid/Solid Sorption Techniques, *Spectrochim. Acta Part B At. Spectrosc.* 62 (2007) 970–977. <https://doi.org/10.1016/j.sab.2007.07.009>.
- [83] M.K. Uroic, E.M. Krupp, C. Johnson, J. Feldmann, Chemotrapping-Atomic Fluorescence Spectrometric Method as a Field Method for Volatile Arsenic in Natural Gas, *J. Environ. Monit.* 11 (2009) 2222. <https://doi.org/10.1039/b913322d>.
- [84] M. Cachia, H. Carrier, B. Bouyssiere, P. Le Coustumer, P. Chiquet, G. Caumette, I. Le Hecho, Solid Particles in Natural Gas from a Transportation Network: A Chemical Composition Study, *Energies.* 12 (2019) 3866. <https://doi.org/10.3390/en12203866>.
- [85] M. Schweigkofler, R. Niessner, Removal of siloxanes in biogases, *J. Hazard. Mater.* 83 (2001) 183–196. [https://doi.org/10.1016/S0304-3894\(00\)00318-6](https://doi.org/10.1016/S0304-3894(00)00318-6).
- [86] D. Papurello, L. Tomasi, S. Silvestri, I. Belcari, M. Santarelli, F. Smeacetto, F. Biasioli, Biogas Trace Compound Removal with Ashes Using Proton Transfer Reaction Time-of-Flight Mass Spectrometry as Innovative Detection Tool, *Fuel Process. Technol.* 145 (2016) 62–75. <https://doi.org/10.1016/j.fuproc.2016.01.028>.
- [87] D. Papurello, A. Lanzini, S. Fiorilli, F. Smeacetto, R. Singh, M. Santarelli, Sulfur Poisoning in Ni-Anode Solid Oxide Fuel Cells (SOFCs): Deactivation in Single Cells and a Stack, *Chem. Eng. J.* 283 (2016) 1224–1233. <https://doi.org/10.1016/j.cej.2015.08.091>.
- [88] S. Mariné, M. Pedrouzo, R.M. Marcé, I. Fonseca, F. Borrull, Comparison Between Sampling and Analytical Methods in Characterization of Pollutants in Biogas, *Talanta.* 100 (2012) 145–152. <https://doi.org/10.1016/j.talanta.2012.07.074>.
- [89] M. Aghar, B. Wens, K.H. Stollenwerk, G. Spalding, S. Yüce, T. Melin, Suitability of Tedlar® Gas Sampling Bags for Siloxane Quantification in Landfill Gas, *Talanta.* 82 (2010) 92–98. <https://doi.org/10.1016/j.talanta.2010.04.001>.
- [90] M. Harper, Review. Sorbent Trapping of Volatile Organic Compounds from Air, *J. Chromatogr. A.* 885 (2000) 129–151. [https://doi.org/10.1016/S0021-9673\(00\)00363-0](https://doi.org/10.1016/S0021-9673(00)00363-0).
- [91] K. Haas, J. Feldmann, Sampling of Trace Volatile Metal(loid) Compounds in Ambient Air Using Polymer Bags: A Convenient Method, *Anal. Chem.* 72 (2000) 4205–4211. <https://doi.org/10.1021/ac000313c>.
- [92] V. Camel, M. Caude, Review: Trace Enrichment Methods for the Determination of Organic Pollutants in Ambient Air, *J. Chromatogr. A.* 710 (1995) 3–19.

[https://doi.org/10.1016/0021-9673\(95\)00080-7](https://doi.org/10.1016/0021-9673(95)00080-7) .

[93] M. Sulyok, C. Haberhauer-Troyer, E. Rosenberg, M. Grasserbauer, Investigation of the Storage Stability of Selected Volatile Sulfur Compounds in Different Sampling Containers, *J. Chromatogr. A.* 917 (2001) 367–374. [https://doi.org/10.1016/S0021-9673\(01\)00654-9](https://doi.org/10.1016/S0021-9673(01)00654-9) .

[94] M. Enrico, A. Mere, H. Zhou, H. Carrier, E. Tessier, B. Bouyssiére, Experimental Tests of Natural Gas Samplers Prior to Mercury Concentration Analysis, *Energy Fuels.* (2019). <https://doi.org/10.1021/acs.energyfuels.9b03540> .

[95] T. Larsson, W. Frech, E. Björn, B. Dybdahl, Studies of Transport and Collection Characteristics of Gaseous Mercury in Natural Gases Using Amalgamation and Isotope Dilution Analysis, *Analyst.* 132 (2007) 579–586. <https://doi.org/10.1039/B702058A> .

[96] M.C. Leuenberger, M.F. Schibig, P. Nyfeler, Gas Adsorption and Desorption Effects on Cylinders and Their Importance for Long-Term Gas Records, *Atmospheric Meas. Tech.* 8 (2015) 5289–5299. <https://doi.org/10.5194/amt-8-5289-2015> .

PART 2 – STATE OF THE ART

CHAPTER 1 – BIOGAS AND BIOMETHANE PRODUCTION

ABBREVIATIONS CHAPTER 1

CHP	Combined heat and power
GHG	Greenhouse gas(es)
LCV	Lower calorific value
MSW	Municipal solid waste
PBR	Photobioreactor
SNG	Synthetic natural Gas
VOC	Volatile organic compound(s)

I. BIOGAS DEFINITION

Biogas is a colorless flammable gas mixture produced by the anaerobic digestion of humid organic matter by microbial communities and in particular by methanogenic bacteria. This biochemical mechanism is called methanization [1–4] and spontaneously occurs in the nature in organic matter rotting piles, anaerobic sediments or flooded soils. The methanization mechanism has been studied for a long time [5] and is now reproduced at large scale in biogas production facilities (anaerobic digester tanks) where the organic matter feedstocks ideally stem from anthropogenic organic wastes: agricultural residues, manure, food-processing and catering residues, organic and green municipal and household wastes, sewage sludge. Next to biogas, the anaerobic digestion of organic matter gives birth to another valuable product, the digestate. This is the solid-liquid fraction remaining after the digestion, consisting of undigested organic matter and (dead) micro-organisms and representing about 90 %_{vol} of the initial organic matter volume injected in the digester [6,7]. Digestates are nutrient-rich (nitrogen, phosphorus, potassium...) and are nowadays used as substitutes to chemical fertilizers in the agricultural sector [8–11]. Concerns about trace contaminants in digestates (metals, organics, pesticides, pathogenic bacteria) that could percolate through agricultural fields restrain however the enthusiasm for this solution [9,12].

Biogas is also spontaneously generated in landfills (landfill gas) wherein the compaction of the dumped wastes ensures the absence of oxygen, allowing the specific microbiota to anaerobically digest the degradable waste fraction [13–18].

Next to the two major constituents CH₄ (at least 50 %_{vol}) and CO₂ (maximal 50%_{vol}), biogas and landfill gas contain minor constituents like N₂, H₂O, H₂S, NH₃, H₂, CO and potential traces of O₂, hydrocarbons, halogenated hydrocarbons, siloxanes, organic and inorganic Sulphur compounds, oxygenated organic compounds [2,3,10,19–21] as well as potential traces of volatile metals and metalloid (As, Bi, Cd, Cu, Hg, Mo, Ni, Pb, Sb, Se, Sn, Te, V, W, Zn) [20,22–25]. The proportion of CH₄ and CO₂ in biogas as well as its composition regarding the minor constituents, are strongly dependent on the organic matter being digested and on the physico-chemical parameters driving the anaerobic digestion (hydraulic retention time, temperature, humidity, pH ...) [2–5,10,19,20,22].

Thanks to the relatively high Lower Calorific Value (LCV) of the pure methane fraction ($\sim 36 \text{ MJ}\cdot\text{m}^{-3} \text{ CH}_4$ at standard temperature (0°C) and pressure (1 bar_a) conditions) it contains, biogas is an energetic gas with a LCV of $\sim 20\text{-}25 \text{ MJ}\cdot\text{m}^{-3}$ biogas for a CH_4 fraction of 60-65%_{vol} [2,5,10,17,19]. As a comparison, natural gas has an LCV of $\sim 31\text{-}38 \text{ MJ}\cdot\text{m}^{-3}$ [10,26]. Biogas has been used for centuries as a heat and power (electricity) source as its energy-content suffices to fuel combustion engines [5,19]. Today's biogas applications include different types of heat and power generation [4,8,17,19,27-29]:

- heat production from its combustion in gas boilers (water heating, space heating) and cookers
- electricity production from its combustion in internal combustion engines or in other electricity generators (gas turbines, steam turbines) [19,30]
- electricity production from its use as a fuel in direct biogas fuel cells [17,19,31-33]
- combined heat and power (CHP) generation from its combustion in CHP engines (cogeneration units) [19,34]. Yet the total electrical efficiency of such engines generally does not exceed 40% [19,27,35-37] and the thermal efficiency 50-60% [36,38], CHP generation is nowadays the most common biogas valorization way in 'developed' countries [17,27,35]. The generated heat is often used on the biogas production site to preheat the organic feedstocks before their injection in the digester, or to heat the digester [27,39]. For a proper microbial digestion of the organic matter, the microbiota environment (i.e. the digester tank) needs indeed to be kept at mesophilic ($20\text{-}40^\circ\text{C}$) or thermophilic ($>40^\circ\text{C}$) conditions [1,5,10,40]. Alternatively, the biogas-derived heat can also be destined to dry the digestates to reduce their volume or can be sent to local heat distribution networks. Concerning the co-generated electricity: it first powers the biogas plant operation electricity needs [11] after what the remaining electricity is sold and sent to the electricity distribution grid to contribute feeding local electricity demands [27,35,41].
- hydrogen or syngas production by steam reforming of its methane fraction [42]
- biomethane production by its upgrading [2,4,10,20,43-45]. Biogas upgrading to biomethane is the process where the CO_2 and minor compounds (H_2S , N_2 , H_2O , NH_3 , siloxanes...) of biogas are separated from the CH_4 fraction. This pure CH_4 fraction is then called biomethane and detains similar calorific properties as natural gas once sufficiently purified from remaining trace compounds [4,8,20,35,46-48]. Biomethane is then intended to be either injected in the natural gas transport and distribution grid, or to be compressed and used as vehicle fuel [4,8,13,17,19,35,45,49-52]. Today biogas producing plants valorizing biogas via CHP generation outnumber plants upgrading biogas to biomethane [17,53,54]. Indeed, the technologies required to purify biogas to pipeline- or vehicle-quality gas are much more expensive and complex to operate than CHP generating units, and biomethane retail prices are currently too low to outcompete natural gas [17,27,29,45,48].

Note that even for direct biogas applications, a biogas treatment is advised to dry the gas and protect the engines, boilers or fuel cells from fine particles, corrosive (H_2S , NH_3 ...), acidic or abrasive compounds or from compounds generating solid deposits upon combustion (siloxanes) [2,17].

II. BIOMETHANE DEFINITION

'Biomethane' commonly refers to the purified methane fraction of biogas or landfill gas obtained by its separation from the carbon dioxide fraction and from the minor compounds of those gases in an upgrading process.

Additionally, research is being conducted to produce other types of 'bio-methane', i.e. methane produced on a renewable way to substitute natural gas, in one of the following ways:

- by pyrogasification and methanation of dry ligneous-cellulosic biomass. The methane obtained is then often called 'synthetic natural gas'.
- by methanation of hydrogen
- from the anaerobic digestion of microalgae as organic matter feedstock in anaerobic digesters. The biogas produced during this methanization is upgraded to CH₄ at one side and CO₂ at the other side. The CO₂ is sent to a next batch of microalgae to enhance their photosynthesis and growth while the CH₄ is used for energy purposes.

Next sections briefly review these different biomethane or bio-methane production pathways.

III. OVERVIEW OF BIO-METHANE PRODUCTION PROCESSES

Biomethane and bio-methane can be produced via different engineered processes described below. This doctoral thesis will however solely focus on biogas and biomethane generated from the methanization of organic feedstocks in controlled anaerobic digester tanks and in landfills.

III.1. Methanization of humid biomass

Methanization is the biological anaerobic digestion (fermentation) of humid organic matter by collaborating bacteria communities, leading to the production of gaseous CO₂ and CH₄ (biogas). Organic matter to feed the bacteria can be gathered from different waste sectors of modern societies:

- Agriculture: straw, crop and fruit residues ...
- Livestock farming: manure ...
- Food processing, beverage industry and catering: all kind of foodstuffs residues (vegetal and animal), raw or processed
- Waste water treatment: sludge
- Paper industry: paper sludge
- Municipal and household waste collection: garbage, compost...
- Gardens and parks maintenance: green wastes

The biochemical humid methanization process in digesters, microbial communities involved [55–57], and biogas-to-biomethane upgrading technologies [2,4,10,16,20,43,58–62] have been extensively studied and will not be further detailed in this chapter.

III.2. Landfill gas extraction

Landfill gas is biogas produced by the spontaneous methanization of the organic (fermentable) fraction of solid wastes buried and compacted in sanitary landfills [14,15,17,63]. In the past, in non-sanitary landfills, wastes were dumped and compacted directly in bare trenches, covered once filled with the excavated earth. Rain and run-off water were percolating through the wastes, getting enriched, via physico-chemical exchanges, with all kinds of contaminants present in the buried wastes [63]. The resulting leachates, consisting of the infiltrated rain water, the liquid fraction of the wastes and moisture produced by biological degradation mechanisms, were further percolating down to the groundwater, leading to serious pollution issues [63]. Today's sanitary landfills are engineered dumps (Fig.1.1 - 1.2): upon excavation of the future landfill area, clayey geotextiles and high-density plastic liners are laid down on the bottom to protect the underground and groundwater from polluting leachates seeping out of the subsequently buried wastes. Drainage pipes are installed on these liners to collect the leachates and send them to a waste water treatment unit [13,63]. Discarded wastes are progressively compacted in cells of defined volumes; once a cell is filled, it is covered by some of the excavated earth and the next cell begins being loaded, as such gradually filling the whole landfill (Fig.1.2). Rain water will always be allowed to percolate through the cells as long as the landfill is not eventually closed with semi-hermetic materials (Fig.1.1).

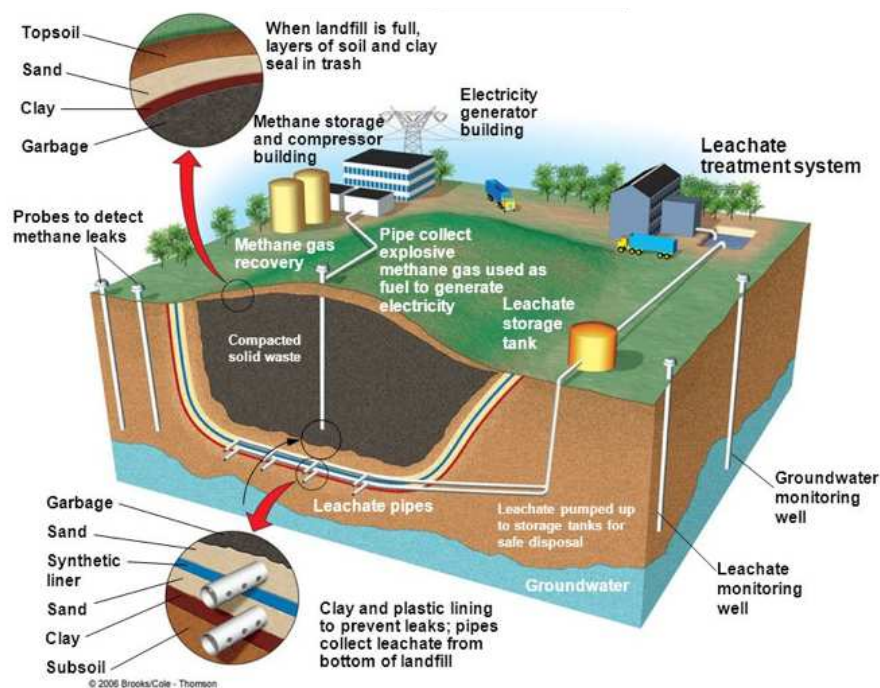


Figure 1.1: Sanitary landfills are equipped with underground protective liners and leachate- and gas collection systems.

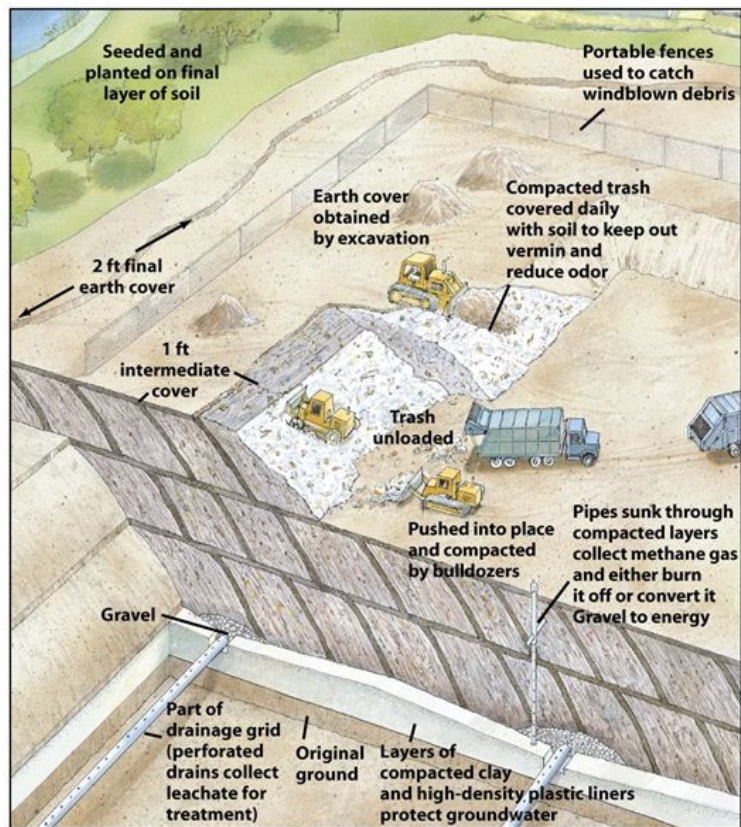


Figure 24-3b Environment, 5/e
© 2006 John Wiley & Sons

Figure 1.2: Progressive filling of a sanitary landfill, equipped with underground protective liners and leachate- and gas collection systems.

Landfill gas can be produced both under aerobic and anaerobic digestion [17]. The aerobic gas generation occurs in recently closed cells or in open cells where oxygen is still present, but this production does not last long and does not generate a high energy content gas. On the contrary, in older well compacted closed cells where anaerobic conditions rule over, the gas production is long-lasting (up to 15-25 years [63]) and the energy content and methane fraction of the gas are higher. Since this anaerobic digestion is microbially driven, anaerobic landfill gas production is enhanced under humid conditions and when the organic fraction of the buried wastes increases [63–65]. Sanitary landfills produce therefore more gas than non-sanitary ones since the leachates and rain water are collected at the bottom and can be re-injected in the cells to keep the wastes moisturized and further stimulate the gas production [17,66]. Other factors impacting the gas production are the temperature in the waste cells (the higher the temperature, the more favorable for the microbiota, the more gas produced), the pH and the type and age of the wastes [17,21,63–65]. The production rate and composition of landfill gas evolve during the landfill lifetime [63,64]. Generally, significant gas production starts after 1 to 3 years of waste burial, peaks after 5-7 years and continues at appreciable levels up to 20 years after waste dumping. Limited gas volumes may further still be produced during up to more than 50 years. Depending on the volume of a waste cell and on the packing pattern of the wastes in this cell, some portions of wastes may be in different degradation stages, leading to discrepancies in gas production levels inside a given cell [17,64]. The evolution of the landfill gas composition over time is depicted in Fig.1.3 [55,56,60,64].

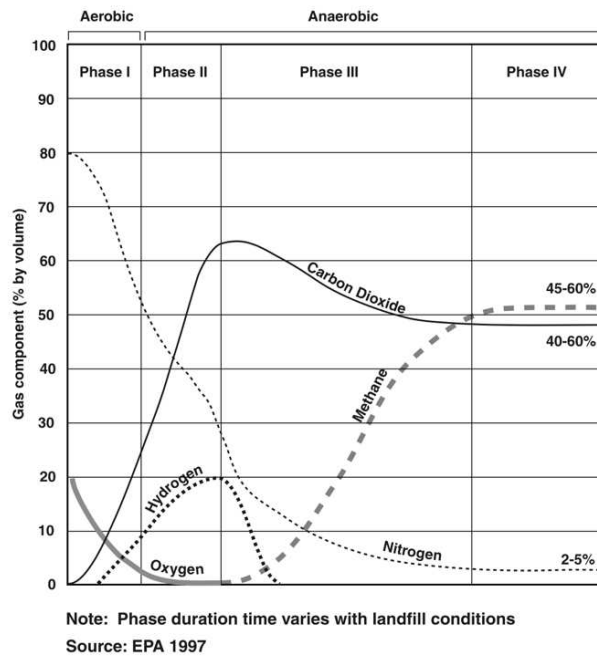


Figure 1.3: Landfill gas composition evolution over time (time scale being different for each single landfill)

In a first phase, oxygen is still present among the wastes (open or recently closed cells, loosely compacted wastes ...) and aerobic bacteria degrade (hydrolyze) the long molecular chains of the wastes (carbohydrates, proteins, lipids...) to smaller molecules (sugars, fatty acids, amino acids...), H₂ and CO₂. This process goes on until all oxygen is depleted. Once anaerobic conditions are reached (phase 2), anaerobic bacteria develop and further degrade the metabolites of phase 1 into even smaller units (typically acetic, lactic and formic acids, methanol and ethanol) with a side production of CO₂ and H₂ gas (acidogenesis). This acidic environment together with the moisture enhances the dilution of nutrients like nitrogen and phosphorus, stimulating the growth of other anaerobic bacteria. Phase 3 starts when those latter metabolize the acids and alcohols produced in phase 2 into acetate, a precursor for methane (acetogenesis). As the pH increases due to the consumption of the acidic compounds, ultimate methanogenic bacteria can develop, consuming H₂ and acetate to produce methane and CO₂ (methanogenesis). The fourth phase of the gas composition evolution in a landfill is characterized by a steady production level and rate of CH₄ and CO₂, that can last for 20 years or more depending on the percentage organic fraction in the wastes, the moisture level, the temperature and the compaction degree of the wastes. A too strong waste compaction restrains gas production as it decreases the water infiltration rate through the waste (rain water, water produced by the biodegradation reactions...), while the microbial waste degradation is precisely enhanced under moist conditions. Leachate collection and re-injection in the waste cells, or permeable landfill covers can help gaining sufficient moisture levels in the cells. Concerning the temperature inside the landfill, it is largely influenced by external weather conditions for shallow and poorly insulated landfills. Bacterial activity will considerably be reduced under 10°C. In deeper and well insulated (earth cover and top liners) landfills on the contrary, the temperature is relatively independent from the external ambient temperatures. This leads, together with the heat released by the bacterial activity, to higher and more constant gas production levels [55,56,60,64].

As solid wastes are progressively digested, the produced biogas accumulates in the landfill and migrates from high pressure (high production level) to low pressure zones (low production level) along paths of least resistance throughout the wastes [17]. Pressure build-up of this inflammable gas can become such that landfill explosions or fires ensue [14,17,63,64] if the gas is not continuously monitored and evacuated. Sanitary landfills are therefore equipped with deep gas collecting wells (Fig.1.1 – 1.2) where through the gas is extracted thanks to the natural pressure gradient or by pulling a light vacuum. This biogas is then often used on site as fuel to generate electricity mainly in CHP engines [17], ideally after a preliminary treatment. Alternatively, this gas can be upgraded to biomethane. Since landfill gas is water-saturated, as it is generated in moist conditions, the deep extraction wells are gridded with downwards sloped lateral pipes allowing the condensation, forming as the gas cools by contact with the pipes, to drain down to a sump [17]. Factors impacting landfill gas recovery efficiency include landfill depth, capping, moisture level and compaction [17]:

- deep landfills sealed with liners lead to better collection efficiencies
- high water levels boost gas production but impede efficient gas collection by obstructing pores in the gas extraction wells
- high waste compaction grade leads to less gas production and to weaker gas diffusion towards the extraction wells

To conclude, landfill gas recovery in sanitary landfills has several advantages:

- Avoiding landfill explosions [14,63,67]. This avoids material losses; atmospheric pollution due to the emanation of greenhouse gases (GHG) (CH_4 and CO_2), toxic gases (CO , H_2S), volatile compounds contained in landfill gas (hydrocarbons, chlorinated compounds like dioxins, oxygenated hydrocarbons like furans, polyaromatic hydrocarbons...) and fine dust particles; and human health damages [63,67].
- Avoiding olfactory nuisance and poor air quality stemming from the emanation of Sulphur compounds and diverse volatile compounds generated upon waste degradation [14,21,67,68].
- Avoiding GHG emissions to the atmosphere [13–15,63,67]. Landfill gas (biogas) is composed of roughly 40% CO_2 and 60% CH_4 , two important GHG. In the U.S.A., municipal solid waste (MSW) receiving landfills are the third-largest source of anthropogenic CH_4 emissions, accounting for ~16% of those emissions in 2017 and representing 107.7 Mton CO_2 -eq GHG emissions [67,69]. In the European Union, solid waste disposal (landfill) sites related GHG emissions amounted to ~101 Mton CO_2 -eq in 2017 [70]. Collecting and flaring landfill gas already reduces the GHG emissions since, in the case of complete combustion, CH_4 is oxidized to CO_2 , having a lower global warming potential than CH_4 . When landfill gas is recovered and sent to an energy conversion system (e.g. CHP engine), GHG emissions are further directly reduced by burning CH_4 to CO_2 and H_2O , and indirectly reduced by avoiding the use of conventional (non-renewable) energy sources when landfill gas-based energy is used instead [67,71]. The CO_2 remaining from the energy-conversion of landfill gas can even itself be valorized e.g. as carbon supplement for horticultural plant growth [72]. Despite landfill gas collection, methane will often still escape from the landfill at some locations. Depending on the gas collection and energy

conversion systems design and efficiency, only 60 to 90% of the landfill gas are captured [67].

- Generating renewable electricity or energy [14,17,63,67]. For a landfill gathering MSW, about 8.5 Nm³ landfill gas are produced per minute per million ton MSW [67]. Just as for the biogas generated in anaerobic digesters, electricity generation from this landfill gas occurs mainly via 3 technologies: combustion in internal combustion engines, gas turbines or microturbines. CHP engines are widely used. Landfill gas can also be directly used in boilers and steam turbines [67]. The generated electricity and heat are ideally used on site or in nearby located factories. Direct heat valorization applications include [67]:
 - leachate evaporation: the heat released upon landfill gas combustion is used to reduce the volume of landfill leachates, improving the cost-efficiency of leachate management (epuration, disposal...)
 - (waste water treatment) sludge drying for the same purpose
 - running kilns, furnaces, forges, for the pottery, brick, cement or metal industry, running process heaters, paint shop ovens...

Landfill gas can also be upgraded to biomethane (pipeline quality gas).

III.3. Pyrogasification and methanation of dry biomass

Dry, lignocellulosic biomass (wood, straw, olive stones...) can be converted into synthetic natural gas (SNG) via a complex industrial thermo-chemical process whose main steps can be summarized as follows. The plant receives dry biomass which is mechanically sorted to remove too big pieces or eventual inorganic materials like metals or plastic objects [73]. The admitted biomass is sent to the first conversion step called pyrogasification. In the gasifier reactor, biomass is turned into a synthetic gas consisting mainly of H₂ and CO but also containing some CO₂ and impurities like Sulphur and Nitrogen compounds, condensable hydrocarbons (tars), HCl, VOC, siloxanes, inorganic compounds and particulate matter... [73–78]. As those impurities cause severe damages on the next process steps, this gas must be cleaned and conditioned to only keep H₂ and CO [73–75,77–82]. In the next step, the purified synthetic gas is sent to the methanation reactor where it is catalytically converted into methane (SNG), eventually upgraded to a certain purity level depending on the ultimate targeted SNG application (e.g. grid injection) [73–81]. Each of these process phases is now explained in more details.

Dry biomass input

Suitable biomass feedstocks for gasification and subsequent methanation are dry solid lignocellulosic biomaterials (wood, straw, fruit stones...) [73,76,78,81]. At the Gothenburg Biomass Gasification (GoBiGas) demonstration plant in Sweden, the adequacy and gasification performance of several woody feedstocks have been tested: wood pellets, wood chips (from poor quality residual logs), shredded bark (from a paper pulp factory), sawmill residues and recovered wood (e.g. pallets, wood from the construction sector, though without any paint or chemical treatment). It was found that drying those “dry” feedstocks was fundamental to achieve a satisfactory biomass to SNG conversion efficiency (70%). Unsheltered outdoor drying was not

sufficient for an efficient gasification. Feedstocks with the least inherent moisture content (like wood pellets: 8-9%_w moisture) enabled the most productive and steady plant operation [81].

Pyrogasification: thermochemical biomass conversion

In this step, the selected dry biomass enters a gasification reactor where it is converted into a combustible gas via several complex thermochemical reactions. Gasification actually includes four stages or reactions, each taking place in different zones of the reactor in case a fixed-bed reactor is used: biomass drying, pyrolysis, combustion and reduction (Fig.1.4) [76,77]. In the gasifier reactor, operated at temperatures between 600 and 1500°C, those reactions are triggered by a gasifying agent such as steam, air, enriched air, oxygen, carbon dioxide or a combination of steam and oxygen [74,76,78]. Four main types of gasifier reactors are used: fixed bed updraft (counter-current) or downdraft (co-current) reactors, fluidized bed and entrained flow gasifiers. In updraft and downdraft reactors, biomass is fed respectively counter-currently and co-currently to the gasifying agent flow and to the flow of produced gas (Fig.1.5) [76,77].

During the drying step, biomass moisture is evaporated thanks to the heat released by the other ongoing reactions and by the flow of produced gas (Fig.1.4 – 1.5). The generated water vapor is valorized in the reduction reaction in the reduction zone [77].

The dried biomass then undergoes pyrolysis. During pyrolysis, biomass is thermally broken down or 'devolatilized' in the absence of oxygen (endothermic reaction, the exact chemical mechanisms are still unclear) [76,77]. In the biomass, lignin, cellulose and hemicellulose each decompose at different rates as the pyrolysis goes along. Bond-breakage, formation of free radicals and carbonyl groups with a corresponding release of H₂O, CO and CO₂ occur in a first stage (120-200°C). When the temperature further increases (2nd stage), the biomass weight decreases considerably as solid decomposition occurs. C-H and C-O bonds are then further cleaved, resulting in the continuous devolatilization of the residual solid material [76]. Pyrolysis generates 3 products [76]:

- Char(coal): the solid, non-volatilized residual biomass material remaining at the end of the pyrolysis. It is a porous carbon structure polluted with mineral impurities and large fractions of hydrogen and oxygen in the case of incomplete pyrolysis. At low pyrolysis temperatures, polycyclic aromatic hydrocarbons (PAH) can be released from this char.
- Bio-oil: a liquid residue especially produced in case of short biomass residence time in the pyrolysis zone or in case of fast cooling of the pyrolysis temperature.
- Gas with as main constituents CO, CO₂, H₂, CH₄ and gaseous condensable hydrocarbons called tars.

Next, the pyrolysis gas, tar and char are combusted by the gasifying agent (oxidation, exothermic). This combustion reaction produces most of the heat serving the drying, pyrolysis and endothermic reactions in the other zones of the reactor. The combustion products (char, tar) further migrate to the reduction zone where they typically undergo water-gas-shift reductions: $C + H_2O \rightleftharpoons H_2 + CO$ (endothermic) and $CO + H_2O \rightleftharpoons H_2 + CO_2$ (exothermic) [76,77]. In Table 1.1 the main thermochemical pyrolysis, oxidation and reduction reactions taking place in the fixed-bed gasifier are listed.

The resulting product gas exiting the gasifier is a combustible mixture. Depending on the gasification temperature, syngas ($>1200^{\circ}\text{C}$) or producer gas ($< 1000^{\circ}\text{C}$) is obtained [74,76]. Syngas is mainly composed of H_2 and CO but also contains some CO_2 and H_2O . Producer gas contains H_2 , CO , CH_4 , CO_2 , H_2O , N_2 , hydrocarbons. Both syngas and producer gas also contain impurities like N-, S- and Cl-compounds (N_2 , NH_3 , HCN , H_2S , COS , HCl), alkaline and tar compounds and particles of char, ashes and soot [74,76,77]. Syngas or producer gas composition is extremely influenced by the feedstock type and its moisture content, by the way feedstock is brought in contact with the gasification agent, by the type of reactor and its operating parameters (temperature, pressure, type gasification agent, residence time) [74,76–78]. Many of the contaminants present in syngas or producer gas induce deficiencies (corrosion, solid deposit formation, deactivation of methanation catalyst...) in the next steps of the biomass to SNG conversion. Cleaning and conditioning those gases is therefore crucial and can be executed e.g. via particle filters, activated carbon beds, water scrubbers [77].

While this thermal gasification process is only suitable for dry (lignocellulosic) biomass inputs, an analogous hydrothermal gasification process is available to convert wet biomass (food residues, crops, sewage sludge, manure...) into SNG. Whereas wet biomass is usually converted to biomethane via anaerobic digestion, it is here directly catalytically converted to CH_4 , CO_2 and H_2O via the hydrothermal gasification using supercritical water [78,79].

Syngas cleaning and conditioning

The next fate of the product gas is to be sent to the catalyzed methanation step. As many impurities in this gas can deactivate the catalysts or induce other negative impacts on the process efficiency, it must be cleaned [73–75,77–82]. The type of catalyst and methanation technology used specifies the maximum tolerable impurities concentration in the product gas at the entrance point to the methanation unit [78]. The most troublesome impurities are: S-compounds (H_2S , COS , CS_2 , mercaptans [80]), chlorines (HCl), NH_3 , siloxanes [75,78], particles and condensable hydrocarbons (tars) [74,78,81].

Gas cleaning involves the physicochemical removal of impurities off the gas [78,79]. Generally the raw product gas exiting the gasifier first passes a high temperature (400°C) gas filter, cyclone or textile bag filter to remove all remaining solid particles (dust, ashes, soot...). A high temperature is important to avoid tar condensation and fouling in the filter [74,81].

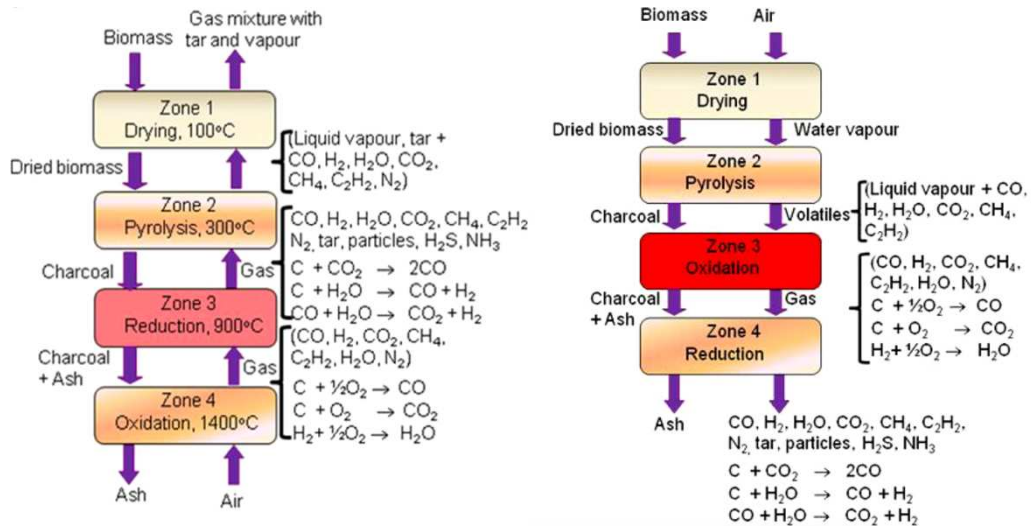


Figure 1.4: Zonal location of the thermochemical reaction processes occurring in updraft (left) and downdraft (right) fixed-bed dry biomass gasification reactors. From [83].

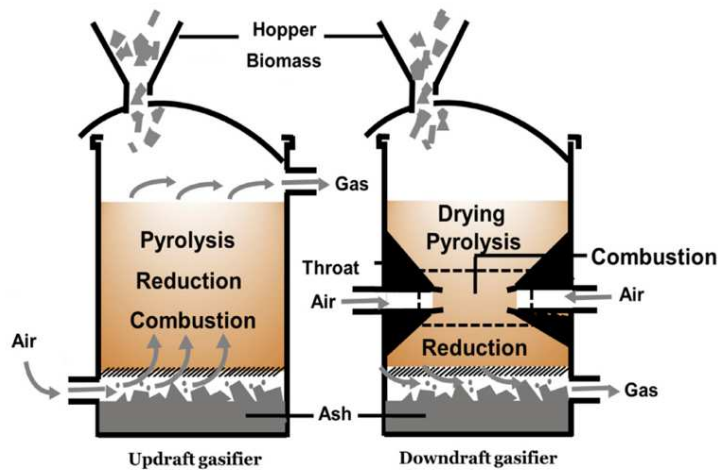


Figure 1.5: Updraft (left) and downdraft (right) fixed-bed dry biomass gasification reactors. Air represents the gasifying agent. From [84].

The next cleaning unit is intended for hydrocarbons (tars, aromatic hydrocarbons) removal. This unit is best operated at a temperature higher than the tar dewpoint to avoid their condensation (typically $>400^{\circ}\text{C}$) [74]. Examples of technologies for hydrocarbon removal include:

- Gas scrubbing with an organic liquid (e.g. rape-methyl-ester) absorbing the tars. Several biomass-to-SNG conversion pilot plants use this technology. Heavy tars are removed by condensation upon contact with the cool oil scrubbing liquid and light tars by absorption in the liquid [74,81]
- Light tars and hydrocarbons like BTEX and naphthalene are removed by sorption on e.g. fixed activate carbon beds in series [81]

Table 1.1: Known thermochemical reactions taking place during dry biomass gasification using steam as gasifying agent in fixed-bed reactors. From [77].

Name of reaction	Chemical reaction	$\Delta H_{r(298)}^0$ (kJ/mol)	$\Delta G_{r(298)}^0$ (kJ/mol)
Pyrolysis	$C_xH_yO_z \rightarrow aCO_2 + bH_2O + cCH_4 + dCO + eH_2 + fC_{2n} + \text{char} + \text{tar}$		
Partial oxidation	$C + 0.5 O_2 \rightarrow CO$	-111	
Complete oxidation	$C + O_2 \rightarrow CO_2$	-394	
Steam-tar reforming	$C_nH_m + 2nH_2O \rightarrow (2n + m/2) H_2 + nCO_2$		
Hydrogenating gasification	$C + 2H_2 \leftrightarrow CH_4$	123.7	168.6
Boudouard equilibrium	$C + CO_2 \leftrightarrow 2CO$	205.3	140.1
Water-gas shift (WGS)	$CO + H_2O \leftrightarrow CO_2 + H_2$	-41.47	-28.5
Heterogeneous WGS	$C + H_2O \leftrightarrow CO + H_2$	130.4	89.8
Steam reforming of methane	$CH_4 + H_2O \leftrightarrow CO + 3H_2$	172.6	118.4
Dry reforming of methane	$CH_4 + CO_2 \leftrightarrow 2CO + 2H_2$	-74.9	-50.3
Ethylene	$2CO + 4H_2 \leftrightarrow C_2H_4 + 2H_2O$	-104.3	-111.6
Ethane	$2CO + 5H_2 \leftrightarrow C_2H_6 + 2H_2O$	-172.7	-212.7
Propane	$3CO + 7H_2 \leftrightarrow C_3H_8 + 3H_2O$	-165.1	-293.2
Butane	$4CO + 9H_2 \leftrightarrow C_4H_{10} + 4H_2O$	-161.9	-376.7
H ₂ S formation	$S + H_2 \rightleftharpoons H_2S$		
H ₂ S-COS equilibrium	$H_2S + CO \rightleftharpoons COS + H_2$		

Removal of S-compounds, NH₃, HCl and other inorganic impurities can occur via water or amine scrubbers or via adsorption beds. ZnO filters are efficient for H₂S removal. Beds of activated carbon or other commercial adsorbents are often used as last guard beds to retain all remaining impurities (H₂S, COS, CS₂, mercaptans, HCl) [74,81].

Once cleaned, the product gas has to be conditioned which implies:

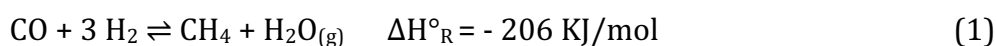
- Enhancing its CO and H₂ concentration and adjusting the CO/H₂ ratio, by converting remaining unsaturated hydrocarbons into convenient CO, H₂ and CH₄ [74,81]. Typical remaining unsaturated hydrocarbons are alkenes, alkynes and aromatic compounds [74]. The prevailing conversion reactions are steam reforming:
 $C_xH_y + x H_2O \rightleftharpoons x CO + [x+(y/2)] H_2$ [78].
- Steam addition to avoid Carbon (soot) formation via the Boudouard reactions [74]:
 $2 CO \rightleftharpoons CO_2 + C$ and $CO + H_2 \rightleftharpoons C + H_2O$. Carbon formation leads to poor conversion efficiency and to soot deposition on and deactivation of the subsequent methanation catalysts. Steam addition inhibits these reactions and the water-gas-shift reaction occurs instead: $CO + H_2O \rightleftharpoons CO_2 + H_2$ [74,78].

Those conditioning operations render the product gas more suitable to enter the methanation step [74,78,81].

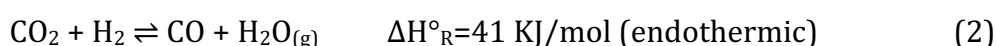
Catalytic methanation

Methanation is the catalyzed hydrogenation of carbon oxides (CO and CO₂) into methane. Carbon oxide-rich gases generated during the thermal gasification of dry biomass (syngas and producer gas) are sent to a methanation reactor, of which several types and concepts exist. CO methanation and CO₂ methanation are distinguished, both being exothermic reactions [74,78,79,82,85]:

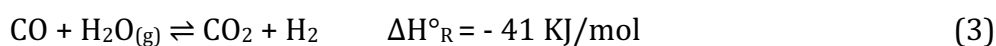
CO methanation:



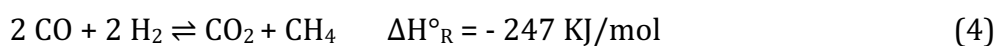
When a Nickel-based catalyst catalyzes this reaction, the reverse of the water-gas-shift reaction (eq. 2) always also takes place simultaneously [82]:



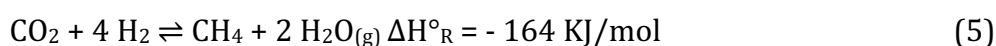
CO methanation reaction runs properly if the stoichiometric ratio of H₂:CO is at least 3:1. Syngas produced from biomass gasification nevertheless often has a lower H₂:CO ratio, typically between 0.3 and 2. By the interplay of the water-gas-shift reaction (eq. 3) and corresponding H₂ generation, this ratio can be adjusted (a water-gas-shift reactor can be placed upstream the methanation reactor) [74,78]:



Note that the linear combination of eqs. 1 and 3 yields another CO methanation reaction (eq. 4) [78]:



CO₂ methanation:



CO₂ methanation is a linear combination of the CO methanation (eq. 1) and reverse water-gas-shift reaction (eq. 2) [82].

Catalysts are essential for the methanation reaction and each specific catalyst also influences the design of the whole methanation unit as well as up- and downstream elements [82]. Most studied and suitable catalysts for syngas methanation are metals: Ni, Co, Fe, Mo, Ru, Rh and Pt, with nickel catalysts being predominantly used in methanation plants [74,75,78–80,82,85]. Catalysts are highly sensitive to carbon and soot depositions and to impurities contained in the gas (H₂S, COS, mercaptans, siloxanes and chlorine [75,78]). Those deposits and impurities can deactivate the catalyst by covering its active surfaces and by adsorbing (physically or chemically) on its active specific sites, impeding the desired reactions to proceed [75]. Bubbling fluidized bed methanation reactors are thought to be less susceptible to deactivation and fouling than fixed bed reactors [80]. The catalytic chemistry of methanation is highly complex and well described in several papers [78,79,82,85].

As methanation reactions are exothermic, accumulation of the produced reaction heat gradually inhibits methane generation and reduces process efficiency in adiabatic reactors. Reactors are hence designed to evacuate the reaction heat via heat exchangers and gas recirculation systems [74,76,78,82]. The simplest design is a series of adiabatic fixed bed methanators with intermediate cooling and gas recycling [74,78,79,82]. Such a design must be operated at relatively low pressures as high pressures will shift the methanation reaction equilibria to more CH₄ production with associated heat release and temperature increase in the reactor, slowing down the conversion and damaging the catalysts [74]. Other reactor configurations include cooled fixed beds with an internal cooling coil, fluidized beds with internal heat exchangers and three-phase methanation where the catalyst is suspended in an inert liquid mineral oil facilitating heat extraction [76,79,82]. The heat removed from methanation reactors can be recovered and valorized as energy source [73,74,81].

To produce SNG via catalytic methanation, carbon oxide rich gases are required. Those can be obtained from the gasification of biomass, but direct catalytic methanation of biogas is also possible [75,80]. Biogas (~40%_{mol} CO₂) from anaerobic digestion plants can directly be methanized, but its CO₂ fraction can also first be isolated and then methanized. In this latter case, biomethane production from a given biomass amount can be increased by up to 60% since on the one hand biomethane is produced from the anaerobic digestion and subsequent biogas upgrading, and on the other hand the isolated CO₂ fraction of the upgraded biogas is not thrown away in the atmosphere but valorized into methane via CO₂-methanation [80]. For this biogenic-CO₂ catalytic methanation to succeed, an external H₂ source is indispensable to fulfill the methanation reaction according to equation 5 [75]. Hydrogen can be supplied via the Power-to-Gas concept, where electricity surpluses electrolyze water into hydrogen and oxygen. In this case CO₂ methanation becomes synonym of chemical electricity storage since the produced methane is a storable source of energy, and since the methanation products (CH₄ and H₂O) can also be turned back into H₂ via steam reforming, and H₂ back into electricity via fuel cells [80,82]. Again, as biogas or the CO₂ fraction of this latter can contain catalyst poisons (impurities like H₂S, siloxanes...), biogas cleaning is required prior to methanation [75,80].

Next to thermochemical catalytic methanation, typically operated at temperature >250°C in fixed or fluidized bed reactors, biological methanation also exists and is typically operated at temperatures <70°C in stirred tank reactors or trickle bed reactors [75,80,82]. Biological methanation of biogas is currently at the research stage [59,80,86].

The final methanation product, raw SNG, is a gas mixture composed of mainly CH₄, H₂O_(g) and CO₂, requiring a final upgrading step to meet natural gas quality specifications and comply with gas grid injection obligations [74,75,78,79]. The water vapor is typically removed via condensation in a cooling unit (gas drying). Depending on the reactor and catalyst used, the gas may need to be filtered to remove remaining catalyst particles [75]. To eventually achieve a pure methane flow, the CO₂ is removed via usual technologies like membrane filtration, water scrubbing, pressure swing adsorption, chemical absorption ... [2,4,20,79]. Remaining traces of H₂ and other components are gotten rid of via adsorption, absorption or membranes [79]. Ultimately, upgraded SNG can be compressed to a convenient pressure for injection in the natural gas grid [74,75].

Fig.1.6 summarizes the different ways to produce SNG discussed in this section.

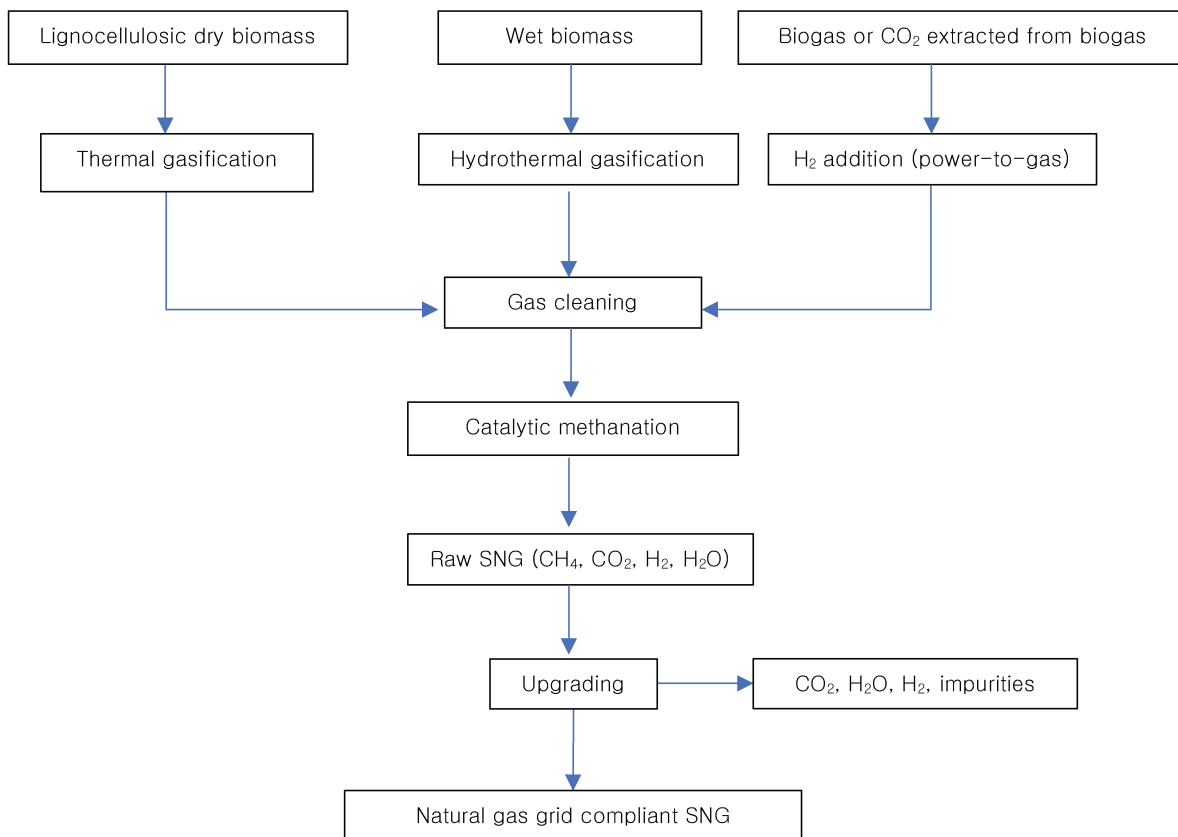


Figure 1.6: Overview of different pathways to produce SNG. Adapted from [79].

Biomass methanation plants with production of SNG at the experimental or demonstration scale began to pop up in the 2000's [73–75,77,78,80,81], based on the technologies developed since the 1970's for coal gasification and methanation [76,78,82]. Examples of today's biomass gasification and methanation (experimental) plants and research centers are:

- The Energy Research Center of the Netherlands [74]
- The Center for Solar Energy and Hydrogen Research in Germany [78,87]
- The Paul Scherrer Institute in Switzerland [75,78,80]
- The GoBiGas project in Sweden [81]. Launched in 2005, this was the first demonstration plant for the production of SNG from woody biomass at industrial scale. In 2013 the plant was operational and in 2014, SNG was fed to the local gas grid.
- The GAYA project in France [73], launched in 2010 to generate SNG from dry biomass (wood residue, olive stones, almond shells, bark, inedible straw) at the industrial scale. This project is currently in its optimization phase.

III.4. Micro- and macro-algae methanization

Lastly, biomethane could be produced from the anaerobic digestion of microalgae or macroalgae (seaweeds). Due to the complex biology of macro- and microalgae, this process is currently not yet operational at industrial scale as will be discussed below [88–98]. A possible configuration for such biomethane production (in pilot or demonstration plants) can be summarized as follows (Fig.1.7). The starting point is often an existing methanization unit valorizing ‘traditional’ organic matter feedstocks (energy crops or organic wastes) into biogas and biomethane. Both the produced biogas and digestate are used to grow algae in photobioreactors (PBR) or open raceway ponds exposed to sunlight: biogas injected in the PBR provides the CO₂ required for the photosynthesis while the digestate provides the essential macro- (nitrogen, phosphorus, potassium...) and micronutrients (metals,...) [89,90,97,99]. Growing algae this way simultaneously (partially) upgrades the biogas since its CO₂ fraction is consumed for the photosynthesis (photosynthetic biogas upgrading). The CH₄ fraction, being less water soluble than CO₂ and being left aside by the algae, is recovered at the exit of the PBR and further purified to biomethane. The grown algal biomass is periodically harvested out of the PBR and conditioned [90,91,93,95] to eventually be fed in turn as feedstock in the initial anaerobic digester, closing the process loop [97]. Growing algae on the liquid digestate fraction has the advantage of removing excess nutrients and metals this latter contains inasmuch as algae consume those nutrients and metals, rendering the digestate safer and better suited for use as a fertilizer on agricultural fields [89,99]. The challenge however to grow algae in digestate is the high turbidity of this latter, impeding light penetration, its high NH₃ content, high chemical oxygen demand and the presence of foreign potentially pathogenic bacteria and viruses inhibiting algal growth. Digestate is therefore often diluted with wastewater or seawater depending on the algal species concerned [89,99,100]. Another alternative is to pre-treat the digestate by ammonia stripping and adsorption on activated carbon beds to help lowering turbidity and organic load of digestates [89,101].

While some seaweeds can be monodigested on the long-term (used as the sole feedstock in the digester), monodigestion of microalgae is much less straightforward as will be discussed below [98]. Microalgae are actually best digested together with other feedstock types (co-digestion) to achieve acceptable CH₄ production levels [91,94,98].

Compared to traditional anaerobic digesters converting edible energy crops (maize, triticale, winter wheat, beet, sugar cane, rapeseed, clover, sunflower...) to biogas [93,102–104], anaerobic digestion of micro- or macroalgae is more sustainable. Algae are not (yet) a main food source and their cultivation does not necessitate arable lands, hence their exploitation as fuel feedstock does not exacerbate the food versus fuel controversy. Micro- and macro algae are furthermore characterized by higher growth rates and photosynthetic yields than traditional terrestrial crops [89,90,92,93,95,97,98] as well as less water requirements [95]. Additionally, growing algae on industrial CO₂ effluents can alleviate atmospheric CO₂ emissions by photosynthetically converting it into biomass [89,90,95]. Anaerobic digestion of microalgae was first proposed in 1956 by Golueke et al. [105] and since then many studies have been led in an attempt to optimize the process [88–97]. Examples of micro- and macroalgae used for anaerobic digestion are [98]:

- Microalgae: *Chlorella sorokiniana*, *Chlorella vulgaris*, *Spirulina dunaliella*, *Spirulina maxima*, *Scenedesmus obliquus*, *Euglena gracilis*, *Durvillea antarctica*, *Nannochloropsis oculata*
- Macroalgae: *Laminara saccharina*, *Laminara digita*, *Ascophyllum nodosum*, *Ulva lactuca*, *Saccharina latissimi*, *Macrocystis pyrifera*, *Himanthalia elongate*, *Saccorhiza polyschides*

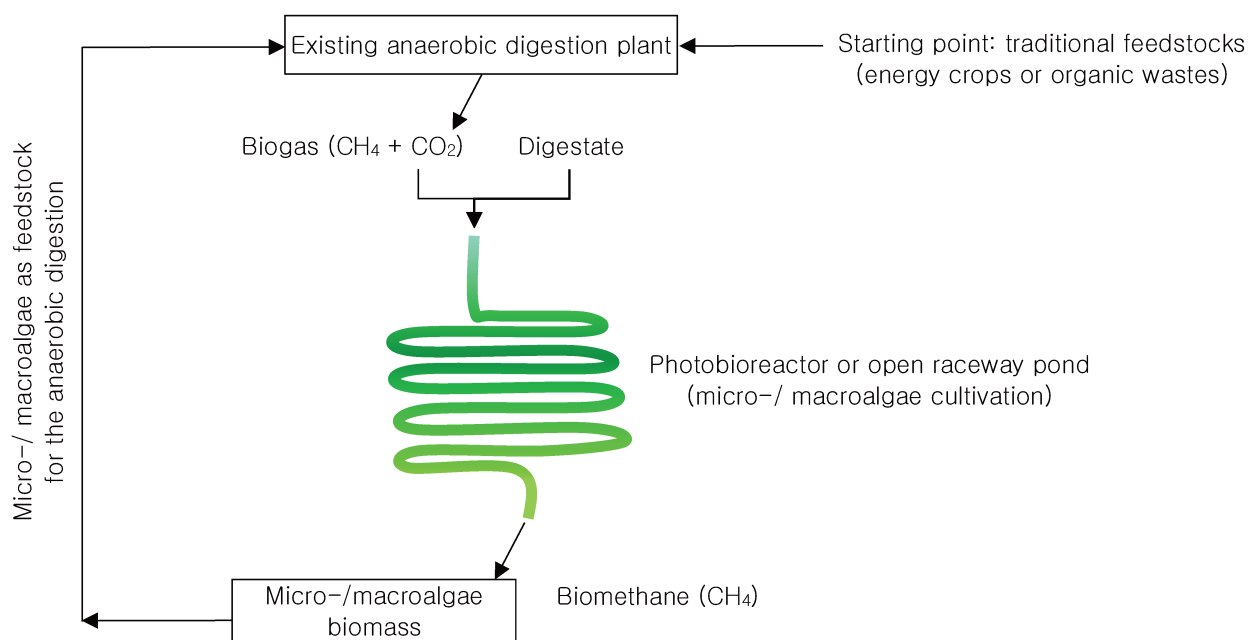


Figure 1.7: Simplified closed-loop example of biomethane production based on the anaerobic digestion of algae grown on the digestate and CO₂ of the produced biogas.

The main hurdle in anaerobic digestion of algae is the resistance of the cell wall of some species to hydrolytic bacterial degradation in the digester and hence their limited digestibility [89,91–95,98,99,105]. In their first experiments, Golueke et al. [105] microscopically examined digestates from the anaerobic digestion of algae (*Scenedesmus* spp. and *Chlorella* spp.) and observed considerable amounts of intact green cells in it. It seemed that, in spite of the unfavorable living conditions in the digester, algae cells did either not die or did die inside the unaffected cell wall. The microalgal cell wall is composed of glycolipids, glycoproteins, polysaccharides, ligno-cellulosic compounds and biopolymers assembled in a structure resistant to hydrolytic degradation in the first anaerobic digestion step. The more readily digestible organic intracellular fractions of microalgae are thus unavailable for digester's bacteria [89,91,92,98,99]. Furthermore, the intracellular microalgal content is characterized by a high carbohydrate, protein and lipid content. When cells eventually do degrade in the anaerobic digester, breakdown of the considerable protein content leads to ammonia (NH₃) production and to a low C:N ratio (typically <10), both being extremely detrimental to methanogen bacteria [89,92,94,98,99,105]. As the population methanogen bacteria diminishes, volatile fatty acids (VFA), being the previous metabolites in the digestion process, accumulate and inhibit the whole digestion process [98,99]. Continued mono-digestion of microalgae is therefore burdensome [94,98]. On the contrary, macroalgae cell walls do not contain hydrolysis resistant lignin and

their cells contain less proteins and lipids than those of microalgae, resulting, for certain macroalgae species, in a more favorable C:N ratio for anaerobic digestion. Those macroalgae can therefore be mono-digested in the long-term with acceptable CH₄ production levels [89,92,98].

As every single micro- or macro-algae species has its very own cellular composition, growth kinetics and growth-response to environment conditions (cultivation method, pH, salinity, temperature, sunlight, nutrient availability, time of harvest, hydraulic retention time...), the specific biomethane potential of each species is different and the suitability of a given algae species for anaerobic digestion must be studied individually depending on the cultivation and anaerobic digestion system configurations available [89,92,93,96,98].

To remedy the negative impacts of micro- and macro-algal cell-composition on the anaerobic digestion process efficiency and CH₄ yields, numerous investigations have been launched to establish adequate pre-treatment operations to help disrupting the compact and resistant cell walls to increase the availability of the intracellular organic components for the microorganisms executing the anaerobic digestion [89,92,93,95,98,99]. Thorough literature reviews have been published on the different convenient pre-treatment methods [98,106–108]. Pre-treatment methods can be categorized into four types: physical (thermal or mechanical), chemical (alkaline or acidic), biological (microbial or enzymatic digestion) and combined (steam explosions, thermo-chemical or biochemical) processes, all aiming at rupturing the cell wall [89,95,98,99,106]. The energy requirement for some of those pre-treatment operations may be considerable and may jeopardize the CH₄ production economic viability (low energy return on investment) [92]. Energy-efficient and affordable pre-treatment options include enzymatic digestion of algal cells [109,110] or the solar-driven hydrothermal pre-treatment system proposed by Xiao Chao et al. [95]. Alternatively, the selection of algae strains without cell walls or with protein-based cell walls can help avoid energy-intensive pre-treatment methods as far as those strains give acceptable biomethane yields [93]. Each pre-treatment's performance relies on the algae type concerned, on its economic and energetic viability and on the type and amount wastes it produces [98].

Next to a pre-treatment aiming at opening the cell wall of micro- and some macroalgae, a complementary way to boost the methanization potential of protein-rich micro- and macroalgae is to co-digest them with carbon-rich materials to increase the resulting C:N ratio obtained during the digestion and to avoid inhibiting NH₃-conditions for methanogen bacteria [89,92,94,98,99]. Acceptable C:N ratio's yielding stable biogas production levels lie in the 20-30 range [92,98]. Carbon rich materials used as co-feedstock with those algae are for instance straw, waste paper, switchgrass, beet silage, manure, sewage sludge [94,98], activated sludge, septic tank sludge, waste fats, oils and greases [94]. Septic tank sludge has been found to be particularly efficient as co-substrate with microalgae inasmuch as it contains hydrolytic enzymes and bacteria able to hydrolyze cellulose (*Clostridium acetobutylicum*, *Clostridium cellulolyticum* and *Acetivibrio cellulolyticus*), actively contributing to the lysis of algal cell walls, enhancing their accessibility to digestion [94]. Another advantage of co-digesting protein-rich algae with other substrates is that the amount unfavorable compounds released during the degradation of those algae (like NH₃ for protein-rich micro- and macro-algae, salt, Sulphur and polyphenols for some seaweeds [89,92,98]), is diluted in a larger volume, keeping their

concentrations below the toxicity levels for the microbiota performing the anaerobic digestion [92,98]. Additionally, favoring a microbiota inoculum able to acclimatize to higher NH_3 and salt concentrations will help stabilize the algae digestion process [89,98].

Next to growing algae in a closed loop system as depicted in Fig.1.7, several other configurations of growing or gathering algae are exploited to produce biomethane. Algae can be farm-cultivated or can be harvested from bays and estuaries where they overgrow other species or cause eutrophication [89,92]. These options may however negatively impact the environment wherein they are cultivated or wherefrom they are harvested, and harvesting seaweeds on bays and estuaries may be burdensome and expensive [89]. Another alternative for algae cultivation involves integrated multi-trophic aquacultures (IMTA) where fish farming and algae growth are combined [89,111]. In this system, algae are grown on the nutrient-rich wastewater wherein fishes were grown, simultaneously purifying the water. Analogously, algae can be grown in municipal wastewater treatment ponds [92].

When photosynthetic biogas upgrading is carried out, algae are fed with the CO_2 of biogas and for every mol CO_2 consumed, one mol O_2 is released according to the oxygenic photosynthesis reaction [89,99]. As biogas upgrading often aims at producing grid-compliant biomethane, the presence of oxygen in the gas is firmly unwanted as strict specifications define maximal oxygen concentrations tolerated in biomethane for grid injection [89,99,112]. This issue can for instance be solved by the combined action of Sulphur-oxidizing bacteria present in the algae growth medium, using the generated O_2 to oxidize H_2S present in the biogas into sulphates [89,113].

Another technical and economic bottleneck regarding microalgae cultivation is their harvest from their liquid growth medium wherein they are relatively diluted ($0.5 - 5 \text{ g}\cdot\text{L}^{-1}$) and in view of their small cell sizes ($3-50 \mu\text{m}$) and low densities [88,90,92]. Efficient biogas production will only succeed if the algal biomass is concentrated, which can be achieved via filtration [93], centrifugation [90,93,97,105] natural settling [90,97] or flocculation [88,97,105].

So far, no or very few industrial-scale plants exist where algae are cultivated and anaerobically digested into biomethane [88,97,98]. Aside from the different bio-technical burdens discussed above, the expenses for the required infrastructures, maintenance and upscaling of algae cultivation, harvesting and pre-treatment may be unaffordable without incentives [88,99]. Currently the configuration the closest to commercialization is that depicted in Fig.1.7 where an existing biogas plant integrates algae cultivation by growth on digestate and photosynthetic biogas upgrading [92,97,99]. However, this configuration is not standardized yet and determining the most appropriate algae species, cultivation conditions, harvesting and pre-treatment methods and anaerobic digestion parameters is becoming urgent to evaluate the global potential of this circular process for energy-efficient biomethane production [99].

IV. REFERENCES CHAPTER 1

- [1] V. Nallathambi Gunaseelan, Anaerobic Digestion of Biomass for Methane Production: A Review, *Biomass Bioenergy*. 13 (1997) 83–114.
- [2] I. Angelidaki, L. Treu, P. Tsapekos, G. Luo, S. Campanaro, H. Wenzel, P.G. Kougias, Biogas Upgrading and Utilization: Current Status and Perspectives, *Biotechnol. Adv.* 36 (2018) 452–466. <https://doi.org/10.1016/j.biotechadv.2018.01.011>.
- [3] INERIS, Étude De La Composition Du Biogaz De Méthanisation Agricole Et Des Émissions En Sortie De Moteur De Valorisation. Rapport d'étude n° DRC-09-94520-13867A, (2009).
- [4] R. Augelletti, M. Conti, M.C. Annesini, Pressure Swing Adsorption for Biogas Upgrading. A New Process Configuration for the Separation of Biomethane and Carbon Dioxide, *J. Clean. Prod.* 140 (2017) 1390–1398. <https://doi.org/10.1016/j.jclepro.2016.10.013>.
- [5] T. Bond, M.R. Templeton, History and Future of Domestic Biogas Plants in the Developing World, *Energy Sustain. Dev.* 15 (2011) 347–354. <https://doi.org/10.1016/j.esd.2011.09.003>.
- [6] M. Vondra, M. Touš, S.Y. Teng, Digestate Evaporation Treatment in Biogas Plants: A Techno-Economic Assessment by Monte Carlo, Neural Networks and Decision Trees, *J. Clean. Prod.* 238 (2019) 117870. <https://doi.org/10.1016/j.jclepro.2019.117870>.
- [7] Anaerobic Digestion, Digestate | Anaerobic Digestion, AD Off. Inf. Portal Anaerob. Dig. (2019). <http://www.biogas-info.co.uk/about/digestate/> (accessed December 11, 2019).
- [8] L. Blaisonneau, M. Faure, A. Gondel, E. Julien, L. Rakotojaona, Overview of the Biomethane Sector in France and Ideas for Its Development, (2017).
- [9] E. Govasmark, J. Ståb, B. Holen, D. Hoornstra, T. Nesbakk, M. Salkinoja-Salonen, Chemical and Microbiological Hazards Associated with Recycling of Anaerobic Digested Residue Intended for Agricultural Use, *Waste Manag.* 31 (2011) 2577–2583. <https://doi.org/10.1016/j.wasman.2011.07.025>.
- [10] I. Angelidaki, L. Xie, G. Luo, Y. Zhang, H. Oechsner, A. Lemmer, R. Munoz, P.G. Kougias, Chapter 33 - Biogas Upgrading: Current and Emerging Technologies, in: *Biofuels Altern. Feedstock Convers. Process. Prod. Liq. Gaseous Biofuels*, Elsevier, 2019: pp. 817–843. <https://doi.org/10.1016/B978-0-12-816856-1.00033-6>.
- [11] E. Saracevic, D. Koch, B. Stuermer, B. Mihalyi, A. Miltner, A. Friedl, Economic and Global Warming Potential Assessment of Flexible Power Generation with Biogas Plants, *Sustainability*. 11 (2019). <https://doi.org/10.3390/su11092530>.
- [12] B. Stürmer, E. Pfundtner, F. Kirchmeyr, S. Uschnig, Legal Requirements for Digestate as Fertilizer in Austria and the European Union Compared to Actual Technical Parameters, *J. Environ. Manage.* 253 (2020) 109756. <https://doi.org/10.1016/j.jenvman.2019.109756>.
- [13] P.Y. Hoo, H. Hashim, W.S. Ho, Opportunities and Challenges: Landfill Gas to Biomethane Injection into Natural Gas Distribution Grid Through Pipeline, *J. Clean. Prod.* 175 (2018) 409–419. <https://doi.org/10.1016/j.jclepro.2017.11.193>.

- [14] M. Schweigkofler, R. Niessner, Determination of Siloxanes and VOC in Landfill Gas and Sewage Gas by Canister Sampling and GC-MS/AES Analysis, *Environ. Sci. Technol.* 33 (1999) 3680–3685. <https://doi.org/10.1021/es9902569>.
- [15] A.C. Elwell, N.H. Elsayed, J.N. Kuhn, B. Joseph, Design and Analysis of Siloxanes Removal by Adsorption from Landfill Gas for Waste-to-Energy Processes, *Waste Manag.* 73 (2018) 189–196. <https://doi.org/10.1016/j.wasman.2017.12.021>.
- [16] M. Beil, W. Beyrich, Chapter 15 - Biogas Upgrading to Biomethane, in: A. Wellinger, J. Murphy, D. Baxter (Eds.), *Biogas Handb.*, Woodhead Publishing, 2013: pp. 342–377.
- [17] M.A. Goossens, Landfill Gas Power Plants, *Renew. Energy.* 9 (1996) 1015–1018. [https://doi.org/10.1016/0960-1481\(96\)88452-7](https://doi.org/10.1016/0960-1481(96)88452-7).
- [18] K. Arrhenius, U. Johansson, Characterisation of Contaminants in Biogas Before and After Upgrading to Vehicle Gas. Rapport SGC 246, (2012). http://www.sgc.se/ckfinder/userfiles/files/SGC246_eng.pdf (accessed June 20, 2021).
- [19] L. Pizzuti, C.A. Martins, P.T. Lacava, Laminar Burning Velocity and Flammability Limits in Biogas: A Literature Review, *Renew. Sustain. Energy Rev.* 62 (2016) 856–865. <https://doi.org/10.1016/j.rser.2016.05.011>.
- [20] G. Leonzio, Upgrading of Biogas to Bio-Methane with Chemical Absorption Process: Simulation and Environmental Impact, *J. Clean. Prod.* 131 (2016) 364–375. <https://doi.org/10.1016/j.jclepro.2016.05.020>.
- [21] M.R. Allen, A. Braithwaite, C.C. Hills, Trace Organic Compounds in Landfill Gas at Seven U.K. Waste Disposal Sites, *Environ. Sci. Technol.* 31 (1997) 1054–1061. <https://doi.org/10.1021/es9605634>.
- [22] M. Cachia, B. Bouyssiere, H. Carrier, H. Garraud, G. Caumette, I. Le Hécho, Characterization and Comparison of Trace Metal Compositions in Natural Gas, Biogas, and Biomethane, *Energy Fuels.* 32 (2018) 6397–6400. <https://doi.org/10.1021/acs.energyfuels.7b03915>.
- [23] J. Feldmann, I. Koch, W.R. Cullen, Complementary Use of Capillary Gas Chromatography–Mass Spectrometry (ion Trap) and Gas Chromatography–Inductively Coupled Plasma Mass Spectrometry for the Speciation of Volatile Antimony, Tin and Bismuth Compounds in Landfill and Fermentation Gases, *The Analyst.* 123 (1998) 815–820. <https://doi.org/10.1039/a707478f>.
- [24] J. Feldmann, Determination of Ni(CO)₄, Fe(CO)₅, Mo(CO)₆, and W(CO)₆ in Sewage Gas by Using Cryotrapping Gas Chromatography Inductively Coupled Plasma Mass Spectrometry, *J. Environ. Monit.* 1 (1999) 33–37. <https://doi.org/10.1039/A807277I>.
- [25] J. Feldmann, W.R. Cullen, Occurrence of Volatile Transition Metal Compounds in Landfill Gas: Synthesis of Molybdenum and Tungsten Carbonyls in the Environment, *Environ. Sci. Technol.* 31 (1997) 2125–2129. <https://doi.org/10.1021/es960952y>.
- [26] International Energy Agency, Eurostat, OECD, *Energy Statistics Manual*, OECD, 2004. <https://doi.org/10.1787/9789264033986-en>.
- [27] W.M. Budzianowski, D.A. Budzianowska, Economic Analysis of Biomethane and

- Bioelectricity Generation from Biogas Using Different Support Schemes and Plant Configurations, *Energy*. 88 (2015) 658–666. <https://doi.org/10.1016/j.energy.2015.05.104>.
- [28] E. Finocchio, T. Montanari, G. Garuti, C. Pistarino, F. Federici, M. Cugino, G. Busca, Purification of Biogases from Siloxanes by Adsorption: On the Regenerability of Activated Carbon Sorbents, *Energy Fuels*. 23 (2009) 4156–4159. <https://doi.org/10.1021/ef900356n>.
- [29] D.-H. Lee, Evaluation the Financial Feasibility of Biogas Upgrading to Biomethane, Heat, CHP and AWR, *Int. J. Hydrog. Energy*. 42 (2017) 27718–27731. <https://doi.org/10.1016/j.ijhydene.2017.07.030>.
- [30] P. Jaramillo, H.S. Matthews, Landfill-Gas-to-Energy Projects: Analysis of Net Private and Social Benefits, *Environ. Sci. Technol.* 39 (2005) 7365–7373. <https://doi.org/10.1021/es050633j>.
- [31] D. Papurello, L. Tomasi, S. Silvestri, M. Santarelli, Evaluation of the Wheeler-Jonas Parameters for Biogas Trace Compounds Removal with Activated Carbons, *Fuel Process. Technol.* 152 (2016) 93–101. <https://doi.org/10.1016/j.fuproc.2016.06.006>.
- [32] Y. Shiratori, T. Oshima, K. Sasaki, Feasibility of Direct-Biogas SOFC, *Int. J. Hydrog. Energy*. 33 (2008) 6316–6321. <https://doi.org/10.1016/j.ijhydene.2008.07.101>.
- [33] N. de Arespacochaga, C. Valderrama, C. Mesa, L. Bouchy, J.L. Cortina, Biogas Deep Clean-up Based on Adsorption Technologies for Solid Oxide Fuel Cell Applications, *Chem. Eng. J.* 255 (2014) 593–603. <https://doi.org/10.1016/j.cej.2014.06.072>.
- [34] D. Topić, D. Šljivac, L. Jozsa, S. Nikolovski, M. Vukobratović, Cost–Benefit Analysis of Biogas CHP (combined Heat and Power) Plant, in: 2010. <https://doi.org/10.13140/2.1.4026.0168>.
- [35] W.M. Budzianowski, M. Brodacka, Biomethane Storage: Evaluation of Technologies, End Uses, Business Models, and Sustainability, *Energy Convers. Manag.* 141 (2017) 254–273. <https://doi.org/10.1016/j.enconman.2016.08.071>.
- [36] F. Teymoori Hamzehkolaei, N. Amjady, A Techno-Economic Assessment for Replacement of Conventional Fossil Fuel Based Technologies in Animal Farms with Biogas Fueled Chp Units, *Renew. Energy*. 118 (2018) 602–614. <https://doi.org/10.1016/j.renene.2017.11.054>.
- [37] S.E. Hosseini, M.A. Wahid, Development of biogas combustion in combined heat and power generation, *Renew. Sustain. Energy Rev.* 40 (2014) 868–875. <https://doi.org/10.1016/j.rser.2014.07.204>.
- [38] Electricity and Heat Production from Biogas CHP: Discover Technologies, *BiogasWorld*. (2017). <https://www.biogasworld.com/news/biogas-chp-discover-technologies/> (accessed December 11, 2019).
- [39] Viking Strategies, Biogas Association, Farm To Fuel Developers’ Guide To Biomethane, (2012).
- [40] A.-M. Pourcher, C. Druilhe, Impact Du Compostage Et De La Méthanisation Sur Les Pathogènes Et L’antibiorésistance, (n.d.).
- [41] F. Cucchiella, I. D’Adamo, Technical and Economic Analysis of Biomethane: A Focus on

the Role of Subsidies, *Energy Convers. Manag.* 119 (2016) 338–351.

<https://doi.org/10.1016/j.enconman.2016.04.058>.

[42] M. Ashrafi, C. Pfeifer, T. Pröll, H. Hofbauer, Experimental Study of Model Biogas Catalytic Steam Reforming: 2. Impact of Sulfur on the Deactivation and Regeneration of Ni-Based Catalysts, *Energy Fuels*. 22 (2008) 4190–4195. <https://doi.org/10.1021/ef8000828>.

[43] Z. Bacsik, O. Cheung, P. Vasiliev, N. Hedin, Selective Separation of CO₂ and CH₄ for Biogas Upgrading on Zeolite NaKa and SAPO-56, *Appl. Energy*. 162 (2016) 613–621. <https://doi.org/10.1016/j.apenergy.2015.10.109>.

[44] M. Schweigkofler, R. Niessner, Removal of siloxanes in biogases, *J. Hazard. Mater.* 83 (2001) 183–196. [https://doi.org/10.1016/S0304-3894\(00\)00318-6](https://doi.org/10.1016/S0304-3894(00)00318-6).

[45] F. Ferella, F. Cucchiella, I. D'Adamo, K. Gallucci, A Techno-Economic Assessment of Biogas Upgrading in a Developed Market, *J. Clean. Prod.* 210 (2019) 945–957. <https://doi.org/10.1016/j.jclepro.2018.11.073>.

[46] M. Ghidotti, D. Fabbri, C. Torri, Determination of Linear and Cyclic Volatile Methyl Siloxanes in Biogas and Biomethane by Solid-Phase Microextraction and Gas Chromatography-Mass Spectrometry, *Talanta*. 195 (2019) 258–264. <https://doi.org/10.1016/j.talanta.2018.11.032>.

[47] A.M.H. Van Der Veen, C. Chamorro, F. Lestremau, F. Pérer Sanz, Final Publishable JRP Report Metrology for Biogas, ENG54 Biogas, (2018). <http://projects.npl.co.uk/metrology-for-biogas/>.

[48] D.L. Saber, S.F. Takach, Pipeline Quality Biomethane: North American Guidance Document for Introduction of Dairy Waste Derived Biomethane into Existing Natural Gas Networks. Technology Investigation, Assessment and Analysis. Task 1 Final Report, GTI Project Number 20614, (2009). <http://www.agriwasteenergy.com/pdf/FINALTASK1FINALREPORT-REFORMATTED.pdf> (accessed December 12, 2019).

[49] A.M.H. Van Der Veen, A.S. Brown, J. Li, A. Murugan, M. Heinonen, F. Haloua, K. Arrhenius, Measurement Requirements for Biogas Specifications, 17th Int. Congr. Metrol. 08006. (2015) 7. <https://doi.org/10.1051/metrology/201508006>.

[50] Y. Karagöz, Analysis of the Impact of Gasoline, Biogas and Biogas + Hydrogen Fuels on Emissions and Vehicle Performance in the WLTC and NEDC, *Int. J. Hydrog. Energy*. 44 (2019) 31621–31632. <https://doi.org/10.1016/j.ijhydene.2019.10.019>.

[51] T. Lönnqvist, S. Anderberg, J. Ammenberg, T. Sandberg, S. Grönkvist, Stimulating Biogas in the Transport Sector in a Swedish Region – an Actor and Policy Analysis with Supply Side Focus, *Renew. Sustain. Energy Rev.* 113 (2019) 109269. <https://doi.org/10.1016/j.rser.2019.109269>.

[52] R. Hernández-Gómez, T. Fernández-Vicente, D. del Campo, M. Val'ková, M. Chytil, C.R. Chamorro, Characterization of a Biomethane-Like Synthetic Gas Mixture Through Accurate Density Measurements from (240 to 350) K and Pressures up to 14MPa, *Fuel*. 206 (2017) 420–428. <https://doi.org/10.1016/j.fuel.2017.06.040>.

[53] Présentation De L'observatoire Du Biogaz En France, ATEE Club Biogaz Assoc. Tech.

- Energ. Environ. (n.d.). <http://atee.fr/biogaz/observatoire-du-biogaz-en-france> (accessed July 26, 2019).
- [54] ATEE Club Biogaz, Statistiques Filière Biogaz – Juillet 2018, (2018).
- [55] A. Anukam, A. Mohammadi, M. Naqvi, K. Granström, A Review of the Chemistry of Anaerobic Digestion: Methods of Accelerating and Optimizing Process Efficiency, *Processes*. 7 (2019) 504. <https://doi.org/doi:10.3390/pr7080504>.
- [56] J.N. Meegoda, B. Li, K. Patel, L.B. Wang, A Review of the Processes, Parameters, and Optimization of Anaerobic Digestion, *Int. J. Environ. Res. Public. Health*. 15 (2018) 2224. <https://doi.org/doi:10.3390/ijerph15102224>.
- [57] V. Nallathambi Gunaseelan, Anaerobic Digestion of Biomass for Methane Production: A Review, *Biomass Bioenergy*. 13 (1997) 83–114.
- [58] H. Porté, P.G. Kougias, N. Alfaro, L. Treu, S. Campanaro, I. Angelidaki, Process Performance and Microbial Community Structure in Thermophilic Tricking Biofilter Reactors for Biogas Upgrading, *Sci. Total Environ*. 655 (2019) 529–538. <https://doi.org/10.1016/j.scitotenv.2018.11.289>.
- [59] I. Bassani, P.G. Kougias, L. Treu, H. Porté, S. Campanaro, I. Angelidaki, Optimization of Hydrogen Dispersion in Thermophilic up-Flow Reactors for Ex Situ Biogas Upgrading, *Bioresour. Technol*. 234 (2017) 310–319. <https://doi.org/10.1016/j.biortech.2017.03.055>.
- [60] D. Nagarajan, D.-J. Lee, J.-S. Chang, Integration of Anaerobic Digestion and Microalgal Cultivation for Digestate Bioremediation and Biogas Upgrading, *Bioresour. Technol*. 290 (2019) 121804. <https://doi.org/10.1016/j.biortech.2019.121804>.
- [61] M. Prussi, M. Padella, M. Conton, E.D. Postma, L. Lonza, Review of Technologies for Biomethane Production and Assessment of Eu Transport Share in 2030, *J. Clean. Prod*. 222 (2019) 565–572. <https://doi.org/10.1016/j.jclepro.2019.02.271>.
- [62] M.R. Atelge, H. Senol, M. Djaafri, T.A. Hansu, D. Krisa, A. Atabani, C. Eskicioglu, H. Muratçobanoğlu, S. Unalan, S. Kalloum, N. Azbar, H.D. Kıvrak, A Critical Overview of the State-of-the-Art Methods for Biogas Purification and Utilization Processes, *Sustainability*. 13 (2021). <https://doi.org/10.3390/su132011515>.
- [63] M.D. Vaverková, Landfill Impacts on the Environment—Review, *Geosciences*. 9 (2019) 431. <https://doi.org/10.3390/geosciences9100431>.
- [64] US EPA, Chapter 2: Landfill Gas Basics. In *Landfill Gas Primer - An Overview for Environmental Health Professionals*, (2008). https://www.atsdr.cdc.gov/HAC/landfill/PDFs/Landfill_2001_ch2mod.pdf (accessed January 27, 2020).
- [65] S. Rasi, J. Läntelä, J. Rintala, Trace Compounds Affecting Biogas Energy Utilisation – A Review, *Energy Convers. Manag*. 52 (2011) 3369–3375. <https://doi.org/10.1016/j.enconman.2011.07.005>.
- [66] C. Guyot, Terralia ISDND, Aire sur l'Adour, France. Oral communication., (2019).
- [67] US EPA, LFG Energy Project Development Handbook. Landfill Methane Outreach Program, (2017).

- [68] R. Chiriac, J. Carre, Y. Perrodin, L. Fine, J.-M. Letoffe, Review: Characterisation of VOCs Emitted by Open Cells Receiving Municipal Solid Waste, *J. Hazard. Mater.* 149 (2007) 249–263.
- [69] US EPA, EPA 430-R-19-001- Inventory of U.S. Greenhouse Gas Emissions and Sinks: 1990–2017, (2019). <https://www.epa.gov/ghgemissions/inventory-us-greenhouse-gas-emissions-and-sinks> ; <https://www.epa.gov/ghgemissions/inventory-us-greenhouse-gas-emissions-and-sinks-1990-2017>.
- [70] EEA (European Environmental Agency), Eurostat, Greenhouse Gas Emissions By Source Sector (source: EEA), Eurostat - Data Explor. (2019). https://appsso.eurostat.ec.europa.eu/nui/show.do?query=BOOKMARK_DS-089165_QID_30E84690_UID_-3F171EB0&layout=TIME,C,X,0;GEO,L,Y,0;UNIT,L,Z,0;AIRPOL,L,Z,1;SRC_CRF,L,Z,2;INDICATORS,C,Z,3;&zSelection=DS-089165INDICATORS,OBS_FLAG;DS-089165UNIT,THS_T;DS-089165AIRPOL,GHG;DS-089165SRC_CRF,TOTX4_MEMONIA;&rankName1=TIME_1_0_0_0&rankName2=UNIT_1_2_-1_2&rankName3=GEO_1_2_0_1&rankName4=SRC-CRF_1_2_-1_2&rankName5=AIRPOL_1_2_-1_2&rankName6=INDICATORS_1_2_-1_2&sortC=ASC_-1_FIRST&rStp=&cStp=&rDCh=&cDCh=&rDM=true&cDM=true&footnes=false&empty=false&wai=false&time_mode=ROLLING&time_most_recent=false&lang=EN&cfo=%23%23%23%2C%23%23%23.%23%23%23 (accessed January 28, 2020).
- [71] L. Lombardi, E. Carnevale, A. Corti, Greenhouse Effect Reduction and Energy Recovery from Waste Landfill, *Energy*. 31 (2006) 3208–3219. <https://doi.org/10.1016/j.energy.2006.03.034>.
- [72] A. Jaffrin, N. Bentounes, A.M. Joan, S. Makhlof, Landfill Biogas for Heating Greenhouses and Providing Carbon Dioxide Supplement for Plant Growth, *Biosyst. Eng.* 86 (2003) 113–123. [https://doi.org/10.1016/S1537-5110\(03\)00110-7](https://doi.org/10.1016/S1537-5110(03)00110-7).
- [73] ENGIE, Gaya, Turning Dry Biomass Into Green Gas, (2014). <http://www.projetgaya.com/en/> (accessed February 17, 2020).
- [74] R. Zwart, H. Boerrigter, E. Deurwaarder, C. Van der Meijden, S. Van Paasen, Production of Synthetic Natural Gas from Biomass. Development and Operation of an Integrated Bio-SNG System. Non Confidential Version., (2006).
- [75] A.S. Calbry-Muzyka, A. Gantenbein, J. Schneebeli, A. Frei, A.J. Knorpp, T.J. Schildhauer, S.M.A. Biollaz, Deep Removal of Sulfur and Trace Organic Compounds from Biogas to Protect a Catalytic Methanation Reactor, *Chem. Eng. J.* 360 (2019) 577–590. <https://doi.org/10.1016/j.cej.2018.12.012>.
- [76] Y. Chhiti, M. Kemiha, Thermal Conversion of Biomass, Pyrolysis and Gasification: A Review, *Int. J. Eng. Sci.* 2 (2013) 75–85.
- [77] K. Koido, T. Iwasaki, Chapter 7 - Biomass Gasification: A Review of Its Technology, Gas Cleaning Applications, and Total System Life Cycle Analysis, in: M. Poletto (Ed.), *Lignin - Trends Appl., InTech*, 2018. <https://doi.org/10.5772/intechopen.70727>.
- [78] J. Kopyscinski, T.J. Schildhauer, S.M.A. Biollaz, Production of Synthetic Natural Gas (SNG) from Coal and Dry Biomass – a Technology Review from 1950 to 2009, *Fuel*. 89 (2010) 1763–

1783. <https://doi.org/10.1016/j.fuel.2010.01.027>.

[79] T.J. Schildhauer, S.M. Biollaz, *Synthetic Natural Gas: From Coal, Dry Biomass, and Power-to-Gas Applications*, John Wiley & Sons, Paul Scherrer Institut, Villigen, Switzerland, 2016.

[80] J. Witte, A. Calbry-Muzyka, T. Wieseler, P. Hottinger, S.M.A. Biollaz, T.J. Schildhauer, Demonstrating Direct Methanation of Real Biogas in a Fluidised Bed Reactor, *Appl. Energy*. 240 (2019) 359–371. <https://doi.org/10.1016/j.apenergy.2019.01.230>.

[81] A. Larsson, I. Gunnarsson, F. Tengberg, *The GoBiGas Project: Demonstration of the Production of Biomethane from Biomass via Gasification*, (2018). <https://doi.org/10.13140/RG.2.2.27352.55043>.

[82] S. Rönsch, J. Schneider, S. Matthischke, M. Schlüter, M. Götz, J. Lefebvre, P. Prabhakaran, S. Bajohr, Review on Methanation – from Fundamentals to Current Projects, *Fuel*. 166 (2016) 276–296. <https://doi.org/10.1016/j.fuel.2015.10.111>.

[83] M. Asadullah, Barriers of Commercial Power Generation Using Biomass Gasification Gas: A Review, *Renew. Sustain. Energy Rev.* 29 (2014) 201–215. <https://doi.org/10.1016/j.rser.2013.08.074>.

[84] V.S. Sikarwar, M. Zhao, P.S. Fennell, N. Shah, E.J. Anthony, Progress in Biofuel Production from Gasification, *Prog. Energy Combust. Sci.* 61 (2017) 189–248. <https://doi.org/10.1016/j.pecs.2017.04.001>.

[85] M.C. Seemann, T.J. Schildhauer, S.M.A. Biollaz, Fluidized Bed Methanation of Wood-Derived Producer Gas for the Production of Synthetic Natural Gas, *Ind. Eng. Chem. Res.* 49 (2010) 7034–7038. <https://doi.org/10.1021/ie100510m>.

[86] B. Lecker, L. Illi, A. Lemmer, H. Oechsner, Biological Hydrogen Methanation – a Review, *Bioresour. Technol.* 245 (2017) 1220–1228. <https://doi.org/10.1016/j.biortech.2017.08.176>.

[87] ZSW Zentrum für Sonnenenergie- und Wasserstoff-Forschung Baden-Württemberg, ZSW: Biomass-to-Fuels, Thermochemical conversion, (2020). <https://www.zsw-bw.de/en/research/renewable-fuels/topics/biomass-to-fuels.html> (accessed February 17, 2020).

[88] E. Jankowska, M. Zieliński, M. Dębowski, P. Oleśkiewicz-Popiel, Chapter 15 - Anaerobic Digestion of Microalgae for Biomethane Production, in: A. Basile, F. Dalena (Eds.), *Second Third Gener. Feedstock*, Elsevier, 2019: pp. 405–436. <https://doi.org/10.1016/B978-0-12-815162-4.00015-X>.

[89] D.M. Wall, S. McDonagh, J.D. Murphy, Cascading Biomethane Energy Systems for Sustainable Green Gas Production in a Circular Economy, *Bioresour. Technol.* 243 (2017) 1207–1215. <https://doi.org/10.1016/j.biortech.2017.07.115>.

[90] P. Collet, A. Hélias, L. Lardon, M. Ras, R.-A. Goy, J.-P. Steyer, Life-Cycle Assessment of Microalgae Culture Coupled to Biogas Production, *Bioresour. Technol.* 102 (2011) 207–214. <https://doi.org/10.1016/j.biortech.2010.06.154>.

[91] M. Wang, E. Lee, M.P. Dilbeck, M. Liebelt, Q. Zhang, S.J. Ergas, Thermal Pretreatment of Microalgae for Biomethane Production: Experimental Studies, Kinetics and Energy Analysis, *J. Chem. Technol. Biotechnol.* 92 (2017) 399–407. <https://doi.org/10.1002/jctb.5018>.

- [92] J.J. Milledge, V.B. Nielsen, S. Maneein, J.P. Harvey, A Brief Review of Anaerobic Digestion of Algae for Bioenergy, *Energies*. 12 (2019). <https://doi.org/10.3390/en12061166>.
- [93] J.H. Mussnug, V. Klassen, A. Schlüter, O. Kruse, Microalgae as Substrates for Fermentative Biogas Production in a Combined Biorefinery Concept, *J. Biotechnol.* 150 (2010) 51–56. <https://doi.org/10.1016/j.jbiotec.2010.07.030>.
- [94] D. Lu, X. Liu, O.G. Apul, L. Zhang, D.K. Ryan, X. Zhang, Optimization of Biomethane Production from Anaerobic Co-Digestion of Microalgae and Septic Tank Sludge, *Biomass Bioenergy*. 127 (2019) 105266. <https://doi.org/10.1016/j.biombioe.2019.105266>.
- [95] C. Xiao, Q. Liao, Q. Fu, Y. Huang, H. Chen, H. Zhang, A. Xia, X. Zhu, A. Reungsang, Z. Liu, A Solar-Driven Continuous Hydrothermal Pretreatment System for Biomethane Production from Microalgae Biomass, *Appl. Energy*. 236 (2019) 1011–1018. <https://doi.org/10.1016/j.apenergy.2018.12.014>.
- [96] S. Perazzoli, B.M. Bruchez, W. Michelon, R.L.R. Steinmetz, M.P. Mezzari, E.O. Nunes, M.L.B. da Silva, Optimizing Biomethane Production from Anaerobic Degradation of *Scenedesmus* Spp. Biomass Harvested from Algae-Based Swine Digestate Treatment, *Int. Biodeterior. Biodegrad.* 109 (2016) 23–28. <https://doi.org/10.1016/j.ibiod.2015.12.027>.
- [97] X. Wang, E. Nordlander, E. Thorin, J. Yan, Microalgal biomethane production integrated with an existing biogas plant: A case study in Sweden, *Appl. Energy*. 112 (2013) 478–484. <https://doi.org/10.1016/j.apenergy.2013.04.087>.
- [98] R.G. Saratale, G. Kumar, R. Banu, A. Xia, S. Periyasamy, G.D. Saratale, A Critical Review on Anaerobic Digestion of Microalgae and Macroalgae and Co-Digestion of Biomass for Enhanced Methane Generation, *Bioresour. Technol.* 262 (2018) 319–332. <https://doi.org/10.1016/j.biortech.2018.03.030>.
- [99] A. Bose, R. O’Shea, R. Lin, J.D. Murphy, A Perspective on Novel Cascading Algal Biomethane Biorefinery Systems, *Bioresour. Technol.* 304 (2020) 123027. <https://doi.org/10.1016/j.biortech.2020.123027>.
- [100] A. Xia, J.D. Murphy, Microalgal Cultivation in Treating Liquid Digestate from Biogas Systems, *Trends Biotechnol.* 34 (2016) 264–275. <https://doi.org/10.1016/j.tibtech.2015.12.010>.
- [101] F. Marazzi, C. Sambusiti, F. Monlau, S.E. Cecere, D. Scaglione, A. Barakat, V. Mezzanotte, E. Ficara, A Novel Option for Reducing the Optical Density of Liquid Digestate to Achieve a More Productive Microalgal Culturing, *Algal Res.* 24 (2017) 19–28. <https://doi.org/10.1016/j.algal.2017.03.014>.
- [102] C. Gissén, T. Prade, E. Kreuger, I.A. Nges, H. Rosenqvist, S.-E. Svensson, M. Lantz, J.E. Mattsson, P. Börjesson, L. Björnsson, Comparing Energy Crops for Biogas Production – Yields, Energy Input and Costs in Cultivation Using Digestate and Mineral Fertilisation, *Biomass Bioenergy*. 64 (2014) 199–210. <https://doi.org/10.1016/j.biombioe.2014.03.061>.
- [103] R. Braun, P. Weiland, A. Wellinger, Biogas From Energy Crop Digestion. Task 37 - Energy From Biogas and Landfill Gas, (n.d.).
- [104] ADEME, Life Cycle Analysis of the Biogas Originating from Energy Crops Recovered as

Vehicle and Boiler Fuel, After Injection into the Natural Gas Grid. Final Definitivie Report, (2011).

[105] C.G. Golueke, W.J. Oswald, H.B. Gotaas, Anaerobic Digestion of Algae, *Appl. Microbiol.* 5 (1957) 47–55.

[106] E. Jankowska, A.K. Sahu, P. Oleskowicz-Popiel, Biogas from Microalgae: Review on Microalgae's Cultivation, Harvesting and Pretreatment for Anaerobic Digestion, *Renew. Sustain. Energy Rev.* 75 (2017) 692–709. <https://doi.org/10.1016/j.rser.2016.11.045>.

[107] V.T. de C. Neves, E.A. Sales, L.W. Perelo, Influence of Lipid Extraction Methods as Pre-Treatment of Microalgal Biomass for Biogas Production, *Renew. Sustain. Energy Rev.* 59 (2016) 160–165. <https://doi.org/10.1016/j.rser.2015.12.303>.

[108] S. Maneein, J.J. Milledge, V.B. Nielsen, J.P. Harvey, A Review of Seaweed Pre-Treatment Methods for Enhanced Biofuel Production by Anaerobic Digestion or Fermentation, *Fermentation.* 4 (2018). <https://doi.org/10.3390/fermentation4040100>.

[109] F. Passos, A. Hom-Diaz, P. Blaquez, T. Vicent, I. Ferrer, Improving Biogas Production from Microalgae by Enzymatic Pretreatment, *Bioresour. Technol.* 199 (2016) 347–351. <https://doi.org/10.1016/j.biortech.2015.08.084>.

[110] S. Kavitha, P. Subbulakshmi, J.R. Banu, M. Gobi, I.T. Yeom, Enhancement of Biogas Production from Microalgal Biomass Through Cellulolytic Bacterial Pretreatment, *Bioresour. Technol.* 233 (2017) 34–43. <https://doi.org/10.1016/j.biortech.2017.02.081>.

[111] A. Jacob, A. Xia, D. Gunning, G. Burnell, J.D. Murphy, Seaweed Biofuel Derived from Integrated Multi-Trophic Aquaculture, *Int. J. Environ. Sci. Dev.* 7 (2016) 805.

[112] Teréga, Prescriptions Techniques Applicables Au Raccordement D'un Ouvrage Tiers Au Réseau De Transport De Gaz Naturel De Teréga, (2017).

[113] A. Toledo-Cervantes, C. Madrid-Chirinos, S. Cantera, R. Lebrero, R. Muñoz, Influence of the Gas-Liquid Flow Configuration in the Absorption Column on Photosynthetic Biogas Upgrading in Algal-Bacterial Photobioreactors, *Bioresour. Technol.* 225 (2017) 336–342. <https://doi.org/10.1016/j.biortech.2016.11.087>.

CHAPTER 2 – REVIEW OF GAS SAMPLING AND PRECONCENTRATION TECHNIQUES FOR THE DETERMINATION OF TRACE COMPOUNDS IN METHANE-LIKE FIELD GAS SAMPLES

– Submitted as a review article in *Analytica Chimica Acta* on March 28th 2022 –

Aurore Lecharlier^{1,2}, Hervé Carrier¹, Isabelle Le Hécho^{2*}

¹ Université de Pau et des Pays de l'Adour, E2S UPPA, CNRS, TOTAL, LFCR UMR 5150, BP 1155 avenue de l'Université, 64013 Pau Cedex, France

² Université de Pau et des Pays de l'Adour, E2S UPPA, CNRS, IPREM UMR 5254, Technopôle Hélioparc, 2 avenue du Président Angot, 64053 Pau Cedex 09, France

* Corresponding author : Isabelle Le Hécho • isabelle.lehecho@univ-pau.fr

ABSTRACT

Worldwide, the valorization of landfill gas, biogas and biomethane is getting momentum as circular economies and energy transition are triggered. The anaerobic digestion of anthropogenic organic wastes in landfills or in controlled digesters concomitantly addresses these two challenges by converting wastes into renewable energy in the form of methane contained in these gases. Their sustainable integration into today's energy mix nevertheless requires their quality to be controlled regarding their major (CH₄; CO₂), minor and trace constituents to preserve the integrity of engines, boilers and infrastructures wherein they are burned, transported or stored. Field gas sampling is the first and most critical step of the analytical chain to characterize trace compounds in such gases. A large array of gas sampling techniques is available yet choosing the most suitable one is complex, especially when targeting trace compounds (< ng·Nm⁻³ to mg·Nm⁻³) which often require a preconcentration step to be detectable. Sampled trace compounds must be kept stable (no loss, no degradation, no contamination) during the storage phase between sampling and analysis and all materials of the sampling chain in contact with the gas potentially influence this stability.

This chapter aims at reviewing available gas sampling and preconcentration techniques for the determination of trace compounds in methane-like gas samples. Techniques reviewed include 1) whole gas sampling methods (gas sampling bags, gas cylinders, canisters) and 2) gas sampling methods with preconcentration on solid media (sorbent tubes for physisorption or chemisorption, amalgamation, solid phase microextraction); gas sampling methods with preconcentration in liquid media (absorption in impingers); and gas sampling methods with cryogenic preconcentration. These techniques are reviewed for the sampling of non-metal(loid) volatile organic trace compounds (aliphatic, aromatic, halogenated and oxygenated species;

organic Silicon-compounds (siloxanes, silanes), and (in)organic Sulphur-compounds) as well as for volatile (in)organic metal(loid) compounds. The section on adsorbent tubes for the preconcentration of non-metal(loid) trace compounds is extensively discussed as it has been found to be the most robust and most applied technique for the field preconcentration of these trace compounds in landfill gas, biogas and biomethane. Appropriateness for given families of trace compounds, storage stability issues, considerations on the ease of field implementation, advantages and disadvantages are discussed for all presented sampling and preconcentration methods. Not any of them is able to trap and recover all families of trace compounds in view of the diversity in physicochemical properties of trace compounds often present in landfill gas, biogas and biomethane (volatility, polarity, reactivity...), resulting in different affinities and stabilities in the sampling entities.

This review highlights the intricate complexity of sampling trace compounds and is closed by a list of recommendations to select proper sampling units, materials and parameters and to apply suitable sample transport and storage conditions to safeguard the integrity of samples.

KEYWORDS

Biogas and biomethane

Trace compounds

Whole gas sampling

Preconcentration

Volatile organic compounds

Volatile metal(loid) compounds

ABBREVIATIONS CHAPTER 2

AD	Anaerobic digestion
AES	Atomic emission spectrometry
BTEX	Benzene; Toluene; Ethylbenzene; <i>o</i> -, <i>m</i> -, <i>p</i> -Xylene
BV	Breakthrough volume
b.p.	Boiling point
CT	Cryotrapping
D3	Hexamethylcyclotrisiloxane
D4	Octamethylcyclotetrasiloxane
D5	Decamethylcyclopentasiloxane
D6	Dodecamethylcyclohexasiloxane
DMDS	Dimethyldisulfide ((CH ₃) ₂ S ₂)
DMS	Dimethylsulfide ((CH ₃) ₂ S)
ECD	Electron capture detector
FID	Flame ionization detector
GC	Gas chromatography
HPLC	High pressure liquid chromatography
ICP	Inductively coupled plasma
ID	Internal diameter
L2	Hexamethyltrisiloxane
L3	Octamethyltrisiloxane
L4	Decamethyltetrasiloxane
L5	Dodecamethylpentasiloxane
OD	Outer diameter
LOD	Limit of detection
MS	Mass spectrometry
MSW	Municipal solid waste
OES	Optical emission spectrometry
PTFE	Polytetrafluoroethylene
RH	Relative humidity
SPME	Solid phase microextraction
SSV	Safe sampling volume
TD	Thermal desorption

TMA	Trimethylarsine
(H)VOC	(Halogenated) Volatile organic compounds
VMS	Volatile methyl siloxane
VSC	Volatile Sulphur compound
WWTP	Wastewater treatment plant

I. INTRODUCTION

The metrological analysis of trace compounds in biogas (including landfill gas) and biomethane matrices is intricate due to the low concentrations concerned ($< \text{ng}\cdot\text{m}^{-3}$ to $\text{mg}\cdot\text{m}^{-3}$), the variability in composition of biogases and biomethane and due to the complex nature of these gas matrices [1–3]. First, to be detectable, the low concentrations of targeted trace compounds often request specific preconcentration operations to reach higher concentration levels and bridge the limits of detection of currently available analytical apparatuses. Determining the most appropriate preconcentration technique is a delicate enterprise in view of the broad diversities in physico-chemical behaviors of targeted compounds. Next, biogases may contain condensate phases, relative high water content [1,4,5], complex mixtures of volatile organic and organometallic compounds having different volatilities and polarities [1,2,5–7], counting many isomers and functional groups, rendering their analysis challenging and laborious [1,6,8]. Additionally, searching for trace compounds as it is aimed to in this project, is not evident inasmuch as the aim is not to monitor one narrow family of compounds nor to follow the composition of biogas with respect to one given chemical element or compound, but rather is to screen as much as possible different compounds from different families, hence searching for the unknown. As biogas and biomethane can be produced from a wide variety of feedstocks (municipal and household wastes, manure, agricultural and food-processing residues, waste water treatment sludge...) [5,9–12], under many different conditions [5,11–20] and at different places [20], their composition, especially in trace elements, is highly variable [5,12] and the probability is high that unknown compounds are present. Finally, analytical standard gases are necessary to calibrate analytical instruments and validate the applicability of elaborated methods. Producing such standard gases is a delicate task since they have to contain targeted analytes in a concentration range close to that present in real gases (which may be unknown for certain compounds), and this composition must be stable in time [7,8]. A systemic analytical chain must therefore be carefully followed to come to reliable results [7,11]. Gas sampling is the first salient step in this chain, followed by analysis, generally in the lab [5,7,11,21–23]. Once targeted compounds are preconcentrated on a dedicated support, several analytical techniques are available, each with their advantages and disadvantages, to segregate, detect, speciate and quantify them.

In this chapter, the state-of-the-art gas sampling and preconcentration techniques for the determination of trace compounds in methane-like gas samples are reviewed. Inasmuch as biogas and biomethane sampling and analysis is a relatively recent endeavor not yet benefitting from standardized methods, natural gas sampling and (trace-compounds) analysis methods, being already well standardized (EN ISO 10715:2000 [24]; ISO 6974 [25]; ISO 6975 [26]; ISO 6978 [27,28]), are referred to in this review as suitable for biogas and biomethane in view of the similarity of the matrices (CH_4) and of some trace compounds of those three gases. Standardized methods for ambient air sampling and analysis (EN ISO 16017-1:2000 [29]; EPA Compendium of Methods for the Determination of Toxic Organic Compounds in Ambient Air [30,31]) are also pointed out as suitable for biogas and biomethane. Whereas the matrices of air and biogas or biomethane differ, common families of trace compounds are targeted both in air and biogas or biomethane (volatile organic compounds, siloxanes, volatile metal(loid) compounds...).

Therefore, efficient sampling techniques applied for those compounds in air are also expected to be suitable and efficient for biogas and biomethane.

Gas sampling is the first and most decisive step of the analytical chain towards trace compounds determination in biogas and biomethane inasmuch as any sampling method implies at least one element in the sampling line where through targeted analyte loss or sample contamination is possible (analyte or ambient air permeation through the container walls, leaks at valves, analyte condensation, sorption of analytes on sampling lines or on container's walls, chemical reactions between sampled compounds inside the container leading to analyte degradation or conversion...) [5,7,11,21–23]. Establishing the most suitable sampling container and procedure is hence intricate: the sampling device must be handleable on field, the composition of collected samples must be representative of that of the studied gas and must remain as unchanged as possible until effective analysis; the sample must be easily transportable to the lab; the recovery of targeted analytes from the sampling vessel must be maximal; and finally the whole sampling procedure must be economically affordable [5,11,23].

There are currently two gas sampling approaches: whole gas sampling and gas sampling with enrichment (preconcentration) of targeted analytes [5,32,33]. In the first one, a whole bulk gas volume is sampled in a dedicated container (gas bags, canisters or cylinders) without enrichment of the targeted trace analytes, with subsequent transport of the container to the lab. The next crucial step is an analyte enrichment step [7] aiming at isolating the targeted trace compounds from the sampled gas matrix in a small volume via trapping or preconcentration techniques. Choosing the proper preconcentration procedure is a complex task in view of the broad diversities in physico-chemical behaviors of targeted compounds. Whole gas sampling and subsequent transport to the lab not only implies potential contaminations and artifacts related to the sampling, transport, storage and sample preparation proceedings, but also implies a delayed preconcentration with associated risks of analyte loss or composition alteration due to chemical reactions inside the sampling container [5,11,21,22]. The second sampling approach involves sampling with direct enrichment (preconcentration, trapping) of targeted analytes on a dedicated support (solid adsorbent tubes, impregnated surfaces or fibers, liquid absorbent, cryogenic trapping). On the contrary to whole gas sampling, the gas matrix (e.g. CH₄, CO₂) is not sampled as it is not retained and passes through the preconcentration unit retaining solely the targeted analytes. To avoid disadvantages related to the use of whole gas sampling containers, the development of direct *in situ* preconcentration techniques for targeted analytes and of *in situ* direct analysis methods is being more and more considered and recommended [4,5,11,34,35].

In the next sections, techniques for biogas and biomethane sampling without and with enrichment are critically described. Section III.1.1 on solid adsorbent tubes is particularly extensively discussed as this sampling/preconcentration media will be used in the presented doctoral thesis work. In the discussions, 'semi volatile', 'volatile' and 'very volatile' organic compounds will be dealt with. According to the U.S. Environment Protection Agency (EPA), semi volatile compounds have boiling points ranging from 240-260°C to 380-400°C. Volatile compounds have boiling points ranging from 50-100°C to 240-260°C. Very volatile compounds have boiling points < 50-100°C.

II. GAS SAMPLING WITHOUT ENRICHMENT (WHOLE GAS SAMPLING)

Sampling without enrichment of targeted analytes involves whole gas sampling in gas bags, canisters or cylinders, without discrimination between sampled compounds [5,11,32]. Such sampling methods are attractive in view of the ease of sampling: the whole gas matrix is collected together with all contained compounds in their original concentration [23,36–38]. Additionally, gas moisture has little effect on sample integrity and stability [23,37,39,40], and a last benefit is the possibility of repeated analyses of a same sample by multiple withdrawals from the vessel [1,23,36]. Gas bags, cylinders and canisters do nevertheless only allow to sample a defined gas volume so that effective collected quantities of trace compounds may be insufficient to be reliably detected [22]. Whole gas sampling is therefore only to consider either if available analytical devices offer detection limits sufficiently low to detect analytes in the raw sample (direct sample analysis) or if the sample is subsequently preconcentrated in the lab [41]. However, as sample transport to the lab may take days to weeks, the delayed direct analysis or preconcentration of trace compounds from the gas matrix implies the risk of trace analyte loss during the storage period, owing to sorption on or permeation through the sample container's walls, to leaks in the container and to chemical reactions in the container inducing analyte degradation or conversion [5,11,21–23].

Also note that biogas or biomethane filled bags, cylinders and canisters are flammable and accordingly considered as dangerous goods with corresponding restrictive implications for transport to comply with the regulation in place [22].

In the following, the characteristics and use of gas bags, canister and cylinders for biogas and biomethane sampling with an eye on (H)VOC, Si- and S-compounds as well as volatile metal(loid) compound analysis, are discussed.

II.1. Gas sampling bags

Gas sampling bags (Fig.2.1 a) are gas-tight bags equipped with a valve fitting. Bag materials include polyvinyl fluoride (PVF, tradename: Tedlar), polyethyleneterephthalate (PET, tradename: Nalophan), polytetrafluoroethylene and fluorinated ethylene propylene copolymer (PTFE and FEP, tradename: Teflon), polyester aluminum (PEA), polyethyleneterephthalate-nylon-aluminum, polyvinylidene difluoride (PVDF, tradenames: Altef, Kynar, Supel Inert Film) [5,11,21,42–44]. Table 2.1 lists some useful features of sampling bags suitable for ppm to ppb-levels sampling, based on manufacturer's informations. Gas bags are relatively cheap and simple to use and do not require trained personnel [22,23,37,38,42]: a piping is plugged onto the bag valve hose to inflate the bag until a sufficient volume is sampled. Bags exist in volumes from 0.5 to 100 L and even 1000 L depending on the material and manufacturer, and some companies also offer custom-sized bags or polymer film rolls [45–47]. According to manufacturer's specifications, bags must not be filled to more than 80-90% of their volume during sampling, and the inflation pressure must not exceed ~0.14 bar above the atmospheric pressure [45]. Gas sampling bags are hence typically designed for sampling at atmospheric pressure, forbidding a high-pressure-based preconcentration of low-concentrated analytes [48]. Manufacturers

usually recommend to transport filled gas bags in rigid opaque containers to avoid bag perforation or damage, to transport and store them above 0°C to avoid sample condensation, to avoid air-shipping unless in a pressurized zone, to protect them from sunlight and to analyze the sample as soon as possible [45].

Each bag material may be specifically recommended for the sampling of given targeted compounds [5,11,42,49,50] inasmuch as the polymer bag material and impurities inherent to the polymer may be incompatible with the successful sampling of certain chemicals, and in view of potential reactions between sampled compounds and compound-specific permeation and adsorption effects through and on the bag film [11,37,42,49–55]. For instance, Tedlar bags are known to contain traces of dimethylacetamide and phenol while Altec bags do not, but Altec bags are not recommended for sampling of ketones, esters, acetates, H₂S and permanent gases [45,56,57]. The suitability of PEA versus Tedlar bags for the short-term storage of VOC (benzene, toluene, *p*-xylene, styrene, methyl ethyl ketone, methyl isobutyl ketone, butyl acetate, and isobutyl alcohol) in a N₂ matrix has been investigated by Kim et al. [50]. After 3 days of storage in both bag types, their results showed that recoveries of compounds from PEA bags were significantly higher than recoveries from Tedlar bags. Hence, for a N₂ matrix, PEA bags offered more stability than Tedlar bags. Kim [58] also compared the stability of reduced Sulphur compounds (H₂S, CH₃SH (methanethiol), (CH₃)₂S (dimethylsulfide, DMS), (CH₃)₂S₂ (dimethyldisulfide, DMDS)) in PEA and Tedlar bags. Mean recovery results for all compounds from Tedlar bags (87%) were higher than from PEA bags (77%). PEA bags were also studied by Ahn et al. [54] to examine sorption losses of VOC as a function of storage time. Vigilantly consider however that it is not possible to assess a universal suitability of a given bag material for a given (family of) compound(s). Jo et al. [49] compared the storability of several Sulphur compounds in a N₂ matrix in PEA and Tedlar bags. They concluded that the most decisive factor for the storage stability of S-compounds in both bags was the initial concentration and not the bag material. Other factors influencing the stability of S-compounds were the nature and molecular weight of the compound, the storage time and the bag material. Brown et al. [42] also noticed a concentration-dependent adsorption loss pattern for H₂S in CH₄ in FlexFoil and FlexFilm bags. The relative H₂S-loss of their 4.99 μmol H₂S/mol CH₄ mixture was greater than for the 9.95 μmol mol⁻¹ mixture. As both tested bags had similar internal surface areas, this is the consequence of a fixed number of potential sorption sites per m² bag film, which have to be occupied by a fixed amount of (H₂S) molecules to reach saturation [42]. A lower concentrated mixture will henceforth lose relatively more molecules than a higher concentrated mixture before no sorption losses longer occur. Next, Nalophan bags are especially used in odor sampling studies because of their neutral odor background contaminations [43,51,52], but have also been used for biogas sampling and trace compound analysis by several research groups [59–63]. Papurello et al. [63] preferred Nalophan bags to Tedlar bags for sampling of trace compounds such as VOCs, thiols and siloxanes, as it was shown Nalophan bags gave cleaner backgrounds than Tedlar bags that released degradation compounds interfering with the detection of the low amounts targeted compounds [43]. However, the permeability of Nalophan films may be high for some compounds, in particular S-species (H₂S, CH₃SH, CS₂) due to their small molecule dimensions [51,52,55], hence those bags may be unsuitable for sample storage when such compounds are targeted. Teflon bags were used by Badjagbo et al. [64] for biogas sampling. Finally, Mochalski

et al. [55] compared the suitability of Nalophan, transparent Tedlar, black layered Tedlar, Teflon and FlexFoil bags for the sampling and storage of volatile Sulphur compounds (VSC) (H_2S , CH_3SH , $\text{CH}_3\text{-CH}_2\text{-SH}$ (ethanethiol), COS (carbonyl sulfide), $(\text{CH}_3)_2\text{S}$ and CS_2 (carbon disulfide)) in a N_2 (air) matrix. They firstly measured the background emissions of potential contaminants from new, unused bags and found Nalophan, Teflon and Flexfoil did not emit contaminants which could interfere with their target S-analytes, while Tedlar bags did (emission of COS and CS_2). Subsequently, they studied the stability of VSC in each of those bags. Considerable (permeation) losses of VSC were observed within 6 h of storage in Teflon and Nalophan bags, hence they were not recommended for VSC sampling and storage. Transparent and black Tedlar bags gave good VSC stabilities during the first 6h of storage with recoveries > 90%. After 24 h storage, H_2S and COS losses were booked and longer storage gave rise to losses of all VSC. They did not record any significant influence of daylight on the stability of the VSC in transparent Tedlar bags. In Flexfoil bags, H_2S was the only species decreasing during the first 6 h storage, and after 24 h, the concentration of other VSC also decreased. Yet bag reuse is usually not recommended [45,47,53], Mochalski et al. [55] tested the efficiency of several bag cleaning procedures with an eye on bag reuse and concluded that bags could be reused if the following cleaning steps were executed : N_2 flush, heating at 45°C for 6 h, N_2 flush, heating at 45°C for 6 h, N_2 flush. In spite of the above, Tedlar bags are the most widely used bags [5,37,50]. Tedlar bags are generally appropriate for sampling and short-term storage of VSC and are used in industrial routine analyses for this purpose [42,58,65,66], but they have also often successfully been used for biogas and biomethane sampling [3,11,21,22,37,38,67–71]. Black-layered Tedlar bags have also been developed to sample photosensitive compounds. Walls of such bags consist of an inner polyvinyl fluoride layer and an outer light-blocking layer of carbon black. The inner PVF layer theoretically prevents sampled compounds to adsorb into the carbon black material. Nonetheless, permeation of analytes through the first PVF layer can lead to adsorptive losses into the carbon black layer [65]. Sulyok et al. [65] compared standard with black-layered Tedlar bags for the storage of VSC and found better VSC recoveries in the standard Tedlar bags even after 300 h storage while significant losses were observed in the black-layered Tedlar bags after only 1 h. The authors proposed these losses were due to permeation of VSC through the inner Tedlar layer and adsorption in the outer carbon black layer.

Advantageous to gas sampling bags is the ability to, once in the lab, withdraw several samples from the bag for repetitive analyses of the same gas [5,23,50] as long as the sample composition is stable. Indeed, as already partly mentioned, a disadvantage of gas bag sampling is the poor storability of analytes in the bags when effective analysis is delayed due to transport and storage of bags from the field to the lab [5,50]. Analyte loss in gas bags has been proved to be especially caused by adsorption effects on bag walls [11,21,37,49,50,53,72] and on valve fitting materials [37]. Additionally, permeation through the walls [11,21,37,49–52,55], leaks through the septum of the valve [21,50] especially once it has been pierced with a needle or syringe for analysis [65], photochemical degradation (photolysis) when bags are not protected from sunlight [3,23,39,49,67,73], and chemical conversion reactions between sampled compounds [23] also contribute to analyte loss during storage. Gas permeation and diffusivity through polymeric bag films are ruled by the polymer type, its crystalline structure, orientation, molecular cohesion, porosity, free volume, Hydrogen bonding capacity and polarity [52], by the film thickness and

bag dimensions (surface), by the molecular size, volatility and molecular diffusion coefficient of the diffusant in the film and by the concentration gradient of the diffusants across the inner and outer bag sides [51]. Additionally, the relative humidity and temperature of the sample inside the bag and of the atmosphere around the bag also impact the permeation rates [52]. Ambient air from the bag surroundings as well as the bulk gas matrix of the sample inside the bag can also permeate respectively in and out of the bag, affecting the concentrations of stored analytes [37].

The stability of sampled species in gas bags is also influenced by the initial sampled concentration as was proved by Jo et al. [49] for reactive Sulphur compounds in a N₂ matrix in PEA and Tedlar bags: compounds sampled in high concentrations (1 ppm and 10 ppm) disappeared faster than the same compounds sampled in lower concentrations (1, 10 and 100 ppb), due to adsorption and diffusion effects being enhanced for compounds present in high concentration [49]. However, the opposite trend is also often observed: adsorption losses are relatively higher when low analyte concentrations are stored in bags since sorption on inner bag surfaces will occur until occupation of all sorption sites [11]. If the analyte concentration is lower than or equal to the corresponding sorption site capacity, potentially all analyte molecules can be lost to adsorption. Another concentration effect was observed by Arrhenius et al. [11] in a study on the stability of HVOC (1,1,2-trichlorotrifluoroethane, dichloromethane, tetrachloroethylene and m-dichlorobenzene) in Altec bags. All compounds showed a concentration decrease in time but after 4 days, a slight concentration increase was recorded for 1,1,2-trichlorotrifluoroethane and tetrachloroethylene. Authors suggested this concentration increase was due to outgassing of those compounds from bag walls where they initially adsorbed during the first storage days, owing to the gas volume drop in the bag as a result of daily gas withdrawal from the bag for analysis [11]. Why only two out of the four tested HVOC displayed this pattern was not clarified. Next to concentration effects, adsorption effects on bag walls and corresponding analyte losses are also promoted for high molecular weight, less volatile analytes [5,11]. Kim et al. [50] tested the stability of VOCs in PEA and Tedlar bags: lighter compounds such as benzene and toluene were relatively stable after 3 days in both bag types (>86% recovery) while the heavier *p*-xylene and styrene were less stable after 3 days in both bag types (<81% recovery). Similarly, Mariné et al. [21] found that high-molecular weight alkanes in biogas were lost by adsorption on bag walls immediately after sampling in Tedlar bags. Arnold et al. [69] found the concentration of the relatively heavy siloxane D5 in a real biogas sample was only 65% of the initial concentration after 1 day storage in a Tedlar bag, while the concentrations of lighter siloxanes (D4 and L4) were respectively 87 and 88% of the initial concentrations after 1 day in the Tedlar bag. Ajhar et al. [37] also found D5 siloxane, the heaviest siloxanes they studied, was adsorbing the readiliest in Tedlar bags. Arrhenius et al. [11] performed 12-days stability tests of L2, L3, D4 and D5 siloxanes in CH₄ in Altec and Tedlar bags. Light L2 and L3 siloxanes were stable over the whole storage period in both bag types while the response of heavier D4 and D5 markedly decreased during the first storage days in both bags. To limit adsorption losses in bags, on bag valves and in sampling connection tubing, Ajhar et al. [37] suggest to flush the entire bag sampling set-up for 5 min with the gas to sample prior to effective sampling so as to already occupy potential sorption sites. These authors also found a high relative humidity (90% RH) in a standard siloxane mixture in a synthetic biogas matrix stored at 37°C in Tedlar bag lead to less sorption losses of siloxanes as water molecules tended to first

sorb onto the bag surface sorption sites. However, under the same 90% RH condition but at lower temperature (20°C), no effect was observed on the siloxane recoveries from the bag [37]. Tedlar bags may hence be favorable sampling vessels for humid biogases, yet bags should be stored and analyzed at relative high temperatures (50°C was used by Ajhar et al. [37]).

The stability of volatile metal(loid) compounds in Tedlar bags has also been studied. Haas and Feldmann [23] generated standard gases of trace amounts (0.3 to 18 ng L⁻¹) various volatile arsenic, tin and antimony species in moisturized air in Tedlar bags: AsH₃, MeAsH₂, Me₂AsH, Me₃As, SnH₄, MeSnH₃, Me₂SnH₂, Me₃SnH, Me₄Sn, BuSnH₃, SbH₃, MeSbH₂, Me₂SbH, Me₃Sb (Me = methyl group; Bu = butyl group). The authors also sampled sewage sludge digester gas in Tedlar bags. This real gas was known to only contain Me₃Sb, Me₃Bi and Me₂Te. All bags were stored in the dark during the entire stability assessments. Stability of volatile metal(loid)s in standard Tedlar bags was investigated under different conditions: storage of the bags at 20°C during 8 weeks and storage at 50°C during 5 weeks. Tedlar bags containing real gas were stored at 20°C during 48 h. Concentrations of targeted analytes were periodically monitored during these storage periods via cryotrapping-GC-ICP-MS (gas chromatography – inductively coupled plasma – mass spectrometry). Surprisingly high recoveries were obtained for the standard gas: after 8 h both under 20 and 50°C storage, >95% of all metal(loid) analytes were recovered. After 24 h under 20 and 50°C, all analytes were still recovered at 81-99% except Me₃Sb and Me₃As showing considerable losses especially at the higher temperature [23]. In the real gas after 24 h storage, losses of Me₃Bi and Me₂Te amounted to ~10% while losses of Me₃Sb amounted to 44%. The long-term (5-8 weeks) stability study of the standard gases revealed that the central metal atom of each analyte was strongly determining its stability in the bag. All stibines were less stable than As and Sn counterpart species, the most stable species being AsH₃ (75% recovery after 8 weeks at 20°C) and the least stable being Me₃Sb (3% recovery after 4 days at 50°C) [23]. Determining the loss mechanisms of volatile metal(loid) compounds in Tedlar bags is intricate since these compounds are thermodynamically unstable and susceptible to several loss or degradation pathways such as diffusion, oxidation, hydrolysis, photodecomposition, adsorption, absorption, and heterogeneous surface-catalyzed breakdown [23]. The results of Haas and Feldmann nevertheless demonstrated adsorption to bag walls was not the main underlying mechanism for the observed losses in the standard bags (air matrix) [23]. Instead, chemical reactions like oxidative breakdown in the aerobic atmosphere of the standards, oxidation and demethylation were probably responsible for the immobilization and instability of the volatile metal(loid) compounds in the Tedlar bags. Methylated compounds are more prone to degradation reactions as the cleavage of carbon-metal bonds is energetically more favorable than the cleavage of hydrogen-metal bonds in fully hydrogenated metal(loid)s [23]. In accordance with these thermodynamic considerations, all compounds showed poorer stabilities at higher temperatures (50°C), particularly in the long-term storage experiments. Especially fully methylated As and Sb species were less stable at this temperature. The authors concluded Tedlar bags are convenient for sampling of volatile metal(loid) compounds in air if the samples are analyzed within 24 h and transported and stored at low temperatures (20°C) [23]. Accordingly, Feldmann et al. [2] successfully used Tedlar bags to sample biogases with an eye on volatile Sb, Sn and Bi compounds speciation. Another study by Arndt et al. [74] appraised the storage stability of volatile arsenicals in Tedlar bags in the presence of (reactive) gases such as O₂, CO₂,

SO₂ and H₂S. Standard gas mix containing 2 ng·L⁻¹ of each of the following compounds: AsH₃, MeAsH₂, Me₂AsH, and Me₃As, were prepared in Tedlar bags in several synthetic gas matrices: N₂ (reference), 3800 ppm_v CO₂ in N₂, 20% O₂ in N₂ (200 000 ppm_v), 100 ppm_v SO₂ in N₂, and 100 ppm_v H₂S in N₂. Tedlar bags were stored in the dark at 5°C for 21 days. Tedlar bags' arsenic contents were periodically analyzed by cryotrapping and cryofocusing 50 mL of the 2 ng·L⁻¹ gases followed by GC-MS for the speciation or GC-AFS for total arsenic determination. Analysis of the standard As-mix in the reference N₂ matrix revealed no sorption losses nor losses by precipitation of the As-species occurred on the Tedlar bag walls [74] hence agreeing with the results of Haas and Feldmann [23]. Arndt et al. obtained recoveries of AsH₃, MeAsH₂, Me₂AsH from the bags of respectively 106 ± 3%, 103 ± 1%, and 101 ± 4% after 19 days. Me₃As had a mean recovery of 85 ± 3%. This compound probably partly converted into less methylated arsines during the storage period [74] simultaneously explaining its loss and the recoveries >100% for AsH₃, MeAsH₂ and Me₂AsH. Stability results of standard As-species in 3800 ppm_v CO₂ in N₂ and in 20% O₂ in N₂ (synthetic air) after 21 days were very similar to those of As-species in the N₂ reference case since CO₂ is not a reactive gas and O₂ apparently has no effect on the stability of the four target As-species. In the 20% O₂ in N₂ (synthetic air) matrix, Arndt et al. [74] obtained higher recoveries than Haas and Feldmann [23] who experimented the stability of the same As-species in air in Tedlar bags. The higher recoveries of Arndt et al. are due to the lower storage temperature (5°C) than that used by Haas and Feldmann (20 or 50°C). SO₂ however had a strongly detrimental effect on the stability of the As-species [74]. In the SO₂ doped matrix, the recoveries of AsH₃, MeAsH₂, Me₂AsH, Me₃As dropped to respectively 72, 72, 41 and 11% after 21 days. It is unclear whether SO₂ induces those losses by bag wall sorption or by precipitation of arsines into As₂O₃ or As-S compounds. The effect of H₂S was especially pronounced for Me₃As which was only recovered at 67% after 17 days in the H₂S doped standard matrix. Me₂AsH, MeAsH₂ and AsH₃ were recovered at respectively 89, 105 and 123% after 17 days, suggesting H₂S induces the conversion of methylated species to non-methylated ones [74]. Without regard to the matrix of the standard As-mix, the results of Arndt et al. [74] agree with those of Haas and Feldmann [23] concerning the lower stability of increasingly methylated arsines stored in Tedlar bags due to either precipitation or conversion to more stable non-methylated species.

Besides bag walls, the valve fitting material of sampling bags may also influence the stability of sampled compounds, as was demonstrated by Ajhar et al. [37] in a stability study of landfill biogas siloxanes in Tedlar bags equipped either with a polypropylene fitting with integrated PTFE-septum or a dual port stainless-steel fitting with o-ring. It turned out that polypropylene fittings led to much better siloxanes stabilities than stainless-steel ones. Nevertheless, Mochalski et al. [55] compared the stability of VSC in black layered Tedlar bags equipped either with stainless-steel or PTFE valve fittings and found comparable stability results: after 3 storage days, the concentration difference between the two valve materials was < 5%. They concluded losses of VSC due to contact with stainless-steel were insignificant and could be neglected.

Concerning the stability of sampled analytes in function of storage time, the longer the storage period, the more severe analyte losses will be due to the previously mentioned effects [21,49,53–55]. Sorption losses are usually the strongest during the first storage days until sorption-sites on inner bag surfaces reach saturation [11,21,22,49]. However, the storage stability in a given bag type differs for each compound, and the stability of a given compound may differ when stored in

different bag types [50]. Enrico et al. [75] for example determined Hg⁰-doped Argon gas was stable in Tedlar bags for at least 96 h, showing Tedlar films may be inert to Hg.

Finally, re-using gas sampling bags is not recommended [21,45,47,76]. McGarvey et al. [53] investigated the reusability of Tedlar bags used for sampling of VOCs in air. After storage stability tests, bags were cleaned via N₂-flushing and gentle heating in an attempt to desorb VOC's that got adsorbed on the bag walls during the storage phase. These cleaning operations were not sufficient to remove all compounds, in particular styrene, ethylbenzene and methanol were not quantitatively recovered. They concluded that re-using Tedlar bags previously used for long-term storage of VOCs was leading to substantial contamination of subsequent samples via off-gassing of compounds formerly adsorbed on bag walls. Re-using Tedlar bags would only be acceptable if the content of the bag was immediately analyzed after sampling and the bag immediately cleaned by N₂-flushing and heating.

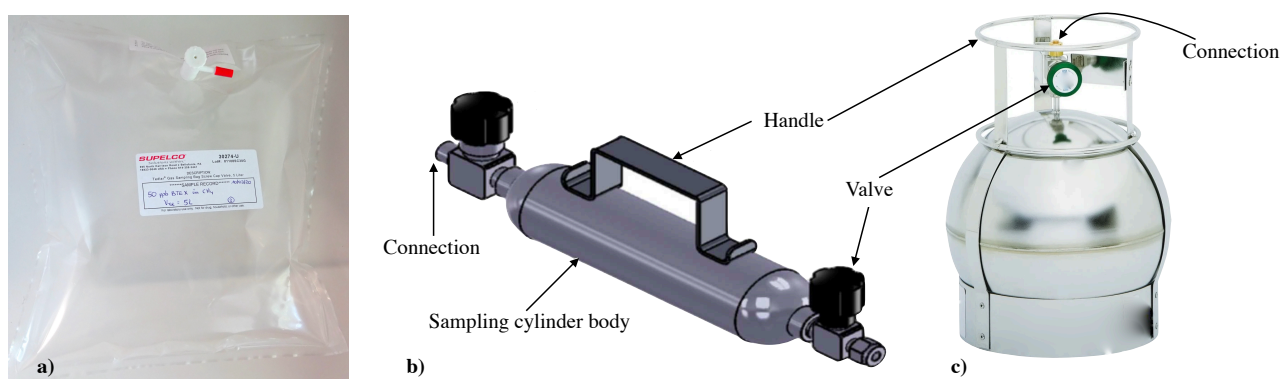


Figure 2.1: Whole gas sampling vessels: a) Polymer bag. b) Cylinder. c) Canister.

Table 2.1: Physico-chemical features of some common gas sampling bags according to manufacturer's informations. Bags with stainless-steel valves usually have a higher maximal working temperature due to the higher thermal resistance of the o-ring in those valves compared to the polypropylene valves with integrated septum.

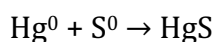
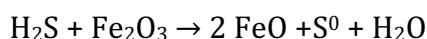
Commercial bag name	Tedlar	Altef	Kynar	Nalophan	Teflon	Teflon
Film composition	polyvinyl fluoride	polyvinylidene difluoride	polyvinylidene difluoride	polyethylene-terephthalate	fluorinated ethylene propylene (FEP)	polytetrafluoroethylene (PTFE)
Available valve materials	PP; SS	PP	PP; SS; PTFE	PP; PTFE; PTFE-coated nylon	PP; PTFE	PP; PTFE, PTFE-coated nylon
Pressure (P) and temperature (T) working range	Max operating T: PP valve 82 °C; SS valve 202 °C	Max operating T: 82 °C	Max operating T: PP valve 93.3°C ; SS and PTFE valves 107.2°C	Not found	PTFE valve working T range: -60°C to +150°C	Not found
	Max filling P relative to atmospheric P: ~ 0.14 bar or ≤80% filled	Max filling P relative to atmospheric P: ~ 0.14 bar or ≤80% filled			Max filling P relative to atmospheric P: 0.06 bar or ≤90% filled	
Available bag volumes	0.5 – 100 L	0.5 – 100 L	0.5 - 1000 L	1 – 60 L and film rolls	0.5 – 100 L	Not found
Measured permeability to permanent gases at 1 bar filling	O₂: 50 cc/m ² /day H₂O vapor: 9–57 g/m ² /day CO₂: 172 cc/m ² /day	O₂: 58 cc/m ² /day H₂O vapor: 12-15 g/m ² /day CO₂ : 172 cc/m ² /day	Not found	Not found	O₂ : 2400cc/m ² /day H₂O vapor: 1.3g/m ² /day	Not found
Remarks	Background levels of dimethyl-acetamide and phenol	Lower VOC and Sulfur background contamination than Tedlar (no dimethyl-acetamide nor phenol background) Not recommended for ketones, esters, acetates, hydrogen sulfide, permanent gases	Low VOC and Sulfur background Resistant to corrosion Good stability for VOCs, CO, CO ₂ , CH ₄ Good 24-h storage stability for some S-compounds	Especially used and recommended for odors sampling for gases with moderate H ₂ S and VOC contents being analyzed within less than 6h after sampling Not recommended for samples being processed more than 6 h after sampling, nor for samples with high humidity, high H ₂ S, high VOC because of poor stability of those compounds due to high permeability rates and adsorption effects	Suitable for corrosive and reactive compounds Suitable for VOCs samples Low adsorbability of compounds on bag walls	Suitable for VOC and S-compounds including H ₂ S Excellent stability for CO,CO ₂ , CH ₄ , SF ₆ Resistant to contamination, low adsorbability of compounds on bag walls, hence possible cleaning and reuseability Not recommended for samples processed more than 30 h after sampling
References	[45]	[45]	[47]	[43,46,47,51,52,73]	[47]	[46]

PP: polypropylene. SS: stainless-steel. PTFE: polytetrafluoroethylene.

II.2. Gas cylinders

Gas sampling cylinders (Fig.2.1 b) allow to collect gas under high pressure [5] (up to 5000 psi = 344 bar) [77–79] and exist both in aluminum or stainless-steel [42,80,81] in volumes from 40 to 3785 cm³ [77–79]. Stainless-steel cylinders are generally used and have long been used for the sampling of natural gas [4,5,34,82] and natural gas fractions (e.g. condensate [4]). As biogas and biomethane are predominantly produced at near-atmospheric pressure, cylinders have seldomly been relevant for biogas or biomethane sampling [5]. However, cylinder-sampling of compressed grid-quality biomethane at the injection point in the gas grid is relevant to subsequently proceed to biomethane quality verifications.

A well-known concern with cylinders is the adsorption (physi- or chemisorption) of compounds on the inner cylinder walls and hence their loss [11,34,42,68,75,79,81]. The surface-iron atoms of stainless-steel inner walls can act as active sites for sorption and catalysis phenomena. Reactive VSC (e.g. H₂S, COS, CS₂, CH₃S, (CH₃)₂S, (CH₃)₂S₂) [42,65,75,79] as well as volatile arsenicals [34] sampled in cylinders have especially been found to be lost by adsorption on cylinder walls. Larsson et al. [83] found low recoveries of gaseous mercury (Hg⁰) when collected over stainless-steel surfaces. In natural gas containing H₂S, they propose stainless-steel may act as a sink for Hg⁰ through the following reactions involving first a reaction of H₂S with stainless-steel iron, and then a reaction between the resulting gaseous Sulphur and the gaseous mercury, causing the formation of solid mercuric sulfide (HgS):



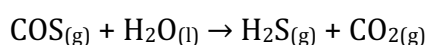
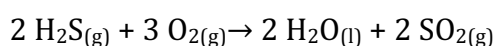
Also, as the majority of trace compounds in biogas and biomethane are reactive species, they are particularly predisposed to sorption on inner surfaces of sampling cylinders (and of any other sampling vessels) [11]. Surface treatment and passivation technologies have therefore gradually been developed to render the inner cylinder walls more inert to targeted analytes. An example of treatment technology is the polishing of the walls to reduce the internal surface area and as such the number of sorption sites [42]. Surface passivation technologies involve coating or chemically treating the inner cylinder walls [11,42] to occupy and obstruct active sorption areas on the walls (creation of a smooth surface) and as such minimize adsorption of targeted compounds [11]. Several commercial passivation processes exist such as Spectraseal (BOC) [84], Experis (Air Products) [85], Aculife (Scott Speciality Gases) [86], AlphaTec (Air Liquide), SilcoNert (SilcoTek® Corporation) [87] and Silonite (Entech Instruments Inc.) [88], each being recommended for the safe sampling of specific targeted compounds [11,34,42]. Other gas sampling cylinder suppliers propose PTFE coatings offering smooth non-sticking surfaces [77]. The SilcoTek Corporation is a leader in such high-performance coatings that they apply by chemical vapor deposition (layer thickness ~nm) onto the cylinders. Currently, their SilcoNert®1000 (formerly known as SilcoSteel®) and SilcoNert®2000 (formerly known as Siltek® and Sulfinert™), made of amorphous silicon (plus functionalization for SilcoNert®2000), offer among the most inert coatings. SilcoNert®2000 is especially advised when dealing with trace levels (ppb) of active species like H₂S, mercaptans, NH₃, NO_x, SO_x and mercury [79,87]. This coating prevents adsorption and memory effects, keeping the analytes stable in the vessel.

The maximal working temperature for SilcoNert®2000 is 450°C [87]. SilcoNert®2000 has also been found suitable for stable sampling and storage of other compounds with reactive functional groups such as siloxanes, CS₂, (CH₃)₂S, (CH₃)₂S₂ and tetrahydrothiophene [11,89]. However, during short term stability tests, Arrhenius et al. [11] found BTEX sampled in Sulfinert (SilcoNert®2000) coated gas cylinders were not stable: the concentrations of all BTEX decreased, especially during the first day. After one storage day, the BTEX levels had decreased by 15% (benzene), 25% (toluene), 40% (ethylbenzene) and 45% (*o*-xylene) as compared to the initial concentrations. They concluded Sulfinert (SilcoNert®2000) coating is not suitable for gas sampling and storage when BTEX are targeted. Note the order of decrease percentages of BTEX follows the molecular weights of BTEX, heavier compounds being more prone to sorption effects than lighter ones. Next, the Silonite coating has been found suitable for the same compounds as SilcoNert®2000, i.e. compounds with reactive functional groups such as oxygen, nitrogen, siloxanes, H₂S, CS₂, CH₃SH, (CH₃)₂S, (CH₃)₂S₂ and tetrahydrothiophene, but this coating is not suitable for BTEX [11,89]. A more convenient coating for storage of BTEX would be the Experis passivation [11]. Compounds with polar functional groups are however unstable in Experis-passivated cylinders [11].

Some examples of successful use of passivated cylinders are now given. Sulyok et al. [65] investigated the stability of several VSC (CH₃SH, CH₃CH₂SH, DMS, ethylmethylsulfide, diethylsulfide, 2-propylmercaptan, 1-propylmercaptan, 2-butylmercaptan, 1-butylmercaptan at 1 mg·m⁻³ each in nitrogen) in SilcoSteel® cylinders. Recoveries measured after a few hours were significantly >100% for all compounds except methanethiol (~100%), and after 200 h, all compounds were still recovered at ~100% or more except 1-butylmercaptan recovered at <95 %. As the authors flushed the cylinders with their multicomponent standard gas prior to effectively filling the cylinder for storage assessments, they propose the overestimation of initial recoveries is due to enrichment of analytes from the standard gas on cylinder and system walls during the pre-flush operation, and to subsequent outgassing of these analytes due to pressure drop in the cylinder during the analysis period (sample withdrawal) [65]. Nonetheless, they concluded SilcoSteel® cylinders were appropriate for sampling VSC.

In a study on the determination of volatile arsenic species, Krupp et al. [4,34] sampled pressurized natural gas in stainless-steel SilcoSteel® or Sulfinert™ passivated cylinders, as the use of non-passivated cylinders had been found to induce losses of arsenic species or speciation modifications. Cryotrapping-GC-ICP-MS allowed them to identify trimethylarsine (TMA) with a detection limit of 200 pg As as TMA/L gas for an injection volume of 50 mL [4].

Suitably passivated cylinders are however not a stability guarantee for all compounds, depending on the gas sampled, as chemical conversion or degradation reactions can occur in the cylinder between unstable or reactive sampled compounds. For instance, in the case biogas would be sampled in a cylinder suitably passivated against Sulphur compounds, those latter could still react with the water and oxygen present in the biogas, for instance through those equations [42]:



Furthermore, in view of the diversity of targeted trace components in biogas and biomethane and of the diversity in their boiling points, polarities, water solubilities, and reactivities [5], determining one optimal cylinder passivation treatment allowing to reliably sample them, is extremely challenging [11]. Instead, sampling biogas or biomethane in cylinders should be carried out using several cylinders with different passivation treatments to obtain a sufficient storage stability level for the different targeted analyte families [11]. Another example of chemical reactions impacting the stability of samples in cylinders is given by Enrico et al. [75]. The authors found an oxidized Hg species was formed during storage of Hg⁰-doped Argon gas in silicon- and PTFE-passivated cylinders having already been used in the past for natural gas sampling. The underlying reaction mechanism they propose is as follows: reduced Sulphur compounds from previous natural gas samples (H₂S, natural thiophenes, added tetrahydrothiophene...) remain adsorbed onto the cylinder walls despite the passivation, and act as suitable sorption sites for subsequently added gaseous Hg⁰. This physically adsorbed Hg⁰ is then oxidized and undergoes further complexation with the reduced Sulphur compounds on the cylinder walls. They [75] as such proved silicon- and PTFE-passivated cylinders presumably inert towards Hg, are actually not inert and do not allow reliable sampling and storage of real gases when targeting Hg-species. Additionally, Enrico et al. [75] demonstrated outgassing (desorption) of previously adsorbed Hg-species from used cylinders could falsify analytical speciation and quantification results of future samplings.

The relative extent of analytes losses due to adsorption effects on (passivated) cylinders has furthermore been proved to be linked to the initial sample concentration. After a given time period, the recovery percentages of compounds initially present in low concentrations in the cylinder, or sampled at low pressures, are lower than the recovery percentages of the same compounds initially present in higher concentrations or sampled initially at higher pressures [11,42]. This effect seems to be due to the presence of a fixed number of active sorption sites on the cylinder walls, and to a fixed number of a given molecular species needed to saturate all those sites by adsorbing on it [11]. Losses of a given species occur by adsorption on each of those individual sites until all sites are saturated. Therefore, when low initial concentrations are sampled, relatively high losses are observed since the proportion of analytes adsorbing on the sorption sites until saturation may be great compared to the total analyte quantity present. According to this simplified model, losses can even be total if the initial concentration is lower than or equal to the total sorption site capacity. Analyte losses decrease as their initial concentrations exceed the sorption site capacity, since larger and larger proportions of analytes then remain unadsorbed. Following this theory, Barone et al. [90] found an 11 ppb_v mixture of H₂S and CH₃SH was stable for a longer period (14 days) in a Sulfinert™ cylinder than the same mixture at 1.5 ppb_v (6 days). Arrhenius et al. [11] also found much better stabilities for siloxanes and Sulphur-compounds when sampled and stored at higher pressures (> 6 MPa) in conveniently passivated cylinders than at lower pressures (0.8 MPa). In case of biogas and biomethane cylinder sampling, they accordingly recommend to sample at > 5-6 MPa to ensure reliable storage. Sampling at lower pressures and especially < 1MPa would lead to an underestimation of the concentrations of targeted compounds upon analysis, due to the discussed concentration-dependent adsorption effect. Further, such concentration-dependent sorption losses are strictly species-specific, i.e. ruled by the species-sorption sites affinity, and

also impacted by the presence of other species in the sample. For silicon- and PTFE passivated cylinders, Enrico et al. [75] found the sorption losses of mercury in natural gas or Argon test gas increased if the cylinder had previously been used for natural gas sampling. They argue the reduced Sulphur compounds present in natural gas (H_2S , thiophenes, added tetrahydrothiophene) would first adsorb onto the cylinder surface to further create suitable sorption sites for gaseous Hg^0 , meaning Hg^0 does not sorb directly to the cylinder surface but is lost as a consequence of the presence of Sulphur compounds. As the inertness of passivated cylinders towards S-compounds is not perfect, even <1% Sulphur adsorption on the inner walls can suffice to deplete sampled gaseous Hg-concentration as a result of the above mentioned mechanisms [75].

An improvement towards undesired sorption effects is to condition the cylinders prior to sample collection to avoid both underestimation of compounds (due to adsorption) and overestimation of other compounds (due to outgassing of previously adsorbed compounds) [11]. Heating the cylinder (within the material and passivation coating working temperature range) and flushing with a pure N_2 -stream will greatly contribute to clean the cylinder walls by triggering the desorption of previously sorbed compounds. It is additionally advised to flush the cylinder with the gas to be sampled just before sample collection [65], so as to already occupy the potential sorption sites on the cylinder walls and hence to avoid analyte losses in the effective sample. This can nevertheless lead to over-estimation of analyte recoveries inasmuch as the compounds adsorbed during this pre-operation, can in turn desorb and outgas from the walls upon pressure drop in the cylinder during sample withdrawal for analysis [65].

II.3. Canisters

Canisters (Fig.2.1 c) are stainless-steel whole gas sampling containers with specifically passivated internal surfaces, commercially available in volume from 0.4 to 15 L [5,36,45,91] or up to 100 L [6]. Canisters do not allow pressurized gas sampling. Small canisters are rather used for concentrated gas samples, larger ones for lower concentrated samples [91]. Canister sampling has especially been used for air sampling and monitoring [23,36,39,40,76,92,93] since scientists first started investigating freons and other VOC in air responsible for ozone depletion in the upper atmosphere [94]. In the 1980's, the first US EPA Compendium of methods for the determination of VOC in ambient air [30] was introduced, preconizing the use of SUMMA® passivated canisters to reliably measure a broad set of VOC [95]. Indeed, as for cylinders, the surface-iron atoms of stainless-steel inner walls act as active sites for sorption and catalysis phenomena [94]. Polishing and passivation of the inner surfaces has hence been found necessary to avoid analyte loss by sorption, analyte conversion due to reactions catalyzed by iron sites inside the canister, and corrosion of the steel by corrosive or acidic sampled compounds like moisture, CO_2 , ozone, NO_x , O_2 and other oxidizing compounds in air. The first canister passivation treatment was SUMMA® (also TO-Can®) [91,94]: stainless-steel is electropolished and coated with a 500-1000 Å thick Nickel Chromium oxide (NiCrOx) layer in a liquid deposition bath. This coating aims particularly at covering iron sites on stainless-steel to prevent them from catalyzing reactions with sampled compounds such as VOC and halogenated VOC (HVOC) and to

avoid steel corrosion by reactions between surface iron atoms and corrosive sampled compounds [94]. The NiCrOx metal oxide passivation layer itself can however also act as catalyzer or adsorb polar and aromatic VOC as well as reactive Sulphur and amine compounds, which are not stable in SUMMA canisters unless the sampled gas contains enough water vapor to saturate the sorption sites on the NiCrOx layer [96]. SUMMA or TO-Can are general-purpose canisters recommended in air sampling and VOC-analysis methods such as US EPA methods TO-14A [97] and TO-15 [98]. A more recent canister passivation treatment is Silonite™ (Entech Instruments): a chemical vapor deposited silica layer offering even more inert surfaces than the SUMMA process and consequently enabling to reliably sample, store and recover a broader range of reactive analytes [94,96]. A canister passivation similar to Silonite is Siltek® (SilcoCan® canister, by Restek Corporation): an inert fused silica layer is chemically bound to the inner stainless-steel walls. The excellent inertness of this Siltek coating, compared to SUMMA or TO-Can, enables to sample, store and reliably recover low concentration levels (ppb) of compounds usually reactive with metal surfaces, such as polar-, halogenated- and Sulphur-compounds [39,91].

Two sampling approaches are possible with canisters: either active or passive sampling [91]. In both cases, prior to sampling, the canister is vacuumed to 10-50 mTorr ($1.3 \cdot 10^{-5}$ to $6.6 \cdot 10^{-5}$ bar) and equipped with a pressure gauge, a flow restricting device or a mass flow meter [5,91,95]. Canisters can hold < 10 mTor ($1.3 \cdot 10^{-5}$ bar) vacuum and can maximally be filled to 40 psig (2.75 bar) [91]. In active sampling, the gas sample is pumped into the canister with a pumping device, enabling to slightly sur-pressurize the sample (up to ~ 2 bar) and to double the sampled volume [36,91]. Passive sampling requires no pump: the pressure gradient between the vacuumed canister and the gas to sample causes the sample to flow into the canister. In passive 'grab' sampling, the gas is collected at an uncontrolled rate over 10 – 30 s until pressure equilibrium is reached between the canister and the atmosphere of the gas. This easy sampling method, typically used for qualitative measurements when unknown analytes are sampled, has the advantage not requiring any additional equipment such as flowmeters. Besides, in 'time-integrated' passive sampling, a flow restrictor is used to guarantee a constant flow rate of gas into the canister during the entire sampling time interval (minutes to days) to ensure a representative, time-weighted average gas composition is sampled despite the progressive pressure increase in the canister (indicated by the vacuum gauge) and environmental parameters variations (temperature, humidity...) [5,91,95]. Technical guides provide extensive practical information on the canister-components, and their assembly, required for a full canister sampling train; important is that all components are made of properly passivated stainless-steel [91,95]. One such essential component is a particle filter ($\sim 30\mu\text{m}$), installed upstream flow controlling units to prevent dust particles in the gas to foul or damage valves, obstruct flow paths, alter flow rates and enter the canister [5,91,99]. Canisters are reusable and proper canister cleaning is crucial prior to and between sampling campaigns to ascertain actual samples are not contaminated with residues from previous samplings or laboratory air contaminants. Cleaning procedures are for instance described in US EPA method TO-14A [97], in a technical guide of Restek [91] and in scientific publications [1] and mainly involves purging the whole sampling train and canister with humidified pure N₂ or air with simultaneous heating, sonicating the disassembled pieces in a solvent like methanol to remove possibly condensed high

boiling compounds and oven baking pieces to discard residual organic vapors. Different passivation treatments require different cleaning procedures. Once cleaned, filling the canister with humidified air, passing the air through an adsorbent trap and analyzing the air towards targeted compounds should give the spectrum of eventual residual contaminants. Cleanliness certification depends on the expected concentration level of future targeted analytes. Schweigkofler and Niessner [1] however found a simpler cleaning procedure was sufficient for canisters where landfill and sewage biogases had been collected: six cycles of canister evacuation and flushing with dry pure N₂ without heating yielded very low blanks.

Similarly to gas cylinders, disadvantages to canisters are economical (high purchase, transport and cleaning costs) [5,38,93] as well as related to the poor stability and recovery of high boiling, high polarity or water soluble reactive compounds. Polar VOC are especially those with oxygen, nitrogen and Sulphur groups, rendering them reactive. VOC stability in canisters is negatively affected by physical adsorption or absorption effects on inner canister walls, dissolution in condensed water, compound instability and by chemical conversions due to reactions between sampled compounds [1,5,39,40,92,100,101]. Coutant [101] found the losses of (polar) VOC due to physical adsorption in canisters were strongly related to a complex interaction of compound-specific physico-chemical properties such as polarizability, equilibrium vapor pressure, temperature and sample vapor concentration. Adsorption losses seem to decrease when a relatively high water vapor level is present in the sample, as water then occupies the sorption sites on inner canister walls [39,40]. Furthermore, polarity, water solubility, aqueous reactivity and reactivity of the compound with other species in the sample, competitive adsorption of the compound on the inner walls relative to that of water vapor and trace compounds in the sample, as well as characteristics of the canister surface (e.g. passivation treatment), usage history of the canister, sample humidity, canister pressure and temperature during sampling and storage, are all factors interactively influencing the storage stability of VOC in canisters [39,40,101]. Dissolution of compounds in condensed water inside a canister can lead to recoveries' over-estimations of concerned compounds inasmuch as the amount condensed water diminishes as the pressure drops in the canister upon sample withdrawal for analysis, increasing the concentration of concerned compounds [39,101]. Compounds unlikely to be stable in canisters are those with relatively high polarity, water solubility, Henry constant, reactivity (with water or other compounds) and boiling point. Inorganic volatile compounds such as Cl₂, HF, N₂H₄ and PH₃ are also unlikely to be stable in canisters due to their high reactivity, water solubility and propensity to adsorption in spite of their high vapor pressures [40]. In view of all factors influencing compounds stability in canisters, one should always test the stability of targeted compounds prior to sampling, under the same conditions as the future sample. Hsieh et al. [39] compared Summa and SilcoCan canisters for the storage of 56 VOC found in air (alkanes, alkenes, aromatics and biogenics) at 5-30 ppb_v levels and at different temperature (25 and 35°C) and relative humidity (30 and 90% RH) conditions combinations. According to a first order decay model, the authors found the fastest compound losses occurred at the higher temperature and lower RH (35°C and 30%) condition for all VOC tested in both canisters. Hence low temperatures and high relative humidity storage conditions were advised to enhance the stability of VOC. The favorable effect of low temperatures was explained by lower degradation rate constants at lower

temperatures; the favorable effect of high relative humidities was explained by fewer adsorption losses as more water molecules then occupy potential sorption sites on inner canister walls [39].

Moreover, reliably assessing the extent of compound loss after a certain storage period in a canister requires previous standard stability tests and hence standard gas generation in the canister. Achieving reproducible replicates of gas standards is a challenging task especially when low concentrations of targeted compounds are to be introduced in the canister, and this variability in standard initial concentration affects the stability testing reliability [40]. Schweigkofler et al. [1] successfully prepared a calibrated mixture of 30 compounds susceptible to be found in biogases (siloxanes, HVOC, organosulfurs, alkanes, terpenes and aromatic compounds, dissolved in pentane) in an evacuated canister by vaporizing 1.5 μL of the mixture with a dry N_2 stream, filling the canister to ambient pressure. After 2 h equilibration, this standard gas was analyzed via GC-MS/AES and recoveries >90% were found for all compounds except for high boiling siloxanes D5 (bp 210°C, 85% recovery) and L5 (bp 223°C, 35% recovery). The poor recovery of L5 was due to adsorption on inner canister walls, and the authors predicted that larger, less volatile siloxanes such as D6 would also not be satisfyingly recoverable from canisters for the same reason. Concerning the precision of their standards, six replicates of the 30-component standard in canister were analyzed within 8 h after preparation. They found relative standard deviations < 5.1% for all compounds except for L5 for the mentioned reason. Saeed et al. [99] also prepared siloxane gas standards in Summa canisters. They first prepared an 8-siloxanes standard solution in hexane. After heating the injection port of the canister to 140-150°C with heat tape, they injected the standard solution in the canister by means of a micro-syringe. Finally, they pressurized the canister to 5 psig with pure dry N_2 , agitated it for 8 h to enhance the vaporization of the higher boiling siloxanes, and let the canister further stabilize for 24 h where after it could be used. The authors mentioned that in spite of these precautions, high boiling siloxanes may never totally vaporize due to preferential sorption effects, leading to erratic recoveries.

Biogas and biomethane have seldomly been sampled in canisters and studies found using canisters were all targeting siloxanes [1,72,99,100,102]. Hayes et al. [100] and Saeed et al. [99] compared the performance of Summa canister sampling with other sampling techniques with direct analyte enrichment (methanol impingers and charcoal adsorbent cartridges) in terms of ease of sampling, representative sample collection and siloxane recovery. According to these authors, the greatest advantages of canisters are the ease of sampling and short sampling time when performing grab sampling, as well as straight transport to the lab. Moreover, canister sampling enables to withdraw several batches of samples from the same sampled volume for repeated lab analysis, and canisters are reusable after proper cleaning [1,36]. On the contrary, sampling in impingers or on sorbent tubes requires more training and flow metering equipment, can last minutes to days, requires specific transport on ice beds to preserve sample integrity [100] and sorbent tubes only allows for one single sample run since the entire sample is desorbed at one time [36]. Nevertheless, a disadvantage of canister grab sampling Hayes et al. [100] highlight is the poor time representativeness of the sampled gas composition. This latter often varies in time, which is especially true for biogases, whereas grab sampling involves instantaneous canister filling, hence only reflecting the gas composition at the sampling time t . Time-integrated passive canister sampling can however solve this problem, inasmuch as a flow

restriction device is set up to gradually fill the canister over a wished time interval, as is done for impingers and sorbent tubes. Besides, the siloxane recovery efficiency of canisters has been found better for light, volatile siloxanes than for heavier, less volatile ones [1,99,100] due to the previously discussed wall adsorption effects increasing for compounds with relative high boiling points and polarities. Hayes et al. [100] and Saeed et al. [99] found methanol-impingers were better than canisters for the sampling of heavier siloxanes like D4, D5 and D6, while Summa canisters were better suited for light siloxanes like D3 and pentamethyldisiloxane. Consequently, as D4 and D5 siloxanes have been found abundant siloxanes in biogases [1,37,61,103,104], Saeed et al. [99] concluded canisters were not convenient for reliable and representative siloxanes sampling from biogases. Analogously, Eichler et al. [72] compared the performance of Summa canisters, Tedlar bags, methanol impingers and thermal desorption tubes to sample and store a standard gas of D5 siloxane in N₂. They interestingly described and quantified the adsorption process of the semi-volatile D5 (bp 210°C, vapor pressure 20.4 Pa at 25°C) onto the inner Summa canister surfaces. To this aim, the authors performed a three-fold experiment:

- flushing the canister with the reference D5 gas (640 cm³·min⁻¹) to enable adsorption to occur while recovering the outlet gas in sorption tubes to subsequently quantify the exiting D5 level in function of time. During the first 60 minutes of this operation, the canister walls act as a sorption sink for D5, where after all sorption sites seemed to be saturated (equilibrium between gas phase concentration and surface-sorbed concentration) as the D5 level exiting the canister reached a steady state with a ~95% recovery of the incoming reference concentration (Fig.2.2).
- flushing the canister with pure N₂ (640 cm³·min⁻¹) to empty the canister and trigger the desorption of adsorbed D5, while recovering the outlet gas in sorption tubes to subsequently quantify the exiting D5 level in function of time. After 60 minutes desorption, the D5 level exiting the canister reached ~2% of the initial concentration (Fig.2.2).
- solvent (methanol)-extraction of the remaining D5 more strongly adsorbed onto inner canister surfaces. About 4% of the initial D5 concentration were extracted this way.

The authors then choose a model to describe the equilibrium partitioning of D5 between gas phase and canister surface, assuming linear and instantaneously reversible equilibrium [72]:

$$\ln\left(\frac{y}{y_0}\right) = -\left(\frac{Q}{V + K_s A_s}\right) t$$

with y the D5 gas phase concentration at the canister outlet, y_0 the steady state D5 gas phase concentration, Q the gas flowrate (640 cm³·min⁻¹), V the canister volume, A_s the inner surface area of the canister, K_s the partition coefficient (D5 surface concentration (ng·m⁻²) on D5 gas phase concentration (ng·m⁻³)) and t the time (min). The partition coefficient K_s was found by plotting $\ln(y/y_0)$ against t and filling in the values of Q , V and A_s in the resulting slope term. In this case K_s was = 0.0171 (ng D5·m⁻²)/(ng D5·m⁻³): per ng D5 in 1 m³ gas phase, 0.0171 ng is adsorbed onto 1 m² inner canister walls, which is not negligible. Eichler et al. [72] hence concluded Summa canisters were not suited for D5 sampling and storage as quantitative desorption is unlikely,

resulting in underestimation of sampled concentrations. A drawback of their study is however that pure D5 in a pure N₂ matrix was used as the sole test gas, being non-representative of real biogas samples in a humid CH₄/CO₂ matrix containing a broad range of other species which may compete or interfere with the described sorption process of D5.

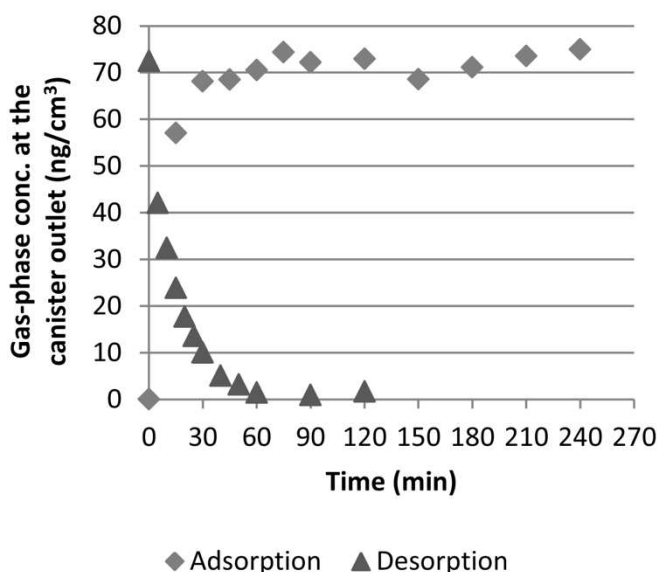


Figure 2.2: Adsorption and desorption results of D5 siloxane in a Summa canister according to the Eichler et al. [72] experiment (figure from [72]).

Finally, a study by Khan et al. [105] gives some insight on the relevance of reusing old canisters. They investigated the storage losses of a mixture of 10 nL·L⁻¹ reduced Sulphur compounds in air (H₂S, COS, CH₃SH, DMS, CS₂) in 6-years old versus 1-year old (new) commercial SilcoCan canisters. Both canister generations have been electropolished and coated with amorphous silicon but newest canisters have a thicker silica layer purported to improve the inertness of the inner canister walls [105]. In the old canister, >50% of H₂S and CH₃SH were lost after 1 storage day while other compounds remained stable in this vessel for 10 more days. Furthermore, the authors observed the formation of DMDS concurrently to the disappearance of H₂S and CH₃SH. They suggested these two compounds were quantitatively converted to the more stable DMDS. Past usage history of the old canister may also have induced cracks in the old coating, possibly contributing to analyte losses. On the contrary, >96% of COS, DMS and CS₂ and > 85% of H₂S and CH₃SH were recovered in the new canister after 7 storage days, confirming that recently coated SilcoCan canisters were more inert towards trace levels of reduced Sulphur compounds [105].

III. GAS SAMPLING WITH ENRICHMENT (PRECONCENTRATION)

On the contrary to whole gas sampling vessels limited in sampleable volumes and inducing analyte losses during transport and storage periods due to wall-effects and reactions between unstable sampled compounds, sampling with direct on-site enrichment not only allows to sample considerable gas volumes [23] but above all enables to preconcentrate low-concentrated analytes by selective isolation from the gas matrix in- or onto a small dedicated volume. This purposeful enrichment aims at reaching analytes concentrations superior to the available analytical detection limits [41]. Sampling with preconcentration is based on three main selective analyte-trapping methods: trapping on solid media (physical or chemical adsorption, amalgamation), trapping in liquid media (absorption, bubbling) and cryogenic trapping ('cryotrapping', condensation) [5,41]. In each of those approaches the gas matrix actively flows through, but is not retained in, the trapping system as long as required to trap sufficient amounts targeted compounds [22]. The more diluted the compounds, the larger the gas volume required, the longer the sampling will last. The sampling support whereon analytes are fixed is then generally transported to the lab for analysis. For biogas and biomethane samples, as the flammable methane matrix is not contained in the trapped sample, traps are usually not considered as dangerous goods and their transport does not require specific consignments as is the case for whole gas sampling vessels [22]. Nevertheless, just as the length of the transport and storage period preceding analysis was critical for the stability of compounds sampled in whole gas sampling vessels, the storage period of trapped analytes should be kept as short as possible even though analyte stability should be better on the dedicated selective traps than in bags, cylinders or canisters [21]. Importantly, appropriate conditions (temperature, humidity...) governing the stability of analytes in their trapping media have to strictly be respected during transport and storage.

Drawbacks to almost all preconcentration sampling techniques include:

- *Analyte breakthrough* [6,23,32,36,41]: trapping media, especially solid adsorbents and liquid absorbents, have limited trapping capacities towards targeted molecules. During sampling, when the sampled gas volume exceeds the corresponding saturation point of the trapping media relative to a targeted analyte, further analyte molecules will not be trapped, leading to an underestimation of the analyte concentration. Saturation of solid adsorbents results from the saturation of all sorption sites by either the targeted analyte or competing analytes. Saturation of liquid absorbents is rather linked to the solubility limit of analytes. When dealing with gases of unknown composition, breakthrough is usually avoided by placing several traps in series so as to recover analytes breaking through the previous trap.
- *Negative effect of moisture upon sampling* [22,23,32,37]: a high humidity percentage in the gas is harmful when sampling on (hydrophilic) sorbent tubes as water will compete with targeted analytes for the sorption sites or even saturate the sorption sites of the adsorbent. This effect can be weakened by using hydrophobic adsorbent materials. In cryotraps, ice blocks can form when sampling humid gases. This can nevertheless also be avoided for instance by a preliminary gas drying or by putting two cryotraps in series [3,8,33].

- *Complex field implementation requiring trained personnel* [22,23,37,42]: to accurately measure sampled gas volumes, on-line equipment such as flowmeters, flow regulators, electricity/batteries, cryogen vessels for cryotrapping... are needed as well as equipment to properly store and transport traps back to the lab. Biogas and biomethane sampling normally do not require pumps for sampling as the production pressure at the sampling point usually suffices to draw the gas through the trapping system.
- *Time consuming sampling* [37]: the more diluted the analytes, the larger the gas volume to be sampled to collect a sufficient amount targeted analytes, the longer the sampling will last at a given flow rate.
- *Impossibility of repeated sample analysis* [23,32]: on the contrary to a single whole gas sample wherefrom several batches of gas can be analyzed, each preconcentration support is individualized (sorbent tube, SPME fiber, impinger bottle, cryotrap...) and can only be analyzed once, implying numerous replicates have to be sampled to assess the robustness of trace compounds characterization results.

The next sections critically review available techniques for biogas or biomethane sampling with enrichment of targeted compounds such as (H)VOC, volatile Si- and S-compounds as well as volatile metal(loid) compounds.

III.1. Trapping on solid media

III.1.1. Adsorbent tubes

Trapping gaseous analytes on solid sorbent powders packed into tubes involve sorption mechanisms (Fig.2.3). Sorption refers either to absorption or adsorption. Absorption involves the permeation or dissolution of adsorbates (atoms, ions or molecules from the gas) into the volume of a liquid or solid adsorbent. Adsorption on the other hand involves the layered adhesion of adsorbates (atoms, ions or molecules from the gas) onto the surface of a solid adsorbent due to surface energy forces. Because surface atoms of the adsorbent are not fully surrounded by other adsorbent atoms, they can attract adsorbates [81]. One further distinguishes physical or chemical adsorption, respectively referred to as physisorption and chemisorption. Physisorption is ruled in particular by Van der Waals forces: numerous weak electrostatic interactions between electron configurations of both the adsorbate and the adsorbent lead to the assembly of mono- or multilayers of adsorbates on the adsorbent surface (binding energies are relatively weak: 1 – 10 kJ·mol⁻¹). Physisorption is favored at low (room) temperatures [81]. Chemisorption in contrast relies on the creation of a kind of ionic or covalent chemical bond between adsorbate and adsorbent, whose chemical structures are therefore decisive. Those chemical bonds often need some (thermal) activation energy to appear and the associated binding energies are accordingly high (100-1000 kJ·mol⁻¹). This process only leads to monolayers on the adsorbent surface [81].

Whereas sorption is the process of interest during the sampling phase, desorption enables recovering sorbed analytes from the sorption medium to analyze them. Different desorption approaches exist (solvent or thermal desorption) and will be dealt with in time. Importantly,

desorption especially from solid sorbents is not always quantitative: the desorbed quantity may be lower than the initially sorbed quantity (hysteresis) [81].

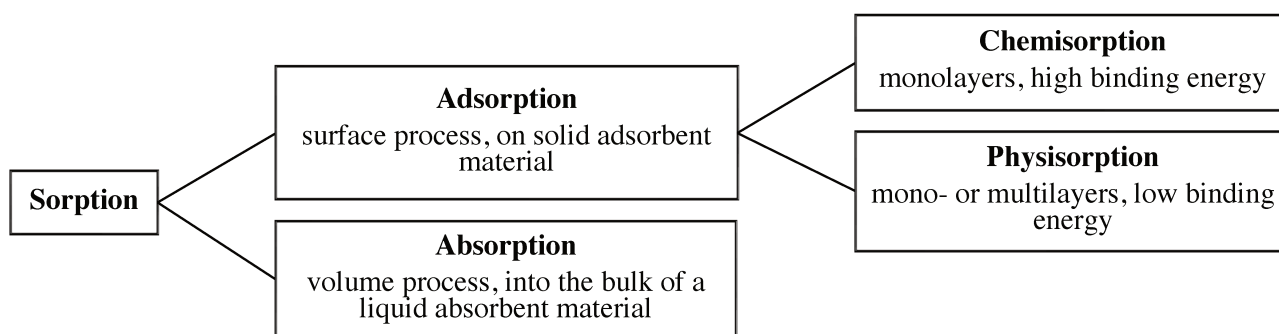


Figure 2.3: Sorption mechanisms. Adapted from [81].

Sorbent tubes are borosilicate glass or surface-passivated stainless-steel tubes packed with one or several solid (powdered) adsorbent materials (Fig.2.4) [5,6,11,21,32,76,106–108]. During sampling, gas actively flows through the tubes while targeted analytes are selectively sorbed in the adsorbent bed. Adsorbents are especially suited to trap intermediate-, semi- or very-volatile (halogenated) organic compounds [5,6,21,22,42,106,109–113], volatile Sulphur compounds [6,21,42,113–119] and volatile Silicon compounds such as siloxanes [5,6,21,37,61,113,120–122], with various polarities and volatilities. Adsorbents can nevertheless not be used to sample volatile metal(loid) compounds [23]. The physico-chemical interactions required for such unstable analytes to be caught in the adsorbent are too strong and would inevitably lead to irreversible adsorption or analyte degradation during desorption, alteration of the chemical speciation of the analytes or artifacts build-up [23]. Sorbent tubes are also not intended to trap permanent inorganic gases [21,76].

A multitude of commercial solid adsorbents exist and choosing the most appropriate adsorbent material for the trapping of given targeted compounds is by far the most delicate task regarding tube assembly as will be discussed below [32,33,110,120,123]. In the following, sorbent tube assembly, adsorbent conditioning, desorption considerations and adsorbent choice are discussed. Usage of sorbent tubes for biogas and biomethane sampling will then be reviewed.

Sorbent tube self-assembly and adsorbent conditioning

Numerous ready to use sorbent tube configurations are commercially available. However, it has been shown the background contaminations of commercial sorbent tubes were higher than that of self-assembled tubes, leading to higher detection limits and restricting their use for high-ppb concentration samples [6]. Therefore, sorbent tube self-assembly is reviewed here to provide insight into preparation steps critically influencing the final background contamination level of sorbent tubes. Fig.2.4 depicts required sorbent tubes constituents. Typical commercial tube dimensions are 6.35 mm OD, 4 mm ID (for glass tubes) or 5 mm ID (for stainless-steel tubes), 89 mm length [6,21,22,32,76,93,106,107,124]. Both tube extremities should be equipped with detachable sealing connection accessories. Sorbent tubes are usually fitted with stainless-steel,

brass or PTFE Swagelok® gas-tight screw-fittings (ferrules and nuts) [6,21,32,93,106] enabling easy field connection. Alternatively, especially glass sorbent tubes can be fitted with crimp caps with central septa, requiring specific needles for sampling and analysis operation.

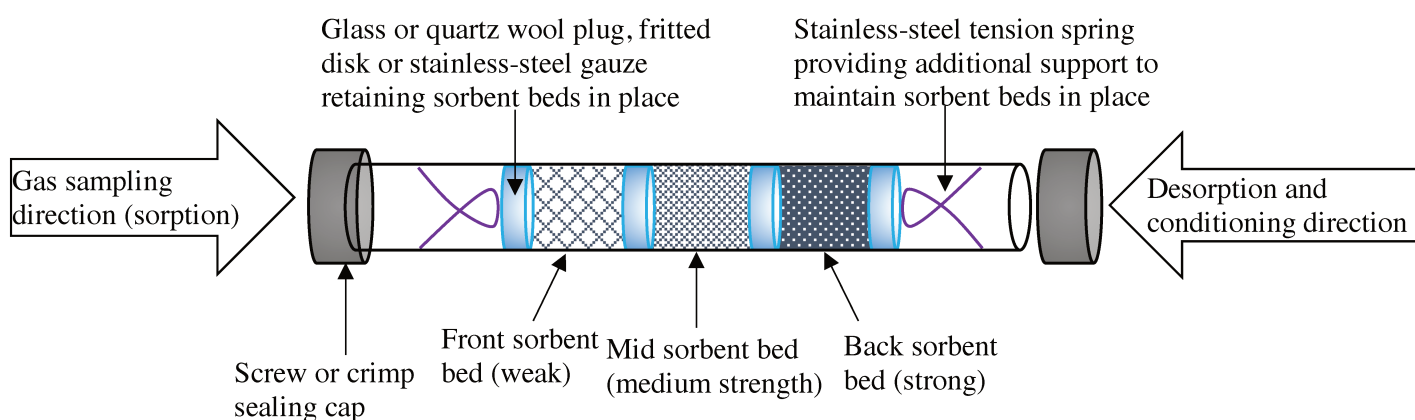


Figure 2.4: Schematic of a multitubed sorbent tube. 100 mesh stainless-steel gauzes and tension springs are typically used together in stainless-steel tubes whereas unsilanized glass or quartz wool plugs are used in glass tubes to secure adsorbent beds [107]. Constriction of the tube internal diameter at the tube extremities can additionally help securing the sorbent beds. The desorption direction is always the reverse of the sampling direction even for single bed tubes [110].

As any part constituting a sorbent tube may be a source of contamination, it is strongly advised to clean all of them prior to tube assembly and to always handle them with disposable gloves in order to obtain the lowest blanks [6,106,107]. Note that the tube material itself may also act as sorption and catalysis surface, as studied by Arnts for untreated stainless-steel versus Sulfinert™ or SilcoSteel® passivated stainless-steel tubes [108]. It is advised, when using stainless-steel sorbent tubes, to opt for surface-passivated stainless steel [21,108]. Helmig [106] sonicated all metal (stainless-steel tube, tension springs, gauzes and sealing ferrules and nuts) and PTFE (alternative sealing caps) parts in methanol before use and stainless-steel parts were additionally baked at 150°C for 4 h. Glass or quartz wool plugs used to secure adsorbent beds in glass tubes should also be pre-cleaned by thermal conditioning to remove any impurity trapped in the wool [107]. Sheu et al. [6] thermally cleaned all loose parts and empty tubes in dedicated ovens with simultaneous high-purity N₂ flow. They stressed out thermally pre-cleaning the ovens and gas capillary lines used is also crucial, in their case a Lindberg/Blue M Mini-Mite Thermo Fisher tube furnace was used and pre-cleaned in air at 450°C for 8 h with N₂ flow [6]. Before packing adsorbents in tubes, Sheu et al. [6] also thermally cleaned all adsorbents by placing them in the tube furnace at their material-specific maximal temperatures (Table 2.2) with simultaneous high-purity nitrogen flow (0.5 – 1 L·min⁻¹) during several hours to induce the desorption of contaminants from the adsorbents. A method by the UK Health and Safety Executive [124] also recommends to precondition all adsorbents before packing the tubes, by heating them at their material-specific temperature in an inert atmosphere for 16 h.

Actual tube packing and assembly begins by placing the first sorbent bed retaining hardware [106] (100 mesh stainless-steel gauzes and tension springs are typically used together in stainless-steel tubes whereas glass or quartz wool plugs are used in glass tubes [107]). Adsorbent bed(s) needs then to be packed in the tube. The adsorbent mass or volume to be loaded is determined by the tube geometry, the number of sorbent beds placed in series in the

tube, the adsorbent sorption capacity properties and by the concentration of analytes targeted in the future gas to be sampled [76]. As will be clarified later, extraction of trapped analytes from sampled sorbent tubes can occur via solvent or thermal desorption. For thermal desorption, it is of prime importance that the total length of (successive) sorbent bed(s) is within the central zone of the tube that will later on be heated by the thermal desorption device [107,124,125]. A technical report of Supelco [125] therefore suggests to pack the tubes with a fixed volume V of each adsorbent so that all beds occupy the same length. Collecting the chosen volume V of adsorbent powder is possible by constructing a vessel of volume V , filling it with adsorbent, vibrating it to ensure homogeneous packing of the powder and finally pouring the content into the sorbent tube [125,126]. Alternatively, the mass m of adsorbent corresponding to the fixed volume V can be calculated with the packing density (ρ) data of adsorbents (Table 2.2): $m = \rho \cdot V$. Because of packing density discrepancies among adsorbents, packing those on a fixed weight basis is not convenient since in this case adsorbents with low ρ would cause the sorbent bed length to extend past the heated zone limits, and inversely adsorbents with high ρ would occupy a too small volume to obtain robust tubes [125]. During packing, care must be given not to compress adsorbent materials excessively to prevent tube impedance and later head losses during gas sampling or desorption operations [107,126]. For multibed assembly, each adsorbent should be kept in a discrete bed sufficiently separated from the others by glass / quartz wool plugs (3 mm length) [107,127], glass-fiber filter discs [106] or any other suitable fritted disks or gauze. Mind however that quartz and glass wool may act as sorbents for intermediate or semi-VOC and that glass wool tends to physically degrade at elevated temperatures [6,108]. Also, silanized glass wool releases siloxanes upon heating during the thermal desorption, contaminating the sample and falsifying results when targeting siloxane analytes [6]. Using high purity unsilanized quartz wool is henceforth preferable [6,107,125]. If fritted disks are used, their porosity should not be too low to prevent disadvantageous head losses. If metallic gauzes are used, one should expect potential negative sorption and desorption interferences since high boiling, heavier compounds are prone to sorption on metallic surfaces, as was discussed for non-passivated stainless-steel cylinders and canisters (whole gas sampling vessels). Additionally the inertness of such gauzes upon heating is poorly documented and metallic compounds could be released in the sample. Finally, the plugs or discs used should mechanically withstand the gas pressure applied during sampling and (thermal) desorption. With this respect, quartz or glass wool plugs are known to easily blow out of the tube or to move inside the tube, affecting the adsorbent bed packing quality and in worst cases leading to adsorbent and sample loss [128]. Securing the plugs with tension springs or constricting the inner diameter of the tube extremities are possible solutions [6,125].

Adsorbents in a multibed (up to 4 beds in the central zone of 89 mm long tubes) must be arranged in order of increasing sorption strength (Fig.2.4) [41,76,107,110,125]. Because no single adsorbent is universal enough to individually accommodate the sorption of all analytes, multibeds are especially attractive as they enable quantitative adsorption and desorption of volatile compounds over a wider volatility and polarity range than single beds do, in one single sampling run [6,21,32,41,76,107,125,127,129,130]. When sampling multicomponent gases, high molecular weight compounds with low volatilities (high boiling point) are easily trapped onto the weakest front adsorbent bed and their later desorption is quantitative. Very volatile

compounds however are not trapped yet as the sorption strength of front adsorbents is not sufficient to retain them. Those light compounds therefore further flow in the tube and gradually reach stronger adsorbents whereon they are trapped. This way, heavy compounds never meet strong adsorbents that they quickly would saturate and whereon they would be irreversibly or too strongly adsorbed to be further quantitatively desorbed. Back strong adsorbents are hence dedicated to the sorption of (very) volatile species whose later desorption is possible [32,41,107,110,125]. Sorption strength relates to the affinity of sorbents for volatile analytes, and is generally roughly positively related to the surface area of given adsorbents (Table 2.2) [107]. When preparing a multibed, selecting adsorbents with similar conditioning and desorption temperatures (Table 2.2) is crucial or conditioning of the most thermally stable adsorbent will be impossible without exceeding the maximum recommended temperature of and hence degrading the least thermally stable adsorbent [107]. Lastly, when dealing with humid gas samples such as biogas, selecting hydrophobic adsorbents is clever to avoid water collection in the sorbent tube and water-saturation of the sorbent beds [6,93,110]. However, when dealing with very volatile compounds, hydrophobic adsorbents which are weak or medium strength sorbents (Table 2.2), will not suffice and using stronger, hydrophilic sorbents is inevitable.

The step following sorbent tube packing is tube conditioning. Adsorbent tubes are mounted on a manifold and heated at the adsorbent material-specific conditioning temperature (Table 2.2) under a continuous clean gas (N_2 or He) stream for several hours to induce the desorption of contaminants passively adsorbed onto the adsorbents during tube assembly. The temperature and gas flow during conditioning must always be more stringent than during effective tube (thermal) desorption and analysis [93,106]. Importantly, multibeds must be placed so that the gas flows from the strongest to the weakest adsorbent bed [106,110] to avoid high molecular weight impurities desorbed from the weak sorbents, to encounter strong adsorbents where on they probably would adsorb. Table 2.3 reviews some sorbent tube conditioning parameters (conditioning temperature, gas flowrate and duration) used by several authors.

The oven wherein tubes are conditioned should be clean and programmed to gradually ($5-10^{\circ}C\ min^{-1}$) reach the material-specific temperature of adsorbents. Commercial multi-position tube conditioning oven systems exist. During tube conditioning, adsorbents must absolutely be shielded from contact with air or oxygen to avoid adsorbent oxidation and degradation [41,106]. Helmig [106] filtered the N_2 conditioning gas through a hydrocarbon scrubber, a high-capacity oxygen trap and an indicating oxygen trap and connected the tube outlets to stainless-steel tubing to prevent air from diffusing into the back of the sorbent tubes. At the end of the conditioning program, sorbent tubes should be taken off the oven as soon as possible while still hot (to avoid passive adsorption of new air contaminants) and immediately sealed with cleaned air-tight caps to avoid passive sampling via ambient air diffusion [6,106]. Stainless-steel Swagelok-like caps detached from the tubes can also be conditioned in the oven [106]. Another way to pre-clean the caps is to rinse them in an organic solvent (e.g. 50:50 acetone:hexane) and to subsequently bake them (e.g. for 90 min at $150^{\circ}C$) [109].

The efficiency of adsorbent tube conditioning can be verified by thermodesorbing one tube per conditioning batch, typically in a thermodesorber device mounted on a GC-MS, at the material-

specific desorption temperature to scan potential contaminants still remaining in the tube after conditioning [6,124]. Artifacts inherent to adsorbents and present in tube blanks must however be distinguished from contaminants [107].

Freshly conditioned and sealed sorbent tubes must properly be stored if not immediately used for sampling. Sorbent tubes are generally stored in refrigerators at $\leq 4^{\circ}\text{C}$ or in freezers at $\leq -30^{\circ}\text{C}$ in clean air-tight recipients (e.g. glass jar) with desiccant material [6,21,44,106,107] since it has been proven that cold temperature storage reduces the formation of adsorbent artifacts contributing to background contamination [6,106]. Refrigerators and recipients wherein tubes are stored must be free of any volatile chemical or concentrated standards, i.e. no solvent bottles or samples must be stored in the same fridge as the tubes to avoid passive tube contamination by these volatiles compounds [6,107]. Helmig [106] stored conditioned tubes at -30°C in a glass jar in a freezer and also placed commercial activated charcoal adsorption cartridges (opened) in the jars to keep the headspace above the tubes hydrocarbon-free, as also suggested by others [32,93]. The shelf-life of rightly assembled, pre-conditioned and stored tubes may last several months [32,93], though after 30 days storage re-conditioning may be recommended right before using the tube [32]. Finally, it is analogously advised to store and transport *sampled* sorbent tubes at cold temperatures ($\leq 4^{\circ}\text{C}$ [21,107,111,130]; -18°C [59,61]; -20°C [131] or -30°C [6,106]) in hermetically sealed vessels with desiccants if desorption and analysis of sampled analytes cannot be executed immediately after sampling as cold temperatures inhibit desorption, chemical reactions and analyte diffusion processes in the tubes [6]. Note that the storage stability of sampled single bed sorbent tubes is better than that of multibeds since the risk exists that analytes trapped in multibeds migrate from one bed to another via diffusion processes in the tube during the storage period. Multibeds should therefore always be analyzed sooner than single beds, ideally within 30 days [93,107,110]. Countless studies examined the storage stability of targeted analytes from air matrices (ambient air, industrial emissions, workplace air...) or synthetic gases trapped on adsorbent tubes, e.g. [111,118,132]. It is nevertheless beyond the scope of this work to review all of them. Furthermore, no universal storage stability recommendation can be given since stability results are highly dependent on targeted analytes, on each particular adsorbent tube configuration, on adsorbate-adsorbent affinities and interactions, sampling conditions, potential contaminations during sampling, transport or storage, and on the analytical method used. The only valid rule is to analyze sampled sorbent tubes as soon as possible. For instance, Ramírez et al. [111] investigated the storage stability of 90 VOC (ranging in volatility from iso-pentane (b.p. 28°C) to methyl-naphthalene (b.p. 240°C) and including carbon disulphide, halogenated hydrocarbons (e.g. dichloromethane and bromobenzene), N-containing compounds (e.g. propionitrile), oxygenated compounds (e.g. dioxane), hydrocarbons (e.g. alkanes, aromatic hydrocarbons)) from industrial wastewater plant air emissions trapped on multibeds composed of Tenax TA and Carbograph 1TD. Sorbent tubes were analyzed via thermal desorption-GC-MS and results indicated a complete stability for all targeted compounds after 3 storage days. Only after 7 days did the response of some compounds (hexane and carbonyl sulfide) vary. Authors hence recommended to analyze tubes within 3 days after sample collection [111].

Next page:

Table 2.2: Properties of common commercial adsorbents used in thermodesorption applications.

Adsorbents are listed in order of increasing sorption strength. Data compiled from [33,107,110,125,129,133–137]. The sole difference between Carbotraps and Carbopacks is the mesh size: Carbotraps are 20/40 mesh size ($420\ \mu\text{m} < \text{particle diameter} < 841\ \mu\text{m}$) and Carbopacks are 40/60 mesh ($250\ \mu\text{m} < \text{particle diameter} < 420\ \mu\text{m}$) or smaller [125,133]. Note that sorption strength categories are not strictly defined. In particular, Carbopack X, Carbotrap X, Carbograph 5 and Carboxen 569 are often considered as “strong” adsorbents. However, in this table, the sorbent strength criteria proposed in the US EPA method TO-17 [107] are chosen to distinguish weak, medium and strong adsorbents based on their surface areas: adsorbents with surface area $< 50\ \text{m}^2\cdot\text{g}^{-1}$: weak; surface area between 100 and $500\ \text{m}^2\cdot\text{g}^{-1}$: medium; surface area $> 1000\ \text{m}^2\cdot\text{g}^{-1}$: strong. Note that adsorbents with pore diameters $> \sim 1000\ \text{Å}$ are considered as non-porous. Trademarks: Carbopack, Carbotrap, Carboxen, Carbosieve: Sigma-Aldrich Co.; Carbograph: LARA s.r.l, Italy; Anasorb: SKC, Inc.; Spherocarb: Analabs Inc.; Tenax: Enka Research Institute, The Netherlands; Porapak: Waters Corporation; Chromosorb: Celite Corporation, USA; HayeSep: Hayes Separation Inc.; Amberlite: Rohm and Haas; UniCarb: Markes International.

Table 2.2

Adsorbent name	Adsorbent class \diamond	Packing density (g·cm ⁻³)	Conditioning T (°C)	Desorption T (°C)	Approximate surface area (m ² ·g ⁻¹)	Mean pore diameter (Å)	Sorbent strength	Hydrophobic / Hydrophilic
Glass Beads	SiO ₂	1.68	350	330	<5	>3000		
Quartz Wool	SiO ₂				<5	-		
Carbopack F	GCB	0.81	350	330	5	1000-3000	Very weak	
Carbograph 3	GCB				5	1000-3000		
Carbopack C	GCB	0.85	350	330	10	2000		
Carbograph 2	GCB		350	330	10	2000		
Anasorb GCB2	GCB		350	325	12	2000		
Tenax GR	PP	0.41	320	300	24	200-1000	Weak	
Carbopack Y	GCB	0.51	350	330	24	1000-3000		
Tenax TA	PP	0.28	320	300	35	720		
Carboxen-1016	CMS	0.48	350	330	75	-		
Carbopack B	GCB	0.43	350	330	100	3000	Weak	
Carbograph 1	GCB		350	330	100	3000	/	
Anasorb GCBI	GCB		350	325	100	3000	Medium	
Carbopack X	GCB	0.58	350	330	240	100		hydrophobic
Carbograph 5	GCB		350	330	240			
PoraPak N	PP	0.37	190	180	300	75		
Amberlite XAD 2	PP		190	180	300	10-20		
Chromosorb 102	PP		250	225	350	90	Medium	
Carboxen-564	CMS	0.59	350	330	400	6-9		
Carboxen-569	CMS	0.61	350	330	485	5-8		
Carboxen 1001	CMS	0.58	350	330	500	5-8		
Carboxen-563	CMS	0.55	350	330	510	7-10		
PoraPak Q	PP		250	225	550	75		
Carboxen-1018	CMS	0.80	350	330	700	6-8	Medium	
Chromosorb 106	PP	0.30	190	180	750	50	/	
Amberlite XAD 4 *	PP		140	130	750	50	Strong	
Hayesep D	PP	0.35	190	180	795			
Anasorb CMS	CMS		350	325	800			
Carbosieve S-III	CMS	0.76	350	330	820	4-11		
Carboxen-1003	CMS	0.45	350	330	1000	5-8		
Petroleum A.C. *	Charcoal	0.50	190	180	1050	4-20		
Coconut A.C. *	Charcoal	0.57	190	180	1070	4-20	Strong	relatively hydrophilic
Carboxen-1002	CMS	0.46	350	330	1100	10-12		
Spherocarb	CMS		400	390	1200	13-15		
Carboxen-1000	CMS	0.52	350	330	1200	10-12		
UniCarb (SulfiCarb)	CMS		350	330	1200			

\diamond GCB: graphitized carbon black. PP: porous polymer. CMS: carbon molecular sieve.

* Not compatible with thermal desorption (charcoals and Amberlite resins) yet still given as indication.

Table 2.3: Examples of sorbent tube conditioning parameters

Adsorbent tube composition	Conditioning T (°C)	Conditioning gas	Conditioning gas flowrate (mL·min ⁻¹)	Conditioning duration	Reference
Multibeds: • Quartz wool – glass beads – Tenax TA • Quartz wool – glass beads – Tenax TA – Carbopack X	material-specific	N ₂	500	> 6 h	[6]
Tenax GR	300	N ₂	Not mentioned	8 h	[61]
Single bed: Tenax TA or Carbosieve III	330	He	100	15 min	[71]
Multibed: Carbotrap C – Carbotrap (B) – Carbosieve S-III	300	N ₂	100	> 8 h	[106]
General prescription	350 or material-specific	He	50 – 100	> 2 h	[107]
Multibed: Carbotrap B – Carboxen 1000	370	He	100	1 h	[109]
Single beds: • Tenax TA or Tenax GR • Carbotrap C, Carbopack B or Anasorb 747 • Chromosorb 102 or Anasorb 727 • Porasil C/n-octane	300 350 250 170	He	30-40	12 h	[112]
Single beds : • Tenax TA, Carbotrap (B), Carbotrap C, Carbosieve SIII or Carboxen 1000 • Chromosorb 106	300 250	N ₂	50-60	3 h	[120]
General prescription (see Table 2.2)	material-specific	N ₂	Not mentioned	> 8 h	[125]
Multibeds: • Tenax TA – Amborsorb XE-340 – activated charcoal • Carbotrap C – Carbotrap – Carbosieve II • Chromosorb 106 – Carbotrap B – Carbosieve SII	300 300 265	N ₂	50	30 min	[127]
Multibed: Tenax TA – Carbograph 1TD	100 200 325	N ₂	100	15 min 15 min 30 min	[131]
Tenax GC	300	N ₂	10	48 h	[138]
Multibeds • 2x Tenax TA • 2x Anasorb CMS • Tenax TA – Anasorb CMS	320	N ₂	35	≥ 4 h	[139]
Single beds : Tenax TA, Tenax GR, Carbotrap (B), Chromosorb 106	material-specific	He	35	≥ 16 h	[140]

Sorbent tube desorption methods

Adsorbent choice depends on the nature of targeted analytes (and in particular their boiling points) while desorption method choice (solvent or thermal) depends on targeted concentrations and desired analytical sensitivity. Not all adsorbent materials are compatible with both solvent and thermal desorption [32]. Therefore this section first clarifies the distinction between both desorption processes when desorption occurs into a gas chromatograph (GC). When screening gases with unknown composition such as biogas or biomethane, containing a complex mixture of trace compounds from different chemical families differing in volatilities (alcohols, ketones, aldehydes, esters, glycol ethers, halogenated organic compounds, amines, sulphides, volatile fatty acids, mercaptans...), GC coupled with mass spectrometry detection (MS) is the analytical technique the most widely agreed upon when

using sorbent tubes to separate, identify and quantify the individual compounds of the mix [12,32,76,93,108,127]. Adsorbent materials, their physico-chemical properties (porosity, surface area, strength, hydrophobicity...) and compatibility with one or both desorption means are then reviewed.

Solvent desorption of sampled sorbent tubes can occur by dosing and passing a certain volume of extraction solvent through the tube in the reverse direction as compared to the sampling direction [141]. However, solvent desorption more often typically implies carefully breaking the tubes, transferring each individual adsorbent bed into a separate glass vial (e.g. 2 mL capped vials), adding 1 mL of a suitable desorption solvent to each vial, immediately capping the vials and waiting (e.g. 30 min, with or without shaking) for desorption to take place by partitioning of the analytes from the solid sorbent to the liquid solvent. 1 μ L of each obtained extract is then withdrawn with a syringe and in turn injected via liquid injection in the heated GC inlet port where the sample is vaporized before entering the GC-column [76,104,131]. Each sorbent bed in a multibed is hence analyzed separately with an analyte:solvent dilution ratio of 1:1000 [32,41,131]. As this analyte dilution is detrimental to the analytical sensitivity, evaporation of the solvent is sometimes performed to enrich the analytes [142] yet this has severe drawbacks as a procedure involving preconcentration, dilution and re-concentration is very prone to errors, compound loss (volatile target analytes can evaporate as well), contamination and artifacts formation [32,134]. Solvents for such extraction procedures must strip the analyte(s) from the adsorbent material with a high degree of efficiency and a high degree of reproducibility, and as considerable solvent volumes are used (solvent:analyte ratio at least 1000:1), suitable extraction solvents must be compatible with the GC column and must not interfere with the detection of analytes [32,41]. Carbon disulfide (CS_2) is a suitable solvent when used with flame ionization detectors (FID) and has been widely used to extract apolar hydrocarbons from activated carbon (polar adsorbent) adsorbent tubes for air monitoring purposes [32,76,129,131]. The charcoal-stripping efficiency of CS_2 is nevertheless impacted by the analyte type (e.g. CS_2 can react with amines, interfere with the detection of some chlorinated hydrocarbons, and polar compounds are not soluble in CS_2), by the analyte-to-sorbent mass ratio (lower desorption efficient for low ratios), by analyte-to-solvent mass ratio (higher desorption efficiency for lower ratios), by the presence, type and quantity of other trapped compounds (e.g. water vapor) and by the type of activated charcoal sorbent (e.g. petroleum or coconut-based). Note that using less sorbent or more solvent in an attempt to get higher recoveries leads to respectively higher risks of analyte breakthrough in the sorbent tube and lower analytical sensitivities (higher analyte dilution). Additionally, CS_2 is not compatible with electron capture detectors (ECD) [32]. Solvent desorption of polar analytes from humid gases trapped on polar adsorbent beds such as activated charcoals, is impeded by the propensity of polar analytes to hydrogen-bond to sorbed water molecules or to the polar adsorbent surface. Yet apolar solvents may displace this phase, polar compounds will remain in the water phase and will hence not be analyzed. Therefore, two-phase desorbing solvents are used, typically a mix of an apolar solvent (e.g. CS_2) with a polar co-solvent (e.g. isopropanol, 2-butanol, 2-propanol, methanol, amyl and hexyl alcohols, dimethylsulfoxide, dimethylformamide), and both solvents are analyzed independently [32,129]. Dimethylformamide may also be used as sole solvent, stripping polar as well as apolar compounds from charcoal beds [32]. Baya and Siskos [139] also used another

single extraction solvent, namely acetone, together with vibration for the desorption of pentane, hexane, heptane, octane, isooctane, nonane, decane, dodecane, cyclohexane, dichloromethane, toluene, propylbenzene, ethylbenzene and methylcyclohexane from multibeds composed of Tenax TA and Anasorb CMS. Wang et al. [132] also used successfully used acetone to desorb coconut activated carbon adsorbent tubes and silica gel adsorbent tubes sampled with siloxanes from a synthetic biogas. Next to GC, solvent-desorbed analyte extracts may be injected in high pressure liquid chromatographs (HPLC). CS₂ is not a suitable solvent in this case and charcoal sorbent beds are also less often used. Instead, silica gel sorbent tubes and methanol or acetonitrile as desorption solvents are used [32]. Concerning advantages, solvent desorption enables the analysis of very high molecular thermally unstable compounds for which thermal desorption would lead to alteration [131]. Moreover, solvent desorption enables repeated analysis of the analyte extract since a relatively large extract volume is generated (~mL) while only small quantities (~µL) are analyzed at a time [41,134]. Disadvantages to solvent desorption are:

- Sorbent tubes are not reusable when solvent-extracted [32,41]
- The consumption of relatively large volumes of toxic solvents often having objectionable odors [32,129]
- Poor desorption efficiency of polar and reactive compounds and absence of universal solvent able to quantitatively desorb all polar species [41,131]
- Poor analytical sensitivity and low method detection limit (analyte:solvent dilution ratio at least 1:1000 and the solvent peak may mask analyte peaks in chromatograms). Solvent desorption is therefore only suited for relatively high concentrated VOC samples (~1ppm) and not advised for trace compounds analysis below high ppb levels [32,76] unless very large gas volumes are preconcentrated [131]
- Incompatibility with mass spectrometry (MS) detection due to solvent interferences [76]
- No automated desorption/injection in the analytical finish [41,76]

Thermal desorption is typically hyphenated with GC and requires a thermal desorption (TD) unit serving as GC-injector. Unlike adsorption, desorption is an endothermic process. TD thus involves placing the sorbent tube in a geometrically compatible TD unit in the reverse direction as compared to the sampling direction (Fig.2.4), and heating the tube to the adsorbent material specific desorption temperature (Table 2.2). Note that Table 2.2 mentions the maximal ('default') desorption temperatures allowable above which thermal degradation of the adsorbent material starts to occur. In cases where one is only interested in the desorption of particular analytes of known boiling points, the lowest desorption temperature quantitatively eluting the targeted analytes from the adsorbent is preferred to using the default desorption temperature in order to avoid premature adsorbent material degradation and sample decomposition [123]. When the sample composition is unknown however, the default desorption temperature is used to enhance the chances of desorption of even the less volatile analytes. For multibeds, the global desorption temperature must not exceed the material-specific desorption temperature of any of the sorbent beds. As heat triggers the desorption of analytes to the gas phase, the carrier gas (He) connected to the TD and GC blows the desorbed analytes from the strongest to the weakest sorbent bed into the GC-column [32,76]. However, since the heat diffusion inside the tube is relatively slow owing to the radial tube geometry (the

center of the tube warms up later than the external sides) and in view of the diversity in analyte volatilities, a certain time (5-15 min [6,41]) and a certain carrier gas volume (some mL [124], depending on the carrier gas flow rate, e.g. 30 mL·min⁻¹ as recommended in the US EPA method TO-17 [107]) is required to desorb and transfer all analytes from the tube to the GC-column [32,41]. Synchronizing desorption and injection would therefore lead to dispersion of the analytes in a relative high carrier gas volume [41], leading to broad analyte peaks (poor resolution) in the GC [93,124]. To avoid this, most TD methods use a second, smaller (1-2 mm ID), sorbent focusing trap maintained at low temperatures (near ambient or sub-ambient temperatures, e.g. -30°C [41,44,71,124,130], -10°C [6,21], -5°C [131], usually obtained by electrical Peltier cooling effect [41,76]), placed downstream the sampled sorbent tube [22,32,93,134]: the sampled sorbent tube is heated ('primary TD') and thermally desorbed analytes, blown by the carrier gas, move to the second cold adsorbent trap whereon they adsorb in order of decreasing volatility (analyte 're-focusing' or 're-collection'). Once desorption from the initial sample tube is complete, the second cold focusing trap is rapidly heated ('secondary TD', e.g. 40°C·s⁻¹ [41,71], up to 100°C·s⁻¹ [76]) to the material specific desorption temperature of the sorbent(s) used in the trap, quickly thermally desorbing all re-focused analytes thus being instantly injected into the GC-column ('plug' injection) via a heated (~200°C) transfer line [6,32,41,76,124]. The smaller internal diameter of this second trap provides for a higher linear velocity of the analytes at a given carrier gas flow rate, realizing the rapid desorption [129]. Heating the transfer lines avoids adsorption and condensation of volatile species onto tubing [6]. Note the second focusing trap is also desorbed in the reverse direction as compared to the sampling (re-focusing) direction. At the end of the secondary TD, a 10 min high temperature hold can be applied to the focusing sorbent trap to ensure all least volatile analytes are desorbed and to simultaneously thermally clean the trap [6,41,44]. In modern TD units, the total carrier gas volume eventually injecting the refocused analytes into the GC can be as small as 100-300 µL, meaning analytes are concentrated in a tiny volume. The ratio of the initial sampled gas volume to this tiny injection volume hence determines the final concentration enhancement factor and the method sensitivity [76]: e.g. if the analytes from a 100 L sample are splitlessly transferred to the GC column in 100 µL of carrier gas, the concentration enhancement factor is 10⁶. There are two alternatives to second sorbent cold refocusing traps. The first one is to thermally desorb the sampled sorbent tube directly in the GC where analytes are concentrated at the entrance of the GC-column by holding this latter at an initial low temperature (typically 10°C) [124,129,134]. The second alternative is to use a cryofocusing trap. Here the refocusing of analytes thermally desorbed from the initial sampled sorbent tubes takes place by freezing them in a trap maintained at temperatures close to that of liquid nitrogen (~ -196°C) by means of liquid cryogen [32,138]. Drawbacks to this method are however the consumption of large volumes cryogen (expensive, energy intensive) and above all the blockage of transfer lines due to ice formation when dealing with humid samples [32,93,108,112,140]. Two-phase desorption with a second sorbent cold focusing trap is therefore preferred as furthermore the milder cold temperatures achieved by Peltier cooling suffice to quantitatively collect all volatile analytes. These second sorbent traps generally contain smaller amounts of sorbent than the effective sampling tubes, typically less than 100 mg [93] (e.g. 40 mg [124]). The chosen sorbent must quantitatively adsorb and desorb re-focused analytes over their whole volatility range and must withstand rapid heating rates or broad analyte peaks will be recorded. Two commercially

available and often used second sorbent traps are ~50 mg Tenax GR for analytes ranging in volatility from benzene to polychlorinated biphenyls and polycyclic aromatic hydrocarbons, and a dual-bed of carbon black and carbon molecular sieve sorbents for analytes ranging in volatility from C2 to n-C12 [41,93]. Table 2.4 lists some configurations of second cold focusing sorbent traps used by several authors for the thermal desorption analysis of air or biogas trace compounds sampled on adsorbent tubes.

Table 2.4: Examples of second cold focusing sorbent traps used for the thermal desorption analysis of air or biogas trace compounds sampled on adsorbent tubes. (H)VOC: halogenated volatile organic compounds.

Analyzed gas	Targeted analytes	Sampled adsorbent tube	Second cold focusing sorbent trap	Reference
Air	(H)VOC	Multibeds: • Quartz wool – glass beads – Tenax TA • Quartz wool – glass beads – Tenax TA – Carboxen X	Multibed : Quartz wool – Tenax TA – Carboxen X	[6]
Biogas	(H)VOC, mercaptans, siloxanes (mass range 35-290 a.m.u.)	Multibed: Tenax TA – Unicarb	Multibed : Tenax TA – Unicarb	[21]
Biogas	(H)VOC, siloxanes (mass range 20-450 a.m.u.)	Multibed: Carbotrap B – Carboxen X – Carboxen 569	Multibed : Tenax TA – Carbotrap B	[44]
Landfill gas	(H)VOC, dimethylsulfide, siloxanes (mass range 30-300 a.m.u)	Two single bed tubes in series: Tenax TA and Carboxen III	Tenax TA	[71]
Air	(H)VOC (mass range 30 - 200 a.m.u)	Multibeds: • Tenax TA – Amborsorb XE-340 – activated charcoal • Carbotrap C – Carbotrap – Carboxen II • Chromosorb 106 – Carbotrap B – Carboxen SII	Multibed : Tenax TA – Carbotrap B – Porasil® – activated charcoal	[127]
Landfill gas	(H)VOC (mass range 20-250 a.m.u.)	Multibed: Tenax TA – Chromosorb 102 – Carboxen SIII	Tenax TA	[130]
Air	(H)VOC (mass range 35 to 280 a.m.u)	Multibed: Tenax TA – Carbograph 1TD	Multibed : Tenax TA – Carbograph 1TD	[131]

Thermal desorption is not suited for thermally unstable compounds nor for very high boiling compounds (b.p. >300°C) since complete desorption is then not guaranteed but also because of the specific temperature limitations of adsorbent materials (Table 2.2) [131]. A method for tube thermal desorption efficiency determination is given in [124]. Unlike solvent extracted tubes, thermally desorbed tubes are reusable as TD is non-destructive: tubes undergo thermal regeneration upon each TD-run (same method as initial tube conditioning, see first section of this paragraph), theoretically removing all trapped analytes [5,32,76,93,108,131]. Some high boiling analytes may nonetheless be poorly desorbed and appear as contamination in subsequent samples trapped with the same tube [32]. Performing a second tube analysis to check remaining signals or systematically reconditioning tubes between sampling campaigns may be necessary to obtain the lowest background contamination levels [21,124]. Moreover, physical and chemical sorbent bed degradation occurring with time and as a result of reuse, limits tube reusability [32].

A last relevant consideration is the thermal desorption of tubes where on / in moisture has been trapped. When sampling humid gases, it is indeed sometimes inevitable to use hydrophilic adsorbents as they offer the strongest sorptive strength (Table 2.2) for the uppermost volatile species. During TD, any water trapped on the hydrophilic adsorbent will be transferred to the refocusing trap and to the GC, negatively impacting the retention of analytes on the GC column and interfering with the analysis [32,127]. A form of tube drying is hence necessary and two options are available. If the target analyte concentrations are sufficiently high to apply a split ratio of > 50:1 in the GC inlet port without compromising detection limits, desorbed water moisture should not interfere with the analysis. The sample should be split both at the sorbent tube and at the second refocusing trap for optimum effect [110]. When dealing with very low analyte concentrations, a lower split ratio or a splitless mode is preferred, in which case water moisture has to be removed from the sorbent tube via dry purging prior to TD and injection [32,41,93,109,110,112,127]. Dry purging involves purging the sampled sorbent tube with a flow of ~300 mL (at e.g. 50 mL·min⁻¹ [109]) dry pure inert carrier gas at ambient temperature (e.g. 27°C) in the sampling direction. Because the strong hydrophilic adsorbents for which this procedure may be required still have more binding affinities for the organic molecules trapped, even the polar ones, than for water, dry purging results in water being selectively vented off the tube without removal of even the most volatile and polar trapped analytes [32,93,110].

TD disadvantages are:

- Cost of thermal desorption unit [131]
- No possible repeated analysis of one given sampled sorbent tube [32,129,131,134]. All the sample is desorbed in one analysis. Nonetheless, depending on the sampled concentrations and GC-split ratio's used, modern thermal desorption equipment allow to recollect the split sample onto a fresh sorbent tube for immediate or delayed 'replicate' analysis [32,110,131]. This solution is however only feasible for relatively high concentrated samples necessitating a split in order not to saturate GC signals. Very low concentrated samples may need a splitless analysis in which case such sample recollection is not possible.
- Progressive degradation of adsorbent materials along with the reuse of tubes, leading to artefacts generation and higher blank levels [32,131]

TD advantages are:

- Sorbent tubes are reusable when thermally desorbed [5,32,76,93,108,131]
- 1000 fold higher analytical sensitivity compared to solvent desorption and hence lower gas volume need to be sampled compared to solvent desorption [32,76,110,131]
- No use of solvents, hence no corresponding interference with solvent signals masking analyte peaks in detectors [110,127,129,131]
- Possible automated desorption and injection [76] (commercial automated thermodesorbers available)
- Good desorption efficiency for polar as well as apolar (thermally stable) compounds [131]

Adsorbent material choice

Commercially available adsorbent materials suitable for respectively solvent or thermal desorption have been reviewed by Harper [32]. Owing to the greater analytical sensitivity and other advantages of TD compared to solvent desorption, TD is preferred for biogas and biomethane trace compounds characterization. Consequently, solely adsorbent materials suitable for TD are discussed here (Table 2.2).

Since adsorption is a surface phenomenon, the surface area effectively available for adsorption, determining the 'sorbent strength', is the most critical factor to consider when choosing adsorbents for a given application [32]. The surface area is a function of the material porosity: the smaller and the more numerous the pores, the higher the surface area, the stronger the adsorbent. Microporous sorbents (pore diameter < 2 nm) have therefore higher surfaces than mesoporous materials (2 nm < pore diameter < 50 nm) and macroporous materials (pore diameter >50 nm). Upon sampling on sorbent tubes, pores become covered with mono- or multilayers of analyte molecules, multilayers can especially form in macropores [32]. In micropores, each trapped molecule is close to all pore walls and experiences hence more surface-forces (Van der Waals forces) than in larger pores. Moreover, the presence of adjacent molecules in the micropore reinforces the overall adsorption strength [32]. Molecules are thus more strongly retained in micropores. Microporous materials have hence the highest sorption strengths and are accordingly used to trap the most volatile, smaller species. Microporous materials are also used for their molecular sieve behavior, i.e. molecules larger than the pore are not retained. Lastly, different pore shapes exist (tapered, pore opening smaller than pore body ...), also influencing pore filling mechanisms [32].

For each given gas sampling application on sorbent tubes, the analytical sensitivity is determined by the sampling and desorption efficiencies. Chosen adsorbents must be strong enough to completely remove and retain targeted analytes from the gas stream during sampling, and must be weak enough to enable the quantitative desorption (recovery) of the analytes upon TD [76,93,110]. Recoveries >80% are usually required in TD-methods. Recoveries between 20 and 80% indicate either analytes are too strongly retained or analyte broke through the sorbent bed, while recoveries < 20% indicate either irreversible adsorption or absence of sorption [125]. Selecting an adsorbent of appropriate strength (porosity) and appropriate adsorbent-adsorbate interactions and affinities (surface complexation, ion-exchange...) is therefore crucial, but sorbent strength has also to be considered with regards to breakthrough volumes during sampling [76,110,123]. The breakthrough volume (BV, L/g adsorbent) is the volume of a gas with a constant concentration, passed through the sorbent tube before a detectable level of analyte (typically 5% of the initial concentration) is detected at (elutes from) the outlet of the tube [32,93,107,120]. In general, stronger adsorbent materials have greater breakthrough volumes, allowing to sample larger gas volumes than weaker adsorbents [107]. An analyte breaking through a sorbent tube indicates the sorbent material(s) in the tube are saturated with respect to that analyte or that the analyte was displaced by another compound having stronger binding affinity [32]. Further sampling is no longer representative since concerned analytes are no longer trapped while the total gas volume passed is still recorded, leading to an underestimation of the analyte concentration. To avoid effective breakthrough and analyte loss

during sampling, a *safe sampling volume* (SSV), rather than the breakthrough volume, should be sampled and not be exceeded:

$SSV = \frac{2}{3} \times BV$ [107,124]. Determining breakthrough volumes is hence important but not straightforward since it is influenced by several factors such as:

- The adsorbent material used. Its porosity, surface area, chemical composition, hydrophobicity or polarity, particle mesh size... influence its capacity and affinity for given analytes [32,93,123,134,139]
- The mass of adsorbent packed in the tube and the tube geometry [134,139]. The higher the mass of adsorbent, the higher the BV. There is however for each adsorbent material a minimum mass required under which BV is 0, i.e. breakthrough occurs instantaneously. Adsorbent masses usually packed (~100 mg) in commercial tubes of typical dimensions (89 mm length, 4 or 5 mm ID) normally exceed the minimum required masses [32].
- The configuration (single- or multibed) of the adsorbent tube. Multibeds have higher BV than single beds, as demonstrated by Gallego et al. [143] in a comparison of single Tenax TA beds (200 mg) versus multibeds composed of Carbotrap B (70 mg), Carbopack X (100 mg) and Carboxen 569 (90 mg) for the trapping of VOC in air. Multibeds normally always have a higher total surface area than single beds (e.g. ~70 m² for the multibed versus ~ 7 m² for the Tenax bed of Gallego et al. [143]) and have therefore higher adsorption capacities.
- The temperature during sampling [120,123]. When sampling above 20°C, the BV is reduced by a factor 2 for each 10°C rise in temperature [124] (very approximate rule [110]) since adsorption is an exothermic process.
- The gas flow rate. Over the range 5 to 500 mL·min⁻¹ gas flow rate, the BV for tubes of typical commercial dimensions (89 mm length, 4 or 5 mm ID) is independent on the flow rate and only dependent on the total volume passed. However, at gas sampling flow rates < 5 mL·min⁻¹ or >500 mL·min⁻¹, the BV is substantially reduced [32,124]. Sampling should hence occur between 5 and 500 mL·min⁻¹, with 50 mL·min⁻¹ often mentioned as the optimal sampling flow rate (for air samples) for tubes of typical commercial dimensions (89 mm length, 4 or 5 mm ID) [22,76,93,124]. Other suitable sampling flow rate ranges mentioned are 5-200 mL·min⁻¹ [93], 10-200 mL·min⁻¹ [22,110] or 20-200 mL·min⁻¹ [76]. Note however that Gallego et al. [143] observed lower BV for air VOC with b.p. > 100°C on Tenax TA tubes (90 mm length, 6mm OD, 200 mg Tenax TA) when sampling a total volume of 90 L at 90 mL·min⁻¹ than when sampling 90 L at 70 mL·min⁻¹. They nevertheless did not observe BV differences when sampling 90 L air VOC at 90 or 70 mL·min⁻¹ on multibeds composed of Carbotrap B (70 mg), Carbopack X (100 mg) and Carboxen 569 (90 mg) [143].
- The analyte nature, its volatility and its concentration. On a given adsorbent, more volatile species have lower BV than less volatile ones [143]. The more concentrated an analyte, the lesser its BV. The BV of Sphero carb, a carbon molecular sieve adsorbent, for instance, is reduced by a factor 2 when high concentrations VOC are sampled [124]. Baya and Siskos [139] also measured lower BV at higher concentrations of octane and dichloromethane on Anasorb CMS. They suggest that at high concentrations, the first

(mono-) layer of adsorbates gets covered by a second layer of adsorbates, whereafter subsequent molecules are unable to interact with and sorb on active adsorbent sites. They alternatively suggest that at high adsorbate concentrations, the pores of the adsorbent material get filled and “closed” for subsequent adsorbates [139].

- The composition of the gas. The presence of competing analytes and especially the presence of water vapor in the gas can affect the BV of hydrophilic adsorbents [32,93,110] such as the strong carbon molecular sieves (e.g. Sphero carb): water vapor will tend to occupy sorption sites, impeding the sorption of targeted analytes and accordingly reducing their BV. At high relative humidity (95%) the BV of such strong carbonaceous adsorbents can be reduced by a factor 10 as compared to a low humidity scenario, while the BV of more hydrophobic porous polymer adsorbents is only reduced by a factor 2 [124]. Other sources report the BV of hydrophobic adsorbent materials (graphitized carbons, porous polymers) is not affected by relative humidities even up to 90% [110]. When sampling humid gas, it is therefore advised to determine BV using humidified calibration gases [32].

Safe sampling volume or breakthrough volume data for the sorption of a wide list of different (H)VOC on different adsorbent supports at 20°C and how to determine them is available in the literature (e.g. [29,93,120,124]). Apart from limiting the sampled volume to the SSV, breakthrough can be circumvented by placing several sorbent tubes in series ('backup' tubes) and analyzing all tubes or by placing a backup sorbent section in a same tube [32]. If breakthrough has occurred on the front sorbent bed/tube, only 5% of the initial analyte concentration is found on the backup bed/tube which can further efficiently adsorb the analyte. When more than 20-25% of the total analyte level is sorbed on the backup section, sampling on both the front and backup sections become inefficient and non-representative [32]. Also, when the SSV of a given analyte on a given sorbent (multi)bed is lower than 2 L, it is advised to use stronger adsorbent(s) [93].

A last consideration relating to sorbent strength concerns the mass of adsorbent packed in a tube. A small mass of an adsorbent of appropriate strength typically suffices to quantitatively adsorb and desorb trapped analytes [32,93]. If a too weak adsorbent is chosen, one may be tempted to increase its mass in the tube or to use larger tubes with high adsorbent masses to achieve quantitative sorption and less breakthrough. Oversizing sorbent beds compromises nevertheless the final analytical sensitivity. The thermal desorption of larger beds requires more time, leading to slow, less efficient analyte transfer to the GC with as result broader analyte peak bands in the chromatograms. Additionally, heating during TD is uneven in large tubes since the center of the tube may not reach the desired desorption temperature and consequently not desorb the analytes, while the outer parts may experience excessive temperatures and start to degrade. If the adsorbent bed length furthermore exceeds the limits of the zone heated during TD, desorption efficiency will be even poorer. Large tubes with high adsorbent masses are also difficult to stringently condition, giving higher contamination, artefacts and blank levels, and gas flow in such tubes may be heterogeneous and impeded by the thick packing [93,110]. Therefore, if it is noticed an adsorbent is too weak for a given application, it is preferable to substitute it by a (slightly) stronger adsorbent without exceeding optimal tube dimensions and packing mass instead of increasing its mass in the sampling tube or of choosing a tube with a larger diameter

[93]. Note however that, *if appropriate*, a weaker adsorbent is always preferred to a stronger one in order to ensure quantitative adsorption during sampling but especially a quantitative and rapid desorption during analysis [110].

Table 2.2 lists commercially available TD-compatible adsorbents of weak, medium and strong adsorptive strength usable for biogas and biomethane trace compounds sampling. Several adsorbent material classes exist: quartz or glass wool and glass beads (very weak, hydrophobic), porous polymers (weak or medium strength, hydrophobic), graphitized carbon blacks (GCB) (weak to medium strength, hydrophobic) and carbon molecular sieves (CMS) (strong, relatively hydrophilic). The formation mechanism and structure of carbon sorbents (GCB, CMS and porous carbons) has been reviewed by Matisová et al. [129]. All adsorbents differ in their physicochemical properties (density, temperature stability, surface area, surface functionalities and polarity, pore dimensions, hydrophobicity, chemical inertness...) and the resulting differences in kinetic and thermodynamic behaviors (breakthrough volumes, adsorption isotherms, adsorbent-adsorbate interactions ...) greatly influence their preconcentration and desorption efficiencies and hence the adsorbent choice for a given application [129]. As a general rule, the (surface) polarity of an adsorbent material governs its affinity for the sorption of given adsorbates, while the surface area of the adsorbent material determines the quantity of a given adsorbate that can be retained in the adsorbent (capacity). The ideal adsorbent would be one that is fully hydrophobic, that has infinite breakthrough volume, zero artefacts, that is chemically inert, able to quantitatively adsorb and desorb very low levels of volatile, semi-volatile, polar and non-polar compounds, that is thermally stable and stable upon storage. Such adsorbent does however not exist [112,120], motivating the use of multibed sorbent tubes to combine the properties of several adsorbents.

Quartz wool, although used as sorbent bed securing plug, also acts as weak adsorbent for intermediate or semi-volatile, relatively large or functionalized, species [6,108]. Sheu et al. [6] used it as very front bed in multibeds further packed with glass beads, Tenax TA and Carbopack X. The weak quartz wool/glass beads/Tenax TA trio was intended to collect large VOC's (C7+) while the stronger Carbopack X was supposed to collect small volatile VOC (C4-C10).

Polymeric adsorbents often derive from copolymers of polydivinylbenzene (DVB), have a weak to medium sorption strengths and include Tenax, Chromosorb, PoraPak, HayeSep and Amberlite XAD families. **Tenax TA** (replacing Tenax GC), a semi-crystalline macroporous polymer of 2,6-diphenyl-*p*-phenylene oxide (Fig.2.5 a) with a low surface area ($15\text{-}35\text{ m}^2\cdot\text{g}^{-1}$ [32,125,143]) and associated low adsorption capacity, is a weak adsorbent rather suited for trapping of large, less volatile compounds (b.p. > 50-100°C). Very volatile compounds such as pentane and dichloromethane are not retained on Tenax TA [125,139]. The diversity in pore sizes and especially the relatively large pores of Tenax TA enable it to trap and efficiently release adsorbates of various sizes (and associated volatilities) and bulkiness such as the bulky isooctane molecule [139] and large siloxanes [11]. Further, the inertness and high temperature stability of Tenax TA (Table 2.2) enable effective desorption of a wide range of intermediate or semi volatile species including Sulphur compounds [11,42,108,112] and halogenated VOC [11], and enable stringent conditioning leading to low background levels. In view of its high temperature stability and rapid desorption kinetics, Tenax TA can also be combined with the

strongest adsorbents, also having high desorption temperatures, in multibeds. For the same reasons, Tenax TA is also widely used in secondary cold focusing sorbent traps [32]. The inherent background contamination level of Tenax TA is low [110] although thermal desorption of Tenax TA at 300°C often generates trace amounts of thermal degradation by-products being typically benzene, toluene, ethylbenzene, xylene isomers, phenylethyne, styrene, naphthalene, biphenyl and phenol with benzene and toluene being the most abundant thermal degradation products of Tenax TA [144,145]. Also, the formation of artefacts in Tenax TA beds, such as acetophenone, benzaldehyde, benzacetaldehyde, phenol, nonanal and decanal from reactions with ozone or other oxidants (OH, NO₃, NO/NO₂), and 2,6-diphenyl-*p*-benzoquinone from reactions with air-borne nitrogen oxides is a limitation when sampling air [6,32,129,146] but should not when sampling biogas or biomethane. Tenax TA is theoretically hydrophobic and its sorption affinity for volatile polar compounds such as alcohols (e.g. isopropanol, 2-propanol), esters, ethers and ketones (e.g. acetone), is therefore poor [41,110,112,124,129,143]. The hydrophobicity of Tenax TA makes it however suitable to sample humid gases such as biogas, yet its adsorption capacity for polar compounds such as alcohols has been observed to increase at high moisture levels, suggesting some water retention [32,112]. Sunesson et al. [112] also shown the storage stability of organic vapors in a gas matrix with 85% relative humidity on Tenax TA beds was high after a storage period of 2 weeks in a freezer. **Tenax GR** is a mixture of various proportions of Tenax TA and graphite (e.g. 70% Tenax TA and 30% graphite) [32,147] with a lower surface area than Tenax TA alone but an even high temperature stability (Table 2.2) enabling it to trap and desorb heavy molecules. It is not clear however whether this combined adsorbent has a greater sorption efficiency than separate beds of Tenax TA and a graphitized adsorbent placed in series [32]. Sunesson et al. [112] additionally shown that Tenax TA and GR had similar sorption and desorption properties. **Chromosorb** adsorbents (from Celite Corporation, USA) are porous and 8 types exist (Chromosorb 101 to 108) [147]. Types 101, 103, 104 and 108 have low surface areas (<100 m²·g⁻¹) and thus weak sorption properties [134]. Chromosorb 106 (commercial equivalent: Anasorb 727 from SKC, Inc.) is a hydrophobic mesoporous copolymer of polystyrene-divinylbenzene with a higher sorption capacity and sorption strength than Tenax TA (surface area 750 m²·g⁻¹) [32,125]. It can accordingly sample higher concentrations without breakthrough. However, its thermal stability is lower (Table 2.2) and it can therefore not be used to sample semi-volatile compounds with boiling points higher than its temperature limit and also not be used in combination with strong sorbents in multibeds. Chromosorb 106 is better suited for (very) volatile species but only in relatively high concentrations (> ppb) as this adsorbent exhibits high blank background levels even after stringent conditioning [5,32,140,148]. Chromosorb 102 (styrene-divinylbenzene copolymer) has a lower surface area but a higher temperature stability than the 106 version, rendering it more suitable for semi-volatile compounds. Sunesson et al. [112] shown Chromosorb 102 and Anasorb 727 retain some water but a dry purge prior to TD-GC-MS could remove it. They also shown those materials efficiently sorbed and desorbed 2-propanol (while Tenax TA did not). **PoraPak** porous polymers (from Waters Corporation) are spherical beads with medium surface areas and temperature stabilities meaning they cannot be used to trap semi-volatile species with boiling points > ~200°C when TD is applied (Table 2.2). Eight commercial types exist (P, PS, Q, QS, R, S, N, T) covering a broad range of polarities and surface areas (from ~100 to 600 m²·g⁻¹), PoraPak Q (composed of ethylvinylbenzene and divinylbenzene) and PoraPak N (composed of

polyvinyl pyrrolidone and divinylbenzene) [147] being the most broadly used for TD applications. PoraPak Q is suitable to trap a wide range of VOC, oxygenated compounds and nitrogen oxides [107]. Brookes and Young [149] used Porapak Q sorbent tubes to trap acid, neutral and low molecular weight (volatile) compounds in landfill emissions and analyzed the traps via TD-GC-MS. These authors also investigated background contamination of Porapak Q blank tubes and found alkylstyrene artefacts [149]. PoraPak N efficiently traps and desorbs volatile nitriles, acrylonitrile, propionitrile, pyridine, volatile alcohols as well as a wide range of (H)VOC ranging in volatilities from chloroethane to hexachlorobutadiene [107,125], such as aldehydes, ketones, esters and ethers [150]. **HayeSep** porous polymer adsorbents (from Hayes Separation Inc.) consist of more than 10 types. HayeSep D is the most widely used in TD applications. It is hydrophobic, has a relatively high surface area ($795 \text{ m}^2\cdot\text{g}^{-1}$) making it a medium-strong adsorbent but its relatively low temperature stability (max. desorption temperature 180°C) does not allow the desorption of compounds with boiling points higher than 180°C (Table 2.2). A technical report by Supelco shown HayeSep D is nevertheless very suitable for efficient adsorption and desorption of a wide range of (H)VOC ranging in volatilities from chloroethane to hexachlorobutadiene [125]. **Amberlite XAD** polymers (from Rohm and Haas) are non-ionic hydrophobic or hydrophilic macroreticular resins where the surface sorption mechanism is based on Van der Waals and hydrophobic or hydrophilic interactions (H-bonding, dipolar interactions...) but not on ion exchange nor on pore size exclusion mechanisms. Several XAD types exist, differing in polarity and surface area. All XAD resins have low temperature stabilities ($<200^\circ\text{C}$) as a consequence of which they have rather been used with solvent-desorption applications [33,134,141]. Careful thermodesorption applications are nonetheless possible [151]. XAD 2 and XAD 4 are non-polar (hydrophobic) styrene-divinylbenzene crosslinked copolymers. The crosslinked structure gives a relatively high surface area, degree of porosity, rigidity, and mechanical strength to these resins. Their hydrophobicity results from the high number of aromatic benzene rings on the material surfaces. In view of their low temperature stabilities ($<200^\circ\text{C}$) they can only efficiently desorb light (low boiling) compounds. XAD 4 has a greater surface area ($750 \text{ m}^2\cdot\text{g}^{-1}$) than XAD 2 ($300 \text{ m}^2\cdot\text{g}^{-1}$) hence XAD 4 is better suited for very volatile species than XAD 2. Note that the manufacturing process of Amberlite resins leaves residues of preservative agents and monomers in the porous structure. Washing the resins prior to use is therefore necessary [134,151] if one does not purchase the available purified commercial versions available (e.g. Supelpack-2® from Supelco) to avoid interferences with manufacturing impurities.

Graphitized carbon blacks (GCB) are granular friable particles including Carbotraps, Carbopacks (from Sigma-Aldrich Co.) and Carbographs (from LARA s.r.l., Italy). Note that the sole difference between Carbotraps and Carbopacks is the mesh size: Carbotraps are 20/40 mesh size ($420 \mu\text{m} < \text{particle diameter} < 841 \mu\text{m}$) and Carbopacks are 40/60 mesh ($250 \mu\text{m} < \text{particle diameter} < 420 \mu\text{m}$) or smaller [125,133]. Carbographs are equivalents to Carbopacks/Carbotraps:

Carbograph 1 ~ Carbotrap / Carbopack B
 Carbograph 2 ~ Carbotrap / Carbopack C
 Carbograph 3 ~ Carbotrap / Carbopack F

Carbograph 4 ~ Carbopack Z
 Carbograph 5 ~ Carbotrap / Carbopack X

Other commercial equivalents to Carbotrap/Carbopack exist: Anasorb GCB1 and GCB2 (from SKC, Inc.) are respectively the equivalents of Carbotrap / Carbopack B and C. GCB are non-porous materials except for Carbotrap/Carbopack X and its equivalents: they are porous with closed-pores [133]. Very weak, weak, medium and strong GCB exist yet never being as strong as carbon molecular sieves (Table 2.2). The adsorbent-adsorbate interactions in GCB are solely non-specific, i.e. London dispersion and Van der Waals forces [44,129], with London forces prevailing in Carbopack B due to its non-polar surface [152]. The weakest GCB do not retain very volatile species but do retain intermediate or semi-volatiles species that they also effectively desorb thanks to their high temperature stability (Table 2.2). Weak and medium-strength GCB are accordingly often used as front beds in multibeds [32,109,125]. Carbopack C and B are among the most widely used GCB and are often used together in multibeds in view of their complementarity in the range of analyte they retain and effectively desorb [125,133]. GCB are hydrophobic in theory and their sorption affinity for polar compounds is therefore low [33,133]. Sunesson et al. [112] shown the sorption and TD-desorption recovery of 2-propanol on Carbopack B and Carbotrap C were respectively only 12% and 7%. Dimethyl sulfide was also poorly recovered from these adsorbents. However, GCB can retain some water especially when the relative humidity of the gas becomes high (>50%) [32,112,131]. Note also that as GCB derive from charcoal [129], some metal active sites may still remain on the material surface after the graphitization process. GCB may therefore not behave suitably with reactive or labile species such as reactive Sulphur compounds, terpenes and amines [110]. GCB may also catalyze reactions with α -pinene and aldehydes during thermal desorption [112]. The carbon black backbone of GCB (Fig.2.5 b) renders them extremely friable and prone to fines formation, especially upon tube ageing, increasing the bed resistance to gas flow. Fine particles may also enter TD-GC units and cause pollution or blockage. Over-compression of these adsorbents during tube packing and sharp knocks on packed tubes must thus be avoided [110]. Supelco launched a new product line of **spherical graphitized polymer carbon** (SGPC) adsorbents under the trademark Graphsphere™. Surface sorption on these materials occurs only via dispersion (London) forces and Graphsphere particles are spherical, yielding better packing performance than the granular shape of GCB, hard and non-friable [133]. SGPC offer similar sorption properties (hydrophobic, similar sorption strength) compared to GCB and are hence a great alternative for the granular and friable GCB.

Carbon molecular sieves (CMS): a CMS is the microporous carbon skeletal framework remaining after pyrolysis of a polymeric precursor. The packing bed performance of the as such obtained spherical particles is better than that of granular particles, and the particles are non-friable [133]. CMS materials are microporous (very) strong adsorbents and numerous commercial variations and equivalents exist (Carbosieve and Carboxen series (from Sigma-Aldrich), Sphero carb (from Analabs Inc.), Anasorb 747 and Anasorb CMS (from SKC, Inc.) ...). Carboxen® adsorbents have tapered (closed- or through-) pores given them excellent adsorption *and* desorption thermodynamic properties for very low boiling compounds. Adsorbent-adsorbate interaction in CMS are both non-specific (London and Van der Waals forces) and specific (e.g. dipole-dipole interactions) [44,129]. Carboxen 569 is the less hydrophilic material amongst the Carboxen family. Carbosieve® materials, prepared from polyvinylidene chloride, have non-tapered pores and extremely strong adsorption strength. Carbosieve S-III has closed-

pores and is a very strong sorbent (used e.g. for chloromethane sampling) although relatively hydrophilic [133]. CMS have among the highest temperature stabilities (Table 2.2) and are particularly used as the rear end of multibeds where they adsorb very volatile compounds (analytes with size relative to C₂-C₅ n-alkanes [133]). In multibeds, such strong sorbents have absolutely to be guarded by front weaker adsorbents that aim at retaining the high boiling compounds that would otherwise get irretrievably adsorbed on the strong back sorbent [32,125]. Note that all CMS are relatively hydrophilic [32,110,112] and that strong variations in sorbent strength, owing to differences in surface area's (Table 2.2), can occur among series, e.g. the Carboxen series, and among types, pointing at the difference between all CMS materials [32]. Lamaa et al. [120] shown that Carbosieve SIII had very low breakthrough volumes (< 0.3 L.g⁻¹) for volatile methyl siloxanes (trimethylsilanol and various siloxanes: L2, L3, L4, L5, D3, D4, D5, D6) whereas Carboxen 1000 had high breakthrough volume (~10⁴ L.g⁻¹) for those compounds. The inability of Carbosieve SIII to retain those volatile compounds was explained by the fact that the size of the compounds was larger than the opening size of the Carbosieve micropores (molecular sieve effect). Carbosieve SIII has only micropores while Carboxen 1000 has both micro- and mesopores, enabling the trapping of the compounds at least in the mesopores [120]. Baya and Siskos [139] evaluated the breakthrough volume of several compounds on 100 mg Anasorb CMS. They found isooctane quasi immediately broke through the adsorbent bed even at relatively low concentrations (2900 mg.m⁻³). The reason is that isooctane has a bulky structure not fitting in the small pores of Anasorb CMS. On the contrary, the same concentration of the octane isomer had a breakthrough volume of 1 L/100 mg Anasorb CMS thanks to its straight-chain shape enabling it to enter the slit-like pores of the adsorbent [139]. Other bulky compounds such as methylcyclohexane, ethylbenzene, decane and dodecane broke quasi instantaneously through or had low breakthrough values on Anasorb CMS. The C₆-ring in methylcyclohexane or in ethylbenzene probably would fit into the pores of Anasorb CMS but the aliphatic side groups seem to hinder it. The long aliphatic decane and dodecane chains can exist in different more or less bulky conformations, hindering their fitting into the Anasorb CMS pores [139].

Note that activated carbons are not suited for TD applications for the following reasons. First of all activated carbons have high contamination backgrounds owing to their complex surface structure displaying several functional groups [129]. Activated carbons are strongly hydrophilic because of polar surface groups (especially carbonyl and carboxyl groups) and of metallic and ionic salts in the material [129]. Hydrophilicity leads water to compete for sorption sites, decreasing the adsorption capacity of the adsorbent for a given analyte by occupying sorption sites or by removing sorbed adsorbates. Water can also cause interferences during the heating TD-step and GC analysis [125,134]. Activated carbons have extremely high surface areas and numerous differently functionalized sorption sites, causing irreversible adsorption, especially of polar compounds, owing to the strength of the multiple binding interactions (hydrophobic interactions, charge-transfer complexation, hydrogen bonding, cation exchange...) [129]. The thermal desorption of those and other compounds would require such high temperatures that compounds decomposition and artifact formation would occur, moreover without certainty of complete desorption [125,129,134]. Some charcoals naturally contain metals able to catalyze the degradation of trapped analytes under the high temperatures applied during TD [93,107].

Nonetheless, activated carbons may be used, only as the rearmost section of a multibed tube, for the trapping and thermal desorption of very volatile compounds such as halocarbon 12 (CCl_2F_2) and chloromethane when keeping the TD temperature below 200°C (Table 2.2) [125].

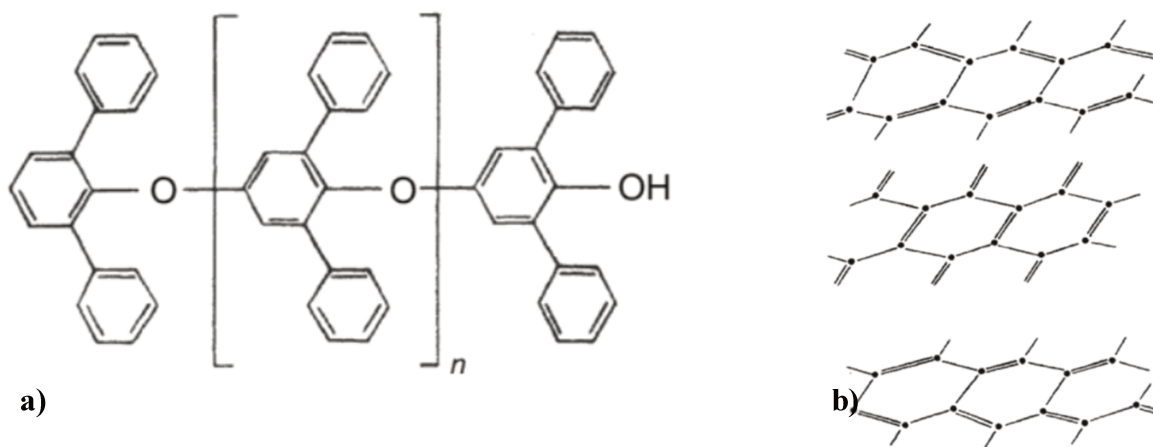


Figure 2.5: Chemical structure of two commonly used adsorbents: a) Tenax TA (poly-2,6-diphenyl-p-phenylene oxide). b) Carbotrap B (graphitized carbon black). Adapted from [153].

As discussed above for concerned adsorbent families, other factors than sorbent strength and breakthrough volumes are to consider when selecting adsorbents, such as chemical surface inertness of the adsorbent, its temperature stability, hydrophobicity, mechanical strength (friability) and inherent artefacts or artefacts formation [93,110,129]. Note that Chromosorb, PoraPak, HayeSep and Amberlite polymeric adsorbent families have higher inherent artefact levels than Tenax TA, causing more background signals in chromatograms which may interfere with the detection of targeted trace compounds if present in similar concentrations than the artefacts. GCB and CMS have the lowest inherent artefact levels when properly conditioned [110]. Stringent adsorbent tube packing, conditioning, sealing and storage is the key to minimize artefacts, yet tube materials (fittings, sorbent bed retaining gauzes...) also influence the level of artefacts [93]. The adsorbent particle size and shape (granular, spherical...) also influences the efficiency of the sorption-desorption process. Spherical particles pack better than granular ones [133] and small particles (smaller mesh size) having a higher surface-to-volume ratio yield higher sorption efficiencies [129].

Some important points are also worth mentioning concerning the choice of adsorbents when aiming at multibed preparation [110]. The volatility range of targeted analytes should be estimated and corresponding adsorbents should be chosen. When compatible, weaker adsorbents are always preferred so as to ensure quantitative desorption and to avoid water retention (as the hydrophobicity of adsorbents increases with increasing weakness). As already mentioned, adsorbents chosen to be assembled in a same tube must have the same temperature stabilities or it will not be possible to quantitatively desorb one bed without exceeding the maximum temperature of other bed(s). A last crucial aspect to consider is the risk of analyte migration from one bed to another via diffusion effects during storage of sampled multibeds. If a multibed is composed only of a short, weak front adsorbent (e.g. Tenax TA) directly followed by a very strong adsorbent (e.g. e strong CMS), large, heavier analytes initially trapped on the front weak bed can migrate to the strong bed and get irreversibly adsorbed to it. To avoid this,

multibeds should either contain a first, long bed of weak adsorbent followed by a strong sorbent, or contain an intermediate bed of medium strength.

Common multibed configurations aiming at screening gases of unknown compositions include [93,110]:

- Tenax TA (weak) – Carbopack B or equivalent (medium strength) – Carboxen 1000 or equivalent (strong), all in equal bed lengths. This combination is applicable to a broad range of analytes from very volatile to semi-volatile species, although each bed has its limitation (e.g. Carbopack (GCB) are not totally inert to reactive Sulphur species, terpenes, amines... and Carboxen 1000 (CMS) is relatively hydrophilic).
- Quartz wool (very weak) – Tenax TA (weak) – Carbopack X or equivalent (medium strength) with the Tenax bed slightly longer than the Carbopack X bed (e.g. length ratio 3.5:2). This multibed configuration is totally hydrophobic in theory but does not allow to trap the uppermost volatile species.
- Carbopack B or equivalent (medium strength) – Carboxen 1003 or equivalent (strong) with bed length proportions 2:1 or 1:1. This configuration targets volatile to very volatile species, with the disadvantage of the hydrophilicity of the Carboxen.
- Carbopack C or equivalent – Carbopack B or equivalent – Carboxen 1000 or equivalent. This is suitable to trap intermediate to very volatile species. Mind the hydrophilicity of Carboxen.

A wide range of ready-to-use commercial multibeds is available for numerous applications.

Bishop and Valis [127] compared three multibed configurations for TD-GC-MS analysis of organic vapors in air ($10 \mu\text{g}\cdot\text{mL}^{-1}$): Tube A: Tenax TA – Amborsorb XE-340 – activated charcoal. Tube B: Carbotrap C – Carbotrap B – Carbosieve II. Tube C: Chromosorb 106 – Carbotrap B – Carbosieve SII. The blank background signal of the 3 types of tube was satisfactory yet chromatograms of tubes A displayed some extraneous peaks. Studied analytes were: ethanol, methyl acetate, 2-butanone, tetrahydrofuran, cyclohexane, trichloroethylene, 1-nitropropane, pyridine, toluene, chlorobenzene, n-decane. Ethanol has the lowest recoveries on the three tube types. Tubes A were more effective than tubes B and C to retain polar compounds, but all types of tubes were more efficient in retaining non-polar compounds than polar ones. The authors also performed a storage stability test: one set of each tube type was spiked with the analytes and analyzed only after 1 month (storage in the dark at room temperature). Comparing the TD-GC-MS results of these tubes with tubes analyzed directly after being spiked shown that the most volatile and polar species had been partly lost during the 1 month storage. The tube A type shown less loss than the others. The loss mechanism (migration, moisture, long-term effects from co-adsorption of multiple compounds, oxidation, or other factors) was unclear [127]. The authors also tested the influence of water moisture in the gas on the adsorption efficiency of tube types A and B and found the retention of polar compounds on tube B was significantly affected by the presence of water moisture while tube A was not. Tube B contains indeed somewhat hydrophilic Carbosieve sorbent. They concluded tube type A has the largest potential for sampling of various analytes differing in polarities and volatilities even under humid conditions and under different concentrations [127].

Another example of successful multibed tube configuration used for sampling a wide range of VOC (halogenated alkanes and alkenes, ethers, alcohols, nitriles, esters, ketones, aromatics, a disulfide and a furan) in ambient air is given by Pankow et al. [109]. Tubes composed of 50 mg Carbotrap B and 280 mg Carboxen 1000 were used to trap the most volatile targeted species while tubes of 180 mg Carbotrap B and 70 mg Carboxen 1000 were used to trap less volatile species. Tubes were analyzed via TD-GC-MS and LOD's found ranged from 0.01 ppb_v for chlorobenzene to 0.4 ppb_v for bromomethane. After 8 and 27 days, the analyte storage stability on each multibed tube configuration was excellent to satisfying: >94% recovery for all compounds after 8 days except for chloroethene (89%) and 1,2-dibromo-3-chloropropane (90%); > 70% recovery for all compounds after 27 days, except for bromomethane which was only recovered at 52% [109].

Sorbent tube field considerations for biogas and biomethane sampling

When sampling humid gases such as biogas, sorbent tubes and all parts of the sampling train must be kept at a temperature slightly higher than the sampled gas to avoid any condensation of water or semi-volatile compounds on cold parts [107,110]. It is not advised to place a water retaining tube or membrane upstream of the sorbent tube insofar as water retaining materials (Nafion membranes, ascarite (NaOH coated silica), charcoal, drierite (CaSO₄), sodium carbonate, sodium sulfate, magnesium perchlorate, calcium chloride, calcium sulfate...) will also trap targeted analytes and prevent them from being sampled [6,127,154–157], even though some authors have advised the use of anhydrous calcium chloride before sampling siloxanes from wet synthetic biogas on silica gel adsorbent tubes [132].

When dry gases are sampled however, such as grid quality biomethane, it may be advantageous to electrically cool sorbent tubes to 5-15°C during sampling since adsorption is exothermic [6]. Another tricky precaution is to place a particle filter upstream the sorbent tube to avoid fine particles in the gas to enter the adsorbent beds where they could also act as adsorbing surface for targeted analytes, although the particle filter itself (e.g. a 2 µm Teflon mesh; a glass wool plug) can also adsorb targeted analytes and hence prevent their sampling [107].

Although this is more relevant for air monitoring purposes, sealed blank sorbent tubes identical to sorbent tubes planned to be used for sampling, can be taken to the field and handled in the same way as sampled sorbent tubes (transport, storage...) except for the actual sampling operation [32,93,124]. This helps to take passive contamination from the field area, transport and storage into account.

Next to restraining gas sampling volumes to calculated safe sampling volumes, analyte loss owing to breakthrough on field can be avoided by placing several (multibed) sorbent tubes in series. Also, high accuracy mass-flow controllers or flow regulators should be connected downstream the sorbent tube to stringently control flow rates and record sampled gas masses or volumes [6,107]. Because each analyte has a different breakthrough volume on each adsorbent, it is recommended to sample at low flow rates to prevent breakthrough, e.g. 50 - 100 mL·min⁻¹ [6,12,21,107,126,130,158,159]. The less volatile the analytes to sample, the lower the sampling flow rate should be [107]. Another tip is to sample an overall gas volume ≤ 80% of the safe sampling volume of the most volatile analyte [107].

Advantages and disadvantages of sorbent tube sampling

The greatest advantage of adsorbent tubes is their small size and associated fast sampling, easy handling, transport and storage [5,22,33,44,71,93]. As furthermore the flammable gas matrix (CH₄ for biomethane) is not trapped in the sample, no special transport for dangerous goods is required. Transport of sampled tubes to the lab offers a high flexibility in the type of analytical instruments and detectors to be used, since instruments unavailable for field deployment can be employed, allowing to identify and quantify a potentially broader range of compounds by combination of e.g. several detectors [6]. For sampling of biogas or biomethane, the production pressure may suffice to push the gas through the tubes so that no sampling pumps are required. Another advantage in the case of biogas and biomethane sampling is that permanent gases such as CH₄ and CO₂ (the gas matrices) are not retained on adsorbents, enabling the preconcentration of the constituting trace compounds. Analyte losses as was the case for gas bags, cylinders or canisters owing to surface loss mechanisms, is also avoided with adsorbent tubes and analytes in sampled sorbent tubes are therefore more stable in time [21].

The main disadvantage of sorbent tube sampling is the poor average time-representativeness of the composition of the studied gas. Since the sorbent tube is filled at one point in time, sampled analytes do not give information on the time-related composition variations of the gas, unless sampling campaigns are systematically repeated, or the gas is sampled at a very low flow rate during a long period [32,159]. Another disadvantage is that no single adsorbent combination is able to efficiently trap all analytes and that some reactive species (e.g. Sulphur compounds like CS₂, H₂S, mercaptans) are not stable on any adsorbent [32,42,118]. Other potential issues with adsorbent tubes include [129]: competition between untargeted and targeted analytes for sorption sites, especially for highly volatile targeted species with a weaker propensity to remain adsorbed; poor storage stability of analytes on adsorbent tubes due to contamination, irreversible adsorption, modification of sampled analytes and generation of “new” analytes by polymerization reactions on the adsorbent’s surface (e.g. siloxanes polymerization to silicone on silica gel [160]) or other reactions like hydrolysis [109] or oxidation in the sample [140]. Degradation of the adsorbent material, initiated during adsorbent conditioning, can lead to the release of degradation products during storage, increasing the background artifact level, falsifying the composition of the sampled gas and impoverishing the analyte stability [140]. The blank artifact level of some adsorbents, such as Tenax TA, may however be significantly lower than the sampled analyte concentration levels, in which case artifact build-up is less problematic even if artifact compounds are identical to some sampled targeted compounds [140]. Other constraints of adsorbent tubes are the limited adsorption capacity of an adsorbent for a given adsorbate and associated limited sampleable volumes before occurrence of breakthrough. The sampling flowrate through adsorbent tubes must also be adapted to each tube configuration, which requires preliminary calibrations to determine the optimal flowrate to ensure efficient adsorption and avoid premature adsorbent saturation or breakthrough [129].

Landfill gas, biogas and biomethane trace compounds sampling via adsorbent tubes

While a massive amount of publications deals with the analysis of trace compounds in air by preconcentration on adsorbent tubes and subsequent TD-GC-MS analysis (e.g. [109,143,148,161–163]), the number of publications on this topic but for trace compounds in

biogas or biomethane is much more reduced. Adsorbent tubes have nevertheless also been used in several studies to sample biogases and biomethane and characterize their trace constituents, those studies are reviewed in Table 2.5. Pioneering work in this regard aimed at identifying and quantifying trace compounds found in landfill gas emissions and being responsible for odoriferous and toxicological nuisances and associated health and environmental hazards due to poor atmospheric quality around landfills [149,164–166]. Importantly, all studies presented in Table 2.5 sampled landfill gas, biogas or biomethane at near atmospheric pressure. No single pressurized (biomethane) sample has been collected.

In 1983, Brookes and Young [149] established a method to sample landfill gas inside the fill via drive-in perforated piezometer probes able to reach depths from 1 to 4.3 m. A PTFE tubing connected to the probe further led the gas to the gas collection unit of this sampling train, either a grab collection unit or an adsorption tube. Two adsorbents were separately used in single bed tubes: Tenax GC (130 mg, 60/80 mesh, in a 6-mm OD glass tube) and Porapak Q (1 g, 60/80 mesh, in a 12-mm OD stainless-steel tube). Tenax GC was intended to retain non-polar species as well as a large spectrum of other compounds while Porapak Q was intended to retain acid, neutral and low molecular weight (volatile) compounds. The full sampling operation consisted of subsequently loading 3 individual Tenax GC tubes with 25 mL landfill gas at ambient temperature, and 2 individual Porapak Q tubes with 100 mL landfill gas at -80°C . The cold temperature during sampling of Porapak Q tubes was achieved by covering the second half of the tube's length with powdered solid CO_2 . For both Tenax GC and Porapak Q tubes, the gas was drawn through the tubes by means of a downstream-located gas syringe. The adsorbent tubes were analyzed by TD-GC-MS with a cryogenic trap between TD and GC injection. Tenax GC tubes were analyzed on a SE30 capillary column (50 m x 0.3 mm ID) while Porapak Q tubes were analyzed on a 80/100 mesh Chromosorb 101 packed column (1 m x 2 mm ID). Detection limits for the least traceable analytes (free acids, amines, alcohols) were $< 1 \text{ mg}\cdot\text{m}^{-3}$. For the other compounds, a LOD of $0.1 \text{ mg}\cdot\text{m}^{-3}$ was obtained. Concerning sampled sorbent tubes stability, the authors observed no adverse effects on samples stored at room temperature until analysis, but stressed out it was better to store them at cold temperatures in solid CO_2 [149]. The authors also analyzed artefacts and background contamination on both Porapak Q and Tenax GC blank tubes. Alkylstyrene compounds were found in the blank chromatograms of Porapak Q. C1 and C2 alkylbenzenes were found in very small quantities in Tenax GC but did not interfere with targeted analytes [149]. The sampling and analytical method developed in [149] was applied on field by Young and Parker [164] to identify and quantify trace compounds in landfill gas from 6 sites burying various types of domestic or industrial wastes. About a hundred different trace compounds were characterized, belonging to several chemical families such as alkanes, cycloalkanes, alkenes, esters, ethers, ketones, alcohols, terpenes, aromatic hydrocarbons, halogenated hydrocarbons and organosulphur compounds. Concentrations found ranged from 2.6 to $650 \text{ mg}\cdot\text{m}^{-3}$ and were dependent on the type and age of wastes in the landfill [164].

Assmuth et al. [166] also investigated hazardous trace compounds in landfill gas from active and closed municipal solid waste (MSW) and industrial waste landfills where no gas collection systems had yet been installed. Gas was collected from wells in the landfills and sampled on baked steel Tenax GC sorbent tubes at $10 - 15 \text{ mL}\cdot\text{min}^{-1}$ during 72 h by means of electric suction pumps connected via Telfon™ tubing. Before effective sampling, the sampling train, with

exception of the Tenax GC tubes, was flushed with landfill gas to avoid cross-contamination between study sites [166]. Such a pre-flush allows sorption- and sink-sites on inner surfaces of sampling equipment to already get occupied by potential targeted analytes or by other compounds so as to avoid targeted analytes losses by sorption upon effective sampling. Sampled sorbent tubes were stored at cold temperature and in the dark until analysis. The authors tested two storage temperatures: 4°C and -20°C and found 4°C was sufficient to guarantee sample integrity [166]. Sorbent tubes were analyzed via TD-GC-FID. Over 30 trace compounds were characterized with concentrations ranging from < 0.01 to 143 mg·m⁻³: 12 halogenated aliphatic hydrocarbons (chloromethanes, chloroethenes, chlorofluorohydrocarbons...); 10 aromatic hydrocarbons and phenolic compounds (BTEX, styrene, cresol...); 9 halogenated benzenes (including mono- and dichlorobenzene). The concentrations found for chlorofluorohydrocarbons were potentially underestimated since those compounds are not effectively retained on Tenax GC [166]. Styrene and *o*-, *m*- and *p*-cresol were detected but could not be quantified. Again, the authors found strong variations in trace compounds species and concentrations between different landfill sites, the type and age of wastes as well as sample representativity being influential factors.

Allen et al. [130,167] characterized trace (H)VOC in landfill gases using multibed adsorbent tubes and TD-GC-MS. The multibed was composed of Tenax TA (80/100 mesh), Chromosorb 102 (80/100 mesh) and Carbosieve SIII (60/80 mesh) in 1:1:1 volume ratio. Sampling involved passing 500 mL landfill gas through the sorbent tube at 50 mL·min⁻¹. Sampled tubes were stored at 4°C and analyzed within 24 h. The tube configuration yielded no breakthrough during sampling and all analytes could be recovered with ~100% from the adsorbents. Tubes were thermally desorbed via 2-step desorption with a secondary trap filled with Tenax TA. Method LOD was 0.1 and 0.02 mg·m⁻³ for respectively dichloromethane and decane. Landfill gas was sampled at seven sites and over 140 VOC were identified and quantified. Groups and concentrations found were [130]: alkanes (302-1543 mg·m⁻³); aromatic compounds (94-1906 mg·m⁻³); cycloalkanes (80-487 mg·m⁻³); terpenes (35-652 mg·m⁻³); alcohols and ketones (2-2069 mg·m⁻³); halogenated compounds (327-1239 mg·m⁻³).

Narros et al. [71] compared three different *in situ* sampling methods for VOC and siloxanes in landfill gas: whole gas sampling in 10 L Tedlar bags; adsorbent tube sampling on two different single bed tubes assembled in series (Tenax TA (60/80 mesh) and Carbosieve III (60/80 mesh)); and sampling via absorption in methanol impingers. Once in the lab, landfill gas sampled in Tedlar bags was intended to be transferred either to methanol impingers or to the adsorbent tubes to study the difference between direct absorption or adsorption on site or first whole gas sampling and then preconcentration. Liquid extracts from the methanol impingers were directly injected in a GC-MS while the adsorbent tubes were analyzed via TD-GC-MS. Adsorbent tubes were prepared in commercial stainless-steel tubes for Tenax TA and commercial glass tubes for Carbosieve III, each packed with a bed length of 6 cm and sealed with Teflon analytical caps and brass storage caps. For *in situ* sampling, a Tenax TA tube and a Carbosieve III tube were assembled in series and 100 mL gas was sampled via a manual pump. Tubes were thermally desorbed via 2-step desorption with a refocusing trap of Tenax TA. The authors targeted the following compounds in landfill gas: saturated hydrocarbons (heptane, octane, nonane, decane, undecane), aromatic hydrocarbons (benzene, toluene, ethyl benzene, *p*-xylene, propyl benzene,

p-cymene, styrene, cumene), sulphur compounds (dimethyl sulphide), halogenated compounds (tetrachloroethylene, 1,4-dichlorobenzene), ketones (acetone, 2-butanone, methyl isobutyl ketone), alcohols (ethanol, isopropanol, 1-butyl alcohol, 1-propyl alcohol, 2-butyl alcohol, isobutyl alcohol), esters (ethyl acetate, propyl acetate, methyl butanoate, butyl acetate, ethyl butanoate, butyl hexanoate), terpenes (α -pinene, limonene), siloxanes (hexamethyldisiloxane (L2), hexamethylcyclotrisiloxane (D3), octamethyltrisiloxane (L3), octamethylcyclotetrasiloxane (D4), decamethyltetrasiloxane (L4), decamethylcyclopentasiloxane (D5), trimethylsilanol (TMS)). Concentrations found ranged from <0 to $320 \text{ mg}\cdot\text{Nm}^{-3}$ [71]. After comparison of the analytical results from the 3 gas sampling methods, the authors concluded direct *in situ* sampling with adsorbent tubes was the best option [71]. Tenax TA and Carbosieve III enabled to sample simultaneously VOC, siloxanes and TMS (trapped on Tenax TA) while methanol impingers could not trap TMS. Adsorption tubes also gave higher quantitative results than the impingers for the most volatile siloxanes L2 and D3, but lower results for the less volatile siloxanes D4 and D5, probably due to difficulties to quantitatively desorb those more heavy species from the adsorbents [71].

A similar study was led by Raich-Montiu et al. [104] to preconcentrate and analyze siloxanes and trimethylsilanol in biogas generated from sludge digestion at different wastewater treatment plants. The authors compared *in situ* direct biogas sampling and preconcentration on adsorbent tubes and in impingers with whole gas sampling in a 200 L Tedlar bag (filled on the same day as the adsorbents and impingers) followed by laboratory preconcentration of the bag content on the same adsorbent tubes and impinger configurations. Impingers used were filled with n-hexane as absorption solvent. Adsorbent tubes used were commercial large ORBO 32 tubes packed with an activated coconut charcoal matrix (24–40 mesh) divided into beds A (400 mg) and B (200 mg) (Sigma–Aldrich). 10 L gas were sampled on the tubes at a flowrate of $1 \text{ L}\cdot\text{min}^{-1}$ and the tubes were analyzed via solvent desorption in n-hexane and GC-MS. Five different GC-columns (HP-5MS, TRB-G43, DB-1701, SUPELCOWAX 10, DB-624) were evaluated to determine the one resolving TMS and siloxanes the best. Biogas samples were eventually analyzed on a DB-624 column and the MS was operated in simultaneous scan (m/z 70-450 a.m.u.) and selected ion monitoring (SIM) mode. Statistical analysis showed there was no significant difference (significance level 0.05) between the results from the direct biogas sampling on adsorbent tubes (or impingers) and the results from biogas sampling in Tedlar bag and subsequent transfer to adsorbent tubes (or impingers). Concerning the effectiveness of the ORBO 32 adsorbent tubes, for each siloxane sampled the back-up bed (B) contained no or less than 10% of the content detected in the front bed (A), indicating a suitable tube configuration and no analyte loss during sampling. The authors therefore validated direct biogas sampling in adsorbent tubes was suitable for siloxane and TMS analysis, as furthermore transport and storage of the tubes were convenient [104]. Eight siloxanes (L2, L3, L4, L5, D3, D4, D5, D6) and TMS were successfully detected and quantified from adsorbent tubes at five different wastewater treatment plants. Concentration ranges determined were as follows ($\text{mg}\cdot\text{Nm}^{-3}$): TMS: $<0.02 - 0.9$; L2: <0.01 ; L3: $0.05 - 0.28$; L4: $<0.01 - 0.31$; L5: $<0.0 - 0.8$; D3: $<0.01 - 0.2$; D4: $1.5 - 10.1$; D5: $12.5 - 124$; D6: $0.4 - 0.5$ [104]. For samples taken directly at the biogas source, adsorbent tubes yielded higher concentrations than impingers for D4 and D5, hence adsorbent tubes can contribute avoiding underestimations of siloxanes potentially harmful for biogas energy conversion systems.

Rey et al. [113] investigated the trace compounds composition of MSW landfill gas and targeted VOC including halogenated compounds and siloxanes. Landfill gas was sampled into 1 or 2 L Tedlar bags and subsequently transferred to a preconcentration system. The authors compared different preconcentration systems and the analytical results respectively obtained: commercial adsorbent tubes (two adsorbent tube configurations were individually tested: Tenax TA and Carbotrap 349, the latter being a multibed packed with Carbopack Y, Carbopack B, Carboxen 1003), carboxen-polydimethylsiloxane (CAR-PDMS) SPME fibers, and activated carbon columns inserted in a special device intended to analyze halogenated components (Total Organic Halogen Analyzer, TOX-100 Mitsubishi Chemical Corporation). Adsorbent tubes were sampled according to the 8260 US EPA method and were analyzed via TD-GC-MS. SPME fibers were desorbed and analyzed via GC-MS. The results indicated that the SPME-GC-MS method was the easiest one. However, yet the majority of halogenated compounds could be detected via SPME, more compounds were chromatographically resolved, detected and quantified via the adsorbent tubes. 119 VOC including aliphatic and aromatic compounds, alcohols, ketones, esters, ethers, carbamates, terpenes, siloxanes, (in)organic Sulphur compounds and halogenated compounds were characterized via the Tenax TA tubes only, with concentrations ranging from $1.85 \cdot 10^{-2}$ to $72.6 \text{ mg} \cdot \text{Nm}^{-3}$. The multibed Carbotrap 349 adsorbed more compounds than Tenax TA thanks to the different adsorbent strengths of its constituting materials (Carbopack Y, Carbopack B, Carboxen 1003), but desorption from Carbotrap 349 was not always evident [113].

Arnold et al. [69] compared direct on-line measurement (no preconcentration) of siloxanes and VOC from biogases and landfill gases via a field-GC and a photo-ionization detector (PID), with their preconcentration on Tenax TA (sampling of 100 mL gas at $100 \text{ mL} \cdot \text{min}^{-1}$) and subsequent TD-GC-MS. For the direct on-line field measurements, the field GC was equipped with a Supelcowax 10 and a Carbopack B column and the detection limit in a biogas matrix was 0.01 ppm for siloxanes and VOC. Trimethylsilanol and halogenated VOC could however not be determined via this method and were only determined via adsorption on Tenax TA and TD-GC-MS. Siloxanes were determined with both methods. The Tenax TA method-LOD for siloxanes was $30 \text{ } \mu\text{g} \cdot \text{m}^{-3}$ and for halogenated compounds $100 \text{ } \mu\text{g} \cdot \text{m}^{-3}$. With the Tenax TA method, following concentration ranges were obtained ($\text{mg} \cdot \text{m}^{-3}$): siloxanes: 0.04 – 27.05; trimethylsilanol: $<0.01 - 2$; halogenated VOC: $<0.1 - 7$. In comparison with the results obtained from the direct on-line measurement method for siloxanes, the Tenax TA method yielded surprisingly lower concentrations [69]. The authors suggested these inconsistent results could be due to the small gas volume (100 mL) sampled on the Tenax TA tubes, and to natural variations in the biogases composition between the time of direct measurement and the time of Tenax TA sampling [69].

For the trapping and determination of siloxanes in landfill gas, Kim et al. [121] compared the conventional impinger technique (absorption in methanol) with adsorption on solid adsorbents. They evaluated three adsorbents: coconut-activated carbon (10-25 mesh), coal-activated carbon (10-25 mesh) and silica gel (5-10 mesh) intended for solvent desorption. The authors first validated the methods in the laboratory and used octamethylcyclotetrasiloxane (D4) as model compound since this siloxane is typically found in the highest concentrations in landfill gas. For the absorption method, 18 L of a standard D4 gas in N_2 was circulated at $150 \text{ mL} \cdot \text{min}^{-1}$ over three impingers each filled with 6 mL methanol and placed in series. The sampling procedure on the adsorbent tubes was passing 18 L of this standard gas at $600 \text{ mL} \cdot \text{min}^{-1}$ through three adsorbent

tubes (glass tubes, 7 cm length, 8 mm ID) of the same adsorbent material placed in series. D4 standard gases of 10, 30, 50, and 100 ppb ($\text{mg}\cdot\text{m}^{-3}$) were analyzed with both methods and each test was repeated 30 times. Tubes were desorbed by solvent (methanol) desorption with subsequent GC-MS analysis. For all D4-concentrations tested, results indicated coconut activated carbon yielded the highest reproducibility, accuracy, precision and recovery of the adsorbents tested, and the closest results to the conventional impinger method. The worst reproducibility was obtained for silica gel [121]. All investigated siloxane trapping methods were then applied to a real landfill gas sample under the same experimental conditions as the laboratory validation experiments. Average concentrations of total siloxanes in $\text{mg}\cdot\text{Nm}^{-3}$ were 8.91 ± 1.26 for the methanol impinger, 7.91 ± 1.86 for the coconut-activated carbon, 7.67 ± 2.12 for the coal-activated carbon and 5.54 ± 2.53 for the silica gel. The results obtained with coconut and coal activated carbon sorbent tubes were not significantly different from the impinger method while those obtained with silica gel were significantly different (lower) at the significance level $\alpha = 0.05$ [121]. Since adsorbent tube sampling is less labor intensive, requires less equipment and is faster than impinger sampling, the authors suggested that coconut-activated carbon adsorbent tube sampling was a reliable and suitable alternative for accurate quantification of siloxanes in biogas since this method gave high reproducibilities and recoveries.

Tansel et al. [122] also investigated the suitability of activated carbon sorbent tubes for the preconcentration of siloxanes from landfill gas and biogas from anaerobic digesters, with subsequent TD-GC-MS analysis. The sampling consisted in placing 4 carbon sorbent tubes (each packed with ~ 700 mg activated carbon) in series and drawing gas through them at $200 \text{ mL}\cdot\text{min}^{-1}$. One set of 4 tubes was sampled during 30 min, collecting 6 L gas, another set of 4 tubes was sampled for 1 h, collecting 12 L gas. This longer sampling was intended to provide information on the saturation potential (breakthrough) of the activated carbon. Also, placing 4 tubes in series was intended to provide information on the feasibility of single sorbent tube sampling by observation of analyte breakthrough to the subsequent tubes. The tubes in series also allowed to determine the selectivity and sorption efficiency of activated carbon for siloxanes in biogases. Results highlighted that a single activated carbon sorbent tube of ~ 700 mg was sufficient to quantitatively retain the light compounds trimethylsilanol (TMS; $3800 \mu\text{g}\cdot\text{m}^{-3}$ in landfill gas, $195 \mu\text{g}\cdot\text{m}^{-3}$ in digester biogas) and hexamethyldisiloxane (L2; $313 \mu\text{g}\cdot\text{m}^{-3}$ in landfill gas, $16 \mu\text{g}\cdot\text{m}^{-3}$ in digester biogas), but could not quantitatively trap other targeted siloxanes (octamethyltrisiloxane (L3), hexamethylcyclotrisiloxane (D3), octamethylcyclotetrasiloxane (D4), decamethylcyclopentasiloxane (D5) and dodecamethylcyclohexasiloxane (D6)) which were also found in various percentages on the second, third or even fourth tubes. Even with 4 tubes in series, the heavier D5 was not quantitatively retained neither from biogas nor from landfill gas. The first carbon tube of the series only retained 30% of the total detected D5 amount. For D3, D4 and D6 from landfill gas however, the first tube trapped respectively 100, 95 and 80% of the total amounts detected. For the digester biogas, the first tube trapped respectively 70%, 65%, 63% and 49% of the total amounts of D3, L3, D4 and D6. D3, L3 and D4 were fully trapped in the second tube. The heavy D6 was still present on the fourth tube after biogas sampling, indicating it was not quantitatively retained. The inability of activated carbon tubes to quantitatively retain heavy siloxanes was not so much related to very high concentrations in the gas nor to too high sampled volume causing analyte breakthrough, but, according to the authors,

rather to a lower affinity of activated carbon for high molecular weight siloxanes [122]. This assertion is however contradictory with the common theory that the sorption affinity and capacity of an adsorbent material for a compound rise with increasing molecular weight, density and boiling point, a theory that the authors themselves cite in their publication [122]. The fact that heavier siloxanes D5 and D6 are not quantitatively adsorbed on the activated carbon tubes may alternatively be caused by competitive sorption effects. In the landfill gas and digester biogas studied, a high concentration of relatively light compounds ($3800 \mu\text{g}\cdot\text{m}^{-3}$ TMS in landfill gas; $2725 \mu\text{g}\cdot\text{m}^{-3}$ D4 in digester biogas) was quantitatively adsorbed in the first or second tube. Those light compounds may limit the number available sorption sites for heavier compounds [122].

Arrhenius et al. led several studies to characterize trace compounds in biogas and biomethane by means of adsorbent tubes [22,168,169]. One of these studies [168] focused on the formation of terpenes in biogas produced from food waste digestion and their effects on gas processing equipment and workplace environment. Biogas and biomethane samples were collected in Altef bags from anaerobic digestion plants where food wastes are digested. The sampled gas was subsequently transferred to Tenax TA adsorbent tubes at a controlled flow over 1-2 minutes. Tenax TA tubes were analyzed via TD-GC-MS/FID with two-stage TD (cold refocusing trap between the Tenax TA tubes and the GC). For analyte detection, the GC column effluent was split into one stream going to the FID for quantification and one stream going to the MSD for identification. The Tenax TA trapping efficiency for the targeted terpenes (*p*-cymene, d-limonene, α -pinene, camphene, β -myrcene, β -pinene, α -terpinene, γ -terpinene, eucalyptol, 3-carene) and the method were first validated in the lab with a standard mixture of the targeted compounds prepared in an Altef bag. Results showed terpenes were quantitatively recovered from the Tenax TA tubes (recovery >85%). *p*-Cymene and d-limonene displayed slightly lower recoveries, likely due to sorption effects on bag walls since those compounds were present in higher concentration in the standard [168]. Results from the terpenes quantification in real biogas and biomethane samples indicated four dominant terpenes were present: d-limonene, *p*-cymene, β -pinene, α -pinene. Concentrations found (total terpenes) in raw biogas ranged from 360 to $1650 \text{ mg}\cdot\text{m}^{-3}$ and are influenced by the type of food waste (especially citrus fruits give rise to high terpenes concentrations), the share of food wastes in the digester and the digester operation temperature. The concentration range of total terpenes found in upgraded biogas (biomethane) was lower than in raw biogas: 5 to $240 \text{ mg}\cdot\text{m}^{-3}$ and was found to be dependent on the upgrading technique used [168]. The second study of Arrhenius et al. [22] also involved collecting real biogas or biomethane in 3 L Altef gas sampling bags (with polypropylene fittings) with immediate transfer to stainless-steel Tenax TA adsorbent tubes for VOC analysis. They demonstrate this two-step sampling and preconcentration procedure combines the advantages of sampling bags and sorbent tubes while eliminating their disadvantages. Gas bags can be filled at any flowrate, even at unstable rates, but the main disadvantage of gas bags is the poor short-term storage stability of trace compounds. On the other hand, the short-term storage stability of analytes trapped on an adsorbent material is very good, but the main disadvantage of adsorbent tube sampling is the requirement of a constant gas flowrate through the tubes during sampling. Gas transfer from the Altef bags to the Tenax TA tubes was executed via 3 methods, each time transferring 100 mL of the gas to a single Tenax TA tube at a controlled flowrate. Method 1 used

a 100 mL gas-tight syringe to draw the gas through the tube at 200 mL·min⁻¹. Method 2 used a commercial “easy-VOC” grab sampler (Markes International), a kind of syringe regulating the gas flowrate through the sorbent tube independently of the force used to pull the gas through by means of an internal restrictor. Flowrates obtained are ~500–600 mL·min⁻¹. Method 3 used a universal sampling pump to draw the gas through the tube. An upstream laminar flowmeter calibrated for the composition of biogas or biomethane ensured a flowrate of 50 mL·min⁻¹. The adsorbent tubes were analyzed within 1 day after sampling via two stage thermal desorption-GC-MS/FID. The GC column effluent is split, one part being quantified in the FID, the other being identified in the MSD. About 130 VOC were quantified from the biogas and biomethane samples, in concentrations ranging from 30 to 35 000 µg·m⁻³. Families and compounds found were alkanes (heptane, octane, decane, undecane, dodecane, tridecane, tetradecane, decahydronaphthalene and methyldecahydronaphthalene), aromatic hydrocarbons (toluene, *o*-xylene), terpenes (α -pinene, β -pinene, camphene, 3-carene, d-limonene, *p*-cymene), alcohols (1-propanol, 2-butanol), ketones (2-butanone, 3-pentanone, 2-pentanone), esters (ethyl propanoate, ethyl butanoate, ethyl pentanoate), furans (2-methylfuran, ethyl-furan) and Sulphur compounds (dimethylsulphide, dimethyldisulphide, thiophene, 2-methylthiophene, tetrahydrothiophene, 1-propanethiol). Concerning the three methods for biogas or biomethane drawing from the bags through the tubes, very similar results were obtained for the syringe and the “easy VOC” grab sampler. With the sampling pump method however, the authors observed identical results compared to the syringe and the “easy VOC” grab sampler only if the sampled gas has high humidity content. In gas samples with low humidity, low boiling analytes (up to 120°C b.p) were quantified similarly to the two other methods, but heavier, higher boiling analytes were underestimated. These results were explained by the lower flowrate used in the sampling pump method and by water adsorption effects in the Altec gas collection bags [22]. At low humidity, sorption sites on inner bag wall surfaces are not saturated with water and remain available for especially less volatile analyte sorption, causing their loss for analysis. Low sampling flowrates from the bags do probably not trigger the desorption of the compounds retained on bag walls while higher flowrates do. Authors hence advised sampling gas from the bags through the sorbent tubes using a high flowrate (>300 mL·min⁻¹) especially for gases with low moisture content [22]. In the last study of Arrhenius et al. [169], aiming at characterizing trace contaminants in biogas before and after upgrading to vehicle-quality biomethane, biogas and biomethane samples from different sources were sampled directly on Tenax TA adsorbent tubes at a controlled flowrate during 1-4 min. Tenax TA was intended to retain volatile and semi-volatile nonpolar or slightly polar compounds with boiling points ranging from 70 to 320°C. The analytical methodology is the same as in the other two studies: two step TD-GC-MS/FID with a quantification limit at ppb (mg·m⁻³) level. Results showed *p*-cymene (~60 – 190 ppm) and d-limonene (~10 – 30 ppm) were dominant trace compounds in raw biogases from household waste digestion. Other VOC were present at ~0-40 ppm levels. In raw biogas from sewage sludge digestion, the dominant trace compounds were toluene (~1 – 12 ppm), siloxane D5 (~1 – 2 ppm), linear, branched and aromatic hydrocarbons C9-C13 (~15 – 46 ppm), undecane (~2 – 3 ppm), decane (~1 – 3 ppm), dodecane (~1 – 2 ppm). Sulphur compounds, chlorinated hydrocarbons and dioxolanes were also found in lower concentrations. Much lower concentrations VOC were found in raw biogas from the digestion of industrial food residues and energy crops. The dominant species there were: 2-butanone (~1.25 – 1.75 ppm), pentanones

(~0.1 – 0.7 ppm), methylfurans (~0.2 – 1.5 ppm), toluene (~0.1 – 0.2 ppm), methylmercaptan (~ < 0 – 1.55 ppm), dimethylsulfide (~<0 – 1.95 ppm), dimethyldisulfide (~<0 – 0.6 ppm). The total concentration VOC in studied biomethanes was generally < 10 mg·m⁻³ [169].

Rasi et al. led two studies [59,61] where biogases from different sources (landfill, sewage sludge digestion, farm, co-digestion) were first sampled in Nalophan gas sampling bags and subsequently transferred to Tenax GR adsorbent tubes at 90 mL·min⁻¹. Tubes were capped and stored at -18°C until analysis via TD-GC-MS. The first study [59] aimed at trapping VOC from biogas on a Tenax GR tube. Total VOC concentrations recovered from biogases are given as results and were found to lie between 5 and 268 mg·m⁻³ depending on the biogas origin. Aliphatic and aromatic hydrocarbons, organic silicon, halogenated and reduced Sulphur compounds were amongst the most dominant compounds in landfill and sewage sludge digestion derived biogases. Benzene and toluene were detected in all samples in concentrations from respectively 0.1 – 2.3 mg·m⁻³ and 0.2 – 11.8 mg·m⁻³. Concentrations halogenated compounds found in landfill and sewage digester biogas ranged respectively from 0.3 – 1.3 mg·m⁻³ and <0.1 mg·m⁻³. Concentrations organosilicon compounds found in landfill gas ranged from 0.7 to 4 mg·m⁻³, in the sewage digester gas from 1.5 to 10.6 mg·m⁻³ and in the farm biogas < 0.4 mg·m⁻³. Their second study [61] focused on the determination of siloxanes and TMS. Two Tenax GR sorbent tubes (each containing 200 mg Tenax GR) were placed in series to sample the biogas from the Nalophan bag. The second tube aimed at capturing analytes having broken through the first tube. A two stage thermal desorption was operated with a cryogenic trap (-120 °C) before GC injection. Detection limits for the targeted compounds were (µg·m⁻³): TMS and L2: 0.65; D3: 0.83; L3: 0.77; D4: 0.57; L4: 0.71; D5: 1.30; L5: 0.64. All targeted siloxanes and TMS were detected and quantified in the real biogas samples. The total concentration siloxanes and TMS in the analyzed biogases ranged from 24 to 2460 µg·m⁻³ depending on the type substrate used for biogas production. Concentrations individual organosilicon compounds ranged from 1 µg·m⁻³ (L2) to 1.27 mg·m⁻³ (D5).

Hilaire et al. [12] were the first to analyze trace compounds of raw biogases, treated biogases and biomethanes from several sources, trapped on adsorbent tubes, with two-dimensional gas chromatography (GCxGC). It is often the case with single GC that compounds close in boiling point co-elute in a same chromatographic peak, hampering their distinction. GCxGC overcomes this problem by using two different columns: analytes first pass through a non-polar column (here Agilent DB-5MS) and then through a more polar one (here Agilent DB-17). Analytes co-eluting from the first column are normally resolved on the second column, enhancing the overall resolution of the analysis. The authors validated their GCxGC method with MS detection, with a liquid standard containing 89 compounds of 10 chemical families (each compound 10 µg·mL⁻¹ in 1:1 acetone/dichloromethane (v/v)) susceptible to be found as trace compounds in biogas and biomethane (17 monoaromatic hydrocarbons, 5 polyaromatic hydrocarbons, 10 alkanes, 6 cycloalkanes, 3 alcohols, 3 ketones, 4 esters, 3 furans, 2 aldehydes, 6 organosulphur compounds, 15 organic halogenated compounds, 2 alkenes, 5 terpenes, 9 siloxanes). Real gases were sampled on site on separate commercial ORBO 609 Amberlite XAD-2 and ORBO Charcoal tubes (Supelco). Each of those tubes is composed of two beds of the mentioned adsorbent. Flowrates through each tube were 100 mL·min⁻¹ for raw biogas (1 to 5 L collected) and 500 mL·min⁻¹ for treated biogases and biomethane (20 L collected). Adsorbent tubes were desorbed via pressurized

liquid extraction (solvent desorption) in acetone:dichloromethane (1:1 volume ratio). The first bed of each tube gave information on the amount trapped compounds while the second bed gave information on analyte breakthrough from the first bed. The extracts from the solvent desorption were then analyzed by GCxGC-MS. Analysis of the blanks of the Amberlite XAD-2 and Charcoal tubes indicated XAD-2 had 33 background contaminants while charcoal had 47 of them. Among these background contaminants, 4 compounds detected from the XAD were also targeted analytes, and charcoal had 12 background compounds common to the targeted analytes. ORBO Amberlite XAD-2 tubes were therefore preferred since they gave less contamination. ORBO Amberlite XAD-2 tubes proved furthermore to be more efficient in the trapping and recovery of biogas trace compounds: for a biogas sample, 216 chromatographic peaks were detected with the XAD-2 tube against 98 peaks with the ORBO Charcoal tubes [12]. For validation of the GCxGC method, the real gas samples trapped on sorbent tubes and solvent desorbed in the same way as above were also analyzed via the conventional single GC-MS method with a DB-5MS column to compare the results. Results clearly show co-elutions observed with the conventional single GC are resolved when using GCxGC. Overall, the adsorbent sampling, solvent desorption and GCxGC-MS method enabled the successful characterization of biogas and biomethane trace compounds with detection limits $< \mu\text{g}\cdot\text{Nm}^{-3}$. More than 100 compounds were detected from the samples, belonging to oxygenated-organic compounds, halogenated compounds, mono- and poly-aromatic hydrocarbons (e.g. toluene, ethylbenzene, *p*-cymene, α -pinene and d-limonene), alkanes, cycloalkanes, alkenes, terpenes and siloxanes. Total VOC concentrations for raw biogas samples for each family ranged as follows ($\text{ng}\cdot\text{mL}^{-1}$) : oxygenated compounds: $<0 - 300$; halogenated compounds: $<0 - 300$; monoaromatic hydrocarbons: $0 - 16000$; alkanes: $<0 - 1400$; terpenes: $0 - 4200$; siloxanes: $0 - 1300$ [12].

Mariné et al. [21] compared sampling of biogas from sewage sludge digestion in Tedlar bags and in multibed adsorbent tubes. The multibeds were prepared in SilcoSteel® passivated stainless-steel tubes (89 mm length, 6 mm OD) packed with Tenax TA as front bed and Unicarb as back bed (total adsorbent mass: 400 mg). For biogas sampling on adsorbent tubes, tubes were connected to the field biogas pipe via PTFE tubing and 500 mL gas was drawn through the tubes via a sampling pump at $500 \text{ mL}\cdot\text{min}^{-1}$. Tubes were immediately sealed and capped (PTFE ferrules) after sampling, stored at 4°C and analyzed within 3 days via TD-GC-MS. Two-step TD was operated with a cold refocusing trap also composed of Tenax TA and Unicarb. Tedlar bags (dual port stainless-steel fitting and polypropylene septum, 1.2 L) were connected the same way to the biogas pipes for sampling and stored at room temperature. The authors first compared the storage stability of biogas targeted trace compounds over a 4 days-period in Tedlar bags versus adsorbent tubes, by means of a standard containing siloxanes, alkanes, mercaptans and VOC. Fifteen freshly conditioned adsorbent tubes were loaded with the standard. Two tubes were directly analyzed and the others were stored at 4°C for delayed analysis after 1, 2, 3 and 4 days. As expected, storage stability was better on adsorbent tubes (insignificant analyte loss after 3 days) than in Tedlar bags (significant analyte loss after 1 day). Only after 4 days storage on adsorbent tubes did some compounds have a lower recovery response (e.g. the recovery of nonadecane, nonane or ethylmercaptan decreased by 30-50%) [21]. Note that siloxanes could not be determined via adsorption on tubes and TD-GC-MS due to incomplete desorption from the sampled tubes or from the refocusing trap, as also ascertained by Schweigkofler et al. [1,102].

They could only be determined and quantified (LOD $0.6 \text{ mg}\cdot\text{m}^{-3}$) via transfer from the Tedlar bag and direct GC injection. Mercaptans, VOC and alkanes (C8-C20) were however successfully quantified via the tube-TD-GC-MS method with even lower LOD than when sampled in Tedlar bags and injected onto the cold refocusing trap before GC injection. LOD of tube-TD-GC-MS method ranged from $2\cdot 10^{-5} \text{ mg}\cdot\text{m}^{-3}$ for dodecane, tridecane and tetradecane, to $2.5\cdot 10^{-3} \text{ mg}\cdot\text{m}^{-3}$ for limonene, dimethylsulfide and ethylmercaptan. LOQ for this method ranged from $1\cdot 10^{-4} \text{ mg}\cdot\text{m}^{-3}$ for several compounds to $0.01 \text{ mg}\cdot\text{m}^{-3}$ for ethylmercaptan [21]. Mercaptans, VOC, terpenes and alkanes from real biogas samples were successfully analyzed via the adsorbent tube-TD-GC-MS method, with concentrations ranging from 0.005 to $95 \text{ mg}\cdot\text{m}^{-3}$.

Gallego et al. [44] analyzed VOC including siloxanes in biogas from a mechanical-biological waste treatment plant by first sampling the gas in PVDF gas sampling bags (1 L Supel™ Inert Film bags, Supelco) and then immediately transferring the gas at $100 \text{ mL}\cdot\text{min}^{-1}$ via a pump to a multibed adsorbent tube (90 mm length, 6 mm OD glass tube) composed of Carbotrap B (20/40 mesh, 70 mg), Carbopack X (40/60 mesh, 100 mg) and Carboxen 569 (20/45 mesh, 90 mg), each bed separated with unsilanized glass wool. To establish the optimal gas volume to draw through the adsorbent tube, drawing 100 and 250 mL was evaluated. Additionally, analyte loss by breakthrough was checked by connecting two multibed tubes in series via a short PTFE connector. Adsorbent tubes were analyzed via TD-GC-MS. Two-stage TD was applied with a cold refocusing trap composed of 15 mg Tenax TA and 15 mg Carbotrap B. Targeted trace compounds were VOC (alkanes, aromatic hydrocarbons, ketones, halocarbons, aldehydes, esters, terpenes), trimethylsilanol and siloxanes. Method detection limits ranged “0.01– 0.8 ng per sample”. During real biogas analyzes, 117 compounds were identified: alkanes, aromatic hydrocarbons, alcohols, ketones, furans, halocarbons, aldehydes, esters, terpenes, chlorinated compounds, siloxanes, TMS, Sulphur and Nitrogen compounds [44]. The concentrations found were significantly different (significance level 0.01) between the 100 mL and 250 mL sampling case for 50% of the evaluated analytes, and the concentrations of the 100 mL case were higher. Total concentrations found in the 100 mL loaded tubes ranged from $1.3 \text{ }\mu\text{g}\cdot\text{m}^{-3}$ (1-methylnaphthalene) to $458\ 000 \text{ }\mu\text{g}\cdot\text{m}^{-3}$ (*p*-cymene) while the range was $1 \text{ }\mu\text{g}\cdot\text{m}^{-3}$ (1-methylnaphthalene and 2-methylnaphthalene) to $340\ 000 \text{ }\mu\text{g}\cdot\text{m}^{-3}$ (*p*-cymene) for the 250 mL loaded tubes. Detailed concentrations found for each compound in the 100 or 250 mL loaded tubes are given in the paper [44]. These results (higher concentrations in the 100 mL loaded tubes) were explained by the breakthrough experiments: slightly higher breakthrough percentages were observed in the case 250 mL gas was loaded on the tubes than in the 100 mL case. Especially very volatile compounds like acetaldehyde, carbon disulphide, ethanol and 1,3-butadiene were observed to have high breakthrough percentages (>5% and even more in the 250 mL case). The high breakthrough percentage recorded for ethanol may partly be caused by inefficient adsorption of this highly volatile compound in the cold refocusing trap. Thermal desorption of targeted analytes from the adsorbent tubes was found to be very efficient (99-100 % for most compounds) for both evaluated tube loading volumes (100 and 250 mL). Lower desorption efficiencies were nevertheless recorded for some analytes like benzene (90-92%), methylnaphthalenes (90-93%), phenol (90-95%) and carbon disulphide (71-85%). The authors therefore concluded both 100 and 250 mL gas loading on the multibed adsorbent tubes was

convenient for biogas sampling and trace compound analysis with respect to desorption efficiency [44]. However, to avoid breakthrough, the 100 mL case is more advised.

Salazar Gómez et al. [170] monitored 51 VOC (Silicon-organic compounds, terpenes, BTEX, furanes, ketones, alcohols, alkanes, esters and Sulphur-organic compounds) in biogases from 3 anaerobic digestion plants using different substrates and process conditions during 6 months to investigate correlations between substrates composition and trace VOC present as well as to evaluate seasonal effects on VOC concentrations and composition. Biogas was sampled on commercial single bed 200 mg Tenax TA adsorbent tubes (35/60 mesh, inert coated stainless-steel tubes, 8.89 mm length, 6.35 mm ID) at 100 mL·min⁻¹ during 1 min on two of the biogas plants and during 30 s on the last plant where VOC concentrations were higher so as to avoid breakthrough of the most volatile species. Identification and quantification of preconcentrated VOC's was performed by TD-GC-MS using a GC-MS prototype specifically designed for the simultaneous analysis of major and trace compounds in biogases. The adsorption-TD-GC-MS system was calibrated by spiking vaporized standard solutions of each of the 51 compounds prepared in methanol (except for TMS and siloxane D3 prepared in hexane) into sorbent tubes. LOD (mg·Nm⁻³) ranged 0.002 for ethylbenzene to 0.046 for octamethyltrisiloxane (L3) and all 51 target compounds could be detected across the biogas samples yet small alcohols, aldehydes and some thiols could not be quantified on the Tenax TA sorbent tubes.

Huppman et al. [141] investigated siloxanes in biogas from wastewater treatment plant (WWTP) sludge digestion using Amberlite XAD-2 or XAD-4 resins, activated carbon type F-400 or polyurethane foam as adsorbents, individually packed in glass tubes (155 mm length, 5 mm ID or 190 mm length, 14 mm ID) and fixed with glass wool plugs on both extremities. Biogas was first sampled in 60 L polyethyleneterephthalate gas sampling bags (supposedly inert to siloxanes) and then transferred through adsorbent tubes at 500 mL·min⁻¹. Solvent desorption was used to analyze the tubes content. Two solvent desorption approaches were compared: percolating the solvent through the tube in the reverse direction as compared to the sampling direction, or transferring the adsorbent materials into flasks wherein the solvent was added and the whole mixture ultra-sonicated to aid the solvent extraction. Three solvents were evaluated for the percolating extraction: hexane, cyclohexane, hexamethyldisiloxane. For the solvent extraction method with sonication, only hexane was used as solvent. Analysis was performed via GC to resolve the analytes and FID or MSD as detector. Results from the volatile cyclic siloxanes (D3, D4, D5, D6) used as standards and from the biogas samples indicated adsorption on XAD-2 with hexane desorption with ultra-sonification and GC-FID was the optimal method for quantitative preconcentration, desorption (recovery >95%) and quantification of the samples. The percolation method with hexane or cyclohexane for XAD-4 gave recoveries < 65% and with XAD-2 and hexane, at least 3 extraction steps had to be repeated to obtain recoveries > 90%. Percolation with hexamethyldisiloxane solvent on XAD-2 only gave 67% recovery after 3 extraction steps. With the polyurethane foam, the recovery was 0% when using hexane solvent and the percolation method. With activated carbon and XAD-4, the recoveries were respectively 91 and 78% when using hexane with the ultra-sonification method [141].

In a study on the removal of siloxanes from biogases for purification, Schweigkofler and Niessner [102] evaluated the siloxane adsorption capacity and the regenerability by thermal desorption

of several individual adsorbents: Tenax TA (60/80 mesh), Amberlite XAD-2 (20/60 mesh), zeolite molecular sieve 13X (45/60 mesh), silica gel (particle size 1–3 mm), activated charcoal (particle size 2.5 mm) and Carbopack B (60/80 mesh). The authors first handled two model siloxane compounds: a high volatility siloxane (L2) and a low volatility siloxane (D5), both prepared in a N₂ gas matrix at 1 g·m⁻³. Adsorption experiments were performed by drawing those standard gases at 200 mL·min⁻¹ through adsorbent tubes (120 mm length, 5 mm ID) each packed with 500 mg of one of the adsorbents to test, until 5 mg siloxane has been passed. Siloxanes escaping at the outlet of the tubes were absorbed in an organic solvent being regularly analyzed by GC-FID for tube breakthrough control. Adsorbent tubes were analyzed by TD-GC-MS/AES. It appeared from these standard tests that all adsorbents had a sufficiently high adsorption capacity for the high boiling siloxane D5 as no breakthrough was observed after passing 5 mg of the siloxane on the adsorbents, except on Tenax TA and molecular sieve 13X where a slight breakthrough was observed after passing 4.5 mg D5 [102]. However, the adsorption capacities of the adsorbents were lower for the low boiling siloxane L2. Especially XAD-2 was unsuitable to retain L2: 55% of the initial L2 amount was found in the tube effluent only after passing 0.5 mg L2 through the tube. Breakthrough also occurred on Carbopack B, Tenax TA and molecular sieve 13 X after passing respectively 0.5 mg, 1 mg and 1 mg L2 on the tubes. Only silica gel and activated charcoal were able to retain the 5 mg L2 without breakthrough. Thermal regeneration of adsorbents was only evaluated for silica gel and activated charcoal since only those were able to quantitatively trap both L2 and D5. Thermal regeneration of silica gel adsorbent tubes loaded with siloxanes L2 and D5 occurred by heating the tubes at 250°C during 20 min and flushing them with 200 mL·min⁻¹ carrier gas in the reverse sampling direction. L2 and D5 desorption recoveries were > 95%. Under the same conditions, the thermal regeneration of activated charcoal was less efficient: although L2 desorption recovery reached > 95%, the desorption recovery of the heavier D5 was only 74-83%. Authors concluded activated charcoal is not suitable for practical siloxane removal in biogases since relatively heavy siloxane species such as D4, D5 and D6 are abundant in biogases, which would imply a frequent replacement of activated charcoal units due to poor regeneration regarding heavy siloxanes [102]. After these laboratory validation experiments, the authors sampled biogas from a sewage treatment plant directly into evacuated 15 L stainless-steel Tekmar canisters. Raw biogas (relative humidity at 20°C RH_{20°C} >85%) and biogas dried by refrigeration (RH_{20°C}=38%) were sampled. These biogases were then drawn at 1L·min⁻¹ through an adsorbent tube (200 mm, 12 mm ID) packed with 2 g silica gel. Analysis revealed total siloxane (L2, D3, D4, D5) concentrations in raw biogas was 16.2 mg·m⁻³ and in dried biogas 14.8 mg·m⁻³ [102]. Although this study rather focused on breakthrough volumes of siloxanes in biogas drawn through silica gel beds for large-scale siloxane removal purposes, and on the negative influence of the biogas humidity on the siloxane removal (adsorption) efficiency due to the hydrophilicity of silica gel, the study shows silica gel can be a suitable adsorbent for screening analysis of siloxanes over a broad range of volatilities and polarities. It also shows silica gel adsorbent tubes can be thermally desorbed. However, in a similar study by Sigot et al. [160], it is stressed out silica gel thermal regeneration can be ineffective due to siloxane polymerization to silicone on the surfaces of the adsorbent. They propose easy to desorb hydrogen bonds form between siloxanes and silica gel at low siloxane uptake, while stronger bonds are created by surface polymerization at higher siloxanes loads, hampering their desorption [160].

Paolini et al. [171] sampled biogas and biomethane before and after the upgrading unit (a vacuum swing adsorption on synthetic zeolite 13x) at a waste water treatment plant with anaerobic sludge digestion to investigate the technical feasibility of the upgrading process and its efficiency in achieving low levels of trace compounds in the biomethane to meet compliance requirements to current regulation for biomethane use as vehicle or injection in the natural gas grid. For the analysis of VOC and siloxanes, biogas and biomethane were sampled on carbon cartridges filled with graphitized and activated carbon similar to those used by Tansel and Surita [122]. Sampled cartridges were analyzed by TD-GC-MS and a cryogenic (liquid N₂) 100% polydimethylsiloxane (PDMS) transfer line was used to re-focus the analytes after thermal desorption of the sampled cartridges and before injection in the DB1-MS GC column. A PDMS re-focusing transfer line was chosen because of its low siloxane bleeding levels. However, owing to its poor chromatographic separation of VOC and siloxanes, the PDMS transfer line had to be cryogenic to re-focus the analytes and improve the chromatographic resolution [171].

Tassi et al. [172] compared the use of solid phase microextraction (SPME, using a 50-30µm Divinylbenzene -Carboxen-Polydimethylsiloxane fiber), and multibed adsorbent tubes composed of 3 beds (Carbosieve 111 - Carboxen B - Carboxen C) for the preconcentration of VOC in volcanic gases and landfill gas. They found SPME and multibed adsorbent tubes were both efficient and provided comparable VOC compositions in the analyzed gases (37 VOC amongst linear and cyclo- alkanes, alkenes, aromatics, poly aromatics, furans, halogenated, aldehyde, alcohols, organosulphur compounds).

Lastly, dimethylmercury in MSW landfill biogas is the sole metallic trace compound having successfully been sampled on adsorbent tubes. Mercury-species (gaseous Hg⁰, monomethylmercury and dimethylmercury) in MSW landfill stem from Hg-bearing materials such as fluorescent lamps, alkaline batteries, electrical and ignition switches, electronics (computer monitors), thermometers, thermostats, barometers, manometers, paint residues, and depending on national legislation, from dredge spoil of Hg-contaminated sediments and solid residues from fossil fuel combustion and oil refineries [173-176]. Biogeochemical processes (microbial or abiotic) taking place in landfills under aerobic or anaerobic conditions convert mercury from those materials into volatile Hg-species [175,176]. In landfill gas, gaseous Hg⁰ is the most abundant mercury species. Lindberg et al. [173,174] preconcentrated dimethylmercury in landfill gas from several landfills on Carbotrap™ adsorbent tubes (40-60 mesh, 10 cm × 4 mm ID adsorbent bed, packed between silanized glass wool plugs in a silanized glass tube) having high adsorption affinity and capacity for dimethylmercury while not retaining the most abundant Hg⁰. Carbopack™ blank tubes only shown small inherent Hg⁰ background likely arising from the thermal reduction of inorganic Hg contained in the adsorbent material, but it was demonstrated that this Hg⁰ background was not converted into dimethylmercury on the adsorbent surface during analyses [173]. For sampling, as landfill gas is humid, Carbotrap™ tubes were placed downstream condensate traps and were purged with dry nitrogen immediately after sampling to expel residual water. In [174], Carbotrap™ tubes were also maintained in a heated probe at few degrees above ambient temperature to prevent water condensation on the adsorbent during sampling. Additionally, a 5 µm Teflon filter and a guard column (OV-3 on Chromasorb WAW-DMCS 80/100 mesh) were placed upstream each Carbotrap™ tube to respectively retain particulate matter and other semi-volatile organic trace

compounds and prevent their sorption on the Carbotrap™. Carbotrap™ tubes were usually sampled with 5L landfill gas at 300 mL·min⁻¹ and subsequently protected from light and refrigerated for transport and storage until analysis. Together with purging the sampled tubes with an inert dry gas (nitrogen or argon, 10 min at 100-200 mL·min⁻¹) right after sampling, those precautions have been proved to safeguard high dimethylmercury stability on the Carbotrap™ tubes during >28 days [177]. Recovery of trapped dimethylmercury occurred via thermal desorption of the Carbotrap™ tubes (45 s at a 25°C to 450°C ramp) hyphenated with gas chromatography – cold vapor atomic fluorescence spectrometry (TD-GC-CVAFS). The GC was operated in isothermal mode (80 ± 2°C; 1 m × 4 mm ID column of 15% OV-3 on Chromasorb WAW-DMCS 80/100 mesh) and the methylated mercury eluting the GC is sent to a pyrolytic cracking column (700°C) converting it to elemental Hg⁰ required for detection by CVAFS [173]. Mean dimethylmercury concentrations found were ~30 ng·m⁻³ in the studied landfill gases [173,174]. In [174], the authors pointed out the recovery of dimethylmercury from Carbotrap™ was higher at smaller sampled gas volumes (0.92 L > 3.6 L > 7.1 L), probably due to the displacement, when large gas volumes are sampled, of the relatively weakly bound dimethylmercury by other trace compounds in the landfill gas (in spite of the guard column) having stronger binding affinities with Carbotrap™ [177]. In [177], the authors investigated the influence of sampling flowrate and volume, temperature and humidity on breakthrough of dimethylmercury through the Carbotrap™ tubes. At ambient temperature and humidity and a dimethylmercury concentration of 5–6 ng·m⁻³ in air, breakthrough volume was 100 L over a flowrate range of 0.025 – 0.13 L·min⁻¹. Total volume sampled was more critical than flowrate for the breakthrough determination. The breakthrough volume was sharply decreasing at high humidities (>70%_{RH}) and temperatures (>35°C). Finally, other adsorbent matrices were considered in [177] for the preconcentration of dimethylmercury: Tenax™, Carbosieve™ S-III, Carboxen™-563, Carboxen™-564 and Carboxen™-569. None of them were suitable: Tenax™ did not adsorb dimethylmercury while this latter was too strongly adsorbed on all carbon molecular sieves tested with non-quantitative recovery as result.

Table 2.5: Review of studies using adsorbent tubes to sample and preconcentrate trace compounds in landfill gas, biogas and biomethane. All gas samples were taken at near atmospheric pressure.

MSW = municipal solid waste. AD: anaerobic digestion. WWTP = waste water treatment plant (anaerobic digestion of WWTP sludge). TD-GC-MS = thermal desorption – gas chromatography – mass spectrometry. FID = flame ionization detector. ATD = automated thermal desorption system. TDS = thermal desorption system. ToF-MS: time-of-flight mass spectrometry. TMS = trimethylsilanol. VMS = volatile methyl siloxane. RH = relative humidity.

Adsorbent tube composition	Sampled gas	Sampling conditions	Characterized compounds	Concentration range observed	Analytical method	References
Single beds: Tenax GC (0.13 g, 60/80 mesh) or Porapak Q (1 g, 60/80 mesh)	Landfill gas	Tenax GC tubes: 25 mL gas drawn through the tube at ambient temperature, via a syringe; Porapak Q tubes: 100 mL gas drawn through the tube at -80°C, via a syringe	alkanes, cycloalkanes, alkenes, aromatic hydrocarbons, terpenes, halogenated hydrocarbons, alcohols, ketones, esters, ether, organosulphur compounds	2.6 to 650 mg·m ⁻³	TD – GC – MS (GC with 80/100 mesh Chromosorb 101 packed column (1 m x 2 mm ID) for analysis of the Porapak Q tubes, and SE30 capillary column (50 m x 0.3 mm ID) for the analysis of the Tenax GC tubes – VG Micromass MM16F MS)	[149,164]
Tenax GC	Landfill gas	Sampling at 10 - 15 mL·min ⁻¹ during 72 h by means of electric suction pump	12 halogenated aliphatic hydrocarbons; 10 aromatic hydrocarbons and phenolic compounds; 9 halogenated benzenes	< 0.01 – 143 mg·m ⁻³	TD – GC – FID	[166]
Multibed (1:1:1 volume ratio): Tenax TA (80/100 mesh) + Chromosorb 102 (80/100 mesh) + Carbosieve SIII (60/80 mesh)	Landfill gas	500 mL landfill gas passed through the sorbent tube at 50 mL·min ⁻¹ Tubes stored at 4°C and analyzed within 24 h	Over 140 VOC, belonging to several chemical groups: alkanes, aromatic compounds, cycloalkanes, terpenes, alcohols and ketones, halogenated compounds	alkanes (302-1543 mg·m ⁻³); aromatic compounds (94-1906 mg·m ⁻³); cycloalkanes (80-487 mg·m ⁻³); terpenes (35-652 mg·m ⁻³); alcohols and ketones (2-2069 mg·m ⁻³); halogenated compounds (327-1239 mg·m ⁻³)	TD-GC-MS (Perkin Elmer ATD 50 with second refocusing trap Tenax TA – HP 5890 GC with Restek RTX-1 column (60 m x 0.32 mm x 1.5 μm) – HP 5970 MS) LOD between 0.02 (decane) and 0.1 mg·m ⁻³ (dichloromethane)	[130,167]
Two different single bed tubes in series: Tenax TA (60/80 mesh) and Carbosieve III (60/80 mesh)	Landfill gas	100 mL gas drawn through the tubes via a manual sampling Gastec pump	Alkanes, aromatic hydrocarbons, organosulphur compounds, halogenated compounds, ketones, alcohols, esters, terpenes, siloxanes, trimethylsilanol	< 0 to 320 mg·Nm ⁻³	TD-GC-MS (Perkin Elmer TurboMatrix 650 ATD – Perkin Elmer Clarus 600 GC with Supelco Equity-1 column 60 m x 0.25 mm x 1.0 μm – Perkin Elmer Clarus 600T MS)	[71]
Commercial ORBO 32 tubes (activated coconut charcoal matrix (24–40 mesh) divided into beds A (400 mg) and B (200 mg) (Sigma–Aldrich)	WWTP biogas	10 L sampled at 1 L·min ⁻¹	Siloxanes (L2, L3, L4, L5, D3, D4, D5, D6) and TMS	(mg·Nm ⁻³): TMS: <0.02 – 0.9; L2: <0.01; L3: 0.05 – 0.28; L4: <0.01 – 0.31; L5: <0.0 – 0.8; D3: <0.01 – 0.2; D4: 1.5 – 10.1; D5: 12.5 – 124; D6: 0.4 – 0.5.	Solvent desorption – GC – MS (n-hexane as solvent – Agilent 6890N GC with DB-624 column (6%-cyanopropylphenyl-94%-dimethylpolysiloxane 30 m x 0.25 mm x 1.4 μm) – Agilent 5975B MS). LOQ : 0.02 mg·m ⁻³ for TMS and 0.01 mg·m ⁻³ for the siloxanes	[104]

Table 2.5: continued

Adsorbent tube composition	Sampled gas	Sampling conditions	Characterized compounds	Concentration range observed	Analytical method	References
Single bed: Tenax TA or Carbotrap 349 (multibed packed with Carboxen Y, Carboxen B, Carboxen 1003)	Landfill gas	1-2 L Tedlar bag and subsequent transfer to sorbent tube (8260 US EPA method)	119 VOC including aliphatic and aromatic compounds, alcohols, ketones, esters, ethers, carbamates, terpenes, siloxanes, (in)organic Sulphur compounds and halogenated compounds.	$1.85 \cdot 10^{-2}$ to $72.6 \text{ mg} \cdot \text{Nm}^{-3}$ Total halogen content in all the samples was $< 22 \text{ mg Cl} \cdot \text{Nm}^{-3}$	TD-GC-MS (horizontal Gerstel TDS-2 – Agilent 6890N GC with Agilent DB-624 column (30 m x 0.25 mm x 1.4 μm) – Agilent 5973N MS)	[113]
Tenax TA (60/80 mesh)	AD biogas and MSW landfill gas	100 mL, sampled at $\sim 100 \text{ mL} \cdot \text{min}^{-1}$	Siloxanes (L2, L3 L4, D3, D4, D5), trimethylsilanol and halogenated compounds	Siloxanes: $0.04 - 27.05 \text{ mg} \cdot \text{m}^{-3}$; Trimethylsilanol: $< 0.01 - 2 \text{ mg} \cdot \text{m}^{-3}$; Halogens: $< 0.1 - 7 \text{ mg} \cdot \text{m}^{-3}$	TD-GC-MS (Perkin Elmer ATD 400 – HP 5890 GC – HP 5972 MS) LOD for siloxanes: $30 \mu\text{g} \cdot \text{m}^{-3}$; for halogenated compounds: $100 \mu\text{g} \cdot \text{m}^{-3}$	[69]
Three tubes of one and the same adsorbent in series. Three adsorbents evaluated: coconut-activated carbon (10-25 mesh), coal-activated carbon (10-25 mesh), silica gel (5-10 mesh)	Landfill gas	sampling 18 L of gas for 30 min ($600 \text{ mL} \cdot \text{min}^{-1}$)	Siloxanes (total)	Average concentrations total siloxanes in $\text{mg} \cdot \text{Nm}^{-3}$: * Coconut- activated carbon: 7.91 ± 1.86 * Coal-activated carbon: 7.67 ± 2.12 * Silica gel: 5.54 ± 2.53	Solvent desorption – GC – MS (HPLC-grade methanol as solvent – Agilent 6890 GC with Agilent HP-1MS column (300 m x 0.25 mm x 0.25 μm) – Agilent 5973N MS) LOD of the targeted siloxanes range from 0.88 to $2.46 \mu\text{g} \cdot \text{mL}^{-1}$	[121]
Four activated carbon tubes in series ($\sim 700 \text{ mg}$ activated carbon per tube)	Landfill gas and AD biogas	Sampling at $0.2 \text{ L} \cdot \text{min}^{-1}$ flow rate. 6 L gas sampled on one set of 4 tubes in series; 12 L gas sampled on another set of 4 tubes in series	Siloxanes (trimethylsilanol, L2, D3, L3, D4, D5, D6)	TMS : $195 - 3800 \mu\text{g} \cdot \text{m}^{-3}$; L2 : $16 - 313 \mu\text{g} \cdot \text{m}^{-3}$; D3 : $190 - 203 \mu\text{g} \cdot \text{m}^{-3}$; L3 : $111 \mu\text{g} \cdot \text{m}^{-3}$; D4 : $550 - 2725 \mu\text{g} \cdot \text{m}^{-3}$; D5 : $609 - 724 \mu\text{g} \cdot \text{m}^{-3}$; D6 : $60 - 253 \mu\text{g} \cdot \text{m}^{-3}$	TD – GC – MS (Tekmar Autocan TDS – HP5890 II GC – HP5972 MS)	[122]
Tenax TA	AD biogas and biomethane (food wastes)	Altef bag sampling and subsequent transfer to sorbent tube at a controlled flow over 1-2 min	Terpenes (dominant species were d-limonene, <i>p</i> -cymene, α -pinene, β -pinene)	Total terpene concentration: In biogas: $360 - 1650 \text{ mg} \cdot \text{m}^{-3}$ In biomethane: $5 - 240 \text{ mg} \cdot \text{m}^{-3}$	TD – GC – MS/FID (Markes TD100 – Agilent 6890N GC with 5% phenyl polysilphenylene-siloxane, BPX5, 50 m x 0.32 mm x 1 μm column – Agilent 5975C MS or FID)	[168]

Table 2.5: continued

Adsorbent tube composition	Sampled gas	Sampling conditions	Characterized compounds	Concentration range observed	Analytical method	References
Tenax TA	Biogas and biomethane	Altef bag sampling and subsequent transfer to sorbent tubes via 3 methods, each one transferring 100 mL gas from the bag to the sorbent tube: 1) gas-tight syringe, flowrate 200 mL·min ⁻¹ 2) “easy VOC™ grab sampler”, flowrate 500-600 mL·min ⁻¹ 3) laminare flowmeter + sampling pump, flowrate 50 mL·min ⁻¹	130 VOC from different families: alkanes (heptane, octane, decane, undecane, dodecane, tridecane, tetradecane, decahydronaphthalene and methyldecahydronaphthalene), aromatic hydrocarbons (toluene, <i>o</i> -xylene), terpenes (α -pinene, β -pinene, camphene, 3-carene, d-limonene, <i>p</i> -cymene), alcohols (1-propanol, 2-butanol), ketones (2-butanone, 3-pentanone, 2-pentanone), esters (ethyl propanoate, ethyl butanoate, ethyl pentano-ate), furans (2-methylfuran, ethyl-furan) and sulphur compounds (dimethylsulphide, dimethyl disulphide, thiophene, 2-methylthiophene, tetrahydrothiophene, 1-propanethiol)	30 $\mu\text{g}\cdot\text{m}^{-3}$ to 35 $\text{mg}\cdot\text{m}^{-3}$	TD – GC – MS/FID (Markes TD100) – Agilent 6890N GC with column BPX5 (5% phenyl polysilphenylene-siloxane, polysilphenylene-siloxane, 50 m x 0.32 mm x 1 μm) – Agilent 5975C MS or FID)	[22]
Tenax TA	Biogas and biomethane from different sources (landfills, WWTP, AD of energy crops, byproducts from food industry and manure)	A controlled flow of the gas passed through the adsorbent over a short time (1-4 min)	VOC with boiling point in the range 70-320°C : Alkanes (nonane, decane, undecane, dodecane, tridecane); linear, branched or cyclical hydrocarbons (C5 to C13, decahydronaphthalene, methyl decahydronaphthalene ...); aromatic hydrocarbons (benzene, toluene, xylenes, trimethylbenzenes, tetramethylbenzenes ...); terpenes (<i>p</i> -cymene, d-limonene, α -pinene, β -pinene, 3-carene, santolina triene); chlorinated and fluorinated hydrocarbon; esters; ketones (2-butanone, pentanones, hexanones and heptanones, furans); Sulphur compounds (methylmercaptan, DMS, DMDS); dioxolanes; siloxanes (decamethylcyclopentasiloxane (D5)); Nitrogen compound ethylmethylpyridine	Concentration individual compounds in biogases : <0 – 190 $\text{g}\cdot\text{m}^{-3}$. Typical total VOC concentrations in biogases: 20 - 700 $\text{mg}\cdot\text{m}^{-3}$ Typical total VOC concentrations in biomethanes: <10 $\text{mg}\cdot\text{m}^{-3}$	TD – GC – MS/FID (Perkin Elmer TurboMatrix 650 TDS – Agilent 6890N GC with column 5% phenyl polysilphenylene-siloxane, BPX5, 50 m x 0.32 mm x 1 μm) -Agilent 5975C MS of FID)	[169]

Table 2.5: continued

Adsorbent tube composition	Sampled gas	Sampling conditions	Characterized compounds	Concentration range observed	Analytical method	References
Tenax GR	Biogases from different sources (landfill, WWTP and farm AD)	Nalophan bag sampling and subsequent transfer to adsorbent tubes at 90 mL·min ⁻¹	VOC including organic Silicon compounds	Total VOC concentration : 5 – 268 mg·m ⁻³ ; Benzene: 0.1 – 2.3 mg·m ⁻³ ; Toluene: 0.2 – 11.8 mg·m ⁻³ ; Halogenated compounds: <0.1 – 1.3 mg·m ⁻³ ; Organosilicon compounds: <0.4 – 10.6 mg·m ⁻³	TD – GC – MS (Tekmar Purge & Trap Concentrator 3000 TDS – Agilent 6890+ GC – Agilent 5973 N MS)	[59]
Two Tenax GR (200 mg/tube) tubes in series	Biogases from different sources (WWTP, landfills, co-digestion plants)	Nalophan bag sampling and subsequent transfer to 2 sorbent tubes in series at 90 mL·min ⁻¹	Siloxanes (L2, D3, L3, D4, L4, D5, L5) and TMS	Concentration total organic silicon compounds varied from 24 to 2460 µg·m ⁻³ . Concentration individual organic silicon compounds ranged from 1 µg·m ⁻³ (L2) – 1.27 mg·m ⁻³ (D5)	TD-GC-MS (Tekmar Purge & Trap Concentrator 3000 – Agilent 6890+ GC with Agilent HP5 column (30 m x 0.25 mm x 1 µm) – Agilent 5973N MS)	[61]
Two commercial (Supelco) tube compositions tested, each containing two beds of the sorbent: ORBO 609 Amberlite XAD-2 tube or ORBO Charcoal tube	MSW landfill gas (raw and treated), WWTP and AD biogas and biomethane	Raw biogas: 100 mL·min ⁻¹ through each individual tube. 1 – 5 L collected Treated biogas and biomethane: 500 mL·min ⁻¹ through each individual tube. 20 L collected	Oxygenated-organic compounds, halogenated compounds, mono- and poly-aromatic hydrocarbons, alkanes, cycloalkanes, alkenes, terpenes, siloxanes, Sulphur compounds	Raw biogases: total concentration ranges (ng·mL ⁻¹) : oxygenated compounds: <0 – 300; halogenated compounds: <0 – 300; monoaromatic hydrocarbons: 0 – 16000; alkanes: <0 – 1400; terpenes: 0 – 4200; siloxanes: 0 – 1300	Solvent desorption – GCxGC – MS (Pressurized Liquid Extraction, Dionex™ ASE 200 system with acetone/dichloromethane in 1:1 volume ratio – TRACE GC × GC™ Thermo-Fischer Scientific. First dimension column: Agilent nonpolar DB-5MS (30 m x 0.25 µm; 0.25 µm); second dimension column: Agilent semi-polar DB-17 (1.35 m x 0.1 µm; 0.1 µm)) – ISQ™ quadrupole MS)	[12]
					LOD: 1 ng·Nm ⁻³ for octamethylcyclotetrasiloxane, and 9 ng·Nm ⁻³ for toluene LOQ: 1.5 ng·Nm ⁻³ for octamethylcyclotetrasiloxane and 14 ng·Nm ⁻³ for toluene	
Multibed bed: Tenax TA and Unicarb (400 mg total)	WWTP biogas	500 mL biogas sampled through the tube via a sampling pump at 50 mL·min ⁻¹	Volatile organic and inorganic Sulphur compounds; (H)VOC; terpenes; alkanes	0.005 – 95 mg·m ⁻³	TD – GC – MS (Unity TDS + Ultra A automatic sampler from Markes International – Agilent 7890A GC – Agilent 5975C MS)	[21]
Multibed: Carbotrap B (20/40 mesh, 70 mg) + Carbopack X (40/60 mesh, 100 mg) + Carboxen 569 (20/45 mesh, 90 mg)	WWTP biogas	Supel™ Inert Film bag sampling and immediate transfer to sorbent tubes via a pump, at 100 mL·min ⁻¹ . Drawing 100 and 250 mL gas through the sorbent tubes was evaluated	VOC (alkanes, aromatic hydrocarbons, alcohols, ketones, furans, halocarbons, aldehydes, esters, terpenes, chlorinated compounds); Sulphur and Nitrogen compounds; VMS (TMS, linear and cyclic siloxanes). Total amount identified compounds: 117	100 mL drawn through tube: 1.3 µg·m ⁻³ (1-methylnaphthalene) to 458 000 µg·m ⁻³ (<i>p</i> -cymene); 250 mL drawn through tube: 1 µg·m ⁻³ (1-methylnaphthalene and 2-methylnaphthalene) to 340 000 µg·m ⁻³ (<i>p</i> -cymene).	TD – GC – MS (Perkin Elmer ATD 400 – Thermo Quest Trace 2000 GC with column DB-624, 60 m x 0.25 mm x 1.4 µm – Thermo Quest Trace Finnigan MSD)	[44]

Table 2.5: continued

Adsorbent tube composition	Sampled gas	Sampling conditions	Characterized compounds	Concentration range observed	Analytical method	References
Tenax TA (30/60 mesh, 200 mg) in inert coated stainless-steel tubes (8.89 mm length, 6.35 mm ID)	AD biogas (from 3 different AD plants)	100 mL·min ⁻¹ during 30 s or 1 min	51 VOC (Silicon-organic compounds, terpenes, BTEX, furanes, ketones, alcohols, alkanes, esters and Sulphur-organic compounds)	0.01 mg·Nm ⁻³ (decamethyltetrasiloxane) to 359.84 mg·Nm ⁻³ (<i>p</i> -cymene)	TD-GC-MS (Shimadzu TD20 – Shimadzu QP2010Plus with column Restek Rxi-5MS 60 m x 0.25 mm x 1 μm)	[170]
Different adsorbents evaluated: Amberlite XAD-2 or XAD-4, activated carbon type F-400, polyurethane foam	WWTP biogas	Polyethyleneterephthalate bag sampling with subsequent transfer through adsorbent tube at 500 mL·min ⁻¹	Siloxanes (D3, D4, D5, D6)	Not mentioned	Solvent desorption – GC – FID/MS (hexane, cyclohexane or hexamethyldisiloxane as solvent – Varian 3700 GC with SE 54 fused-silica capillary column 50 m, 0.32 mm, 0.25 μm (CS Chromatographie Service Germany) – FID or TSQ 70 MSD)	[141]
Silica gel (2 g)	WWTP biogas. Raw biogas (RH _{20°C} >85%) and biogas dried by refrigeration (RH _{20°C} =38%) were sampled	Sampling into evacuated 15 L stainless-steel Tekmar canisters with subsequent transfer through adsorbent tube at 1L·min ⁻¹	Siloxanes (L2, D3, D4, D5)	Total siloxane concentrations: raw biogas: 16.2 mg·m ⁻³ ; dried biogas: 14.8 mg·m ⁻³	TD – GC – MS/AES (Tekmar 6000 TD unit with Tekmar cryofocusing module – HP 5890 II GC with DB-5 column 30 m x 0.32 mm x 0.25 μm – HP 5971 A MS operated in parallel with a HP 5921 A AES)	[102]
Carbon cartridges filled with graphitized and activated carbon	WWTP biogas and biomethane	Different volumes sampled in the range 40 mL – 2 L	Siloxanes, VOC (aromatics, terpenes, alkanes, halogenated compounds, organosulphur compounds)	total volatile silicon in biogas: >2 mg·m ⁻³ ; in biomethane: > 0.03 mg·m ⁻³ Aromatics in biogas: 225 μg·m ⁻³ ; in biomethane: 0.8 μg·m ⁻³ Terpenes in biogas: 65.9 μg·m ⁻³ ; in biomethane: <0.5 μg·m ⁻³ Alkanes in biogas: 1540 μg·m ⁻³ ; in biomethane: <1 μg·m ⁻³ Halogenated in biogas: 184 μg·m ⁻³ ; in biomethane: <3 μg·m ⁻³ Organosulphur in biogas: 114 μg·m ⁻³ ; in biomethane: <0.5 μg·m ⁻³	TD-GC-MS (Chrompack CP 4020 TD unit – Trace Ultra GC with DB1-MS column (50 m length, 0.25 mm inner diameter, 0.25 mm film thickness) – SQ MS (Thermo Fisher Scientific, 168 3rd Ave, Waltham, MA 02451 USA).	[171]

Table 2.5: continued

Adsorbent tube composition	Sampled gas	Sampling conditions	Characterized compounds	Concentration range observed	Analytical method	References
Multibed: Carbosieve 111 + Carboxen B + Carboxen C	MSW landfill gas	Pre-evacuated glass vial sampling with subsequent pumped transfer to the tubes (2 L at 200 mL·min ⁻¹)	VOC (linear and cyclo- alkanes, alkenes, aromatics, poly aromatics, furans, halogenated, aldehyde, alcohols, organosulphur compounds)	0.6 – 102000 ppb	TD-GC-MS (DANI Master TD including a 3-phase quartz refocusing trap (-5°C) – GC column TR-V1 30 m x 0.25 mm ID x 1.4 μm film thickness (Thermo))	[172]
XAD-2	WWTP, landfill and AD biogas and biomethane	1 L·min ⁻¹ during 1 h	Semi-VOC	0.10–647.9 ppb _v	Solvent desorption (ethyl acetate) – GC – ToF-MS (Agilent 7890 gas chromatograph and Agilent 7200 quadrupole time-of-flight mass spectrometer)	[178]
Carbotrap™ (40-60 mesh, 10 cm × 4 mm ID adsorbent bed, packed between silanized glass wool plugs in a silanized glass tube)	MSW landfill gas	Upstream the adsorbent tube: condensate trap + 5 μm Teflon particle filter + guard column (OV-3 on Chromasorb WAW-DMCS 80/100 mesh). 5L landfill gas sampled at 300 mL·min ⁻¹ and subsequently purged with dry N ₂ + protected from light and refrigerated until analysis	Dimethylmercury	~30 ng·m ⁻³	TD – GC – CVAFS (isothermal GC 80 ± 2°C; 1 m × 4 mm ID column of 15% OV-3 on Chromasorb WAW-DMCS 80/100 mesh) + GC output to pyrolytic cracking column (700°C)	[173,174,177]

Table 2.5 indicates most studies considered biogas or landfill gas, while biomethane has been barely investigated. Note that critically and relevantly comparing the results obtained in studies appraised in Table 2.5 is difficult if not impossible since limits of detection or of quantification are only rarely given and since every study targets distinct analytes employing a unique set of adsorbent material and tube configuration, sampling conditions and analytical methods. **The absence of standardized methods is striking.** The sole perhaps meaningful comparison to be drawn from the above concerns siloxanes. Hilaire et al. [12], Raich-Montiu et al. [104], Kim et al. [121], Tansel and Surita [122], Paolini et al. [171] and Arnold et al. [69] and have investigated siloxanes in landfill gas, biogas or biomethane. With the exception of Arnold et al. that used Tenax TA, they all successfully used activated carbon or charcoal cartridges for the preconcentration of siloxanes with solvent or thermal desorption (Table 2.5). The lowest LOD ($1 \cdot 10^{-6} \text{ mg} \cdot \text{Nm}^{-3}$) was obtained for siloxane D4 by Hilaire et al. [12] using commercial ORBO-609 Amberlite XAD-2 adsorbent tubes with solvent extraction (1 acetone : 1 dichloromethane) and GCxGC-MS. Raich-Montiu et al. [104] also obtained low LOD's with commercial ORBO-32 coconut activated charcoal tubes and solvent (n-hexane) desorption followed by GC-MS: $3.3 \cdot 10^{-4} \text{ mg} \cdot \text{m}^{-3}$ for siloxanes and $6.6 \cdot 10^{-4} \text{ mg} \cdot \text{m}^{-3}$ for trimethylsilanol. With Tenax TA and TD-GC-MS, Arnold et al. [69] obtained a LOD = $3 \cdot 10^{-2} \text{ mg} \cdot \text{m}^{-3}$ for siloxanes L2, L3, L4, D3, D4, D5. The LOD's for total siloxanes obtained by Kim et al. [121] with coconut activated carbon sorbent tubes and solvent (methanol) desorption-GC-MS, were the highest: 880 – 2460 $\text{mg} \cdot \text{m}^{-3}$. Note however it can not straightforwardly be assessed which analytical method is the best to analyze trace levels of siloxanes in biogases since each of those four studies uses different adsorbents and sampling conditions (Table 2.5). For any target analyte, the optimal adsorbent tube configuration, sampling conditions, desorption and analytical methods should be systematically and independently evaluated.

Special cases of adsorbent sampling of volatile metal(loid) compounds

Although it has been said before that adsorbent tubes could not be used for the trapping of volatile metal(loid) compounds, some publications did address this topic for volatile mercury (Hg), lead (Pb) and arsenic (As) traces in gaseous matrices.

Ballantine and Zoller [179] evaluated the trapping efficiency, breakthrough volume and desorption efficiency of several adsorbent phases for methylmercury chloride (MMC) and dimethyl-mercury (DMM) in atmospheric air: 5% FFAP on Gas Chrom Q; 20% Carbowax 20M on Supelcoport; 3% OV-1 on Gas Chrom Q; 3% Hi-eff 8BP on Gas Chrom Q; Chromosorb 101, Chromosorb NAW; Porapak P; Amberlite XAD-2; Tenax GC. Glass tubes of 4 mm ID were packed with 2-6 cm of those materials and two stage thermal desorption followed by GC-MPD (microwave argon plasma detector) was the analytical method used. Evaluation of the breakthrough volumes at 25°C indicated Chromosorb 101 was the sole material able to significantly retain MMC and DMM. For thermal desorption of MMC-loaded Chromosorb 101 tubes, a second refocusing trap was installed to re-collect MMC desorbed from Chromosorb 101 prior to GC injection. Both 5% FFAP on Gas Chrom Q or Tenax GC traps were efficient. The global collection efficiency of Chromosorb 101 for MMC at 25°C was $95 \pm 3\%$ and was found being independent on the relative humidity of the sampled air [179]. The trapping of DMM (more

volatile than MMC) on Chromosorb 101 was not efficient at ambient temperature (25°C) (low breakthrough volume). Therefore, when targeting this compound, the Chromosorb 101 tubes were cryogenically maintained at -60°C and a drying tube containing drierite was placed upstream the adsorbent tube to trap humidity and avoid ice clogging or condensation in the adsorbent tube. The drying tube did not retain DMM. This way the collection efficiency of Chromosorb 101 for DMM was $96 \pm 2\%$ when air flowrates of $1\text{-}3 \text{ mL}\cdot\text{min}^{-1}$ were applied. Upon thermal desorption, the water condensation present in the DMM-loaded Chromosorb 101, as a result of the drierite drying tubes not retaining 100% of the water vapor in the sample, lead to the extinction of the plasma of the detector. Therefore, a second refocusing trap (blank Chromosorb 101) was placed to recollect DMM eluting from the sampled Chromosorb 101 tube before injection in the GC. The method developed enabled the separation and speciation of the two mercury species and had a detection limit for real atmospheric samples of organic mercury of $0.1 \text{ ng}\cdot\text{m}^{-3}$ [179].

Nerin et al. [142] compared the suitability of several adsorbents (Porapak, Amberlite XAD-2, XAD-4 and XAD-7, Tenax, Chromosorb, active charcoal and polyurethane foam (PUF)) to trap tetraalkyllead compounds in ambient air. Single bed adsorbent tubes (glass tubes, 6.4 mm ID x 110 mm length (except for PUF tubes: 22 mm ID x 100 mm length)) were packed with a bed of 65 mm length of each adsorbent. A synthetic air doped with tetraethyllead (Et_4Pb) was loaded on each adsorbent tube, the total mass Pb passing through each tube was $0.127 \mu\text{g}$. Solvent tube desorption was chosen. Different extraction solvents (chloroform, hexane, dichloromethane) were tested. It appeared Tenax and PUF materials were soluble in chloroform and dichloromethane. Adsorbent tubes were henceforth extracted with hexane in an ultrasonic bath. The obtained extracts needed to be re-concentrated which was done by evaporation of hexane under a current of N_2 at 25°C. Eventually, $2 \mu\text{L}$ of the re-concentrated extract were analyzed via high resolution (HR) GC-MS. Recovery results of Et_4Pb shown Porapak and Tenax were the only suitable adsorbents, with recoveries of respectively ~ 92 and $\sim 96\%$. The recovery percentages from PUF, XAD-4, XAD-2, XAD-7, activated charcoal and Chromosorb were respectively <10 , <20 , <5 , <5 , <30 and $<60\%$ [142]. To simulate a real air containing hydrocarbons, the authors also used synthetic gases doped with different concentrations of gasoline and tetramethyllead (TML), trimethylethyllead (TMEL), dimethyldiethyllead (DMDEL), methyltriethyllead (MTEL), and tetraethyllead (TEL or Et_4Pb). This gas was loaded on Porapak and on Tenax tubes. Recoveries of Et_4Pb from both adsorbents were lower than when using a pure Et_4Pb synthetic air, probably owing to hydrocarbons outcompeting Et_4Pb off the adsorption sites. Further, Tenax did not trap the more volatile TML and TMEL as efficiently as Porapak did. Tenax was however more efficient than Porapak in trapping and desorbing the less volatile DMDEL, MTEL and TEL. Therefore a multibed tube was prepared with Tenax as front bed and Porapak as back bed. The gasoline mixture with the 5 tetraalkyllead compounds was loaded on this multibed which gave higher recovery percentages than the apart Tenax and Porapak beds for the 5 tetraalkyllead compounds. The authors hence concluded the Tenax-Porapak multibed is especially suited for trapping tetraalkyllead compounds in real air matrices [142].

Other authors investigated the trapping volatile tetraalkyllead compounds in air on adsorbent tubes. Hewitt and Harrison [180] sampled air through adsorbent tubes (stainless-steel, 7.8 mm length x 4.8 mm ID) filled with 0.5 g Porapak Q to determine TML, TMEL, DMDEL, MTEL and

TEL in air. All sampled adsorbent tubes were stored at -10°C prior to analysis. Two stage thermal desorption was used to desorb the Porapak tubes with a cryogenic trap (filled with 4% Apiezon M on Chromosorb P, 60-80 mesh) refocusing the analytes before injection in a GC and detection via atomic absorption spectrometry (AAS). Desorption efficiencies from the tubes were $> 90\%$ compared with direct injections of TML and TEL into the GC. Limits of detection obtained were $\sim 250 \text{ pg Pb}\cdot\text{m}^{-3}$ for TML and $\sim 375 \text{ pg Pb}\cdot\text{m}^{-3}$ for TEL in an air sample of 80 L. The authors found the breakthrough volume of TML at ambient temperature was 89 L for 0.45 g of Porapak Q. Sampling of 80 L air on 0.5 g Porapak Q tubes was therefore chosen as safe [180] yet this volume is higher than the theoretical *safe sampling volume* (as defined in the section “Adsorbent material choice”) that in this case would be 66 L air per 0.5 g adsorbent. The storage of adsorbent tubes at -10°C for 14 days did not lead to sample loss [180]. Nielsen et al. [181] also sampled atmospheric air (generally 80 to 90 L) through stainless-steel tubes (50 cm x 6.3 mm ID) packed with $\sim 3.2 \text{ g}$ Porapak N or Porapak QS to determine TML and TEL. Tubes were desorbed via two stage thermal desorption with a cryofocusing trap filled with filled with 4% Apiezon M on Chromosorb P-AW-DCMS (60-80 mesh). The isotope dilution technique and GC-MS were used to analyze the desorbed analytes. Isotope dilution implied adding d_{12} -TML and d_{20} -TEL on the adsorbent tubes in advance to correct for potential decomposition of TML and TEL during sampling or analysis. The detection limit was $20 \text{ pg TML}\cdot\text{m}^{-3}$. Porapak QS seemed more suitable for the trapping of TML: the breakthrough volume of TML at 30°C was $170\text{L}\cdot\text{g}^{-1}$ Porapak QS against $64 \text{ L}\cdot\text{g}^{-1}$ Porapak N. Desorption efficiencies (recovery %) were also higher for TML than for TEL: $102 \pm 4\%$ for TML and $52 \pm 11\%$ for TEL on Porapak QS versus $92 \pm 3\%$ for TML and $73 \pm 5\%$ for TEL on Porapak N. Porapak N seemed more efficient for the successful recovery of TEL than Porapak QS [181].

Arndt et al. [74] considered the suitability of needle trap devices (NTD) to sample volatile arsenic in volcanic gases. NTD are hollow stainless-steel tubes whose inner surfaces are coated with an adsorbent; they in fact are the opposite configuration as solid phase micro-extraction (SPME) fibers where an adsorbent is coated on the external side of the fiber. The same adsorbents are used in NTD and SPME and common ones are polydimethylsiloxane, divinylbenzene, Carboxen X and Carboxen matrices. Yet SPME fibers have successfully been used to trap volatile arsenicals [182,183], Arndt et al. [74] preferred NTD. NTD have a higher mechanical strength and associated higher robustness for field utilization than SPME fibers, but their main advantage is the easier quantification of trapped analytes. SPME are passive sorption tools where the quantification of sorbed analytes is prone to large uncertainties since it implies the calculation of the gas diffusion flux on and around the fiber during sampling. NTD on the contrary allows active pumped sampling of a defined gas volume through the needle, facilitating the quantification of (quantitatively) adsorbed analytes [74]. Arndt et al. [74] evaluated the following NTD multibed adsorbent coatings where each adsorbent is coated on 1 cm length of a needle: PDMS + Carboxen 1000 (PC), PDMS + DVB (PD), PDMS + Carboxen X (PX), PDMS + Carboxen 1000 + DVB (PCD), PDMS + Carboxen X + Carboxen 1000 (PXC). Single adsorbent NTD were also studied, with 3 cm length coating of either Carboxen 1000 or Carboxen X. All NTD were preconditioned by heating for 15 min under He flow at 280°C (for PD, PCD) or 300°C (for PC, PX, PXC) which resulted in good NTD blanks. A standard gas mix prepared in a Tedlar bag and containing $50 \text{ ng}\cdot\text{L}^{-1}$ of each of the following compounds in dry N_2 : AsH_3 , CH_3AsH_2 ,

$(\text{CH}_3)_2\text{AsH}$, and $(\text{CH}_3)_3\text{As}$, was pumped through the NTD at $5 \text{ mL}\cdot\text{min}^{-1}$ during 8 min (2 ng of each As-species loaded per NTD). NTD were thermally desorbed and volatile As-species were characterized by GC-MS in electron impact mode for the speciation and by GC-AFS for total arsenic quantification (GC-EI-MS/AFS). Desorption temperatures were initially set at 280°C (for PD, PCD) or 300°C (for PC, PX, PXC) but in view of the relatively low thermal stability of AsH_3 (230°C), a lower desorption temperature (220°C) was also tested [74]. Characterization of the standard arsenic compounds from the multibed NTD totally failed: with a desorption at 280 or 300°C , no single species was detected. Single beds NTD and a desorption temperature of 220°C yielded better yet unsatisfactory results: trimethylarsine was the sole species partly recovered from both single adsorbent NTD (Carboxen 1000 or Carbopack X). The analysis of a liquid N_2 cryotrap placed downstream the single bed NTD to monitor eventual As-species coming out of the NTD revealed the most volatile AsH_3 , CH_3AsH_2 and $(\text{CH}_3)_2\text{AsH}$ were not adsorbed at all by the single bed NTD and the relatively less volatile $(\text{CH}_3)_3\text{As}$ was only partly adsorbed on those NTD. Furthermore, 220°C was insufficient to quantitatively desorb trimethylarsine from the NTD. Quantitative desorption of trimethylarsine was only reached at a temperature of 300°C which however is incompatible with the least thermally stable AsH_3 . The authors concluded NTD with the chosen adsorbents were not a viable alternative to the state-of-the-art cryogenic preconcentration (cryotrapping) of volatile arsenic since none of the targeted species could be quantitatively trapped nor desorbed [74].

Finally, the NIOSH method 6001 for trapping gaseous arsine (AsH_3) in air [184] recommends the use of solid sorbent tubes (glass tubes, 7 cm long, 6-mm OD, 4-mm ID) filled with two beds of activated coconut shell charcoal (front bed = 100 mg; back bed = 50 mg). With a sampling flowrate comprised between $0.01 - 0.2 \text{ L}\cdot\text{min}^{-1}$ and a sampled volume of $0.1 - 10 \text{ L}$ for a concentration range $0.001 - 0.2 \text{ mg}\cdot\text{m}^{-3}$, the sample stability on the tubes is guaranteed by the method to be at least 6 days at 25°C . Charcoal beds are solvent desorbed in 0.01 M HNO_3 with sonication and the extracts are analyzed by atomic absorption spectrophotometry with graphite furnace. Note other As-species can adsorb onto the charcoal beds and the analysis technique is not species specific so only total As content is reported, with a limit of detection of $\sim 0.004 \mu\text{g As}$ per tube [184].

III.1.2. Chemisorption (chemotrapping) and on-tube derivatization

In contrast to physical sorption, chemical sorption (chemisorption) involves a chemical reaction, with associated bond-breaking and -creation, between the target analyte and a specific chemical (derivatizing agent) immobilized on a solid sorbent material placed in a tube ("chemotrap"). The purpose is to produce a target analyte derivative whose stability is enhanced (e.g. lower vapor pressure) or whose analysis is facilitated compared to the parent analyte. This approach is welcome in cases an analyte is not retained by physisorption on solid adsorbents due to lack of affinity for the adsorbent material or due to a very high volatility [32,41,76]. Ideally, parent target analytes are quantitatively stripped off the sampled gas and the generated derivative preserves identity characteristics of the parent analyte so that post-trapping speciation is secured [185]. In air monitoring, a derivatizing agent commonly used is 2,4-

dinitrophenylhydrazine (DNPH) which derivatizes carbonyl compounds (e.g. aldehydes) into hydrazones [32,41,76]. Sorbents with large, open pores such as silica gel and Chromosorb W are often used as support for the derivatizing agent: the wider pore space facilitates reactions, enables to load more derivatizing agent and provides more potential sorption sites for the reaction product. Note the occurrence of chemical reactions in chemisorption potentially results in slower kinetics than in physisorption, therefore lower sampling flowrates or larger sorbent beds are advised to reach sufficient contact times between analytes and derivatizing agents and as such to complete the reactions. Solvent desorption of the chemotraps is the state-of-the art technique since the excess derivatizing agent would cause analytical problems upon thermal desorption [4,32,34]. Chin et al. [178] applied this approach and sampled 23 biogas and biomethane samples from various production sites (landfills, waste water treatment plants and anaerobic digestion plants treating diverse feedstocks) through DNPH-loaded silica sorbent tubes at $1 \text{ L}\cdot\text{min}^{-1}$ during 1 min for the targeted preconcentration of carbonyls. Acetonitrile was used as solvent to extract carbonyls from the DNPH-silica tubes, followed by liquid chromatography – time-of-flight mass spectrometry (LC-ToF-MS).

In the field of biogas and biomethane, one element for which chemisorption with on-tube derivatization is particularly interesting, is arsenic (As) and its different volatile species. Volatile Arsenic species are present in biogas and biomethane as a result of the microbially-driven biovolatilization and bioalkylation of (inorganic) As-traces in wastes landing up in landfills, sewage sludge and anaerobic digesters [67,186–188]. The similarity of the As-biovolatilization and biomethylation mechanisms with the methanogenesis driven by methanoarchaea during the anaerobic biomethanization process suggests those mechanisms are at least partly performed by these microorganisms [186–188]. Sulfate reducing bacteria are also involved in the anaerobic biovolatilization of arsenic [187]. Arsenic in landfills originates from glasses (As_2O_3), metal alloys, semi-conductors (GaAs), wood impregnated with preservatives (As_2O_5 in chromated copper arsenate), herbicides or insecticides (monomethyl arsonic acid; dimethylarsinic acid). Arsenic in anaerobic digesters can originate from rice straw from rice grown in areas with heavy mining or smelting industries (e.g. in China)[187], and from swine and poultry wastes and -manure when the animals have been doped with organo-arsenical antibiotics such as roxarsone and p-arsanilic acid [186,187]. Chicken manure can contain $1 - 70 \text{ mg As}\cdot\text{kg}^{-1}$ and swine manure $1 - 7 \text{ mg As}\cdot\text{kg}^{-1}$ [187]. Pinel-Raffaitin et al. [67] semiquantified several arsine species in landfill biogas ($0-15 \text{ }\mu\text{g As}\cdot\text{m}^{-3}$): $\text{As}(\text{CH}_3)_3$, $\text{As}(\text{CH}_3)_2\text{H}$, $\text{As}(\text{CH}_3)_2(\text{C}_2\text{H}_5)$, $\text{As}(\text{CH}_3)(\text{C}_2\text{H}_5)_2$, and $\text{As}(\text{C}_2\text{H}_5)_3$, trimethylarsine being the most dominant species. In the biogas from a model anaerobic digester, $\text{As}(\text{CH}_3)_3$, $\text{As}(\text{CH}_3)_2\text{H}$ and AsH_3 were found by Mestrot et al. [187]. Monitoring gaseous arsenicals in landfill's or digester's biogas is crucial because of the toxicity and corrosive nature of certain volatile arsenic species and their ability to form precipitates under particular conditions [4,34,67,189]. However, the sampling and analysis of such species in the complex biogas matrices is as challenging as it is in natural gas, where most of the knowledge comes from, in view of the very low concentrations, low boiling points, high reactivities when in contact with e.g. H_2S or SO_2 , possible interferences with other components, lack of reliable analytical methods with sufficiently low detection limits and lack of gas-phase arsenic standards [34,74,189,190].

A successful preconcentration method for gas phase volatile arsenicals is chemotrapping. Several liquid or solid agents such as H_2O_2 , NaOCl , $\text{Hg}(\text{NO}_3)_2$, activated charcoal, KI , HNO_3 and AgNO_3 react with and have been used to chemotrap volatile As-species [185,186]. Mestrot et al. [185] and Uroic et al. [34] used the same AgNO_3 impregnated silica gel tube method to quantitatively chemotrap volatile arsenic from respectively paddy soils emissions and natural gas. While Uroic et al. [34] only looked at total As from spiked trimethylarsine, the chemotrapping mechanism used by Mestrot et al. relied on oxidation of the volatile arsenicals to their pentavalent oxy-species (arsine to arsenate, methylarsine to monomethylarsonic acid, dimethylarsine to dimethylarsinic acid, and trimethylarsine to trimethylarsine oxide) which preserve the As-C bond and thus the speciation of the parent analytes so that species qualification and quantification could be performed post trapping [185]. Silver nitrate impregnated silica gel absorption tubes were prepared on commercial silica gel tubes (glass tubes, 6 mm OD, 70 mm length, 225 mg silica gel split up into 2 compartments and plugged with active charcoal foam and glass wool) where on different concentrations of silver nitrate solutions (0%, 0.001%, 0.01%, 0.1% and 1% (m/v), corresponding to 0.006, 0.06, 0.6 and 6 mg AgNO_3) were impregnated for the natural gas study [34]. Natural gas samples were collected from gas fields in Sulfinert™ surface treated gas cylinders at the pipeline pressure and subsequently transferred to the AgNO_3 -silica gel tubes for preconcentration of the arsenicals. Liquid desorption with boiling hot nitric acid was used to extract the trapped arsenicals from the tubes: 0.6 mL boiling hot 5%_{m/v} HNO_3 was first injected in the tubes and left for 5 min whereafter tubes were flushed with 2.5 mL boiling hot 1%_{m/v} HNO_3 and flushed with 2.5 mL air. Extraction efficiencies of > 90% were reached this way and total Arsenic content in extracts was determined by online photo-oxidation hydride generation atomic fluorescence spectrometry (UV-HG-AFS) [34]. Krupp et al. [4] which introduced the silver nitrate impregnated silica gel tubes as chemotrapping method for volatile arsenicals in natural gas and its condensate phases, point out that the non-100% extraction efficiency of alkylated arsenicals from the chemotraps can be due to incomplete sorption on the tubes owing to their non-polarity and low boiling point, or to irreversible sorption. Uroic et al. [34] first developed their chemotrapping-UV-HG-AFS method with TMA gas standards prepared in Tedlar bags in N_2 and in natural gas matrices, and validated the method by comparison with the state-of-the art cryotrapping - gas chromatography - inductively coupled plasma - mass spectrometry reference method (CT-GC-ICP-MS). Absorption efficiency of TMA on the chemotraps in function of the impregnated AgNO_3 concentration was studied by injecting 100 mL 1060 ng As/L TMA standard on the chemotrap tubes and subsequently analyzing the gas at the outlet of the tubes by CT-GC-ICP-MS. An absorption of 10.3% TMA was already recorded for non-impregnated silica gel but 98% absorption was reached in silica gel tubes impregnated with 0.01% (60 μg) AgNO_3 . However, to keep breakthrough <1% of the loaded TMA amount and hence guarantee an absorption efficiency of >99.5% TMA, the impregnated AgNO_3 concentration has to be at least 0.1%_{m/v} (0.6 mg). Silica gel tubes impregnated with 1%_{m/v} (6 mg) AgNO_3 could quantitatively accumulate up to 4.8 μg As without breakthrough (>99.8% absorption efficiency), which is a sufficient achievement since the authors found real natural gas samples did not contain more than 2.8 μg As per chemotrap for 20 L gas samples [34]. The authors also found hydrocarbons and volatile Sulphur compounds present in real natural gas had no effect on the absorption efficiency of TMA in the AgNO_3 -silica gel chemotraps yet especially Sulfides were thought to potentially react with

the silver. More, for real natural gas samples containing no arsenicals but spiked with TMA, higher As recoveries from the tubes were obtained for low TMA loads (20 ng TMA; up to 113% recovery) than for high TMA loads (2 µg TMA; 90±5% recovery). Thus the method developed allows to trap, desorb and quantify TMA in a large concentration range in natural gas (linear absorption range: 20-2000 ng As), with a limit of detection (LOD) of 20 ng As as TMA (1 mg As·m⁻³ in a 20 L gas sample) for the blank chemotrap tubes and UV-HG-AFS [34]. Yet this LOD is satisfactory for gas industry requirements [34], it is relatively high and Mestrot et al. [185] which had a similar LOD (17.7 ng As) therefore searched which part of the blank AgNO₃-impregnated silica gel tubes were responsible for the Arsenic source. They found the glass wool of the tubes was the main As contamination source (146 ng As per tube); the foam contained 6.6 ng As per tube and the AgNO₃-impregnated silica gel 4.2 ng As per tube.

The great advantage of the preconcentration in (AgNO₃-impregnated silica gel) chemotraps as compared to preconcentration via cryotrapping is the easy field deployability of the chemotraps. Yet cryotrapping-GC-ICP-MS is the most robust technique in terms of selectivity, sensitivity, repeatability, linearity and individual species quantification and qualification, it is not or difficultly field-implementable in view of the complex technical sophistication level and the requirement of cryogenes. Furthermore, ICP-MS is negatively impacted by the matrix effects of CO₂-rich gases such as biogases. Chemotrapping-UV-HG-AFS can reach high levels of robustness, sensitivity and selectivity and allows real time monitoring of gas composition on site since not only the preconcentration step but also the analytical apparatus setup are field-deployable [4,34,185]. This in-situ preconcentration method hence also avoids risks of sample deterioration during transportation between whole gas sampling and effective preconcentration and analysis in the lab.

Mestrot et al. [187] further employed their AgNO₃-impregnated silica gel chemotraps to study the arsenic volatilization in the biogas of model anaerobic digesters as a function of the initial As-species (Roxarsone, monomethylarsonic acid (MMA(V)), As(V) or no initial As) amended in the organic matter. The model organic matter was composed of fresh pig manure (2.4 ± 0.3 mg As·kg⁻¹ dw), milled and dried rice straw (2.3 ± 0.3 mg As·kg⁻¹ dw), fresh beer residues from a brewery (0.06 ± 0.02 mg As·kg⁻¹ dw) and water. The evolution of volatile As-species from the anaerobic digestion of this matter was monitored by placing AgNO₃-impregnated silica gel traps on the outlet of the model reactors. Total As analysis and speciation analysis were performed every 2 weeks from the harvested traps, respectively by acid digestion of impregnated silica gel followed by ICP-MS and by hot boiling water elution of the traps followed by anion exchange HPLC. Over a 42 days period, the authors found model digesters volatilized 25 ± 4 ng As (non As-amended, n=3), 51 ± 23 ng As (Roxarsone-amended, n=3), 177 ± 28 ng As (As(V)-amended, n=3) and 413 ± 148 ng As (MMA(V)-amended, n=3) with trimethylarsine being the dominant species in all cases [187].

Further, gaseous mercury can also be trapped via chemisorption on iodine (I₂) impregnated silica gel, where it is retained as HgI₂, as worked out in the ISO 6978-1:2003 standard method for determination of mercury in natural gas [27,191]. No speciation can be done with this method as all Hg-species are reduced to Hg⁰. Sampling pressures on the chemotraps can go up to 400 bar and the method is convenient for Hg concentrations in the range 0.1 – 5000 µg·m⁻³.

Total Hg content is quantified by measuring the absorbance or fluorescence of Hg⁰ vapor at 253.7 nm. Similarly, Lindberg et al. [173,174] collected total gaseous mercury (Hg⁰, Hg(II) and organic Hg-species) in landfill gas at 400 mL·min⁻¹ through activated iodated charcoal traps that were heated slightly above landfill gas temperatures (~50°C) to avoid condensation of compounds onto the sorption sites. Mercury species were recovered from the iodated charcoal traps by acid leaching the traps in a hot-refluxing HNO₃/H₂SO₄ system. The acid leachate from that system was further oxidized by a 0.01 N BrCl solution. Both acid and oxidized leachates were then analyzed by cold vapor–atomic fluorescence spectrometry (CV–AFS) at 253.7 nm.

III.1.3. Amalgamation: trapping of volatile Mercury species

Mercury species (metallic, organic or inorganic) occur at ng·m⁻³ to mg·m⁻³ levels in natural gas [83,192,193] and in landfill gas where they volatilize from dumped alkaline batteries, fluorescents light bulbs, electrical and ignition switches, electronics (computer monitors), thermometers, thermostats, barometers, manometers, paint residues [173–176,194,195]. Mercury species, both elemental (Hg⁰) and organic or inorganic forms such as CH₃HgCl or HgCl₂, can specifically be preconcentrated from those gases by the chemical amalgamation reaction between mercury and other noble metals like gold (Au), platinum (Pt), silver (Ag), palladium (Pd), copper (Cu) [192,194–197]. Quartz gas sampling tubes (e.g. ID 5 mm, L 160 mm) packed with noble metal-coated sand beds or containing noble metal gauzes have especially been used for that purpose [192]. For an amalgam to be formed, both mercury and the noble metal must be in their elemental state [196] although noble metals such as Au and Au/Pt alloys also react with inorganic and organic Hg-species [191,192]. Frech et al. [192] evaluated the efficiency of several noble metals (Au, Ag, Au/Pt alloy) for the amalgamation of gaseous elemental mercury (Hg⁰) and dimethylmercury ((CH₃)₂Hg) in natural gas: crumpled Au wire, Ag wire, Au/Pt wire or coiled Au/Pt gauzes were packed in quartz test-tubes. For Hg⁰, silver was found to yield poorer amalgamation efficiencies than gold and gold/platinum alloy. The Au/Pt test-tubes quantitatively trapped Hg⁰ at flowrates up to 9.3 L·min⁻¹, compared with 8.0 and 2.0 L·min⁻¹ for respectively Au and Ag test-tubes. Inasmuch as silver is also known to inefficiently amalgamate organic Hg-species, the authors concluded silver was an unsuitable material for both species-specific and total Hg characterization. Au/Pt tubes proved to collect metallic Hg⁰ more efficiently than Au tubes in real natural gas, and the organic (CH₃)₂Hg species in natural gas was also quantitatively amalgamated onto Au/Pt tubes [192] although less efficiently than metallic Hg⁰ [191]. The noble metal alloy Au/Pt hence seems to deliver the highest quantitative amalgamation efficiencies for both metallic and organic Hg-species [192]. Nevertheless, simple Au tubes have been most often used for both natural gas and landfill gas mercury investigations [48,75,173,194,195].

Preconditioning and properly storing newly assembled amalgamation tubes is as important as it is for adsorbent tubes. New amalgamation tubes are typically blanked at 500°C [83,195,198,199] or 800°C [192] under a continuous Hg-free gas flow (e.g. Ar, N₂, air) during several hours. As substantial Hg background levels can be released from the tube materials, this initial blanking is best conducted outside the analytical gas train [198]. Sealing blanked

amalgamation tubes to avoid passive uptake of Hg traces from the ambient atmosphere is most efficient with gas-tight Teflon plugs [195,198,199] and refrigerating the tubes during the storage period until utilization was found to guarantee blank levels up to 600 hours [198].

To recover amalgamated Hg-species from the tubes and regenerate those latter for re-use in subsequent sampling runs, the amalgam has to be decomposed which occurs by heating the sampling tubes. During this thermal desorption, inorganic and organic Hg-species are reduced and released as gaseous Hg⁰ [191]. A two-stage amalgamation-thermal desorption procedure is often appropriate: the sampled noble metal packed tubes are first thermally desorbed at 400 – 800°C during 50-100 s while a Hg-free carrier gas (Ar, e.g. 220 ml·min⁻¹) blows the released mercury to a second calibrated amalgamation trap, typically packed with Au or Au/Pt and permanently installed in the analytical device [75,192,196,198]. This tube is itself subsequently quickly thermally desorbed (e.g. 500 °C for 15 s [75]) and as such recovered total Hg⁰ vapor is carried to the detector, typically either a cold vapor atomic absorption spectrometer (CVAAS) or a cold vapour atomic fluorescence spectrometer (CVAFS) operated at 253.7 nm, to be quantified. This method has been validated and standardized for field measurements of Hg in natural gas in the norm ISO 6978-2:2003 [28]. The speciation of distinct Hg-species is more complex and was reviewed by [191]. Two stage amalgamation-thermal desorption has two advantages: Firstly, total Hg⁰ amounts are quickly introduced into the detector from a single, well calibrated trap leading to high precision and accuracy. Secondly, other non-Hg organic compounds from the gas sample (that could have been retained in the sampling amalgamation tube), are separated from the total generated Hg⁰ vapor during the re-amalgamation on the second calibrated trap. This prevents them to enter the detector and falsify Hg⁰ signals by absorbing at the same wavelength (253.7 nm) as Hg⁰ [192,198]. As such, sub-ng Hg⁰ levels can be detected [198]. Notwithstanding, Liang and Bloom [199] challenged the benchmark two-stage amalgamation-thermal desorption and argued single-stage amalgamation on a sampling Au-coated sand trap with direct thermal desorption in a CVAFS detector reduced the overall analysis time while providing the same precision, accuracy and detection limits as the two-stage approach when the sampling trap was oriented in the same gas flow direction during both sampling and analysis and when peak area instead of peak height was considered in the detected signal.

Important practical considerations for the optimal use of noble metal (Au/Pt) tubes for the amalgamation of Hg⁰ and (CH₃)₂Hg in natural gas were highlighted by Frech et al. [192]. Firstly, the highest quantitative trapping efficiencies are obtained for both Hg-species when the Au/Pt tubes are heated to 80 °C, since such temperatures inhibit the condensation of other organic natural gas constituents on the noble metal surfaces, which would otherwise cover and passivate the amalgamation sites. Temperatures up to 197°C can even be used as the Hg-amalgamation efficiency was independent of the temperature up to 197°C for Au/Pt tubes. Authors hence suggest to place the amalgamation tubes in a heated box during sampling. After sampling, tubes can be washed with few mL isooctane and methanol to eliminate potential condensates, and surplus washing solvent can then be removed by flushing the tubes with Hg-free air. Secondly, as noble metal surfaces gradually get covered and inactivated by other natural gas constituents than Hg ones during sampling, sampled volumes should be limited to ~10 L (for tubes packed with 1.5 – 4.5 g Au/Pt wire) to guarantee a quantitative Hg-trapping efficiency and minimize breakthrough of Hg-species. Also, sampling flowrates should be kept low (2 or 3 L·min⁻¹ for tubes

packed with 1.5 – 4.5 g Au/Pt wire) to increase the residence time of Hg-species in the tube and thus increase the contact opportunities with amalgamation sites. Finally, as amalgamated Hg tends to migrate into the inner layers of the noble metal surfaces, especially when thermal desorption of the tubes is not performed within hours after sampling, and to only slowly get released from these inner layers during thermal desorption, memory effects can build up across repeated use of amalgamation tubes. Such undesirable effects can be mitigated by coating support materials such as sand, silica or glass beads with highly dispersed thin noble metals layers e.g. via vapor deposition of noble metal wire [192,198], concomitantly increasing the available amalgamation surface area of the noble metal. Too tightly packed noble metal coated sand beds can nevertheless lead to adverse pressure drops upon gas sampling, leading to the condensation of e.g. hydrocarbons of natural gas on the noble metal surfaces [192]. In that respect, Larsson et al. [83] investigated three Au/Pt amalgamation tube designs for the preconcentration of gaseous elemental Hg⁰ in different gases including natural gas: ‘Standard tubes’ were 150 mm long quartz tubes (4 mm ID) packed with 2 m crumpled Au/Pt alloy wire (0.1 mm diameter) eventually occupying a length of 50 mm in the tube. ‘Compact tubes’ were obtained by further compressing the crumpled Au/Pt wire so that it only occupied a 10 mm length in the tube. Finally, to simulate a poorly packed or a collapsed noble metal structure, ‘tubes with orifice’ were prepared as the ‘compact tubes’ but with an additional piercing of a 2 mm wide orifice through the Au/Pt wire filling. The collection efficiency (amalgamation and recovery) of Hg⁰ was evaluated at different flowrates of various gases through the different tube designs. ‘Standard tubes’ gave a quantitative collection when either air or CH₄ containing 1% H₂S, both enriched with Hg⁰, were sampled at 1 L·min⁻¹ but at 10 L·min⁻¹ the collection efficiency was ~90%. Thus the collection efficiency was independent of nature of the gas tested, even in the presence of H₂S. At 10 L·min⁻¹, the ‘compact tubes’ performed better than the ‘standard tubes’ with collection efficiencies ~95%, which contrasts with the results of Frech et al. [192] that coped with reduced efficiencies when using more densely packed tubes due to pressure drops and related condensation of non-Hg species passivating amalgamation sites. However, comparing collection efficiencies of various tube configurations is only relevant if the studied gas is the same, which is not the case between the study of Larsson et al. [83] and that of Frech et al. [192], as the chemical composition of each (natural) gas might vary and influence the collection efficiencies of Hg⁰. In that respect, Fernández-Miranda et al. [196] found higher mercury retention percentages on noble metal coated materials when acid gases like SO₂, HCl were present in the sampled gas, indicating those gases could contribute to another mercury capture mechanism than the sole amalgamation mechanism. For the ‘tubes with orifice’, Hg⁰ collection efficiencies rose from 29 to 44% when the gas sampling flowrate increased from 1 to 10 L·min⁻¹. A transition from laminar to turbulent gas flow regime within the orifice in the Au/Pt filling could explain the higher collection efficiencies at higher flowrates, with a larger fraction of the gas penetrating the compacted Au/Pt material surrounding the orifice owing to the higher pressure under turbulent flow conditions. This highlights the importance of homogeneously packing amalgamation tubes.

Lastly, Hg species have also been preconcentrated by amalgamation using the solid-phase microextraction (SPME) approach by coating fibers with noble metals. Romero et al. [197] compared three palladium (Pd) supports for the SPME of Hg⁰ vapors: a pure Pd-wire, a Pd-coated

stainless-steel wire and a Pd-coated silica fiber, all three implemented as the 'fiber' in the needle of a typical SPME device. After 30 min contact with Hg-loaded gases during which Hg⁰ amalgamated on the Pd-support, those modified SPME fibers were thermally desorbed at 250°C and released Hg-species were analyzed by atomic absorption spectrometry. Hg⁰ amalgamation onto the Pd-wire yielded the highest performance regarding limit of detection, sensitivity and fiber lifetime, nonetheless the mechanical resistance of such noble metal wires was too weak for a routine assembly in a SPME device. Since Pd-coated stainless-steel wires had short lifetimes and gave low Hg-collection efficiencies, Pd-coated silica fibers, yielding high Hg-collection performances and easy assembly in a SPME needle, were the best compromise.

III.1.4. Solid Phase Microextraction

Solid phase microextraction (SPME) is a preconcentration technique based on the passive absorption or adsorption of analytes (from a gaseous or liquid sample) onto a fused silica or metal alloy fiber coated with a thin stationary phase layer. The stationary phase coating (thickness ranging 7 – 100 µm) is either a polymeric film for the *absorption* of analytes or a polymeric film embedding adsorbent particles for the *adsorption* of analytes. Commercially available absorption coatings are based on polydimethylsiloxane (PDMS), polyacrylate (PA), and polyethylene glycol (PEG), while commercially available adsorption coatings embed porous adsorbent particles of divinylbenzene (DVB), Carboxen® (CAR) or a combination of both, usually bound in a PDMS film. Selecting the most appropriate SPME fiber coating is crucial yet delicate [200]. Next to existing literature [201], manufacturers such as Supelco (Bellefonte, PA, USA) provide SPME fiber selection guides depending on the nature and polarity of targeted analytes. Typically, a SPME fiber is ~ < 5 cm long, the stationary phase coating is generally 1 or 2 cm long on the fiber. The fiber is anchored in a hollow protective needle device (outer diameter < 1mm): when not in use, the fiber is retrieved inside the protective needle to keep the stationary phase coating under safe storage conditions. As the fiber is mechanically extremely weak, the needle is used to pierce e.g. the septum of a glass vial or of a gas bag containing a gas to analyze. Then the fiber is exposed to the gas (atmospheric pressure) allowing analytes to sorb onto the stationary phase coating. For optimal sorption and interpretation of quantities sorbed, a partition equilibrium has to be reached between analytes present in the bulk gas phase in the sample, and analytes sorbed on the fiber. Determining this equilibrium and the appropriate exposure time period (from seconds to ~30 min) is complex as it depends on the distribution constant or partition coefficient of each analyte, their concentration, the thickness of the stationary phase, the temperature, humidity and volume of the gas surrounding the fiber, as reviewed by [201–203]. At the end of the fiber exposure time, the fiber is retrieved in the needle, the SPME needle device is withdrawn from the sample and then generally put in the injection port of a GC (the needle pierces the GC inlet septum) for thermal desorption of the fiber coating in the heated inlet and immediate injection of desorbed analytes in the GC capillary column, generally coupled with a mass spectrometer (GC-MS). Main shortcomings of SPME are the limited variety of commercially available coatings and the poor mechanical strength of the fibers (breakage, stripping of coatings) and of the needle (bending) [197]. Nonetheless, SPME is promoted as being

an easy and rapid concomitant sampling and preconcentration system with a longer life-time (numerous sorption-desorption cycles) than adsorbent tubes and no clogging issues [7]. Critical comparisons between SPME and adsorbent tubes are available in [38,113,172].

The application of SPME has been extensively evaluated and reviewed for the determination of volatile organic trace compounds in gaseous matrices, especially atmospheric, indoor or workplace air [7,32,201,204–207]. A broad range of other compound classes can be determined via SPME: polyaromatic hydrocarbons, halogenated volatile organic compounds, oxygenated organic compounds, pesticides and drugs [7,201], Sulphur compounds [42,208], siloxanes [38], organic or inorganic metals and metalloids (Sn, Hg, Se, As, Pb, Mn...) [197,201].

Table 2.6 reviews publications on the use of SPME for the determination of trace compounds in biogas, biomethane and landfill gas.

Table 2.6: Review of the applications of SPME for the determination of trace compounds in biogas, biomethane and landfill gas.

SPME fiber coating	Sampled gas	Sampling conditions	Targeted and characterized compounds	LOD	Analysis	Reference
65 µm PDMS/DVB	AD and WWTP biogas and biomethane	Tedlar bag sampling with subsequent SPME within a day (various exposure times: 1, 5, 10, 20 and 50 min)	Linear (L2 – L5) and cyclic (D3 – D5) volatile methyl siloxanes. Additional compounds identified: D-limonene, α- and β-pinene, camphene, terpinenes, β-caryophyllene	mg·m ⁻³ L2 0.0036 L3 0.0075 L4 0.0031 L5 0.0050 D3 0.0084 D4 0.0091 D5 0.0150	GC-MS	[38]
3 fibers tested in the lab: 100 µm PDMS; 85 µm PDMS/CAR; 50-30µm DVB/CAR/PDMS; 50-30µm DVB/CAR/PDMS used for real landfill samples	Odorant emissions from landfills	Nalophan bag sampling with subsequent SPME within 30 h (exposure 30 min)	Over 100 VOC (alkanes, alkenes, terpenes, halogenated, oxygenated, aromatics) and dimethyl disulfide	<0.1 ppb for VOC; 50 ppb for dimethyldisulfide	GC-MS	[73]
CAR/PDMS	Landfill gas	Tedlar bag sampling with subsequent SPME (exposure time 2 h)	VOC (amines, sulphur compounds, alkanes, alkenes, terpenes, halogenated, oxygenated, aromatics, siloxanes)	Not available	GC-MS	[113]
Not available	AD and WWTP biogas and biomethane	Not available	Volatile sulfur compounds (H ₂ S, COS, methanethiol, dimethyl sulfide, dimethyl disulfide) and oxygenated organic compounds (ketones, alcohols, and esters)	Not available	GC-MS	[208]
50-30µm DVB/CAR/PDMS	Landfill gas	250 mL pre-evacuated glass vial sampling with subsequent SPME (exposure time 30 min at 20°C)	VOC (linear and cyclo-alkanes, alkenes, aromatics, poly aromatics, furans, halogenated, aldehyde, alcohols, sulphur compounds)	Not available	GC-MS	[172]

LOD: limit of detection. **PDMS:** polydimethylsiloxane. **DVB:** divinylbenzene. **CAR:** Carboxen[®]. **WWTP:** waste water treatment plant (anaerobic digestion of WWTP sludge). **AD:** anaerobic digestion. **GC-MS:** gas chromatography-mass spectrometry.

III.2. Trapping in liquid media: absorption in bubbling traps (impingers)

Another technique to preconcentrate trace compounds from gaseous samples involves bubbling the gas through one or a series of purpose-built bubbling traps ('impingers'), generally made of glass, containing a solvent solution and a built-in fritted bubbler nozzle to generate gas bubbles as small as possible so as to maximize the gas-liquid exchange surface area and stimulate the dissolution and absorption of targeted trace compounds in the solvent. To avoid solvent losses by evaporation or transfer to the gas phase, a high-boiling solvent can be chosen [33] but since low boiling solvents such as methanol are predominantly used, it must be chilled [72,100,121]. Solvent nature, volume and temperature, gas bubbling flowrate and total gas sampling volume must be optimally determined depending on the gas composition, concentrations, targeted compounds... This preconcentration technique can be directly implemented on field although it is not very handy as the sampling connection train can be complex, installation is time-consuming [72,121] and implies handling potentially dangerous solvents (e.g. acids, AgNO₃) [4,48,89] and since additionally a cooling bath is often requested to chill the solvent [100]. The trace compounds enriched solvent is subsequently analyzed via appropriate analytical methods (Table 2.7): GC has chiefly been coupled with MS detector for the determination of siloxanes (insofar as MS gives lower LOD than other detectors and qualitative as well as quantitative analysis) although other detectors have been (successfully or not) coupled to GC, namely AAS, AED, FID, FT-IR, atmospheric pressure chemical ionization/tandem mass spectrometry (APCI-MS/MS) [100,132]. Liquid chromatography can also be used [33], and ICP-MS [35,48,178,189] is especially used for the analysis of metal(loid) species.

Critical comparisons between impinger-, adsorbent tube-, gas sampling bag- or canister-gas sampling are available in [4,71,72,99,100,104,121,132]. Publications on the use of impingers for the determination of trace compounds in biogas, biomethane, landfill gas or natural gas are reviewed in Table 2.7.

The suitability of the impinger method has especially been extensively evaluated for volatile methyl-siloxanes in biogas matrices, where methanol, acetone and n-hexane have been found best and most often used solvents (Table 2.7). Methanol has successfully been used as absorption medium for siloxanes (L2, L3, L4, L5, D3, D4, D5, D6) in biogas, landfill gas and synthetic test gases, with recoveries >80% upon analysis [71,72,99,100,121,209]. Whereas Saeed et al. [99,100] highlighted methanol could not stabilize nor quantitatively recover pentamethyldisiloxane and hexamethylcyclotrisiloxane (D3), Wang et al. [209] were able to quantitatively trap and recover D3 from methanol impingers using the more sensitive Purge and Trap-GC-MS analytical system. Narros et al. and Kim et al. [71,121] also identified D3 from methanol impingers using GC-MS. Narros et al. [71] nevertheless pointed out methanol impingers were not able to recover trimethylsilanol, another relevant silicon-compound in biogases. Despite solubility differences between trimethylsilanol and other siloxanes [120], trimethylsilanol could be recovered, together with other siloxanes, in acetone [210] and in n-hexane [104]. Piechota et al. [210–213] investigated the use of various impinger solvents, namely acetone, methanol, n-hexane and dodecane for the preconcentration of siloxanes in landfill gas and biogases. Their work systematically reveals acetone solvates the best siloxanes from the gas samples (L2, L3, L4, D3, D4, D5, D6 and trimethylsilanol) while yielding the highest

recoveries upon GC-MS analysis. In [211] they demonstrate acetone was able to absorb and recover all siloxanes while methanol and n-hexane did not enable the detection of respectively L3 and L4, and L4 and D6. Also, when arranging 3 impingers in series with each containing a different solvent, total siloxanes levels were recovered as follows from each solvent: configuration acetone – methanol – n-hexane: 91.7%–7.37% – 0.92%; configuration methanol – acetone – n-hexane: 81.37%– 18.63% – <0.1%; configuration n-hexane – methanol – acetone: 64.28%– 26.53% – 9.18%. In [213] they had a concentration of siloxanes in acetone globally 81% higher than that quantified in methanol and dodecane was unable to detect most siloxanes at concentrations $\sim <1 \text{ mg}\cdot\text{m}^{-3}$, pointing out the importance of using relatively polar solvents such as acetone for the solvation of siloxanes. However, in a study using a synthetic gas (N_2 containing L2, D3, D4, D5 siloxanes at $600 \text{ mg}\cdot\text{Nm}^{-3}$), Wang et al. [132] also used acetone (two chilled 10 mL impingers in series) and found relatively low recoveries for D3 (45%) and L2 (64%) while fair recoveries for D4 (86%) and D5 (92%) (GC-MS analysis). They also evaluated the efficiency of the acetone impingers for preconcentrating the siloxanes from the wetted synthetic gas and found lower siloxane recoveries than from the dry gas especially for L2, which could be a consequence of competitive adsorption between L2 and water in acetone. Raich-Montiu et al. [104] used n-hexane for the absorption of siloxanes in biogas, and they detected all siloxanes (L2, L3, L4, L5, D3, D4, D5, D6) and trimethylsilanol using n-hexane, on the contrary to Piechota et al. [211] where n-hexane did not enable the detection of L4 and D6. Oshita et al. [214] also successfully used n-hexane impingers to study siloxanes in an experimental biogas generated from the anaerobic digestion of a sludge whose siloxane levels were reduced via a preliminary thermal treatment with gas stripping. Lastly, impinger preconcentration with subsequent derivatization of absorbed analytes has been proposed for the determination of total silicon content in biogas or biomethane [89]. The gas is first bubbled at $10 \text{ mL}\cdot\text{min}^{-1}$ through a heated HNO_3 filled impinger whereafter an 8 M NaOH and a HF solution are added to trigger derivatization, leading to total Si recoveries of 65 – 88 %. ICP-AES or GC-ICP-MS is then used for respectively total Si quantification or identification and quantification of individual silicon-compounds.

Next to siloxanes, bubbling traps have been used for the preconcentration of metals and metalloids (Table 2.7). Whereas gases are generally bubbled through the impingers by means of a pump when the feed line is not pressurized enough, for instance at biogas or landfill gas plants [100,104,174,209], Cachia et al. [48] developed a high-pressure bubbling sampling train to preconcentrate metals and mercury from pressurized gases such as natural gas or compressed biomethane by directly connecting the impinger train to the field gas pipeline for pressures up to 100 bar_a. Acidic solutions specific for metals or mercury (Table 2.7) were used in three impingers in series; impingers are made of an inner Teflon cylinder avoiding metal sorption on impinger walls, circled by a stainless-steel cylinder withstanding working pressures $\leq 100 \text{ bar}_a$. For a Hg^0 spiked Argon gas, laboratory validation experiments indicated >96% of Hg^0 was trapped in the acid solution at various sampling pressures (6 and 50 bar_a), with >90% of the Hg^0 trapped in the first impinger. The 3 high-pressure impingers were then used on field to sample a natural gas at 60 bar_a at $20 \text{ L}\cdot\text{min}^{-1}$ during 1 day for mercury and during 5 days for other metals. Such long sampling times were operated to collect large gas volumes to preconcentrate sufficient metals and have a time-weighted average representation of the gas composition. The efficiency

of the high-pressure impinger train was confirmed yet was found to be metal-dependent as all metals (Ba, Sn, As, Cu, Al, Se, Zn) and mercury were predominantly trapped in the first impinger, going from 51% total Se to 93% total As trapped in the first impinger [48]. The authors then used this high-pressure impinger sampling train to sample metals and metalloids in biomethane and landfill gas [35] and quantified the following metals: Se, Cd, Ni, Sb, As, Zn, Pb, Sn, Cr, Ba, Al, V, Mo, Cu, Ag (in biomethane: $10^{-1} - 10^2$ ng·Nm⁻³; in raw landfill gas: 1 – 100 µg·Nm⁻³). Using similar acidic impinger solutions (Table 2.7), Chin et al. [178] also determined metals and metalloids in 23 biogas and biomethane samples from various production sites (landfills, waste water treatment plants and anaerobic digestion plants treating diverse feedstocks). Gaseous monomethyl mercury has also been preconcentrated from landfill gas using aqueous 0.001 M HCl solution in impingers [174]. On field, the entire sampling train (tubing, impingers...) were shielded from light to avoid the photolytic degradation of monomethyl mercury and the photo-induced conversion of other Hg-compounds (e.g. dimethylmercury) into monomethyl mercury. The analysis of the sampled impinger solutions was quite complex and involved chronologically adding concentrated HCl to reach 0.4%_{vol} HCl, distillation, ethylation, preconcentration on Carbotrap™ tubes, thermal desorption of those tubes, gas-chromatography, thermal conversion and CVAFS detection [174]. These authors also used methanol impingers to trap dimethylmercury from landfill gas as they argued this compound is highly soluble and stable in methanol. Methanol impinger solutions were then analyzed by spiking Carbotrap™ tubes with small aliquots of the methanol solution followed by thermal desorption of the tubes and gas chromatography – cold vapor atomic fluorescence spectrometry (TD-GC-CVAFS) [174]. Next, Krupp et al. [4] developed a field method specific to volatile arsenic species by preconcentration in 200 mL 2%_{vol} silver nitrate impingers. Ensuing gas bubbling through the impingers, 7 mL of the AgNO₃ solution were mixed with 1.5 mL HNO₃ and 1.5 mL H₂O₂ and this mixture was then digested in a microwave. Total arsenic content in the digested solution was determined by Furnace Atomic Absorption Spectroscopy (FAAS). Authors indicated this analytical technique gave quantification results ~30 % lower than those determined with GC-ICP-MS, probably owing to incomplete absorption of the non-polar As-species (trimethylarsine) in the impinger solution and to sorption losses on impinger container walls [4]. Xu et al. [189] further explored this arsenic bubbling method and compared the efficiency of aqueous solutions of AgNO₃ versus HNO₃ as absorbing media. Concentrations of 2% AgNO₃ and 50% HNO₃ yielded the highest trapping efficiencies for trimethylarsine. The AgNO₃ solution systematically gave higher arsenic trapping efficiencies than the HNO₃ solution, except when high H₂S levels were present in the sampled gas. Indeed, silver ions in the AgNO₃ solution have a higher oxidability than HNO₃, oxidizing As-species such as trimethylarsine into AsO₄³⁻, and silver ions can additionally undergo a coordination reaction with trimethylarsine. HNO₃ has nevertheless a better As-absorption efficiency than AgNO₃ when H₂S-rich natural gas was sampled insofar as the reaction between AgNO₃ and H₂S generates black silver sulfide (Ag₂S) solid particles interfering with any further analytical step [189].

Recoveries of trace analytes from impingers not only depend on the affinity with the solvent but also on the impinger storage conditions (duration, temperature, exposure to light...) handled between sampling and analysis. For siloxanes, Saeed et al. [99] found siloxane-sampled methanol impingers kept the siloxanes stable during 21 days (recoveries > 80% after 21 days).

Ajhar et al. [37] nonetheless discouraged the storage of siloxanes in methanol as they observed low recoveries for D3 (16%), L2 (57%) and L3 (76%) after 23 days storage at 4°C. Generally, sampled impinger solutions should be analyzed as soon as possible while stored at 0 – 4°C for siloxanes [209,210] as well as for metal(loid)s [35], and in the dark to avoid photolytic degradation reactions of targeted analytes [174]. For preconcentrated metal(loid)s, it is advised to transfer the solutions into trace-metals cleaned amber glass bottle for transport and storage [4,174]. Besides, to avoid loss of analytes by saturation of the solvent and breakthrough upon sampling, several impingers are often placed in series using appropriate solvent volumes and gas flowrates and volumes (Table 2.7). The second impinger enables determining whether targeted analytes were quantitatively trapped in the first impinger.

A general observation from Table 2.7 reveals impinger sampling times are generally long, going from 10 min to 5 days but most often during several hours, inasmuch a large gas volumes (from 10 L to 140 000 L) have to be bubbled at low and constant flowrates to guarantee sufficient contact between gas and absorbing solvent and to guarantee preconcentrated analyte levels are sufficient to be detectable. This is a major drawback to the impinger method, especially when replicates have to be taken on field and when several field locations have to be sampled. Also, due to the relatively large solvent volumes used (up to 200 mL), detection limits are high. For instance, for an impinger containing 20 mL n-hexane for the preconcentration of siloxanes, Raich-Montiu et al. [104] diluted the siloxane-loaded 20 mL n-hexane to 25 mL with clean n-hexane, and 2 µL of that resulting solution were eventually injected into the GC-MS.

Table 2.7: Review of the applications of impingers for the determination of trace compounds in biogas, biomethane and landfill gas.

LOD: limit of detection. WWTP: waste water treatment plant (anaerobic digestion of WWTP sludge). AD: anaerobic digestion. GC: gas chromatography. MS: mass spectrometry. FID: flame ionization detector. ICP: inductively coupled plasma. AES: atomic emission spectrometry. FAAS: Furnace Atomic Absorption Spectroscopy. TD-GC-CVAFS: thermal desorption – GC – cold vapor atomic fluorescence spectrometry

Solvent *	Sampled gas	Sampling conditions	Targeted compounds	Compounds identified \diamond	LOD (unless otherwise stated)	Analysis	Reference
6 mL methanol (chilled at 4±2°C)	WWTP biogas	2 impingers in series. 20 L gas bubbled (3 h at 112 mL·min ⁻¹)	Volatile methyl-siloxanes	L2 L3 D4 D5 D6	1µg per mL solvent (~50 ppbv)	GC-MS	[99,100]
30 g acetone (chilled at 0°C)	Landfill gas; WWTP and AD biogas	2 impingers in series. 20 L gas bubbled (40 min at 0.5 L·min ⁻¹)	Volatile methylsiloxanes, trimethylsilanol	L2 L3 L4 D3 D4 D5 D6 Trimethylsilanol	0.01µg per g acetone Siloxanes: 0.04 - 0.11 mg·Nm ³ gas Trimethylsilanol 0.08 - 0.12 mg·Nm ³ gas	GC-MS	[210,212]
acetone; n-hexane; or methanol (chilled at 0°C)	WWTP biogas	3 impingers in series	Volatile methyl-siloxanes	L2 L3 L4 D3 D4 D5 D6	GC/MS : 0.01–0.03 µg·g ⁻¹ GC/FID : 0.05–0.09 µg·g ⁻¹	GC-MS GC-FID	[211]
Acetone; methanol; or dodecane (chilled at 0°C)	Landfill gas; WWTP and AD biogas	2 impingers in series. 20 L gas bubbled (40 min at 0.5 L·min ⁻¹)	Volatile methylsiloxanes	L2 L3 L4 D3 D4 D5 D6	0.01 – 0.03 mg·m ⁻³	GC-MS	[213]
Front impinger: 30 g solvent; back impinger: 10 g solvent		Micro-impingers also evaluated (scaled at the ratio 1:2, v/v, including solvent mass and gas flow)					
6 mL methanol (chilled in ice bath)	Landfill gas	3 impingers in series. 18 L gas bubbled (2 hours at 150 mL·min ⁻¹)	Volatile methyl-siloxanes	L2 L3 L4 L5 D3 D4 D5	Method detection limit: 0.88-2.46 µg per mL methanol	GC-MS	[121]

Table 2.7: continued

Solvent *	Sampled gas	Sampling conditions	Targeted compounds	Compounds identified \diamond	LOD (unless otherwise stated)	Analysis	Reference
Methanol (chilled in ice-water bath)	Landfill gas	2 impingers in series	33 VOC (alkanes, aromatics, terpenes, halogenated, ketones, alcohols, esters, dimethyl sulphide) and 6 siloxanes (L2, L3, L4, D3, D4, D5, trimethylsilanol)	L2 L3 L4 D3 D4 D5		GC-MS	[71]
20 ml n-hexane (chilled in ice-water bath)	WWTP biogas; landfill gas	2 impingers in series. 10 L gas bubbled (10 min at 1 L·min ⁻¹)	Volatile methylsiloxanes, trimethylsilanol	L2 L3 L4 L5 D3 D4 D5 D6 trimethylsilanol	Trimethylsilanol: 0.04 ng per L n-hexane Siloxanes: 0.02 ng per L n-hexane	GC-MS	[104]
10 mL methanol (chilled in ice bath)	Landfill gas	2 impingers in series. 12 L gas bubbled (1 hour at 0.2 L·min ⁻¹)	Volatile methyl-siloxanes	L2 L3 L4 L5 D3 D4 D5 D6	6.9 – 73.2 ng per L methanol	Purge and trap – GC-MS	[209]
100 mL n-hexane	Experimentally generated AD biogas	Aluminum gas bag sampling (2 L) and subsequent transfer to 2 impingers in series	Volatile methyl-siloxanes	L2 L3 L4 L5 D3 D4 D5 D6	Not available	GC-MS	[214]
Concentrated HNO ₃ at +60°C	Biogas or biomethane	Impinger, gas bubbling rate: 10 mL·min ⁻¹	Total silicon	Not available	Not available	ICP-AES or GC-ICP-MS	[89]

Table 2.7: continued

Solvent *	Sampled gas	Sampling conditions	Targeted compounds	Compounds identified \diamond	LOD (unless otherwise stated)	Analysis	Reference
50 mL HNO ₃ 10% _w + H ₂ O ₂ 5% _w in milli-Q water	Natural gas	3 high-pressure impingers in series. Gas bubbled at 60 bar _a during 5 days at 20 L·min ⁻¹ (~140 Nm ³ collected)	Metals and metalloids	Ba Sn As Cu Al Se Zn	Limit of quantification (μ g per liter solvent): 10 ⁻¹ for Al and Mn; 10 ⁻² for Se, Ba, Zn, Cu, Ni, Cr 10 ⁻³ for Mo, Ag, Cd, Sn, Pb, V, As	ICP-MS	[48]
50 mL KMnO ₄ 1% _w + H ₂ SO ₄ 5% _w in milli-Q water	Natural gas	3 high-pressure impingers in series. Gas bubbled at 60 bar _a during 1 day at 20 L·min ⁻¹ (~40 Nm ³ collected)	Mercury	Hg	Limit of quantification: 0.6 μ g per liter solvent	ICP-MS	[48]
50 mL HNO ₃ 10% _w + H ₂ O ₂ 5% _w in milli-Q water	AD biomethane and raw and pre- treated landfill gas	3 high-pressure impingers in series. ~140 Nm ³ gas bubbled at 1-4 bar _a (landfill gas) or 40 bar _a (biomethane) during 5 days at 20 L·min ⁻¹	Metals and metalloids	Se Cd Ni Sb As Zn Pb Sn Cr Ba Al V Mo Cu Ag	Limit of quantification (μ g per liter solvent): 10 ⁻¹ for Se, Al, Zn, Cu 10 ⁻² for As, Sb, Sn, Mo, Cd, Ba, Ni, Cr 10 ⁻³ for Ag, Pb, V	ICP-MS	[35]
20 mL HNO ₃ 5% + H ₂ O ₂ 10% in double deionized water	WWTP, landfill and AD biogas and biomethane	3 impingers in series. 30 L gas bubbled (1 h at 0.5 L·min ⁻¹)	Metals and metalloids	Be Cr Mn Co Ni Cu Zn As Se Sr Mo Cd Sb Ba Hg, Tl, Pb	Limit of quantification: 0.005 – 0.1 μ g·m ⁻³	ICP-MS	[178]

Table 2.7: continued

Solvent *	Sampled gas	Sampling conditions	Targeted compounds	Compounds identified \diamond	LOD (unless otherwise stated)	Analysis	Reference
0.001M HCl in double deionized water	Landfill gas	3 impingers in series, followed by a water condensation trap. 16 L gas bubbled (20 min at 0.8 L·min ⁻¹)	Monomethylmercury	Monomethylmercury (Hg(CH ₃))	Not available	distillation, ethylation, Cabotrap TM preconcentration, TD-GC, thermal conversion and CVAFS detection	[174]
Methanol	Landfill gas	Impinger. 11 L gas bubbled.	Dimethylmercury	Dimethylmercury (Hg(CH ₃) ₂)	Not available	Preconcentration on Carbotrap TM + TD-GC-CVAFS	[174]
200 mL 2% _{vol} AgNO ₃ in doubled distilled water	Natural gas	2 impingers in series. 40 L gas bubbled (20 min at 2 L·min ⁻¹)	Volatile arsenic species (trialkylated As species)	Mainly trimethylarsine (As(CH ₃) ₃)	Total As content: 5.0 µg per L solvent	FAAS	[4]
50% HNO ₃ or 2% AgNO ₃ (aqueous solutions)	Natural gas (site A and site B)	Site A: 2 impingers in series. 150 L gas bubbled (~ 1 h at ~ 2L·min ⁻¹) Site B: 2 impingers in series. 450 L gas bubbled (5 h at 1.5 L·min ⁻¹)	Trimethylarsine	Total arsenic	Total As content: 9.0 µg per L solvent	ICP-MS	[189]

* Solvent volumes mentioned are volumes brought in each impinger of the series when several impingers are placed in series, unless otherwise stated

\diamond **Siloxane abbreviations:** L2: Hexamethyldisiloxane; L3: Octamethyltrisiloxane; L4: Decamethyltetrasiloxane; L5: Dodecamethylpentasiloxane; D3: Hexamethylcyclotrisiloxane; D4: Octamethylcyclotetrasiloxane; D5: Decamethylcyclopentasiloxane; D6: Dodecamethylcyclohexasiloxane

III.3. Cryogenic preconcentration (cryotrapping)

A last preconcentration technique is the cryogenic trapping ('cryotrapping') of targeted trace compounds by cooling the gas sample at a temperature such that the volatile trace compounds condense but not the gas matrix (CO₂, CH₄, N₂...). In cryotrapping, the gas is typically passed through a U-shaped tube (glass or stainless-steel, example 1/8" ID (~ 3 mm) × 6" (~15 cm) length) immersed in liquid cryogen, e.g. liquid nitrogen (-196°C) or liquid argon (-186°C) when dealing with air samples [33]. When dealing with methane/carbon dioxide samples (landfill gas, sewage gas, biogas, biomethane), the cryogen temperature should be higher than the methane boiling point (-161.5 °C at 1 atm) and carbon dioxide freezing point (-78.5°C at 1 atm) to avoid CH₄ and CO₂ condensation. For instance, Feldmann et al. [8,215] used an acetone/liquid nitrogen cryogen temperature of - 80°C, or an acetone/dry ice slush at -78°C [216,217] to sample landfill and sewage gases.

Cryotrap do usually not contain adsorbent nor absorbent material, but can be packed with some untreated quartz wool, glass beads or other light inert silica-material (e.g. diatomite [215]) secured between quartz or glass wool plugs to increase the cryogenic surface area and hence increase the trapping efficiency [33]. The absence of sorbent material in the tube allows recovery of the trapped analytes by heating the tube at a moderate temperature (e.g. 40-100°C) [23,33] to non-destructively re-gasify the analytes and transfer them either to a re-focusing trap (itself a cryotrap, e.g. [67,216]) and then to the analytical unit, or directly to the analytical unit, typically a gas chromatograph (GC). The main drawback of cryotrapping is the formation of ice blocks of water in the cryotrap-tube when sampling humid gases, obstructing further gas flow. Upon thermal desorption of the tube, ice will get back to liquid state and water may be transferred to the analytical system, leading to dramatic interferences. This shortcoming can be avoided by drying the gas before cryotrapping (e.g. using anhydrous calcium chloride tubes which concomitantly remove aerosol particles [8,215]) or by adding a second 'analytical' cryogenic trap (re-focusing trap) at the entry of the analytical device [33]: the first 'sampling' cryotrap, where on water potentially got collected, is slowly heated so that water vapor is evacuated and prevented from being transferred to the second re-focusing trap, while targeted analytes are transferred [218]. The re-focusing trap is itself quickly thermally desorbed into the GC to yield high-resolution narrow chromatographic bands [23,33]. Since stable storage of sampled cryotrap is delicate, uncertain and energy-consuming, cryotrap are sampled while directly hyphenated with the analytical system. This renders *in situ* field utilization of cryotrap burdensome if not infeasible in view of the need of substantial volumes liquid cryogen, pumps and associated power supplies on-site, and of hazards related to transport of cryogens [4,23].

Cryotrapping hyphenated with gas chromatography - inductively coupled plasma - mass spectrometry (CT-GC-ICP-MS) was introduced in the 1990's to improve sampling and characterization approaches for inorganic or organic volatile metal(loid) species in environmental gas samples. Volatile metal(loid) species are thermodynamically unstable and are usually present in complex environmental gas matrices containing a multitude of other (in)organic substances wherein their stability is poorly understood [217]. Qualifying and quantifying those species is thus challenging as furthermore to date no reference materials are

available to generate standard gas mixtures wherein the stability of trace concentrations (e.g. $\text{pg}\cdot\text{L}^{-1}$) of those species would moreover be compromised by sorption effects on gas container walls. CT-GC-ICP-MS enables, in a one-stage cryogenic sampling, the concomitant kinetic stabilization and preconcentration of the volatile metal(loid) species by applying low temperatures ($\leq -80^\circ\text{C}$) and has proved to be the most robust and sensitive technique to separate, detect and semi-quantify distinct volatile metal(loid) species in complex gases, even those like biogas containing ICP-interfering CO_2 [8,215,219,220].

Table 2.8 reviews studies using CT-GC-ICP-MS to preconcentrate (in)organic volatile metal(loid) species in landfill gas, biogases and natural gas. Feldmann et al. [2,8,23,215–217,220–223] pioneered this domain and led numerous surveys at various landfill and bio-gas production sites. As however CT-GC-ICP-MS is not field-deployable, gases are often first field sampled in Tedlar bags then transported to the lab for ensuing transfer to the CT-GC-ICP-MS unit (Table 2.8). Since Haas and Feldmann [23] demonstrated most volatile metal(loid) species sampled in Tedlar bags are stable during at least 24 h when stored at 20°C , this sampling approach is an attractive compromise to benefit from the cryogenic preconcentration, the GC segregation and ICP-MS detection power. Generally, Tedlar bags should be shielded from light to prevent UV-induced degradation of the samples, stored at 4°C and analyzed as soon as possible [216,217]. If cryotrap are nevertheless sampled directly *in situ*, they should be gas-tightly closed and stored in liquid nitrogen (-196°C) [8]. The most often determined compounds include hydrides and alkylated species of As, Bi, Cd, Hg, Pb, Se, Sb, Sn, Te, and in [216,217] Feldmann et al. evidenced for the first time the occurrence of carbonyls of the (transition) metals nickel, molybdenum and tungsten ($\text{Ni}(\text{CO})_4$, $\text{Mo}(\text{CO})_6$ and $\text{W}(\text{CO})_6$) in landfill gas and sewage sludge biogas (Table 2.8). They used a non-polar Chromosorb packing in the cryotrap which, after sampling, was heated from -78°C to 150°C . The as-such re-gasified analytes were transferred to a second colder (-196°C) Chromosorb cryotrap, itself also further thermally desorbed at 150°C to the GC-ICP-MS [216,217]. Interestingly, Feldmann et al. [2] considered capillary GC ion-trap electron-impact tandem mass spectrometry (cGC-MS-MS) and GC-ICP-MS as complementary detection systems for enhanced characterization of volatile metal(loid) species in landfill gas and biogas. In a next study [221] they evaluated another detection system, namely time-of-flight mass spectrometry (ToF-MS) and compared CT-GC-ICP-ToF-MS to the standard CT-GC-ICP-MS (quadrupole MS). In particular, they pointed out the high precision and suitability of ToF-MS for multi-isotope ratio determinations of multi-elemental volatile metal(loid)s gas mixtures, and for quantification of the volatile metal(loid)s via isotope dilution. This can be useful to decipher isotope fractionation effects of metal(loid)s during their enzymatically driven bio-volatilization in microbial anaerobic environments such as landfill and sewage sludge. CT-GC-ICP-ToF-MS was also used in [222] to sample an experimental biogas containing volatile metal(loid)s. Cryotrapping occurred at -80°C or at -196°C . At that lower temperature, required to efficiently trap the most volatile metal(loid)s such as stannane (SnH_4) [8], CO_2 ice-blocks in the cryotrap were avoided by placing a NaOH-pellets cartridge, which retains CO_2 , upstream the cryotrap. Methane is not retained by NaOH but is also not efficiently condensed in the -196°C cryotrap and it did not cause major interferences in the ICP since it is much more volatile than the targeted volatile metal(loid)s and hence eluted in the ICP-plasma long before the metal(loid)s, leaving time for re-stabilization of the plasma. The NaOH cartridge reacted however with some volatile metal(loid)s, especially

antimony ones (trimethylantimony, stibine), which dramatically decreased their recovery [222]. The effects of CO₂ in the gas on the ICP-plasma performance and of NaOH cartridges on the recovery of targeted trace metal(loid)s were studied in greater detail in [220]. Further, Krupp et al. [4,34] used CT-GC-ICP-MS as a robust reference method to investigate and validate new preconcentration methods for volatile arsenic species in (natural) gas, easier to handle on field for on-line monitoring, such as chemotrapping on AgNO₃-impregnated silica gel tubes and absorption in AgNO₃ impingers, as discussed earlier in this chapter. Pinel-Raffaitin et al. also studied volatile organic arsenic and tin species in landfill gas and landfill leachates [67,224] and volatile organometal(loid)s including selenium and tellurium species in biogas [3] using CT-GC-ICP-MS for the gas samples in an attempt to determine the parameters influencing their occurrence and volatilization. Following Tedlar bag sampling, the gases were first passed through an empty glass tube at -20°C to condense water and dry the gas. Preconcentration then occurred at -80°C in a glass wool packed cryotrap. The cryotrap was immediately stored in a dry atmosphere cryogenic container. In the lab, cryotrap was flash-desorbed and re-gasified species were again cryo-focused on the packed GC-column (Chromosorb WHP, 60-80 mesh, 10% SP2100) initially maintained at -196°C and then slowly thermally desorbed to 250°C.

Next to volatile metal and metalloid species, cryotrapping has also been occasionally used for the preconcentration of siloxanes and volatile organic compounds. Grümping et al. [225] sampled landfill gas and sewage sludge biogas in gas sampling bags for subsequent cryogenic preconcentration at -100°C. Cryotrap consisted of glass tubes packed either with a silicon-containing material (3% SP-2100 on Supelcoport, 80/100 mesh) or with a silicon-free material (5% Carbowax on Carbo-pack, 60/80 mesh). By slowly heating the cryotrap from -100°C to 165°C and using a GC-ICP-OES (optical emission spectrometry) combined with a GC-MS, they successfully determined volatile organosilicon compounds including trimethylsilanol and siloxanes (L2, D3, L3, D4, L4, D5, D6) in the ng·m⁻³ to µg·m⁻³ range using either the silicon-material or the silicon-free material in the cryotrap. Finally, Schweigkofler and Niessner [1] sampled landfill gas and sewage sludge biogas in evacuated 15 L stainless-steel canisters before cryogenic preconcentration, GC segregation and concomitant mass spectrometry / atomic emission spectrometry detection (GC-MS/AES). Up to 200 mL gas from the canister was injected on the -85°C cryotrap consisting of a nickel tube packed with fine glass beads. The cryotrap was desorbed at 250°C and analytes were re-focused on a second -150°C cryotrap itself desorbed at 250°C in the GC. More than 80 volatile organic and organosilicon compounds were identified: alkanes (C5-C12), terpenes (R-pinene, camphene, limonene, terpinene), aromatic compounds, ketones (acetone, butanone), alcohols, furans (tetrahydrofuran), trimethylsilanol and siloxanes (L2, L3, L4, D3, D4, D5, D6).

Table 2.8: Review of the applications of cryotrapping – gas chromatography – inductively coupled plasma – mass spectrometry (CT-GC-ICP-MS) for the determination of traces of (in)organic volatile metals and metalloids in biogas, landfill gas and natural gas.

LOD: limit of detection. WWTP: waste water treatment plant (anaerobic digestion of WWTP sludge). AD: anaerobic digestion

Sampled gas	Sampling conditions	Cryotrap	Targeted compounds	Compounds identified	LOD	Reference
Landfill gas	20 L gas; 20 mL·min ⁻¹ ; CaCl ₂ drying tube upstream cryotrap	– 80°C; packed with Supelcoport (10% SP-2100, 60/80 mesh, Supelco)	Volatile metals and metalloids	Volatile species (hydrides and alkylated) of As, Bi, Hg, Sb, Sn, Te (ng to µg·m ⁻³)	Not available	[215]
Landfill gas, WWTP biogas	20 L gas; CaCl ₂ or Mg(ClO ₄) ₂ drying tube upstream cryotrap	2 cryotrap in series; – 80°C; packed with Supelcoport (10% SP-2100, 60/80 mesh, Supelco)	Volatile metals and metalloids	Volatile species (hydrides and alkylated) of: Landfill gas: As, Bi, Hg, Pb, Sb, Se, Sn, Te WWTP biogas: As, Bi, Cd, Hg, Pb, Sb, Sn, Te (ng to µg·m ⁻³)	Not available	[8]
Landfill gas	Tedlar bag (4 L) with subsequent transfer to cryotrap	– 78°C; packed with Chromosorb (10% SP-2100, 60/80 mesh, Supelco)	Volatile metals, metalloids and transition metals	Volatile species (hydrides and alkylated) of As, Bi, Hg, Pb, Sb, Se, Sn, Te; Transition metal carbonyls: Mo(CO) ₆ , W(CO) ₆ (Mo: 0.2-0.3 µg·m ⁻³ ; W: 0.005-0.01 µg·m ⁻³)	Not available	[216]
WWTP biogas	Tedlar bag (80 L) with subsequent transfer to cryotrap	– 78°C; packed with Chromosorb (10% SP-2100, 60/80 mesh, Supelco)	Volatile transition metal carbonyls	Ni(CO) ₄ (0.5-1.0 µg·m ⁻³); Mo(CO) ₆ (3.0-3.6 µg·m ⁻³); W(CO) ₆ (0.01-0.015 µg·m ⁻³)	Ni: 0.01 µg·m ⁻³ gas	[217]
Landfill and WWTP biogas	4 – 20 L	–78°C or –80°C; packed with 10% SP-2100 on either Chromosorb or Supelcoport	Volatile bismuth species	Trimethylbismuth (Bi(CH ₃) ₃ , up to 25 µg·m ⁻³)	Not available	[223]
Landfill gas and WWTP biogas	Tedlar bag with subsequent transfer to cryotrap	– 78°C; packed with Chromosorb (10% SP-2100, 45/60 mesh, Supelco)	Volatile metals and metalloids	Volatile species (hydrides and alkylated) of Sb, Sn, Bi species	~ µg·m ⁻³ gas	[2]
WWTP biogas	Tedlar bag (10 L) with subsequent transfer to cryotrap	–80°C; fused silica column	Volatile metals and metalloids	Trimethylantimony (5 ng·L ⁻¹); trimethylbismuth (18 ng·L ⁻¹); dimethyltellurium	Not available	[23]
Landfill gas	Tedlar bag (5 – 10 L) with subsequent transfer of 500 mL to cryotrap	–80°C; fused silica column	Volatile metals and metalloids	Volatile alkylated species of As, Bi, Pb, Sn, Sb, Te	Not available	[221]

Table 2.8: continued

Sampled gas	Sampling conditions	Cryotrap	Targeted compounds	Compounds identified	LOD	Reference
Experimental AD biogas	NaOH-pellets cartridge to absorb CO ₂ and H ₂ O upstream cryotrap	–196°C	Volatile metals and metalloids	Volatile species (hydrides and alkylated) of: As, Sb, Sn	Not available	[220,222]
	if not:	–80°C				
Natural gas	Pressurized stainless-steel gas cylinder (SilcoSteel® surface treatment) with subsequent depressurization and transfer of 50 mL to the cryotrap	–120°C; SilcoSteel® tubing	Volatile arsenic compounds	Trimethylarsine (TMA) <18 µg·m ⁻³ gas	0.2 µg TMA · m ⁻³ gas	[4]
Natural gas	Pressurized stainless-steel gas cylinder (Sulfinert™ surface treatment) with subsequent depressurization and transfer of 50 mL to the cryotrap	–80°C; SilcoSteel® tubing	Volatile arsenic compounds	Trimethylarsine (TMA) 3 – 130 µg·m ⁻³ gas	0.2 µg TMA · m ⁻³ gas	[34]
Landfill gas	Tedlar bag (10 L) with subsequent transfer to a H ₂ O-condensation tube (–20°C) before transfer to the cryotrap	–80°C; Packed with glass wool	Volatile (in)organic arsenic compounds	Volatile alkylated arsenic species (0 – 15 µg As · m ⁻³ gas)	0.1 ng As · m ⁻³ gas	[67]
Landfill gas	Tedlar bag (10 L) with subsequent transfer to a H ₂ O-condensation tube (–20°C) before transfer to the cryotrap	–80°C; Packed with glass wool	Volatile (in)organic tin compounds	Volatile alkylated tin species 0.01 – 20 µg Sn · m ⁻³ gas	0.25 ng Sn · m ⁻³ gas	[224]
Compost (pine shavings, duck feathers, duck excreta) biogas	Tedlar bag (10 L) with subsequent transfer to a H ₂ O-condensation tube (–20°C) before transfer to the cryotrap	–80°C; Packed with silanized glass wool	Volatile metals and metalloids	Volatile alkylated species of As, Bi, Pb, Sb, Se, Sn, Te (Se and Te: 0.01 – 2.3 µg·m ⁻³ gas)	Bi: 1.2 pg·m ⁻³ gas Se: 799 pg·m ⁻³ gas	[3]

IV. CONCLUSIONS AND RECOMMENDATIONS

This chapter highlighted the diversity of available gas sampling techniques, either whole gas sampling or gas sampling with preconcentration of trace compounds. Most of those techniques have been applied for biogas and biomethane sampling, as recently reviewed by Bragança et al., 2020 [226]. Importantly, as stressed out by Arrhenius et al. [5], above discussions suggest there is no universal sampling vessel nor preconcentration technique able to quantitatively sample and recover all (families of) trace compounds. The materials used in the sampling chain (tubing, polymer film and valve fitting material of gas bags, passivation treatment in stainless-steel cylinders and canisters, adsorbent material and sorbent bed retaining hardware in sorbent tubes; absorption solvent in impingers, packing material in cryotrap...), the pressure at which gas is sampled, the transport and storage conditions of samples (duration, temperature, humidity, exposure to light...), the gas composition and trace compounds nature and concentrations are all influencing the integrity, stability and recovery of trace compounds in and from their sampling unit. High boiling and polar compounds are for instance less stable in whole gas sampling vessels owing to, respectively, their propensity for wall sorption and dissolution in condensed water. The stability of volatile metal(loid) compounds in whole gas vessels may depend on the central metal atom. Reactive analytes could undergo conversion or degradation reactions with other sampled compounds especially inside whole gas sampling vessels. In those vessels, the initial sampled analyte concentration and moisture level as well as sampled volume and sample pressure critically influence wall sorption effects.

In addition to the lack of 'universal' sampling devices, this review suggests there is a lack of techniques allowing to directly preconcentrate trace compounds from pressurized gases *in situ* on the gas pipes at the working pressure to avoid drawbacks and shortcomings diverted from the depressurization of gas samples.

If a singular trace compound or chemical family is targeted, the most appropriate sampling chain can be chosen based on existing literature and on preliminary validation experiments. Nonetheless, when a global screening of trace compounds in a gas sample is desired, coupling several sampling methods is perhaps the best compromise to increase the chances that each considered sampling method will suitably retain a given family of trace compounds.

Some general recommendations can be drawn from the above to optimize sampling procedures.

- The sampling vessel or preconcentration unit should be chosen based on the preliminary evaluation of the short-term (~24 h) storage stability and recovery of targeted analytes in/from that sampling unit and of the achievable analytical detection limits. Reference, calibrated gas mixtures prepared in biogas matrices and containing model targeted compounds should be used to accurately and robustly validate the methods. Suitable methods for biogas should also be appropriate for biomethane as this purified gas is dry and should contain lower concentrations trace compounds than biogas. However, more stringent detection limits are requested for biomethane [5].
- Tubing and connectors used in the field sampling chain and in the lab analytical chain should be of inert and clean materials and leak-free to avoid trace compounds losses.

Polytetrafluoroethylene (PTFE) tubing is generally advised as it is considerably less adsorptive than stainless-steel, copper or Tygon tubing [5,42]. Silicon tubing should especially be avoided when targeting siloxanes, for which silicon-free tubing must be used [104]. When stainless-steel collection or tubing material is used, it should be surface-treated or coated with appropriate passivation technologies to limit surface wall sorption and reactions with the stainless-steel iron [42].

- The field sampling chain should be as short as possible by using tubing as short as possible to limit trace compounds sorption losses.
- The field sampling chain should be flushed with the gas to sample during several minutes to hours before effective sampling, to condition and 'accustom' the tubing to the trace compounds and saturate potential sinks (sorption sites).
- Gas samples should be analyzed as soon as possible after sampling, usually within 24 h to avoid or minimize artifacts and analytes losses during storage phases. If possible, direct *in situ* analysis should be performed, e.g. using field-portable gas chromatographs.
- If sample storage is inevitable, the gas sample should be stored at cold temperatures (from <0°C for adsorbent tubes to <20°C for Tedlar bags), shielded from sun light to avoid UV-induced degradation reactions and stored in a dry and solvent-free and vapor-free environment.

To conclude, Table 2.9 displays an overview of important features of gas sampling techniques with and without enrichment.

Table 2.9: Global features of gas sampling techniques: whole gas sampling and gas sampling with enrichment.

Sampling technique	Whole gas sampling			Sampling with enrichment				
	no analyte breakthrough; fast sampling; only defined gas volumes can be sampled; especially suitable for very volatile permanent gases (N₂, CO₂, CH₄, O₂...)			breakthrough possible; time-consuming; large gas volumes can be sampled; flammable gas matrix (CH ₄) not sampled; especially suitable for trace compounds				
Sampling support	Gas bag	Passivated cylinder	Passivated canister	Adsorbent tubes	Solid Phase Microextraction	Absorption (impinger)	Cryogenic trapping	Amalgamation and Chemotrapping
Allowed sampling pressure	Slightly above P _{atm}	≤ 344 bar _a	≤ 2.75 bar	Slightly above P _{atm} ; ≤ 200 bar _a (this PhD thesis)	P _{atm}	P _{atm} ; ≤ 100 bar _a [48]	Slightly above P _{atm}	Slightly above P _{atm}
Maximal sampleable gas volume (†)	100 L	3785 cm ³ at 124 bar _a max [77]	Up to 100 L at max 2.75 bar _a	No theoretical limit. Analytically relevant volume function of analyte breakthrough volume at a given sampling rate, temperature and moisture level	Not applicable (exposure time)	No theoretical limit. Analytically relevant volume function of analyte breakthrough volume at a given sampling rate, temperature and moisture level		
Advantages << Disadvantages >>	Cheap, easy use << Sorption losses on vessel walls	Pressurized sampling << Sorption losses on vessel walls; expensive	Easy use << sorption losses on vessel walls; expensive	Small size; easy handling, transport and storage; high storage stability; possibility of multibed for enlarged affinities << No repeated sample analysis; trained personnel required	Small size; easy handling; fast << Fragile; not for field utilization unless field-GC	>< Installation time consuming; handling of solvents; cooling bath required; trained personnel required	Reference method for volatile metal(loid)s << energy intensive (cryogen); cryogen handling; trained personnel required; not field-deployable	Specific for given elements e.g. Hg, As << Complex preparation; trained personnel required
Sampleable chemical families	(H)VOC VSC, VSiC VMC	VOC VSC, VSiC VMC	(H)VOC VSC, VSiC	(H)VOC VSC, VSiC VMC	(H)VOC VSC, VSiC	VOC VSiC VMC	VSiC VMC	VMC
Reusable	Not recommended	Yes with cleaning (but old cylinders give artifacts [75])	Yes with cleaning (but older canister do not keep analytes as stable as new canisters do [105])	Yes if thermally desorbed; no if solvent-desorbed	Yes (thermal reconditioning)	No	Yes (thermal reconditioning)	Yes (thermal reconditioning)

(H)VOC: (halogenated) volatile organic compounds; VSC: volatile Sulphur compounds; VSiC: volatile silicon compounds; VMC: volatile metal(loid) compounds.

(†) Maximal sampleable gas volumes for whole gas sampling vessels indicate standard commercially available vessel sizes. Custom-sized bags, cylinders and canisters are an alternative.

Authors Informations

* Corresponding Author: Isabelle Le Hécho • isabelle.lehecho@univ-pau.fr • Université de Pau et des Pays de l'Adour, E2S UPPA, CNRS, IPREM UMR 5254, Technopôle HélioParc, 2 avenue du Président Angot, 64053 Pau Cedex 09, France

Note

The authors declare no competing financial interests or personal relationships that could have influenced the work reported in this paper.

Acknowledgements

The authors thank Teréga (40 Avenue de l'Europe, CS 20 522, 64010 Pau Cedex, France) for the financial support.

V. REFERENCES CHAPTER 2

- [1] M. Schweigkofler, R. Niessner, Determination of Siloxanes and VOC in Landfill Gas and Sewage Gas by Canister Sampling and GC-MS/AES Analysis, *Environ. Sci. Technol.* 33 (1999) 3680–3685. <https://doi.org/10.1021/es9902569>.
- [2] J. Feldmann, I. Koch, W.R. Cullen, Complementary Use of Capillary Gas Chromatography–Mass Spectrometry (ion Trap) and Gas Chromatography–Inductively Coupled Plasma Mass Spectrometry for the Speciation of Volatile Antimony, Tin and Bismuth Compounds in Landfill and Fermentation Gases, *The Analyst*. 123 (1998) 815–820. <https://doi.org/10.1039/a707478f>.
- [3] P. Pinel-Raffaitin, C. Pécheyran, D. Amouroux, New Volatile Selenium and Tellurium Species in Fermentation Gases Produced by Composting Duck Manure, *Atmos. Environ.* 42 (2008) 7786–7794. <https://doi.org/10.1016/j.atmosenv.2008.04.052>.
- [4] E.M. Krupp, C. Johnson, C. Rechsteiner, M. Moir, D. Leong, J. Feldmann, Investigation into the Determination of Trimethylarsine in Natural Gas and Its Partitioning into Gas and Condensate Phases Using (cryotrapping)/Gas Chromatography Coupled to Inductively Coupled Plasma Mass Spectrometry and Liquid/Solid Sorption Techniques, *Spectrochim. Acta Part B At. Spectrosc.* 62 (2007) 970–977. <https://doi.org/10.1016/j.sab.2007.07.009>.
- [5] K. Arrhenius, A.S. Brown, A.M.H. van der Veen, Suitability of Different Containers for the Sampling and Storage of Biogas and Biomethane for the Determination of the Trace-Level Impurities – A Review, *Anal. Chim. Acta.* 902 (2016) 22–32. <https://doi.org/10.1016/j.aca.2015.10.039>.
- [6] R. Sheu, A. Marcotte, P. Khare, S. Charan, J.C. Ditto, D.R. Gentner, Advances in Offline Approaches for Chemically Speciated Measurements of Trace Gas-Phase Organic Compounds Via Adsorbent Tubes in an Integrated Sampling-to-Analysis System, *J. Chromatogr. A.* 1575 (2018) 80–90. <https://doi.org/10.1016/j.chroma.2018.09.014>.
- [7] J. Namieśnik, B. Zygmunt, A. Jastrzębska, Application of Solid-Phase Microextraction for Determination of Organic Vapours in Gaseous Matrices, *J. Chromatogr. A.* 885 (2000) 405–418. [https://doi.org/10.1016/S0021-9673\(99\)01157-7](https://doi.org/10.1016/S0021-9673(99)01157-7).
- [8] J. Feldmann, A.V. Hirner, Occurrence of Volatile Metal and Metalloid Species in Landfill and Sewage Gases, *Int. J. Environ. Anal. Chem.* 60 (1995) 339–359. <https://doi.org/10.1080/03067319508042888>.
- [9] T. Bond, M.R. Templeton, History and Future of Domestic Biogas Plants in the Developing World, *Energy Sustain. Dev.* 15 (2011) 347–354. <https://doi.org/10.1016/j.esd.2011.09.003>.

- [10] N. Scarlat, J.-F. Dallemand, F. Fahl, Biogas: Developments and perspectives in Europe, *Renew. Energy*. 129 (2018) 457–472. <https://doi.org/10.1016/j.renene.2018.03.006>.
- [11] K. Arrhenius, H. Yaghooby, L. Rosell, O. Bükler, L. Culleton, S. Bartlett, A. Murugan, P. Brewer, J. Li, A.M.H. van der Veen, I. Krom, F. Lestremau, J. Beranek, Suitability of Vessels and Adsorbents for the Short-Term Storage of Biogas/Biomethane for the Determination of Impurities – Siloxanes, Sulfur Compounds, Halogenated Hydrocarbons, BTEX, Biomass Bioenergy. 105 (2017) 127–135. <https://doi.org/10.1016/j.biombioe.2017.06.025>.
- [12] F. Hilaire, E. Basset, R. Bayard, M. Gallardo, D. Thiebaut, J. Vial, Comprehensive Two-Dimensional Gas Chromatography for Biogas and Biomethane Analysis, *J. Chromatogr. A*. 1524 (2017) 222–232. <https://doi.org/10.1016/j.chroma.2017.09.071>.
- [13] G. Leonzio, Upgrading of Biogas to Bio-Methane with Chemical Absorption Process: Simulation and Environmental Impact, *J. Clean. Prod.* 131 (2016) 364–375. <https://doi.org/10.1016/j.jclepro.2016.05.020>.
- [14] R. Augelletti, M. Conti, M.C. Annesini, Pressure Swing Adsorption for Biogas Upgrading. A New Process Configuration for the Separation of Biomethane and Carbon Dioxide, *J. Clean. Prod.* 140 (2017) 1390–1398. <https://doi.org/10.1016/j.jclepro.2016.10.013>.
- [15] C. Li, G. Liu, I.A. Nges, J. Liu, Enhanced Biomethane Production from Miscanthus Lutarioriparius Using Steam Explosion Pretreatment, *Fuel*. 179 (2016) 267–273. <https://doi.org/10.1016/j.fuel.2016.03.087>.
- [16] H. Porté, P.G. Kougiyas, N. Alfaro, L. Treu, S. Campanaro, I. Angelidaki, Process Performance and Microbial Community Structure in Thermophilic Trickling Biofilter Reactors for Biogas Upgrading, *Sci. Total Environ.* 655 (2019) 529–538. <https://doi.org/10.1016/j.scitotenv.2018.11.289>.
- [17] E. Hosseini Koupaie, S. Dahadha, A.A. Bazyar Lakeh, A. Azizi, E. Elbeshbishy, Enzymatic Pretreatment of Lignocellulosic Biomass for Enhanced Biomethane Production-a Review, *J. Environ. Manage.* 233 (2019) 774–784. <https://doi.org/10.1016/j.jenvman.2018.09.106>.
- [18] L. Ding, J. Cheng, A. Xia, A. Jacob, M. Voelklein, J.D. Murphy, Co-Generation of Biohydrogen and Biomethane Through Two-Stage Batch Co-Fermentation of Macro- and Micro-Algal Biomass, *Bioresour. Technol.* 218 (2016) 224–231. <https://doi.org/10.1016/j.biortech.2016.06.092>.
- [19] X. Kan, J. Zhang, Y.W. Tong, C.-H. Wang, Overall Evaluation of Microwave-Assisted Alkali Pretreatment for Enhancement of Biomethane Production from Brewers' Spent Grain, *Energy Convers. Manag.* 158 (2018) 315–326. <https://doi.org/10.1016/j.enconman.2017.12.088>.

- [20] A.S. Calbry-Muzyka, A. Gantenbein, J. Schneebeli, A. Frei, A.J. Knorpp, T.J. Schildhauer, S.M.A. Biollaz, Deep Removal of Sulfur and Trace Organic Compounds from Biogas to Protect a Catalytic Methanation Reactor, *Chem. Eng. J.* 360 (2019) 577–590.
<https://doi.org/10.1016/j.cej.2018.12.012>.
- [21] S. Mariné, M. Pedrouzo, R.M. Marcé, I. Fonseca, F. Borrull, Comparison Between Sampling and Analytical Methods in Characterization of Pollutants in Biogas, *Talanta*. 100 (2012) 145–152. <https://doi.org/10.1016/j.talanta.2012.07.074>.
- [22] K. Arrhenius, A. Fischer, O. Büker, Methods for Sampling Biogas and Biomethane on Adsorbent Tubes After Collection in Gas Bags, *Appl. Sci.* 9 (2019) 1171.
<https://doi.org/10.3390/app9061171>.
- [23] K. Haas, J. Feldmann, Sampling of Trace Volatile Metal(loid) Compounds in Ambient Air Using Polymer Bags: A Convenient Method, *Anal. Chem.* 72 (2000) 4205–4211.
<https://doi.org/10.1021/ac000313c>.
- [24] International Organization for Standardization, EN ISO 10715:2000: Natural Gas - Sampling Guidelines (ISO 10715:1997), (2000).
- [25] International Organization for Standardization, ISO 6974: Natural gas — Determination of composition and associated uncertainty by gas chromatography, (2012).
- [26] International Organization for Standardization, ISO 6975: Natural Gas - Extended Analysis - Gas-Chromatographic Method (ISO 6975:1997), (1997).
- [27] International Organization for Standardization, ISO 6978-1:2003: Natural Gas - Determination of Mercury - Part 1: Sampling of Mercury by Chemisorption on Iodine, (2003).
- [28] International Organization for Standardization, ISO 6978-2:2003: Natural Gas - Determination of Mercury - Part 2: Sampling of Mercury by Amalgamation on Gold/Platinum Alloy, (2003).
- [29] International Organization for Standardization, ISO 16017-1:2000: Indoor, Ambient and Workplace Air — Sampling and Analysis of Volatile Organic Compounds by Sorbent Tube/Thermal Desorption/Capillary Gas Chromatography — Part 1: Pumped Sampling, (2000).
- [30] US EPA, W. Winberry, N.T. Murpyh, R.M. Riggan, Compendium of Methods for the Determination of Toxic Organic Compounds in Ambient Air (EPA/600/4-89/017), (1988).
- [31] US EPA, Compendium of Methods for the Determination of Toxic Organic Compounds in Ambient Air - Second Edition (EPA/625/R-96/010b), (1999).
- [32] M. Harper, Review. Sorbent Trapping of Volatile Organic Compounds from Air, *J. Chromatogr. A*. 885 (2000) 129–151. [https://doi.org/10.1016/S0021-9673\(00\)00363-0](https://doi.org/10.1016/S0021-9673(00)00363-0).

- [33] V. Camel, M. Caude, Review: Trace Enrichment Methods for the Determination of Organic Pollutants in Ambient Air, *J. Chromatogr. A.* 710 (1995) 3–19.
[https://doi.org/10.1016/0021-9673\(95\)00080-7](https://doi.org/10.1016/0021-9673(95)00080-7).
- [34] M.K. Uroic, E.M. Krupp, C. Johnson, J. Feldmann, Chemotrapping-Atomic Fluorescence Spectrometric Method as a Field Method for Volatile Arsenic in Natural Gas, *J. Environ. Monit.* 11 (2009) 2222. <https://doi.org/10.1039/b913322d>.
- [35] M. Cachia, B. Bouyssiere, H. Carrier, H. Garraud, G. Caumette, I. Le Hécho, Characterization and Comparison of Trace Metal Compositions in Natural Gas, Biogas, and Biomethane, *Energy Fuels.* 32 (2018) 6397–6400.
<https://doi.org/10.1021/acs.energyfuels.7b03915>.
- [36] J.P. Hsu, G. Miller, V. Moran, Analytical Method for Determination of Trace Organics in Gas Samples Collected by Canister, *J. Chromatogr. Sci.* 29 (1991) 83–88.
<https://doi.org/10.1093/chromsci/29.2.83>.
- [37] M. Ajhar, B. Wens, K.H. Stollenwerk, G. Spalding, S. Yüce, T. Melin, Suitability of Tedlar® Gas Sampling Bags for Siloxane Quantification in Landfill Gas, *Talanta.* 82 (2010) 92–98.
<https://doi.org/10.1016/j.talanta.2010.04.001>.
- [38] M. Ghidotti, D. Fabbri, C. Torri, Determination of Linear and Cyclic Volatile Methyl Siloxanes in Biogas and Biomethane by Solid-Phase Microextraction and Gas Chromatography-Mass Spectrometry, *Talanta.* 195 (2019) 258–264.
<https://doi.org/10.1016/j.talanta.2018.11.032>.
- [39] C.-C. Hsieh, S.-H. Horng, P.-N. Liao, Stability of Trace-Level Volatile Organic Compounds Stored in Canisters and Tedlar bags, *Aerosol Air Qual. Res.* 3 (2003) 17–28.
- [40] T.J. Kelly, M.W. Holdren, Applicability of Canisters for Sample Storage in the Determination of Hazardous Air Pollutants, *Atmos. Environ.* 29 (1995) 2595–2608.
[https://doi.org/10.1016/1352-2310\(95\)00192-2](https://doi.org/10.1016/1352-2310(95)00192-2).
- [41] L. Maret, Application De La Technique De Thermodésorption Pour L’analyse De 93 COV Et Le Screening Des COV Dans L’air Des Lieux De Travail. *Chimie Analytique. Université Claude Bernard - Lyon I*, 2013. Français. Nnt: 2013lyo10313 . Tel-01070680, (n.d.).
- [42] A.S. Brown, A.M.H. Van Der Veen, K. Arrhenius, A. Murugan, L.P. Culleton, P.R. Ziel, J. Li, Sampling of Gaseous Sulfur-Containing Compounds at Low Concentrations with a Review of Best-Practice Methods for Biogas and Natural Gas Applications, *TrAC Trends Anal. Chem.* 64 (2015) 42–52. <https://doi.org/10.1016/j.trac.2014.08.012>.

- [43] S. Beghi, J.-M. Guillot, Use of Poly(ethylene Terephthalate) Film Bag to Sample and Remove Humidity from Atmosphere Containing Volatile Organic Compounds, *J. Chromatogr. A*. 1183 (2008) 1–5. <https://doi.org/10.1016/j.chroma.2007.12.051>.
- [44] E. Gallego, F.J. Roca, J.F. Perales, X. Guardino, E. Gadea, Development of a Method for Determination of VOCs (including Methylsiloxanes) in Biogas by TD-GC/MS Analysis Using Supel™ Inert Film Bags and Multisorbent Bed Tubes, *Int. J. Environ. Anal. Chem.* 95 (2015) 291–311. <https://doi.org/10.1080/03067319.2015.1016012>.
- [45] RESTEK Pure Chromatography, Air Sampling, Restek. (2020). <https://www.restek.com/Sample-Handling/Air-Sampling> (accessed April 14, 2020).
- [46] Scentroid, Sampling Bags, Scentroid. (2020). <https://scentroid.com/products/sampling-bags/> (accessed April 14, 2020).
- [47] MediSense Samplebags.eu, The Sample Bag Supplier. Worldwide Delivery and Sharp Prices, Samplebagseu Supplier Gas Sampl. Bags. (n.d.). <https://www.samplebags.eu/> (accessed April 14, 2020).
- [48] M. Cachia, B. Bouyssi re, H. Carrier, H. Garraud, G. Caumette, I. Le H cho, Development of a High-Pressure Bubbling Sampler for Trace Element Quantification in Natural Gas, *Energy Fuels*. 31 (2017) 4294–4300. <https://doi.org/10.1021/acs.energyfuels.6b03059>.
- [49] S.-H. Jo, K.-H. Kim, Z.-H. Shon, D. Parker, Identification of Control Parameters for the Sulfur Gas Storability with Bag Sampling Methods, *Anal. Chim. Acta*. 738 (2012) 51–58. <https://doi.org/10.1016/j.aca.2012.06.010>.
- [50] Y.-H. Kim, K.-H. Kim, S.-H. Jo, E.-C. Jeon, J.R. Sohn, D.B. Parker, Comparison of Storage Stability of Odorous VOCs in Polyester Aluminum and Polyvinyl Fluoride Tedlar® Bags, *Anal. Chim. Acta*. 712 (2012) 162–167. <https://doi.org/10.1016/j.aca.2011.11.014>.
- [51] M. Toledo, J.M. Guillot, J.A. Siles, M.A. Mart n, Permeability and Adsorption Effects for Volatile Sulphur Compounds in Nalophan Sampling Bags: Stability Influenced by Storage Time, *Biosyst. Eng.* 188 (2019) 217–228. <https://doi.org/10.1016/j.biosystemseng.2019.10.023>.
- [52] L. Eusebio, L. Capelli, S. Sironi, H₂S Loss through Nalophan™ Bags: Contributions of Adsorption and Diffusion, *Sci. World J.* 2017 (2017) 9690704. <https://doi.org/10.1155/2017/9690704>.
- [53] L.J. McGarvey, C.V. Shorten, The Effects of Adsorption on the Reusability of Tedlar® Air Sampling Bags, *AIHAJ - Am. Ind. Hyg. Assoc.* 61 (2000) 375–380. <https://doi.org/10.1080/15298660008984546>.

- [54] J.-H. Ahn, A. Deep, K.-H. Kim, The Storage Stability of Biogenic Volatile Organic Compounds (BVOCs) in Polyester Aluminum Bags, *Atmos. Environ.* 141 (2016) 430–434. <https://doi.org/10.1016/j.atmosenv.2016.07.019>.
- [55] P. Mochalski, B. Wzorek, I. Śliwka, A. Amann, Suitability of Different Polymer Bags for Storage of Volatile Sulphur Compounds Relevant to Breath Analysis, *J. Chromatogr. B.* 877 (2009) 189–196. <https://doi.org/10.1016/j.jchromb.2008.12.003>.
- [56] Geotech Environmental Equipment, Tedlar & ALTEF Gas Sampling Bags., (2019). http://www.geotechenv.com/pdf/air_quality/gas_sampling_bags.pdf.
- [57] Uniphos, ALTEF Gas Sampling Bags, Uniphos Envirotronic. (2020). <https://www.uniphosamericas.com/altef-gas-sampling-bags/> (accessed March 31, 2020).
- [58] K.-H. Kim, A Study of Sorptive Loss Patterns for Reduced Sulfur Compounds in the Use of the Bag Sampling Method, *Environ. Monit. Assess.* 123 (2006) 259–269. <https://doi.org/10.1007/s10661-006-9195-8>.
- [59] S. Rasi, A. Veijanen, J. Rintala, Trace Compounds of Biogas from Different Biogas Production Plants, *Energy.* 32 (2007) 1375–1380. <https://doi.org/10.1016/j.energy.2006.10.018>.
- [60] S. Rasi, J. Lantelä, J. Rintala, Trace Compounds Affecting Biogas Energy Utilisation – A Review, *Energy Convers. Manag.* 52 (2011) 3369–3375. <https://doi.org/10.1016/j.enconman.2011.07.005>.
- [61] S. Rasi, J. Lehtinen, J. Rintala, Determination of Organic Silicon Compounds in Biogas from Wastewater Treatments Plants, Landfills, and Co-Digestion Plants, *Renew. Energy.* 35 (2010) 2666–2673. <https://doi.org/10.1016/j.renene.2010.04.012>.
- [62] D. Papurello, A. Lanzini, L. Tognana, S. Silvestri, M. Santarelli, Waste to Energy: Exploitation of Biogas from Organic Waste in a 500 Wel Solid Oxide Fuel Cell (SOFC) Stack, *Energy.* 85 (2015) 145–158. <https://doi.org/10.1016/j.energy.2015.03.093>.
- [63] D. Papurello, L. Tomasi, S. Silvestri, I. Belcari, M. Santarelli, F. Smeacetto, F. Biasioli, Biogas Trace Compound Removal with Ashes Using Proton Transfer Reaction Time-of-Flight Mass Spectrometry as Innovative Detection Tool, *Fuel Process. Technol.* 145 (2016) 62–75. <https://doi.org/10.1016/j.fuproc.2016.01.028>.
- [64] K. Badjagbo, M. Héroux, M. Alae, S. Moore, S. Sauvé, Quantitative Analysis of Volatile Methylsiloxanes in Waste-to-Energy Landfill Biogases Using Direct APCI-MS/MS, *Environ. Sci. Technol.* 44 (2010) 600–605. <https://doi.org/10.1021/es902741k>.

- [65] M. Sulyok, C. Haberhauer-Troyer, E. Rosenberg, M. Grasserbauer, Investigation of the Storage Stability of Selected Volatile Sulfur Compounds in Different Sampling Containers, *J. Chromatogr. A.* 917 (2001) 367–374. [https://doi.org/10.1016/S0021-9673\(01\)00654-9](https://doi.org/10.1016/S0021-9673(01)00654-9).
- [66] Y.K. Lau, Measurement of Sulphur Gases in Ambient Air, *Environ. Monit. Assess.* 13 (1989) 69–74. <https://doi.org/10.1007/BF00398736>.
- [67] P. Pinel-Raffaitin, I. Le Hecho, D. Amouroux, M. Potin-Gautier, Distribution and Fate of Inorganic and Organic Arsenic Species in Landfill Leachates and Biogases, *Environ. Sci. Technol.* 41 (2007) 4536–4541. <https://doi.org/10.1021/es0628506>.
- [68] E.A. Polman, H. Top, B. Gerritsen, A. Rekers, Development of Existing and New Measurement Technologies for Determination of the Gas Composition EDGaR project number 100201910, (2015).
- [69] M. Arnold, T. Kajolinna, Development of on-Line Measurement Techniques for Siloxanes and Other Trace Compounds in Biogas, *Waste Manag.* 30 (2010) 1011–1017. <https://doi.org/10.1016/j.wasman.2009.11.030>.
- [70] A. Ghosh, S.K. Seeley, S.R. Nartker, J.V. Seeley, Analysis of Siloxanes in Hydrocarbon Mixtures Using Comprehensive Two-Dimensional Gas Chromatography, *J. Chromatogr. A.* 1360 (2014) 258–263. <https://doi.org/10.1016/j.chroma.2014.07.062>.
- [71] A. Narros, M.I. Del Peso, G. Mele, M. Vinot, E. Fernández, M.E. Rodriguez, Determination of Siloxanes in Landfill Gas by Adsorption on Tenax Tubes and TD-GC-MS, in: CISA Publisher, Italy, S. Margherita di Pula, Cagliari, Italy, 2009.
- [72] C.M.A. Eichler, Y. Wu, S.S. Cox, S. Klaus, G.D. Boardman, Evaluation of Sampling Techniques for Gas-Phase Siloxanes in Biogas, *Biomass Bioenergy.* 108 (2018) 1–6. <https://doi.org/10.1016/j.biombioe.2017.10.049>.
- [73] E. Davoli, M.L. Gangai, L. Morselli, D. Tonelli, Characterisation of Odorants Emissions from Landfills by SPME and GC/MS, *Chemosphere.* 51 (2003) 357–368. [https://doi.org/10.1016/S0045-6535\(02\)00845-7](https://doi.org/10.1016/S0045-6535(02)00845-7).
- [74] J. Arndt, G. Ilgen, B. Planer-Friedrich, Evaluation of Techniques for Sampling Volatile Arsenic on Volcanoes, *J. Volcanol. Geotherm. Res.* 331 (2017) 16–25. <https://doi.org/10.1016/j.jvolgeores.2016.10.016>.
- [75] M. Enrico, A. Mere, H. Zhou, H. Carrier, E. Tessier, B. Bouyssiere, Experimental Tests of Natural Gas Samplers Prior to Mercury Concentration Analysis, *Energy Fuels.* (2019). <https://doi.org/10.1021/acs.energyfuels.9b03540>.

- [76] E. Woolfenden, Sorbent-Based Sampling Methods for Volatile and Semi-Volatile Organic Compounds in Air: Part 1: Sorbent-Based Air Monitoring Options, *J. Chromatogr. A.* 1217 (2010) 2674–2684. <https://doi.org/10.1016/j.chroma.2009.12.042>.
- [77] Swagelok Company, *Cylindres d'Échantillonnage, Accessoires, Et Tubes De Remplissage*, (2017). <https://www.swagelok.com.fr/downloads/webcatalogs/FR/MS-01-177.PDF> (accessed April 6, 2020).
- [78] Proserv, *Sample Cylinder Catalogue*, (n.d.). <https://www.proserv.com/wp-content/uploads/2019/01/Sample-Cylinder-Catalogue-Rev001.pdf> (accessed April 6, 2020).
- [79] RESTEK Pure Chromatography, *Sample Cylinders*, Restek. (2020). <https://www.restek.com/Sample-Handling/Gas-Sampling/Sample-Cylinders> (accessed April 14, 2020).
- [80] International Organization for Standardization, *ISO 11114-1:2012: Gas Cylinders – Compatibility of Cylinder and Valve Materials with Gas Contents – Part 1: Metallic Materials*, (2012).
- [81] M.C. Leuenberger, M.F. Schibig, P. Nyfeler, *Gas Adsorption and Desorption Effects on Cylinders and Their Importance for Long-Term Gas Records*, *Atmospheric Meas. Tech.* 8 (2015) 5289–5299. <https://doi.org/10.5194/amt-8-5289-2015>.
- [82] A. Attari, S. Chao, *Characterization and Measurement of Natural Gas Trace Constituents*. AICHE Spring National Meeting, Houston, TX, (1993).
- [83] T. Larsson, W. Frech, E. Björn, B. Dybdahl, *Studies of Transport and Collection Characteristics of Gaseous Mercury in Natural Gases Using Amalgamation and Isotope Dilution Analysis*, *Analyst.* 132 (2007) 579–586. <https://doi.org/10.1039/B702058A>.
- [84] BOC, *Stability and SPECTRA-SEAL*, BOC Online UK Ind. Gases. (2020). <https://www.boconline.co.uk/en/contact-and-support/technical-advice/speciality-products-advice/stability-spectraseal/stability-spectraseal.html> (accessed April 7, 2020).
- [85] Air Products and Chemicals, *Experis® Gas Mixtures, Wherever Accuracy, Stability and Reliability Are Essential*, (2007). http://www.airproducts.ae/microsite/ae/expert/PDF/literature/mixture_brochure_EN.pdf (accessed April 7, 2020).
- [86] Air Liquide, *Scott Specialty Gases. Aculife Cylinder Treatment*, *Air Liq. Res. Anal.* (2020). <https://airliquide-expertisecenter.com/scott-specialty-gases/> (accessed April 7, 2020).

- [87] SilcoTek Corporation, SilcoTek Coatings: Inert, Corrosion Resistant, Anti-Coking Solutions, SilcoTek. (2020). <https://www.silcotek.com> (accessed April 7, 2020).
- [88] Entech Instruments, Silonite™ Renew - Inertness Continually Perfected, Entech Instrum. (2019). <https://www.entechinstr.com/featured-products/silonite-coating> (accessed April 7, 2020).
- [89] A.M.H. Van Der Veen, C. Chamorro, F. Lestremau, F. Pérer Sanz, Final Publishable JRP Report Metrology for Biogas, ENG54 Biogas, (2018). <http://projects.npl.co.uk/metrology-for-biogas/>.
- [90] G.A. Barone, D. Shelow, D. Smith, Poster No. 2226P, in: New Orleans, LA, 2000.
- [91] RESTEK Pure Chromatography, Technical Guide. A Guide to Whole Air Canister Sampling. Equipment Needed and Practical Techniques for Collecting Air Samples, (2010). <https://www.restek.com/pdfs/EVTG1073A.pdf> (accessed April 9, 2020).
- [92] D.A. Brymer, L.D. Ogle, C.J. Jones, D.L. Lewis, Viability of Using SUMMA Polished Canisters for the Collection and Storage of Parts per Billion by Volume Level Volatile Organics, *Environ. Sci. Technol.* 30 (1996) 188–195. <https://doi.org/10.1021/es950240s>.
- [93] E. Woolfenden, Monitoring VOCs in Air Using Sorbent Tubes Followed by Thermal Desorption-Capillary GC Analysis: Summary of Data and Practical Guidelines, *J. Air Waste Manag. Assoc.* 47 (1997) 20–36. <https://doi.org/10.1080/10473289.1997.10464411>.
- [94] Entech Instruments, Air Sampling Canisters – Why Coating Is Not Optional. The Lessons Learned from SUMMA® (Nickel Chromium Oxide) and Silonite™ (Ceramic) Canister Passivation Coating Technologies., Entech Instrum. (2019). <https://www.entechinstr.com/summa-canisters/> (accessed April 9, 2020).
- [95] US EPA, SUMMA Canister Sampling. SOP# 1704, REV.# 01, (1995).
- [96] Entech Instruments, Comparing Silonite™ Canisters vs SUMMA & Other TO-15 Canisters for Air Monitoring - What's Best?, Entech Instrum. (2019). <https://www.entechinstr.com/silonite-vs-summa-canisters/> (accessed April 9, 2020).
- [97] US EPA, Compendium of Methods for the Determination of Toxic Organic Compounds in Ambient Air. Second Edition. Compendium Method TO-14A: Determination Of Volatile Organic Compounds (VOCs) In Ambient Air Using Specially Prepared Canisters With Subsequent Analysis By Gas Chromatography (EPA/625/R-96/010b), (1999). <https://www3.epa.gov/ttnamti1/files/ambient/airtox/to-14ar.pdf> (accessed April 9, 2020).

- [98] US EPA, Compendium of Methods for the Determination of Toxic Organic Compounds in Ambient Air. Second Edition. Compendium Method TO-15: Determination Of Volatile Organic Compounds (VOCs) In Air Collected In Specially-Prepared Canisters And Analyzed By Gas Chromatography/Mass Spectrometry (GC/MS) (EPA/625/R-96/010b), (1999). <https://www3.epa.gov/ttnamti1/files/ambient/airtox/to-15r.pdf> (accessed April 9, 2020).
- [99] S. Saeed, S.F. Kao, G.J. Graening, Comparison of Impinger and Canister Methods for the Determination of Siloxanes in Air, in: San Francisco, CA, 2002.
- [100] H. Hayes, G. Graening, S. Saeed, S. Kao, A Summary of Available Analytical Methods for the Determination of Siloxanes in Biogas. Air Toxics Ltd, in: 2003.
- [101] R.W. Coutant, Theoretical Evaluation of Stability of Volatile Organic Chemicals and Polar Volatile Organic Chemicals in Canisters. Final Report to U.S. EPA, Contract No. 68-D0-0007, Work Assignment No. 45, Subtask 2, Battelle, Columbus, Ohio., United States, 1992. <https://www.osti.gov/servlets/purl/5410047>.
- [102] M. Schweigkofler, R. Niessner, Removal of siloxanes in biogases, J. Hazard. Mater. 83 (2001) 183–196. [https://doi.org/10.1016/S0304-3894\(00\)00318-6](https://doi.org/10.1016/S0304-3894(00)00318-6).
- [103] E. Wheless, J. Pierce, Siloxanes in Landfill and Digester Gas - Update, in: 2004: p. 10.
- [104] J. Raich-Montiu, C. Ribas-Font, N. [de Arespachaga, E. Roig-Torres, F. Broto-Puig, M. Crest, L. Bouchy, J.L. Cortina, Analytical Methodology for Sampling and Analysing Eight Siloxanes and Trimethylsilanol in Biogas from Different Wastewater Treatment Plants in Europe, Anal. Chim. Acta. 812 (2014) 83–91. <https://doi.org/10.1016/j.aca.2013.12.027>.
- [105] M.A.H. Khan, M.E. Whelan, R.C. Rhew, Analysis of Low Concentration Reduced Sulfur Compounds (RSCs) in Air: Storage Issues and Measurement by Gas Chromatography with Sulfur Chemiluminescence Detection, Talanta. 88 (2012) 581–586. <https://doi.org/10.1016/j.talanta.2011.11.038>.
- [106] D. Helmig, Artifact-Free Preparation, Storage and Analysis of Solid Adsorbent Sampling Cartridges Used in the Analysis of Volatile Organic Compounds in Air, J. Chromatogr. A. 732 (1996) 414–417. [https://doi.org/10.1016/0021-9673\(95\)01376-8](https://doi.org/10.1016/0021-9673(95)01376-8).
- [107] US EPA, Compendium of Methods for the Determination of Toxic Organic Compounds in Ambient Air. Second Edition. Compendium Method TO-17: Determination of Volatile Organic Compounds in Ambient Air Using Active Sampling Onto Sorbent Tubes (EPA/625/R-96/010b), (1999). <https://www3.epa.gov/ttnamti1/files/ambient/airtox/to-17r.pdf> (accessed April 23, 2020).

- [108] R.R. Arnts, Evaluation of Adsorbent Sampling Tube Materials and Tenax-TA for Analysis of Volatile Biogenic Organic Compounds, *Atmos. Environ.* 44 (2010) 1579–1584. <https://doi.org/10.1016/j.atmosenv.2010.01.004>.
- [109] J.F. Pankow, W. Luo, L.M. Isabelle, D.A. Bender, R.J. Baker, Determination of a Wide Range of Volatile Organic Compounds in Ambient Air Using Multisorbent Adsorption/Thermal Desorption and Gas Chromatography/Mass Spectrometry, *Anal. Chem.* 70 (1998) 5213–5221. <https://doi.org/10.1021/ac980481t>.
- [110] E. Woolfenden, Sorbent-Based Sampling Methods for Volatile and Semi-Volatile Organic Compounds in Air. Part 2. Sorbent Selection and Other Aspects of Optimizing Air Monitoring Methods, *J. Chromatogr. A.* 1217 (2010) 2685–2694. <https://doi.org/10.1016/j.chroma.2010.01.015>.
- [111] N. Ramírez, R.M. Marcé, F. Borrull, Determination of Volatile Organic Compounds in Industrial Wastewater Plant Air Emissions by Multi-Sorbent Adsorption and Thermal Desorption-Gas Chromatography-Mass Spectrometry, *Int. J. Environ. Anal. Chem.* 91 (2011) 911–928. <https://doi.org/10.1080/03067310903584073>.
- [112] A.-L. Sunesson, C.-A. Nilsson, B. Andersson, Evaluation of Adsorbents for Sampling and Quantitative Analysis of Microbial Volatiles Using Thermal Desorption-Gas Chromatography, *J. Chromatogr. A.* 699 (1995) 203–214. [https://doi.org/10.1016/0021-9673\(95\)00025-1](https://doi.org/10.1016/0021-9673(95)00025-1).
- [113] M.D. Rey, R. Font, I. Aracil, Biogas from MSW Landfill: Composition and Determination of Chlorine Content with the AOX (Adsorbable Organically Bound Halogens) Technique, *Energy.* 63 (2013) 161–167. <https://doi.org/10.1016/j.energy.2013.09.017>.
- [114] P. Mochalski, B. Wzorek, I. Śliwka, A. Amann, Improved Pre-Concentration and Detection Methods for Volatile Sulphur Breath Constituents, *J. Chromatogr. B.* 877 (2009) 1856–1866. <https://doi.org/10.1016/j.jchromb.2009.05.010>.
- [115] I. Devai, R.D. DeLaune, Field Sampling of Trace Levels of Hydrogen Sulfide with the Use of Solid Adsorbent Preconcentration, *Field Anal. Chem. Technol.* 1 (1997) 145–149. [https://doi.org/10.1002/\(SICI\)1520-6521\(1997\)1:3<145::AID-FACT4>3.0.CO;2-W](https://doi.org/10.1002/(SICI)1520-6521(1997)1:3<145::AID-FACT4>3.0.CO;2-W).
- [116] I. Devai, R.D. DeLaune, Trapping Efficiency of Various Solid Adsorbents for Sampling and Quantitative Gas Chromatographic Analysis of Carbonyl Sulfide, *Anal. Lett.* 30 (1997) 187–198. <https://doi.org/10.1080/00032719708002300>.

- [117] I. Devai, R.D. Delaune, Evaluation of Various Solid Adsorbents for Sampling Trace Levels of Methanethiol, *Org. Geochem.* 24 (1996) 941–944. [https://doi.org/10.1016/S0146-6380\(96\)00117-9](https://doi.org/10.1016/S0146-6380(96)00117-9).
- [118] K.B. Andersen, M.J. Hansen, A. Feilberg, Minimisation of Artefact Formation of Dimethyl Disulphide During Sampling and Analysis of Methanethiol in Air Using Solid Sorbent Materials, *J. Chromatogr. A.* 1245 (2012) 24–31. <https://doi.org/10.1016/j.chroma.2012.05.020>.
- [119] E. Baltussen, F. David, P. Sandra, C. Cramers, On the Performance and Inertness of Different Materials Used for the Enrichment of Sulfur Compounds from Air and Gaseous Samples, *J. Chromatogr. A.* 864 (1999) 345–350. [https://doi.org/10.1016/S0021-9673\(99\)01066-3](https://doi.org/10.1016/S0021-9673(99)01066-3).
- [120] L. Lamaa, C. Ferronato, L. Fine, F. Jaber, J.M. Chovelon, Evaluation of Adsorbents for Volatile Methyl Siloxanes Sampling Based on the Determination of Their Breakthrough Volume, *Talanta.* 115 (2013) 881–886. <https://doi.org/10.1016/j.talanta.2013.06.045>.
- [121] N.-J. Kim, S.-K. Chun, D.K. Cha, C. Kim, Determination of Siloxanes in Biogas by Solid-phase Adsorption on Activated Carbon, *Bull. Korean Chem. Soc.* 34 (2013) 2353–2357. <http://dx.doi.org/10.5012/bkcs.2013.34.8.2353>.
- [122] B. Tansel, S.C. Surita, Selectivity and Limitations of Carbon Sorption Tubes for Capturing Siloxanes in Biogas During Field Sampling, *Waste Manag.* 52 (2016) 122–129. <https://doi.org/10.1016/j.wasman.2016.03.057>.
- [123] M. Schneider, K.-U. Goss, Systematic Investigation of the Sorption Properties of Tenax TA, Chromosorb 106, Porapak N, and Carbopak F, *Anal. Chem.* 81 (2009) 3017–3021. <https://doi.org/10.1021/ac802686p>.
- [124] UK Health and Safety Executive, Methods for the Determination of Hazardous Substances (MDHS). MDHS 72. Volatile Organic Compounds in Air. Laboratory Method Using Pumped Solid Sorbent Tubes, Thermal Desorption and Gas Chromatography. Her Majesty's Stationary Office: London, Uk, (1992). <https://www.hse.gov.uk/pubns/mdhs/pdfs/mdhs72.pdf> (accessed May 4, 2020).
- [125] J. Brown, B. Shirey, A Tool for Selecting an Adsorbent for Thermal Desorption Applications. Technical Report, (2001). https://www.sigmaaldrich.com/content/dam/sigmaaldrich/docs/Supelco/General_Information/t402025.pdf (accessed April 23, 2020).

- [126] A.C. Marcillo Lara, A GC-MS Method for Volatile Profiling of Odour Compounds After Thermal Desorption from Sample Collection Tubes. Master Thesis Structural Chemistry and Spectroscopy, University of Leipzig. Faculty of Chemistry and Mineralogy, 2015.
- [127] R.W. Bishop, R.J. Valis, A Laboratory Evaluation of Sorbent Tubes for Use with a Thermal Desorption Gas Chromatography-Mass Selective Detection Technique, *J. Chromatogr. Sci.* 28 (1990) 589–593. <https://doi.org/10.1093/chromsci/28.11.589>.
- [128] K. Schultz, J. Brown, Introducing Supelco® Glass-Fritted Thermal Desorption Tubes with Barcode, Sigma-Aldrich Merck. (2020). <https://www.sigmaaldrich.com/technical-documents/articles/reporter-eu/introducing-supelco.html> (accessed April 24, 2020).
- [129] E. Matisová, S. Škrabáková, Carbon Sorbents and Their Utilization for the Preconcentration of Organic Pollutants in Environmental Samples, *J. Chromatogr. A.* 707 (1995) 145–179. [https://doi.org/10.1016/0021-9673\(95\)00347-P](https://doi.org/10.1016/0021-9673(95)00347-P).
- [130] M.R. Allen, A. Braithwaite, C.C. Hills, Trace Organic Compounds in Landfill Gas at Seven U.K. Waste Disposal Sites, *Environ. Sci. Technol.* 31 (1997) 1054–1061. <https://doi.org/10.1021/es9605634>.
- [131] N. Ramírez, A. Cuadras, E. Rovira, F. Borrull, R.M. Marcé, Comparative Study of Solvent Extraction and Thermal Desorption Methods for Determining a Wide Range of Volatile Organic Compounds in Ambient Air, *Talanta.* 82 (2010) 719–727. <https://doi.org/10.1016/j.talanta.2010.05.038>.
- [132] J. Wang, L. Liao, L. Wang, L. Wang, Influence of Sampling Methods and Storage Condition on Volatile Methyl Siloxanes Quantification in Biogas, *Biomass Bioenergy.* 158 (2022) 106347. <https://doi.org/10.1016/j.biombioe.2022.106347>.
- [133] Sigma-Aldrich Co, Supelco® Specialty Carbon Adsorbents. High-Tech Materials Engineered for Applications of This World and Beyond!, (2015). https://www.sigmaaldrich.com/content/dam/sigmaaldrich/docs/Supelco/General_Information/1/specialty-carbon-adsorbents-t410081.pdf (accessed May 11, 2020).
- [134] A.J. Núñez, L.F. Gonzalez, J. Janak, Pre-Concentration of Headspace Volatiles for Trace Organic Analysis by Gas Chromatography, *J. Chromatogr. A.* 300 (1984) 127–162. [https://doi.org/10.1016/S0021-9673\(01\)87583-X](https://doi.org/10.1016/S0021-9673(01)87583-X).
- [135] P.R. Brown, E. Grushka, eds., *Advances in Chromatography*, Taylor & Francis, 2003. <https://books.google.fr/books?id=iIVIVvxqeGUC>.

- [136] Sigma-Aldrich Co, Characterization of Adsorbents for Sample Preparation Processes. Supelco T402026 EQG, (n.d.).
<https://www.sigmaaldrich.com/Graphics/Supelco/objects/11400/11322.pdf> (accessed May 15, 2020).
- [137] V.G. Berezkin, Y.S. Drugov, Gas Chromatography in Air Pollution Analysis, Elsevier Science, 1991. <https://books.google.fr/books?id=0nvn7S2BJCEC>.
- [138] J. LaRegina, J. Bozzelli, R. Harkov, S. Gianti, Volatile Organic Compounds at Hazardous Waste Sites and a Sanitary Landfill in New Jersey. An up-to-Date Review of the Present Situation., Environ. Prog. 5 (1986) 18–27.
- [139] M.P. Baya, P.A. Siskos, Evaluation of Anasorb CMS and Comparison with Tenax TA for the Sampling of Volatile Organic Compounds in Indoor and Outdoor Air by Breakthrough Measurements, The Analyst. 121 (1996) 303–307.
- [140] X.-L. Cao, N. Hewitt, Build-up of Artifacts on Adsorbents During Storage and Its Effect on Passive Sampling and Gas Chromatography-Flame Ionization Detection of Low Concentrations of Volatile Organic Compounds in Air, J. Chromatogr. A. 688 (1994) 368–374.
- [141] R. Huppmann, H.W. Lohoff, H.F. Schröder, Cyclic Siloxanes in the Biological Waste Water Treatment Process – Determination, Quantification and Possibilities of Elimination, Fresenius J. Anal. Chem. 354 (1996) 66–71. <https://doi.org/10.1007/s002169600011>.
- [142] C. Nerin, B. Pons, M. Martinez, J. Cacho, Behaviour of Several Solid Adsorbents for Sampling Tetraalkyllead Compounds in Air, Mikrochim. Acta. 112 (1994) 179–188.
- [143] E. Gallego, F.J. Roca, J.F. Perales, X. Guardino, Comparative Study of the Adsorption Performance of a Multi-Sorbent Bed (Carbotrap, Carbopack X, Carboxen 569) and a Tenax TA Adsorbent Tube for the Analysis of Volatile Organic Compounds (VOCs), Talanta. 81 (2010) 916–924. <https://doi.org/10.1016/j.talanta.2010.01.037>.
- [144] C. Freissinet, D.P. Glavin, P.R. Mahaffy, K.E. Miller, J.L. Eigenbrode, R.E. Summons, A.E. Brunner, A. Buch, C. Szopa, P.D. Archer, H.B. Franz, S.K. Atreya, Organic Molecules in the Sheepbed Mudstone, Gale Crater, Mars, J. Geophys. Res. Planets. 120 (2015).
<https://doi.org/10.1002/2014JE004737>.
- [145] A. Buch, I. Belmahdi, C. Szopa, C. Freissinet, D.P. Glavin, M. Millan, R. Summons, D. Coscia, S. Teinturier, J.-Y. Bonnet, Y. He, M. Cabane, R. Navarro-Gonzalez, C.A. Malespin, J. Stern, J. Eigenbrode, P.R. Mahaffy, S.S. Johnson, Role of the Tenax® Adsorbent in the Interpretation of

the EGA and GC-MS Analyses Performed with the Sample Analysis at Mars in Gale Crater, J. Geophys. Res. Planets. 124 (2019) 2819–2851. <https://doi.org/10.1029/2019JE005973>.

[146] A. Clausen, P. Wolkoff, Degradation Products of Tenax TA Formed During Sampling and Thermal Desorption Analysis: Indicators of Reactive Species Indoors, Atmos. Environ. 31 (1997) 715–725. [https://doi.org/10.1016/S1352-2310\(96\)00230-0](https://doi.org/10.1016/S1352-2310(96)00230-0).

[147] C.F. Poole, ed., Solid-Phase Extraction, Elsevier Science, 2019. <https://books.google.fr/books?id=gzqvDwAAQBAJ>.

[148] R.H. Brown, What is the Best Sorbent for Pumped Sampling-Thermal Desorption of Volatile Organic Compounds? Experience With the EC Sorbents Project, The Analyst. 121 (1996) 1171–1175.

[149] B.I. Brookes, P.J. Young, The Development of Sampling and Gas Chromatography-Mass Spectrometry Analytical Procedures to Identify and Determine the Minor Organic Components of Landfill Gas, Talanta. 30 (1983) 665–676. [https://doi.org/10.1016/0039-9140\(83\)80154-4](https://doi.org/10.1016/0039-9140(83)80154-4).

[150] V.B. Stein, R.S. Narang, Determination of Aldehydes, Ketones, Esters, and Ethers in Air Using Porapak N and Charcoal, Arch. Environ. Contam. Toxicol. 30 (1996) 476–480. <https://doi.org/10.1007/BF00213398>.

[151] J.P. Ryan, J.S. Fritz, Determination of Trace Organic Impurities in Water Using Thermal Desorption from XAD Resin, J. Chromatogr. Sci. 16 (1978) 488–492. <https://doi.org/10.1093/chromsci/16.10.488>.

[152] I. Lara-Ibeas, C. Megías-Sayago, A. Rodríguez-Cuevas, R. Ocampo-Torres, B. Louis, S. Colin, S.L. Calvé, Adsorbent Screening for Airborne BTEX Analysis and Removal, J. Environ. Chem. Eng. 8 (2020) 103563. <https://doi.org/10.1016/j.jece.2019.103563>.

[153] H.J. Hübschmann, Handbook of GC-MS: Fundamentals and Applications. Third Edition., John Wiley & Sons, 2015. <https://books.google.fr/books?id=DJlxBgAAQBAJ>.

[154] M. Kurdziel, The Effect of Different Drying Agents on the Analytical Data for Non-Methane Hydrocarbon Concentrations in Ambient Air Samples, Chem. Anal. (1998) 387–397.

[155] H.L. McDermot, J.C. Arnell, Charcoal Sorption Studies. II the Sorption of Water by Hydrogen Treated Charcoals, J. Phys. Chem. 58 (1954) 492–498. <https://doi.org/10.1021/j150516a011>.

[156] P. Ciccioli, A. Cecinato, E. Brancaleoni, M. Frattoni, A. Liberti, Use of Carbon Adsorption Traps Combined with High Resolution Gas Chromatography - Mass Spectrometry for the

Analysis of Polar and Non-Polar C4-C14 Hydrocarbons Involved in Photochemical Smog Formation, *J. High Resolut. Chromatogr.* 15 (1992) 75–84.

[157] W.F. Burns, D.T. Tingey, R.C. Evans, E.H. Bates, Problems with a Nafion® Membrane Dryer for Drying Chromatographic Samples, *J. Chromatogr. A.* 269 (1983) 1–9.

[https://doi.org/10.1016/S0021-9673\(01\)90777-0](https://doi.org/10.1016/S0021-9673(01)90777-0).

[158] E. Finocchio, T. Montanari, G. Garuti, C. Pistarino, F. Federici, M. Cugino, G. Busca, Purification of Biogases from Siloxanes by Adsorption: On the Regenerability of Activated Carbon Sorbents, *Energy Fuels.* 23 (2009) 4156–4159. <https://doi.org/10.1021/ef900356n>.

[159] R. Chiriac, J. Carre, Y. Perrodin, L. Fine, J.-M. Letoffe, Review: Characterisation of VOCs Emitted by Open Cells Receiving Municipal Solid Waste, *J. Hazard. Mater.* 149 (2007) 249–263.

[160] L. Sigot, G. Ducom, B. Benadda, C. Labouré, Adsorption of Octamethylcyclotetrasiloxane on Silica Gel for Biogas Purification, *Fuel.* 135 (2014) 205–209.

[161] P. Ciccioli, E. Brancaleoni, A. Cecinato, C. di Palo, A. Brachetti, A. Liberti, Gas Chromatographic Evaluation of the Organic Components Present in the Atmosphere at Trace Levels with the Aid of Carboxen B for Pre-Concentration of the Sample, *J. Chromatogr. A.* 351 (1986) 433–449. [https://doi.org/10.1016/S0021-9673\(01\)83521-4](https://doi.org/10.1016/S0021-9673(01)83521-4).

[162] P. Ciccioli, G. Bertoni, E. Brancaleoni, R. Fratarcangeli, F. Bruner, Evaluation of Organic Pollutants in the Open Air and Atmospheres in Industrial Sites Using Graphitized Carbon Black Traps and Gas Chromatographic-Mass Spectrometric Analysis with Specific Detectors, *J. Chromatogr. A.* 126 (1976) 757–770. [https://doi.org/10.1016/S0021-9673\(01\)84118-2](https://doi.org/10.1016/S0021-9673(01)84118-2).

[163] F. Bruner, G. Bertoni, G. Crescentini, Critical Evaluation of Sampling and Gas Chromatographic Analysis of Halocarbons and Other Organic Air Pollutants, *J. Chromatogr. A.* 167 (1978) 399–407. [https://doi.org/10.1016/S0021-9673\(00\)91172-5](https://doi.org/10.1016/S0021-9673(00)91172-5).

[164] P.J. Young, A. Parker, The Identification and Possible Environmental Impact of Trace Gases and Vapours in Landfill Gas, *Waste Manag. Res.* 1 (1983) 213–226.

[https://doi.org/10.1016/0734-242X\(83\)90004-6](https://doi.org/10.1016/0734-242X(83)90004-6).

[165] T. Parker, J. Dottridge, S. Kelly, Investigation of the Composition and Emissions of Trace Components in Landfill Gas. R&D Technical Report P1-438/TR, (2002).

<http://www.gassim.co.uk/documents/P1-438->

[TR%20Composition%20of%20Trace%20Components%20in%20LFG.pdf](http://www.gassim.co.uk/documents/P1-438-TR%20Composition%20of%20Trace%20Components%20in%20LFG.pdf).

- [166] T. Assmuth, K. Kalevi, Concentrations and Toxicological Significance of Trace Organic Compounds in Municipal Solid Waste Landfill Gas, *Chemosphere*. 24 (1992) 1207–1216. [https://doi.org/10.1016/0045-6535\(92\)90047-U](https://doi.org/10.1016/0045-6535(92)90047-U).
- [167] M.R. Allen, A. Braithwaite, C.C. Hills, Analysis of the Trace Volatile Organic Compounds in Landfill Gas Using Automated Thermal Desorption Gas Chromatography-Mass Spectrometry, *Int. J. Environ. Anal. Chem.* 62 (1996) 43–52. <https://doi.org/10.1080/03067319608027051>.
- [168] K. Arrhenius, A. Holmqvist, M. Carlsson, J. Engelbrektsson, A. Jansson, L. Rosell, H. Yaghooby, A. Fischer, Terpenes in Biogas Plants Digesting Food Wastes. Study to Gain Insight into the Role of Terpenes. Energiforsk AB. ISBN 978-91-7673-350-9, (2017).
- [169] K. Arrhenius, U. Johansson, Characterisation of Contaminants in Biogas Before and After Upgrading to Vehicle Gas. Rapport SGC 246, (2012). http://www.sgc.se/ckfinder/userfiles/files/SGC246_eng.pdf (accessed June 20, 2021).
- [170] J.I.S. Gómez, H. Lohmann, J. Krassowski, Determination of Volatile Organic Compounds from Biowaste and Co-Fermentation Biogas Plants by Single-Sorbent Adsorption, *Chemosphere*. 153 (2016) 48–57. <https://doi.org/10.1016/j.chemosphere.2016.02.128>.
- [171] V. Paolini, F. Petracchini, M. Carnevale, F. Gallucci, M. Perilli, G. Esposito, M. Segreto, L.G. Occulti, D. Scaglione, A. Ianniello, M. Frattoni, Characterisation and Cleaning of Biogas from Sewage Sludge for Biomethane Production, *J. Environ. Manage.* 217 (2018) 288–296. <https://doi.org/10.1016/j.jenvman.2018.03.113>.
- [172] F. Tassi, F. Capecchiacci, A. Bucciatti, O. Vaselli, Sampling and Analytical Procedures for the Determination of VOCs Released into Air from Natural and Anthropogenic Sources: A Comparison Between SPME (Solid Phase Micro Extraction) and ST (Solid Trap) Methods, *Appl. Geochem.* 27 (2012) 115–123. <https://doi.org/10.1016/j.apgeochem.2011.09.023>.
- [173] S.E. Lindberg, D. Wallschläger, E.M. Prestbo, N.S. Bloom, J. Price, D. Reinhart, Methylated Mercury Species in Municipal Waste Landfill Gas Sampled in Florida, USA, *Atmos. Environ.* 35 (2001) 4011–4015. [https://doi.org/10.1016/S1352-2310\(01\)00176-5](https://doi.org/10.1016/S1352-2310(01)00176-5).
- [174] S.E. Lindberg, G. Southworth, E.M. Prestbo, D. Wallschläger, M.A. Bogle, J. Price, Gaseous Methyl- and Inorganic Mercury in Landfill Gas from Landfills in Florida, Minnesota, Delaware, and California, *Atmos. Environ.* 39 (2005) 249–258. <https://doi.org/10.1016/j.atmosenv.2004.09.060>.

- [175] Z. Tao, S. Dai, X. Chai, Mercury Emission to the Atmosphere from Municipal Solid Waste Landfills: A Brief Review, *Atmos. Environ.* 170 (2017) 303–311.
<https://doi.org/10.1016/j.atmosenv.2017.09.046>.
- [176] S.-W. Lee, G.V. Lowry, H. Hsu-Kim, Biogeochemical Transformations of Mercury in Solid Waste Landfills and Pathways for Release, *Environ. Sci. Process. Impacts.* 18 (2016) 176–189.
<https://doi.org/10.1039/C5EM00561B>.
- [177] N.S. Bloom, A.K. Grout, E.M. Prestbo, Development and Complete Validation of a Method for the Determination of Dimethyl Mercury in Air and Other Media, *Anal. Chim. Acta.* 546 (2005) 92–101. <https://doi.org/10.1016/j.aca.2005.04.087>.
- [178] K.F. Chin, C. Wan, Y. Li, C.P. Alaimo, P.G. Green, T.M. Young, M.J. Kleeman, Statistical Analysis of Trace Contaminants Measured in Biogas, *Sci. Total Environ.* 729 (2020).
<https://doi.org/10.1016/j.scitotenv.2020.138702>.
- [179] D.S. Ballantine, W.H. Zoller, Collection and Determination of Volatile Organic Mercury Compounds in the Atmosphere by Gas Chromatography with Microwave Plasma Detection, *Anal. Chem.* 56 (1984) 1288–1293. <https://doi.org/10.1021/ac00272a022>.
- [180] N. Hewitt, R.M. Harrison, A Sensitive, Specific Method for the Determination of Tetraalkyllead Compounds in Air by Gas Chromatography/Atomic Absorption Spectrometry, *Anal. Chim. Acta.* 167 (1985) 277–287.
- [181] T. Nielsen, H. Egsgaard, E. Larsen, G. Schroll, Determination of Tetramethyllead and Tetraethyllead in the Atmosphere by a Two-Step Enrichment Method and Gas Chromatographic—Mass Spectrometric Isotope Dilution Analysis, *Anal. Chim. Acta.* 124 (1981) 1–13. [https://doi.org/10.1016/S0003-2670\(01\)83893-9](https://doi.org/10.1016/S0003-2670(01)83893-9).
- [182] Z. Mester, R.E. Sturgeon, Detection of Volatile Arsenic Chloride Species During Hydride Generation: A New Prospectus, *J. Anal. At. Spectrom.* 16 (2001) 470–474.
<https://doi.org/10.1039/B100750P>.
- [183] B. Planer-Friedrich, C. Lehr, J. Matschullat, B.J. Merkel, D.K. Nordstrom, M.W. Sandstrom, Speciation of Volatile Arsenic at Geothermal Features in Yellowstone National Park, *Geochim. Cosmochim. Acta.* 70 (2006) 2480–2491. <https://doi.org/10.1016/j.gca.2006.02.019>.
- [184] NIOSH, Method 6001: Arsine, Issue 2, (1994).
<https://19january2017snapshot.epa.gov/sites/production/files/2015-07/documents/niosh-6001.pdf> (accessed November 9, 2020).

- [185] A. Mestrot, M.K. Uroic, T. Plantevin, Md.R. Islam, E.M. Krupp, J. Feldmann, A.A. Meharg, Quantitative and Qualitative Trapping of Arsines Deployed to Assess Loss of Volatile Arsenic from Paddy Soil, *Environ. Sci. Technol.* 43 (2009) 8270–8275.
<https://doi.org/10.1021/es9018755>.
- [186] A. Mestrot, B. Planer-Friedrich, J. Feldmann, Biovolatilisation: A Poorly Studied Pathway of the Arsenic Biogeochemical Cycle, *Environ. Sci. Process. Impacts.* 15 (2013) 1639–1651.
<https://doi.org/10.1039/C3EM00105A>.
- [187] A. Mestrot, W.-Y. Xie, X. Xue, Y.-G. Zhu, Arsenic Volatilization in Model Anaerobic Biogas Digesters, *Appl. Geochem.* 33 (2013) 294–297.
<https://doi.org/10.1016/j.apgeochem.2013.02.023>.
- [188] E.B. Wickenheiser, K. Michalke, C. Drescher, A.V. Hirner, R. Hensel, Development and Application of Liquid and Gas-Chromatographic Speciation Techniques with Element Specific (ICP-MS) Detection to the Study of Anaerobic Arsenic Metabolism, *Fresenius J. Anal. Chem.* 362 (1998) 498–501. <https://doi.org/10.1007/s002160051114>.
- [189] R. Xu, D. Tang, Q. Yan, H. Xu, S. Wang, S. Tao, Z. Han, Exploration of Detection Technology about Arsenic Content in Natural Gas and Application, *Energy Fuels.* 29 (2015) 3863–3869.
<https://doi.org/10.1021/ef5028907>.
- [190] L. Freije-Carrelo, M. Moldovan, J.I. García Alonso, T.D. Thanh VO, J.R. Encinar, Instrumental Setup for Simultaneous Total and Speciation Analysis of Volatile Arsenic Compounds in Gas and Liquefied Gas Samples, *Anal. Chem.* 89 (2017) 5719–5724.
<https://doi.org/10.1021/acs.analchem.7b01082>.
- [191] W. Frech, D.C. Baxter, B. Bakke, J. Snell, Y. Thomassen, Highlight. Determination and Speciation of Mercury in Natural Gases and Gas Condensates, *Anal. Commun.* 33 (1996) 7H-9H. <https://doi.org/10.1039/AC996330007H>.
- [192] W. Frech, D.C. Baxter, G. Dyvik, B. Dybdahl, On the Determination of Total Mercury in Natural Gases Using the Amalgamation Technique and Cold Vapour Atomic Absorption Spectrometry, *J. Anal. At. Spectrom.* 10 (1995) 769–775.
<https://doi.org/10.1039/JA9951000769>.
- [193] M.F. Ezzeldin, Z. Gajdosechova, M.B. Masod, T. Zaki, J. Feldmann, E.M. Krupp, Mercury Speciation and Distribution in an Egyptian Natural Gas Processing Plant, *Energy Fuels.* 30 (2016) 10236–10243. <https://doi.org/10.1021/acs.energyfuels.6b02035>.

- [194] D.A. de la Rosa, A. Velasco, A. Rosas, T. Volke-Sepúlveda, Total Gaseous Mercury and Volatile Organic Compounds Measurements at Five Municipal Solid Waste Disposal Sites Surrounding the Mexico City Metropolitan Area, *Atmos. Environ.* 40 (2006) 2079–2088. <https://doi.org/10.1016/j.atmosenv.2005.11.055>.
- [195] S.E. Lindberg, J.L. Price, Airborne Emissions of Mercury from Municipal Landfill Operations: A Short-Term Measurement Study in Florida, *J. Air Waste Manag. Assoc.* 49 (1999) 520–532. <https://doi.org/10.1080/10473289.1999.10463825>.
- [196] N. Fernández-Miranda, E. Rodríguez, M.A. Lopez-Anton, R. García, M.R. Martínez-Tarazona, A New Approach for Retaining Mercury in Energy Generation Processes: Regenerable Carbonaceous Sorbents, *Energies.* 10 (2017). <https://doi.org/10.3390/en10091311>.
- [197] V. Romero, I. Costas-Mora, I. Lavilla, C. Bendicho, Cold Vapor-Solid Phase Microextraction Using Amalgamation in Different Pd-Based Substrates Combined with Direct Thermal Desorption in a Modified Absorption Cell for the Determination of Hg by Atomic Absorption Spectrometry, *Spectrochim. Acta Part B At. Spectrosc.* 66 (2011) 156–162. <https://doi.org/10.1016/j.sab.2011.01.005>.
- [198] W.F. Fitzgerald, G.A. Gill, Subnanogram Determination of Mercury by Two-Stage Gold Amalgamation and Gas Phase Detection Applied to Atmospheric Analysis, *Anal. Chem.* 51 (1979) 1714–1720. <https://doi.org/10.1021/ac50047a030>.
- [199] L. Liang, N.S. Bloom, Determination of Total Mercury by Single-Stage Gold Amalgamation with Cold Vapour Atomic Spectrometric Detection, *J. Anal. At. Spectrom.* 8 (1993) 591. <https://doi.org/10.1039/ja9930800591>.
- [200] P. Prikryl, J.G.K. Sevcik, Characterization of Sorption Mechanisms of Solid-Phase Microextraction with Volatile Organic Compounds in Air Samples Using a Linear Solvation Energy Relationship Approach, *J. Chromatogr. A.* 1179 (2008) 24–32. <https://doi.org/10.1016/j.chroma.2007.10.016>.
- [201] Jae-Hwan Lee, Seung Man Hwang, Dai Woon Lee, Gwi Suk Heo, Determination of Volatile Organic Compounds (VOCs) Using Tedlar Bag/Solid-phase Microextraction/Gas Chromatography/Mass Spectrometry (SPME/GC/MS) in Ambient and Workplace Air, *Bull. Korean Chem. Soc.* 23 (2002) 488–496. <https://doi.org/10.5012/BKCS.2002.23.3.488>.

- [202] D. Gorlo, L. Wolska, B. Zygmunt, J. Namieśnik, Calibration Procedure for Solid Phase Microextraction—Gas Chromatographic Analysis of Organic Vapours in Air, *Talanta*. 44 (1997) 1543–1550. [https://doi.org/10.1016/S0039-9140\(96\)02176-5](https://doi.org/10.1016/S0039-9140(96)02176-5).
- [203] P.A. Martos, J. Pawliszyn, Calibration of Solid Phase Microextraction for Air Analyses Based on Physical Chemical Properties of the Coating, *Anal. Chem.* 69 (1997) 206–215. <https://doi.org/10.1021/ac960415w>.
- [204] J.A. Koziel, J. Pawliszyn, Air Sampling and Analysis of Volatile Organic Compounds with Solid Phase Microextraction, *J. Air Waste Manag. Assoc.* 51 (2001) 173–184. <https://doi.org/10.1080/10473289.2001.10464263>.
- [205] S. Tumbiolo, J.-F. Gal, P.-C. Maria, O. Zerbinati, Determination of Benzene, Toluene, Ethylbenzene and Xylenes in Air by Solid Phase Micro-Extraction/Gas Chromatography/Mass Spectrometry, *Anal. Bioanal. Chem.* 380 (2004) 824–830. <https://doi.org/10.1007/s00216-004-2837-1>.
- [206] S. Tumbiolo, J.-F. Gal, P.-C. Maria, O. Zerbinati, SPME Sampling of BTEX Before GC/MS Analysis: Examples of Outdoor and Indoor Air Quality Measurements in Public and Private Sites, *Ann. Chim.* 95 (2005) 757–766. <https://doi.org/10.1002/adic.200590089>.
- [207] N. Baimatova, B. Kenessov, J.A. Koziel, L. Carlsen, M. Bektassov, O.P. Demyanenko, Simple and Accurate Quantification of BTEX in Ambient Air by SPME and GC-MS, *Talanta*. 154 (2016) 46–52. <https://doi.org/10.1016/j.talanta.2016.03.050>.
- [208] F.A.T. Andersson, A. Karlsson, B.H. Svensson, J. Ejlertsson, Occurrence and Abatement of Volatile Sulfur Compounds during Biogas Production, *J. Air Waste Manag. Assoc.* 54 (2004) 855–861. <https://doi.org/10.1080/10473289.2004.10470953>.
- [209] N. Wang, L. Tan, L. Xie, Y. Wang, T. Ellis, Investigation of Volatile Methyl Siloxanes in Biogas and the Ambient Environment in a Landfill, *J. Environ. Sci.* 91 (2020) 54–61. <https://doi.org/10.1016/j.jes.2020.01.005>.
- [210] G. Piechota, B. Igliński, R. Buczkowski, Development of Measurement Techniques for Determination Main and Hazardous Components in Biogas Utilised for Energy Purposes, *Energy Convers. Manag.* 68 (2013) 219–226. <https://doi.org/10.1016/j.enconman.2013.01.011>.
- [211] G. Piechota, R. Buczkowski, Development of Chromatographic Methods by Using Direct-Sampling Procedure for the Quantification of Cyclic and Linear Volatile Methylsiloxanes in

Biogas as Perspective for Application in Online Systems., *Int. J. Environ. Anal. Chem.* 94 (2014) 837–851. <https://doi.org/10.1080/03067319.2013.879296>.

[212] G. Piechota, B. Igliński, R. Buczkowski, An Experimental Approach for the Development of Direct-Absorption Sampling Method for Determination of Trimethylsilanol and Volatile Methylsiloxanes by the GC-MS Technique in Landfill Gas, *Int. J. Environ. Anal. Chem.* 95 (2015) 867–877. <https://doi.org/10.1080/03067319.2015.1055473>.

[213] G. Piechota, Siloxanes in Biogas: Approaches of Sampling Procedure and GC-MS Method Determination, *Molecules*. 26 (2021). <https://doi.org/10.3390/molecules26071953>.

[214] K. Oshita, K. Omori, M. Takaoka, T. Mizuno, Removal of Siloxanes in Sewage Sludge by Thermal Treatment with Gas Stripping, *Energy Convers. Manag.* 81 (2014) 290–297. <https://doi.org/10.1016/j.enconman.2014.02.050>.

[215] J. Feldmann, R. Grümping, A.V. Hirner, Determination of Volatile Metal and Metalloid Compounds in Gases from Domestic Waste Deposits with GC/ICP-MS, *Fresenius J. Anal. Chem.* 350 (1994) 228–234. <https://doi.org/10.1007/BF00322474>.

[216] J. Feldmann, W.R. Cullen, Occurrence of Volatile Transition Metal Compounds in Landfill Gas: Synthesis of Molybdenum and Tungsten Carbonyls in the Environment, *Environ. Sci. Technol.* 31 (1997) 2125–2129. <https://doi.org/10.1021/es960952y>.

[217] J. Feldmann, Determination of Ni(CO)₄, Fe(CO)₅, Mo(CO)₆, and W(CO)₆ in Sewage Gas by Using Cryotrapping Gas Chromatography Inductively Coupled Plasma Mass Spectrometry, *J. Environ. Monit.* 1 (1999) 33–37. <https://doi.org/10.1039/A807277I>.

[218] J. Dewulf, H.V. Langenhove, Anthropogenic Volatile Organic Compounds in Ambient Air and Natural Waters: A Review on Recent Developments of Analytical Methodology, Performance and Interpretation of Field Measurements, *J. Chromatogr. A.* 843 (1999) 163–177. [https://doi.org/10.1016/S0021-9673\(99\)00225-3](https://doi.org/10.1016/S0021-9673(99)00225-3).

[219] J. Feldmann, Summary of a Calibration Method for the Determination of Volatile Metal(loid) Compounds in Environmental Gas Samples by Using Gas Chromatography–Inductively Coupled Plasma Mass Spectrometry, *J. Anal. At. Spectrom.* 12 (1997) 1069–1076. <https://doi.org/10.1039/A701264K>.

[220] J. Feldmann, L. Naëls, K. Haas, Cryotrapping of CO₂-Rich Atmospheres for the Analysis of Volatile Metal Compounds Using Capillary GC-ICP-MS, *J. Anal. At. Spectrom.* 16 (2001) 1040–1043. <https://doi.org/10.1039/B102580P>.

- [221] K. Haas, J. Feldmann, R. Wennrich, H.-J. Stärk, Species-Specific Isotope-Ratio Measurements of Volatile Tin and Antimony Compounds Using Capillary GC–ICP–Time-of-Flight MS, *Fresenius J. Anal. Chem.* 370 (2001) 587–596.
<https://doi.org/10.1007/s002160100797>.
- [222] J. Feldmann, K. Haas, L. Naëls, S. Wehmeier, Investigations into Biovolatilization of Metal(loid)s in the Environment by Using GC-ICP-ToF-MS, *Plasma Source Mass Spectrom. New Millenn.* (2001) 361–368.
- [223] J. Feldmann, E.M. Krupp, D. Glindemann, A.V. Hirner, W.R. Cullen, Methylated Bismuth in the Environment, *Appl. Organomet. Chem.* 13 (1999) 739–748.
[https://doi.org/10.1002/\(SICI\)1099-0739\(199910\)13:10<739::AID-AOC925>3.0.CO;2-Z](https://doi.org/10.1002/(SICI)1099-0739(199910)13:10<739::AID-AOC925>3.0.CO;2-Z).
- [224] P. Pinel-Raffaitin, D. Amouroux, I. LeHécho, P. Rodríguez-Gonzalez, M. Potin-Gautier, Occurrence and Distribution of Organotin Compounds in Leachates and Biogases from Municipal Landfills, *Water Res.* 42 (2008) 987–996.
<https://doi.org/10.1016/j.watres.2007.09.013>.
- [225] R. Grümping, D. Mikolajczak, A.V. Hirner, Determination of Trimethylsilanol in the Environment by LT-GC/ICP-OES and GC-MS, *Fresenius J. Anal. Chem.* 361 (1998) 133–139.
<https://doi.org/10.1007/s002160050849>.
- [226] I. Bragança, F. Sánchez-Soberón, G.F. Pantuzza, A. Alves, N. Ratola, Impurities in Biogas: Analytical Strategies, Occurrence, Effects and Removal Technologies, *Biomass Bioenergy.* 143 (2020) 105878. <https://doi.org/10.1016/j.biombioe.2020.105878>.

PART 3 – EXPERIMENTAL SECTION

CHAPTER 3 – ELABORATION AND PRELIMINARY LABORATORY OPTIMIZATION OF MULTIBED ADSORBENT TUBES

ABBREVIATIONS CHAPTER 3

b.p.	Boiling point
MAT	Multibed adsorbent tube
GC	Gas chromatography
MS	Mass spectrometry
PTFE	Polytetrafluoroethylene
SGM	Synthetic gas mixture
TC	Trace compound
TD	Thermal desorption / Thermal desorber
TIC	Total ion current chromatogram

I. INTRODUCTION

Chapter 2 reviewed available gas sampling and preconcentration techniques for the determination of trace compounds in gaseous samples such as landfill gas, biogas and biomethane. This review highlighted not any sampling nor preconcentration unit is able to quantitatively trap and recover all families of trace compounds, and also pointed out whole gas sampling vessels suffer from several drawbacks such as trace compounds instability due to inner wall surface sorption phenomena or due to reactions between analytes in the vessel.

The key objective of this doctoral thesis is to develop a field gas sampling method allowing to characterize an as large as possible range of trace compounds in gases such as landfill gas, biogas and biomethane. The sampling method therefore should answer the five following criteria:

- Criterion a) Enable to collect, in a single sampling run, a large spectrum of trace compounds, whose nature and presence in the gas is not known in advance, belonging to various families including alkanes (linear, cyclic, polycyclic), aromatics, terpenes, alkenes, halogenated organic species, oxygenated organic species (alcohols, aldehydes, esters, furans and ethers, ketones), siloxanes, organic and inorganic Sulphur-compounds;
- Criterion b) Enable to sample pressurized gases such as natural gas grid-injected biomethane, directly at their working pressure and over a large pressure range covering pressures used in transport networks ($\approx 5 - 100 \text{ bar}_a$), to avoid drawbacks diverted from the depressurization of pressurized gas samples;

- Criterion c) Ensure the stability of sampled trace compounds (no loss, no degradation, no contamination) between sampling and analysis;
- Criterion d) Enable to eventually detect the low concentrations expected for such compounds;
- Criterion e) Be built using commercially available materials.

Henceforth, it was soon opted for a direct *in situ* field preconcentration method. Indeed, preconcentration is the most appropriate when aiming at screening (unknown) trace compounds as these latter are directly isolated from the gas matrix and stabilized ('trapped') in a small volume (e.g. sorbent tube, solvents in impingers, cryotrap), avoiding whole gas sampling vessels related drawbacks. Preconcentration furthermore allows to accumulate molecules in the preconcentration unit by sampling appropriate gas volumes, to finally reach sufficient and detectable quantities.

According to the review of gas sampling and preconcentration techniques, multibed adsorbent tubes (MAT) answer the best the five sampling requirement criteria. Indeed:

- Criterion a) The combination of several adsorbents of different materials and complementary strengths in a MAT, enables to trap, in one single sampling run, a wide range volatile trace compounds from diverse chemical families displaying various physicochemical properties and volatilities;
- Criterion b) The robust tube structure of MAT offers opportunities for direct pressurized gas sampling at the pipe working pressure by connecting the MAT in a high-pressure proof envelope, directly to the gas pipes;
- Criterion c) Trace compounds trapped in MAT remain stable after up to several weeks' storage, on the contrary to trace compounds trapped and stored in whole gas sampling vessels;
- Criterion d) The adsorption affinities and capacities of adsorbent materials in the MAT for the targeted families of trace compounds, yield outstanding preconcentration performances (adsorption during sampling and desorption to recover and analyze the sampled trace compounds). MAT allow direct *in situ* field preconcentration without first whole gas sampling;
- Criterion e) A wide variety of commercial adsorbent materials is available for the preconcentration of trace compounds targeted in this doctoral thesis. Other MAT components such as tubes, caps, adsorbent bed retaining wool... are also commercially available.

In addition to answering the five sampling requirement criteria, MAT have the following advantages:

- Small size and easy and fast transport between laboratory and field
- Easy to use on field (on the contrary to impingers and cryotrap)
- Robust (on the contrary to fragile solid phase microextraction fibers)
- Easily allow to collect replicates and to assemble several tubes in series
- Have already been used for landfill gas, biogas and biomethane (see Table 2.5)

Further, it was decided to use thermal desorption (TD) as a recovery means of analytes adsorbed on the MAT. TD is an available analytical technique widely agreed upon for the analysis of adsorbent tubes; it yields lower detection limits than solvent desorption and high chromatographic resolution of compounds. Hyphenating TD to gas chromatography – mass spectrometry (GC–MS) (or two dimensional GC–GC–MS) is a robust method for simultaneous identification and quantification of a wide range of (in)organic chemical compounds such as those targeted in this thesis. TD–GC–MS was therefore chosen as state-of-the-art analytical techniques throughout this work: the analyses were conducted using a new TD prototype device (presented in Chapter 4) and a commercial Agilent GC-MS unit.

As the new TD prototype has unique dimensions and only accommodates purpose-built tubes, and in order to create the most suitable combination of adsorbents in a multibed, MAT for this work were entirely designed and assembled in the laboratory. Based on the review of commercial adsorbent materials available for the preconcentration of non-metal(loid) trace compounds and on the discussion of their physicochemical properties and sorption affinities for given chemical compounds (Table 2.2), four commercial adsorbents, having already been used in the field of landfill gas, biogas and biomethane (Table 2.5), were initially selected and purchased from Supelco, Bellefonte, PA, USA to build MAT and conduct the doctoral thesis experiments:

- Tenax®TA (particle size 60 – 80 mesh (177 – 250 µm)) – polymeric matrix
- Carboxen™B (particle size 60 – 80 mesh (177 – 250 µm)) – graphitized carbon black
- Carboxen™X (particle size 40 – 60 mesh (250 – 420 µm)) – graphitized carbon black
- Carboxen®1000 (particle size 60 – 80 mesh (177 – 250 µm)) – carbon molecular sieve

In this chapter, the choice of these four adsorbents is first motivated whereafter the development of the adsorbent tube assembly- and conditioning-procedures is presented. Preliminary laboratory experiments are then discussed wherein the efficiency of different MAT configurations containing different adsorbents for the adsorption and TD of compounds present at trace concentrations in synthetic gas mixtures, is assessed to eventually design the most suitable MAT for the adsorption – TD of trace compounds targeted in landfill gas, biogas and biomethane in this doctoral thesis.

II. ADSORBENT MATERIAL CHOICE

Tenax®TA, Carboxen™B, Carboxen™X and Carboxen®1000 were chosen for their differences in chemical structures, hydrophobicity, porosity, surface areas and associated adsorption strengths and adsorption affinities for given compounds classes. They were also chosen because of their similar temperature stabilities (conditioning and desorption temperatures identical for Carboxen™B, Carboxen™X and Carboxen®1000 (respectively 350 and 330°C) and similar for Tenax®TA (320 and 300°C)) enabling to assemble them together in MAT and to condition and thermally desorb them without degradation of the material of one or the other adsorbent. On these adsorbents, physisorption, as defined in Chapter 2 – section III.1.1, was assumed as the predominant sorption mechanism as no single derivatization nor impregnating agent was added to the adsorbents.

Tenax®TA was chosen to be systematically used as front bed in MAT in view of its low surface area ($\sim 35 \text{ m}^2 \cdot \text{g}^{-1}$), relatively large pores ($\sim 720 \text{ \AA} \varnothing$) and associated weak sorption strength enabling it to physically retain large, bulky, high-boiling molecules (b.p. $> 50\text{-}100^\circ\text{C}$). Concomitantly and analytically crucial, the high thermal stability of Tenax®TA (max. 320°C) enables the TD of these large molecules, even very high-boiling ones, without degradation of the Tenax matrix. Since landfill gas, biogas and biomethane can contain a wide variety of trace compounds from very volatile to semi-volatile ones, using such a weak though polyvalent adsorbent is decisive to quantitatively trap *and* be able to desorb the largest semi-volatile species which, if only medium-strength or strong adsorbents would be used, could perhaps not be recovered. Furthermore, Tenax®TA is hydrophobic and will therefore barely be affected by the presence of humidity in biogas. Lastly, Tenax®TA is considered as a highly versatile adsorbent and is the most often used polymeric weak adsorbent, also in the field of landfill gas, biogas and biomethane, as demonstrated in Table 2.5.

Carbopack™B is slightly stronger than Tenax®TA since it has a slightly higher surface area ($\sim 100 \text{ m}^2 \cdot \text{g}^{-1}$), yet larger pores ($\sim 3000 \text{ \AA} \varnothing$), making it a weak/medium-strong adsorbent. It was chosen to either be used as front bed in a MAT or as intermediary bed between Tenax®TA and a stronger adsorbent. Similarly to Tenax®TA, Carbopack™B is hydrophobic and rather suited for the adsorption – TD of semi-volatile species. Its graphitized carbon structure, higher surface area and larger pore diameters however must lead to a different sorption behavior than that of Tenax®TA. Thus Carbopack™B was also chosen to challenge Tenax®TA and determine whether one or the other was more appropriate for the sake of this work, or whether they were complementing each other in the range of analytes they can adsorb and desorb.

Next, a medium-strong adsorbent was selected, namely Carbopack™X. It has a higher surface area than Tenax®TA and Carbopack™B, namely $\sim 240 \text{ m}^2 \cdot \text{g}^{-1}$, and smaller pores ($\sim 100 \text{ \AA} \varnothing$), implying it retains (and desorbs) smaller and lower boiling molecules (volatile species) than the two previous adsorbents. Accordingly, it can either be used as intermediary bed between a weaker front bed and a stronger back bed in a MAT. However, in this work it was only selected to be used as a back bed in a MAT. As it theoretically also is hydrophobic, a fully hydrophobic MAT can be set-up with Tenax®TA or Carbopack™B as front or intermediary bed and Carbopack™X as back bed, avoiding humidity issues in biogas.

Finally, the strong Carboxen®1000 carbon molecular sieve adsorbent was chosen to be used exclusively as back bed in MAT. It has the largest surface area ($1200 \text{ m}^2 \cdot \text{g}^{-1}$) and tiniest pores ($10\text{-}12 \text{ \AA} \varnothing$) enabling it to retain the most volatile, small molecules (down to C2 alkanes). Carboxen®1000, which is hydrophilic on the contrary to the other selected adsorbents, was also chosen to be contrasted to Carbopack™X and determine whether one or the other was more appropriate for the sake of this work, or whether they were complementing each other in the range of very volatile analytes they can adsorb and desorb.

III. EVALUATION OF DIFFERENT MULTIBED ADSORBENT TUBE CONFIGURATIONS USING SYNTHETIC GAS MIXTURES

Several MAT configurations have been proposed in the literature when aiming at screening gases of unknown trace compounds composition such as landfill gas, biogas and biomethane [1,2]:

- Tenax®TA (weak) – Carbopack™B or equivalent (weak/medium) – Carboxen®1000 or equivalent (strong), allowing to target a broad range of analytes from very volatile to semi-volatile species. The hydrophilicity of Carboxen materials has to be considered.
- Quartz wool (very weak) – Tenax®TA (weak) – Carbopack™X or equivalent (medium strength), a totally hydrophobic MAT which nevertheless does not allow to trap the uppermost volatile species.
- Carbopack™B or equivalent (weak/medium) – Carboxen®1003 or equivalent (strong), to target volatile to very volatile species, with the disadvantage of the hydrophilicity of the Carboxen.
- Carbopack™C or equivalent (weak) – Carbopack™B or equivalent (weak/medium) – Carboxen®1000 or equivalent (strong), enabling to trap intermediate to very volatile species, keeping in mind the hydrophilicity of Carboxen.

Before conducting effective sampling–preconcentration experiments on landfill gas, biogas and biomethane, it was necessary to assess which MAT configuration would be the most suitable to preconcentrate and recover the largest possible amount of trace compounds from a single sampling run, and to determine whether some MAT configurations were complementing each other in the range of analytes they adsorb and desorb. To this aim, and based on the above list, several MAT configurations combining different of the four selected adsorbents in a tube were tested for the sampling of certified synthetic gas mixtures containing a selection of targeted species at trace concentrations in either a N₂ or a CH₄ matrix.

III.1. Materials and methods

III.1.1. Adsorbent tube assembly and conditioning

MAT had to be manually assembled in purpose-sized tubes fitting in the TD prototype device. Empty amber glass tubes having appropriate dimensions (internal diameter 4.8 mm, length 44 mm) were obtained from ActionEurope, Sausheim, France. To prepare a MAT, a first untreated quartz wool plug is manually inserted into the tube. A determined mass of the first adsorbent bed is then weighted and subsequently sucked up inside the tube by means of a flexible vinyl tubing pushed in the tube extremity and connected to a small volumetric pump. A second untreated quartz wool plug is then manually inserted on top of this adsorbent bed to secure it and separate it from the next adsorbent bed, itself introduced the same way in the tube. Untreated quartz wool (Helios Italquartz™) for the plugs was preferred above e.g. silanized

quartz wool or glass wool since glass wool tends to physically degrade at elevated temperatures and silanized glass wool can release siloxanes upon heating during TD [3]. To optimize the later TD of the MAT, adsorbent masses m were determined for each adsorbent based on a fixed volume $V = 0.05 \text{ cm}^3$ for each bed and on their individual packing density ρ : $m = \rho \cdot V$ (packing densities ($\text{g} \cdot \text{cm}^{-3}$): Tenax[®]TA: 0.28; Carbopack[™]B: 0.43; Carbopack[™]X: 0.58; Carboxen[®]1000: 0.52). As such, each bed occupies a length of $3.4 \pm 0.2 \text{ mm}$ in the tube and it is ensured the total length of all adsorbents in the MAT physically only occupies the central part of the tube that will be heated inside the TD prototype.

Ensuing tube assembly, 20 MAT are placed on a purpose-built 20-positions conditioning support (aluminum 2017A, colorless anodic oxidation) installed in a disused GC oven (Fig.3.1). MAT are then conditioned at 320°C under a continuous pure nitrogen flow (99.999% purity) during 8.5 h. The Tenax[®]TA conditioning temperature (320°C) was used to condition all Tenax[®]TA-containing MAT as conditioning them at the higher Carbopack[™]B, Carbopack[™]X or Carboxen[®]1000 conditioning temperature (350°C) would lead to irreversible thermal degradation of Tenax[®]TA. Each of the 20 positions of the support's bottom plate is provided with an 11 mm o-ring (Dupont[™]Kalrez[®] Spectrum[™]metric o-ring 7075) ensuring the N₂ flow effectively enters every single tube. The oven is gently heated from 25 to 320°C at 10°C·min⁻¹. The N₂ flowrate through each individual tube varies between 140 and 510 mL·min⁻¹ with an average of 375 mL·min⁻¹. As soon as the conditioning sequence is completed and tubes cooled down to a temperature allowing manual grip, tubes are sealed with aluminum crimp caps with 3-layers septa (PTFE/silicone/PTFE; 11 mm, high temperature ultra-low-bleed silicone, ActionEurope) and stored until utilization in individual hermetic polyethylene zip bags in a larger zip bag in a desiccator at 4°C as recommended by [4–6].

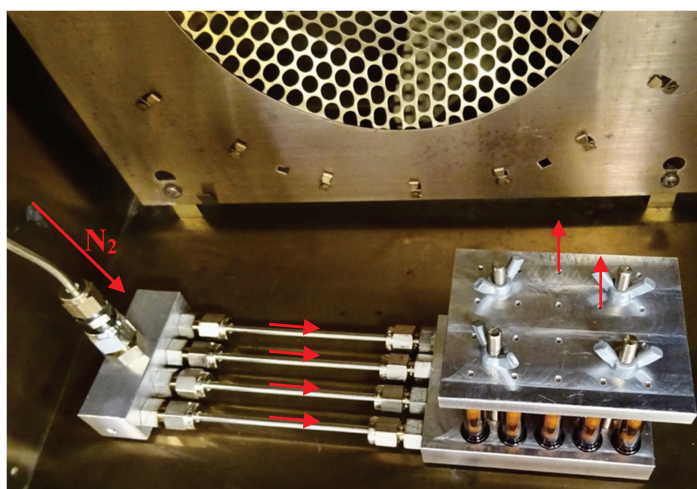


Figure 3.1: Purpose-built 20-positions adsorbent tube conditioning support

III.1.2. Reagents: multibed adsorbent tube configurations and synthetic gas mixtures

Four different MAT configurations were evaluated (Table 3.1). Because the handled adsorbent tubes are relatively short (44 mm), 2-bed MAT were preferred above 3-bed MAT to ensure the total length of all adsorbent beds was well fitting within the heated zone of the TD prototype. One 3-bed MAT was nonetheless evaluated (Table 3.1).

The four MAT configurations were tested for the sampling of four certified synthetic gas mixtures (SGM) containing a selection of targeted species at trace concentrations in either a N₂ or a CH₄ matrix (Table 3.2). Those SGM were custom-made by Air Liquide (France) for the specific requests of this doctoral thesis except for one mixture purchased from Restek France. It was not possible to obtain SGM in a biogas-like matrix (CO₂/CH₄).

Table 3.1: Multibed adsorbent tube (MAT) configurations evaluated

MAT	Composition (± 0.2 mg)		
	Front bed	Intermediary bed	Back bed
TA14-CX26	Tenax®TA 14 mg		Carboxen®1000 26 mg
TA14-CpX29	Tenax®TA 14 mg		Carbopack™X 29 mg
CB21-CX26	Carbopack™B 21 mg		Carboxen®1000 26 mg
TA14-CB21-CX26	Tenax®TA 14 mg	Carbopack™B 21 mg	Carboxen®1000 26 mg

Table 3.2: Certified synthetic gas mixtures (SGM) used. TC: trace compound

SGM	TC composition	TC boiling point range (°C)	Concentration of each TC	Matrix	Provider
OPL	1-Octene α -Pinene d-Limonene	121 – 176	1 ppm _{mol}	CH ₄	Air Liquide
PEO	Pentane Ethylcyclopentane Octane	36 – 125	1 ppm _{mol}	CH ₄	Air Liquide
Chloro	Tetrachloromethane Trichloromethane Dichloromethane Chloromethane Dichloroethane Chloroethane Dichlorobenzene Chlorobenzene	-24 – 180	1 ppm _{mol}	N ₂	Air Liquide
41 HVOC	Dichlorodifluoromethane Chloromethane Chloroethene 1,3-Butadiene 1,2-Dichloro-1,1,2,2-tetrafluoroethane Bromomethane Chloroethane Trichlorofluoromethane 1,1-Dichloroethene Dichloromethane 1,1,2-Trichloro-1,2,2-trifluoroethane 1,1-Dichloroethane <i>cis</i> -1,2-Dichloroethene Trichloromethane 1,1,1-Trichloroethane Tetrachloromethane Acrylonitrile Benzene 1,2-Dichloroethane Trichloroethene 1,2-Dichloropropane <i>cis</i> -1,3-Dichloropropene Toluene <i>trans</i> -1,3-Dichloropropene 1,1,2-Trichloroethane Tetrachloroethene Chlorobenzene 1,2-Dibromoethane Ethylbenzene <i>p</i> -Xylene <i>m</i> -Xylene <i>o</i> -Xylene Styrene 1,1,2,2-Tetrachloroethane 1,3,5-Trimethylbenzene 1,2,4-Trimethylbenzene 1,3-Dichlorobenzene 1,4-Dichlorobenzene 1,2-Dichlorobenzene 1,2,4-Trichlorobenzene Hexachloro-1,3-butadiene	-30 – 215	1 ppm _{mol}	N ₂	Scott Airgas Specialty Gases, Plumsteadville, USA ('TO-14A 41 Component Mix', purchased from Restek, France)

III.1.3. Synthetic gas sampling

To compare the different MAT configurations, the four SGM were individually sampled as outlined in Table 3.3 on one or the other MAT configuration. Although the SGM were provided in pressurized cylinders (from 124 to 200 bar_a), all sampling experiments were performed at near atmospheric pressure by regulating the pressure down to 1.2 bar_a upstream the adsorbent tubes-laboratory sampling chain (Fig.3.2). For all sampling experiments (Table 3.3), three identical MAT were connected in series and 500 mL_N of the SGM were passed through the tubes, in the direction from the weakest to the strongest adsorbent, at 50 mL_N·min⁻¹ by fine-regulating the flowrate using valve n°5 on Fig.3.2. The first MAT was connected to the pressure regulating system by pricking its septa on the gas needle (n°7, Fig.3.2), and the other MAT were linked with para-apical gas needles pricked in their septa. Gas flowrate and total gas volume passed through the MAT were measured via a downstream mass flowmeter (Bronkhorst MassView MV-302) connected via a vinyl tubing to the last MAT of the series (Fig.3.2). Two batches of 3 MAT in series were collected this way for each sampling experiment to obtain two replicates, and for the 41 HVOC SGM sampled on TA14-CX26 and on TA14-CpX29, 10 replicate batches of 3 MAT in series were collected.

All sampling operations were executed at room temperature (20-22°C). Between each sampling experiment with a different SGM, the pressure regulating system (Fig.3.2) was evacuated, flushed with pure N₂ (99.999% purity) (1.3 bar_a) during ≥ 50 min and again evacuated to ensure no residual trace compounds from previously sampled SGM remained in the tubing of the pressure regulating system. Then, before effectively sampling the next SGM onto MAT, the pressure regulating system (without MAT) was flushed during ≥ 5 min with the SGM to sample (regulated to 1.3 bar_a) to saturate potential trace compounds-sorption sites on tubing and connectors surfaces. Whereas adsorbent tubes analyzed by TD can theoretically be re-used after quantitative TD and thermal reconditioning [7-9], here only new MAT were used for all sampling operations to avoid cross-contamination in the case TD of the initial sample was not quantitative and to avoid build-up of thermal degradation artefacts upon repeated conditioning cycles. All sampled MAT were stored in individual hermetic polyethylene zip bags in a larger zip bag in a desiccator at 4°C until TD-GC-MS analysis.

Table 3.3: Sampling experiments of the synthetic gas mixtures on the multibed adsorbent tubes (MAT)

MAT	Synthetic gas mixture*			
	OPL	PEO	Chloro	41 HVOC
TA14-CX26	×	×	×	× ◊
TA14-CpX29				× ◊
CB21-CX26	×	×	×	×
TA14-CB21-CX26			×	×

* OPL, PEO, Chloro, 41HVOC: see Table 3.2

◊ 10 replicate batches of 3 MAT in series

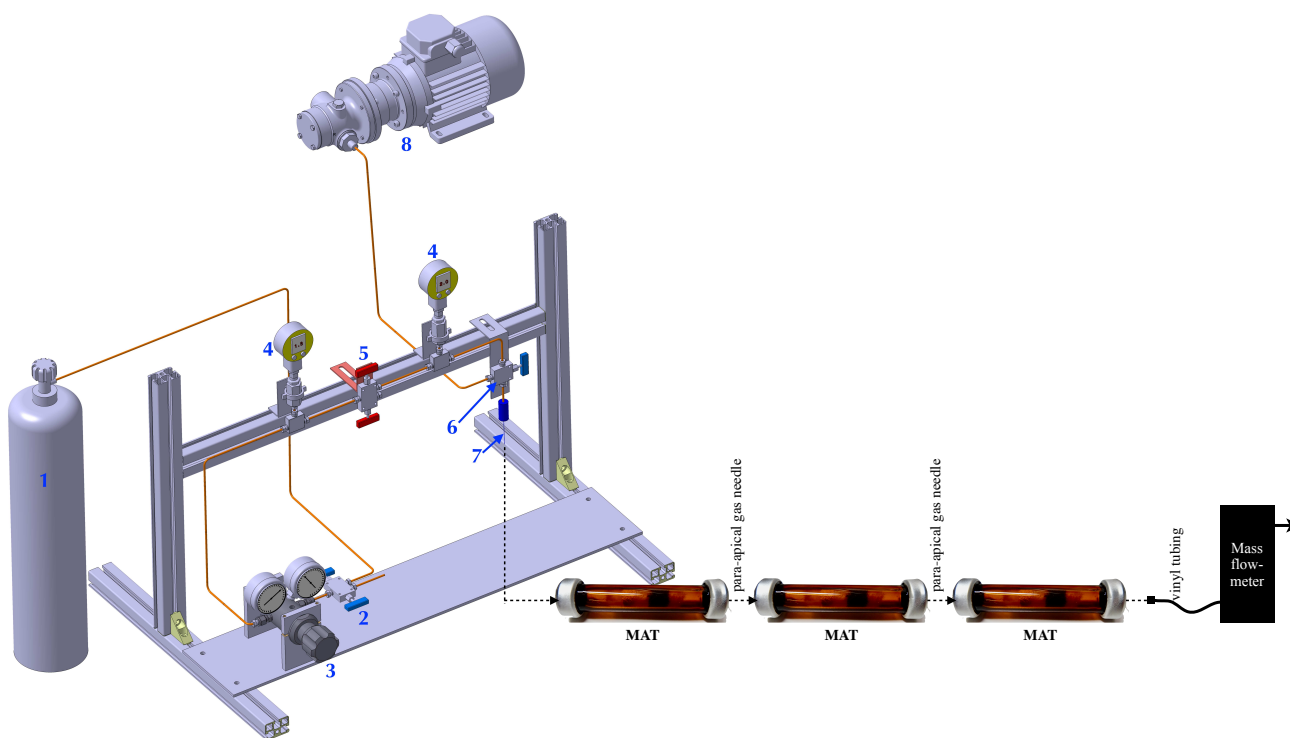


Figure 3.2: Gas pressure regulating system for the sampling of pressurized synthetic gas mixtures on multitubed adsorbent tubes (MAT). Following gas flow: 1: pressurized synthetic gas cylinder, 2: manual high-pressure valve, 3: manometer-gas pressure regulator, 4: manometer, 5: manual micrometric valve, 6: manual valve, 7: gas needle, 8: vacuum pump. All tubing is of stainless-steel 1/8" outer diameter

III.1.4. Analysis

All sampled MAT and new blank MAT were analyzed via TD-GC-MS using the TD prototype device (nC_x Instrumentation, Garlin, France) coupled to an Agilent 6890A GC and an Agilent 5973Network Mass Selective Detector, parametrized as in Table 3.4, using the MSD ChemStation E.02.02.1431 software (Agilent) and the NIST Mass Spectral Search Program version 2.0 d, 2005 for the identification of targeted trace compounds detected in the GC-MS chromatograms.

Each MAT is manually placed in the TD prototype in the reverse direction as compared to the gas sampling direction. Note the 200°C desorption temperature programmed in the TD prototype corresponds to an effective desorption temperature of 300°C inside adsorbent tubes. The desorption temperature was set at 300°C for MAT containing Tenax[®]TA since desorbing them at 330°C (desorption temperature of the other Carboxen's and Carboxen used) would induce thermal degradation of Tenax[®]TA with associated injection of its thermal degradation products in the GC-MS and falsification of the analytical results. The CB21-CX26 MAT was desorbed at 330°C using a 210°C setpoint temperature in the TD prototype.

Table 3.4: TD-GC-MS operational parameters

Instrument	Parameter	Value
TD prototype <i>nCx</i> <i>Instrumentation</i>	Start temperature	35°C
	Desorption temperature *	200°C *
	Stabilization time	15 s
	Injection pressure	1170 mbar
	Injection time	10 s
GC <i>Agilent 6890A</i>	Inlet temperature	230°C
	Inlet septum	Premium Inlet Septa, Bleed/Temp optimized, non-stick (Agilent)
	Inlet liner	Ultra Inert Liner, Splitless, Single taper, no wool, 4 mm ID (Agilent)
	Split ratio	1 :1
	Split flow	1.5 mL·min ⁻¹
	Carrier gas	Helium (quality detector 5.0, Linde, France)
	Gas saver	Off
	Column	HP-5MS, 30 m × 250 µm ID × 0.25 µm film thickness (Agilent)
	Constant flow in column	1.5 mL·min ⁻¹
	Carrier gas linear velocity in column	44 cm·s ⁻¹
	Oven	30°C (4 min) - 10°C·min ⁻¹ - 250°C (5 min)
MS <i>Agilent</i> <i>5973Network Mass</i> <i>Selective Detector</i>	Source temperature	230°C
	Quadrupole temperature	150°C
	GC-MS interface temperature	280°C
	Electron Impact Mode	70 eV
	Electron Multiplier Voltage	Relative voltage (106 = 1871 V)
	Acquisition mode	Scan
	Scan range	10 – 450 a.m.u.
	Sampling rate	3.28 scan·s ⁻¹
	Threshold	100 counts

* 210°C for the CB21-CX26 configuration.

III.2. Results

III.2.1. Multibed adsorbent tube blanks

Fig.3.3 displays the total ion current chromatograms (TIC) obtained from the TD-GC-MS analysis of new blank MAT of each evaluated MAT configuration. For each MAT configuration, the TIC displayed is the average of 3 blank tube replicates. Insofar as this preliminary study only aims at selecting the most suitable MAT configuration, no quantification will be done, hence standard deviations and limits of detection are not given. Six siloxanes appear as contaminants in all MAT configurations; these siloxanes were found to be released during TD from the PTFE/silicone/PTFE septa used to crimp-cap the tubes. The presence of siloxanes is however so far not an issue since no siloxanes are targeted in the SGM used. Besides, both MAT configurations containing Carbopack™B (CB21-CX26 and TA14-CB21-CX26) release a benzene impurity at ~2.7 min, while TA14-CX26 and TA14-CpX29 do not. This suggests the Carbopack™B matrix may unsatisfactorily be conditioned or the Carbopack™B material flask got contaminated during laboratory handling. Aside from this benzene impurity, the absence of background contamination indicates the tube assembly and conditioning procedure is adequate. Notwithstanding, other crimp-cap septa materials should be considered to achieve zero-release of impurities from the tube components while still offering softness and gas-tightness after needle piercing.

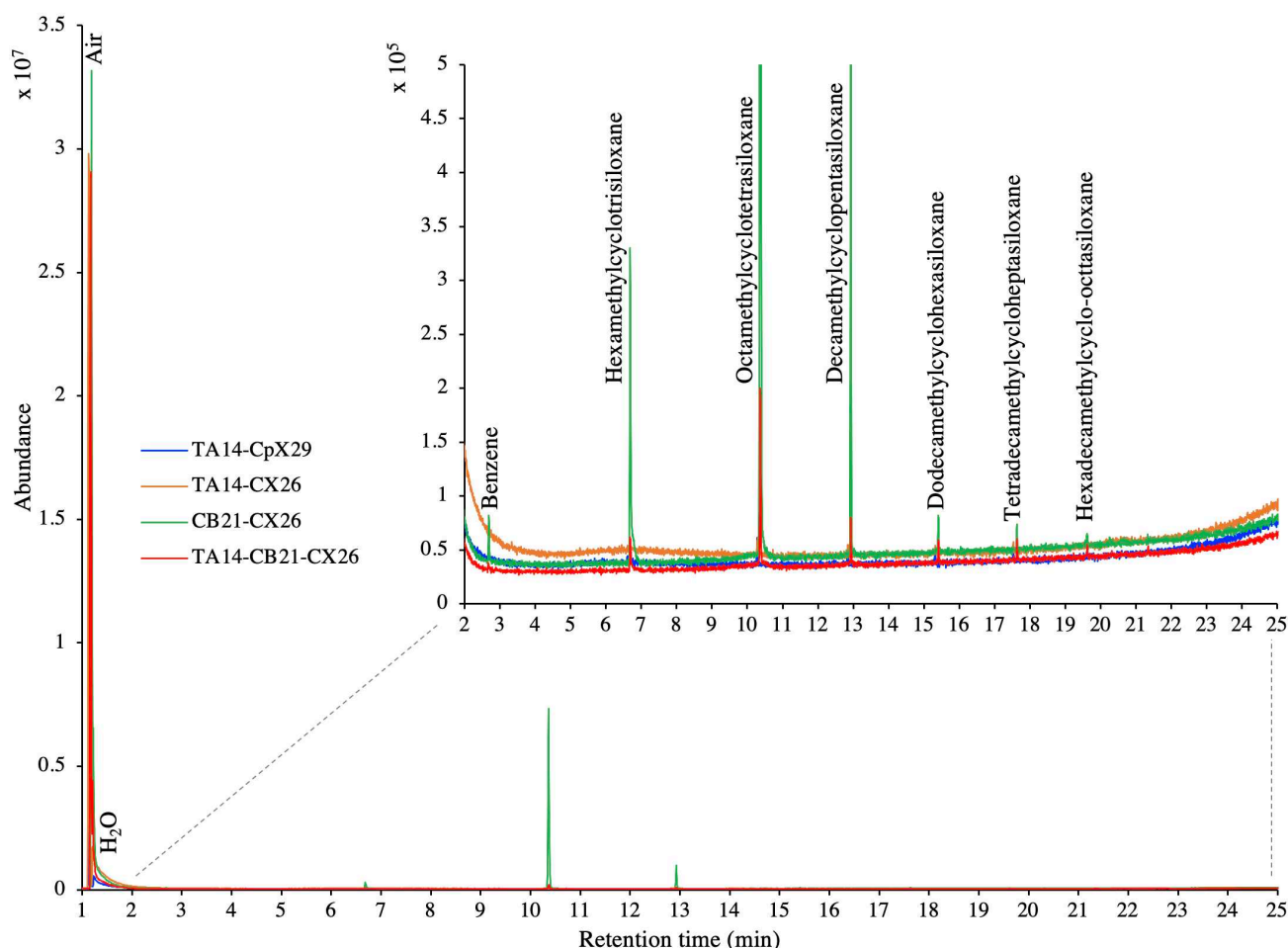


Figure 3.3: TIC of new blank MAT for the four MAT configurations evaluated with indication of inherent background contamination (benzene and septum-released siloxanes)

III.2.2. Efficiency of multibed adsorbent tubes

The efficiency of each MAT configuration in preconcentrating trace compounds in the SGM was assessed by sampling the four SGM on the different MAT configurations (Table 3.3) with each time 3 identical MAT in series. The MAT efficiency criterion was the ability to adsorb, and release upon TD, all trace compounds present in each SGM in a single sampling – TD run.

Table 3.5 summarizes the results of the SGM sampling experiments. For each MAT configuration sampled with a given SGM, it was assessed whether or not all trace compounds present in the SGM were detected in the TD-GC-MS chromatograms of the front MAT of each series. The presence of trace compounds on the second and third MAT of the series was also recorded from the chromatograms to determine whether breakthrough occurred at the sampling conditions handled (500 mL_N at 50 mL_N·min⁻¹, compounds present at 1 ppm_{mol} level).

From the OPL, PEO and Chloro SGM, all targeted trace compounds including the highly volatile chloromethane were recovered and detected on all sampled MAT configurations. No breakthrough of trace compounds in the OPL, PEO and Chloro SGM was witnessed neither for TA14-CX26 nor for CB21-CX26 and TA14-CB21-CX26.

From the 41 HVOC SGM, the TA14-CpX29 MAT configuration was able to recover 39 out of the 41 compounds present in the 41 HVOC SGM. The two missing compounds were chloromethane and 1,2-dichloropropane. The TA14-CX26 was able to recover 36 of the 41 compounds; chloromethane, 1,2-dichloropropane, acrylonitrile and *cis*- and *trans*-1,3-dichloropropane were not recovered. The CB21-CX26 tubes only allowed to recover 24 out of the 41 HVOC, with the following compounds not recovered: chloromethane, 1,3-butadiene, bromomethane, trichlorofluoromethane, dichloromethane, 1,1,2-trichloro-1,2,2-trifluoroethane, trichloromethane, 1,1,1-trichloroethane, tetrachloromethane, acrylonitrile, 1,2-dichloroethane, 1,2-dichloropropane, *cis*- and *trans*-1,3-dichloropropane, 1,1,2-trichloroethane, 1,2-dibromoethane, 1,1,2,2-tetrachloroethane. Finally, the TA14-CB21-CX26 MAT configuration enabled the recovery and detection of 38 out of the 41 HVOC and missing compounds were chloromethane, 1,3-butadiene and 1,2-dichloropropane. The absence of 1,2-dichloropropane was witnessed on all sampling experiments performed with the 41 HVOC SGM on all MAT configurations although all adsorbents used should enable its recovery and detection according to [10]. Albeit a formal composition certification was delivered with the 41 HVOC SGM, 1,2-dichloropropane was ostensibly absent from this SGM or it got converted to another species by reactions with other compounds in the gas cylinder. The absence of chloromethane from all 41 HVOC sampling experiments on all MAT also suggests this compound was absent from the 41 HVOC SGM (or got degraded) in spite of the composition certification insofar as chloromethane was well recovered and detected from the other SGM containing it, namely the Chloro SGM, on the different MAT tested (Table 3.5). Regarding breakthrough, all MAT configurations containing Carboxen®1000 as back bed (-CX26) inhibited the breakthrough of all 41 trace compounds in the 41 HVOC SGM. In contrast, the 14 most volatile trace compounds in the 41 HVOC SGM broke through the first tube of the MAT configuration containing Carbopack™X as back bed (TA14-CpX29), and 7 of these most volatile compounds broke from the second to the third tube of this series (Table 3.5). This properly illustrates the adsorption strength and microporosity of Carboxen®1000 is higher than that of Carbopack™X, with the weaker Carbopack™X being less efficient in retaining very volatile species.

By way of illustration, Fig.3.4 overlays the chromatograms of front tubes of the TA14-CX26 and TA14-CpX29 series sampled with the 41 HVOC SGM. The chromatographic peaks obtained with the TA14-CpX29 MAT are higher than those obtained with TA14-CX26 for all compounds in the 41 HVOC SGM. Table 3.6 lists the corresponding chromatographic retention times of trace compounds in the 41 HVOC SGM detected on TA14-CX26 or TA14-CpX29, highlighting TA14-CX26 did not enable the recovery of acrylonitrile and *cis*- and *trans*-1,3-dichloropropane while TA14-CpX29 did. Retention time differences between those MAT configurations can be due to the manual TD-injections, especially for the most volatile species of the 41 HVOC SGM (Table 3.6).

Table 3.5: Results of the sampling experiments of the synthetic gas mixtures (SGM) on the multibed adsorbent tubes (MAT). TC: trace compound.

SGM *	MAT	Number (and identity) of targeted TC detected in		
		the front MAT of the series	the second MAT of the series	the third MAT of the series
OPL (contains 3 targeted TC)	TA14-CX26	3 / 3	0	0
	CB21-CX26	3 / 3	0	0
PEO (contains 3 targeted TC)	TA14-CX26	3 / 3	0	0
	CB21-CX26	3 / 3	0	0
Chloro (contains 8 targeted TC)	TA14-CX26	8 / 8	0	0
	CB21-CX26	8 / 8	0	0
	TA14-CB21-CX26	8 / 8	0	0
	TA14-CX26	36 / 41	0	0
41 HVOC (contains 41 targeted TC)	TA14-CpX29	39/41	14/41 :	
			Dichlorodifluoromethane	
			Chloroethene	
			1,3-Butadiene	
			1,2-Dichloro-1,1,2,2-tetrafluoroethane	7/41 :
			Bromomethane	Dichlorodifluoromethane
			Chloroethane	Chloroethene
			Trichlorofluoromethane	1,2-Dichloro-1,1,2,2-tetrafluoroethane
			1,1-Dichloroethene	Bromomethane
			Dichloromethane	Chloroethane
1,1,2-Trichloro-1,2,2-trifluoroethane	Dichloromethane			
1,1-Dichloroethane				
cis-1,2-Dichloroethene				
Trichloromethane				
1,2-Dichloroethane				
	CB21-CX26	24/41	0	0
	TA14-CB21-CX26	38/41	0	0

* OPL, PEO, Chloro, 41HVOC: see Table 3.2

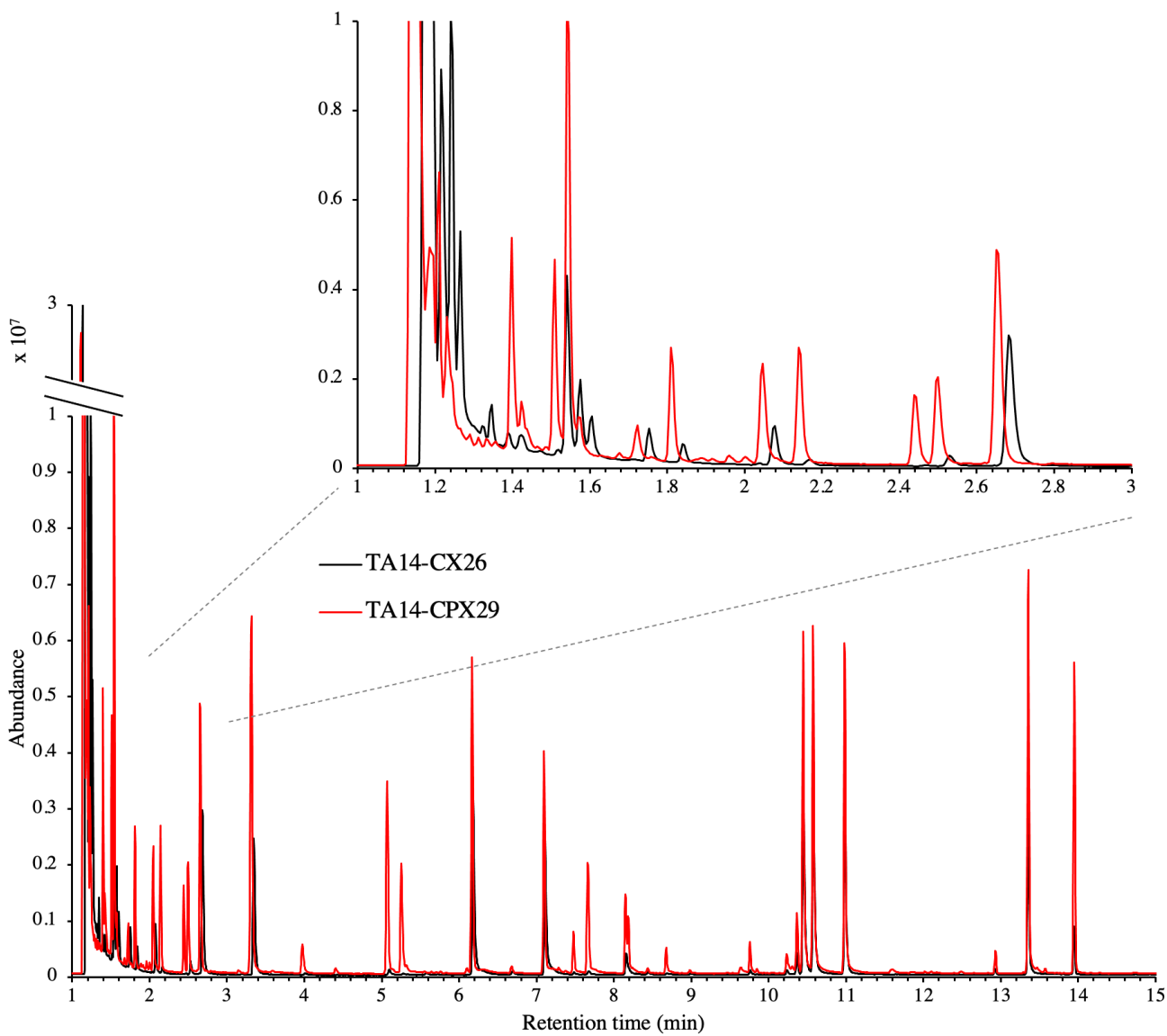


Figure 3.4: TIC of the 41 HVOC synthetic gas mixture sampled on TA14-CX26 and on TA14-CpX29 multibed adsorbent tubes (TIC of the front tubes of the sampling series). Detail of the detected compounds and their retention times is given in Table 3.6.

Table 3.6: Chromatographic retention times of the trace compounds in the 41 HVOC synthetic gas mixture (SGM) sampled on TA14-CX26 and on TA14-CpX29 multibed adsorbent tubes (retention times on the front tubes of the sampling series)

41 HVOC SGM	Retention time (min)	
	TA14-CX26	TA14-CpX29
Dichlorodifluoromethane	1.217	1.195
Chloromethane	*	*
Chloroethene	1.266	1.231
1,3-Butadiene	1.278	1.246
1,2-Dichloro-1,1,2,2-tetrafluoroethane	1.242	1.209
Bromomethane	1.324	1.291
Chloroethane	1.346	1.312
Trichlorofluoromethane	1.423	1.398
1,1-Dichloroethene	1.541	1.509
Dichloromethane	1.605	1.574
1,1,2-Trichloro-1,2,2-trifluoroethane	1.575	1.542
1,1-Dichloroethane	1.841	1.810
<i>cis</i> -1,2-Dichloroethene	2.076	2.046
Trichloromethane	2.168	2.141
1,1,1-Trichloroethane	2.470	2.441
Tetrachloromethane	2.682	2.657
Acrylonitrile	*	2.653
Benzene	2.684	2.654
1,2-Dichloroethane	2.530	2.497
Trichloroethene	3.347	3.315
1,2-Dichloropropane	*	*
<i>cis</i> -1,3-Dichloropropene	*	4.404
Toluene	5.097	5.069
<i>trans</i> -1,3-Dichloropropene	*	5.190
1,1,2-Trichloroethane	5.283	5.253
Tetrachloroethene	6.183	6.168
Chlorobenzene	7.110	7.097
1,2-Dibromoethane	6.120	6.099
Ethylbenzene	7.488	7.479
<i>p</i> -Xylene	7.676	7.663
<i>m</i> -Xylene	7.676	7.663
<i>o</i> -Xylene	8.194	8.185
Styrene	8.161	8.150
1,1,2,2-Tetrachloroethane	8.688	8.676
1,3,5-Trimethylbenzene	9.763	9.759
1,2,4-Trimethylbenzene	10.237	10.234
1,3-Dichlorobenzene	10.450	10.446
1,4-Dichlorobenzene	10.579	10.575
1,2-Dichlorobenzene	10.986	10.982
1,2,4-Trichlorobenzene	13.355	13.355
Hexachloro-1,3-butadiene	13.949	13.950

* Not detected

III.3. Discussion

Table 3.5 indicates the four evaluated MAT configurations successfully enable to acquire information on the major families of trace compounds potentially present in landfill gas, biogas and biomethane (alkenes, terpenes, (cyclo-) alkanes, chlorinated and brominated volatile organic compounds, aromatics with in particular benzene, toluene, ethylbenzene, xylene isomers and styrene) since the trace compounds in all tested SGM could all be adsorbed and recovered in single sampling – TD runs. The chosen gas sampling volume (500 mL_N) and sampling flowrate (50 mL_N·min⁻¹) also seemed suitable to restrict breakthrough as, with the exception of the most volatile species of the 41 HVOC SGM when sampled on TA14-CpX29, no breakthrough of trace compounds was witnessed on the second and third tubes of the sampling series. The breakthrough of the very volatile HVOC species through TA14-CpX29 is due to the weaker sorption strength and wider pores of Carbopack™X compared to Carboxen®1000, with the weaker Carbopack™X being less efficient in retaining very volatile species. Nonetheless, adapting gas sampling volumes and flowrates such that breakthrough no longer occurs, is feasible and could be further optimized for this 41 HVOC SGM (with analytes concentrated at 1 ppm_{mol}) and for other (real) gases.

The sampling experiments with the 41 HVOC SGM give the most noteworthy results in view of the diversity of trace compounds this SGM contains and since all four MAT configurations were sampled with it. The fact that TA14-CX26 disabled the recovery of acrylonitrile and *cis*- and *trans*-1,3-dichloropropane while TA14-CpX29 enabled it indicates Tenax®TA may not be strong enough or may not have high sorption affinities with those compounds to retain them, so that they migrate to the back bed in the MAT. Carboxen®1000 as back bed probably too strongly (irreversibly) retains those volatile compounds, impeding their recovery upon TD. In contrast, using the weaker Carbopack™X as back bed enables their recovery via TD as they are less strongly retained on this material. The three-bed TA14-CB21-CX26 configuration performed slightly better than the TA14-CX26 and enabled to recover acrylonitrile and *cis*- and *trans*-1,3-dichloropropane, likely efficiently trapped and desorbed from the Carbopack™B intermediary bed. Lastly, the CB21-CX26 configuration performed poorly with the 41 HVOC SGM, partly due to analytical and mechanical failures encountered with the TD prototype during the analysis of the CB21-CX26 samples, which may explain the much lower number of trace compounds detected (24/41). Notwithstanding, under proper analytical conditions, it is expected CB21-CX26 would behave similarly to the other two configurations containing Carboxen®1000 as back bed (-CX26) because these configurations performed identically for the other OPL, PEO and Chloro SGM (Table 3.5). Disregarding breakthrough, TA14-CpX29 therefore seems to operate the most efficiently for the 41 HVOC SGM.

The TA14-CpX29 MAT configuration was not sampled with the OPL, PEO and Chloro SGM. However, as it was found being efficient for the 41 HVOC SGM, and as the 41 HVOC SGM contains all trace compounds of the Chloro SGM and that it also covers the volatility range of the trace compounds present in the OPL and PEO SGM (Table 3.2), it is expected TA14-CpX29 will also efficiently adsorb and desorb the (semi-)volatile 1-octene, α -pinene, d-limonene, pentane, ethylcyclopentane and octane, all the more so as the strong Carboxen®1000 was able to recover them, thus the weaker Carbopack™X is certainly able to desorb them upon TD.

In light of above results and discussions, even though all four evaluated MAT configurations proved being conveniently efficient for most targeted trace compounds, it was decided to only keep the TA14-CpX29 and TA14-CX26 MAT configurations for further considerations and experimental work in this thesis. MAT configurations containing Carbopack™B (CB21) were rejected because:

- There was no striking efficiency difference between Tenax®TA or Carbopack™B used as front bed in a MAT, and Tenax®TA has been more often used in the landfill gas, biogas and biomethane literature.
- The analysis of the 41 HVOC SGM with TA14-CB21-CX26 revealed this 3-bed MAT configuration brought a slight efficiency advantage compared to TA14-CX26 but no efficiency advantage compared to TA14-CpX29. As furthermore 2-bed MAT were preferred above 3-bed MAT to ensure the total length of all adsorbent beds was well fitting within the heated zone of the TD prototype, the TA14-CB21-CX26 MAT was rejected.
- The analysis of new blank MAT containing Carbopack™B systematically contained a benzene impurity while benzene is not only targeted in the SGM but is also generally targeted in landfill gas, biogas and biomethane wherein it has often been found and monitored [4,11].

Even though TA14-CpX29 performed better for the 41 HVOC SGM and yielded higher peak heights than TA14-CX26 (Fig.3.4), both TA14-CpX29 and TA14-CX26 configurations were kept because of their potential to complement each other when sampling gases of unknown composition: the strong Carboxen®1000 efficiently retains and releases the most volatile species but with the risk to not efficiently desorb and recover less volatile ones, while Carbopack™X enables sampling very volatile species while simultaneously providing higher guarantee to efficiently desorb less volatiles species and hence avoid information loss on the less volatile species.

Finally, a repeatability study was conducted on the 10 replicate batches of 3 MAT in series for the TA14-CpX29 and TA14-CX26 tubes sampled with the 41 HVOC SGM. The chromatographic peak areas of all trace compounds detected from the 41 HVOC were recorded on all sampled tubes of the series. Results are however unexploitable (and not shown) since unpredictable analytical and mechanical failures of the TD prototype kept on happening. In Chapter 4, where the new TD prototype is presented in detail, some leads are proposed to address and solve the failures of the TD prototype and achieve better repeatabilities for the rest of the doctoral thesis work. In particular, the manufacturer of the TD prototype acknowledged mechanical improvements could be done at the needle injecting the analytes desorbed from the MAT into the gas chromatograph. The needle length, diameter and gas opening width and position on the needle were parameters to work on.

IV. CONCLUSIONS

The four different MAT configurations tested, assembling various combinations of four adsorbents (Tenax®TA, Carbopack™B, Carbopack™X and Carboxen®1000), enabled to preconcentrate major families of trace compounds potentially present in landfill gas, biogas and biomethane. Nevertheless, only two complementary MAT configurations were eventually kept for further considerations and experimental work in this thesis, namely the one containing Tenax®TA (14 mg) – Carbopack™X (29 mg) and the one containing Tenax®TA (14 mg) – Carboxen®1000 (26 mg). Future sampling campaigns of real landfill gas, biogas and biomethane samples will learn whether those two MAT configurations indeed complement each other in the range of trace compounds they enable to adsorb and recover upon thermal desorption and GC-MS analysis.

V. REFERENCES CHAPTER 3

- [1] E. Woolfenden, Monitoring VOCs in Air Using Sorbent Tubes Followed by Thermal Desorption-Capillary GC Analysis: Summary of Data and Practical Guidelines, *Journal of the Air & Waste Management Association*. 47 (1997) 20–36. <https://doi.org/10.1080/10473289.1997.10464411>.
- [2] E. Woolfenden, Sorbent-Based Sampling Methods for Volatile and Semi-Volatile Organic Compounds in Air. Part 2. Sorbent Selection and Other Aspects of Optimizing Air Monitoring Methods, *Journal of Chromatography A*. 1217 (2010) 2685–2694. <https://doi.org/10.1016/j.chroma.2010.01.015>.
- [3] R. Sheu, A. Marcotte, P. Khare, S. Charan, J.C. Ditto, D.R. Gentner, Advances in Offline Approaches for Chemically Speciated Measurements of Trace Gas-Phase Organic Compounds Via Adsorbent Tubes in an Integrated Sampling-to-Analysis System, *Journal of Chromatography A*. 1575 (2018) 80–90. <https://doi.org/10.1016/j.chroma.2018.09.014>.
- [4] S. Mariné, M. Pedrouzo, R.M. Marcé, I. Fonseca, F. Borrull, Comparison Between Sampling and Analytical Methods in Characterization of Pollutants in Biogas, *Talanta*. 100 (2012) 145–152. <https://doi.org/10.1016/j.talanta.2012.07.074>.
- [5] E. Gallego, F.J. Roca, J.F. Perales, X. Guardino, E. Gadea, Development of a Method for Determination of VOCs (including Methylsiloxanes) in Biogas by TD-GC/MS Analysis Using Supel™ Inert Film Bags and Multisorbent Bed Tubes, *International Journal of Environmental Analytical Chemistry*. 95 (2015) 291–311. <https://doi.org/10.1080/03067319.2015.1016012>.
- [6] US EPA, Compendium of Methods for the Determination of Toxic Organic Compounds in Ambient Air. Second Edition. Compendium Method TO-17: Determination of Volatile Organic Compounds in Ambient Air Using Active Sampling Onto Sorbent Tubes (EPA/625/R-96/010b), (1999). <https://www3.epa.gov/ttnamti1/files/ambient/airtox/to-17r.pdf> (accessed April 23, 2020).
- [7] K. Arrhenius, A.S. Brown, A.M.H. van der Veen, Suitability of Different Containers for the Sampling and Storage of Biogas and Biomethane for the Determination of the Trace-Level Impurities – A Review, *Analytica Chimica Acta*. 902 (2016) 22–32. <https://doi.org/10.1016/j.aca.2015.10.039>.
- [8] M. Harper, Review. Sorbent Trapping of Volatile Organic Compounds from Air, *Journal of Chromatography A*. 885 (2000) 129–151. [https://doi.org/10.1016/S0021-9673\(00\)00363-0](https://doi.org/10.1016/S0021-9673(00)00363-0).
- [9] R.R. Arnts, Evaluation of Adsorbent Sampling Tube Materials and Tenax-TA for Analysis of Volatile Biogenic Organic Compounds, *Atmospheric Environment*. 44 (2010) 1579–1584. <https://doi.org/10.1016/j.atmosenv.2010.01.004>.
- [10] J. Brown, B. Shirey, A Tool for Selecting an Adsorbent for Thermal Desorption Applications. Technical Report, (2001). https://www.sigmaaldrich.com/content/dam/sigmaaldrich/docs/Supelco/General_Information/t402025.pdf (accessed April 23, 2020).
- [11] S. Rasi, A. Veijanen, J. Rintala, Trace Compounds of Biogas from Different Biogas Production Plants, *Energy*. 32 (2007) 1375–1380. <https://doi.org/10.1016/j.energy.2006.10.018>.

TRANSITION CHAPTER 3 – 4

In Chapter 3, the methodology for the assembly, conditioning and analysis of multibed adsorbent tubes acting as preconcentration supports for trace compounds in biogas and biomethane, was presented. The regular occurrence of unpredictable analytical and mechanical failures and deficiencies of the thermal desorption (TD) prototype device was evidenced, in particular the inability of the TD prototype to provide repeatable injections in the hyphenated gas chromatograph. These shortcomings will have dramatic impacts on the rest of the thesis experimental results and it is of paramount importance to understand and delineate them to anyhow conduct the thesis with this device. Therefore, the next chapter (Chapter 4) presents, in the form of a published scientific article, an analytical validation study of the TD prototype which was addressed as best as possible while still coping with regular and unpredictable TD prototype failures. The validation study deals with the reliability of the TD prototype functioning and with the qualitative and quantitative repeatability of TD injections in the gas chromatograph. As validation reference, TD injections are compared with direct gas injections in the chromatograph and with solid phase microextraction coupled to gas chromatography.

CHAPTER 4 – PROMISES OF A NEW VERSATILE FIELD-DEPLOYABLE SORBENT TUBE THERMODESORBER BY APPLICATION TO BTEX ANALYSIS IN CH₄

- *Talanta Open* 4 (2021) 100066 • <https://doi.org/10.1016/j.talo.2021.100066> -

Received 28 July 2021; Received in revised form 1 September 2021; Accepted 2 September 2021; Available online 4 September 2021

Aurore Lecharlier^{1,2}, Brice Bouyssiere², Hervé Carrier¹, Isabelle Le Hécho^{2*}

¹ Université de Pau et des Pays de l'Adour, E2S UPPA, CNRS, TOTAL, LFCR UMR 5150, BP 1155 avenue de l'Université, 64013 Pau Cedex, France

² Université de Pau et des Pays de l'Adour, E2S UPPA, CNRS, IPREM UMR 5254, Technopôle Hélioparc, 2 avenue du Président Angot, 64053 Pau Cedex 09, France

*Corresponding Author: Isabelle Le Hécho • isabelle.lehecho@univ-pau.fr

ABSTRACT

Characterizing trace compounds in gaseous matrices such as natural gas is challenging owing to the low concentrations and the intricate interactions between compounds and matrices present. In contrast to whole gas sampling methods, direct *in situ* gas sampling with preconcentration of trace compounds on adsorbent tubes followed by thermal desorption and gas chromatography coupled to mass spectrometry (TD-GC-MS) is a powerful method enabling to screen unknown and targeted trace compounds with low detection limits and where moreover sample transfer and associated loss and contamination risks are avoided. Here, a new versatile, field-deployable thermodesorber prototype ('nCx-TD', *nCx Instrumentation*, Garlin, France) fitted with self-assembled purpose-built Tenax TA adsorbent tubes is presented. Its desorption and GC-injection performances are investigated using a 10 ppm_v BTEX in CH₄ synthetic gas and by contrasting the results to those obtained by solid phase microextraction (SPME) and direct injection of the synthetic gas. Unlike most commercial thermodesorbers, the nCx-TD is characterized by a fast "plug" injection without re-focusing trap, leading to high chromatographic peak resolutions. Between the closely eluting ethylbenzene and *m*- and *p*-xylene isomers, the Gaussian resolution obtained at a concentration of 10 ppm_v with the nCx-TD was 2.9 while that obtained by SPME and direct injection was respectively 1.7 and 1.9. The nCx-TD-obtained peak resolutions increased significantly with the concentration (1 to 10 ppm_v) while the SPME- and direct injection resolutions remained at a low constant level across concentrations tested. A real natural gas sample was sampled through the Tenax TA adsorbent tubes and analyzed via TD-GC-MS using the nCx-TD. More than 50 distinct trace compounds were detected, opening exciting perspectives of adsorbent tube multibed configurations and direct *in situ* field sampling on adsorbent tubes with *in situ* analysis through the nCx-TD and field-portable GC's.

KEYWORDS

Trace compound

Gas sample

Preconcentration

Tenax TA sorbent tube

BTEX

Thermal desorption-GC-MS

ABBREVIATIONS CHAPTER 4

BTEX	Benzene, toluene, ethylbenzene, <i>m</i> -xylene, <i>p</i> -xylene, <i>o</i> -xylene
CAR	Carboxen
GC	Gas chromatography
HS	Headspace sampler
MS	Mass spectrometry
N ₂	Dinitrogen gas
nCx-TD	New thermal desorber prototype by <i>nCx Instrumentation</i>
PDMS	Polydimethylsiloxane
PRS	Pressure regulating system
SPME	Solid phase microextraction
TA15	Self-assembled 15 mg Tenax TA adsorbent tube
TD	Thermal desorption / Thermal desorber

I. INTRODUCTION

Sampling and analysis methods for the characterization of trace constituents in gaseous matrixes have been developed since the 1970's notably by the United States Environmental Protection Agency due to the rising environmental and public health concerns with regards to dramatic atmospheric, workplace or urban air pollution events in the 1950-60's [1-3]. Most studied trace compounds in air are volatile organic compounds (VOC) [4-6], halocarbons [7], volatile Sulphur compounds [8-10] and volatile metals(oids) (As, Sb, Sn, Hg, Pb ...) [11-13]. In parallel, analogous methods began to be developed for the analysis of trace compounds in landfill gas and natural gas owing to industrial, safety and occupational health concerns about the damaging effects of some compounds on the integrity of gas production, transport and final-use infrastructures [14,15]. Trace compounds commonly investigated in natural gas are [14] paraffinic and aromatic hydrocarbons, halocarbons, oxygenated organic compounds, inorganic and organic Sulphur compounds [16], inorganic and organic metallic compounds and metalloid species [17-21].

Gas sampling is the first and most critical analytical step to characterize trace compounds. Gas matrices such as air and natural gas are complex systems consisting of gas-, condensate- (or aerosols) and solid phases (e.g. fine particles) [6,22]. Sampling and monitoring trace compounds is therefore challenging since they may partition into these different phases [20], in view of their low concentrations and the fact they lurk in mixtures of (in)organic, metallic and metalloid species having different physicochemical properties and potentially reacting with each other. Collected samples must be representative of the effective gas composition at a given time and under the prevailing gas pressure and temperature. The sampling procedure must ensure the stability of sampled compounds (no loss, no degradation) during the storage phase between sampling and analysis. Two gas sampling categories are distinguished: whole gas sampling versus gas sampling with enrichment ('trapping', 'preconcentration') of targeted trace compounds [6,12,23,24]. In whole gas sampling a bulk gas volume is collected in a specific vessel: sampling bags made of different polymers, aluminum or stainless-steel canisters or stainless-steel gas cylinders, the inner surfaces of the two latter usually being passivated with specific coatings. Profuse literature is available on the influence of the bag polymer wall type [12,25-30] and of the internal passivation coatings of canisters [31-34] or cylinders [35], on the stability of compounds sampled in such vessels. Disadvantageous to whole gas sampling regarding the determination of trace compounds is the need for subsequent preconcentration to bring analyte levels over the detection limits of analytical apparatuses. Preconcentration of whole gas samples is often done in the lab implying vessel transport (special transport for dangerous, explosive, goods in the case of methane gases) with consequent enhanced risks of target compound losses by sorption on or permeation through the vessel walls, losses by conversion or degradation reactions between reactive species in the vessel and contaminations during sample storage periods and sample transfers [12,24,35]. Direct *in situ* gas sampling with preconcentration is therefore preferred since those issues are avoided [35-37]: the gas is passed through a dedicated small-volume support with specific affinity for only given compounds thus being retained. The gas matrix itself passes through but is not retained, hence trace compounds are preconcentrated. For the preconcentration of (halogenated) volatile organic compounds ((H)VOC), adsorbent tubes [4-6,23,38-41] and solid phase

microextraction (SPME) fibers [42–45] are particularly efficient solid adsorption supports. Adsorbent tubes are nevertheless more suitable for direct field sampling: on the contrary to fragile SPME fibers rather dedicated to lab analyses, these are robust, small size (commercial tubes are typically ~6.35 mm outer diameter, ~9 cm length), easily handleable glass or stainless-steel tubes packed with commercial adsorbents having high sorption affinities and capacities for the targeted compounds.

Shipment of sampled adsorbent tubes to the lab for analysis is easy, fast and secure in view of the absence of the (flammable) gas matrix [4]. Thermal desorption coupled to gas chromatography and mass spectrometry (TD-GC-MS) is the analytical technique the most widely agreed upon for the recovery, segregation, identification and quantification of complex mixtures of low concentrated VOC differing in volatilities and polarities, desorbed from adsorbent tubes [4,46–48]. TD relies on the endothermic desorption of analytes from the adsorbents. Most modern commercial TD units operate a so-called “two-stage desorption”. The sampled sorbent tube is heated up to the adsorbent specific desorption temperature while a controlled flow of inert carrier gas continuously blows the gradually desorbed analytes to the outlet of the tube (‘primary desorption’). Since quantitative desorption of the analytes may require a long time (5-15 min) and large carrier gas volumes depending on their volatilities and on the tube geometry [23,49], injection of this carrier gas now loaded with analytes directly into the GC column would result in the dilution of analytes in the relatively large carrier gas volume and in unfavorable large chromatographic peaks [49]. Therefore, typically only 100-200 mL of the carrier gas loaded with analytes from the primary desorption are sent to a second, smaller, downstream located re-focusing trap [23,46,49]. This trap is a tiny tube filled with similar but lesser amounts of adsorbents as the sampling adsorbent tubes [4,36,41,49–51], of smaller inner diameter (1-2 mm) and maintained at low temperatures (e.g. -30°C [51], -10°C [49], -5°C [50]). Analytes are adsorbed (‘re-focused’) on this trap whereupon it is itself thermally desorbed (‘secondary desorption’) by rapid heating (up to 100°C·s⁻¹ [46]) with an ultra-tiny volume of carrier gas (typically 100-200 µL) instantly transferring the analytes into the GC column via a heated transfer line (~200°C [23,46,49]), as such creating a ‘flash’ or ‘plug’ injection resulting in favorable narrow chromatographic peaks. The preconcentration power of this method is determined by the carrier gas volume eventually injected in the GC by the refocusing trap: if analytes from a 100 L gas sample are quantitatively transferred to the GC column into 100 µL final carrier gas, the concentration enhancement factor is 10⁶ [46].

To the authors’ knowledge, no commercial field-deployable thermodesorber has ever been developed while direct *in situ* analysis of sampled adsorbent tubes with field-deployable TD units coupled to field-portable GC-MS would erase sample transport, storage and associated sample alteration risks. ‘Real time’ assessment of a gas composition can furthermore be crucial to monitor hazardous compounds and take immediate risk management action when measured values exceed a defined level [21].

Therefore, here, a new versatile, single-stage desorption and field-deployable adsorbent tube TD prototype is presented. As a first prototype development step, the ability of the new TD to generate high chromatographic peak resolutions when coupled to a bench-top GC-MS is demonstrated. The new TD prototype is tested by the thermal desorption of a synthetic BTEX (benzene, toluene, ethylbenzene, *m*-xylene, *p*-xylene, *o*-xylene) gas mixture in CH₄

preconcentrated onto self-assembled purpose-built Tenax TA adsorbent tubes. Tenax TA, a macroporous 2,6-diphenyl-*p*-phenylene oxide polymer, is widely used for the preconcentration of semi-VOC in gases [23,38,39]: its relatively low specific surface area (35 m²·g⁻¹ [52]) provides it with a sufficient adsorption strength yet enabling quantitative desorption of semi-VOC such as BTEX (boiling points 80 – 144.4°C at P_{atm}). TD-results are contrasted to direct GC-MS injection and SPME of the synthetic gas. The application potential of the new TD is then illustrated by preconcentrating a real natural gas sample on Tenax TA tubes. BTEX, stemming from crude oil and natural gas [53,54], were used through this study as they have been extensively studied by means of adsorbent tubes [5,37,39,55,56] and on SPME fibers [42,44,57,58] on account of their hazardous effects on human health and environment.

II. MATERIALS AND METHODS

II.1. Thermodesorber prototype

The new adsorbent tube thermodesorber prototype was developed and patented by *nCx Instrumentation*, Garlin, France and will be further referred to as 'nCx-TD'. It works in 'single-stage' desorption mode, meaning no re-focusing nor cryofocusing trap nor heated transfer line are present. Its small size and compatibility to most GC injection ports including miniaturized field-portable GC contribute to its versatility and field-deployability. Fig.4.1 presents the nCx-TD, dimensioned to only accommodate custom-built glass tubes (Fig.4.2). The nCx-TD is screwed on the GC inlet port via an adaptable nut and is connected to its monitor casing where to a carrier gas line (mostly Helium) and a pneumatic line (compressed air) are connected. A sampled adsorbent tube is placed manually into the nCx-TD heating core in the reverse direction as compared to the gas sampling flow direction. A computer software defines the few operational parameters of the nCx-TD (Table 4.S1 in the Supplemental Information). The thermal desorption cycle starts at a defined safe temperature and the heating core is then heated up to the adsorbent material-specific desorption setpoint temperature. The heating rate is not linear but rather follows this pattern at 25°C ambient temperature: from 100 to 200°C: 140°C·min⁻¹, from 200 to 400°C: 100°C·min⁻¹. During this heating phase, analytes are desorbed from the adsorbent material while the carrier gas valve is still closed, meaning volatilized analytes remain trapped in the tube. Once the temperature setpoint is reached, it is maintained during a user-defined time lapse, still without carrier gas flow. When this temperature stabilization phase is over, injection is instantly launched: two injection needles are pneumatically actuated: one piercing the upper septum of the adsorbent tube through which the carrier gas then flows, and one piercing the bottom septum of the tube which is then immediately connected to the GC-column inlet. As such, the carrier gas blows the desorbed analytes from the extremity of the tube directly into the GC column during a user-defined time lapse of as short as 5 seconds. This very fast, 'flash' or 'plug' injection of all analytes in a short time interval leads to narrow chromatographic peaks, justifying the non-necessity of a re-focusing trap.

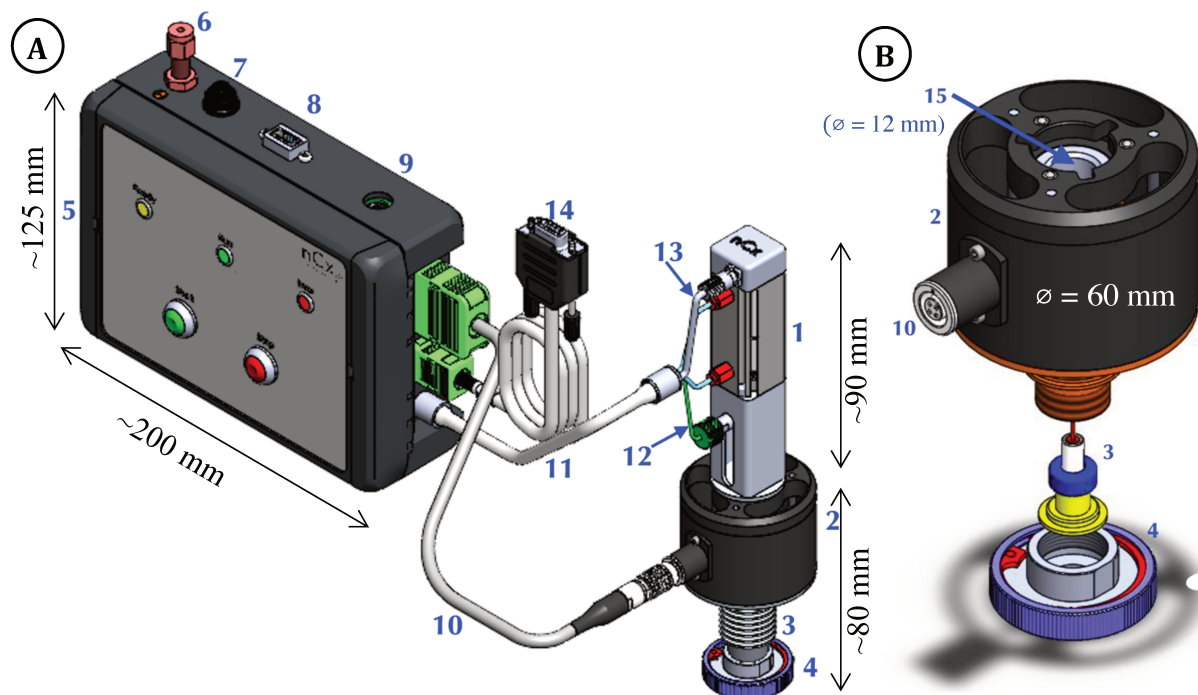


Figure 4.1: Schematic of the nCx-TD. (A) 1= injection head, 2= heating core, 3= injection needle, 4= adaptable GC-fixation nut, 5= monitor casing, 6= carrier gas inlet, 7= compressed air inlet (pneumatic line), 8= USB connection to computer, 9= electrical alimentation, 10= monitor connection to the heating core, 11= monitor connection to the injection head with distribution of the compressed air (12) and carrier gas (13), 14= monitor connection to the GC for synchronization. (B) Detail of the heating core with dismantlement of the injection needle. Same numbering as in (A). 15= adsorbent tube location.

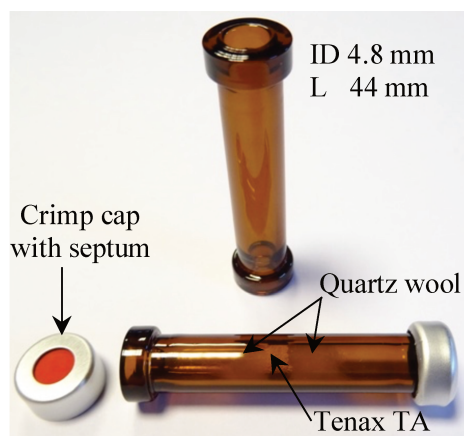


Figure 4.2: Custom-built glass tube intended for packing with adsorbents and thermal desorption in the nCx-TD. ID = internal diameter, L = length.

II.2. Tenax TA adsorbent tube self-assembly

Empty amber glass tubes (ID 4.8 mm, L 44 mm, ActionEurope, Sausheim, France) are packed with 15 mg Tenax TA (60-80 mesh, surface area $35 \text{ m}^2 \cdot \text{g}^{-1}$, Supelco, Bellefonte, PA, USA) retained between two untreated quartz wool plugs (Helios Italquartz™) (Fig.4.2): a first quartz wool plug is manually inserted into the tube where after 15 ± 0.2 mg Tenax TA are sucked up inside the tube by means of a flexible vinyl tubing pushed in the tube extremity and connected to a small volumetric pump (Xylem Flojet, RS Components, Beauvais, France). A second quartz wool plug is then manually inserted on top of the Tenax TA bed to secure it. Thereupon, these 15 mg Tenax TA tubes (here after referred to as “TA15”) are conditioned at 320°C under a continuous pure nitrogen flow (99.999% purity) during 8.5 hours in a purpose-built 20-positions conditioning support (aluminum 2017A, colorless anodic oxidation) installed in a disused GC oven (Fig.4.S1 in the Supplemental Information). Each of the 20 positions of the support’s bottom plate is provided with an 11 mm o-ring (Dupont™ Kalrez® Spectrum™ metric o-ring 7075) ensuring the N_2 flow effectively enters every single tube. The oven is gently heated from 25°C to 320°C at $10^\circ\text{C} \cdot \text{min}^{-1}$. The N_2 flowrate through each individual tube varies between 140 and $510 \text{ mL} \cdot \text{min}^{-1}$ with an average of $375 \text{ mL} \cdot \text{min}^{-1}$. As soon as the conditioning sequence is completed and tubes cooled down to a temperature allowing manual grip, tubes are sealed with aluminum crimp caps with PTFE/silicone/PTFE septa (11 mm, high temperature ultra-low-bleed silicone, ActionEurope) and stored until utilization in individual hermetic polyethylene zip bags in a larger zip bag in a desiccator at 4°C .

II.3. Gas samples

To assess the chromatographic peak resolution of the nCx-TD injections, a synthetic 10 ppm_v BTEX in CH_4 gas mixture (700 L, 140 bar_a , mélange crystal, AirLiquide France Industrie) was sampled on self-assembled TA15 tubes (10 replicates), on a commercial SPME fiber with $75 \mu\text{m}$ thick Carboxen/polydimethylsiloxane (CAR/PDMS) coating (Supelco) (3 replicates) and in 20 mL crimp-cap glass vials (Chromoptic, Courtaboeuf, France) (14 replicates) as follows. The synthetic gas bottle is connected to a pressure regulating system (PRS) lowering the gas pressure to $\sim 1.4 \text{ bar}_a$ and equipped with a final needle “n” allowing gas flow (Fig.4.S2). Each TA15 tube is sampled by pricking one of its septa on this needle “n” and the other septum on a needle with tubing connected to a mass flowmeter (Bronkhorst Mass-View® MV-302) (Fig.4.S2 A). 300 mL_n synthetic gas are passed through each TA15 tube at $50 \text{ mL}_n \cdot \text{min}^{-1}$ and the gas sampling direction through the tube is recorded. Sampled tubes are stored in individual hermetic polyethylene zip bags in a larger zip bag in a desiccator at 4°C until TD-GC-MS analysis. For the other two sampling means, 20 mL glass vials crimp-capped with PharmaFix Butyl/PTFE septa (Chromoptic) are vacuumed to 0.003 bar_a (Fig.4.S2 point 8) and subsequently immediately filled at 1.20 bar_a with the 10 ppm_v BTEX- CH_4 synthetic gas by pricking the vial septum to the needle “n” of the PRS (Fig.4.S2 B). As such filled vials are stored at room temperature until analysis by either direct gas injection in the GC or by SPME. The 10 ppm_v BTEX synthetic gas is sampled on a CAR/PDMS SPME fiber (handled with a SPME fiber holder for use with manual sampling, Supelco) by introducing the fiber in a vial filled as explained and exposing the fiber to the gas during 5.00 minutes where after it is retrieved from the vial and promptly inserted in the heated GC-inlet for analysis.

For calibration purposes, 6 BTEX concentrations C_i with $i=\{1\rightarrow 6\}$ (0, 1, 2.5, 5, 7.5, 10 ppm_v) were generated by volumetric dilution of the 10 ppm_v BTEX in CH₄ synthetic gas in pure synthetic CH₄ ($\geq 99.9995\%$ purity, Linde, France). Each concentration C_i was prepared in a 5L Tedlar bag (Supelco) by transferring adequate volumes of pure CH₄ and of 10 ppm_v BTEX in CH₄ synthetic gas into the bag. To keep the prepared dilutions as fresh and stable as possible in the bags, all analyzes on one concentration C_i were performed before preparing the next concentration C_{i+1} . Sampling of each concentration C_i from its Tedlar bag onto TA15 tubes, SPME and into vials (3 replicates for each sampling means) occurred as follows. 300 mL_n gas is passed through the TA15 tubes at 50 mL_n·min⁻¹ by connecting the Tedlar bag to the TA15 tube via a vinyl tubing with needle and connecting the end of the TA15 tube to a needle with vinyl tubing itself connected to the mass flowmeter (Fig.4.S3 A). A constant force is applied on the bag to trigger the gas flow through the TA15 tube. For the two other sampling means, 20 mL crimp-capped glass vials are first vacuumed to 0.003 bar_a and then connected to the Tedlar bag mouth via a needle (Fig.4.S3 B). The pressure gradient between vacuumed vial and Tedlar bag (~ 1 bar_a) results in the vacuumed vial getting instantly filled with ~ 1 bar_a gas C_i . As such filled vials are stored and analyzed by direct gas injection or SPME as described above.

Lastly, real natural gas from the lab building distribution grid ('NG-A', $P \sim 1.05$ bar_a) was sampled with the three methods on the same day. Ten TA15 tubes were individually loaded at ~ 80 mL_n·min⁻¹ with 500 mL_n NG-A by pricking the tubes to the grid wall valve. NG-A was also sampled in vacuumed glass vials for direct gas injections and SPME analyses (10 vials each) as described above. NG-A samples were stored as explained above until analysis.

All samples were taken at room temperature.

II.4. Analysis

All gas samples were analyzed with their respective injection technique (TD of TA15 tubes; SPME; direct gas injection) via gas chromatography (Agilent 6890A GC) coupled to mass spectrometry detection with quadrupole mass filter (Agilent 5973Network Mass Selective Detector) (GC-MS) programmed as in Table 4.1 using the MSD ChemStation E.02.02.1431 (Agilent) software and the NIST Mass Spectral Search Program version 2.0 d, 2005. Note the 200°C temperature programmed in the nCx-TD corresponds to an effective desorption temperature of 300°C inside the TA15 tube. Glass vials intended for direct gas injection in the GC-MS were placed in an Agilent G1888A Network Headspace Sampler (HS) with a 3 mL sampling loop programmed as in Table 4.1. Glass vials intended for SPME preconcentration are sampled in turn on the CAR/PDMS SPME fiber during 5:00 min as explained above whereupon the fiber is promptly inserted in the heated GC inlet (230°C) for thermal desorption of the analytes from the fiber during the first 5.00 minutes of the GC cycle where after the fiber is removed from the GC inlet. The fiber is reconditioned in the GC inlet at 280°C during ≥ 30 minutes under He flow between each vial. NG-A natural gas sampled on TA15 tubes and NG-A vials for direct injection and SPME were analyzed as in Table 4.1 but with a GC-oven program of 30°C (4 min) – 10°C/min – 250°C (5 min), in split 1:1 and in MS-scan mode (10-450 a.m.u.) with a scan rate of 3.28 scan·s⁻¹.

Table 4.1: Operational parameters for the GC-MS, nCx-TD and Network Headspace Sampler

Instrument	Parameter	Value / reference
GC <i>Agilent 6890A</i>	Inlet temperature	230°C
	Inlet septum for nCx-TD and direct gas injections	Premium Inlet Septa, Bleed/Temp optimized, non-stick (Agilent)
	Inlet septum for SPME injection	Molded Thermogreen® LB-2 septa with injection hole (Supelco)
	Inlet liner for nCx-TD and direct gas injections	Ultra Inert Liner, Splitless, Single taper, no wool, 4 mm ID (Agilent)
	Inlet liner for SPME injection	Inlet Liner, Direct (SPME) Type, Straight Design, 0.75 mm ID (Supelco)
	Split ratio	5 :1
	Split flow	7.5 mL·min ⁻¹
	Carrier gas	Helium (quality detector 5.0, Linde, France)
	Gas saver	Off
	Column	HP-5MS, 30 m × 250 µm ID × 0.25 µm film thickness (Agilent)
	Constant column flow mode	1.5 mL·min ⁻¹
Carrier gas linear velocity in column	44 cm·s ⁻¹	
Oven	30°C (4 min) - 7°C·min ⁻¹ - 180°C (2 min)	
MS <i>Agilent 5973Network Mass Selective Detector</i>	GC-MS interface temperature	280°C
	Electron Impact Mode	70 eV
	Electron Multiplier Voltage	Relative (100)
	Selected Ion Mode (SIM)	Ions: 51, 65, 77, 78, 91, 92, 105, 106
	Dwell time	Peak resolution study: 20 ms (5.37 cycles/s) Calibration curve study: 100 ms (1.21 cycles/s)
Resolution	'Low'	
nCx-TD	Safe temperature	35°C
	Temperature	200°C
	Stabilization time	15 s
	Pressure	1170 mbar
HS <i>Agilent G1888A Network Headspace Sampler</i>	Injection time	10 s
	Oven	70°C
	Loop	90°C
	Transfer line	110°C
	Vial equilibration time	10 min
	Pressurization time	0.15 min
	Loop fill time	0.5 min
	Loop equilibration time	0.1 min
Injection time	0.5 min	

II.5. Calculations

Chromatographic peak resolution

Three chromatographic peak resolution indicators were calculated following the IUPAC recommendations [59] between subsequently eluting BTEX peaks:

- Peak resolution $R = 2 \frac{(t_2 - t_1)}{(\omega_1 + \omega_2)}$ with t_1 and ω_1 respectively the chromatographic retention time and baseline peak width of the first eluting compound and t_2 and ω_2 those of the second eluting compound between which the resolution is calculated;
- Gaussian peak resolution $R_G = 1.18 \frac{(t_2 - t_1)}{(\omega_{0.5h,1} + \omega_{0.5h,2})}$ with t_i as above $\omega_{0.5h,i}$ the half-height peak width;
- Peak separation factor $\alpha = \frac{t_2 - t_0}{t_1 - t_0}$ with t_i as above and t_0 the retention time of a non-retained compound (here the CH₄ matrix of the 10 ppm_v BTEX synthetic gas)

Instrument detection limit

The instrument detection limit (IDL) for each BTEX compound was determined as 3 times the standard deviation of its corresponding peak height in the background noise of 10 blanks for each injection technique using the analytical parameters of Table 4.1. For TA15 tubes, 10 new conditioned tubes were used. For SPME, a single new 75 μm CAR/PDMS fiber was used that was initially pre-conditioned at 300°C in the GC inlet under He flow. The 10 SPME fiber blanks were acquired by reconditioning the fiber between BTEX sorption experiments. For the vials, 10 vials were filled via the PRS with pure CH₄. Further, IDL for TA15 tubes and SPME were also calculated for some compounds determined in NG-A (Table 4.2). 10 new blank TA15 tubes and 10 SPME fiber blanks were acquired as in Table 4.1 but with a GC-oven program of 30°C (4 min) – 10°C/min – 250°C (5 min), in split 1:1 and in MS-scan mode (10-450 a.m.u.) with a scan rate of 3.28 scan·s⁻¹. Then, the target ion of each compound (Table 4.2) was extracted from each scan (Extracted Ion Chromatogram, EIC), each EIC was integrated on the time intervals where its compounds would elute (based on the NG-A sample data) and the corresponding blank background peak heights were recorded for IDL calculation: 3 times the standard deviation on peak heights (n=10).

Table 4.2: Main qualifying ions for the IDL determination of compounds determined in NG-A

<u>Compound</u>	<u>Target ion</u>
Benzene	78
Toluene	91
Ethylbenzene	91
<i>m,p</i> -Xylene	91
<i>o</i> -Xylene	91
Cyclohexane	56
Heptane	43
3-Ethylhexane	43
Octane	43
Thiophene	84
Tetrahydrothiophene	60

Statistical tests

Linear regression analyses (least squares method) and analysis of variance statistical F-tests were performed at a significance level $\alpha = 0.05$ using Microsoft® Excel 16.50 to question the relationship between (1) the concentration (0, 1, 2.5, 5, 7.5, 10 ppm_v) and the average chromatographic peak area of 3 replicates for each BTEX compound for each injection technique (calibration curves) and (2) the concentration (1, 2.5, 5, 7.5, 10 ppm_v) and the average chromatographic Gaussian peak resolution between ethylbenzene and *m*-,*p*-xylene isomers for 3 replicates for each injection technique.

III. RESULTS AND DISCUSSION

III.1. Chromatographic peak resolutions

The chromatographic peak resolution performance of the nCx-TD injections is compared in Fig.4.3 – 4.4 and in Table 4.S2, to the resolution obtained with SPME and HS injections of the 10 ppm_v BTEX-CH₄ synthetic gas. The peak resolution R and the Gaussian peak resolution R_G both measure how well subsequently eluting peaks are distinctly separated in time on the chromatogram. The larger the difference between elution times and the narrower the peaks, the better the resolution. As the SPME-acquired peaks right-tail and do not go back to the original-baseline immediately (Fig.4.3), the peak resolution R relying on the baseline-peak width was not calculated between the three closely eluting ethylbenzene and xylene-isomers since peak-end extrapolations should have been made. For those compounds, the half-height peak width-based Gaussian peak resolution was considered. From Fig.4.3 – 4.4 it is clear nCx-TD injections yield the highest peak resolutions between all BTEX compounds even between ethylbenzene and the co-eluting *p*- and *m*-xylene isomers being close in boiling point (respectively 136, 138.4 and 139°C at P_{atm}). Despite the absence of preconcentration in the HS-injected vials as visible on Fig.4.3 (small, broad peaks), a slightly better resolution is obtained with HS- than with SPME-injections due to the systematic and non-negligible SPME-peak tailing to the right. On the contrary to BTEX on TA15 tubes thermally desorbed and injected via the nCx-TD into the GC-column, thermal desorption and injection of BTEX from the SPME fiber in the heated GC-inlet does not occur in a “flash” mode but in a rather continuous mode during the 5 min the fiber is left in the inlet. BTEX compounds from the fiber get only gradually simultaneously desorbed and injected in the GC-column, with desorption from the inner bulk of the SPME fiber film coating being slower than the almost immediate desorption from the surface of the film coating, leading to long desorption times and associated right-tailing peaks [60,61]. These results point out the preconcentration power of TA15 tubes combined to the flash-injection working mode of the nCx-TD yield highly efficient thermal desorption runs with narrow peaks and corresponding high peak-resolutions.

The peak separation factor α was recorded as well. An α equal to 1.00 indicates the two considered peaks are not separated. The more $\alpha > 1$, the better the peaks are separated in time. As B,T,E,X-retention times do not shift across the three injection techniques tested, α keeps the same value in nCx-TD, SPME and HS injections (Fig.4.4), with α between the closely eluting ethylbenzene and *m*-,*p*-xylene being the closest to one.

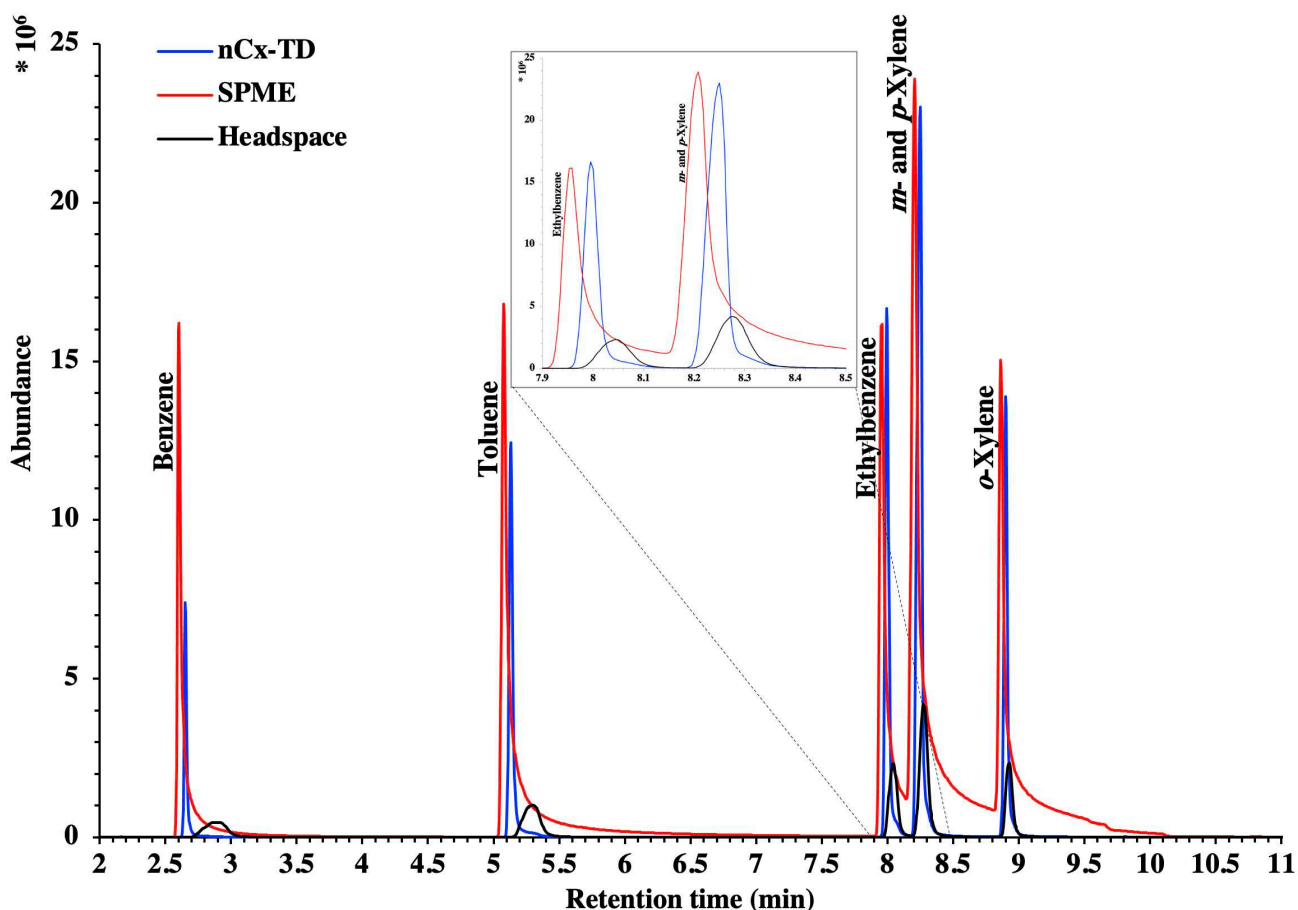


Figure 4.3: Total ion current chromatograms for the determination of the peak resolution between B,T,E,X chromatographic signals obtained from the different injection techniques tested for the 10 ppm_v BTEX-CH₄ synthetic gas.

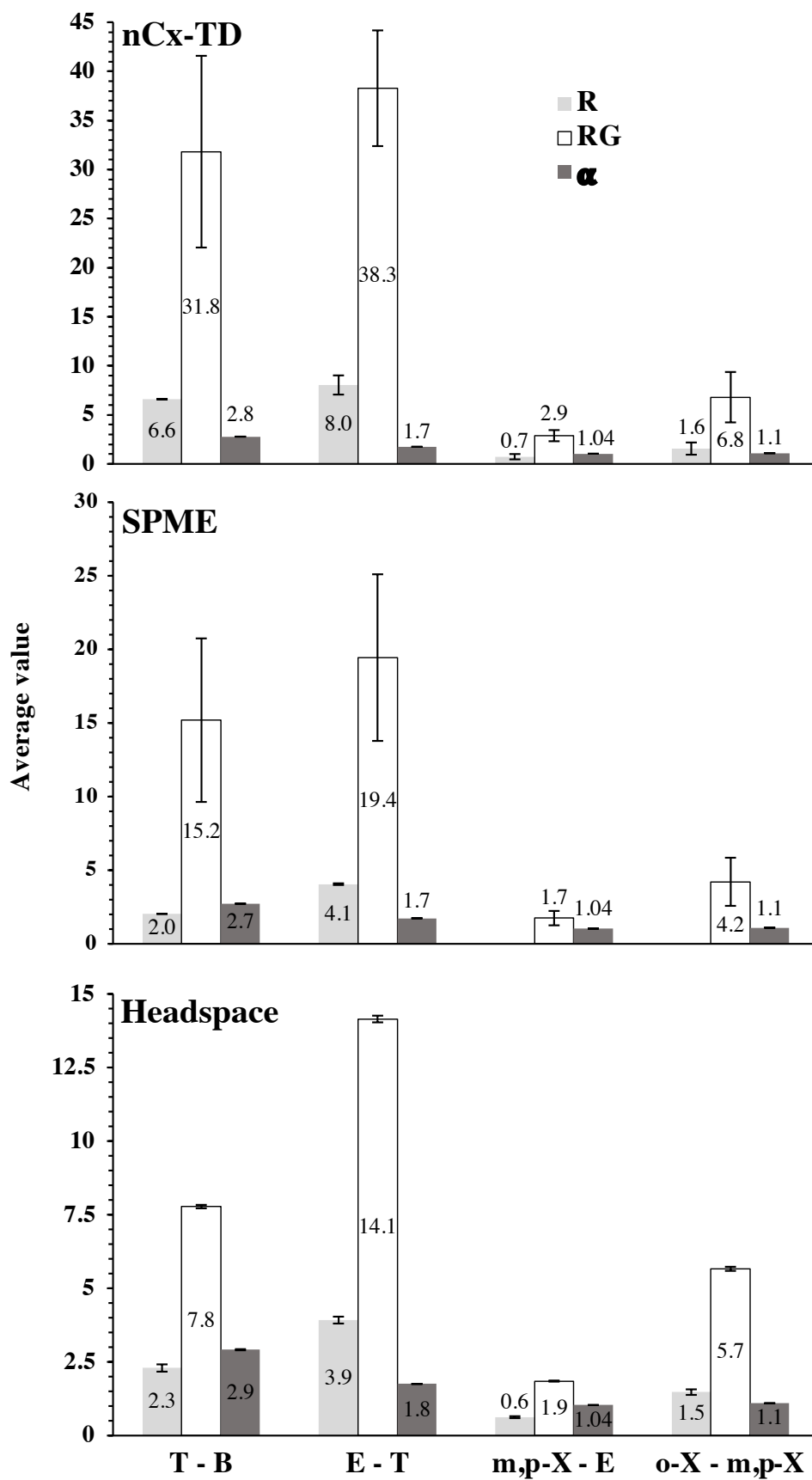


Figure 4.4: Peak resolution R , Gaussian peak resolution R_G and peak separation factor α of 10 ppm_v BTEX-CH₄ synthetic gas injected via the nCx-TD ($n=7$ successful injections on 10 performed), SPME ($n=3$) and Headspace ($n=14$). T - B: resolution between benzene and toluene. E - T: resolution between toluene and ethylbenzene. m,p-X - E: resolution between ethylbenzene and m- and p-xylene. o-X - m,p-X: resolution between m- and p-xylene and o-xylene. Error bars indicate the standard deviation.

III.2. Preconcentration of natural gas trace compounds

The application potential of the nCx-TD is illustrated by the TD-GC-MS analysis of a real natural gas (NG-A) sampled onto TA15 tubes for preconcentration of its trace compounds. NG-A samples were analyzed in MS-scan mode to screen their global trace compounds' composition and not only BTEX, since Tenax TA has a great adsorption potential for many other semi-volatile chemical compounds from different families [16,39,40,62,63]. Inasmuch as this is only a proof of concept, so far no (semi-) quantification was performed on the natural gas samples data.

Fig.4.5 compares the chromatograms of NG-A samples obtained via the three sampling and injection techniques. As no preconcentration occurs in vials with direct gas injection (headspace), the bulk CH₄ matrix of natural gas is injected and generates a broad peak from ~1.30 to 2.60 min hiding at least the main other light hydrocarbons of natural gas (ethane, propane, butane). With the exception of 4 bulky peaks (cyclohexane at 3.10 min; methylcyclohexane at 4.25 min; toluene at 5.38 min; tetrahydrothiophene at 6.31 min), no other compounds are detected and the chromatographic resolution is extremely poor. On the other hand, sampling on the SPME fiber and on TA15 tubes clearly operates a strong preconcentration of natural gas constituents (Fig.4.5). With TA15 tubes, 50 compounds were detected in NG-A against 46 when SPME is used (Table 4.3). The building grid natural gas is globally characterized by aliphatic and cyclic alkanes up to C₉, BTEX and organic Sulphur-compounds related to the natural and artificial odorization of natural gas (thiophene, 2,3-dihydrothiophene, tetrahydrothiophene), corresponding to the literature-mentioned natural gas composition [14,53,64,65]. Across the 10 replicates, the CAR/PDMS 75 µm SPME fiber did not enable to detect thiophene, 2,3-dihydrothiophene, methyloctane isomers, nonane and 1-ethyl-3-methylbenzene while the TA15 tubes did. Also, the SPME chromatographic baseline is higher and noisier than the one of TA15 tubes (Fig.4.5). The diversity of compounds successfully detected from the thermal desorption of NG-A loaded TA15 tubes henceforth demonstrates the efficiency and relevance of the preconcentration and analysis method developed as well as the valuable capacity of the nCx-TD in giving high chromatographic peak resolutions and pure baselines. Furthermore, notwithstanding some analogous qualitative preconcentration performances between TA15 tubes and CAR/PDMS SPME fibers, adsorbent tubes are more solid than fragile SPME fibers and are more convenient for field manipulations with an eye on direct *in situ* preconcentration of trace compounds from gas samples.

What emerges from the results is that on tiny adsorbent tubes packed with as little as 15 mg Tenax TA (whereas the commercial and scientific literature on adsorbent tubes rather refers to adsorbent masses of at least ~100-200 mg [39,41,47]) and where through only 0.5 L_n gas was sampled, more than 50 distinct compounds were detected in the natural gas (Table 4.3). This is a promising fact with an eye on adsorbent tube optimization to sample more complex gases such as biogases and biomethane being composed of a much larger variety trace compounds from diverse chemical families [24,36,37,48] (alkanes, alkenes, terpenes, alcohols, aldehydes, ketones, ethers, esters, aromatics, halogenated-, Nitrogen-, Sulphur-, Silicon-compounds...). In particular, multibed adsorbent tube configurations where an adsorbent with a low sorption strength (lower surface area) is placed first in the tube ("front bed") with respect to the gas sampling direction, and is followed by one or two "mid" and "back" beds made of adsorbents of increasing sorption strengths (increasing surface areas), are extremely useful to

preconcentrate a large number of trace compounds in a wide volatility range and of different families since, upon sampling, heavier compounds get first trapped on the weaker front adsorbents and lighter ones on the stronger downwards located adsorbents [5,23,38,39].

Another advantage of the developed sampling and preconcentration method on tiny adsorbent tubes is the extremely small gas volumes that need to be sampled to trap sufficient amounts of targeted compounds. Here, only 0.5 L_n gas needed to be sampled to acquire a deep characterization of the natural gas sample. Yet the sampling volume has to be optimized for each gas to sample with an eye on breakthrough avoidance, it seems reasonable to declare sampling volumes with the presented adsorbent tubes will be in the range of 0.5 – 2 L_n gas. Smaller gas volumes to sample *in situ* is synonym of less vent CH₄ emissions to the atmosphere during sampling campaigns of e.g. natural gas, biogas or biomethane inasmuch as the CH₄ matrix passes through the adsorbent tubes without being trapped. This contributes to lessen the relative atmospheric pollution generated during such sampling operations.

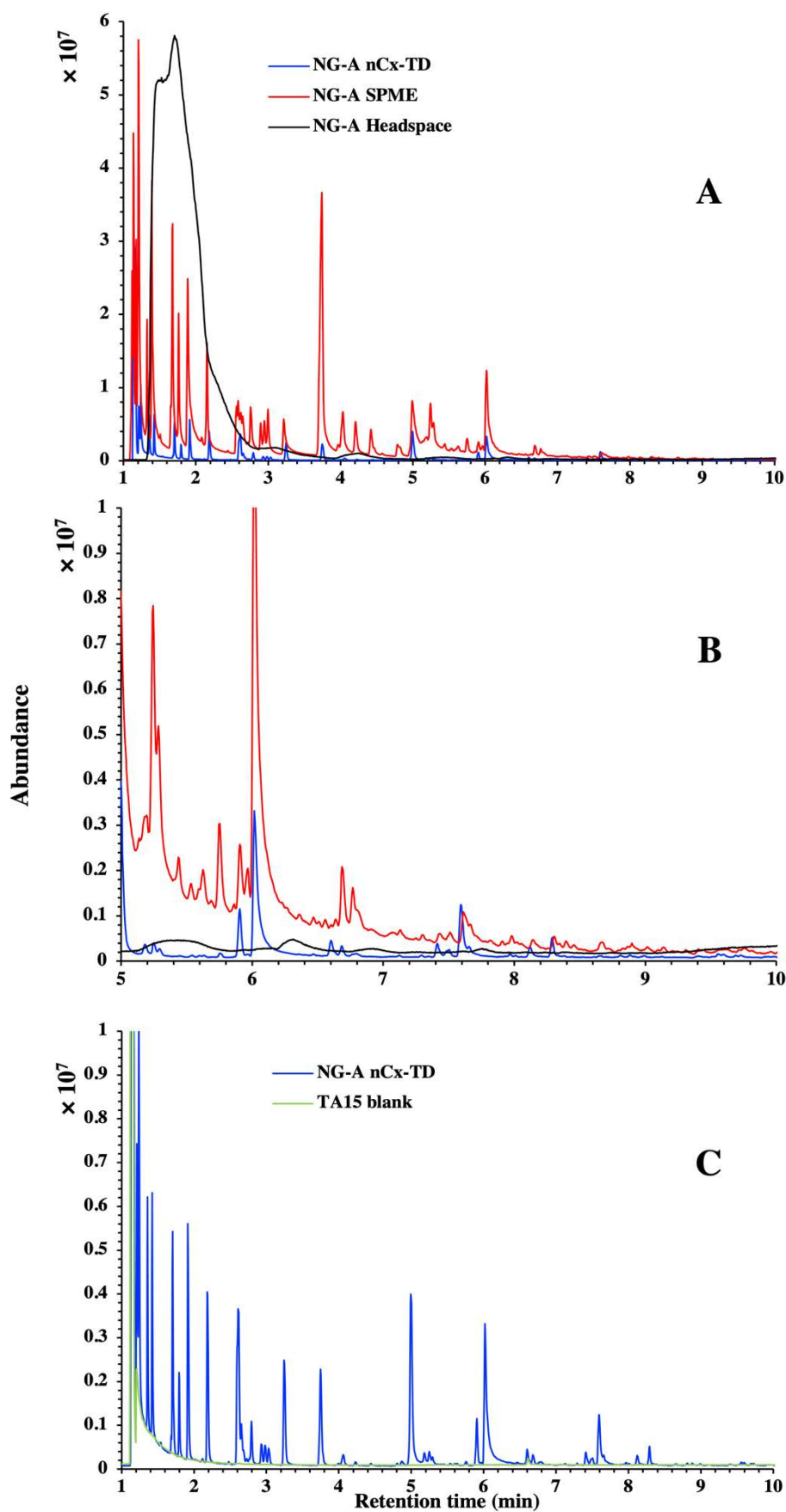


Figure 4.5: A and B: Total ion current chromatograms of the building grid natural gas (NG-A) sampled on TA15 tubes (nCx-TD injection), on the CAR/PDMS 75 μ m SPME fiber and in vials (Headspace injection) on the same day. C: the nCx-TD-GC-MS output of a new blank TA15 tube is contrasted to a NG-A sampled TA15 tube, analyzed with the same parameters. Note a tiny benzene (2.62 min) contamination inherent to new blank TA15 tubes (see section III.3) and hexamethylcyclotrisiloxane (6.61 min) released from the silicone layer of the TA15 tube capping-septum.

Table 4.3: Main trace compounds identified via the NIST-library from the building grid natural gas (NG-A) chromatograms (Fig.4.5) obtained by sampling on TA15 tubes, CAR/PDMS 75 μ m SPME fiber and in headspace vials.

Compound	Retention time (min)		
	TA15 tube	CAR/PDMS SPME	Headspace
Ethane	1.12	1.12	1.62 – 1.71
Propane	1.15	1.14	1.62 – 1.71
Isobutane	1.19	1.17	
Butane	1.22	1.20	1.71
2-methylbutane	1.34	1.33	
Pentane	1.41	1.39	
2,2-dimethylbutane	1.53	1.51	
2,3-dimethylbutane	1.67	1.65	
2-methylpentane	1.69	1.67	
3-methylpentane	1.78	1.76	
Hexane	1.90	1.88	
2,2-dimethylpentane	2.11	2.08	
Methylcyclopentane	2.18	2.15	
Cyclohexane	2.59	2.56	3.10
Benzene	2.61	2.58	
2-methylhexane	2.65	2.62	
2,3-dimethylpentane	2.68	2.65	
Thiophene	2.72		
3-methylhexane	2.79	2.76	
1,2-dimethylcyclopentane (cis/trans)	2.93	2.89	
1,2-dimethylcyclopentane (cis/trans)	2.98	2.95	
1,3-dimethylcyclopentane (cis/trans)	3.03	3.00	
Heptane	3.25	3.22	
Methylcyclohexane	3.75	3.74	4.25
2,5-dimethylhexane	3.99	3.97	
Ethylcyclopentane	4.06	4.03	
1,2,4-trimethylcyclopentane	4.23	4.21	
1,2,3-trimethylcyclopentane	4.45	4.42	
2,3-dimethylhexane	4.80	4.79	
2,3-dihydrothiophene	4.87		
Toluene	5.00	4.99	5.38
3-ethylhexane	5.18	5.19	
1,3-dimethylcyclohexane (cis/trans)	5.25	5.24	
1,4-dimethylcyclohexane (cis/trans)	5.29	5.29	
1,2-dimethylcyclohexane (cis/trans)	5.75	5.75	
Octane	5.90	5.90	
1,4-dimethylcyclohexane (cis/trans)		5.97	
Tetrahydrothiophene	6.02	6.02	6.31
Ethylcyclohexane	6.68	6.69	
1,1,3-trimethylcyclohexane		6.77	
1,2,3-trimethylcyclohexane	7.12	7.13	
Ethylbenzene	7.41	7.43	
4-methyloctane	7.49		
2-methyloctane	7.50		
<i>m</i> - and <i>p</i> -Xylene	7.59	7.61	
1-ethyl-2-methylcyclohexane	7.97	7.98	
1-ethyl-4-methylcyclohexane	8.01	8.02	
<i>o</i> -Xylene	8.12	8.14	
Nonane	8.29		
1-ethyl-3-methylbenzene	9.56		
1,2,3-trimethylbenzene	9.60	9.60	
1,2,4-trimethylbenzene	9.69	9.72	

III.3. Instrument detection limits

Table 4.4 lists the instrument detection limits (IDL) obtained for each BTEX with the three injection techniques (analysis parameters Table 4.1) for each of which a chromatogram of a blank is displayed in Fig.4.6. SPME fiber blanks are free from any BTEX and the low peak-height standard deviations, relatively constant in order of magnitude across all BTEX, indicate a similar background noise on the 10 blanks, so low IDL are obtained (Table 4.4). The slight linear increase in IDL from benzene to *o*-xylene probably comes from the slightly rising blank baseline (Fig.4.6) due to increasing temperatures along the GC cycle. In contrast, new blank TA15 tubes systematically contain inherent benzene, toluene, ethylbenzene, *m*-,*p*-xylene and styrene (co-eluting with *o*-xylene) traces. Now precisely those BTEX compounds with benzene being the most abundant contamination followed by toluene and styrene are well-known typical thermal degradation products of the 2,6-diphenyl-*p*-phenylene oxide Tenax TA matrix [5,66,67] certainly generated during the thermal conditioning of the new TA15 tubes although the Supelco-recommended conditioning specifications for Tenax TA were observed (320°C for at least 8 h under clean nitrogen flow [52]). These inherent contaminations are to bear in mind and the TA15 tube conditioning procedure should be optimized to minimize them. As each single new TA15 tube probably undergoes unique thermal degradation intensities related to its very own location and effective nitrogen flowrate on the 20-positions conditioning support, the BTEX background peak-height standard deviation across the 10 blanks and associated IDL are high especially for the most abundant thermal degradation products benzene, toluene and *o*-xylene (because of its co-elution with styrene). Ethylbenzene and *m*-,*p*-xylene have an IDL of the same order of magnitude as with SPME. Finally, in the pure CH₄ vials for HS injections, relatively high BTEX levels are found due to the vial filling procedure through the PRS where dead volumes in the tubing, despite thorough cleaning procedures, are likely contaminated with minute amounts BTEX from numerous previous gas transfers. Across the 10 'blank' vials, the intensities of ethylbenzene and *m*-,*p*-xylene contaminations look the highest and the least stable, yielding the highest IDL for those species while IDL for benzene, toluene and *o*-xylene are in the same order of magnitude as for SPME.

Table 4.4: Standard deviation (Std dev), relative standard deviation (RSD% = 100 Std dev/average) and instrument detection limit (IDL = 3 Std dev) (signal abundance) of the BTEX background noise (peak height) in 10 blanks of the CAR/PDMS 75 μm SPME fiber, in the blanks of 10 new Tenax TA15 tubes and in 10 vials of pure CH₄ for HS injections.

	Std dev (n=10)			RSD %			IDL		
	CAR/PDMS 75	TA15	Vial	CAR/PDMS 75	TA15	Vial	CAR/PDMS 75	TA15	Vial
Benzene	106.1	18920.8	133.2	17.7	119.0	12.7	318.2	56762.3	399.5
Toluene	125.2	1335.3	106.6	19.7	84.9	5.4	375.6	4005.9	319.7
Ethylbenzene	183.7	306.0	531.6	26.7	38.4	20.2	551.2	917.9	1594.9
<i>m</i>- and <i>p</i>-Xylene	201.9	220.0	772.3	28.5	28.1	21.4	605.8	660.0	2316.8
<i>o</i>-Xylene	219.5	43095.0	216.0	30.7	132.7	19.8	658.6	129285.0	648.0

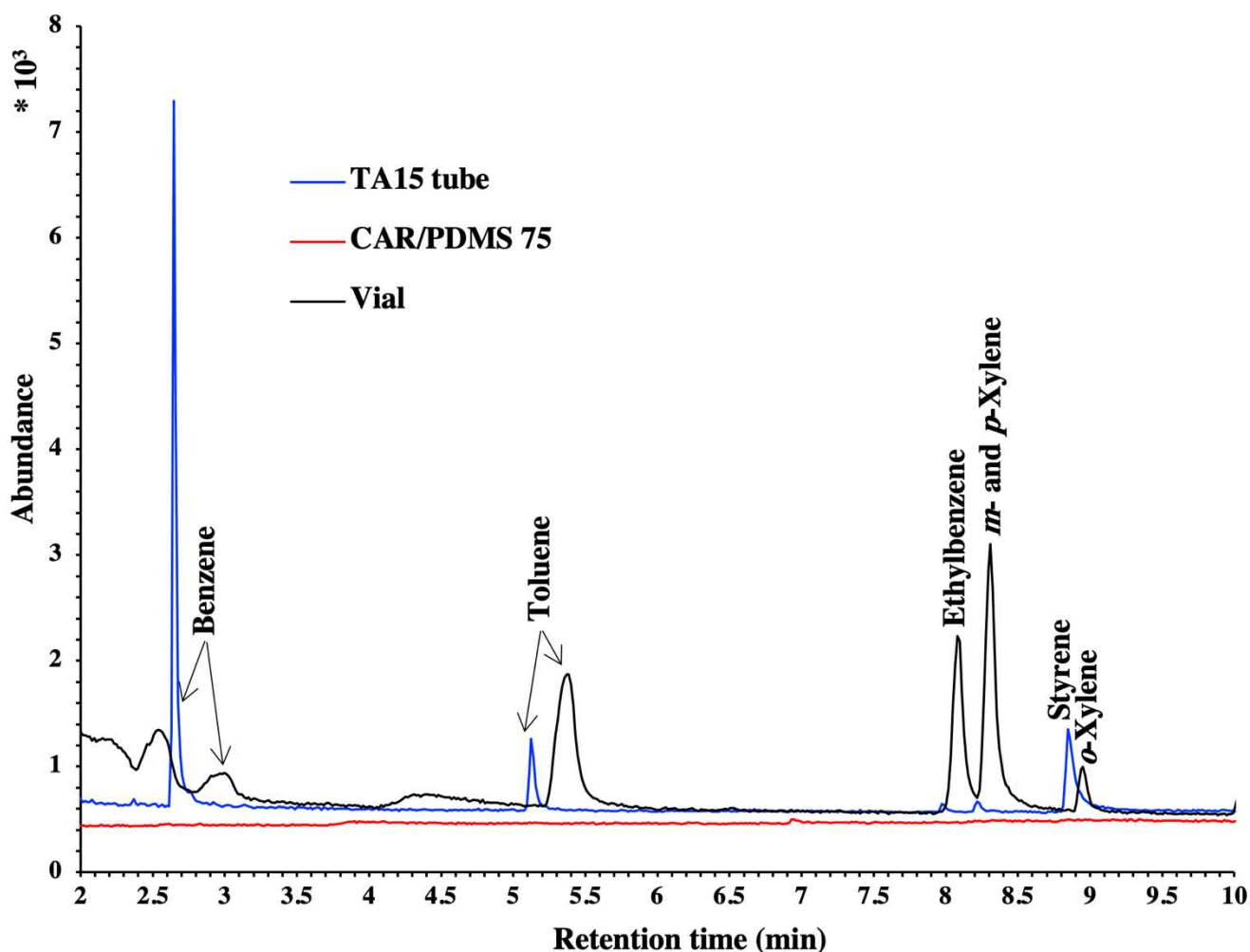


Figure 4.6: Total ion current chromatograms of a blank TA15 tube, a blank of the CAR/PDMS 75 μm SPME fiber and a pure CH_4 -filled vial.

However, when gases are sampled to preconcentrate and screen all their unknown trace compounds without following particular species, GC-MS data is most often acquired in scan mode rather than in SIM mode. New blank TA15 tubes analyzed in scan mode (Fig.4.5 C) only display a small benzene peak surpassing the scan baseline, hence the inherent Tenax-BTEX contaminations reaching high levels in SIM mode, are almost offset. Moreover, the IDL of TA15 tubes for other compounds than BTEX reach satisfying low levels comparable in order of magnitude to or lower than those obtained by SPME, as demonstrated by Fig.4.7 where the IDL of TA15 tubes and of the CAR/PDMS 75 μm SPME fiber were calculated for several compounds identified in NG-A (Table 4.2-4.3) based on the extracted ion chromatograms of the scans of the blank tubes and fiber blanks. Cyclohexane, thiophene and tetrahydrothiophene have lower IDL in TA15 tubes than in SPME while heptane, 3-ethylhexane and octane have an IDL slightly higher yet still of the same order of magnitude compared to SPME. This demonstrates TA15 tubes are highly suitable for the preconcentration of (ultra-) trace amounts of non-BTEX compounds. When targeting (ultra-) trace amounts of BTEX, other adsorbents free of inherent BTEX-contamination should therefore be preferred.

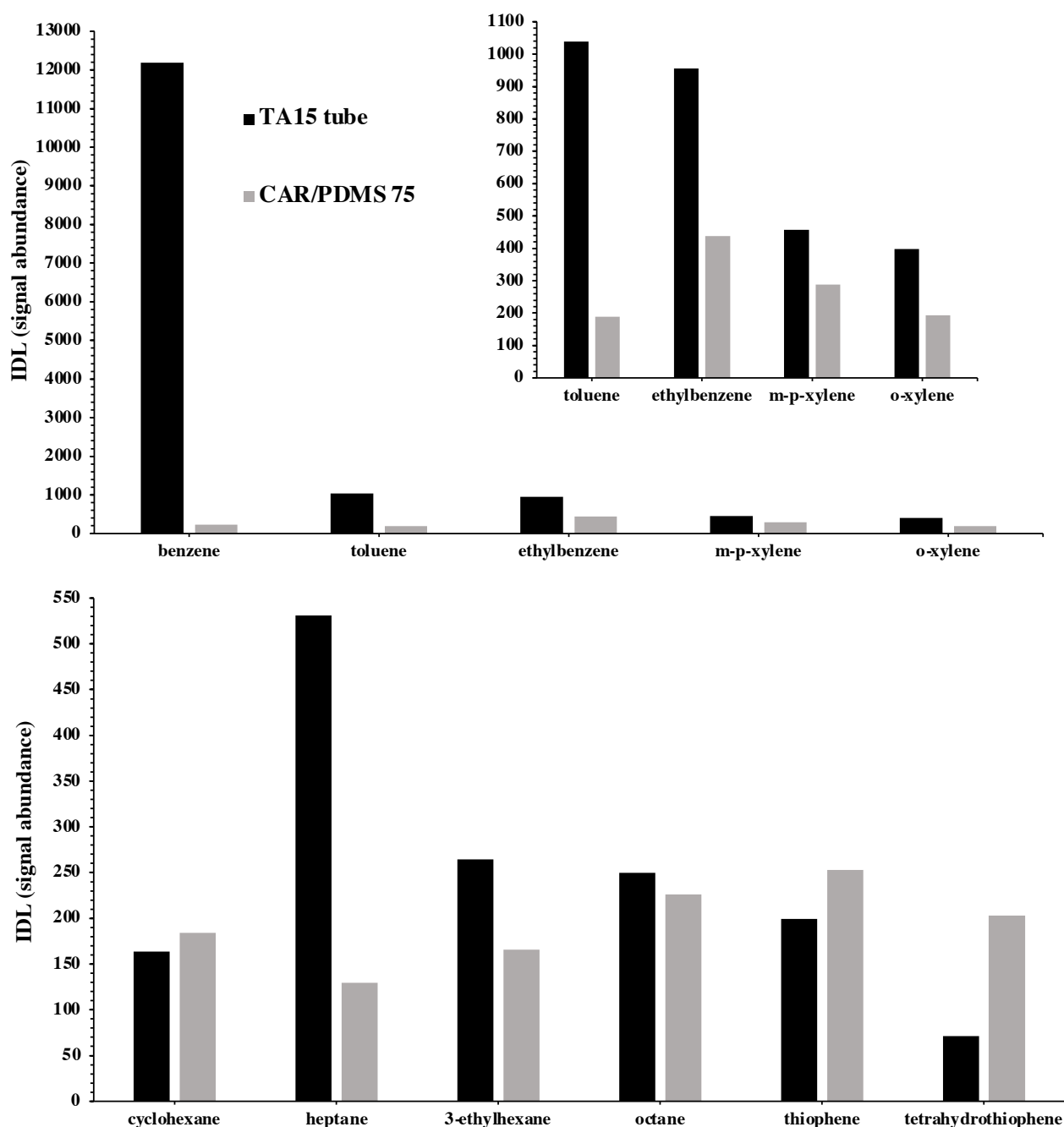


Figure 4.7: Instrument detection limits (peak height signal abundance) of trace compounds determined in the NG-A building grid natural gas sample on TA15 tubes and on the CAR/PDMS 75 μm SPME fiber. Numerical values are available in Table 4.S3.

III.4. A first step towards semi-quantification

The calibration curves built for each BTEX compound and for each injection technique upon the average chromatographic peak area data of 3 replicates at the 6 concentrations (0, 1, 2.5, 5, 7.5, 10 ppm_v) were fitted with a linear regression model (intercept=0) and an F-statistical test at a significance level $\alpha=0.05$ (Table 4.5, Fig.4.S4). The expected positive linear relationship between peak area and concentration for each BTEX compound is verified to be significant for each injection technique by the close-to-one linear determination coefficients R^2 , by the p- (not shown) and significance F-values being $< \alpha = 0.05$ and by the observed F-test values exceeding

the critical F-test value ($F_{1,5}$ at $\alpha = 0.05$ is 6.6079) (Table 4.5). The model fit is nevertheless stronger for SPME and HS injections than for nCx-TD injections. Overall, the significance F-values giving the probability that the analysis of variance model is wrong, are definitely higher for nCx-TD than for other injections (yet still lower than $\alpha = 0.05$ thus enabling to reject the hypothesis that no relationship would exist between nCx-TD obtained peak areas and concentrations). Also, the linear determination coefficients R^2 of each BTEX-calibration curve obtained with the nCx-TD, although relatively high (ranging 0.866 – 0.968), are systematically lower than the R^2 achieved by SPME or HS injections. Further, the F-test values observed for ethylbenzene and xylene isomers with the nCx-TD are only slightly higher than the critical F-value (Table 4.5), indicating a relatively weaker relationship between peak areas and concentrations for nCx-TD injections compared to SPME and HS injections.

What negatively affects the quantitative nCx-TD performance and associated statistics is its low quantitative repeatability as demonstrated by the high relative standard deviations (RSD) obtained (Table 4.S2 and 4.S4).

Firstly, peak resolution experiments on the 10 ppm_v BTEX-CH₄ mixture revealed only 7 on 10 injections occurred successfully and the RSD on the peak areas of the individual BTEX compounds on these n=7 were high: ranging 35% (*m,p*-xylene) to 50% (benzene) (Table 4.S2). Although each TA15 tube has an individual inherent BTEX background contamination level (see section III.3), the contribution of the variability in individual blank BTEX levels to the RSD of BTEX peak areas in the 7 replicates of the 10 ppm_v sampled TA15 tubes is likely negligible: the average peak areas of benzene, toluene, ethylbenzene, *m,p*-xylene and *o*-xylene in the 10 blank TA15 tubes represent respectively only 0.185, 0.007, 0.001, 0.001 and 0.097% of the average peak areas of these compounds in the 7 replicates 10 ppm_v sampled TA15 tubes. Also, in blank TA15 tubes, *o*-xylene has the highest signal and RSD for both peak height (Table 4.4) and peak area (not shown) due to its co-elution with styrene (Tenax TA thermal degradation product), followed by benzene, whereas the highest signals (peak height and area) in 10 ppm_v sampled tubes are recorded for the co-eluting *m*- and *p*-xylenes. Benzene has the lowest signals in those sampled tubes but the highest RSD (Fig.4.3, Table 4.S2). This supports the statement that blank background contamination levels are not a key contributor to the high RSD's observed for sampled TA15 tubes.

Secondly, RSD (n=3) on the nCx-TD BTEX calibration curves range the largest across the 6 concentrations tested: 1 – 62 % against ~ 4 – 35% for SPME and HS (Table 4.S4). The nCx-TD has also the highest RSD's for benzene on all 6 concentrations and the highest RSD's at 5 and 10 ppm_v for all compounds. The reason of this behavior is unclear and can not originate from the Tedlar bag dilution preparations since nCx-TD, SPME and HS samples were taken from the very same bag and RSD's for SPME and HS do not present particular trends at 5 and 10 ppm_v.

Actually, the discussed repeatability issues of the current nCx-TD prototype originate from a too short injection needle (Fig.4.1 point 3) insufficiently penetrating the GC inlet liner, causing the carrier gas to not enter the liner and the column on a repeatable way upon injection. Also, the exact position of the two holes made in each of the upper and bottom adsorbent tube capping septa upon manual sampling and upon thermal desorption was found to influence the injection repeatability of the nCx-TD prototype. Indeed, when upon injection the injection

needle pierces the septum at a location closely adjacent to or overlapping to some extent the hole created during manual sampling, variable proportions carrier gas leaks were observed as a result of septum tearing. When both holes were distinctly away from each other, no carrier gas leak was observed. In spite of these faults, the excellent nCx-TD desorption performance and chromatographic peak resolutions justify the prototype is worth being improved by a lengthened injection needle and by a needle guide to achieve satisfying quantitative repeatabilities.

Notwithstanding the above and the relatively high inherent BTEX contamination levels in new blank TA15 tubes, a simple semi-quantification rule of three based on the BTEX peak areas in the blanks and in the 10 ppm_v BTEX-CH₄ samples (SIM acquisition) indicates blank levels and associated detection thresholds in TA15 tubes can be as low as 0.07 ppb_v for *m*-,*p*-xylene (Table 4.6). As discussed, the thresholds are the highest for benzene (18.52 ppb_v) and *o*-xylene (9.68 ppb_v) owing to the high contamination of those compounds in the blank TA15 tubes (Table 4.4). Table 4.6 also shows the absence of preconcentration in headspace vials, giving detrimental higher detection thresholds.

Table 4.5: Linear regression output (Peak Area = slope a x Concentration) and analysis of variance (F-statistical test) between average peak area of BTEX compounds and concentration, at a significance level $\alpha = 0.05$. The critical F-value $F_{(1,5)}$ at $\alpha = 0.05$ is 6.6079.

	Benzene	Toluene	Ethylbenzene	<i>m,p</i> -Xylene	<i>o</i> -Xylene
nCx-TD					
Slope a	1.3E+07	2.4E+07	1.7E+07	2.4E+07	0.9E+07
R ²	0.954	0.968	0.922	0.878	0.866
Observed F-value	103.1	152.0	59.1	35.9	32.2
Significance F-value	529.5E-06	248.7E-06	1542.0E-06	3901.7E-06	4756.1E-06
SPME					
Slope a	5.8E+07	9.2E+07	4.6E+07	10.5E+07	6.4E+07
R ²	0.994	1.000	0.988	0.982	0.970
Observed F-value	828.4	10207.6	415.9	276.0	163.0
Significance F-value	8.7E-06	0.06E-06	34.1E-06	76.9E-06	216.8E-06
Headspace					
Slope a	0.6E+07	0.8E+07	0.6E+07	1.0E+07	0.4E+07
R ²	0.998	0.999	0.979	0.961	0.937
Observed F-value	2287.1	4406.3	227.6	121.8	74.2
Significance F-value	1.1E-06	0.3E-06	112.5E-06	383.3E-06	997.3E-06

Table 4.6: Semi-quantification (ppb_v) of the BTEX contamination background in new TA15 blank tubes, a blank SPME fiber and 'blank' (pure CH₄) vials based on the BTEX peak areas in 10 ppm_v BTEX-CH₄ samples.

	TA15	CAR/PDMS 75	Vial
Benzene	18.52	0.18	2.62
Toluene	0.67	0.11	7.93
Ethylbenzene	0.10	0.04	6.81
<i>m-p</i> -Xylene	0.07	0.05	5.62
<i>o</i> -Xylene	9.68	0.32	1.40

Lastly, the existence of a relationship between concentration and the chromatographic Gaussian peak resolution R_G between the closely eluting ethylbenzene and *m*- and *p*-xylene isomers was statistically tested (linear regression with intercept and F-test) at a significance level $\alpha = 0.05$ for 5 concentrations (1, 2.5, 5, 7.5, 10 ppm_v) and the three injection techniques handled, taking the average of 3 replicates at each concentration. For SPME and headspace injections, results reveal no significant linear relationship between those variables: the linear determination coefficients R^2 are low (SPME- $R^2=0.018$; HS- $R^2=0.662$), the observed F-test values are lower than the critical F-test value $F_{(1,3)}=10.13$ and the significance F-values are higher than the significance level $\alpha=0.05$ indicating the model is unable to predict the measurements (Table 4.S5 and Fig.4.S5). In contrast, the statistical analysis performed indicates a significant ($R^2=0.852$; observed F-value > critical F-value; significance F-value < $\alpha = 0.05$) yet weak positive linear relationship between concentration and Gaussian peak resolution of nCx-TD-injected ethylbenzene and *m*-,*p*-xylene peaks. Gaussian peak resolutions obtained from the nCx-TD not only are higher than those obtained by SPME and headspace but also improve with the concentrations, once again pointing out the high resolutive power (narrow peaks) of the nCx-TD prototype.

IV. CONCLUSIONS AND PERSPECTIVES

Thermal desorption of purpose-built self-assembled Tenax TA tubes loaded with a synthetic BTEX-CH₄ gas using the new versatile thermodesorber prototype (nCx-TD) has proved to yield much higher chromatographic peak resolutions than thermal desorption of a BTEX-loaded CAR/PDMS 75 μm SPME fiber and than direct BTEX-CH₄ gas injection via a headspace autosampler. Additionally, nCx-TD peak resolutions tend to significantly improve at higher BTEX concentrations (from 1 to 10 ppm_v). The resolutive power of the nCx-TD stems from its fast “plug” injection working mode where furthermore no re-focusing trap is called for. Also, the low adsorbent mass (15 mg) and low sampling volumes (0.5 L_n) required make the whole adsorbent tube sampling operations attractive with regards to economical, practical and environmental considerations. Moreover, the nCx-TD is mountable on the inlet ports of any commercial GC-units and it can be deployed *in situ* on field-portable GC's. To the authors' knowledge, this is the sole thermal desorber device combining all of these qualities and properties. The current nCx-TD prototype version needs however physico-mechanical re-sizing improvements to ensure quantitatively repeatable injections.

Besides, the analysis of a real natural gas sample revealed the future application potential of the self-assembled adsorbent tubes. The Tenax TA tubes allowed to detect thiophene, 2,3-dihydrothiophene, methyloctane isomers, nonane and 1-ethyl-3-methylbenzene while the CAR/PDMS 75 μm SPME fiber did not. Tenax TA is a highly polyvalent adsorbent able to trap a broad range of semi-volatile compounds, and its functionalities could be even further valorized in multibed adsorbent tube configurations for the preconcentration of complex mixtures of trace compounds in gases like biogas and biomethane.

Associated Content

Supplemental Information

Authors Informations

*Corresponding Author : Isabelle Le Hécho • isabelle.lehecho@univ-pau.fr • Université de Pau et des Pays de l'Adour, E2S UPPA, CNRS, IPREM UMR 5254, Technopôle Hélio parc, 2 avenue du Président Angot, 64053 Pau Cedex 09, France

Note

The authors declare no competing financial interests or personal relationships that could have influenced the work reported in this paper.

Acknowledgements

The authors thank *Teréga* (40 Avenue de l'Europe, CS 20 522-64010 PAU Cedex, France) for having financed this study. *nCx Instrumentation* (ZAE Porte du Béarn, 64330 Garlin, France) is also acknowledge for the loan of the thermodesorber prototype.

V. SUPPLEMENTAL INFORMATION CHAPTER 4

Table 4.S1: nCx-TD operational parameters

Parameter	Parameter meaning	Minimal operational value	Maximal operational value
Safe temperature	Start temperature (°C) of the thermal desorption cycle	35	40
Temperature	Target final desorption setpoint temperature (°C)	100	400
Stabilization time	Time interval (s) during which TEMP is held before injection starts	5	60
Pressure	Carrier gas pressure (mbar) at start of injection	500	1600
Injection time	Time interval (s) during which the carrier gas flows through the tube and is injected in the GC	5	60

Table 4.S2: Chromatographic peak areas of 10 ppm_v benzene, toluene, ethylbenzene, m-,p-xylene and o-xylene and chromatographic peak resolutions between toluene and benzene, ethylbenzene and toluene, m-,p-xylene and ethylbenzene, o-xylene and m-,p-xylene acquired at 10 ppm_v from the three injection systems studied (nCx-TD, SPME and Headspace). Std dev: standard deviation. RSD%: relative standard deviation = 100 · Std dev / average. n = number of injections.

	Peak Area			Peak Resolution R			Gaussian Peak Resolution R _G			Separation factor α		
	Average	Std dev	RSD %	Average	Std dev	RSD %	Average	Std dev	RSD %	Average	Std dev	RSD %
nCx-TD (n=7 successful injections on 10 performed)												
Benzene	163.5E+06	81.7E+06	50.0									
Toluene	464.7E+06	193.8E+06	41.7	6.6	1337.4E-03	20.3	31.8	9.8	30.7	2.8	6.2E-03	224.1E-03
Ethylbenzene	615.0E+06	222.2E+06	36.1	8.0	975.9E-03	12.1	38.3	5.9	15.4	1.7	1.5E-03	88.2E-03
m-, p-Xylene	1088.9E+06	386.4E+06	35.5	0.7	270.8E-03	37.0	2.9	0.6	19.7	1.04	0.6E-03	62.0E-03
o-Xylene	528.8E+06	217.4E+06	41.1	1.6	621.5E-03	39.8	6.8	2.6	37.8	1.1	0.7E-03	66.0E-03
SPME (n=3)												
Benzene	306.9E+06	40.5E+06	13.2									
Toluene	413.4E+06	52.0E+06	12.6	2.0	9.2E-03	0.5	15.2	5.6	36.6	2.7	9.3E-03	340.8E-03
Ethylbenzene	245.8E+06	43.3E+06	17.6	4.1	56.9E-03	1.4	19.4	5.7	29.1	1.7	1.8E-03	101.4E-03
m-, p-Xylene	551.6E+06	79.0E+06	14.3	-	-	-	1.7	0.5	28.0	1.04	0.1E-03	10.0E-03
o-Xylene	230.7E+06	36.5E+06	15.8	-	-	-	4.2	1.6	38.8	1.1	0.1E-03	11.6E-03
Headspace (n=14)												
Benzene	93.2E+06	1.3E+06	1.4									
Toluene	150.0E+06	3.5E+06	2.3	2.3	123.5E-03	5.4	7.8	58.9E-03	0.8	2.9	19.7E-03	675.2E-03
Ethylbenzene	159.7E+06	4.9E+06	3.0	3.9	117.1E-03	3.0	14.1	113.5E-03	0.8	1.8	1.7E-03	96.9E-03
m-, p-Xylene	294.4E+06	8.3E+06	2.8	0.6	32.9E-03	5.3	1.9	18.2E-03	1.0	1.04	0.2E-03	17.9E-03
o-Xylene	136.2E+06	4.3E+06	3.1	1.5	94.3E-03	6.4	5.7	69.5E-03	1.2	1.1	0.1E-03	11.3E-03

Table 4.S3: Instrument detection limits (IDL = 3 Std dev) (peak height signal abundance) of trace compounds determined in the NG-A building grid natural gas sample on TA15 tubes and on the CAR/PDMS 75 µm SPME fiber (Fig.4.7 in paper).

Compound	TA15 tubes (n=10)		CAR/PDMS 75 µm SPME (n=10)	
	Std dev	IDL	Std dev	IDL
Benzene	4063.91	12191.74	78.82	236.47
Toluene	346.30	1038.91	63.18	189.54
Ethylbenzene	318.40	955.20	145.99	437.96
<i>m,p</i> -Xylene	152.52	457.56	96.14	288.43
<i>o</i> -Xylene	132.91	398.73	64.40	193.21
Cyclohexane	54.48	163.45	61.33	183.98
Heptane	177.08	531.24	43.21	129.63
3-Ethylhexane	88.12	264.36	55.27	165.81
Octane	83.19	249.57	75.37	226.12
Thiophene	66.38	199.15	84.35	253.06
Tetrahydrothiophene	23.72	71.16	67.62	202.87

Table 4.S4: Relative standard deviations (% ; n=3) of the peak areas obtained for each BTEX compound at the 6 concentrations tested for each injection technique.

Concentration ppmv	Benzene	Toluene	Ethylbenzene	<i>m,p</i> -Xylene	<i>o</i> -Xylene
	nCx-TD				
0	24.6	19.7	45.5	45.3	1.1
1	22.9	10.2	8.3	9.1	9.6
2.5	17.5	12.9	7.8	6.6	7.7
5	34.2	32.3	31.5	31.0	30.7
7.5	12.3	13.0	1.1	4.0	13.2
10	62.1	51.9	45.3	43.3	43.6
	SPME				
0	17.3	17.3	23.6	17.8	19.1
1	20.2	24.7	21.3	29.0	34.1
2.5	13.8	11.8	4.1	8.7	10.1
5	6.9	13.6	18.1	19.8	19.5
7.5	11.1	20.6	24.4	27.6	27.2
10	12.6	16.6	17.2	17.6	16.3
	Headspace				
0	8.1	5.2	22.6	22.9	35.6
1	12.3	17.4	19.7	18.8	20.2
2.5	5.7	9.5	12.2	12.8	12.6
5	4.2	8.4	12.5	12.9	13.3
7.5	12.9	11.4	9.9	9.2	9.3
10	18.1	21.0	24.7	24.7	25.1

Table 4.S5: Linear regression output and analysis of variance (F-statistical test) between concentration (1, 2.5, 5, 7.5, 10 ppm_v) and average Gaussian peak resolution between ethylbenzene and m-, p-xylene, at a significance level $\alpha = 0.05$. The critical F-value $F(1,3)=10.13$ at $\alpha = 0.05$.

	nCx-TD	SPME	Headspace
Slope a	0.049	-0.008	0.017
R ²	0.852	0.018	0.662
Observed F-value	17.278	0.054	5.863
Significance F-value	0.025	0.832	0.094

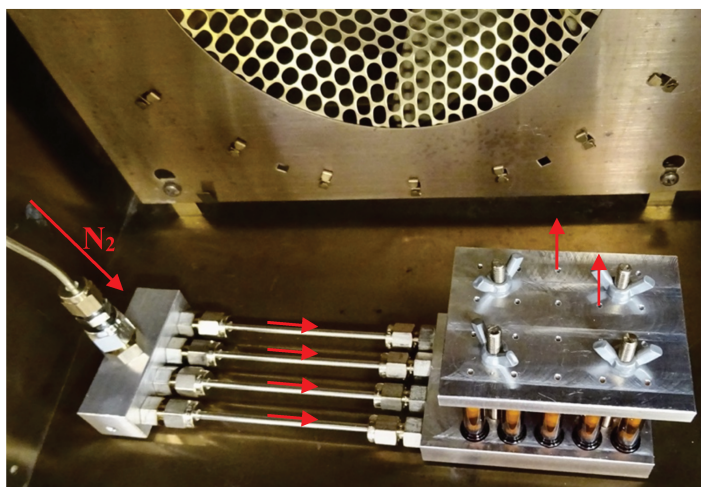


Figure 4.S1: Purpose-built 20-positions adsorbent tube conditioning support.

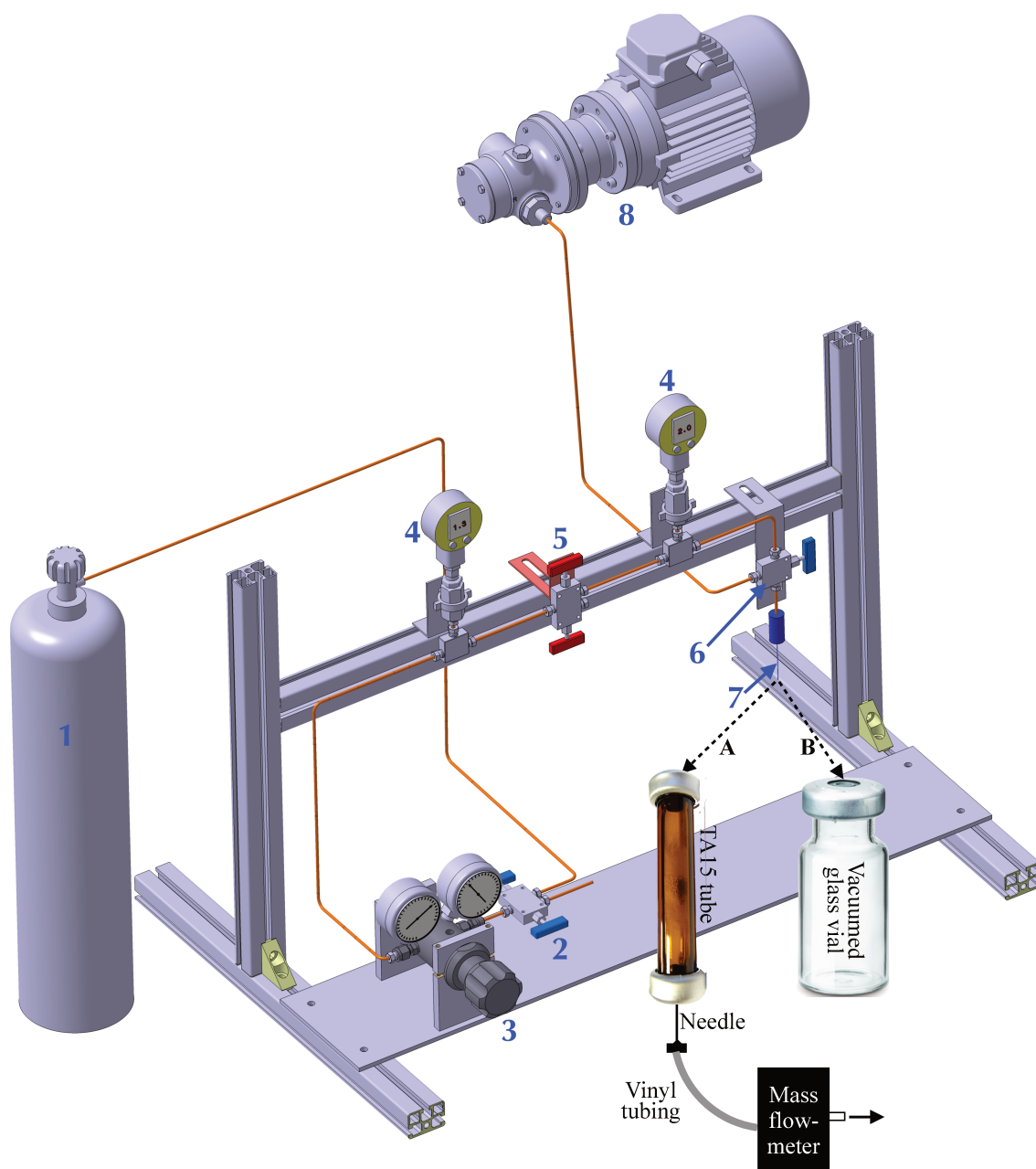


Figure 4.S2: Gas pressure regulating system for the sampling of pressurized gases. 1=pressurized synthetic gas bottle, 2>manual high pressure valve, 3=manometer-gas pressure regulator, 4=manometer, 5>manual micrometric valve, 6>manual valve, 7=gas needle "n", 8=vacuum pump. A=sampling through an adsorbent tube. B=sampling in a vacuumed glass vial.

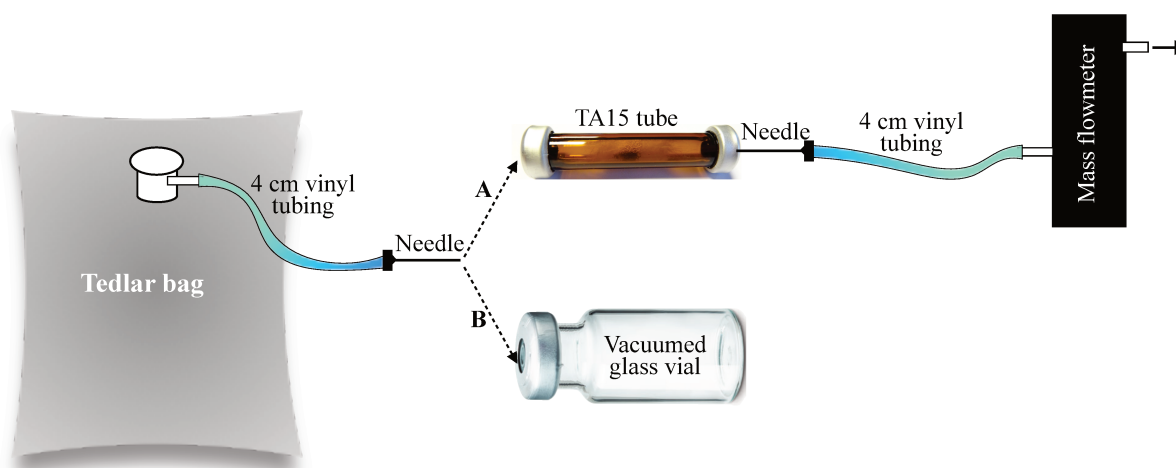


Figure 4.S3: Sampling of gas concentrations C_i from a Tedlar bag (A) through an adsorbent tube or (B) in a vacuumed glass vial.

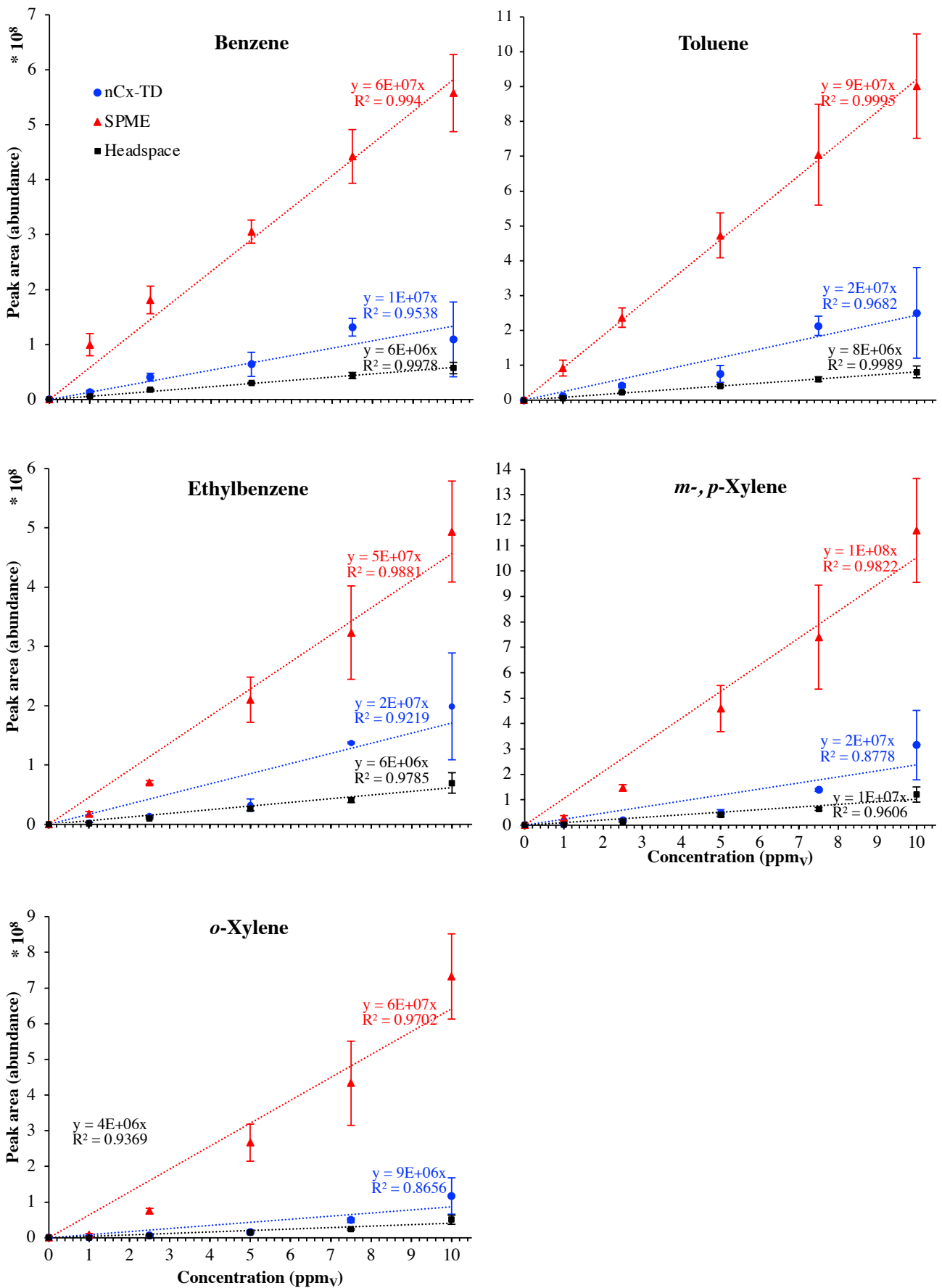


Figure 4.S4: Calibration curves (average chromatographic peak area) for benzene, toluene, ethylbenzene, m- and p-xylene and o-xylene acquired for six concentrations (0, 1, 2.5, 5, 7.5, 10 ppm_v) by different injection techniques (nCx-TD, SPME and headspace). Vertical bars at each concentration indicate the standard deviation (3 replicates at each concentration).

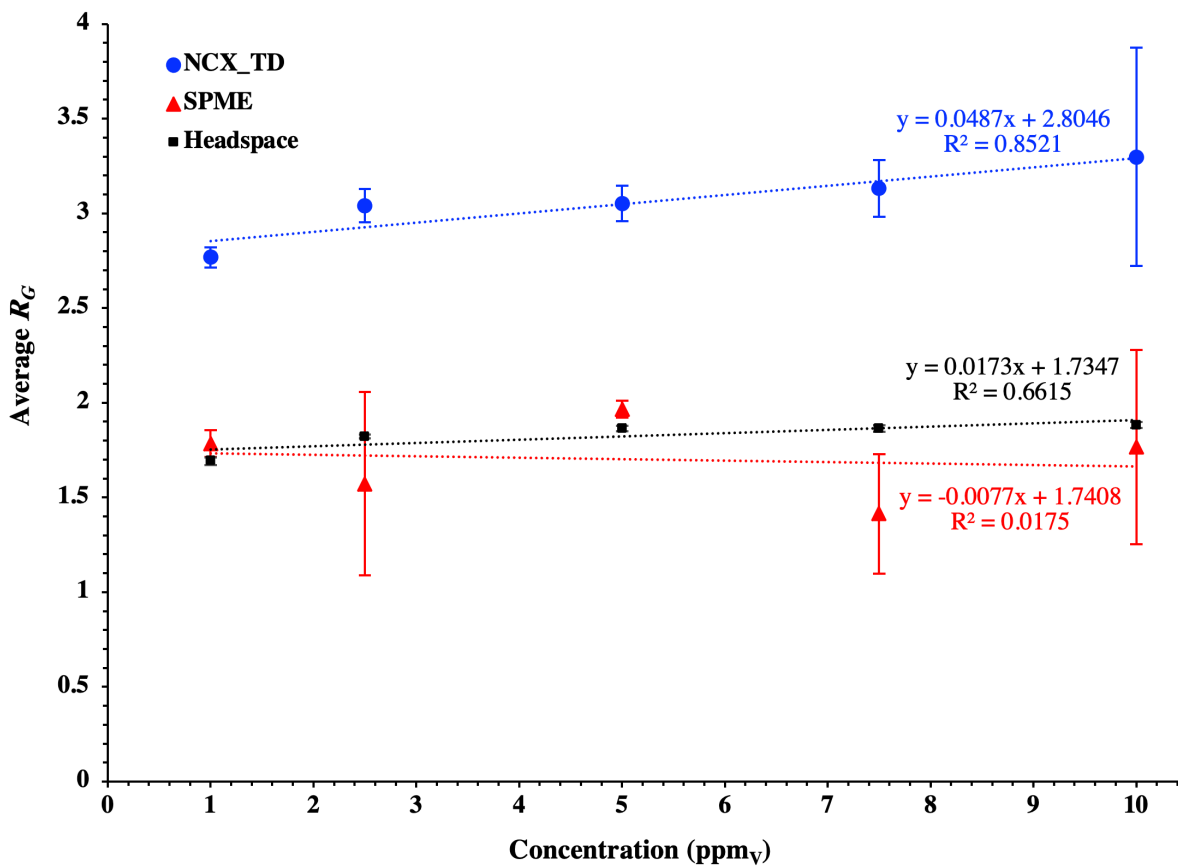


Figure 4.S5: Least squares linear regression model fitted on the average Gaussian peak resolution R_G between ethylbenzene and *m*-, *p*-xylene acquired for six concentrations (0, 1, 2.5, 5, 7.5, 10 ppm_v) by different injection techniques (nCx-TD, SPME and headspace). Vertical bars at each concentration indicate the standard deviation (3 replicates at each concentration).

VI. REFERENCES CHAPTER 4

- [1] L.K. Wang, J.R. Taricska, Y.-T. Hung, K.H. Li, Chapter 1 - Air Quality and Pollution Control, in: L.K. Wang, N.C. Pereira, Y.-T. Hung (Eds.), *Air Pollution Control Engineering*, Humana Press, Totowa, NJ, 2004: pp. 1–57. https://doi.org/10.1007/978-1-59259-778-9_1.
- [2] US EPA, Evolution of the Clean Air Act, US EPA. (2015). <https://www.epa.gov/clean-air-act-overview/evolution-clean-air-act> (accessed February 9, 2021).
- [3] US EPA, Monitoring and Air Quality Trends Report: 1974. EPA-450/1-76-001, (1976). https://www.epa.gov/sites/production/files/2017-11/documents/trends_report_1974.pdf (accessed February 9, 2021).
- [4] E. Woolfenden, Monitoring VOCs in Air Using Sorbent Tubes Followed by Thermal Desorption-Capillary GC Analysis: Summary of Data and Practical Guidelines, *Journal of the Air & Waste Management Association*. 47 (1997) 20–36. <https://doi.org/10.1080/10473289.1997.10464411>.
- [5] J.F. Pankow, W. Luo, L.M. Isabelle, D.A. Bender, R.J. Baker, Determination of a Wide Range of Volatile Organic Compounds in Ambient Air Using Multisorbent Adsorption/Thermal Desorption and Gas Chromatography/Mass Spectrometry, *Anal. Chem.* 70 (1998) 5213–5221. <https://doi.org/10.1021/ac980481t>.
- [6] V. Camel, M. Caude, Review: Trace Enrichment Methods for the Determination of Organic Pollutants in Ambient Air, *Journal of Chromatography A*. 710 (1995) 3–19. [https://doi.org/10.1016/0021-9673\(95\)00080-7](https://doi.org/10.1016/0021-9673(95)00080-7).
- [7] F. Bruner, G. Bertoni, G. Crescentini, Critical Evaluation of Sampling and Gas Chromatographic Analysis of Halocarbons and Other Organic Air Pollutants, *Journal of Chromatography A*. 167 (1978) 399–407. [https://doi.org/10.1016/S0021-9673\(00\)91172-5](https://doi.org/10.1016/S0021-9673(00)91172-5).
- [8] K.B. Andersen, M.J. Hansen, A. Feilberg, Minimisation of Artefact Formation of Dimethyl Disulphide During Sampling and Analysis of Methanethiol in Air Using Solid Sorbent Materials, *Journal of Chromatography A*. 1245 (2012) 24–31. <https://doi.org/10.1016/j.chroma.2012.05.020>.
- [9] E. Baltussen, F. David, P. Sandra, C. Cramers, On the Performance and Inertness of Different Materials Used for the Enrichment of Sulfur Compounds from Air and Gaseous Samples, *Journal of Chromatography A*. 864 (1999) 345–350. [https://doi.org/10.1016/S0021-9673\(99\)01066-3](https://doi.org/10.1016/S0021-9673(99)01066-3).
- [10] M.A.H. Khan, M.E. Whelan, R.C. Rhew, Analysis of Low Concentration Reduced Sulfur Compounds (RSCs) in Air: Storage Issues and Measurement by Gas Chromatography with Sulfur Chemiluminescence Detection, *Talanta*. 88 (2012) 581–586. <https://doi.org/10.1016/j.talanta.2011.11.038>.
- [11] A. Bzezinska, J.V. Loon, D. Williams, K. Oguma, K. Fuwa, I.H. Haraguchi, A Study of the Determination of Dimethylmercury and Methylmercury Chloride in Air, *Spectrochimica Acta Part B: Atomic Spectroscopy*. 38 (1983) 1339–1346. [https://doi.org/10.1016/0584-8547\(83\)80078-0](https://doi.org/10.1016/0584-8547(83)80078-0).

- [12] K. Haas, J. Feldmann, Sampling of Trace Volatile Metal(loid) Compounds in Ambient Air Using Polymer Bags: A Convenient Method, *Anal. Chem.* 72 (2000) 4205–4211. <https://doi.org/10.1021/ac000313c>.
- [13] C. Nerin, B. Pons, M. Martinez, J. Cacho, Behaviour of Several Solid Adsorbents for Sampling Tetraalkyllead Compounds in Air, *Mikrochimica Acta.* 112 (1994) 179–188.
- [14] A. Attari, S. Chao, Sampling and Analysis of Natural Gas Trace Constituents, in: Institute of Gas Technology, Chicago, Illinois 60616, USA, Isfahan, Iran, 1993.
- [15] T. Assmuth, K. Kalevi, Concentrations and Toxicological Significance of Trace Organic Compounds in Municipal Solid Waste Landfill Gas, *Chemosphere.* 24 (1992) 1207–1216. [https://doi.org/10.1016/0045-6535\(92\)90047-U](https://doi.org/10.1016/0045-6535(92)90047-U).
- [16] A.S. Brown, A.M.H. Van Der Veen, K. Arrhenius, A. Murugan, L.P. Culleton, P.R. Ziel, J. Li, Sampling of Gaseous Sulfur-Containing Compounds at Low Concentrations with a Review of Best-Practice Methods for Biogas and Natural Gas Applications, *TrAC Trends in Analytical Chemistry.* 64 (2015) 42–52. <https://doi.org/10.1016/j.trac.2014.08.012>.
- [17] M. Cachia, B. Bouyssière, H. Carrier, H. Garraud, G. Caumette, I. Le Hécho, Development of a High-Pressure Bubbling Sampler for Trace Element Quantification in Natural Gas, *Energy & Fuels.* 31 (2017) 4294–4300. <https://doi.org/10.1021/acs.energyfuels.6b03059>.
- [18] W. Duoyi, D. Meizhou, L. Yinghan, L. Yawei, L. Xingyun, L. Renqi, Discovery of the Metal Trace Elements in Natural Gas and Its Ecological Environment Significance, *Earth Science Frontiers.* 15 (2008) 124–132. [https://doi.org/10.1016/S1872-5791\(09\)60012-9](https://doi.org/10.1016/S1872-5791(09)60012-9).
- [19] M.F. Ezzeldin, Z. Gajdosechova, M.B. Masod, T. Zaki, J. Feldmann, E.M. Krupp, Mercury Speciation and Distribution in an Egyptian Natural Gas Processing Plant, *Energy Fuels.* 30 (2016) 10236–10243. <https://doi.org/10.1021/acs.energyfuels.6b02035>.
- [20] E.M. Krupp, C. Johnson, C. Rechsteiner, M. Moir, D. Leong, J. Feldmann, Investigation into the Determination of Trimethylarsine in Natural Gas and Its Partitioning into Gas and Condensate Phases Using (cryotrapping)/Gas Chromatography Coupled to Inductively Coupled Plasma Mass Spectrometry and Liquid/Solid Sorption Techniques, *Spectrochimica Acta Part B: Atomic Spectroscopy.* 62 (2007) 970–977. <https://doi.org/10.1016/j.sab.2007.07.009>.
- [21] M.K. Uroic, E.M. Krupp, C. Johnson, J. Feldmann, Chemotrapping-Atomic Fluorescence Spectrometric Method as a Field Method for Volatile Arsenic in Natural Gas, *Journal of Environmental Monitoring.* 11 (2009) 2222. <https://doi.org/10.1039/b913322d>.
- [22] M. Cachia, H. Carrier, B. Bouyssièrre, P. Le Coustumer, P. Chiquet, G. Caumette, I. Le Hecho, Solid Particles in Natural Gas from a Transportation Network: A Chemical Composition Study, *Energies.* 12 (2019) 3866. <https://doi.org/10.3390/en12203866>.
- [23] M. Harper, Review. Sorbent Trapping of Volatile Organic Compounds from Air, *Journal of Chromatography A.* 885 (2000) 129–151. [https://doi.org/10.1016/S0021-9673\(00\)00363-0](https://doi.org/10.1016/S0021-9673(00)00363-0).
- [24] K. Arrhenius, A.S. Brown, A.M.H. van der Veen, Suitability of Different Containers for the Sampling and Storage of Biogas and Biomethane for the Determination of the Trace-Level Impurities – A Review, *Analytica Chimica Acta.* 902 (2016) 22–32.

<https://doi.org/10.1016/j.aca.2015.10.039>.

[25] M. Toledo, J.M. Guillot, J.A. Siles, M.A. Martín, Permeability and Adsorption Effects for Volatile Sulphur Compounds in Nalophan Sampling Bags: Stability Influenced by Storage Time, *Biosystems Engineering*. 188 (2019) 217–228.

<https://doi.org/10.1016/j.biosystemseng.2019.10.023>.

[26] L.J. McGarvey, C.V. Shorten, The Effects of Adsorption on the Reusability of Tedlar® Air Sampling Bags, *AIHAJ - American Industrial Hygiene Association*. 61 (2000) 375–380.

<https://doi.org/10.1080/15298660008984546>.

[27] Y.-H. Kim, K.-H. Kim, S.-H. Jo, E.-C. Jeon, J.R. Sohn, D.B. Parker, Comparison of Storage Stability of Odorous VOCs in Polyester Aluminum and Polyvinyl Fluoride Tedlar® Bags, *Analytica Chimica Acta*. 712 (2012) 162–167. <https://doi.org/10.1016/j.aca.2011.11.014>.

[28] C.-C. Hsieh, S.-H. Horng, P.-N. Liao, Stability of Trace-Level Volatile Organic Compounds Stored in Canisters and Tedlar bags, *Aerosol and Air Quality Research*. 3 (2003) 17–28.

[29] M. Ajhar, B. Wens, K.H. Stollenwerk, G. Spalding, S. Yüce, T. Melin, Suitability of Tedlar® Gas Sampling Bags for Siloxane Quantification in Landfill Gas, *Talanta*. 82 (2010) 92–98.

<https://doi.org/10.1016/j.talanta.2010.04.001>.

[30] J.-H. Ahn, A. Deep, K.-H. Kim, The Storage Stability of Biogenic Volatile Organic Compounds (BVOCs) in Polyester Aluminum Bags, *Atmospheric Environment*. 141 (2016) 430–434. <https://doi.org/10.1016/j.atmosenv.2016.07.019>.

[31] D.A. Brymer, L.D. Ogle, C.J. Jones, D.L. Lewis, Viability of Using SUMMA Polished Canisters for the Collection and Storage of Parts per Billion by Volume Level Volatile Organics, *Environ. Sci. Technol.* 30 (1996) 188–195. <https://doi.org/10.1021/es950240s>.

[32] R.W. Coutant, Theoretical Evaluation of Stability of Volatile Organic Chemicals and Polar Volatile Organic Chemicals in Canisters. Final Report to U.S. EPA, Contract No. 68-D0-0007, Work Assignment No. 45, Subtask 2, Battelle, Columbus, Ohio., United States, 1992. <https://www.osti.gov/servlets/purl/5410047>.

[33] T.J. Kelly, M.W. Holdren, Applicability of Canisters for Sample Storage in the Determination of Hazardous Air Pollutants, *Atmospheric Environment*. 29 (1995) 2595–2608. [https://doi.org/10.1016/1352-2310\(95\)00192-2](https://doi.org/10.1016/1352-2310(95)00192-2).

[34] M. Schweigkofler, R. Niessner, Determination of Siloxanes and VOC in Landfill Gas and Sewage Gas by Canister Sampling and GC-MS/AES Analysis, *Environmental Science & Technology*. 33 (1999) 3680–3685. <https://doi.org/10.1021/es9902569>.

[35] M. Enrico, A. Mere, H. Zhou, H. Carrier, E. Tessier, B. Bouyssiére, Experimental Tests of Natural Gas Samplers Prior to Mercury Concentration Analysis, *Energy Fuels*. (2019). <https://doi.org/10.1021/acs.energyfuels.9b03540>.

[36] S. Mariné, M. Pedrouzo, R.M. Marcé, I. Fonseca, F. Borrull, Comparison Between Sampling and Analytical Methods in Characterization of Pollutants in Biogas, *Talanta*. 100 (2012) 145–152. <https://doi.org/10.1016/j.talanta.2012.07.074>.

[37] K. Arrhenius, H. Yaghooby, L. Rosell, O. Büker, L. Culleton, S. Bartlett, A. Murugan, P. Brewer, J. Li, A.M.H. van der Veen, I. Krom, F. Lestremau, J. Beranek, Suitability of Vessels and Adsorbents for the Short-Term Storage of Biogas/Biomethane for the Determination of

- Impurities – Siloxanes, Sulfur Compounds, Halogenated Hydrocarbons, BTEX, Biomass and Bioenergy. 105 (2017) 127–135. <https://doi.org/10.1016/j.biombioe.2017.06.025>.
- [38] E. Woolfenden, Sorbent-Based Sampling Methods for Volatile and Semi-Volatile Organic Compounds in Air. Part 2. Sorbent Selection and Other Aspects of Optimizing Air Monitoring Methods, *Journal of Chromatography A*. 1217 (2010) 2685–2694. <https://doi.org/10.1016/j.chroma.2010.01.015>.
- [39] E. Gallego, F.J. Roca, J.F. Perales, X. Guardino, Comparative Study of the Adsorption Performance of a Multi-Sorbent Bed (Carbotrap, Carbopack X, Carboxen 569) and a Tenax TA Adsorbent Tube for the Analysis of Volatile Organic Compounds (VOCs), *Talanta*. 81 (2010) 916–924. <https://doi.org/10.1016/j.talanta.2010.01.037>.
- [40] R.R. Arnts, Evaluation of Adsorbent Sampling Tube Materials and Tenax-TA for Analysis of Volatile Biogenic Organic Compounds, *Atmospheric Environment*. 44 (2010) 1579–1584. <https://doi.org/10.1016/j.atmosenv.2010.01.004>.
- [41] US EPA, Compendium of Methods for the Determination of Toxic Organic Compounds in Ambient Air. Second Edition. Compendium Method TO-17: Determination of Volatile Organic Compounds in Ambient Air Using Active Sampling Onto Sorbent Tubes (EPA/625/R-96/010b), (1999). <https://www3.epa.gov/ttnamti1/files/ambient/airtox/to-17r.pdf> (accessed April 23, 2020).
- [42] S. Tumbiolo, J.-F. Gal, P.-C. Maria, O. Zerbinati, SPME Sampling of BTEX Before GC/MS Analysis: Examples of Outdoor and Indoor Air Quality Measurements in Public and Private Sites, *Annali Di Chimica*. 95 (2005) 757–766. <https://doi.org/10.1002/adic.200590089>.
- [43] E. Davoli, M.L. Gangai, L. Morselli, D. Tonelli, Characterisation of Odorants Emissions from Landfills by SPME and GC/MS, *Chemosphere*. 51 (2003) 357–368. [https://doi.org/10.1016/S0045-6535\(02\)00845-7](https://doi.org/10.1016/S0045-6535(02)00845-7).
- [44] N. Baimatova, B. Kenessov, J.A. Koziel, L. Carlsen, M. Bektassov, O.P. Demyanenko, Simple and Accurate Quantification of BTEX in Ambient Air by SPME and GC-MS, *Talanta*. 154 (2016) 46–52. <https://doi.org/10.1016/j.talanta.2016.03.050>.
- [45] J. Namieśnik, B. Zygmunt, A. Jastrzębska, Application of Solid-Phase Microextraction for Determination of Organic Vapours in Gaseous Matrices, *Journal of Chromatography A*. 885 (2000) 405–418. [https://doi.org/10.1016/S0021-9673\(99\)01157-7](https://doi.org/10.1016/S0021-9673(99)01157-7).
- [46] E. Woolfenden, Sorbent-Based Sampling Methods for Volatile and Semi-Volatile Organic Compounds in Air: Part 1: Sorbent-Based Air Monitoring Options, *Journal of Chromatography A*. 1217 (2010) 2674–2684. <https://doi.org/10.1016/j.chroma.2009.12.042>.
- [47] R.W. Bishop, R.J. Valis, A Laboratory Evaluation of Sorbent Tubes for Use with a Thermal Desorption Gas Chromatography-Mass Selective Detection Technique, *Journal of Chromatographic Science*. 28 (1990) 589–593. <https://doi.org/10.1093/chromsci/28.11.589>.
- [48] F. Hilaire, E. Basset, R. Bayard, M. Gallardo, D. Thiebaut, J. Vial, Comprehensive Two-Dimensional Gas Chromatography for Biogas and Biomethane Analysis, *Journal of Chromatography A*. 1524 (2017) 222–232. <https://doi.org/10.1016/j.chroma.2017.09.071>.
- [49] R. Sheu, A. Marcotte, P. Khare, S. Charan, J.C. Ditto, D.R. Gentner, Advances in Offline Approaches for Chemically Speciated Measurements of Trace Gas-Phase Organic Compounds

- Via Adsorbent Tubes in an Integrated Sampling-to-Analysis System, *Journal of Chromatography A*. 1575 (2018) 80–90. <https://doi.org/10.1016/j.chroma.2018.09.014>.
- [50] N. Ramírez, A. Cuadras, E. Rovira, F. Borrull, R.M. Marcé, Comparative Study of Solvent Extraction and Thermal Desorption Methods for Determining a Wide Range of Volatile Organic Compounds in Ambient Air, *Talanta*. 82 (2010) 719–727. <https://doi.org/10.1016/j.talanta.2010.05.038>.
- [51] M.R. Allen, A. Braithwaite, C.C. Hills, Trace Organic Compounds in Landfill Gas at Seven U.K. Waste Disposal Sites, *Environmental Science & Technology*. 31 (1997) 1054–1061. <https://doi.org/10.1021/es9605634>.
- [52] J. Brown, B. Shirey, A Tool for Selecting an Adsorbent for Thermal Desorption Applications. Technical Report, (2001). https://www.sigmaaldrich.com/content/dam/sigmaaldrich/docs/Supelco/General_Information/t402025.pdf (accessed April 23, 2020).
- [53] S. Faramawy, T. Zaki, A.A.-E. Sakr, Natural Gas Origin, Composition, and Processing: A Review, *Journal of Natural Gas Science and Engineering*. 34 (2016) 34–54. <https://doi.org/10.1016/j.jngse.2016.06.030>.
- [54] A.L. Bolden, C.F. Kwiatkowski, T. Colborn, New Look at BTEX: Are Ambient Levels a Problem?, *Environ. Sci. Technol.* 49 (2015) 5261–5276. <https://doi.org/10.1021/es505316f>.
- [55] A.N. Baghani, A. Sorooshian, M. Heydari, R. Sheikhi, S. Golbaz, Q. Ashournejad, M. Kermani, F. Golkhorshidi, A. Barkhordari, A.J. Jafari, M. Delikhoon, A. Shahsavani, A Case Study of BTEX Characteristics and Health Effects by Major Point Sources of Pollution During Winter in Iran, *Environmental Pollution*. 247 (2019) 607–617. <https://doi.org/10.1016/j.envpol.2019.01.070>.
- [56] E. Durmusoglu, F. Taspinar, A. Karademir, Health Risk Assessment of BTEX Emissions in the Landfill Environment, *Journal of Hazardous Materials*. 176 (2010) 870–877. <https://doi.org/10.1016/j.jhazmat.2009.11.117>.
- [57] S. Tumbiolo, J.-F. Gal, P.-C. Maria, O. Zerbinati, Determination of Benzene, Toluene, Ethylbenzene and Xylenes in Air by Solid Phase Micro-Extraction/Gas Chromatography/Mass Spectrometry, *Analytical and Bioanalytical Chemistry*. 380 (2004) 824–830. <https://doi.org/10.1007/s00216-004-2837-1>.
- [58] F. Tassi, F. Capecciacci, A. Bucciatti, O. Vaselli, Sampling and Analytical Procedures for the Determination of VOCs Released into Air from Natural and Anthropogenic Sources: A Comparison Between SPME (Solid Phase Micro Extraction) and ST (Solid Trap) Methods, *Applied Geochemistry*. 27 (2012) 115–123. <https://doi.org/10.1016/j.apgeochem.2011.09.023>.
- [59] L.S. Ettre, Nomenclature for Chromatography (IUPAC Recommendations 1993), *Pure and Applied Chemistry*. 65 (1993) 819–872. <https://doi.org/10.1351/pac199365040819>.
- [60] B. Kenessov, J.A. Koziel, N. Baimatova, O.P. Demyanenko, M. Derbissalin, Optimization of Time-Weighted Average Air Sampling by Solid-Phase Microextraction Fibers Using Finite Element Analysis Software, *Molecules*. 23 (2018). <https://doi.org/10.3390/molecules23112736>.
- [61] C.L. Arthur, Janusz. Pawliszyn, Solid Phase Microextraction with Thermal Desorption

Using Fused Silica Optical Fibers, *Anal. Chem.* 62 (1990) 2145–2148.

<https://doi.org/10.1021/ac00218a019>.

[62] A. Narros, M.I. Del Peso, G. Mele, M. Vinot, E. Fernández, M.E. Rodriguez, Determination of Siloxanes in Landfill Gas by Adsorption on Tenax Tubes and TD-GC-MS, in: CISA Publisher, Italy, S. Margherita di Pula, Cagliari, Italy, 2009.

[63] A.-L. Sunesson, C.-A. Nilsson, B. Andersson, Evaluation of Adsorbents for Sampling and Quantitative Analysis of Microbial Volatiles Using Thermal Desorption-Gas Chromatography, *Journal of Chromatography A*. 699 (1995) 203–214. [https://doi.org/10.1016/0021-9673\(95\)00025-I](https://doi.org/10.1016/0021-9673(95)00025-I).

[64] A. Attari, S. Chao, Characterization and Measurement of Natural Gas Trace Constituents. AICHE Spring National Meeting, Houston, TX, (1993).

[65] D. Papurello, S. Silvestri, L. Tomasi, I. Belcari, F. Biasioli, M. Santarelli, Natural Gas Trace Compounds Analysis with Innovative Systems: PTR-ToF-MS and FASTGC. 71st Conference of the Italian Thermal Machines Engineering Association, ATI2016, 14-16 September 2016, Turin, Italy, *Energy Procedia*. 101 (2016) 536–541.

[66] C. Freissinet, D.P. Glavin, P.R. Mahaffy, K.E. Miller, J.L. Eigenbrode, R.E. Summons, A.E. Brunner, A. Buch, C. Szopa, P.D. Archer, H.B. Franz, S.K. Atreya, Organic Molecules in the Sheepbed Mudstone, Gale Crater, Mars, *Journal of Geophysical Research: Planets*. 120 (2015). <https://doi.org/10.1002/2014JE004737>.

[67] A. Buch, I. Belmahdi, C. Szopa, C. Freissinet, D.P. Glavin, M. Millan, R. Summons, D. Coscia, S. Teinturier, J.-Y. Bonnet, Y. He, M. Cabane, R. Navarro-Gonzalez, C.A. Malespin, J. Stern, J. Eigenbrode, P.R. Mahaffy, S.S. Johnson, Role of the Tenax® Adsorbent in the Interpretation of the EGA and GC-MS Analyses Performed with the Sample Analysis at Mars in Gale Crater, *Journal of Geophysical Research: Planets*. 124 (2019) 2819–2851. <https://doi.org/10.1029/2019JE005973>.

TRANSITION CHAPTER 4–5

Chapter 2 reviewed and highlighted the diversity of available gas sampling and preconcentration techniques for the determination of trace compounds in gas samples. The complexity of the choice of an appropriate sampling methodology and sampling unit that would collect a representative sample, preserve the sample integrity and enable quantitative recovery of targeted trace compounds, was also pointed out. Moreover, the review in Chapter 2 suggests there is a lack of techniques allowing to directly preconcentrate trace compounds from pressurized gases *in situ* on the gas pipes at the working pressure to avoid drawbacks and shortcomings diverted from the depressurization of gas samples. For that reason, one of the objectives of this doctoral thesis was precisely to develop a direct *in situ* high-pressure preconcentration sampling chain using existing preconcentration approaches. Henceforth, the next chapter (Chapter 5) presents, as a published scientific article, a new prototype purposely built to accommodate the multibed adsorbent tubes designed in Chapter 3 and to enable pressurized gas streams (up to 200 bar_a) to be sampled through these multibed adsorbent tubes by connecting the prototype directly to field gas pipes. Following presentation of the prototype mechanics, its high-pressure functioning is validated and the effect of pressure on the preconcentration (adsorption and recovery) of trace compounds is investigated using a pressurized certified synthetic gas mixture whereafter the high-pressure prototype is used *in situ* to sample a biomethane stream injected in the natural gas transport grid at 40 bar_a. All laboratory- and field-sampled adsorbent tubes are desorbed and analyzed via the thermal desorption prototype presented in Chapter 4.

CHAPTER 5 – NOVEL FIELD-PORTABLE HIGH-PRESSURE ADSORBENT TUBE SAMPLER PROTOTYPE FOR THE DIRECT *IN SITU* PRECONCENTRATION OF TRACE COMPOUNDS IN GASES AT THEIR WORKING PRESSURES: APPLICATION TO BIOMETHANE

– RSC Advances 12 (2022) 10071-10087 • <https://doi.org/10.1039/d2ra00601d> –
Received 28 January 2022; Accepted 23 March 2022

Aurore Lecharlier^{1,2}, Hervé Carrier¹, Brice Bouyssiere², Guilhem Caumette³, Pierre Chiquet³, Isabelle Le Hécho^{2*}

¹ Université de Pau et des Pays de l'Adour, E2S UPPA, CNRS, TOTAL, LFCR UMR 5150, BP 1155 avenue de l'Université, 64013 Pau Cedex, France

² Université de Pau et des Pays de l'Adour, E2S UPPA, CNRS, IPREM UMR 5254, Technopôle Hélioparc, 2 avenue du Président Angot, 64053 Pau Cedex 09, France

³ Teréga, 40 Avenue de l'Europe, CS 20 522, 64010 Pau Cedex, France

*Corresponding Author: Isabelle Le Hécho • isabelle.lehecho@univ-pau.fr

ABSTRACT

In Europe, renewable energy gases such as biomethane are aimed at substituting natural gas provided their stringent compliance to natural gas quality standards stipulating maximal levels of several chemical trace compounds (TC). Preconcentration is generally required to detect TC and inasmuch as biomethane is compressed for injection in the natural gas grid, preconcentration is commonly either done by collecting the bulk pressurized gas in a high-pressure cylinder or by first depressurizing it to collect a bulk volume in e.g. a gas sampling bag. Such whole gas samples are then transported to the lab and transferred to a preconcentration unit, entailing contamination and TC loss risks. Therefore, here a novel handy field-portable device for the direct *in situ* high-pressure preconcentration of TC is presented, enabling to sample gases at pressures up to 200 bar_a through a self-assembled Tenax[®]TA + Carbopack[™]X multibed adsorbent tube. The effect of the gas sampling pressure on the preconcentration of TC on adsorbent tubes was evaluated using a synthetic gas mixture containing 41 halogenated volatile organic compounds each at 1 ppm_{mol} in N₂. At given normalized sampled volumes and in the pressure range 5 – 100 bar_a handled in French gas transport grids, the pressure had no influence on the preconcentration when the gas circulates through the adsorbent tubes and as long as the adsorbents are not saturated. Next, for the first time, a real biomethane stream was sampled using the novel direct high-pressure preconcentration method on Tenax[®]TA + Carbopack[™]X multibed adsorbent tubes, allowing to preconcentrate, in a single sampling run, a wide range of volatile organic TC. More than 26 distinct TC were detected, belonging to seven chemical families: alkenes, aromatics, alkanes (linear, cyclic and polycyclic), Sulphur-compounds and terpenes, with linear alkanes (pentane, heptane, octane) and terpenes

predominating. Semi-quantification indicated pentane, dimethylcyclopropane, hexane, heptane, octane, α -pinene and camphene are present at a ≤ 1 ppm_{mol} concentration threshold in the biomethane.

KEYWORDS

High-pressure preconcentration

Trace compounds

Multibed adsorbent tube

Gas sampling

Biomethane

TD-GC-MS

ABBREVIATIONS CHAPTER 5

CpX	Carbopack™X
GC	Gas chromatography
HPTS	High-pressure tube sampling prototype
HVOC	Halogenated volatile organic compound
ID	Internal diameter
L	Length
MAT	Multibed adsorbent tube
MS	Mass spectrometry
PTFE	Polytetrafluoroethylene
RA	Relative abundance
SGM	Synthetic gas mixture
TA	Tenax®TA
TC	Trace compound(s)
TD	Thermodesorption
TD-GC-MS	Thermodesorption – gas chromatography – mass spectrometry
THT	Tetrahydrothiophene
TIC	Total ion current chromatogram

I. INTRODUCTION

In the present-day worldwide energy transition context, the share of renewable gases is meant to increase in the energy mix to tackle global greenhouse gases emissions. In France, the goal is to bring this share to 7 to 10% of the total gas consumption by 2030 depending on costs cuts [1]. Biomethane and synthetic natural gas are pure methane (CH_4) renewable gases with the same calorific value as fossil natural gas, produced in anthropogenically optimized processes from different biomass types, ideally from the wastes-sector, simultaneously contributing to the circular economy. Biomethane commonly refers to the purified methane fraction of biogas, a gas mixture composed of mainly $<50\%$ CO_2 and $>50\%$ CH_4 produced by the anaerobic digestion of humid organic matter by a microbially driven biochemical mechanism called methanization in controlled digesters [2,3] or in landfills [4,5]. Organic wastes ('substrates') used in anaerobic digesters include agricultural residues, manure, food-processing and catering wastes, organic and green municipal and household wastes, sewage sludge. Several technologies exist to upgrade biogas to biomethane by separation of the CO_2 and CH_4 fractions [2,6–9]. Synthetic natural gas is obtained by pyrogasification and methanation of dry lignocellulosic biomass (wood, straw, olive stones...) [10–13].

Those renewable methane streams are aimed at substituting or complementing natural gas in any of its applications (engines, boilers, cookers, fuels...). Stringent compliance of their quality to international natural gas quality standards is however required to guarantee their safe and sustainable injection in the natural gas transport grids [14] or their use as vehicle fuels [15]. Next to CH_4 and depending on production conditions (digester or landfill, hydraulic retention time, temperature, humidity, pH...), substrates types, seasonal effects, and upgrading techniques, biomethane can contain low concentrations of various volatile compounds (trace compounds, TC) from diverse chemical families: alkanes, alkenes, terpenes, alcohols, aldehydes, ketones, ethers, esters, aromatics, halogenated organic compounds, organic and inorganic Sulphur- and Silicon-compounds [16–21] and organic or inorganic metal and metalloid species [22–24]. Observed concentrations range $30 - 35000 \mu\text{g}\cdot\text{m}^{-3}$ [19] and $<10 - 700 \text{ mg}\cdot\text{m}^{-3}$ [20] for total volatile organic compounds; $<100 \mu\text{g}_{\text{Si}}\cdot\text{m}^{-3}$ for total siloxanes [20] and $<300 \mu\text{g}_{\text{Si}}\cdot\text{m}^{-3}$ for total volatile methyl siloxanes [17]; and $0.1 - 100 \text{ ng}\cdot\text{Nm}^{-3}$ for metallic trace compounds [22]. Since natural gas grid quality standards stipulate maximal levels of among others ammonia, siloxanes, Sulphur-, Mercury- and halogenated-compounds to avoid those compounds inducing chemical reactions such as corrosion and abrasion that could damage gas infrastructures [25], sampling and quantifying biomethane's TC is crucial before grid injection. Odorant organic compounds of biomethane such as terpenes can also mask the odor of tetrahydrothiophene (THT) added to the gas for the safety of users (olfactive gas leak detection) [26].

Sampling, identification and quantification of biomethane's TC is difficult. The low concentrations not only imply high risks for TC loss by sorption to tubing, connectors and vessels in the sampling and analytical chains [20,27–29], but they often lie below the detection limits of analytical instruments, meaning a 'preconcentration' step is essential (the gas flows through a dedicated small-volume support with specific retention affinity for only given TC. Since the very volatile gas matrix itself (CH_4) is not retained, TC are preconcentrated). Moreover, not any sampling nor preconcentration system is able to quantitatively trap all

families of TC in one run in view of the complexity and diversity in physicochemical properties of the TC present (volatility, polarity, water solubility, reactivity...), resulting in different affinities and stabilities in the sampling entities [20,21,27,29,30]. Lastly, monitoring TC in grid-quality compliant biomethane may imply the gas has already been compressed to the grid pressure (French distribution network: 4-6 bar_a, transportation network: 8-80 bar_a). To the authors' knowledge, biomethane has only been *in situ* sampled directly on the pipelines at the grid pressure (40 bar_a) by Cachia et al. [22] using a high-pressure acid bubbling impinger for the direct preconcentration of metallic TC in gas samples [31]. So far, other reported determinations of TC in high-pressure gases (typically natural gas) have always been carried out by depressurization of the gas and preconcentration at atmospheric pressure: the gas is either depressurized *in situ* from the pipe after what the sampling system is installed at atmospheric pressure [32], or it is sampled at its grid pressure in surface-treated high-pressure stainless-steel cylinders subsequently transported to the lab for depressurization and preconcentration [29,33–36]. Depressurization is detrimental to the preconcentration of TC since, assuming the ideal gas law $PV=nRT$, a dilution factor equal to the ratio of the high pressure to the pressure after depressurization leads to a concentration decrease of the TC, implying larger gas volumes have to be sampled at atmospheric pressure than at high pressure to trap a given amount of TC. Next, a first whole gas sampling step in a high-pressure cylinder, cylinder transport to the lab, and then depressurization and transfer of the gas to the preconcentrating unit (e.g. sorbent tubes [34], cryogenic traps for metallic TC [33], amalgamation traps for mercury-TC [35,36]) has disadvantages. Firstly, transport of cylinders containing compressed flammable gas (CH₄) must observe national regulations for the transport of dangerous goods. Secondly, transport entails a storage phase of the sample until analysis can be executed. Sorption losses of TC onto cylinders' inner surfaces or instabilities have been established for both metallic [34–36] and non-metallic TC [21,29,30,37] when complex gases such as natural gas or biomethane are stored in cylinders, despite appropriate surface polishing or passivation-treatments. Surface-treated cylinders are additionally expensive and the instability and cross-contamination of TC is worse in re-used than in brand new cylinders [36]. Lastly, transfer of the gas from the cylinder to the preconcentration unit also increases the chances of sample loss or contamination due to leaks or sorption of TC on the gas transfer line materials. Having an easily field-implementable device at one's disposal that does not require solvents nor impingers, would avoid drawbacks diverted from the use of pressurized gas samples by enabling to sample target analytes at working pressures without depressurization; would simplify the sampling chain, avoid sample transfers and associated loss and contamination risks, avoid TC dilution by depressurization, diminish minimal sampling volumes and hence reduce sampling duration. To the authors' knowledge, such high-pressure preconcentration device does not exist.

Therefore, in this study, a novel handy field-portable sampling prototype for the direct *in situ* high-pressure preconcentration of non-metallic TC in gas samples at working pressures up to 200 bar_a is presented. To the authors' knowledge, this prototype is the first of its kind. Preconcentration takes place on self-developed multibed adsorbent tubes (MAT) packed with commercial adsorbents (Tenax[®]TA + Carbopack[™]X), placed in the high-pressure sampling prototype. The prototype was first validated by sampling a synthetic gas mixture containing 41 halogenated volatile organic compounds each at 1 ppm_{mol} in nitrogen through the MAT at

pressures ranging 5 – 100 bar_a. The effect of the gas pressure on the adsorption of the compounds was investigated to justify the use of the prototype. Next, biomethane was sampled in the prototype at a natural gas grid injection station at 40 bar_a. Preconcentrated TC were characterized by thermal desorption of the adsorbent tubes hyphenated with gas chromatography and mass spectrometry. It was beyond the scope of this study to quantify TC identified and to determine TC's breakthrough volumes on adsorbent multibeds.

II. MATERIALS AND METHODS

II.1. Multibed adsorbent tubes

Multibed adsorbent tubes (MAT), whose theoretical working principle is explained in the Supplemental Information, were self-assembled and conditioned as described in previous work [38]. Briefly, empty amber glass tubes (ID 4.8 mm, L 44 mm, ActionEurope, Sausheim, France) are manually packed with commercial adsorbents from Supelco, Bellefonte, PA, USA (Table 5.1). The MAT held 14±0.2 mg Tenax[®]TA (front bed) and 29±0.2 mg Carbopack[™]X (back bed) and are further called 'TA14-CpX29'. Each adsorbent is weighted and sucked up in the tube where it is secured between and separated from the other bed by untreated ~4 mm long quartz wool plugs (Helios Italquartz[™]). To optimize the later thermal desorption of the MAT, adsorbent masses m were determined based on a fixed volume $V = 0.05 \text{ cm}^3$ for each bed and on the packing density ρ (Table 5.1): $m = \rho \cdot V$. As such, each bed occupies a length of $3.4 \pm 0.2 \text{ mm}$ in the tube and it is ensured both lengths physically only occupy the central part of the tube that will be heated inside the thermodesorber. After packing, tubes are conditioned at 320°C during 8.5 h under a continuous clean N₂ flow as described earlier [38]. The Tenax[®]TA conditioning temperature (320°C) was used to condition the MAT as conditioning them at the higher Carbopack[™]X conditioning temperature (350°C) would lead to irreversible thermal degradation of TA. As soon as the conditioning sequence is completed, tubes are sealed with aluminum crimp caps with PTFE/silicone/PTFE septa (11 mm, high temperature ultra-low-bleed silicone, ActionEurope) and stored until utilization in individual hermetic polyethylene zip bags in a larger zip bag in a desiccator at 4°C as recommended by [27,39,40]. Despite adsorbent tubes analyzed by thermodesorption can theoretically be re-used after quantitative thermodesorption and thermal reconditioning [20,41,42], here it was decided to only use new tubes for all sampling operations to avoid cross-contamination in the case thermodesorption of the initial sample was not quantitative and to avoid build-up of thermal degradation artefacts upon repeated conditioning cycles.

Table 5.1: Properties of commercial adsorbents used in the MAT.

Adsorbent brand name	Nick-name	Matrix	Mesh size	Surface area (m ² ·g ⁻¹)	Packing density (g·cm ⁻³)	Conditioning T (°C)	Desorption T (°C)	Mass in the MAT (mg)	Position in the MAT
Tenax [®] TA	TA	Macroporous polymer (2,6-diphenyl- <i>p</i> -phenylene oxide)	60-80	35	0.28	320	300	14	Front bed
Carbopack [™] X	CpX	Graphitized carbon black	40-60	240	0.58	350	330	29	Back bed

II.2. High-pressure sampling prototype

The novel field-portable high-pressure tube sampling prototype (HPTS) is derived from an existing patented device [43], both were manufactured by SANCHEZ TECHNOLOGIES (France). The HPTS is a purpose-built stainless-steel cylindrical envelope allowing to sample gas at pressures up to 200 bar_a through a self-assembled adsorbent tube using an equal-pressure gas flow design principle. The central parts AB and BC of the HPTS (Fig.5.1) can be unscrewed to accommodate the adsorbent tube. Once the tube is placed, re-screwing parts AB and BC causes each of the fine beveled hollow needles located in both HPTS extremities (Fig.5.1 A and C), to pierce the inlet and outlet septa of the tube. Equal-pressure in- and outside the tube during sampling is achieved by a clever aperture in the upstream needle's base: when gas enters the HPTS at side A (Fig.5.1), it not only flows throughout the needle and into the tube but also flows out of the needle's base into the space around the tube. The whole system is gas-tight. When the outlet HPTS valve is opened at side C (valves not shown on Fig.5.1), high-pressure gas circulates through the tube and the total volume passed through can be controlled via a downstream flowmeter. The gas around the tube does not circulate. The HPTS itself has no flowrate limitations, those are set by the adsorbent tube adsorption and breakthrough properties.

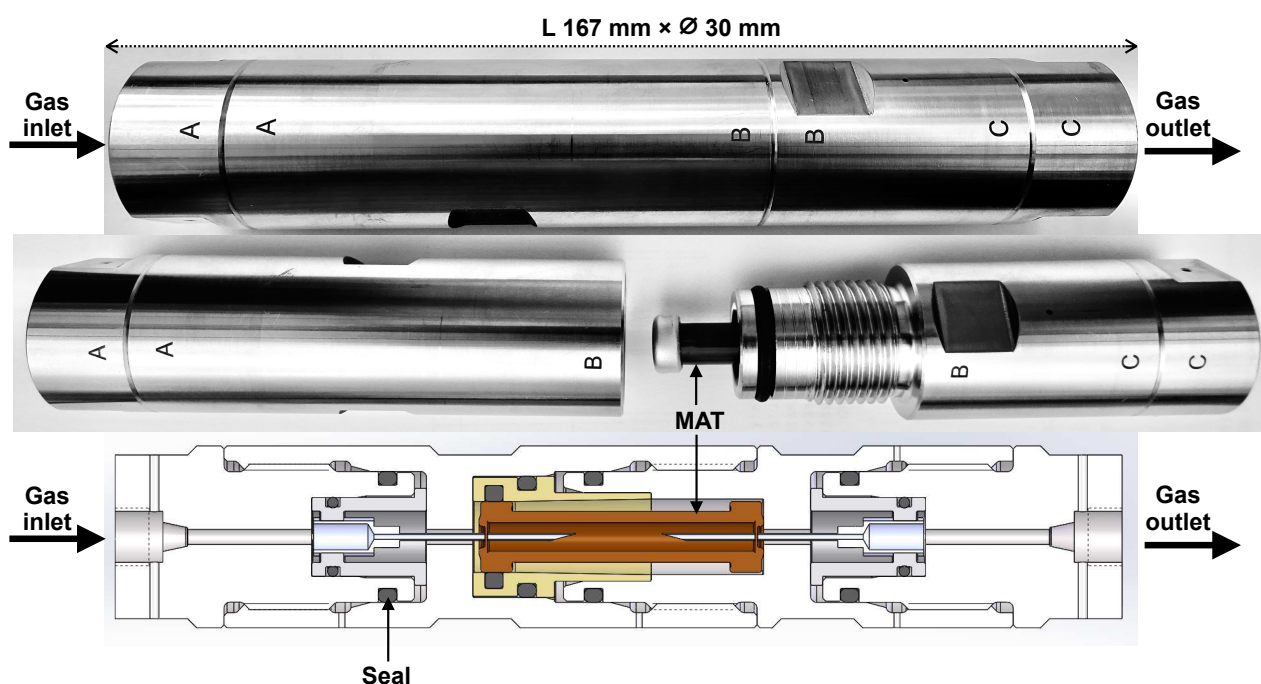


Figure 5.1: The high-pressure tube sampling prototype. Gas sampling direction is from A to C.

II.3. Sampling

The high-pressure preconcentration sampling chain is schematized in Fig.5.2. The pressure of the high-pressure gas (either a synthetic gas cylinder for laboratory tests or a real gas during *in situ* sampling) is measured with a manometer (Leo2-Ei 0-300 bar_a Atex-certified, Keller, Switzerland) before the gas enters the MAT inside the HPTS. The MAT is oriented so that the gas first meets the front weak adsorbent bed (Tenax[®]TA). Downstream preconcentration, the gas is depressurized to atmospheric pressure (250 - 0 bar_a pressure regulator, Swagelok,

France) before entering the drum-type gas meter (TG 0.5-polypropylene, Ritter, Germany). The gas meter is limited to flowrates of $1 \text{ L}_N \cdot \text{min}^{-1}$ and the measure of the gas volume passed is independent on the gas composition. To sample a given gas volume, valves 1 and 2 (Fig.5.2) are opened. Valve 1 is then closed to stop the sampling and the residual volume V_R trapped between valve 1 and the gas meter is also counted as contributing to the total sampling volume although once valve 1 is closed, the V_R circulates following a pressure gradient from the initial sampling pressure to atmospheric pressure. Henceforth, to sample a targeted gas volume V_T , valve 1 has to be closed in advance when a volume $V = V_T - V_R$ has passed through the gas meter. The gas volume effectively sampled under pressure is thus equal to V .

A bench supporting all sampling elements and tubing was built and is used in the lab as well as *in situ*. Connectors used are from Top Industrie (France) and Swagelok (France). Only stainless-steel tubing is used and attention is paid to always use clean tubing upstream the preconcentration in the HPTS. Before sampling a gas onto the MAT in the HPTS, the sampling chain without MAT is flushed with the gas to sample during few minutes to ‘accustom’ the sampling chain elements to the gas and to saturate potential TC-sorption sites on tubing upstream the HPTS. Between subsequent sampling operations of gases of different composition, the HPTS is flushed with pure nitrogen (99.999% purity) during ≥ 60 min to remove residual sample traces and avoid sample cross-contamination. All sampling operations are performed at ambient temperature. All lab- and field-sampled adsorbent tubes were stored in individual hermetic polyethylene zip bags in a larger zip bag in a desiccator at 4°C until analysis and were analyzed within 36 hours as recommended by [27,39,40].

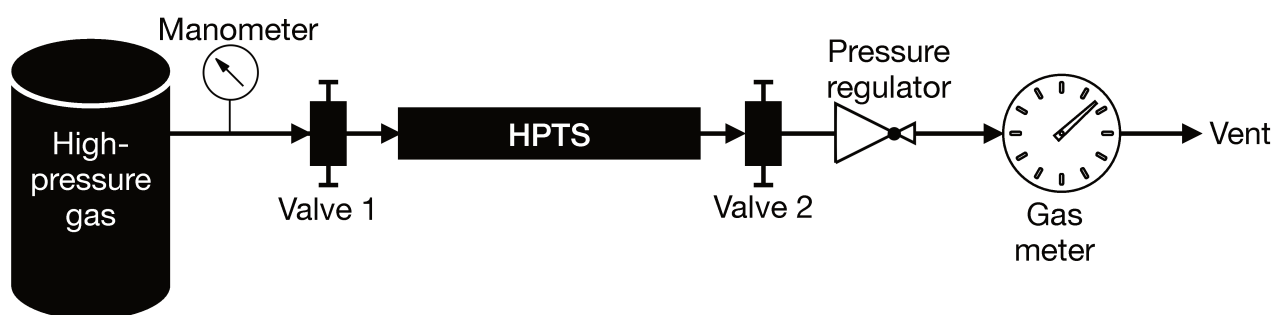


Figure 5.2: High-pressure preconcentration sampling chain.

II.3.1. Synthetic gas sampling

The HPTS containing a TA14-CpX29 MAT was first tested in the lab using a pressurized certified synthetic gas mixture (SGM) containing 41 halogenated volatile organic compounds (HVOC) each at $1 \text{ ppm}_{\text{mol}}$ in nitrogen (Table 5.2) (‘TO-14A 41 Component Mix’, Scott Airgas Specialty Gases, Plumsteadville, USA, purchased from Restek, France). Yet the HPTS withstands up to 200 bar_a , high-pressure sampling tests were only performed up to 100 bar_a at different test-pressures (Table 5.3) covering the pressure range used in the French gas distribution grids ($4\text{--}6 \text{ bar}_a$) and transport grids ($8\text{--}80 \text{ bar}_a$). A high-pressure regulator was connected to the SGM cylinder to achieve the desired test-pressure which was also controlled by a digital pressure sensor (accuracy $\pm 0.05 \text{ bar}_a$) (Scaime).

The effect of the circulating gas pressure on the preconcentration (adsorption) of the 41 HVOC on the MAT was investigated by sampling given gas volumes (2 and 5 L_N) at different test-pressures at a flowrate of 1L_N·min⁻¹ through the MAT. To ensure these pressure-effect tests were performed in conditions of non-saturation of the adsorbents in the MAT, different volumes were also sampled at given pressures (5 and 40 bar_a) at 1L_N·min⁻¹ to verify the saturation point of the breakthrough curve was not reached for the 41 HVOC (Table 5.3). Sampling operations were all executed at constant ambient temperature (20°C).

Table 5.2: The 41 HVOC present in the SGM used, listed in order of increasing boiling points. Note 1,2-dichloropropane was never detected on the TA14-CpX29 MAT despite both adsorbents should enable fair adsorption and recovery (>80%) of this compound [44].

Compound	Boiling point (°C, at P _{atm})	Molecular mass (g·mol ⁻¹)
Dichlorodifluoromethane	-30.0	120.9
Chloromethane	-23.8	50.5
Chloroethene	-13.4	62.5
1,3-Butadiene	-4.4	54.1
1,2-Dichloro-1,1,2,2-tetrafluoroethane	3.6	170.9
Bromomethane	4.0	94.9
Chloroethane	12.5	64.5
Trichlorofluoromethane	23.8	137.4
1,1-Dichloroethene	32.0	96.9
Dichloromethane	39.6	84.9
1,1,2-trichloro-1,2,2-trifluoroethane	48.0	187.4
1,1-Dichloroethane	57.0	99.0
cis-1,2-Dichloroethene	60.2	96.9
Trichloromethane	61.2	119.4
1,1,1-Trichloroethane	74.0	133.4
Tetrachloromethane	76.7	153.8
Acrylonitrile	77.0	53.1
Benzene	80.0	78.1
1,2-Dichloroethane	84.0	99.0
Trichloroethene	87.2	131.4
1,2-Dichloropropane (absent)	96.0	113.0
cis-1,3-Dichloropropene	104.0	111.0
Toluene	111.0	92.1
trans-1,3-Dichloropropene	112.0	111.0
1,1,2-Trichloroethane	112.5	133.4
Tetrachloroethene	121.1	165.8
Chlorobenzene	131.0	112.6
1,2-Dibromoethane	131.5	187.9
Ethylbenzene	136.0	106.2
p-Xylene	138.0	106.2
m-Xylene	139.0	106.2
o-Xylene	144.0	106.2
Styrene	145.0	104.2
1,1,2,2-Tetrachloroethane	146.0	167.8
1,3,5-Trimethylbenzene	164.7	120.2
1,2,4-Trimethylbenzene	170.0	120.2
1,3-Dichlorobenzene	172.0	147.0
1,4-Dichlorobenzene	174.0	147.0
1,2-Dichlorobenzene	180.2	147.0
1,2,4-Trichlorobenzene	213.5	181.4
Hexachloro-1,3-butadiene	215.0	260.8

Table 5.3: Experimental conditions for the HPTS lab validation. n= amount of successful replicates

Test-condition	Test-pressure (± 0.05 bar _a)	Theoretical sampled volume (L _N)	Average effective sampled volume (L _N)	Standard deviation effective sampled volume (L _N)
A	5	2	2.01 (n=3)	0.02
	40		2.06 (n=2)	0.02
	100		2.22 (n=3)	0.57
B	5	5	5.00 (n=4)	0.02
	40 *		4.87 (n=3)	0.05
	68		4.80 (n=1)	/
	74		5.04 (n=1)	/
C	40	1	0.98 (n=2)	0.06
		2	2.06 (n=2)	0.02
		5	5.02 (n=1)	/
D	5	2	2.01 (n=3)	0.02
		5	5.00 (n=4)	0.02
		6	6.01 (n=3)	0.02

* On the n=3 replicates, two were performed at 40 bar_a and one at 39 bar_a.

II.3.2. *In situ* biomethane sampling

Next, the HPTS was used *in situ* to preconcentrate TC in a biomethane injected at 40 bar_a in the French natural gas transport grid. The biomethane sampled is produced by biogas upgrading at an anaerobic digestion plant gathering agricultural, manure (duck, cow, sheep) and food processing residues. Biogas is upgraded by water washing in a fluidized bed (scrubber). Water streams downwards while biogas streams upwards. Water-soluble CO₂ and H₂S gas components dissolve in water while CH₄ does not and moves to the top of the scrubber where it is evacuated towards the natural gas grid injection pool and dried via pressure swing adsorption on regenerable hydrophilic silica beads.

The HPTS containing a TA14-CpX29 MAT was connected to the biomethane grid injection pipe at 40 bar_a using a clean 2.5 m long stainless-steel tube dedicated to this site. The sampling point was located upstream the THT odorization point. 2 L_N were collected through the HPTS directly at 40 bar_a on 6 MAT replicates at 1 L_N·min⁻¹. Six other MAT replicates were sampled after depressurization at 1.45 bar_a with 2 L_N at 1 L_N·min⁻¹ from the same sampling point. All samples were taken the same day within 4 hours at ambient outdoor temperature (8.2 \pm 0.1 °C). Before and after sampling, adsorbent tubes were transported from and to the lab in individual hermetic polyethylene zip bags in a larger zip bag in a polystyrene box filled with carbon dioxide dry ice.

II.4. Analysis

All sampled MAT are analyzed via TD-GC-MS: thermal desorption (nC_x Instrumentation, Garlin, France, 'nC_x-TD' thermodesorber prototype) coupled to gas chromatography (Agilent 6890A GC) and mass spectrometry detection with quadrupole mass filter (Agilent 5973Network Mass Selective Detector) programmed as in Table 5.4 using the MSD ChemStation E.02.02.1431 software (Agilent) and the NIST Mass Spectral Search Program version 2.0 d, 2005. Each MAT is placed in the thermodesorber in the reverse direction as compared to the gas sampling direction. The nC_x-TD prototype was presented in previous work [38] and the chromatographic

peak resolutions, limits of detection and repeatabilities obtained with this TD-GC-MS analytical chain have also been presented in [38]. Note the 200°C temperature programmed in the nCx-TD corresponds to an effective desorption temperature of 300°C inside adsorbent tubes. The MAT desorption temperature is 300°C since desorbing MAT at 330°C (desorption temperature of CpX, Table 5.1) would induce thermal degradation of TA (desorption temperature 300°C) with associated injection of its thermal degradation products in the GC-MS and falsification of the analytical results as well as irreversible TA damage.

Table 5.4: TD-GC-MS instrument parameters

Instrument	Parameter	Value / reference
nCx-TD prototype <i>nCx Instrumentation</i>	Safe temperature	35°C
	Temperature	200°C
	Stabilization time	15 s
	Pressure	1170 mbar
	Injection time	10 s
GC <i>Agilent 6890A</i>	Inlet temperature	230°C
	Inlet septum	Premium Inlet Septa, Bleed/Temp optimized, non-stick (Agilent)
	Inlet liner	Ultra Inert Liner, Splitless, Single taper, no wool, 4 mm ID (Agilent)
	Split ratio	1 :1
	Split flow	1.5 mL·min ⁻¹
	Carrier gas	Helium (quality detector 5.0, Linde, France)
	Gas saver	Off
	Column	HP-5MS, 30 m × 250 µm ID × 0.25 µm film thickness (Agilent)
	Constant flow in column	1.5 mL·min ⁻¹
	Carrier gas linear velocity in column	44 cm·s ⁻¹
Oven	30°C (4 min) - 10°C·min ⁻¹ - 250°C (5 min)	
MS <i>Agilent 5973Network</i> <i>Mass Selective Detector</i>	Source temperature	230°C
	Quadrupole temperature	150°C
	GC-MS interface temperature	280°C
	Electron Impact Mode	70 eV
	Electron Multiplier Voltage	Relative voltage (106 = 1871 V)
	Acquisition mode	Scan
	Scan range	10 – 450 a.m.u.
	Sampling rate	3.28 scan·s ⁻¹
Threshold	100 counts	

II.5. Calculations

In real biomethane samples, the relative abundance (RA , %) of each TC i ($i = \{1 \rightarrow n\}$) identified upon TD-GC-MS analysis of the sampled MAT, was calculated as follows:

$$RA_i (\%) = \frac{100 \cdot A_i}{\sum_{i=1}^n A_i}$$

with A_i the average chromatographic peak area of compound i across all replicates on the total ion current chromatograms (TIC). For the per-chemical family RA (e.g. alkanes), n =the number of alkanes found in the sample. For the global RA in the whole sample, n =the total number of TC identified.

III. RESULTS AND DISCUSSION

III.1. High-pressure sampling prototype validation

The equal-pressure working principle of the novel HPTS allowed to sample pressurized gases through MAT without any physical damage to the glass tubes: tubes do not break and adsorbent beds do not move inside their tubes. The HPTS is handy and field-portable, allowing easy sampling at any gas production site at any pressure up to 200 bar_a. Note the sampling chain in Fig.5.2 is currently equipped to work at 200 bar_a yet it can easily be adapted to work at higher pressures up to 1000 bar_a.

III.2. Multibed adsorbent tubes adequacy

In this study, the SGM used was chosen for its 41 HVOC trace compounds (Table 5.2), some of which may be present in real biomethane samples [16,21,45]. The TA14-CpX29 MAT configuration proved suitable to adsorb and desorb all HVOC present in the SGM at all test-pressures in the range 5 – 100 bar_a with the exception of chloromethane which was never detected (Table 5.SI-1 in the Supplemental Information). Tenax®TA and Carbopack™X are indeed both too weak to adsorb and recover the highly volatile and small chloromethane molecule (recovery < 20% [44]). Stronger adsorbents than Carbopack™X could be used as back bed in MAT when targeting very volatile and small compounds such as chloromethane. Care should nevertheless be taken that such stronger adsorbents also enable recovery of the compounds upon analysis.

New blank TA14-CpX29 MAT were also TD-GC-MS analyzed and were free of any inherent contaminant with the exception of siloxanes released from the PTFE/silicone/PTFE septa used to crimp-cap the tubes (Fig.5.3), indicating the tube assembly and conditioning procedure was adequate. Notwithstanding, other septa materials should be considered to achieve zero-release of impurities from tube materials while still offering softness and gas-tightness after needle piercing.

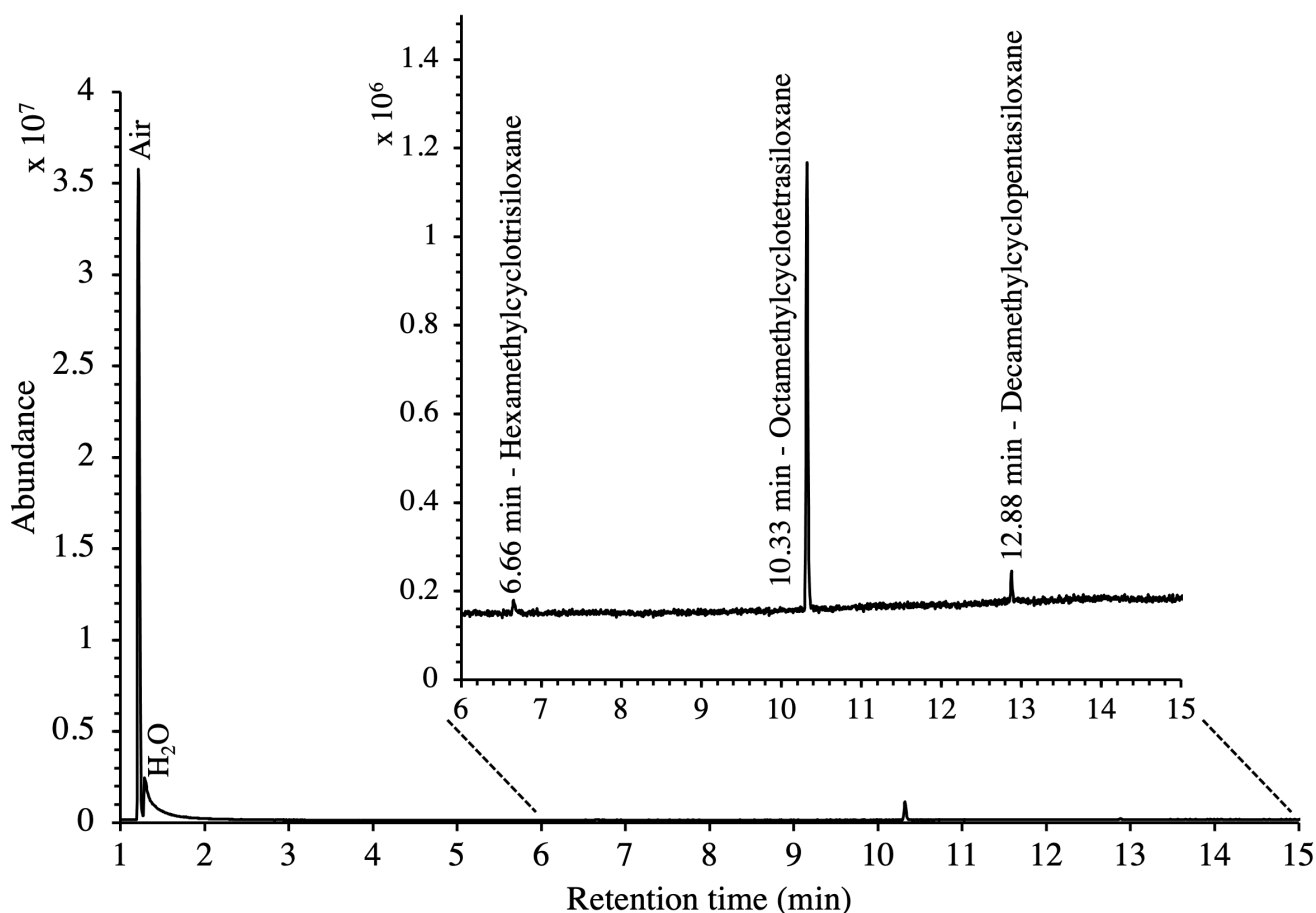


Figure 5.3: TIC of a new blank TA14-CpX29 MAT with indication of septum-released siloxane background contaminants.

III.3. Influence of the gas pressure on the preconcentration

The influence of the gas pressure on the preconcentration of the 41 HVOC of the SGM on the adsorbent materials upon circulating the gas through the HPTS was investigated. In Fig.5.4, the total ion current chromatogram (TIC) obtained from the TD-GC-MS analysis of a TA14-CpX29 MAT sampled with 2 L_N of the 41 HVOC SGM at 100 bar_a is depicted. From the TIC resulting from each high-pressure test-condition listed in Table 5.3, the chromatographic peak areas were recorded for each HVOC. In Fig.5.5 – 5.6, the average chromatographic peak areas for the replicates at test-conditions A and B respectively, have been plotted for each HVOC against the sampling pressure of the SGM on the TA14-CpX29 MAT. Results in Fig.5.5 – 5.6 present relatively high standard deviations due to the poor nCx-TD repeatability which was demonstrated in previous work [38]. In view of the systematic overlap of peak area-error bars (standard deviations) between the different test-pressures in Fig.5.5 (2 L_N sampled at different pressures) and Fig.5.6 (5 L_N sampled at different pressures), no effect of the gas sampling pressure on the preconcentration of the 41 HVOC on the TA14-CpX29 MAT could be established between 5 and 100 bar_a when the gas circulates through the MAT and as long as the MAT are not saturated. Results also demonstrated the gas sampling pressure had no effect on the chromatographic retention time of the HVOC (Table 5.SI-1). The non-saturation of the MAT by the trace HVOC studied was evaluated by test-conditions C and D (Table 5.3) where growing SGM volumes were sampled on the MAT at two given pressures: 1, 2 and 5 L_N at 40 bar_a (Fig.5.7)

and 2, 5 and 6 L_N at 5 bar_a (Fig.5.8) respectively. For each HVOC studied, Fig. 5.7 – 5.8 plot the average chromatographic peak areas for the replicates at test-conditions C and D respectively, against the sampled volume of the SGM on the MAT. While the preliminary shape of a breakthrough curve, or adsorption isotherm, appears for each HVOC in Fig.5.7 – 5.8, it is not possible to identify the isotherm type each compound follows with regards to e.g. the IUPAC adsorption isotherm classification [46] since too few measurement points were obtained to draw a complete isotherm. Nevertheless, it can be claimed that sampling 2 or 5 L_N of the 41 HVOC SGM does not lead to saturation of the sorption sites on the TA14-CpX29 MAT as the pseudo-isotherms in Fig.5.7 – 5.8 do not reach a plateau at those volumes for all HVOC studied. For the most volatile HVOC (from dichlorodifluoromethane to 1,1-dichloroethane in Table 5.2), saturation may start at 6 L_N (Fig.5.8). Dissimilarities in adsorption behavior and adsorbent surface coverage mechanisms between the 41 HVOC studied on the TA14-CpX29 MAT, are suggested by the potentially different adsorption isotherms in Fig.5.7 – 5.8, although investigating those differences goes beyond the scope of this study.

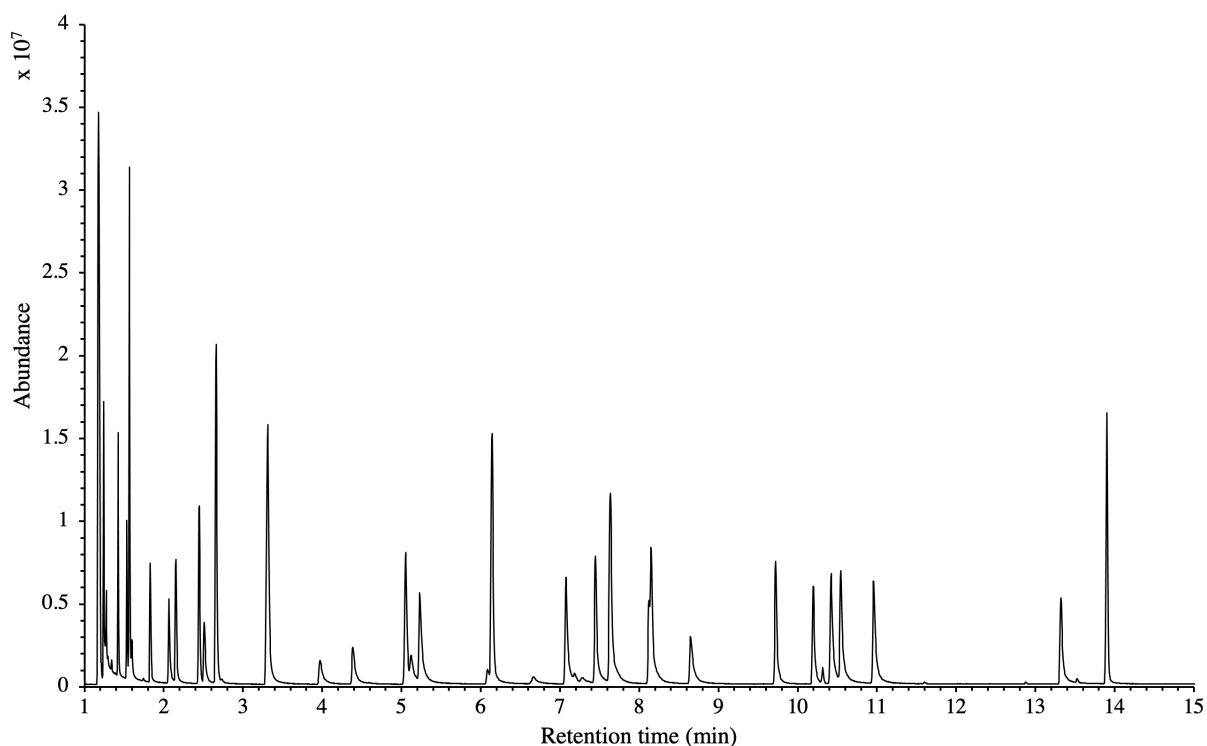


Figure 5.4: TIC of the 41 HVOC SGM sampled (2 L_N) at 100 bar_a on TA14-CpX29 MAT in the HPTS. Retention times are given in Table 5.SI-1.

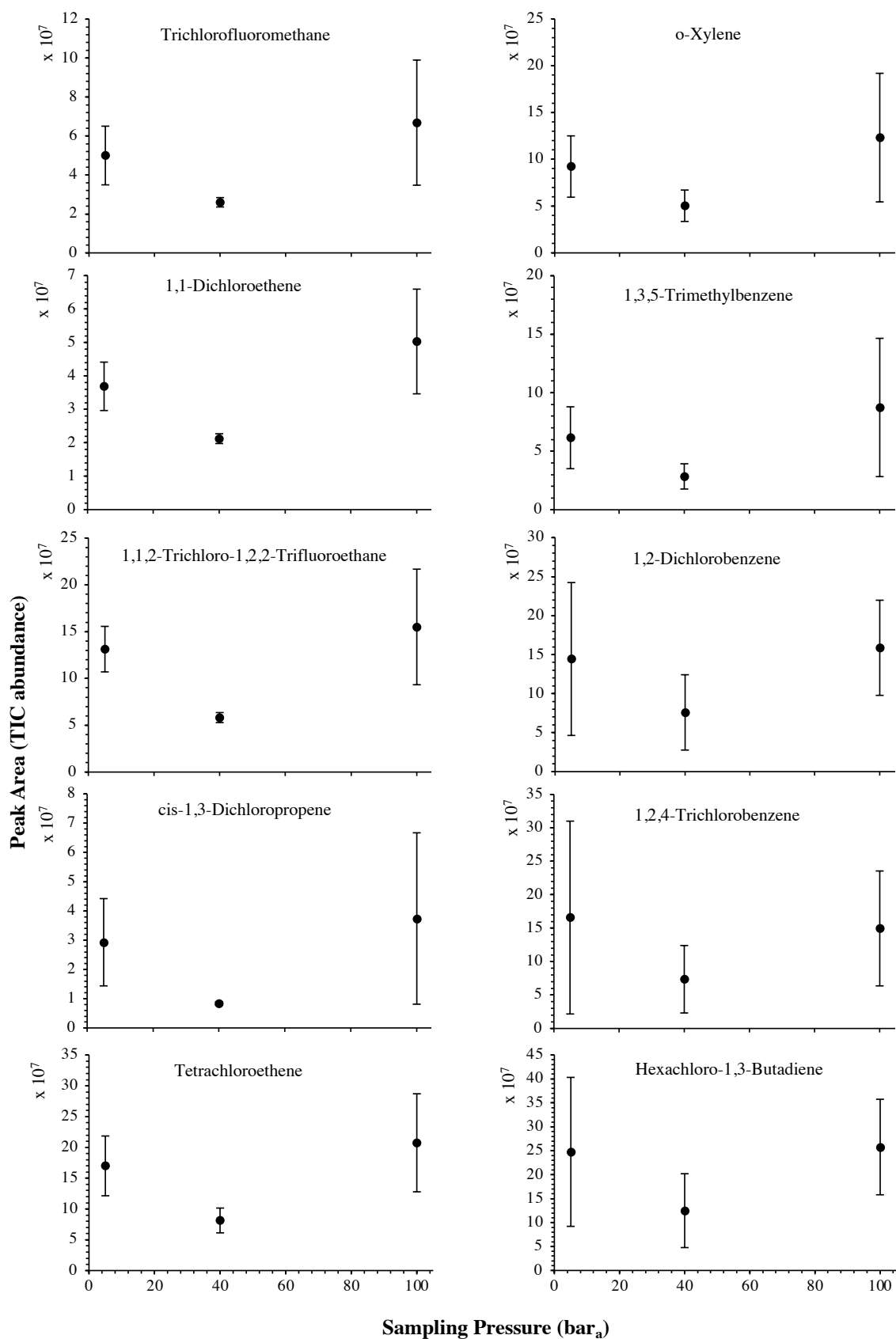


Figure 5.5: High-pressure adsorption isotherms of 10 randomly selected HVOC (out of the 41) for test-condition A ($2 L_N$ of the SGM sampled at 5, 40 and 100 bar_a on TA14-CpX29 MAT). Average peak area with indication of the standard deviation. The remaining HVOC are plotted in the Supplemental Information (SI): Fig.5.SI-1.

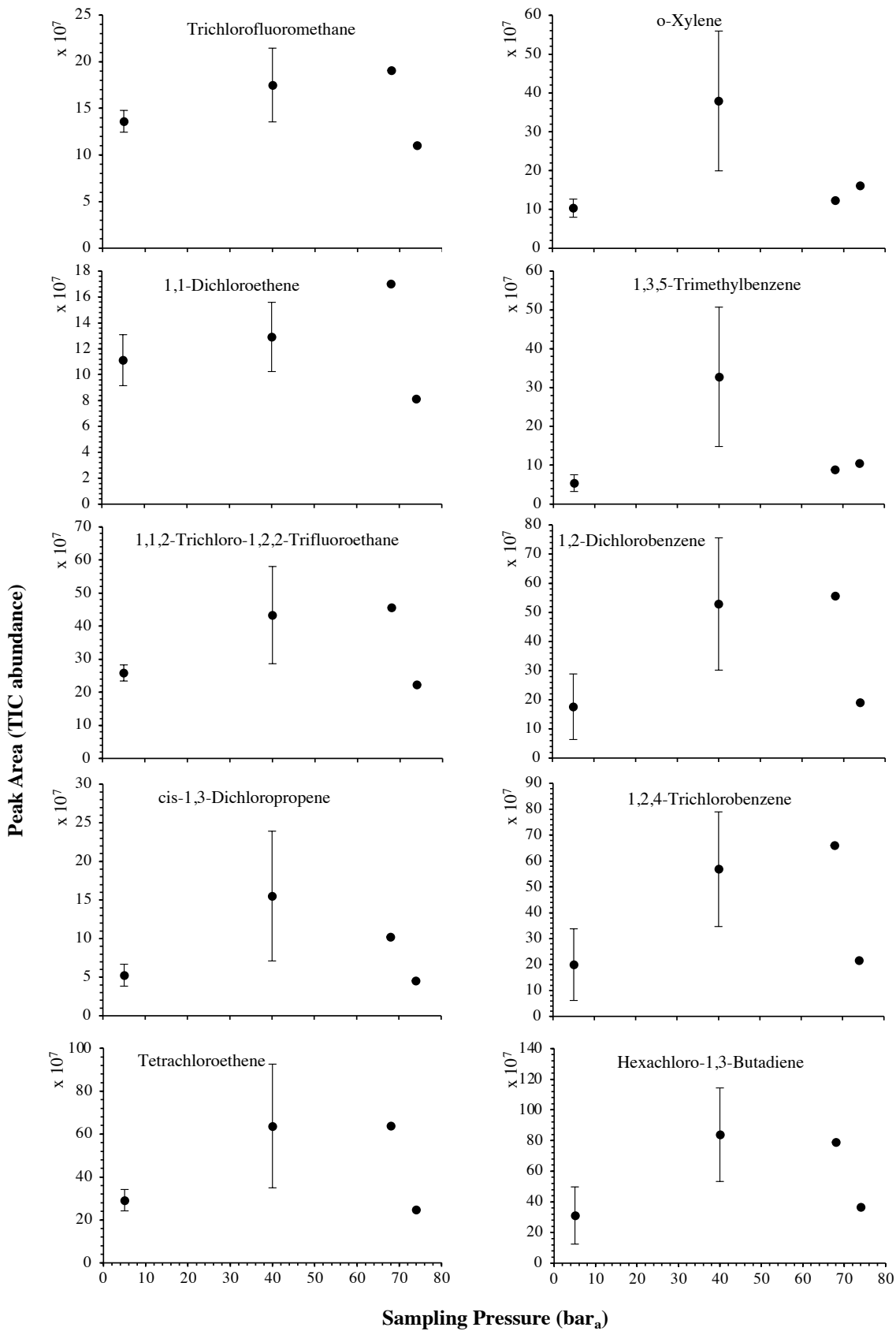


Figure 5.6: High-pressure adsorption isotherms of 10 randomly selected HVOC (out of the 41) for test-condition B (5 L_N of the SGM sampled at 5, 40, 68 and 74 bar_a on TA14-CpX29 MAT). Average peak area with indication of the standard deviation. The remaining HVOC are plotted in Fig.5.SI-2.

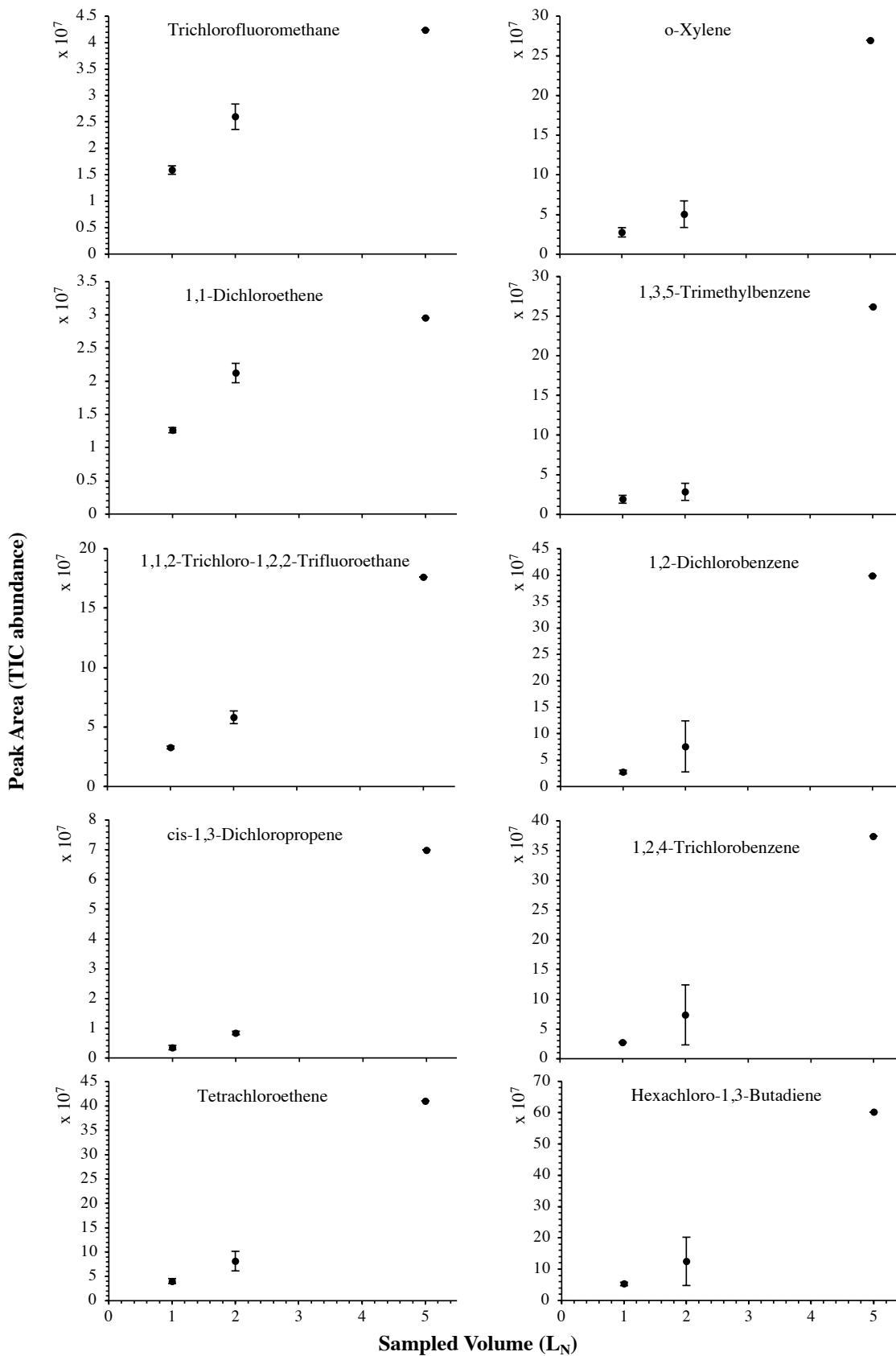


Figure 5.7: Partial breakthrough curves for 10 randomly selected HVOC (out of the 41) for test-condition C (1, 2 and 5 L_N of the SGM sampled at 40 bar_a on TA14-CpX29 MAT). Average peak area with indication of the standard deviation. The remaining HVOC are plotted in Fig.5.SI-3.

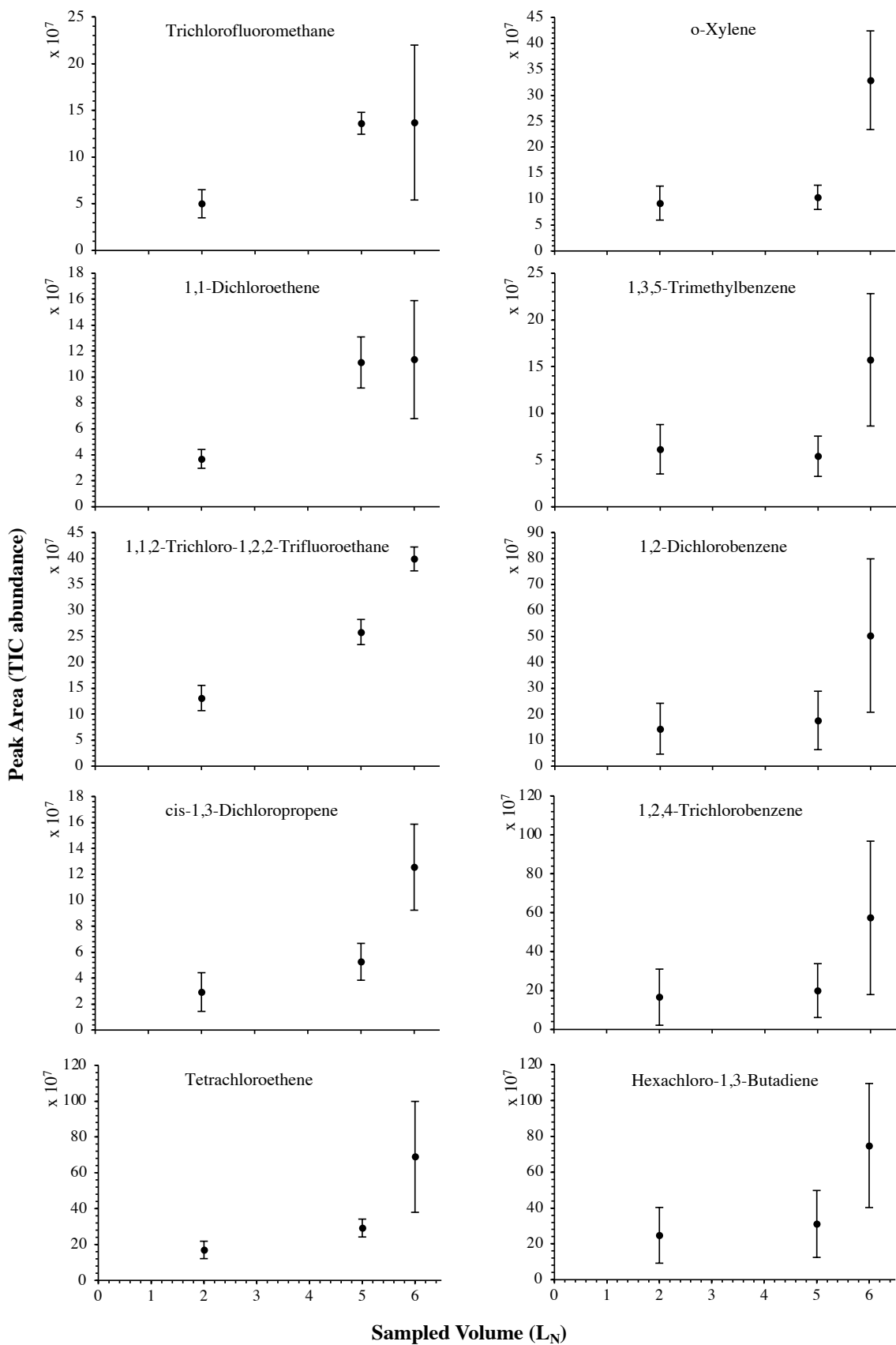


Figure 5.8: Partial breakthrough curves for 10 randomly selected HVOC (out of the 41) for test-condition D (2, 5 and 6 L_N of the SGM sampled at 5 bar_a on TA14-CpX29 MAT). Average peak area with indication of the standard deviation. The remaining HVOC are plotted in Fig.5.SI-4.

To the authors' knowledge, the pressure effect studied here has not been previously investigated. Thermodynamic researches on high-pressure adsorption of gases on microporous adsorbents have mainly focused on gases like N₂, CO₂, CO, CH₄, Ar and H₂ for industrial gas separation or enhanced gas storage purposes [47–49]. Few publications [50] have dealt with other gaseous species such as the 41 HVOC studied here. Furthermore, closed {gas (adsorbate) – adsorbent} systems in equilibrium conditions and at above-critical temperatures are generally assumed. The high-pressure preconcentration system considered in the present study is fundamentally different inasmuch as the gas *circulates* through an adsorbent tube at the same pressure as the pressure surrounding it, under non-equilibrium and non-saturation conditions at ambient temperatures and since adsorbates are not the bulk N₂ nor CH₄ matrix but the 41 HVOC. The absence of pressure effect on adsorption observed here therefore contrasts with the established conclusions from high-pressure adsorption thermodynamics where adsorption of TC tends to increase with the gas pressure [47–50]. The observed absence of pressure effect may be due to several factors. Firstly, the test-pressure range of 5-100 bar_a handled here may possibly be too narrow to reveal any pressure effect. Nonetheless, this pressure range was chosen to represent pressures used in the French gas distribution and transport grid, thus for this application, testing higher pressures may be irrelevant. Secondly, it is questionable whether the pressure could exert a prejudicial influence on the porous structure of the adsorbents in the MAT, such as modifying the specific surface area or the specific pore volume. This last assumption is however unlikely since Salem et al. [47] studied high-pressure induced changes in pore size distribution and in structure of microporous adsorbents (active carbon and zeolite 13X) and found high-pressure adsorption did not modify the porous structure of the microporous adsorbents.

The results presented here therefore suggest an efficient and non-selective preconcentration of TC from gaseous samples on MAT in the HPTS independently from the pressure of the circulating gas since all HVOC studied were equally and proportionately trapped on the MAT at all test-pressures. This high-pressure preconcentration sampling method is hence justified and does not need particular preliminary pressure-dependent calibration operations as long as the gas circulates through the MAT and that the total sampled volume does not saturate the adsorbents.

III.4. High-pressure sampling prototype application to biomethane's trace compounds characterization

TC in the biomethane sampled directly *in situ* at 40 bar_a or after depressurization at 1.45 bar_a on TA14-CpX29 MAT in the HPTS were characterized by TD-GC-MS of the sampled MAT. The goal was to qualitatively screen a large spectrum of TC-families rather than to focus on a single family or a single TC (multibed principle).

Fig.5.9 presents the TIC recorded for one biomethane sample replicate preconcentrated directly at 40 bar_a versus a replicate preconcentrated after depressurization at 1.45 bar_a. Disregarding the toluene peak at 5.03 min being large in the sample preconcentrated after depressurization, the visual evaluation of Fig.5.9 suggests no striking difference in TIC signal

intensities between the two samples, confirming the aforementioned statement (section III.3) that the sampling pressure has *a priori* no significant effect on the preconcentration of TC in gas samples under the sampling conditions handled here (gas circulates through unsaturated adsorbents). The relatively large toluene peak in the sample taken at 1.45 bar_a was confirmed to stem from a toluene-contamination of the tubing and connectors of the depressurization bench (results not shown). This highlights the critical advantage of sampling a compressed gas as close as possible to its source when targeting TC, i.e. at its grid pressure to shorten the sampling chain and avoid contamination risks in surplus equipment. Impressions from Fig.5.9 are corroborated by Fig.5.10 where the average chromatographic peak area of 10 TC identified in all biomethane replicates preconcentrated directly at 40 bar_a versus at 1.45 bar_a, are plotted against the sampling pressure. Again, the overlap of standard deviation error bars and the sometimes increasing – sometimes decreasing peak area trend in Fig.5.10 do not allow to authenticate a significant effect of the sampling pressure on the preconcentration.

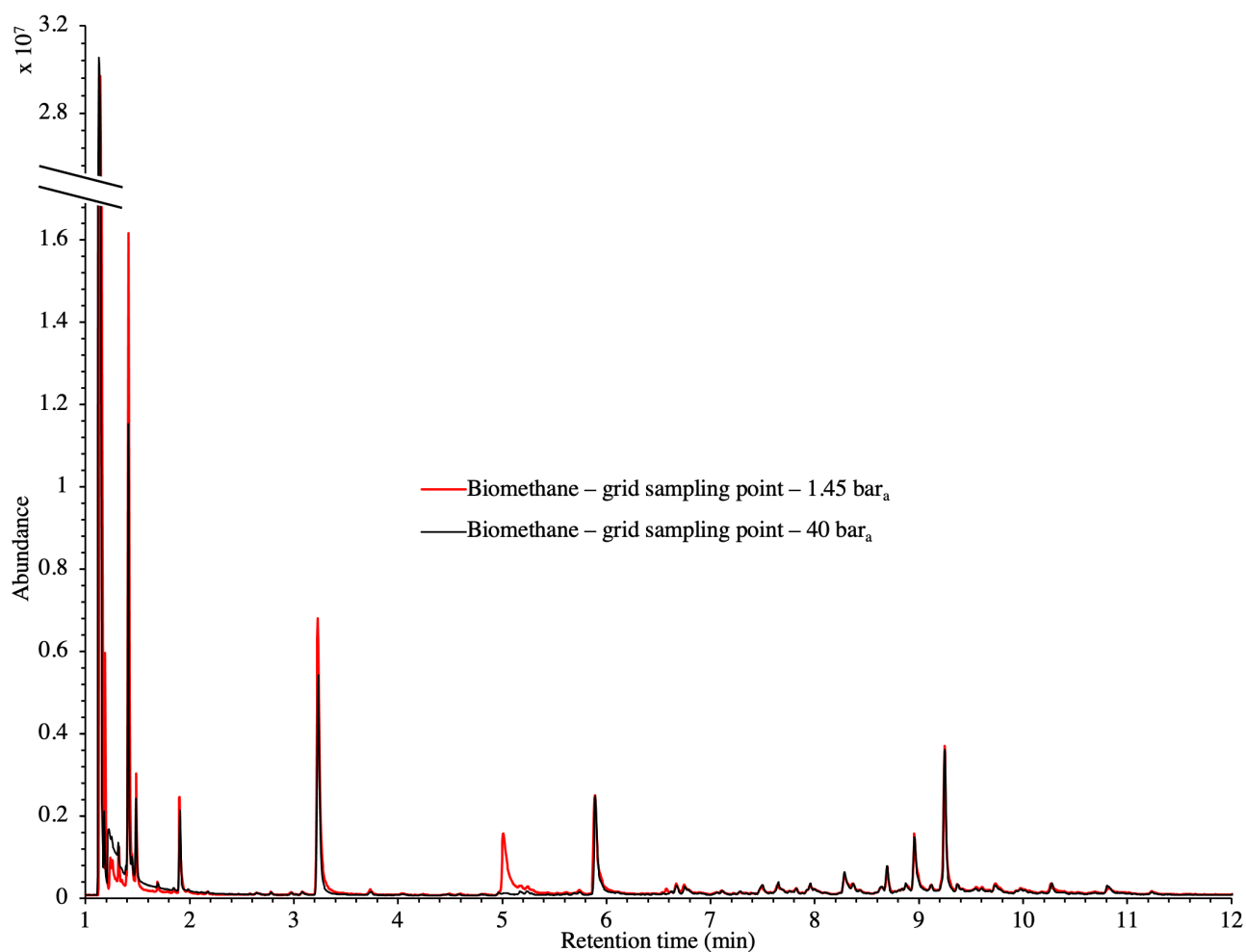


Figure 5.9: TIC of two biomethane samples: 2 L_N collected on TA14-CpX29 MAT at 1 L_N·min⁻¹ at 1.45 bar_a after depressurization versus directly at 40 bar_a in the HPTS.

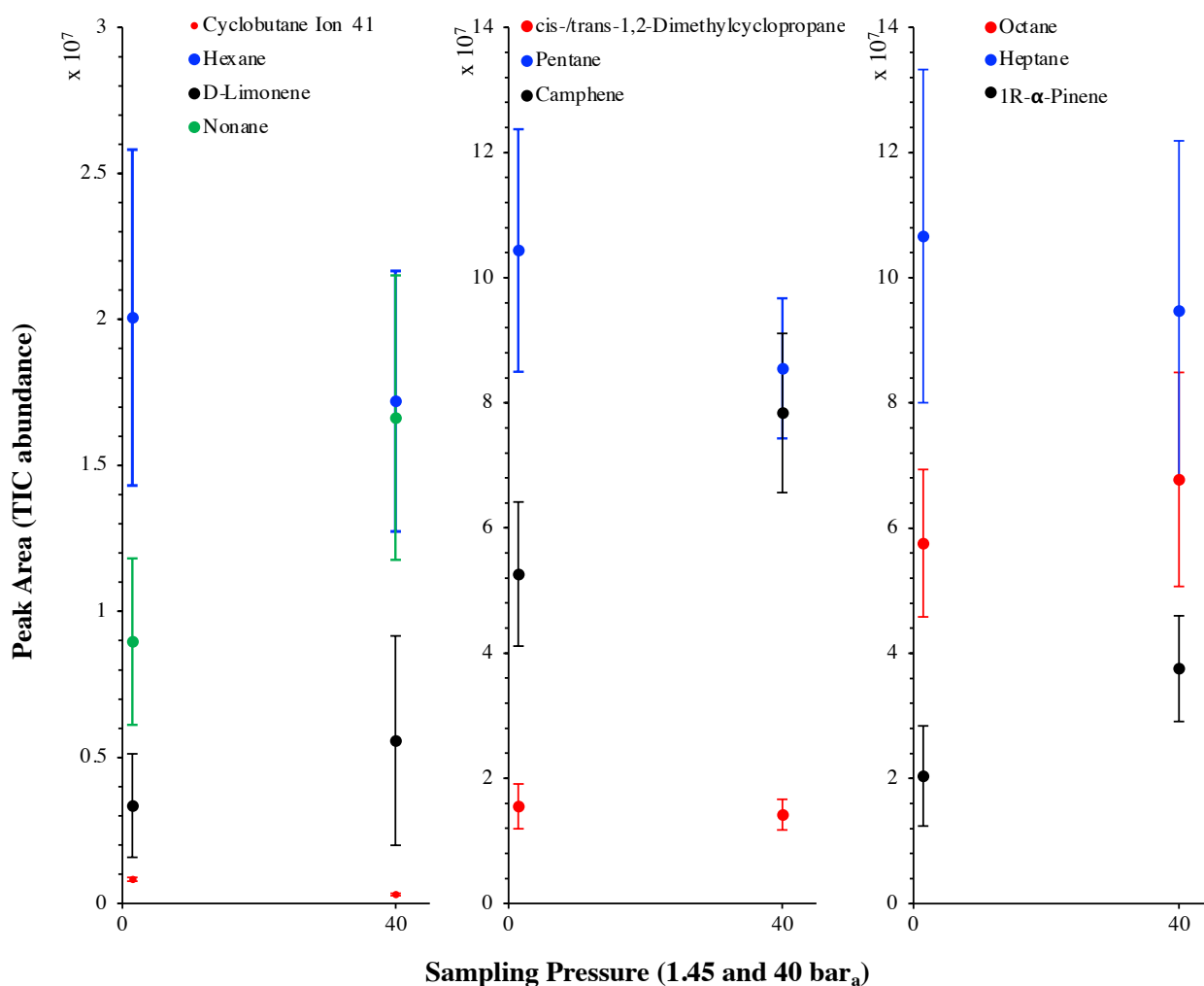


Figure 5.10: Average chromatographic peak area, with indication of the standard deviation, of 10 TC identified in the TIC of both biomethane sample types: 2 L_N collected on TA14-CpX29 MAT at 1 $L_N \cdot \text{min}^{-1}$ at 1.45 bar_a after depressurization ($n=5$ successful replicates) versus directly at 40 bar_a in the HPTS ($n=6$ successful replicates).

The average TC's biomethane composition was determined for the samples preconcentrated at 40 versus at 1.45 bar_a from the peaks identified in the respective replicates (Fig.5.11). Importantly, the HP-5MS chromatographic capillary column used was chosen for its non-polar stationary phase and associated 'universal' retention properties enabling to analyze a wide range of compounds in a broad polarity and volatility range such as found in biomethane samples. Disadvantageous to this column was nevertheless the co-elution of several TC and the difficult unambiguous peak identification with the NIST database. Therefore, for clarity and to avoid misidentification, molecular formulas are given in Fig.5.11 to represent the TC determined. An unequivocal compound identification could be done for those labeled with a "*" on Fig.5.11: benzene, toluene, cyclobutane, pentane, hexane, heptane, octane, nonane, 2-ethyl-1-hexanethiol, camphene, D-limonene. For the other TC whose identification was equivocal between various compounds having the same molecular formula but different structural formulas, the main corresponding compound has been labeled on Fig.5.11 as an indication. The per-family and global relative abundance (*RA*) of each TC (or each molecular formula) are given in Fig.5.11 (chemical families include alkenes, aromatics, cyclo-alkanes, linear alkanes, polycyclic alkanes, Sulphur-compounds, terpenes). For molecular formulas with several occurrences (chromatographic peaks), the average chromatographic peak areas of all

occurrences were summed up ($A_{i,sum}$) and the corresponding RA was calculated as $100 \times A_{i,sum} / \sum_{i=1}^n A_{i,sum}$. Importantly, the RA are only given in Fig.5.11 as a rough guide to decipher notable trends in dominant TC present in the biomethane since so far, no TC quantification was done owing to a lack of time in this research project. RA 's are nowise proportional to TC's concentrations in view of the differences in ionization efficiency between the TC in the mass spectrometer detector yielding signal intensity-differences in the TIC even at equal concentration.

In the biomethane sampled, at least 26 distinct TC were found to belong to seven chemical families: alkenes, aromatics, cyclo-alkanes, linear alkanes, polycyclic alkanes, Sulphur-compounds, terpenes (Fig.5.11). No qualitative composition difference was noticed between the biomethane preconcentrated directly at 40 bar_a and the one preconcentrated after depressurization at 1.45 bar_a with the exception of some C₈H₁₈ linear alkanes absent from the samples taken at 1.45 bar_a. Their absence may be due to sorption losses on tubing and connectors of the depressurization bench, once again underlining the importance of shortening the sampling chain upstream preconcentration. Among alkenes, C₅H₁₀ compounds were dominant. Among aromatics, solely benzene and toluene traces were found, with toluene reaching higher levels (recall the toluene contamination in the sample taken after depressurization). The cyclo-alkanes diversity was the highest with 7 distinct molecular formulas identified from C₄H₈ to C₁₀H₂₀. C₉H₁₈ species were the dominant cyclo-alkanes. Linear alkanes were also diversified with pentane, hexane, heptane, octane and nonane and several other C₇H₁₆, C₈H₁₈ and C₉H₂₀ species. Pentane and heptane were the most abundant linear alkanes. Polycyclic alkanes only counted a C₁₀H₁₈ species, and a single Sulphur-compound was also identified (2-ethyl-1-hexanethiol). Finally, at least 5 terpenes (C₁₀H₁₆) were detected: camphene (the most abundant), D-limonene, α -pinene, 3-carene and ocimene. Regarding global relative abundances (Fig.5.11), and momentarily overlooking the differences in ionization efficiency between the TC, linear alkanes (pentane, heptane, octane) and terpenes seem to be the predominant TC in the biomethane. Those two families are often reported as abundant in biogases and biomethane [16,45], terpenes being known to typically originate from vegetal matter [26,45] which may enter the anaerobic digester considered in this study through the agricultural crop and food processing residues. No Silicon-containing compounds were found in this biomethane, agreeing with other studies on farm- or agricultural-sourced biogas where Silicon-compounds are generally absent or present at lower concentrations than other TC [18].

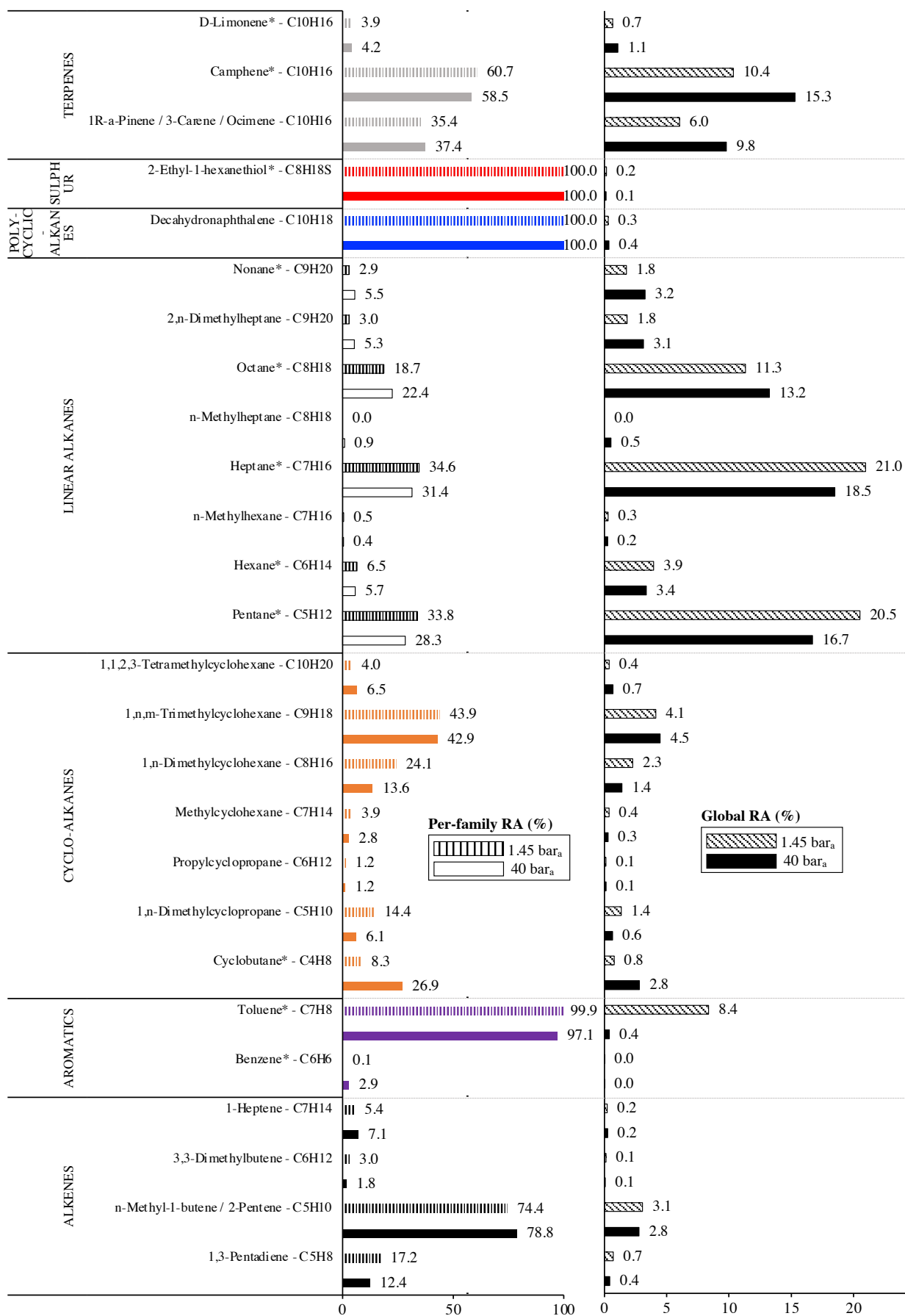


Figure 5.11: Per-chemical family and global relative abundances (RA, %) of molecular formulas, with indication of the potential corresponding TC, identified in both biomethane sample types: 2 LN collected on TA14-CpX29 MAT at 1 LN·min⁻¹ at 1.45 bar_a after depressurization (n=5 successful replicates) versus directly at 40 bar_a in the HPTS (n=6 successful replicates). Compounds marked with a "*" are unequivocally identified.

Finally, to make up for the lacking TC quantification and merely as a semi-quantitative indication, Fig.5.12 compares the TIC of a biomethane sample to the TIC of the 41 HVOC SGM sampled and analyzed under the same conditions (2 L_N collected at 40 bar_a on TA14-CpX29 MAT at 1 L_N·min⁻¹). The relatively high variability in signal intensities between replicates of a given sample in Fig.5.12 is due to the poor nCx-TD prototype repeatability, as demonstrated earlier [38]. Nonetheless, and disregarding differences in ionization efficiencies between TC present in the biomethane sample and in the SGM, the order of magnitude of the concentration threshold at which TC are present in the biomethane can be roughly estimated (50% error) from Fig.5.12 inasmuch as all compounds in the SGM are certified to be present at 1 ppm_{mol}. Most obvious TC in this biomethane sample (labelled on Fig.5.12) hence seem to have a ≤ 1 ppm_{mol} concentration threshold considering the similarity of their peak signal intensities to the peaks of the SGM compounds. Other TC in the biomethane probably lurk at lower concentrations.

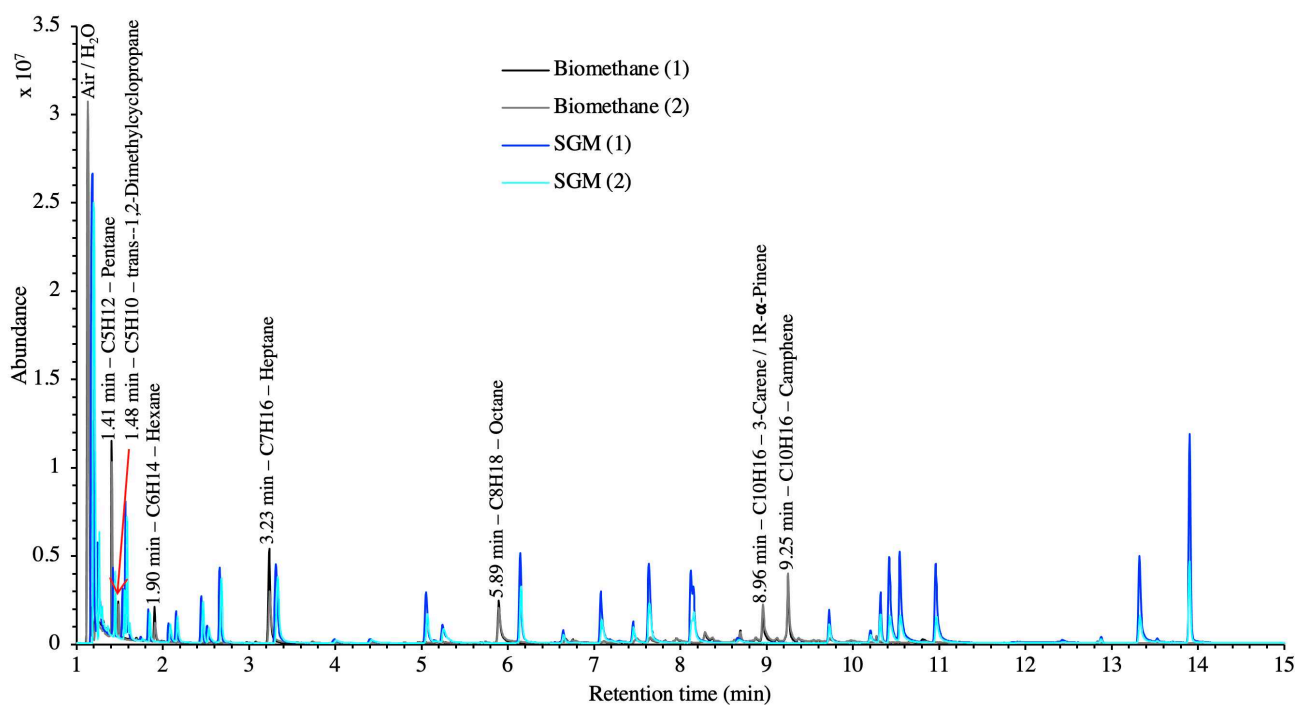


Figure 5.12: TIC of two biomethane replicates preconcentrated directly at 40 bar_a compared to the TIC of two 41 HVOC SGM replicates sampled and analyzed under the same conditions: 2 L_N collected at 40 bar_a on TA14-CpX29 MAT at 1 L_N·min⁻¹ in the HPTS.

IV. CONCLUSIONS AND PERSPECTIVES

A versatile field sampling method to easily preconcentrate trace compounds (TC) in gas samples at high working pressures ($\leq 200 \text{ bar}_a$) directly *in situ* on gas production sites has been presented. The high-pressure adsorbent tube sampling (HPTS) prototype hosting a TA14-CpX29 multibed adsorbent tube has been successfully applied to preconcentrate TC in a pressurized synthetic gas and a grid-injected biomethane. In the pressure range 5 – 100 bar_a , handled in French gas transport grids, the gas sampling pressure had no effect on the preconcentration of TC on the adsorbent tubes when the gas circulates through the tube and as long as the adsorbents are not saturated. The TA14-CpX29 multibed adsorbent tubes were found appropriate to preconcentrate, in a single sampling run, a wide range of volatile organic TC families in the synthetic gas and the biomethane: halogenated compounds, (poly)cyclic- and linear alkanes, alkenes, terpenes, aromatic compounds, Sulphur-compounds. Semi-quantification indicated pentane, dimethylcyclopropane, hexane, heptane, octane, α -pinene and camphene are present at a $\leq 1 \text{ ppm}_{\text{mol}}$ concentration threshold in the biomethane.

Regarding real gas sampling for TC determination, combining an efficient preconcentration support such as multibed adsorbent tubes with the HPTS prototype enables to circumvent the disadvantages of whole gas sampling where transport and subsequent transfer to a preconcentration unit are required. With direct *in situ* high pressure preconcentration of TC in pressurized gases, pressure regulators are bypassed, shortening the sampling line upstream preconcentration, hence diminishing contamination risks and TC loss risks by sorption onto surfaces in surplus valves, connectors and tubing. The preconcentration unit (here a multibed adsorbent tube) is directly plugged into the gas pipeline, avoiding transfers from a whole gas sampling vessel and associated contamination and TC loss risks by sorption to transfer lines. Additionally, adsorbent tubes shipment to the lab is easy, fast and secure in view of their small sizes and of the absence of the flammable gas matrix (in the case of biomethane). As moreover TC stability on adsorbent tubes is higher than in whole gas sampling vessels [21,27], sample storage stability issues are avoided.

It is believed the novel instrumentation presented will substantially help improving field sampling campaigns for the characterization of trace compounds in pressurized gas samples such as biomethane.

Associated Content

Supplemental information

Authors Informations

*Corresponding Author : Isabelle Le Hécho • isabelle.lehecho@univ-pau.fr • Université de Pau et des Pays de l'Adour, E2S UPPA, CNRS, IPREM UMR 5254, Technopôle Hélioparc, 2 avenue du Président Angot, 64053 Pau Cedex 09, France

Note

The authors declare no competing financial interests or personal relationships that could have influenced the work reported in this paper.

Acknowledgements

The authors thank *Teréga* (40 Avenue de l'Europe, CS 20 522, 64010 Pau Cedex, France) for the financial support and *nCx Instrumentation* (ZAE Porte du Béarn, 64330 Garlin, France) for the loan of the thermodesorber prototype. Authors are also grateful to the operators of the biogas-biomethane production plant and to the operators of the biomethane grid injection station for their availability and cooperation during sampling operations and for the technical information provided.

V. SUPPLEMENTAL INFORMATION CHAPTER 5

Theoretical note on multibed adsorbent tubes

Multibed adsorbent tubes (MAT) are attractive preconcentration supports for complex gas samples with unknown composition such as biomethane in view of the large diversity of chemical TC families it can contain [1–6] with associated large boiling points- and polarity-ranges [5,7]. While not any adsorbent is universal enough to adsorb all TC [5,8], the working principle of a MAT precisely enables to preconcentrate a large range of TC in a wide volatility range in one single sampling run. In a MAT, different adsorbents are arranged in order of increasing sorption strength (increasing surface area, decreasing pore size) in the gas sampling direction [9,10]. As the gas matrix (CH₄ in the case of biomethane) passes through the tube without being retained due to its too high volatility, the weak front adsorbent (here Tenax®TA) traps relatively large, heavy, high-boiling TC (boiling point > ~80°C) but is not strong enough to retain small volatile nor very volatile TC (boiling point < ~50 – 80°C). Those hence move onwards to the next gradually stronger adsorbent beds (here Carbopack™X) whereon they eventually get adsorbed. Importantly, thermodesorption of MAT must occur in the reverse direction as compared to the gas sampling direction. Thermodesorbing a MAT in the same direction as sampling would result in the carrier gas of the TD to blow high-boiling compounds desorbed from the weak front bed towards the stronger back bed whereon they could (partly) re-adsorb and not enter the GC-column. The critical benefits of MAT are that (1) the gas matrix is not retained enabling preconcentration ('isolation') of TC, (2) high-boiling TC never meet strong adsorbents whereon they would irreversibly adsorb, impeding their desorption upon analysis, and (3) very volatile TC can be trapped on and desorbed from strong adsorbents. Therefore, MAT enable quantitative adsorption and desorption (which is analytically at least as important as adsorption) of TC over a wider volatility and polarity range than single adsorbent beds do.

References

- [1] F. Hilaire, E. Basset, R. Bayard, M. Gallardo, D. Thiebaut, J. Vial, Comprehensive Two-Dimensional Gas Chromatography for Biogas and Biomethane Analysis, *Journal of Chromatography A*. 1524 (2017) 222–232. <https://doi.org/10.1016/j.chroma.2017.09.071>.
- [2] M. Ghidotti, D. Fabbri, C. Torri, Determination of Linear and Cyclic Volatile Methyl Siloxanes in Biogas and Biomethane by Solid-Phase Microextraction and Gas Chromatography-Mass Spectrometry, *Talanta*. 195 (2019) 258–264. <https://doi.org/10.1016/j.talanta.2018.11.032>.
- [3] S. Rasi, J. Lantela, J. Rintala, Trace Compounds Affecting Biogas Energy Utilisation – A Review, *Energy Conversion and Management*. 52 (2011) 3369–3375. <https://doi.org/10.1016/j.enconman.2011.07.005>.
- [4] K. Arrhenius, A. Fischer, O. B ker, Methods for Sampling Biogas and Biomethane on Adsorbent Tubes After Collection in Gas Bags, *Applied Sciences*. 9 (2019) 1171. <https://doi.org/10.3390/app9061171>.
- [5] K. Arrhenius, A.S. Brown, A.M.H. van der Veen, Suitability of Different Containers for the Sampling and Storage of Biogas and Biomethane for the Determination of the Trace-Level Impurities – A Review, *Analytica Chimica Acta*. 902 (2016) 22–32. <https://doi.org/10.1016/j.aca.2015.10.039>.
- [6] K. Arrhenius, H. Yaghooby, L. Rosell, O. B ker, L. Culleton, S. Bartlett, A. Murugan, P. Brewer, J. Li, A.M.H. van der Veen, I. Krom, F. Lestremau, J. Beranek, Suitability of Vessels and Adsorbents for the Short-Term Storage of Biogas/Biomethane for the Determination of Impurities – Siloxanes, Sulfur Compounds, Halogenated Hydrocarbons, BTEX, Biomass and Bioenergy. 105 (2017) 127–135. <https://doi.org/10.1016/j.biombioe.2017.06.025>.
- [7] E. Gallego, F.J. Roca, J.F. Perales, X. Guardino, E. Gadea, Development of a Method for Determination of VOCs (including Methylsiloxanes) in Biogas by TD-GC/MS Analysis Using Supel™ Inert

Film Bags and Multisorbent Bed Tubes, *International Journal of Environmental Analytical Chemistry*. 95 (2015) 291–311. <https://doi.org/10.1080/03067319.2015.1016012>.

[8] J. Brown, B. Shirey, A Tool for Selecting an Adsorbent for Thermal Desorption Applications. Technical Report, (2001). https://www.sigmaaldrich.com/content/dam/sigmaaldrich/docs/Supelco/General_Information/t402025.pdf (accessed April 23, 2020).

[9] US EPA, Compendium of Methods for the Determination of Toxic Organic Compounds in Ambient Air. Second Edition. Compendium Method TO-17: Determination of Volatile Organic Compounds in Ambient Air Using Active Sampling Onto Sorbent Tubes (EPA/625/R-96/010b), (1999). <https://www3.epa.gov/ttnamti1/files/ambient/airtox/to-17r.pdf> (accessed April 23, 2020).

[10] M. Harper, Review. Sorbent Trapping of Volatile Organic Compounds from Air, *Journal of Chromatography A*. 885 (2000) 129–151. [https://doi.org/10.1016/S0021-9673\(00\)00363-0](https://doi.org/10.1016/S0021-9673(00)00363-0).

Supplemental Tables

*Table 5.SI-1: Chromatographic retention times (min) of compounds identified from the TD-GC-MS analysis of the SGM sampled at different test-pressures and different volumes at 1 L_N·min⁻¹ on the TA14-CpX29 MAT in the HPTS prototype. STDEV : standard deviation. * : absent. ◊ : co-elution of tetrachloromethane, acrylonitrile and benzene*

Sampling pressure (bara)	100		40		1		5		
Sampled volume (L _N)	2		2		5		2		
Replicates	n=3		n=2		n=1		n=2		
Compounds from the SGM	Mean	STDEV	Mean	STDEV	Value	Mean	STDEV	Mean	STDEV
Dichlorodifluoromethane	1.217	0.018	1.227	0.018	1.217	1.250	0.006	1.245	0.030
Chloromethane	*	*	*	*	*	*	*	*	*
Chloroethene	1.270	0.013	1.282	0.025	1.267	1.300	0.005	1.294	0.030
1,3-Butadiene	1.275	0.023	1.283	0.008	1.28	1.311	0.006	1.306	0.030
1,2-Dichloro-1,1,2,2-tetrafluoroethane	1.244	0.017	1.254	0.018	1.245	1.277	0.006	1.271	0.031
Bromomethane	1.325	0.017	1.334	0.017	1.326	1.357	0.006	1.352	0.030
Chloroethane	1.345	0.017	1.354	0.017	1.348	1.377	0.006	1.371	0.029
Trichloromonofluoromethane	1.427	0.016	1.436	0.017	1.429	1.459	0.006	1.453	0.029
1,1-Dichloroethene	1.538	0.015	1.546	0.016	1.54	1.568	0.006	1.563	0.028
Dichloromethane	1.602	0.015	1.611	0.016	1.606	1.633	0.006	1.627	0.027
1,1,2-Trichloro-1,2,2-trifluoroethane	1.569	0.015	1.577	0.016	1.571	1.599	0.006	1.594	0.028
1,1-Dichloroethane	1.833	0.014	1.841	0.016	1.836	1.863	0.006	1.857	0.027
cis-1,2-Dichloroethene	2.070	0.014	2.079	0.015	2.073	2.101	0.006	2.093	0.025
Trichloromethane	2.157	0.014	2.164	0.016	2.159	2.185	0.007	2.178	0.025
1,1,1-Trichloroethane	2.451	0.014	2.457	0.014	2.452	2.479	0.006	2.471	0.025
Tetrachloromethane ◊	2.664	0.013	2.671	0.013	2.666	2.691	0.007	2.684	0.025
Acrylonitrile ◊	2.664	0.013	2.671	0.013	2.666	2.691	0.007	2.684	0.025
Benzene ◊	2.664	0.013	2.671	0.013	2.666	2.691	0.007	2.684	0.025
1,2-Dichloroethane	2.517	0.015	2.525	0.015	2.516	2.548	0.007	2.537	0.024
Trichloroethene	3.317	0.013	3.323	0.014	3.318	3.345	0.008	3.335	0.024
1,2-Dichloropropane	*	*	*	*	*	*	*	*	*
cis-1,3-Dichloropropene	4.401	0.015	4.413	0.014	4.389	4.447	0.001	4.416	0.017
Toluene	5.056	0.011	5.060	0.011	5.058	5.077	0.006	5.068	0.018
trans-1,3-Dichloropropene	5.139	0.017	5.159	0.022	5.119	5.270	0.004	5.149	0.014
1,1,2-Trichloroethane	5.242	0.011	5.251	0.011	5.233	5.201	/	5.250	0.014
Tetrachloroethene	6.145	0.008	6.148	0.007	6.15	6.159	0.004	6.153	0.011
Chlorobenzene	7.080	0.009	7.083	0.008	7.077	7.098	0.001	7.085	0.010
1,2-Dibromoethane	6.103	0.015	6.119	0.007	6.087	6.150	0.008	6.114	0.009
Ethylbenzene	7.452	0.004	7.456	0.004	7.452	7.463	0.001	7.458	0.004
p-Xylene	7.637	0.006	7.639	0.005	7.649	7.648	0.002	7.642	0.007
m-Xylene	7.637	0.006	7.639	0.005	7.649	7.648	0.002	7.642	0.007
o-Xylene	8.149	0.010	8.153	0.005	8.163	8.161	0.001	8.154	0.010
Styrene	8.127	0.010	8.128	0.008	8.13	8.139	0.000	8.130	0.009
1,1,2,2-Tetrachloroethane	8.663	0.013	8.676	0.011	8.638	8.694	0.003	8.661	0.007
1,3,5-Trimethylbenzene	9.724	0.002	9.727	0.002	9.727	9.730	0.001	9.727	0.002
1,2,4-Trimethylbenzene	10.200	0.003	10.204	0.003	10.2	10.207	0.000	10.202	0.001
1,3-Dichlorobenzene	10.423	0.006	10.425	0.006	10.422	10.436	0.000	10.424	0.005
1,4-Dichlorobenzene	10.546	0.005	10.548	0.006	10.547	10.556	0.000	10.548	0.004
1,2-Dichlorobenzene	10.960	0.006	10.963	0.007	10.959	10.974	0.001	10.962	0.006
1,2,4-Trichlorobenzene	13.323	0.005	13.324	0.004	13.324	13.333	0.001	13.324	0.003
Hexachloro-1,3-Butadiene	13.903	0.001	13.904	0.001	13.913	13.904	0.001	13.906	0.002

Supplemental Figures

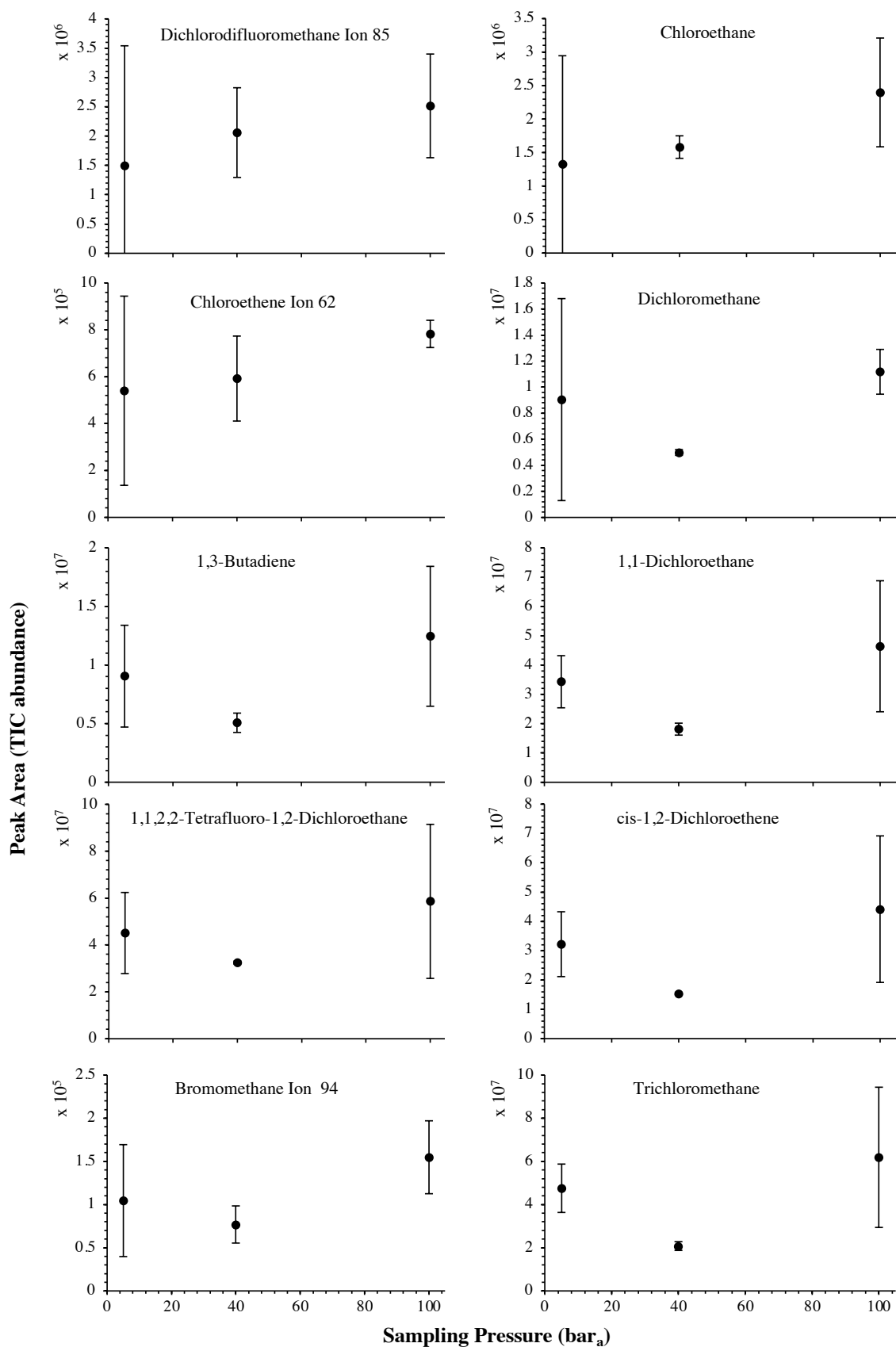


Figure 5.SI-1: High-pressure adsorption isotherms of the HVOC not shown in Fig.5.4 of the core paper for test-condition A (2 L_N of the SGM sampled at 5, 40 and 100 bar_a on TA14-CpX29 MAT). Average peak area with indication of the standard deviation.

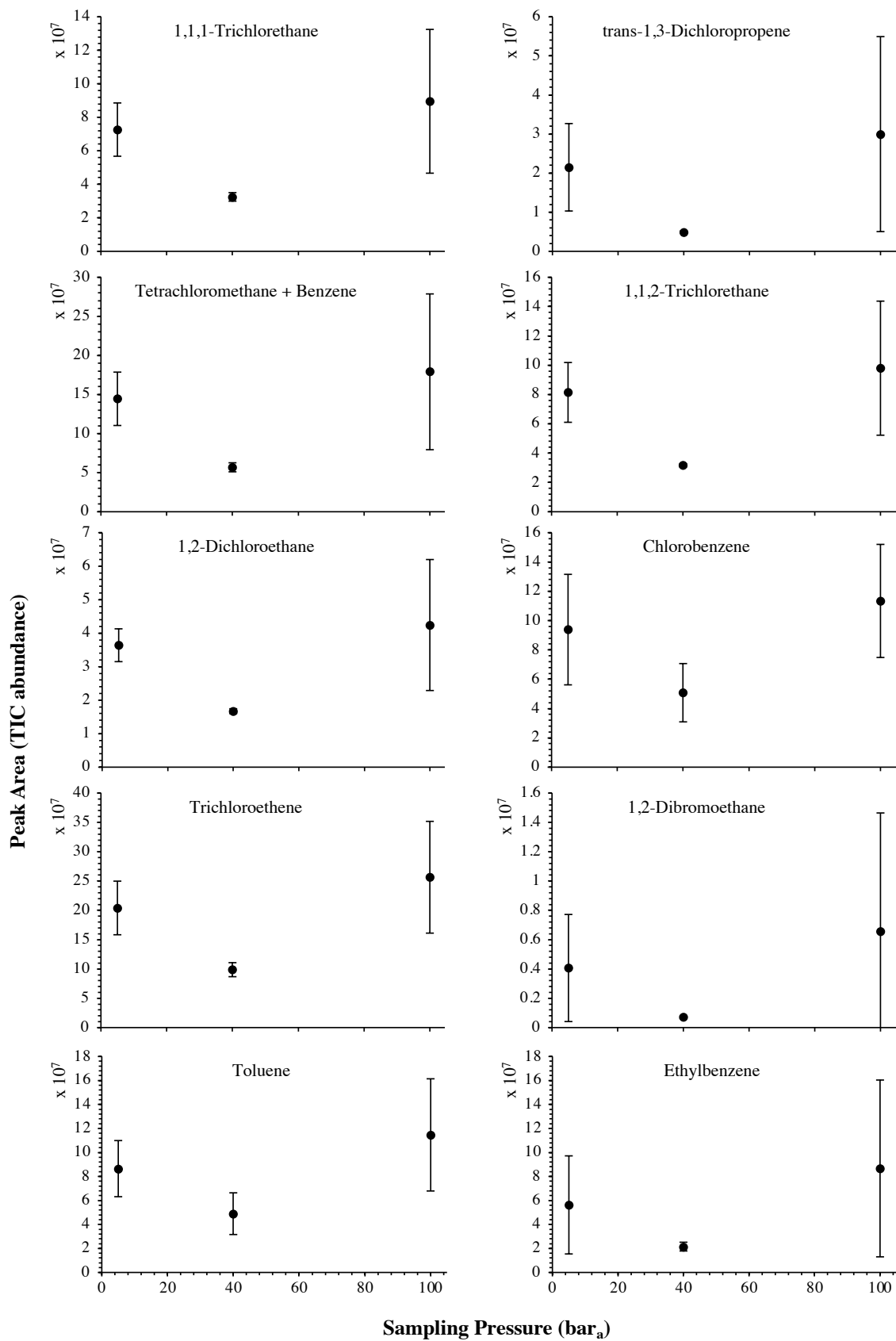


Figure 5.SI-1: continued (1).

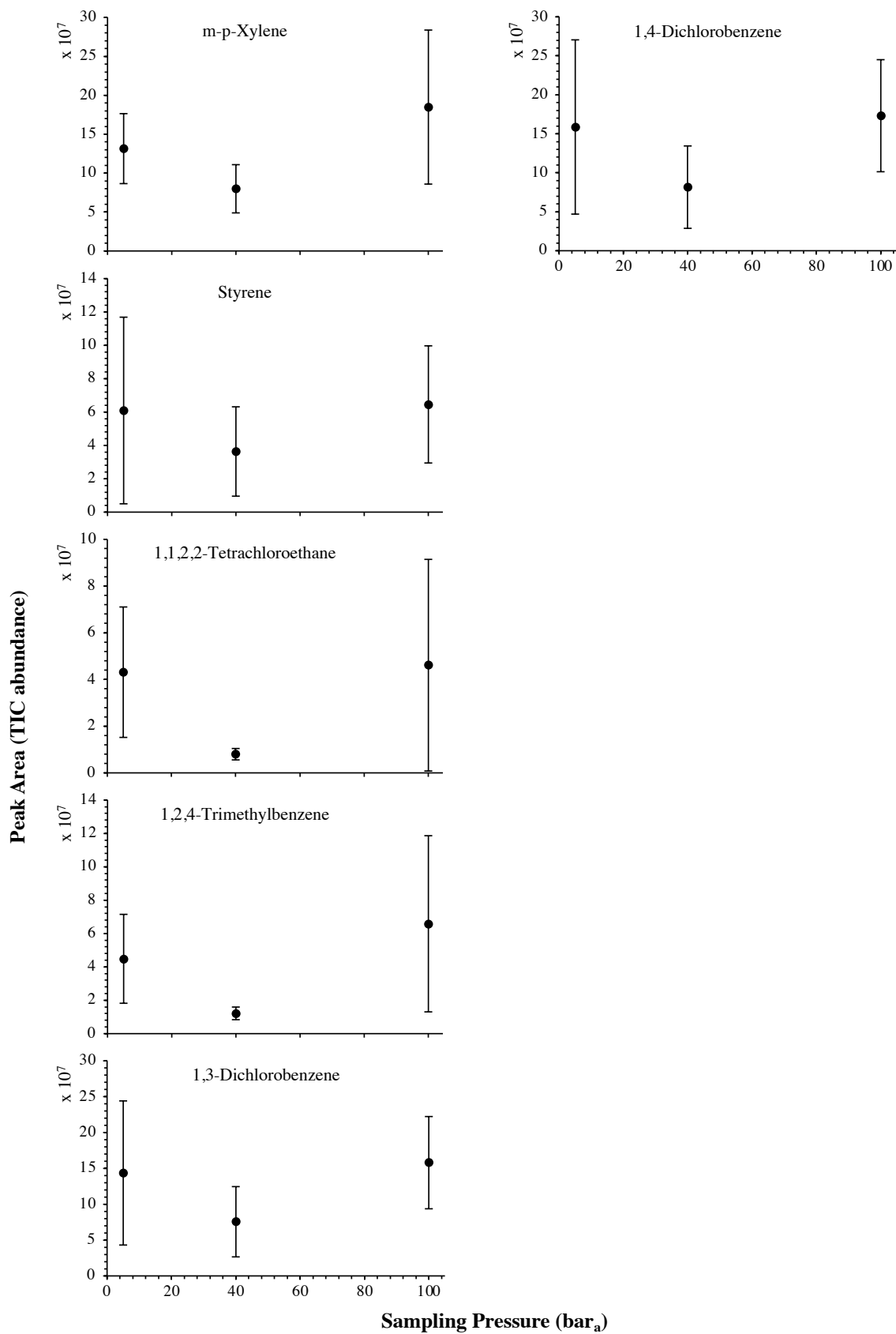


Figure 5.SI-1: continued (2).

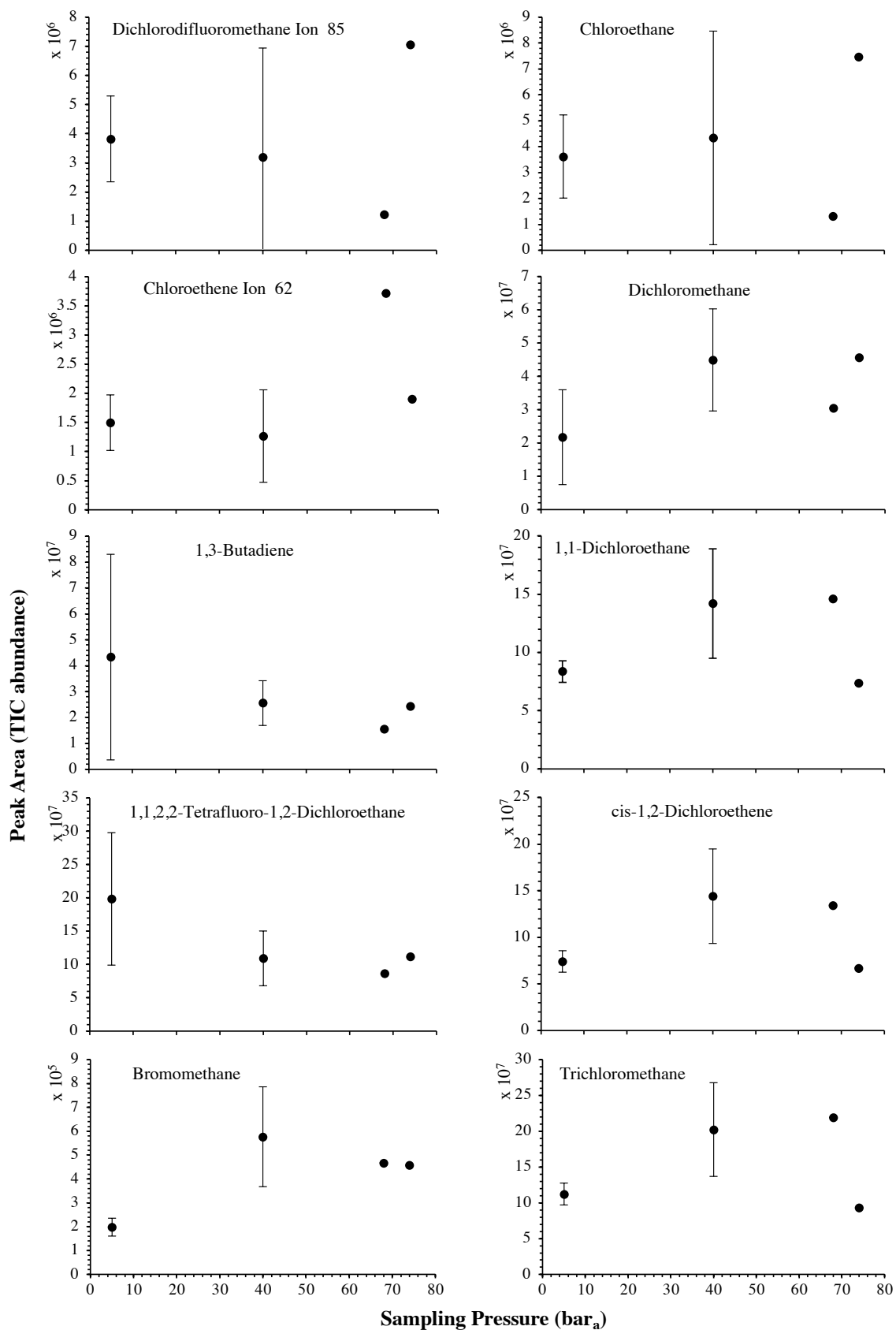


Figure 5.SI-2: High-pressure adsorption isotherms of the HVOC not shown in Fig.5.5 of the core paper for test-condition B (5 L_N of the SGM sampled at 5, 40, 68 and 74 bar_a on TA14-CpX29 MAT). Average peak area with indication of the standard deviation.

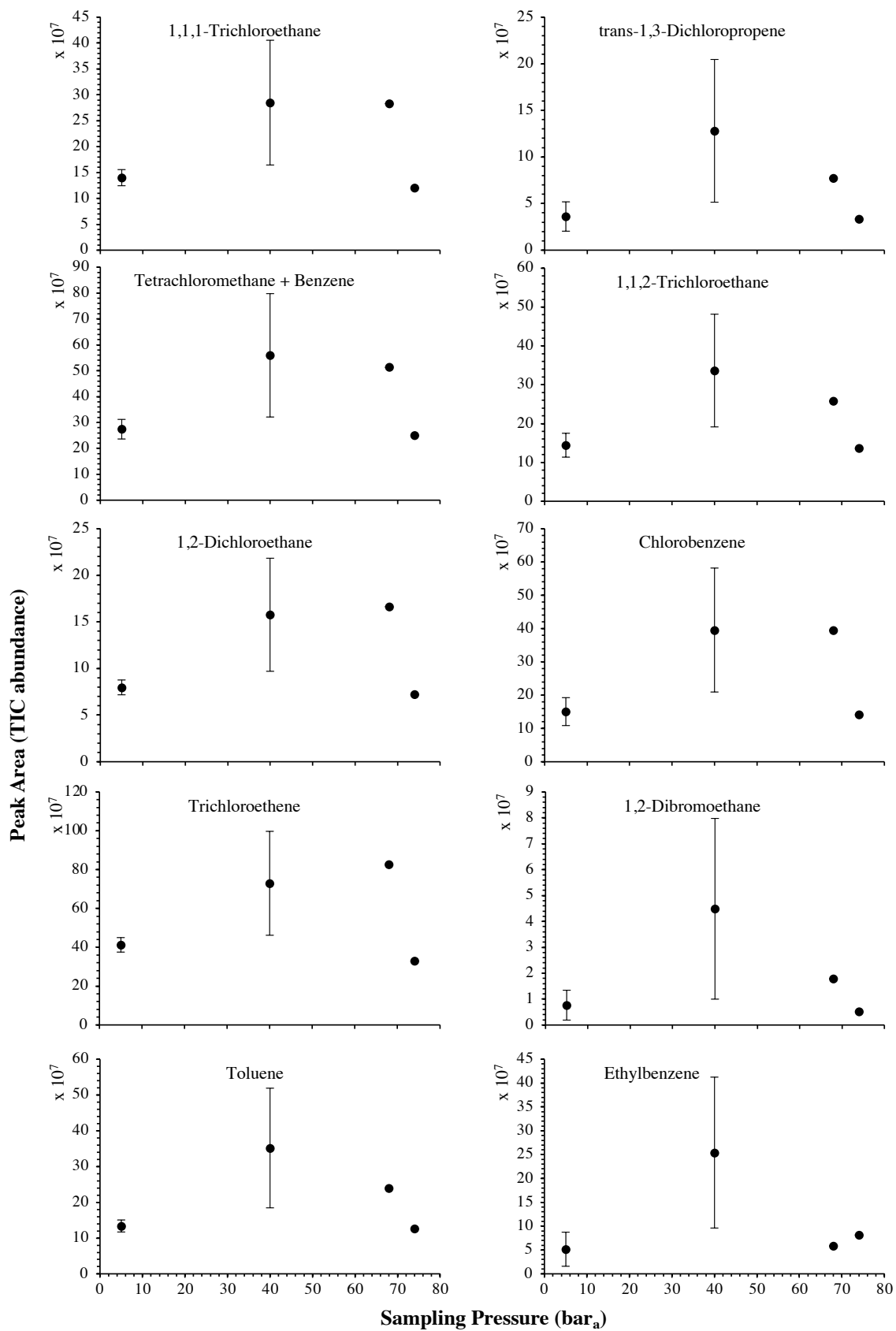


Figure 5.SI-2: continued (1)

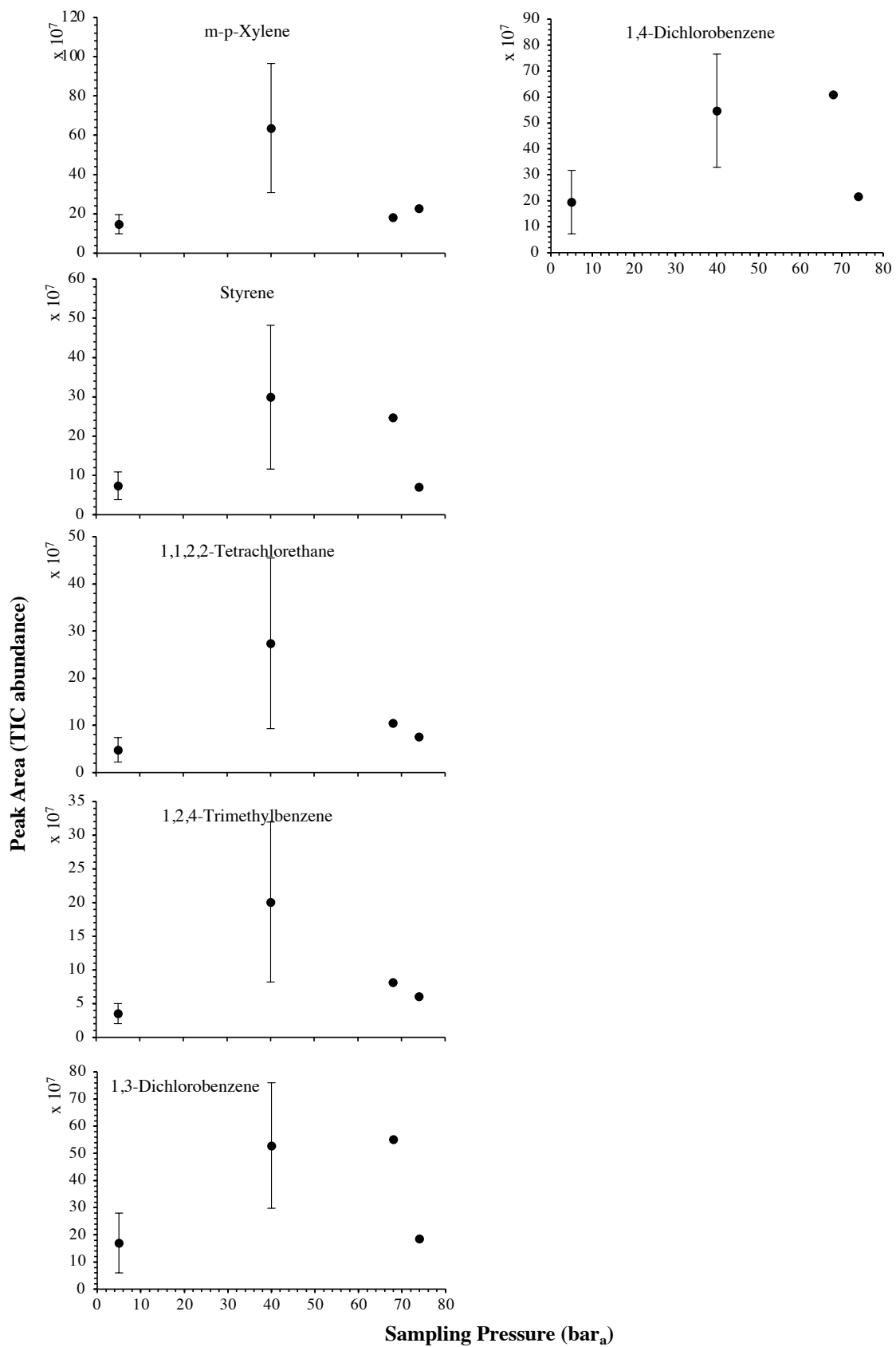


Figure 5.SI-2: continued (2)

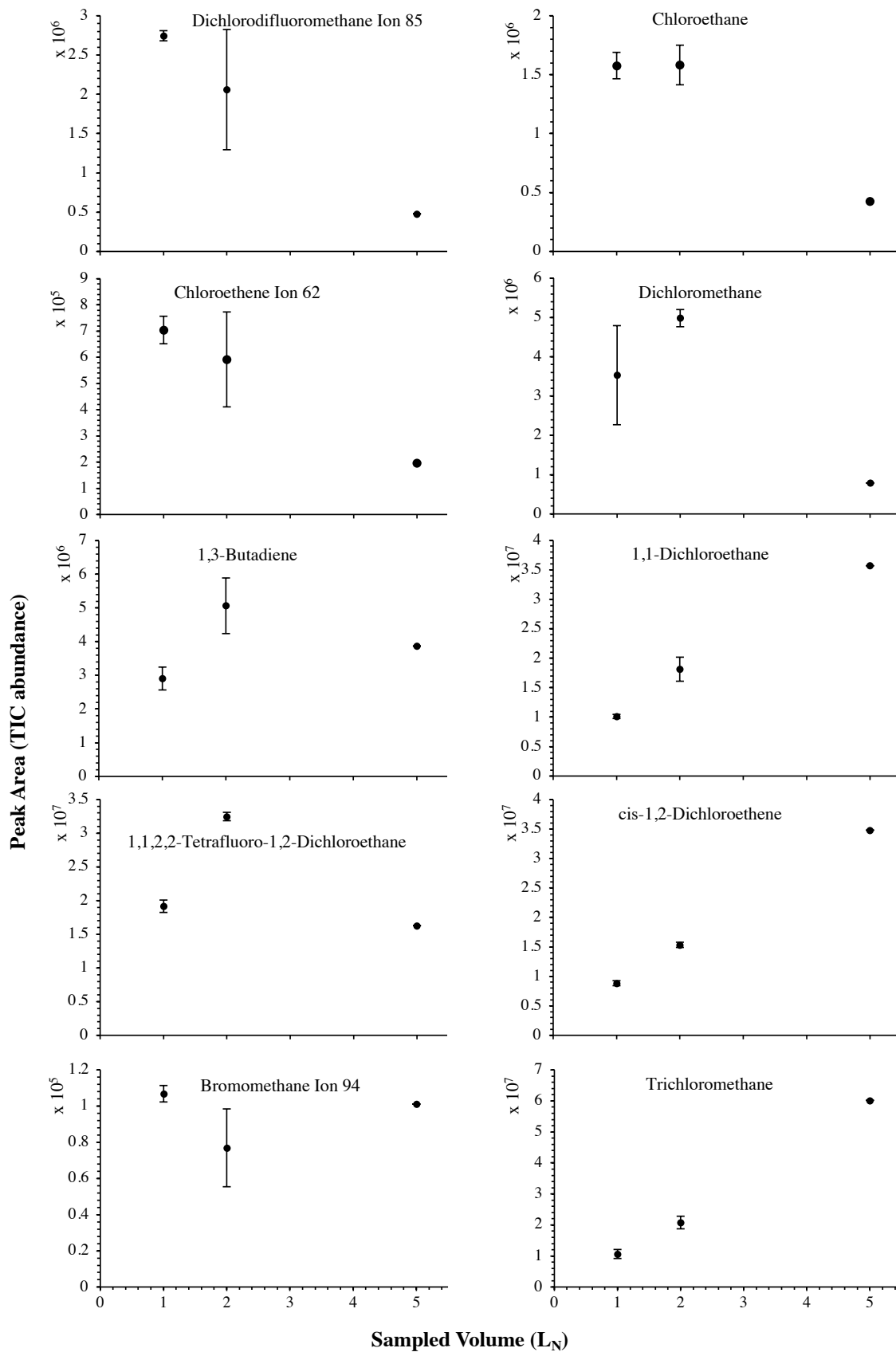


Figure 5.SI-3: Partial breakthrough curves for the HVOC not shown in Fig.5.6 of the core paper for test-condition C (1, 2 and 5 LN of the SGM sampled at 40 bar_a on TA14-CpX29 MAT). Average peak area with indication of the standard deviation.

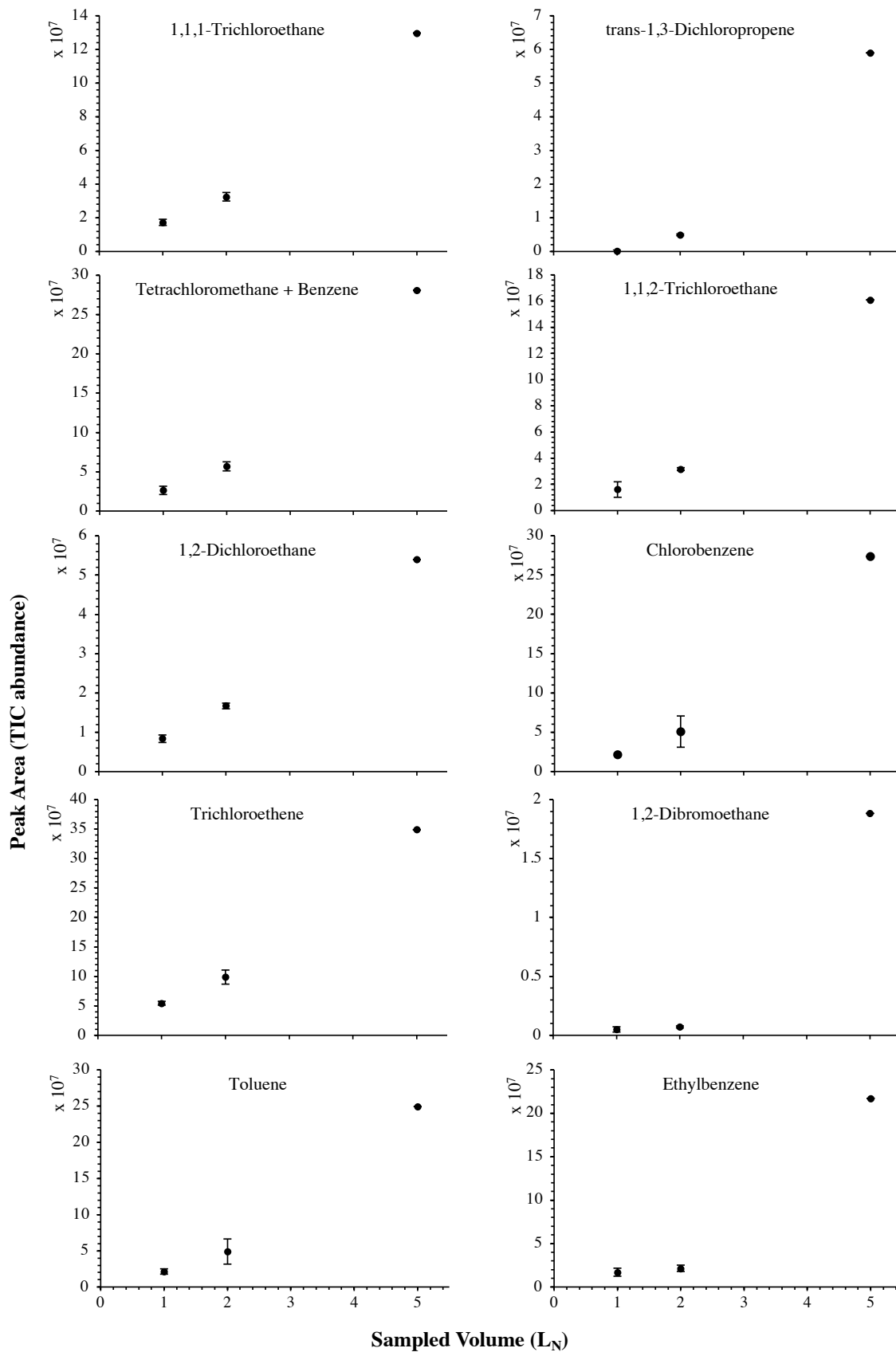


Figure 5.SI-3 : continued (1).

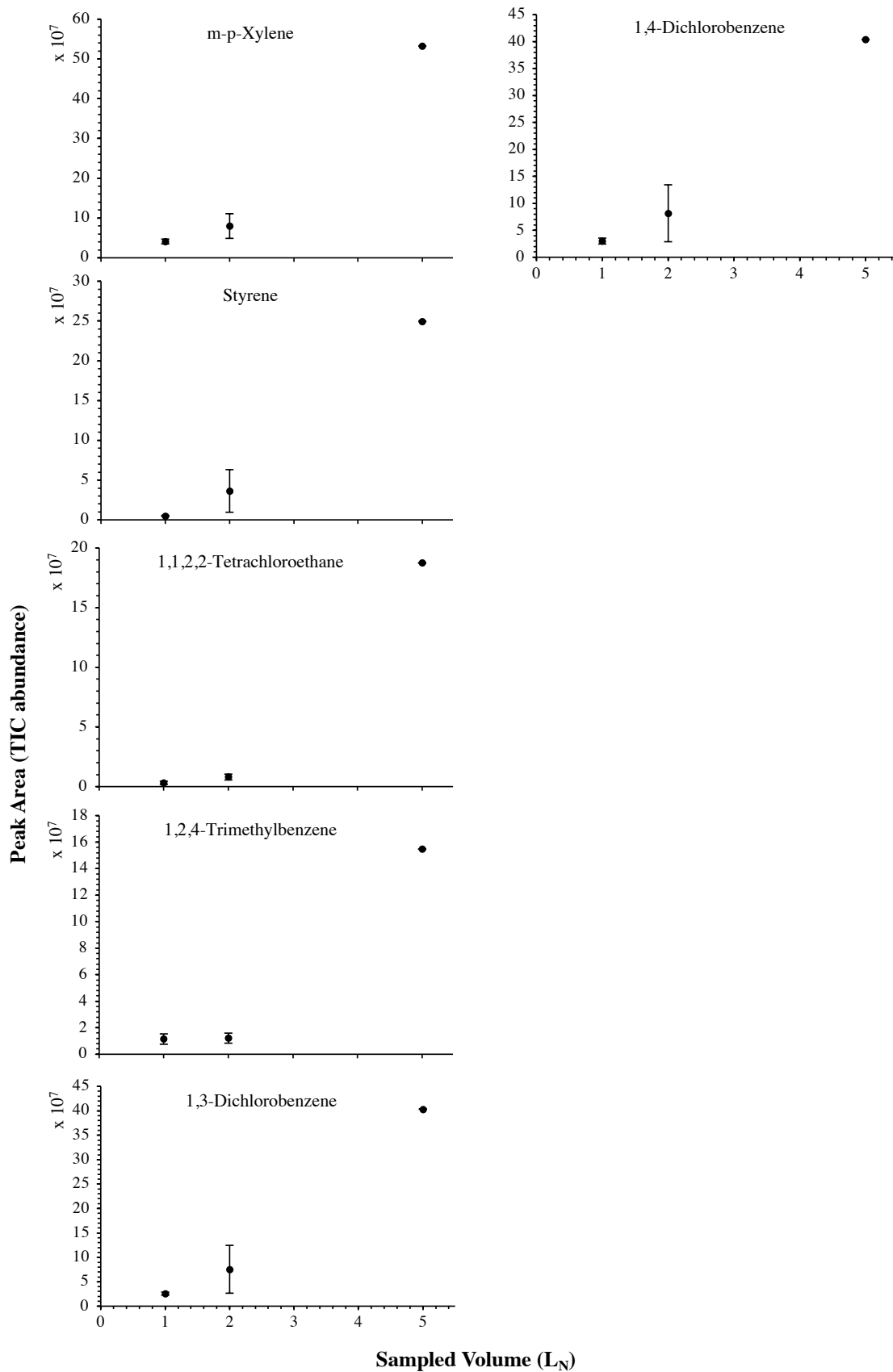


Figure 5.SI-3 : continued (2).

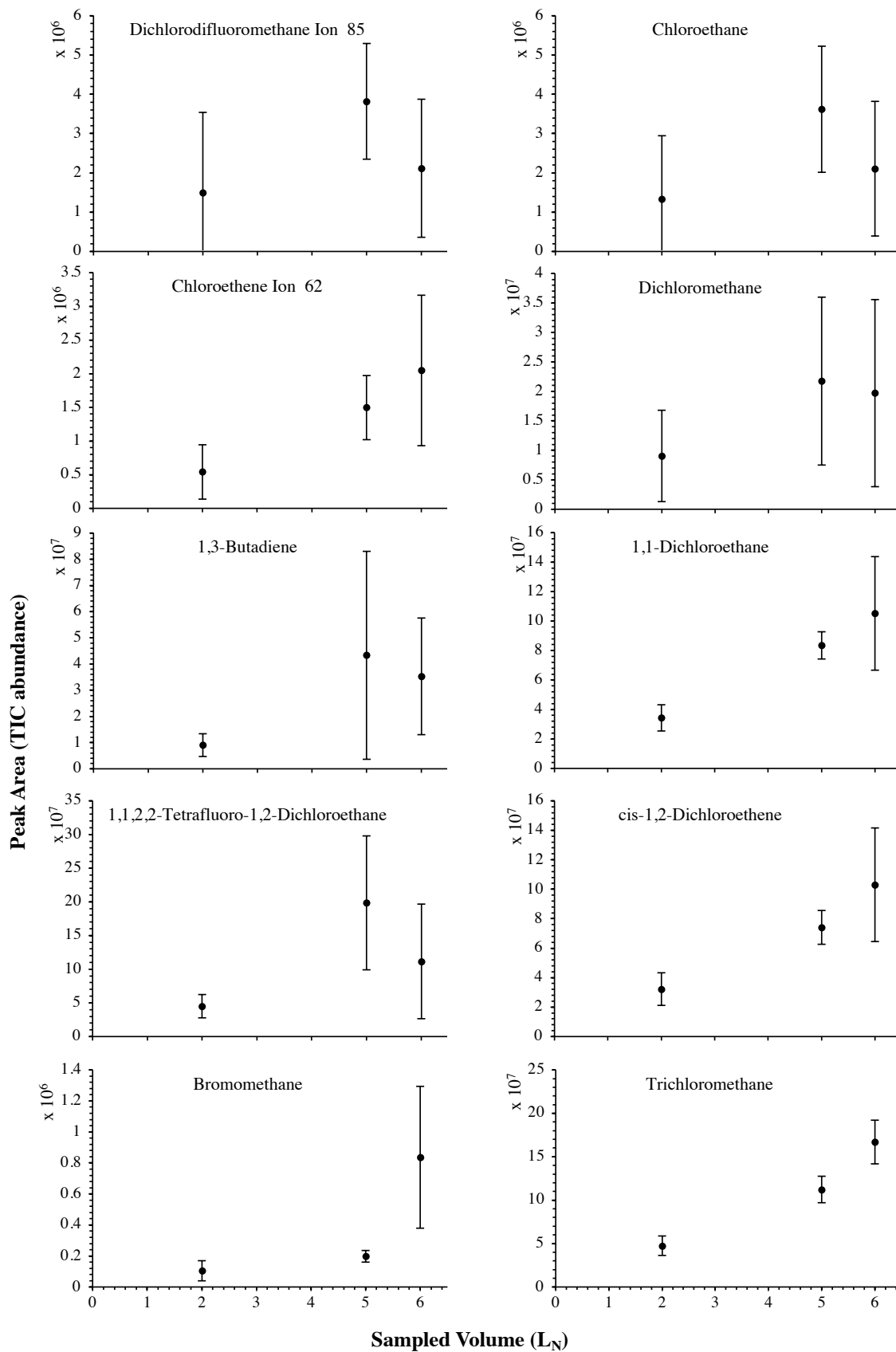


Figure 5.SI-4: Partial breakthrough curves for the HVOC not shown in Fig.5.7 of the core paper for test-condition D (2, 5 and 6 L_N of the SGM sampled at 5 bar_a on TA14-CpX29 MAT). Average peak area with indication of the standard deviation.

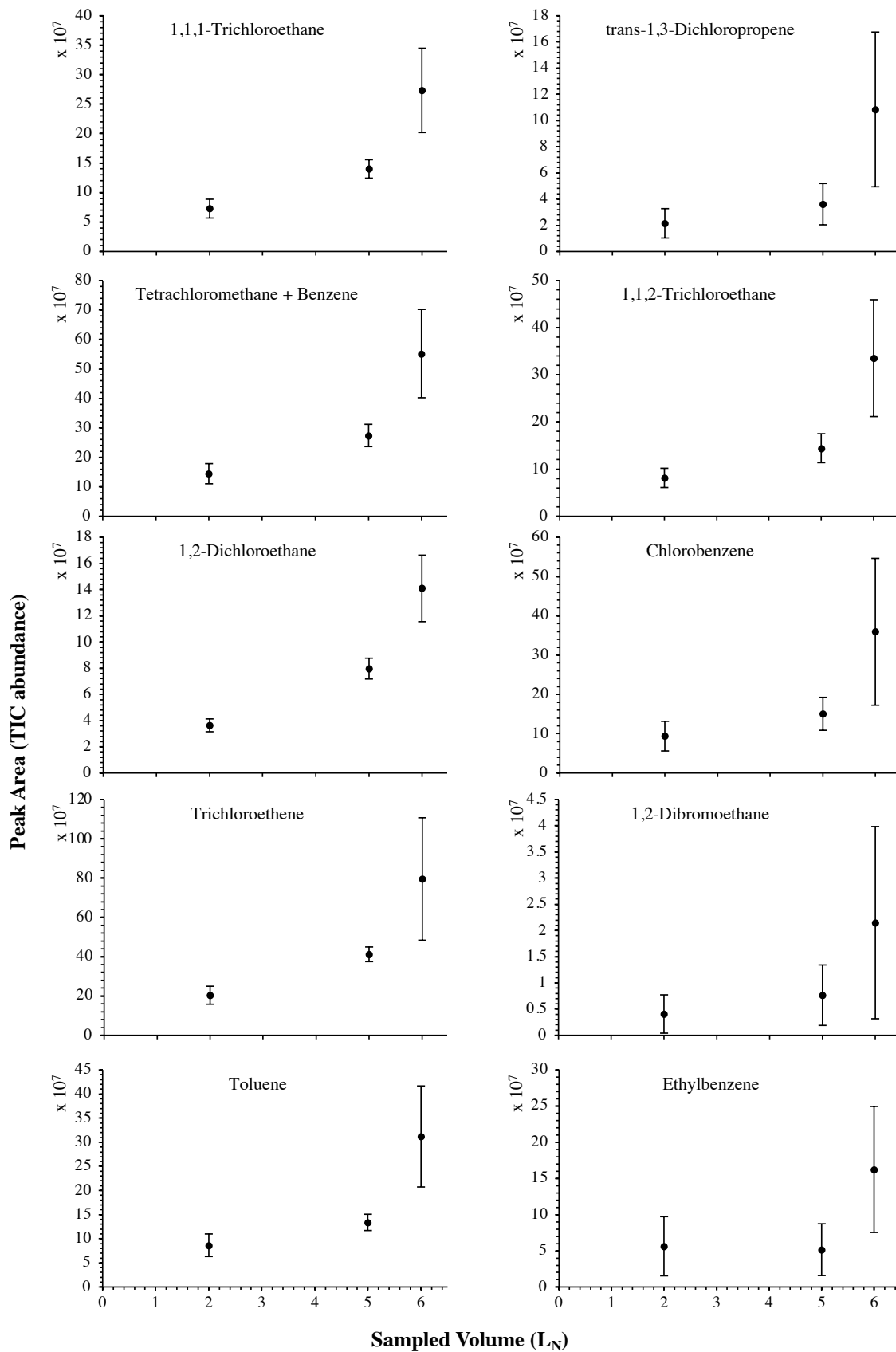


Figure 5.SI-4 : continued (1).

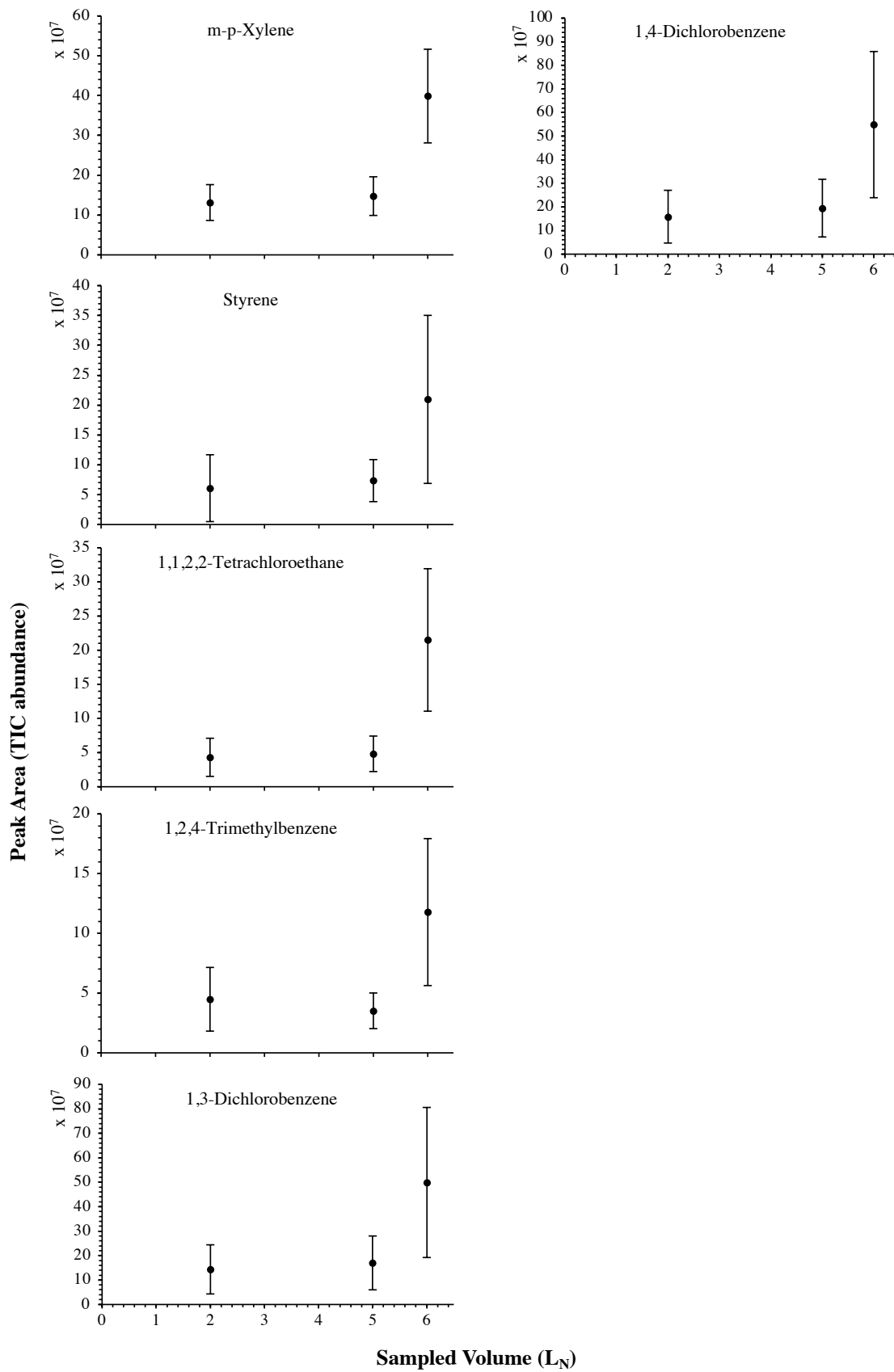


Figure 5.SI-4 : continued (2).

VI. REFERENCES CHAPTER 5

- [1] Ministère de la Transition Ecologique et Solidaire, République Française, Synthèse Stratégie Française pour l'Energie et le Climat - Programmation Pluriannuelle de l'Energie 2019-2023 & 2024-2028, (2018).
- [2] I. Angelidaki, L. Treu, P. Tsapekos, G. Luo, S. Campanaro, H. Wenzel, P.G. Kougias, Biogas Upgrading and Utilization: Current Status and Perspectives, *Biotechnology Advances*. 36 (2018) 452–466. <https://doi.org/10.1016/j.biotechadv.2018.01.011>.
- [3] S. Rasi, A. Veijanen, J. Rintala, Trace Compounds of Biogas from Different Biogas Production Plants, *Energy*. 32 (2007) 1375–1380. <https://doi.org/10.1016/j.energy.2006.10.018>.
- [4] M.R. Allen, A. Braithwaite, C.C. Hills, Trace Organic Compounds in Landfill Gas at Seven U.K. Waste Disposal Sites, *Environmental Science & Technology*. 31 (1997) 1054–1061. <https://doi.org/10.1021/es9605634>.
- [5] P.Y. Hoo, H. Hashim, W.S. Ho, Opportunities and Challenges: Landfill Gas to Biomethane Injection into Natural Gas Distribution Grid Through Pipeline, *Journal of Cleaner Production*. 175 (2018) 409–419. <https://doi.org/10.1016/j.jclepro.2017.11.193>.
- [6] R. Augelletti, M. Conti, M.C. Annesini, Pressure Swing Adsorption for Biogas Upgrading. A New Process Configuration for the Separation of Biomethane and Carbon Dioxide, *Journal of Cleaner Production*. 140 (2017) 1390–1398. <https://doi.org/10.1016/j.jclepro.2016.10.013>.
- [7] G. Leonzio, Upgrading of Biogas to Bio-Methane with Chemical Absorption Process: Simulation and Environmental Impact, *Journal of Cleaner Production*. 131 (2016) 364–375. <https://doi.org/10.1016/j.jclepro.2016.05.020>.
- [8] Z. Bacsik, O. Cheung, P. Vasiliev, N. Hedin, Selective Separation of CO₂ and CH₄ for Biogas Upgrading on Zeolite NaKa and SAPO-56, *Applied Energy*. 162 (2016) 613–621. <https://doi.org/10.1016/j.apenergy.2015.10.109>.
- [9] A. Toledo-Cervantes, C. Madrid-Chirinos, S. Cantera, R. Lebrero, R. Muñoz, Influence of the Gas-Liquid Flow Configuration in the Absorption Column on Photosynthetic Biogas Upgrading in Algal-Bacterial Photobioreactors, *Bioresource Technology*. 225 (2017) 336–342. <https://doi.org/10.1016/j.biortech.2016.11.087>.
- [10] Y. Chhiti, M. Kemih, Thermal Conversion of Biomass, Pyrolysis and Gasification: A Review, *The International Journal of Engineering And Science*. 2 (2013) 75–85.
- [11] K. Koido, T. Iwasaki, Chapter 7 - Biomass Gasification: A Review of Its Technology, Gas Cleaning Applications, and Total System Life Cycle Analysis, in: M. Poletto (Ed.), *Lignin - Trends and Applications*, InTech, 2018. <https://doi.org/10.5772/intechopen.70727>.
- [12] J. Kopyscinski, T.J. Schildhauer, S.M.A. Biollaz, Production of Synthetic Natural Gas (SNG) from Coal and Dry Biomass – a Technology Review from 1950 to 2009, *Fuel*. 89 (2010) 1763–1783. <https://doi.org/10.1016/j.fuel.2010.01.027>.
- [13] S. Rönsch, J. Schneider, S. Matthischke, M. Schlüter, M. Götz, J. Lefebvre, P. Prabhakaran, S. Bajohr, Review on Methanation – from Fundamentals to Current Projects, *Fuel*. 166 (2016) 276–296. <https://doi.org/10.1016/j.fuel.2015.10.111>.

- [14] European Committee for Standardization, EN 16723-1 Natural Gas and Biomethane for Use in Transport and Biomethane for Injection in Natural Gas Network - Part 1: Specifications for Biomethane for Injection in the Natural Gas Network, (2016).
- [15] European Committee for Standardization, EN 16723-2 Natural Gas and Biomethane for Use in Transport and Biomethane for Injection in the Natural Gas Network - Part 2: Automotive Fuels Specification, (2017).
- [16] F. Hilaire, E. Basset, R. Bayard, M. Gallardo, D. Thiebaut, J. Vial, Comprehensive Two-Dimensional Gas Chromatography for Biogas and Biomethane Analysis, *Journal of Chromatography A*. 1524 (2017) 222–232. <https://doi.org/10.1016/j.chroma.2017.09.071>.
- [17] M. Ghidotti, D. Fabbri, C. Torri, Determination of Linear and Cyclic Volatile Methyl Siloxanes in Biogas and Biomethane by Solid-Phase Microextraction and Gas Chromatography-Mass Spectrometry, *Talanta*. 195 (2019) 258–264. <https://doi.org/10.1016/j.talanta.2018.11.032>.
- [18] S. Rasi, J. Läntelä, J. Rintala, Trace Compounds Affecting Biogas Energy Utilisation – A Review, *Energy Conversion and Management*. 52 (2011) 3369–3375. <https://doi.org/10.1016/j.enconman.2011.07.005>.
- [19] K. Arrhenius, A. Fischer, O. Büker, Methods for Sampling Biogas and Biomethane on Adsorbent Tubes After Collection in Gas Bags, *Applied Sciences*. 9 (2019) 1171. <https://doi.org/10.3390/app9061171>.
- [20] K. Arrhenius, A.S. Brown, A.M.H. van der Veen, Suitability of Different Containers for the Sampling and Storage of Biogas and Biomethane for the Determination of the Trace-Level Impurities – A Review, *Analytica Chimica Acta*. 902 (2016) 22–32. <https://doi.org/10.1016/j.aca.2015.10.039>.
- [21] K. Arrhenius, H. Yaghooby, L. Rosell, O. Büker, L. Culleton, S. Bartlett, A. Murugan, P. Brewer, J. Li, A.M.H. van der Veen, I. Krom, F. Lestremau, J. Beranek, Suitability of Vessels and Adsorbents for the Short-Term Storage of Biogas/Biomethane for the Determination of Impurities – Siloxanes, Sulfur Compounds, Halogenated Hydrocarbons, BTEX, Biomass and Bioenergy. 105 (2017) 127–135. <https://doi.org/10.1016/j.biombioe.2017.06.025>.
- [22] M. Cachia, B. Bouyssiére, H. Carrier, H. Garraud, G. Caumette, I. Le Hécho, Characterization and Comparison of Trace Metal Compositions in Natural Gas, Biogas, and Biomethane, *Energy & Fuels*. 32 (2018) 6397–6400. <https://doi.org/10.1021/acs.energyfuels.7b03915>.
- [23] J. Feldmann, Determination of Ni(CO)₄, Fe(CO)₅, Mo(CO)₆, and W(CO)₆ in Sewage Gas by Using Cryotrapping Gas Chromatography Inductively Coupled Plasma Mass Spectrometry, *Journal of Environmental Monitoring*. 1 (1999) 33–37. <https://doi.org/10.1039/A807277I>.
- [24] J. Feldmann, I. Koch, W.R. Cullen, Complementary Use of Capillary Gas Chromatography–Mass Spectrometry (ion Trap) and Gas Chromatography–Inductively Coupled Plasma Mass Spectrometry for the Speciation of Volatile Antimony, Tin and Bismuth Compounds in Landfill and Fermentation Gases, *The Analyst*. 123 (1998) 815–820. <https://doi.org/10.1039/a707478f>.
- [25] European Committee for Standardization, EN 16726 Gas Infrastructure - Quality of Gas

- Group H, (2015).

[26] K. Arrhenius, A. Holmqvist, M. Carlsson, J. Engelbrektsson, A. Jansson, L. Rosell, H. Yaghooby, A. Fischer, Terpenes in Biogas Plants Digesting Food Wastes. Study to Gain Insight into the Role of Terpenes. Energiforsk AB. ISBN 978-91-7673-350-9, (2017).

[27] S. Mariné, M. Pedrouzo, R.M. Marcé, I. Fonseca, F. Borrull, Comparison Between Sampling and Analytical Methods in Characterization of Pollutants in Biogas, *Talanta*. 100 (2012) 145–152. <https://doi.org/10.1016/j.talanta.2012.07.074>.

[28] M. Ajhar, B. Wens, K.H. Stollenwerk, G. Spalding, S. Yüce, T. Melin, Suitability of Tedlar® Gas Sampling Bags for Siloxane Quantification in Landfill Gas, *Talanta*. 82 (2010) 92–98. <https://doi.org/10.1016/j.talanta.2010.04.001>.

[29] A.S. Brown, A.M.H. Van Der Veen, K. Arrhenius, A. Murugan, L.P. Culleton, P.R. Ziel, J. Li, Sampling of Gaseous Sulfur-Containing Compounds at Low Concentrations with a Review of Best-Practice Methods for Biogas and Natural Gas Applications, *TrAC Trends in Analytical Chemistry*. 64 (2015) 42–52. <https://doi.org/10.1016/j.trac.2014.08.012>.

[30] M. Sulyok, C. Haberhauer-Troyer, E. Rosenberg, M. Grasserbauer, Investigation of the Storage Stability of Selected Volatile Sulfur Compounds in Different Sampling Containers, *Journal of Chromatography A*. 917 (2001) 367–374. [https://doi.org/10.1016/S0021-9673\(01\)00654-9](https://doi.org/10.1016/S0021-9673(01)00654-9).

[31] M. Cachia, B. Bouyssière, H. Carrier, H. Garraud, G. Caumette, I. Le Hécho, Development of a High-Pressure Bubbling Sampler for Trace Element Quantification in Natural Gas, *Energy & Fuels*. 31 (2017) 4294–4300. <https://doi.org/10.1021/acs.energyfuels.6b03059>.

[32] M.F. Ezzeldin, Z. Gajdosechova, M.B. Masod, T. Zaki, J. Feldmann, E.M. Krupp, Mercury Speciation and Distribution in an Egyptian Natural Gas Processing Plant, *Energy Fuels*. 30 (2016) 10236–10243. <https://doi.org/10.1021/acs.energyfuels.6b02035>.

[33] E.M. Krupp, C. Johnson, C. Rechsteiner, M. Moir, D. Leong, J. Feldmann, Investigation into the Determination of Trimethylarsine in Natural Gas and Its Partitioning into Gas and Condensate Phases Using (cryotrapping)/Gas Chromatography Coupled to Inductively Coupled Plasma Mass Spectrometry and Liquid/Solid Sorption Techniques, *Spectrochimica Acta Part B: Atomic Spectroscopy*. 62 (2007) 970–977. <https://doi.org/10.1016/j.sab.2007.07.009>.

[34] M.K. Uroic, E.M. Krupp, C. Johnson, J. Feldmann, Chemotrapping-Atomic Fluorescence Spectrometric Method as a Field Method for Volatile Arsenic in Natural Gas, *Journal of Environmental Monitoring*. 11 (2009) 2222. <https://doi.org/10.1039/b913322d>.

[35] T. Larsson, W. Frech, E. Björn, B. Dybdahl, Studies of Transport and Collection Characteristics of Gaseous Mercury in Natural Gases Using Amalgamation and Isotope Dilution Analysis, *Analyst*. 132 (2007) 579–586. <https://doi.org/10.1039/B702058A>.

[36] M. Enrico, A. Mere, H. Zhou, H. Carrier, E. Tessier, B. Bouyssiere, Experimental Tests of Natural Gas Samplers Prior to Mercury Concentration Analysis, *Energy Fuels*. (2019). <https://doi.org/10.1021/acs.energyfuels.9b03540>.

[37] M.C. Leuenberger, M.F. Schibig, P. Nyfeler, Gas Adsorption and Desorption Effects on Cylinders and Their Importance for Long-Term Gas Records, *Atmospheric Measurement*

- Techniques. 8 (2015) 5289–5299. <https://doi.org/10.5194/amt-8-5289-2015>.
- [38] A. Lecharlier, B. Bouyssiere, H. Carrier, I.L. Hécho, Promises of a New Versatile Field-Deployable Sorbent Tube Thermodesorber by Application to BTEX Analysis in CH₄, *Talanta Open*. 4 (2021) 100066. <https://doi.org/10.1016/j.talo.2021.100066>.
- [39] E. Gallego, F.J. Roca, J.F. Perales, X. Guardino, E. Gadea, Development of a Method for Determination of VOCs (including Methylsiloxanes) in Biogas by TD-GC/MS Analysis Using Supel™ Inert Film Bags and Multisorbent Bed Tubes, *International Journal of Environmental Analytical Chemistry*. 95 (2015) 291–311. <https://doi.org/10.1080/03067319.2015.1016012>.
- [40] US EPA, Compendium of Methods for the Determination of Toxic Organic Compounds in Ambient Air. Second Edition. Compendium Method TO-17: Determination of Volatile Organic Compounds in Ambient Air Using Active Sampling Onto Sorbent Tubes (EPA/625/R-96/010b), (1999). <https://www3.epa.gov/ttnamti1/files/ambient/airtox/to-17r.pdf> (accessed April 23, 2020).
- [41] M. Harper, Review. Sorbent Trapping of Volatile Organic Compounds from Air, *Journal of Chromatography A*. 885 (2000) 129–151. [https://doi.org/10.1016/S0021-9673\(00\)00363-0](https://doi.org/10.1016/S0021-9673(00)00363-0).
- [42] R.R. Arnts, Evaluation of Adsorbent Sampling Tube Materials and Tenax-TA for Analysis of Volatile Biogenic Organic Compounds, *Atmospheric Environment*. 44 (2010) 1579–1584. <https://doi.org/10.1016/j.atmosenv.2010.01.004>.
- [43] H. Carrier, I. Le Hécho, J.-L. Daridon, Device for Collecting a Sample of Elements of Interest Present as Traces in a Pressurized Gas. Terega/UPPA patent (France), Patent n° WO 2020217031, 2020.
- [44] J. Brown, B. Shirey, A Tool for Selecting an Adsorbent for Thermal Desorption Applications. Technical Report, (2001). https://www.sigmaaldrich.com/content/dam/sigmaaldrich/docs/Supelco/General_Information/t402025.pdf (accessed April 23, 2020).
- [45] J.I.S. Gómez, H. Lohmann, J. Krassowski, Determination of Volatile Organic Compounds from Biowaste and Co-Fermentation Biogas Plants by Single-Sorbent Adsorption, *Chemosphere*. 153 (2016) 48–57. <https://doi.org/10.1016/j.chemosphere.2016.02.128>.
- [46] M. Thommes, K. Kaneko, A.V. Neimark, J.P. Olivier, F. Rodriguez-Reinoso, J. Rouquerol, K.S.W. Sing, Physisorption of Gases, with Special Reference to the Evaluation of Surface Area and Pore Size Distribution (IUPAC Technical Report), *Pure and Applied Chemistry*. 87 (2015) 1051–1069. <https://doi.org/10.1515/pac-2014-1117>.
- [47] M.M.K. Salem, P. Braeuer, M. v. Szombathely, M. Heuchel, P. Harting, K. Quitzsch, M. Jaroniec, Thermodynamics of High-Pressure Adsorption of Argon, Nitrogen, and Methane on Microporous Adsorbents, *Langmuir*. 14 (1998) 3376–3389. <https://doi.org/10.1021/la970119u>.
- [48] Y. Zhou, L. Zhou, Fundamentals of High Pressure Adsorption, *Langmuir*. 25 (2009) 13461–13466. <https://doi.org/10.1021/la901956g>.
- [49] P. Bénard, R. Chahine, Modeling of High-Pressure Adsorption Isotherms above the Critical Temperature on Microporous Adsorbents: Application to Methane, *Langmuir*. 13

(1997) 808–813. <https://doi.org/10.1021/la960843x>.

[50] G.L. Aranovich, M.D. Donohue, Adsorption Isotherms for Microporous Adsorbents, *Carbon*. 33 (1995) 1369–1375. [https://doi.org/10.1016/0008-6223\(95\)00080-W](https://doi.org/10.1016/0008-6223(95)00080-W).

TRANSITION CHAPTER 5 – 6

In the next and last experimental chapter, as a crowning achievement of three years' research, all previous analytical and instrumental developments are combined and ultimately implemented on field. Namely, different landfill gas, biogas and biomethane streams are sampled using the developed direct *in situ* high-pressure preconcentration method using the TA14-CX26 and TA14-CpX29 multibed adsorbent tubes which are directly connected to field gas pipe with tubing as short as possible. When sampling compressed biomethane at a natural gas grid injection station, the multibed adsorbent tubes were placed in the high-pressure tube sampling prototype.

CHAPTER 6 – TRACE COMPOUNDS DETERMINATION IN LANDFILL GAS, BIOGAS AND BIOMETHANE BY DIRECT *IN SITU* PRECONCENTRATION AT THE PREVAILING GAS PRODUCTION PRESSURE

- To be submitted to *Chemosphere* -

Aurore Lecharlier^{1,2}, Hervé Carrier¹, Brice Bouyssiere², Guilhem Caumette³, Pierre Chiquet³, Isabelle Le Hécho^{2*}

¹ Université de Pau et des Pays de l'Adour, E2S UPPA, CNRS, TOTAL, LFCR UMR 5150, BP 1155 avenue de l'Université, 64013 Pau Cedex, France

² Université de Pau et des Pays de l'Adour, E2S UPPA, CNRS, IPREM UMR 5254, Technopôle Hélioparc, 2 avenue du Président Angot, 64053 Pau Cedex 09, France

³ Teréga, 40 Avenue de l'Europe, CS 20 522, 64010 Pau Cedex, France

* Corresponding Author: Isabelle Le Hécho • isabelle.lehecho@univ-pau.fr

ABSTRACT

In pursuance of enhancing knowledge on biogas and biomethane's trace compounds to help guarantee their sustainable integration in today's European energy mix, non-metallic trace compounds in biogas and biomethane samples from a landfill and two anaerobic digestion plants treating diverse feedstocks, were qualitatively determined by thermodesorption – gas chromatography – mass spectrometry following their direct *in situ* preconcentration on self-assembled multibed adsorbent tubes using an improved safer and shortened field sampling set-up. A grid-injected biomethane (40 bar_a) was also sampled and preconcentrated the same way using a novel high-pressure tube sampling prototype. Two different multibed adsorbent tube configurations were compared, namely Tenax®TA-Carbopack™X and Tenax®TA-Carboxen®1000 and the first one proved having a higher preconcentration versatility enabling the recovery of more trace compounds than the other configuration. The narrow dimensions of multibed adsorbent tubes enabled to sample gas volumes as low as 0.5 – 2 L_N and to detect in a single sampling run a wide range of trace compounds in a variety of chemical families (alcohols, aldehydes, alkenes, aromatics, cyclo-alkanes, esters, furans and ethers, halogenated species, ketones, linear alkanes, polycyclic alkanes, Sulphur-compounds, siloxanes and terpenes). Differences in trace compounds composition were evidenced between the gases of the different plants and potential correlations between feedstocks nature, treatment processes implemented and trace compounds present were discussed. In particular, the substantial generation of the mono-terpene *p*-cymene and of other terpenes has been evidenced for the anaerobic digestion plant treating principally food-wastes. It is believed the shortened and high-pressure-proof sampling procedure presented here can contribute facilitating field sampling operations for the determination of trace compounds in complex gas matrices such as biogas and biomethane.

KEYWORDS

Biogas and biomethane

Trace compounds

Direct *in situ* preconcentration

Multibed adsorbent tubes

TD-GC-MS

ABBREVIATIONS CHAPTER 6

CpX	Carbopack™X
CX	Carboxen®1000
GC	Gas chromatography
HPTS	High-pressure tube sampling prototype
MAT	Multibed adsorbent tube
MF	Molecular formula
MS	Mass spectrometry
PTFE	Polytetrafluoroethylene
RA _F	Per-family relative abundance
RA _G	Global relative abundance
SGM	Synthetic gas mixture
TA	Tenax®TA
TC	Trace compounds
TD	Thermal desorption
THT	Tetrahydrothiophene
TIC	Total ion current chromatogram

I. INTRODUCTION

Worldwide, modern societies and economies have placed biogas and biomethane at the crossroads of two contemporary challenges, namely valorizing the continually growing amounts of organic municipal and industrial wastes (circular economy) while simultaneously generating more sustainable energy to tackle global greenhouse gases emissions (energy transition) [1,2].

Biogas is a flammable gas mixture produced by the anaerobic digestion of humid organic matter by microbiota including methanogenic bacteria. This biochemical mechanism called methanization takes place in controlled 'digesters' or 'methanizers' [2,3] or spontaneously in landfills ('landfill gas') wherein the compaction of dumped wastes ensures the absence of oxygen [4–7]. Next to its two major constituents CH_4 ($\geq 50\%_{\text{vol}}$) and CO_2 ($< 50\%_{\text{vol}}$), biogas contains minor constituents like N_2 , H_2O , H_2S , NH_3 , H_2 , CO , O_2 and traces of volatile compounds ('trace compounds', TC) from various families: alkanes, alkenes, terpenes, aromatics, alcohols, aldehydes, ketones, esters, ethers, halogenated organic compounds, organic and inorganic Sulphur- and Silicon- compounds including siloxanes and silanes [2,6–15] and (in)organic metal(loid) species [9,16–20]. This biogas composition is strongly dependent on the organic matter being digested and on the physicochemical and mechanical parameters driving the anaerobic digestion (temperature, humidity, pH, season, digester hydraulic retention time and mixing regime ...) [12,14,21–23]. Ideally, organic matter ('feedstocks') brought in digesters stem from the wastes sector and include agricultural residues, manure, food-processing and catering residues, organic and green municipal and household wastes, sewage sludge.

The interest of biogas lies in the calorific value of its methane content. Today's direct biogas applications include heat and power generation by its combustion in boilers, cookers [24], internal combustion engines [25,26], (solid oxide) fuel cells [27–29] and combined heat and power generation engines [26,30–32]. Alternatively, biogas can be upgraded via well-established technologies involving the separation of CO_2 and CH_4 to obtain a pure methane stream, 'biomethane', a renewable gas having the same calorific value as natural gas (fossil methane) [2,33–37]. According to the European Biogas Association, 18943 biogas production plants and 725 biomethane production plants were in service across Europe by the end of 2019 [38] with $\sim 10\%$ of the biogas production upgraded to biomethane. By 2030, up to 20% of the biogas production could be upgraded to biomethane [1,39]. Provided its stringent compliance to natural gas quality standards stipulating maximal levels of several chemical compounds (in France: total Sulphur $< 30\text{ mg}\cdot\text{Nm}^{-3}$, H_2S and COS $< 5\text{ mg}\cdot\text{Nm}^{-3}$, CO_2 $< 2.5\%_{\text{mol}}$, CO $< 2\%_{\text{mol}}$, O_2 $< 0.001\%_{\text{mol}}$, H_2 $< 6\%_{\text{mol}}$, NH_3 $< 3\text{ mg}\cdot\text{Nm}^{-3}$, Hg $< 1\text{ }\mu\text{g}\cdot\text{Nm}^{-3}$, chlorinated species $< 1\text{ mg}\cdot\text{Nm}^{-3}$, fluorinated species $< 10\text{ mg}\cdot\text{Nm}^{-3}$, siloxanes $< 5\text{ mg}\cdot\text{Nm}^{-3}$) [40], biomethane is intended for injection in the existing natural gas transport grid [41] to gradually substitute natural gas in any of its applications and in particular as transport fuel [1,42] for terrestrial as well as marine vehicles [43].

Depending on the energy application, removal of minor- and trace compounds in biogas and biomethane is crucial inasmuch as compounds such as H_2S , NH_3 , COS , CS_2 , thiols, halogenated compounds, siloxanes, aromatic hydrocarbons can have deleterious effects (acid corrosion, abrasion, fouling, depositions, catalyst deactivation...) in boilers, engines and fuel cells upon

combustion of the gas [7,13,21,22,28,44–47]. Odorous compounds like terpenes are also known to attack rubber seals and to mask the tetrahydrothiophene artificial odor of grid-injected biomethane [48]. Determining suitable abatement techniques requires the preliminary characterization of TC, which is a difficult task owing to their low concentrations, the complexity of the gas mixture and the high variety in physicochemical properties amongst TC, complicating the choice of an appropriate sampling methodology [8,49–53]. A common sampling practice is to collect a bulk gas sample in a whole gas sampling vessel (canister, gas sampling bag, gas cylinder) subsequently transported to a laboratory where the gas is transferred to a preconcentration unit (e.g. adsorbent tubes [51]) having specific retention affinity for only given TC thus being isolated from the non-retained gas matrix. This procedure nevertheless entails risks of TC losses during transport and storage until analysis by sorption to or permeation through the whole gas sampling vessel walls, as well as loss and contamination risks during transfer to the preconcentration unit, endangering sample stability and TC recovery [6,49,50]. Additionally, transport of whole gas samples containing flammable gas (CH₄) must observe national regulations for the transport of dangerous goods and is therefore costly.

Therefore, this work presents a field gas sampling method seeking to improve existing ones by preconcentrating TC directly *in situ* with a shortened sampling chain to avoid sample transfers and minimize contaminations and TC losses. Six different landfill gas, biogas and biomethane streams, including a natural gas transport grid-injected biomethane (40 bar_a), were collected at a landfill plant and at two anaerobic digestion plants treating diverse feedstocks. The non-metallic TC in each gas have been preconcentrated directly *in situ* on self-developed multibed adsorbent tubes connected as straightly as possible to the gas pipes without gas depressurization using a novel high-pressure tube sampling prototype [53] when working pressures exceeded 2 bar_a. Two multibed adsorbent tubes configurations were studied. Preconcentrated TC were qualitatively characterized by thermal desorption of the adsorbent tubes using a new thermodesorber prototype [54] hyphenated with gas chromatography and mass spectrometry (TD-GC-MS). Based on the diversity of TC identified in the different gases, potential correlations between feedstocks nature, gas treatment processes implemented and TC composition in the gases were discussed.

II. MATERIALS AND METHODS

II.1. Multibed adsorbent tubes

Trace compounds in gas samples are preconcentrated onto self-assembled purpose-built multibed adsorbent tubes (MAT). MAT are assembled by manually packing empty amber glass tubes (ID 4.8 mm, L 44 mm, ActionEurope, France) with appropriate commercial macro- and microporous adsorbents from Supelco, Bellefonte, PA, USA. Two MAT configurations were prepared ('TA14-CX26' and 'TA14-CpX29'), each MAT containing two adsorbent beds: a front weak bed (Tenax®TA in both MAT configurations) and a back strong bed (Carboxen®1000 in TA14-CX26 or Carbopack™X in TA14-CpX29) (Table 6.1). Each adsorbent bed is secured

between and separated from the other bed by ~4mm long untreated quartz wool plugs (Helios Italquartz™). Adsorbent masses corresponding to a fixed bed volume of 0.05 cm³ are weighted and sucked up in the tube via a flexible tubing plugged on the tube extremity and connected to a pump (Xylem Flojet). Each bed occupies 3.4 ± 0.2 mm length in the tube. Thereupon, packed MAT are conditioned at 320°C during 8.5 hours under a continuous pure nitrogen flow (99.999% purity, averagely 375 mL·min⁻¹) in a purpose-built 20-positions conditioning support as described in [54]. Immediately after conditioning, MAT are sealed with aluminum crimp caps with 3-layers septa (polytetrafluoroethylene/silicone/polytetrafluoroethylene, 'PTFE/Si/PTFE', high temperature ultra-low-bleed silicone, ActionEurope, France) and stored until utilization in individual hermetic polyethylene zip bags in a larger zip bag in a desiccator at 4°C as recommended [52,55].

Particular considerations on MAT design, working principle, conditioning and operating parameters were described in previous work [53].

Table 6.1: Composition and properties of multibed adsorbent tubes (MAT) configurations.

MAT configuration	MAT composition		Adsorbent matrix	Mass in MAT (±0.2 mg)	Mesh size	Surface area (m ² ·g ⁻¹)	Recommended conditioning T (°C)	Recommended desorption T (°C)
	Bed	Adsorbent						
TA14-CX26	Front	Tenax®TA	2,6-diphenyl- <i>p</i> -phenylene oxide polymer (macroporous)	14	60-80	35	320	300
	Back	Carboxen®1000	Carbon molecular sieve (microporous)	26	60-80	1200	350	330
TA14-CpX29	Front	Tenax®TA	2,6-diphenyl- <i>p</i> -phenylene oxide polymer (macroporous)	14	60-80	35	320	300
	Back	Carbopack™X	Porous graphitized carbon black	29	40-60	240	350	330

II.2. Sampling

Six different landfill gas, biogas and biomethane streams were sampled at three distinct French production plants (A, B, C) treating diverse feedstocks (Table 6.2 – 6.3). Plant A is a landfill opened in 2014. Since it only dumps inorganic wastes refused from other municipal solid waste valorization pathways, landfill gas production is slow and only started around 2017. The drainage network extracting gas from the waste-cells was installed in two 7-years old waste-cells. A desulfurization unit was installed on March 31st 2021 downwards the gas extraction network, i.e. between the first and second sampling campaigns (Table 6.3). Plant B is a methanization plant converting mainly agricultural residues and manure into biogas with upgrading to biomethane. Upgrading occurs via water washing in a fluidized bed (scrubber) where biogas and water flow countercurrently. CO₂ and H₂S biogas-components dissolve in water while CH₄ does not. This CH₄ (biomethane) is evacuated towards a drying step (pressure swing adsorption on regenerable hydrophilic silica beads) before compression to 40 bar_a. Compressed biomethane is then odorized with tetrahydrothiophene (THT) and injected into the natural gas transport grid. Plant C is a methanization plant converting mainly food and vegetal residues into biogas. Raw biogas is dried by condensation at 12°C before passing through an activated carbon column for pre-treatment aiming at removing primarily H₂S.

Each gas stream is sampled directly *in situ* on a MAT connected as straightly as possible to the gas pipe sampling point. The MAT is always oriented so that the gas first meets the front weak adsorbent bed (Tenax®TA). For gas streams at pressures $\leq 1.1 \text{ bar}_a$, an as short as possible piece of 1/4" or 1/8" new clean and inert tubing (polytetrafluoroethylene (PTFE, Approflon, France), perfluoroalkoxyalkane (PFA, Swagelok Lyon, France) or vinyl (Swagelok Lyon, France) depending on the site, Table 6.3) was connected to the sampling point either via stainless-steel Swagelok connectors or directly on hose barb fittings installed at the sampling point. A stainless-steel male luer-lock needle (nCx Instrumentation, France) fitted to the tubing was used to pierce the inlet MAT septum and allow gas to flow in the tube. The exit MAT septum was simultaneously also pierced by a similar needle connected to a tubing leading the circulating gas to the gas flowmeter (Bronkhorst Mass View MV-302 or Ritter TG 0.5 PP). When the gas sampling pressure exceeded 2 bar_a , the MAT was placed in a novel high-pressure tube sampling prototype (HPTS) presented earlier [53]. The HPTS was straightly connected to the gas sampling point via a clean stainless-steel tubing as in [53], enabling to directly preconcentrate TC in the gas at its effective pipe pressure up to 200 bar_a . Gas is only depressurized downstream the HPTS-MAT preconcentration unit to further flow to the gas flowmeter. Before effectively sampling a gas onto a MAT, the sampling chain without MAT was flushed during 15 – 45 min with the gas to sample to saturate potential TC-sorption sites on tubing and connectors surfaces upstream the MAT. No pump was used to drive the gases through the MAT during sampling operations. Solely the actual gas pressure was relied on to that purpose. When the gas pressure was sufficient ($\geq 1.1 \text{ bar}_a$, plants B and C), sampling flowrates were controlled upstream the MAT preconcentration to reach desired values ranging 50 – 100 $\text{mL}_N \cdot \text{min}^{-1}$ for biogases and non-grid biomethane and ranging 55 – 1600 $\text{mL}_N \cdot \text{min}^{-1}$ for the 40 bar_a grid-biomethane (i.e. 1.37 – 40 $\text{mL} \cdot \text{min}^{-1}$ on the MAT under the actual 40 bar_a pressure conditions) (Table 6.3). On plant A however, the landfill gas production pressure was low despite the booster-pump sucking up the gas from the landfill waste-cells, leading to very low and fluctuating inflicted flowrates (down to $\sim 3 \text{ mL}_N \cdot \text{min}^{-1}$) (Table 6.3).

Three new blank MAT of both configurations (TA14-CX26 and TA14-CpX29) were always brought to the field for each sampling day. All sampling operations were performed at outside ambient temperature (Table 6.3). Despite adsorbent tubes analyzed by thermodesorption can theoretically be re-used after quantitative thermodesorption and thermal reconditioning [49], here only new MAT were used for all sampling operations to avoid cross-contamination in the case thermodesorption of the initial sample was not quantitative and to avoid build-up of thermal degradation artefacts upon repeated conditioning cycles. Before and after sampling, MAT were transported from and to the lab in individual hermetic polyethylene zip bags in a larger zip bag in a polystyrene box filled with carbon dioxide dry ice. Back in the lab, sampled and blank MAT were stored in their zip bags in a desiccator at 4°C until analysis as recommended [52,55]. With the exception of MAT sampled at plant C which could only be analyzed within 6 days, all other MAT were analyzed within 1 and 3 days after sampling as recommended [52].

Table 6.2: Gas production plants where landfill gas, biogas and biomethane samples were collected. THT= tetrahydrothiophene.

Plant	Description	Feedstock	Gas sampled	Main gas compounds (mean values)	Gas destiny
A	Landfill	Inorganic municipal solid wastes	Landfill gas	41.5 % _{vol} CH ₄ 34.4 % _{vol} CO ₂ 2.2 % _{vol} O ₂ 0.01 % _{vol} H ₂ 10960 ppm H ₂ S * 4.6 g H ₂ O·Nm ⁻³	Flare stack; heat of combustion dries up landfill leachates
B	Wet mesophilic anaerobic digestion	<ul style="list-style-type: none"> • Agricultural residues • Manure (cow, duck, sheep) • Food-processing residues including greases (hygienization prior to transfer to digester)	Raw biogas	64.5 % _{vol} CH ₄ 35.5 % _{vol} CO ₂	Upgrading to biomethane
			Dried biomethane	96.3 % _{vol} CH ₄ 1.9 % _{vol} CO ₂ 0.4 % _{vol} O ₂ 0.3% _{vol} N ₂ 6·10 ⁻³ ppm _{vol} H ₂ S	Compression (40 bar _a)
			Grid-biomethane (upstream THT odorization)	96.3 % _{vol} CH ₄ 1.9 % _{vol} CO ₂ 0.3 % _{vol} O ₂ 7·10 ⁻⁴ ppm _{vol} H ₂ S	THT odorization and natural gas transport grid injection
C	Wet mesophilic anaerobic digestion	<ul style="list-style-type: none"> • (Mass) catering residues and unsold food including meat • Food-processing residues including pork gelatin, greases • Vegetal biomass • Manure (hygienization prior to transfer to digester)	Dried raw biogas	59.6 % _{vol} CH ₄ 0.2 % _{vol} O ₂ 5 ppm _{vol} H ₂ S	Pre-treatment on activated carbon
			Pre-treated biogas	59.6 % _{vol} CH ₄ 0.2 % _{vol} O ₂ 0 ppm H ₂ S	Combined heat and power generation

* H₂S levels upstream or before installation of the desulfurization unit

Table 6.3: Operational sampling parameters. P= pressure. MAT= multibed adsorbent tube. V= volume. n= number of MAT replicates taken. Q= flowrate. T= temperature. L= length. THT= tetrahydrothiophene. PTFE= polytetrafluoroethylene. PFA= Perfluoroalkoxy-alkane. SS= stainless-steel.

Plant	Gas sampled	Sampling date (2021)	Gas sampling P (bar _a)	MAT	Sampled V (L _N)	n	Sampling Q (± 0.5 mL _N ·min ⁻¹)	Ambient T (°C)	Gas T (°C)	Connecting tubing (L)
A	Landfill gas	March 8	≤ 1.05	TA14-CX26	0.5	n ₁	17.0	9.0 ± 0.1	13	Vinyl (20 cm)
						n ₂	17.0			
		Nov 15	≤ 1.05	TA14-CX26	0.5	n ₁	7.5	11.2 ± 0.5	17	Vinyl (2 m)
						n ₂	11.0			
				TA14-CpX29	0.5	n ₃	3.8			
						n ₁	3.2			
B	Raw biogas	March 22	1.1	TA14-CX26	0.5	n ₁	75.0	18.3 ± 0.2	12	PTFE (20 cm)
						n ₂	70.5			
				TA14-CpX29	0.5	n ₁	75.0			
						n ₂	75.0			
	Dried biomethane	March 22	6.1	TA14-CX26	1	n ₁	50.0	15.8 ± 0.1	12	PFA (5 m)
						n ₂	50.0			
				TA14-CpX29	1	n ₁	50.0			
						n ₂	50.0			
	Grid-biomethane (upstream THT odorization)	April 6	40.0	TA14-CpX29	1.2	n ₁	55.0	12.6 ± 1	12	SS (2.5 m)
						n ₂	55.0			
						n ₃	55.0			
		May 10	40.0	TA14-CpX29	1.5	n ₁	500.0	24.2 ± 3	26	SS (2.5 m)
n ₂						500.0				
n ₃						500.0				
				n ₄	500.0					
				n ₅	500.0					
				n ₆	200.0					
C	Dried raw biogas	March 24	1.1	TA14-CpX29	0.5	n ₁	85.7	19.5 ± 0.1	24	PTFE (20 cm)
						n ₁	60.8			
	Pre-treated biogas	March 24	1.1	TA14-CpX29	1	n ₁	61.5	17.3 ± 0.2	24	PTFE (20 cm)
						n ₂	62.2			

II.3. Analysis

All field-sampled and blank MAT were analyzed via TD-GC-MS parametrized as in Table 6.4 using the Agilent MSD ChemStation E.02.02.1431 software. Thermal desorption was performed using a new thermodesorber (TD) prototype (nC_x Instrumentation, France) presented elsewhere [54]. Each MAT is placed in the TD in the reverse direction as compared to the gas sampling direction. Note the 200°C temperature programmed in the TD corresponds to an effective desorption temperature of 300°C inside adsorbent tubes. This desorption temperature is handled since desorbing MAT at 330°C (desorption temperature of Carboxen[®]1000 and Carbopack[™]MX matrices, Table 6.1) would induce thermal degradation of Tenax[®]TA (desorption temperature 300°C) with associated injection of its thermal degradation products in the GC-MS and falsification of the analytical results.

Trace compounds detected in the chromatograms were identified using the NIST Mass Spectral Search Program version 2.0 d, 2005. In view of the co-elution of several TC and of the difficult unambiguous peak identification with the NIST database, identified TC will be given in terms of molecular formulas in the presented results for clarity and to avoid misidentification. For TC whose identification was equivocal between various species having the same molecular formula but different structural formulas, the main potentially corresponding compound will be given as an indication. As for TC labeled with a “*”, they could be unequivocally identified.

Table 6.4: TD-GC-MS instrument parameters

Instrument	Parameter	Value / reference
TD prototype <i>nCx Instrumentation</i>	Safe temperature	35°C
	Temperature	200°C
	Stabilization time	15 s
	Pressure	1170 mbar
	Injection time	10 s
GC <i>Agilent 6890A</i>	Inlet temperature	230°C
	Inlet septum	Premium Inlet Septa, Bleed/Temp optimized, non-stick (Agilent)
	Inlet liner	Ultra Inert Liner, Splitless, Single taper, no wool, 4 mm ID (Agilent)
	Split ratio	1 : 1
	Split flow	1.5 mL·min ⁻¹
	Carrier gas	Helium (quality detector 5.0, Linde, France)
	Gas saver	Off
	Column	HP-5MS, 30 m × 250 µm ID × 0.25 µm film thickness (Agilent)
	Constant flow in column	1.5 mL·min ⁻¹
	Carrier gas linear velocity in column	44 cm·s ⁻¹
Oven	30°C (4 min) - 10°C·min ⁻¹ - 250°C (5 min)	
MS <i>Agilent 5973Network</i> <i>Mass Selective Detector</i>	Source temperature	230°C
	Quadrupole temperature	150°C
	GC-MS interface temperature	280°C
	Electron Impact Mode	70 eV
	Electron Multiplier Voltage	Relative voltage (106 = 1871 V)
	Acquisition mode	Scan
	Scan range	10 – 450 a.m.u.
	Sampling rate	3.28 scan·s ⁻¹
	Threshold	100 counts

II.4. Calculations

For each identified TC i ($i = \{1 \rightarrow n\}$), the per-chemical family relative abundance ($RA_{F,i}$, %) and the global relative abundance ($RA_{G,i}$, %) were calculated as follows:

$$RA_{G,i} (\%) = \frac{100 \cdot A_i}{\sum_{i=1}^n A_i}$$

with A_i the average chromatographic peak area of TC i integrated from the total ion current chromatograms (TIC) of all replicates of a sample. For $RA_{F,i}$, n considers only the TC belonging to the concerned family found in the sample. For $RA_{G,i}$, n considers the total number of TC identified in the sample, all families taken together. For molecular formulas MF with several occurrences (chromatographic peaks i) of equivocally identified compounds inside a given chemical family, the respective average chromatographic peak areas of all occurrences i were summed up ($A_{MF,sum} = \sum_{i=1}^n A_{MF,i}$) and the corresponding RA of that MF was calculated as $100 \times A_{MF,sum} / \sum_{i=1}^n A_i$.

III. RESULTS AND DISCUSSION

III.1. Multibed adsorbent tube blanks

The TD-GC-MS analyses of new blank MAT of both configurations reveal they are free of any background contamination aside from cyclic siloxanes released from the PTFE/Si/PTFE tube sealing septa, as depicted by their TIC in Fig.6.1.

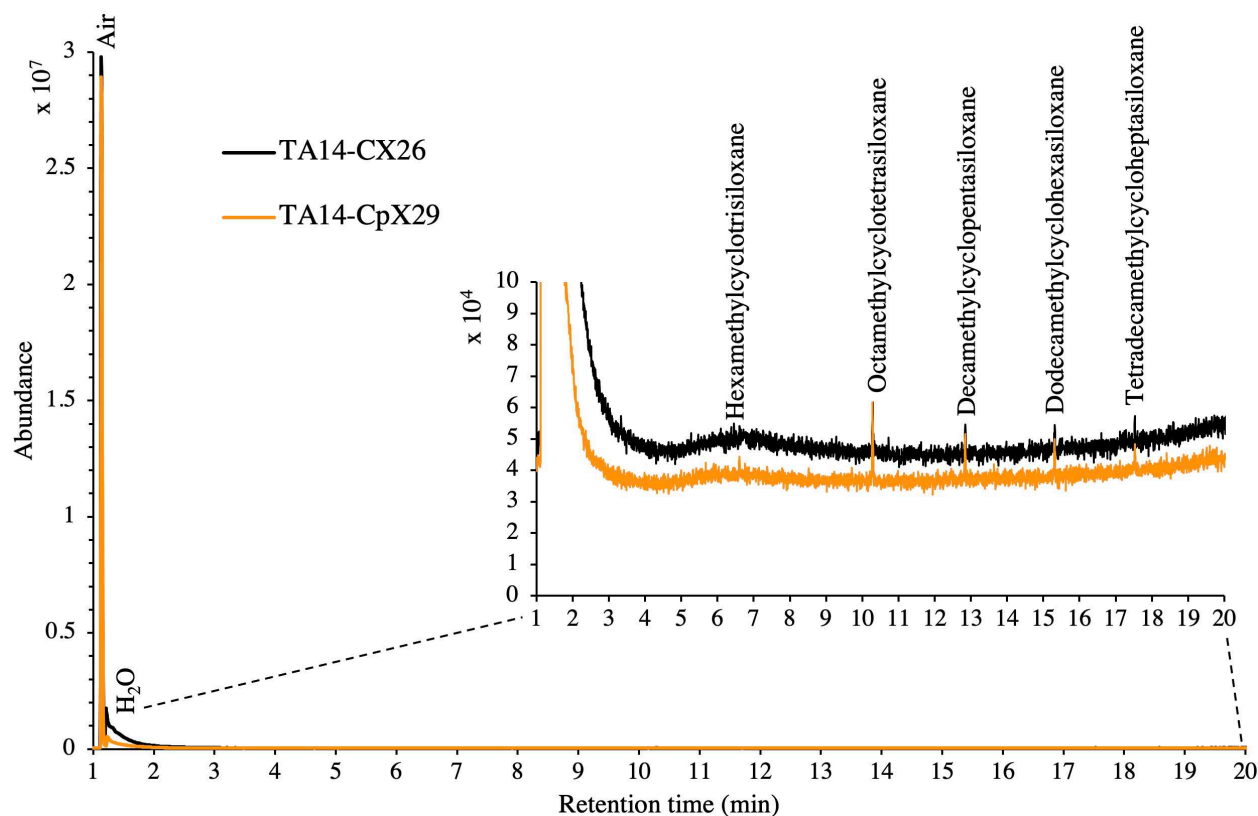


Figure 6.1: TIC of a new blank TA14-CX26 and a new blank TA14-CpX29 MAT with indication of septum-released siloxane background contaminants.

III.2. Sampled volumes

Effective sampled volumes presented in Table 6.3 were chosen based on the results of preliminary field sampling experiments where 3 identical MAT were placed in series to evaluate the breakthrough of TC from the front- towards the mid- and back-MAT of each test-series upon sampling a certain gas volume through it. This was done for several batches of 3 TA14-CX26 in series and 3 TA14-CpX29 in series for the raw biogas in plant B ($0.5 L_N$ raw biogas sampled through each series at $75 \pm 0.5 \text{ mL}_N \cdot \text{min}^{-1}$) (Fig.6.SI-1, 6.SI-2); for the dried raw biogas in plant C ($1 L_N$ dried raw biogas sampled through each series at $60 \pm 0.5 \text{ mL}_N \cdot \text{min}^{-1}$) (Fig.6.SI-3, 6.SI-4); and for the pre-treated biogas in plant C ($1 L_N$ sampled through each series at $65 \pm 0.5 \text{ mL}_N \cdot \text{min}^{-1}$) (Fig.6.SI-5, 6.SI-6). These relatively small volumes ($0.5 - 1 L_N$) were initially chosen in view of the small size of and the low adsorbent masses in the MAT. Figures 6.SI-1 to 6.SI-6 in the Supplemental Information overlay for each of these preliminary breakthrough experiments, the TIC of the front, mid and back adsorbent tubes. For all three gases investigated and for both MAT configurations, volumes of 0.5 or $1 L_N$ never led to breakthrough of TC downstream the front adsorbent tube of the series inasmuch as the TIC of mid- and back-tubes are always 'blank' with the exception of the siloxane impurities released from the tubes septa as demonstrated in section III.1. Additionally, a previous study [53] has shown that sampling up to $5 L_N$ of a synthetic gas mixture containing potential biogas TC (41 halogenated volatile organic compounds each at $1 \text{ ppm}_{\text{mol}}$ in N_2) onto TA14-CpX29 MAT did not lead to saturation of the adsorbents in the MAT. Therefore, depending on the gas stream, volumes of 0.5 up to $2.3 L_N$ were effectively sampled during field operations listed in Table 6.3 since those volumes were considered as safe (no breakthrough, no saturation) and sufficient to preconcentrate detectable amounts of TC.

For landfill gas (plant A) and raw biogases (plants B and C), the lowest volumes were sampled ($0.5 L_N$) as it was hypothesized they would contain a relatively high load of TC from diverse chemical families in view of their 'raw' status, especially the landfill gas, so that this limited volume would be safe and sufficient. In plant C, an additional $1 L_N$ dried raw biogas sample was taken to contrast it with the $0.5 L_N$ sample and determine whether or not a higher TC resolution was obtained with $1 L_N$ (Fig.6.2). Fig.6.2 indicates all TC detected in the $1 L_N$ sample were also detected in the $0.5 L_N$ sample albeit TC eluting from the GC after 8 min were characterized by higher signal intensities in the $1 L_N$ sample yet without a particularly higher resolution. The TC eluting at ~ 10.8 min already displayed some saturation in the $0.5 L_N$ sample and got even more saturated at $1 L_N$. Sampling a volume of $0.5 L_N$ henceforth appeared sufficient.

For biomethane (plant B) and pre-treated biogas (plant C) samples, higher volumes were sampled ($\geq 1 L_N$) as it was hypothesized they would contain lesser amounts of TC in view of their 'purified' status so that $0.5 L_N$ may be insufficient to preconcentrate detectable levels of some TC. For the grid-biomethane in plant B, a larger volume was sampled in December ($2.3 L_N$) since the April and May samples ($1.2 - 1.5 L_N$) had shown relatively low TC levels without saturation (see section III.4).

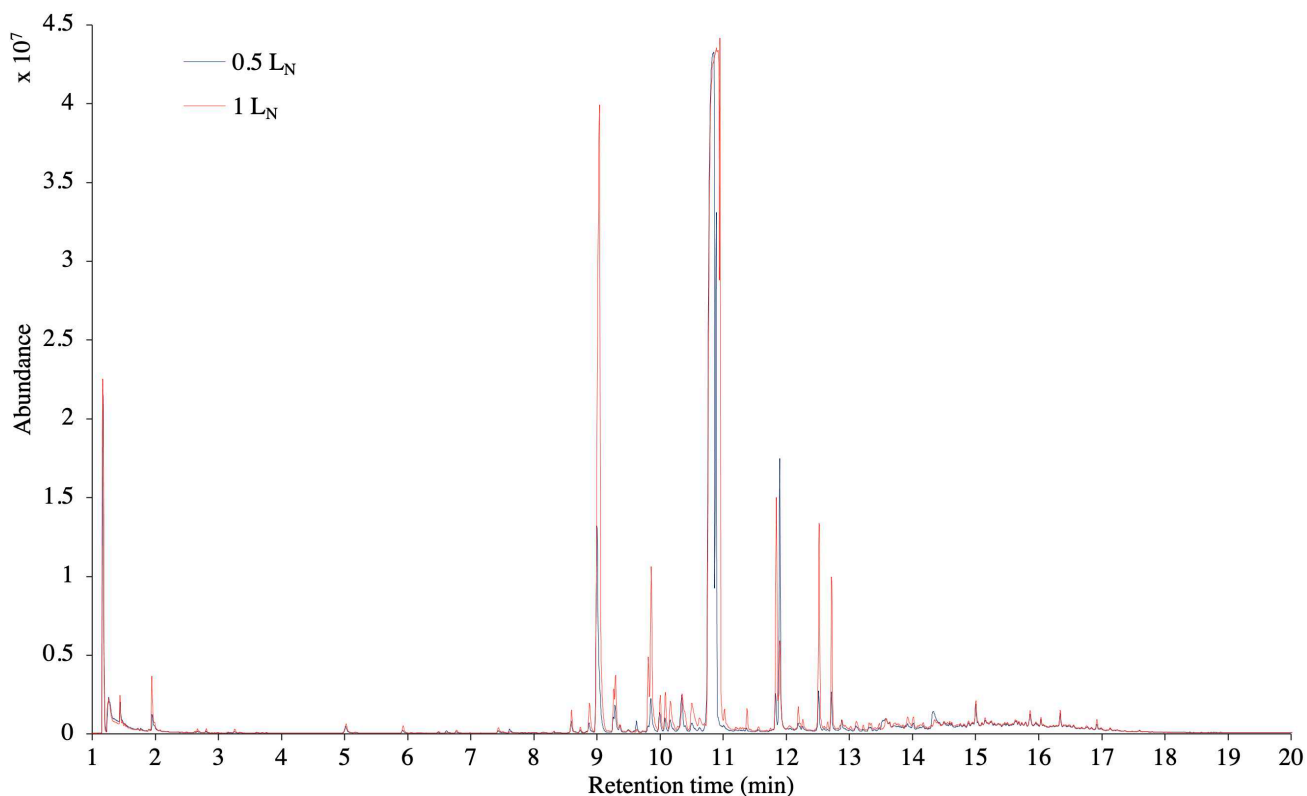


Figure 6.2: TIC of 0.5 versus 1 L_N dried raw biogas of plant C sampled on individual TA14-CpX29 MAT.

III.3. Multibed adsorbent tube configuration appropriateness

The interest of using both TA14-CX26 and TA14-CpX29 MAT to sample a given gas, since both configurations could be complementary in the spectrum of TC they preconcentrate and enable to recover, was evaluated for the landfill gas in November and for the raw biogas and dried biomethane of plant B in March 2021 (Table 6.3). Fig.6.3 overlays for each of those gases the TIC of the gas sampled with TA14-CX26 versus sampled with TA14-CpX29. Fig.6.4, 6.5, 6.6 depict the corresponding per-family relative abundances of TC identified in each of those gases sampled with one or the other MAT configuration. $RA_{F,i}$ are only given as a rough guide to decipher notable trends in TC present in the gases but are in no way proportional to TC concentrations.

For all three gases, TA14-CX26 samples give lower signal intensities after 2 min on the TIC and less compounds are detected than with TA14-CpX29 (Fig.6.3). In the landfill gas, 90 distinct TC (40 identified molecular formulas) belonging to 10 families were detected in the TA14-CpX29 sample against only 23 TC (16 molecular formulas) in 6 families in the TA14-CX26 sample (Fig.6.4). In the landfill TA14-CX26 TIC, no signal is detected after 7 min (except for the septum-siloxanes) while the TA14-CpX29 TIC reveals peaks up to 14 min (Fig.6.3). In the raw biogas of plant B, 93 distinct TC (36 molecular formulas) belonging to 11 chemical families were detected in the TA14-CpX29 sample against only 37 TC (14 molecular formulas) in 6 families in the TA14-CX26 sample (Fig.6.5). In the dried biomethane of plant B, 140 distinct TC (33 molecular formulas) belonging to 7 families were detected in the TA14-CpX29 sample against 109 TC (32 molecular formulas) in 9 families in the TA14-CX26 sample (Fig.6.6).

The TA14-CpX29 MAT configuration proved having a greater adsorption-desorption versatility. For all three gas samples, this MAT configuration enables to detect more chemical families and a larger diversity of TC are detected over a wider volatility range than with TA14-CX26. For instance, Sulphur-compounds from SO₂ up to C₈H₁₈S₂; alkanes from C₅H₁₂ to C₁₄H₃₀; cycloalkanes from C₃H₆ to C₁₀H₂₀; alkenes from C₅H₈ to C₉H₁₆; polycyclic-alkanes from C₁₀H₁₈ to C₁₂H₂₂ and diverse halogenated compounds and furans are found with TA14-CpX29. In contrast, the TA14-CX26 configuration proved rather suitable for lighter TC such as SO₂, CS₂, dimethylsulfide (C₂H₆S), butane (C₄H₁₀), cyclobutane and n-butene (C₄H₈) and dichlorofluoromethane (CHCl₂F) although some of those compounds (SO₂, CS₂, cyclobutane, n-butene) were also detected from TA14-CpX29 samples (Fig.6.4 – 6.6). Those divergent preconcentration behaviors straightly stem from the nature of Carbopack™X in TA14-CpX29 and of Carboxen®1000 in TA14-CX26. Carbopack™X is a porous graphitized carbon black with a moderate specific surface area (240 m²·g⁻¹, Table 6.1) enabling an efficient adsorption and desorption of very light up to relatively heavy compounds (50 to 260 g·mol⁻¹ in a boiling point range of -30 to 215°C) [56]. Carboxen®1000 on the other hand is a carbon molecular sieve with a great specific surface area (1200 m²·g⁻¹, Table 6.1) and micro- and mesopores [57] designed to only reversibly retain small volatile compounds lighter than ~130 g·mol⁻¹ with boiling points < 85 °C [56]. In both MAT, the Tenax®TA front bed is a weak adsorbent supposed to retain less-volatile and semi-volatile molecules (boiling point > ~80°C) to prevent them from reaching the next stronger adsorbents. Certain semi-volatile molecules can nevertheless migrate through it and reach the back bed. If the strong Carboxen®1000 is used, those semi-volatile molecules may get irreversibly adsorbed on Carboxen®1000, impeding their subsequently desorption and detection. On the contrary, when Carbopack™X is used, those semi-volatile molecules will be reversibly adsorbed as the adsorption strength of this material is lower, enabling more compounds to be detected.

Thusly, there exists a complementarity in the spectrum of TC each MAT is able to preconcentrate, albeit a limited one since most TC specifically detected via the TA14-CX26 tubes could also be detected from the TA14-CpX29 tubes, the opposite being untrue. Generally, there were more preconcentration-advantages to using the TA14-CpX29 configuration. Henceforth, for the subsequent sampling campaigns of grid-biomethane at plant B and of dried raw and pre-treated biogases at plant C, it was decided to only sample the gases through TA14-CpX29 MAT (Table 6.3).

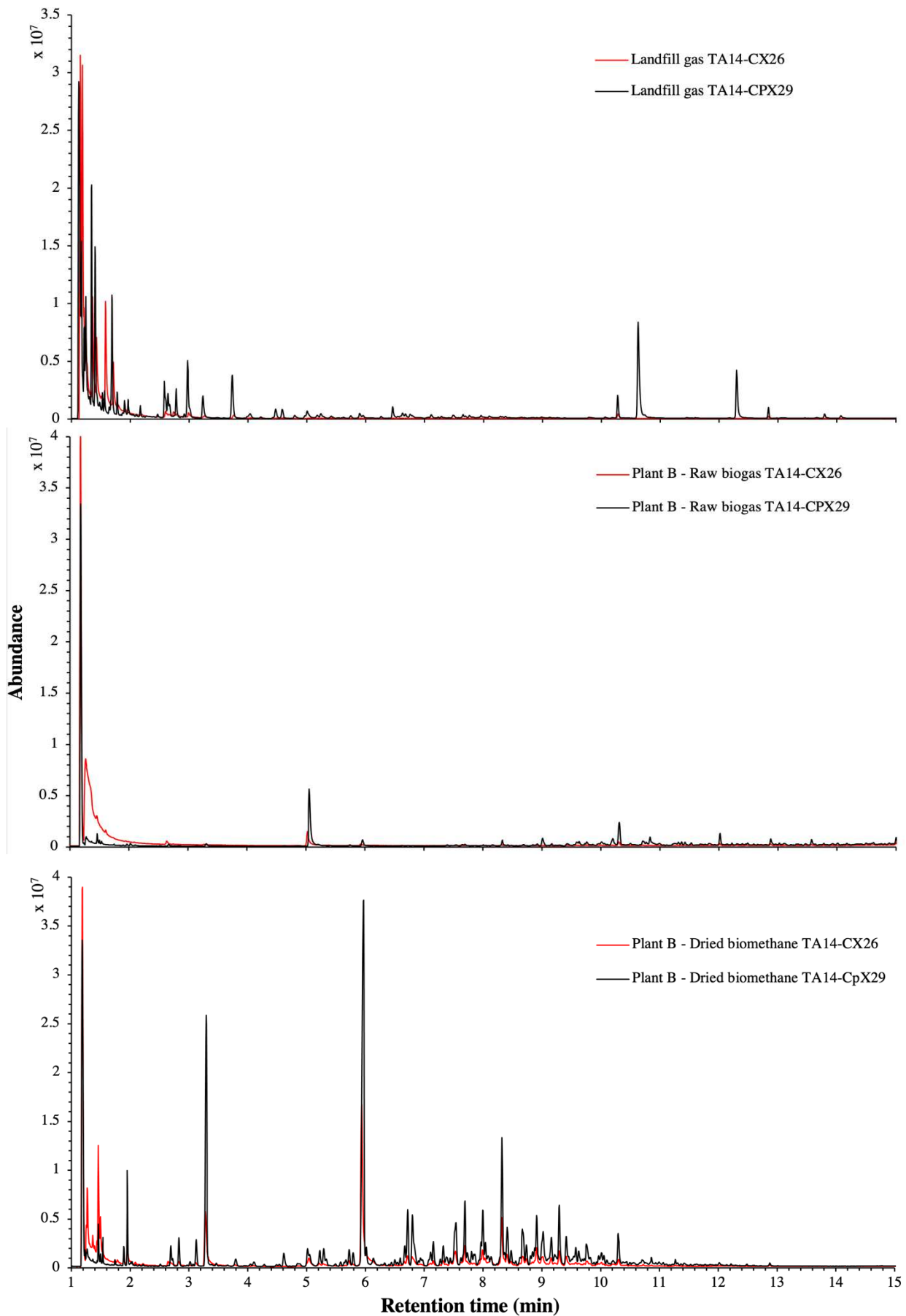


Figure 6.3: TIC of landfill gas (plant A, November 2021), raw biogas (plant B, March 2021) and dried biomethane (plant B, March 2021) sampled on TA14-CX26 or on TA14-CpX29 MAT as described in Table 6.3.

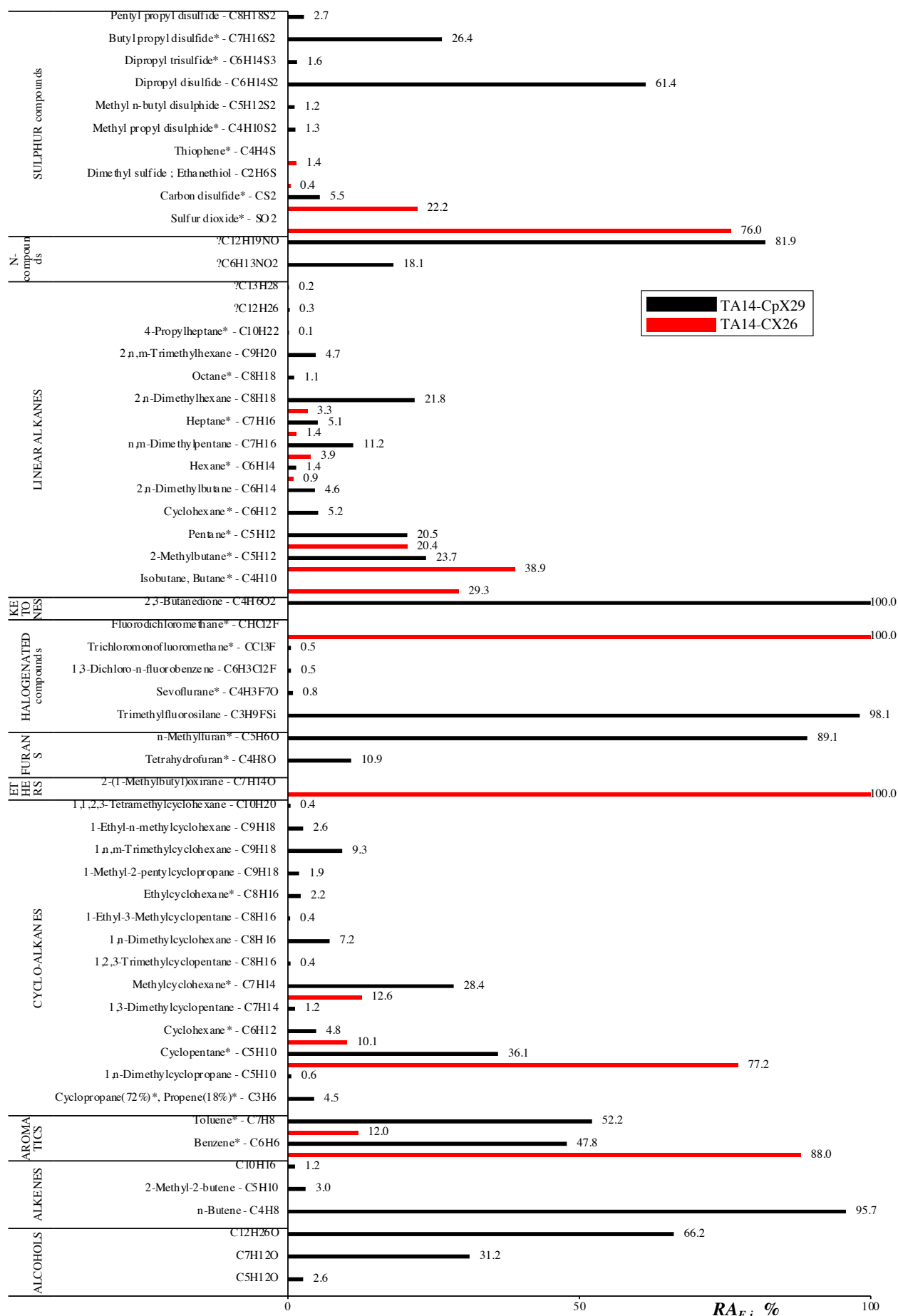


Figure 6.4: Per-family relative abundance (%) of trace compounds identified in the landfill gas of plant A sampled on TA14-CX26 versus on TA14-CpX29 MAT. Compounds marked with a "*" are unequivocally identified.

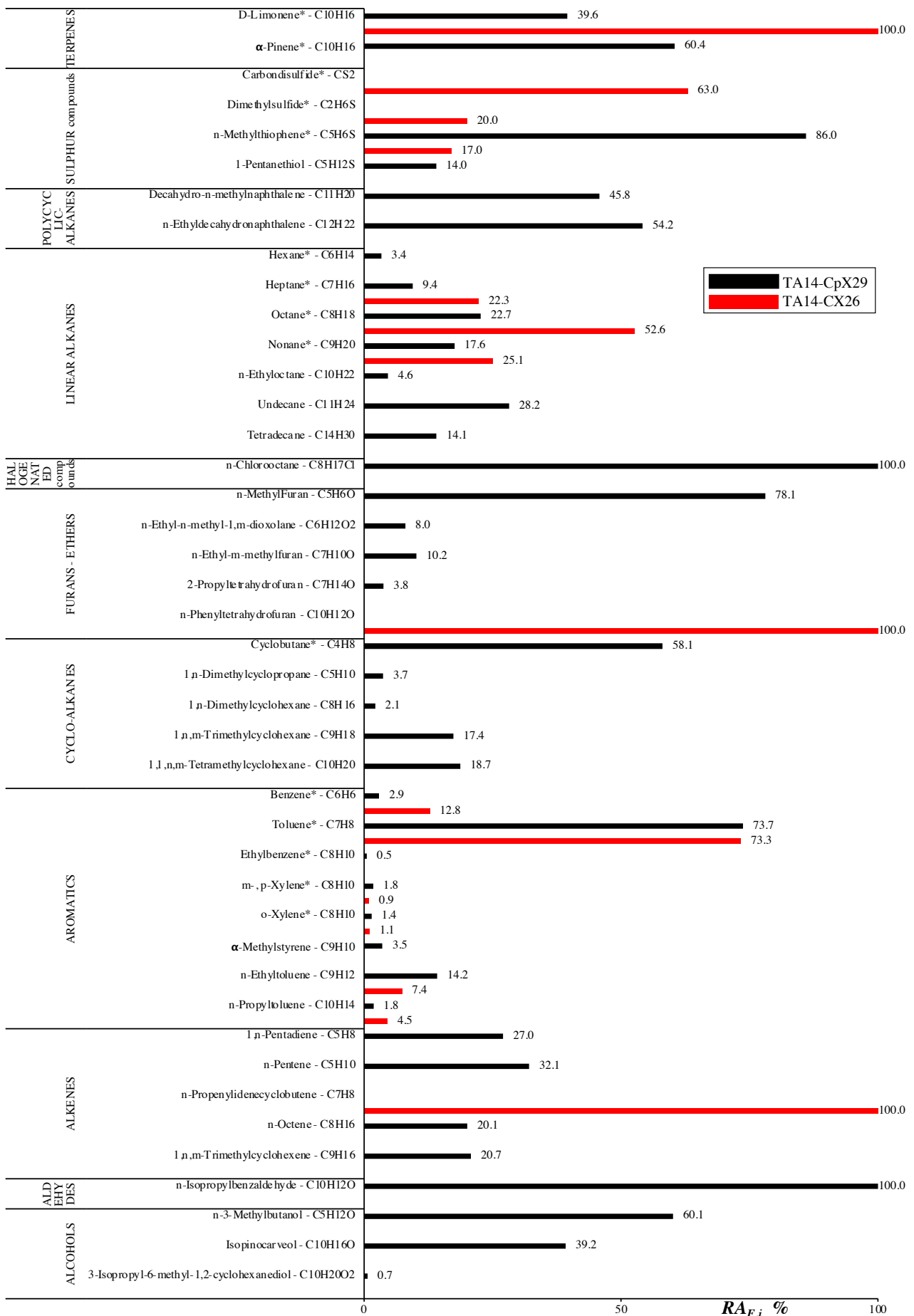


Figure 6.5: Per-family relative abundance (%) of trace compounds identified in the raw biogas of plant B sampled on TA14-CX26 versus on TA14-CpX29 MAT. Compounds marked with a "*" are unequivocally identified.

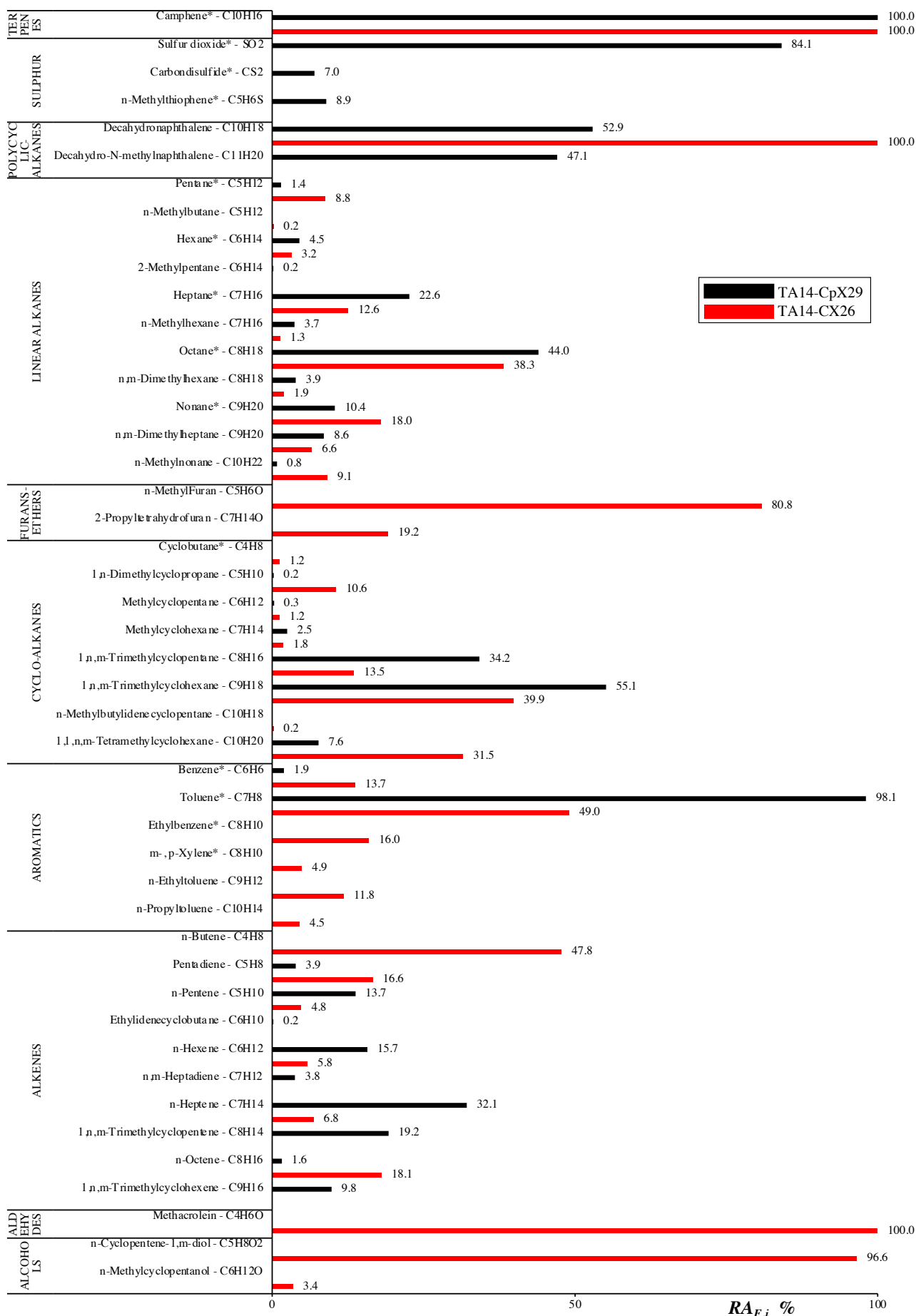


Figure 6.6: Per-family relative abundance (%) of trace compounds identified in the dried biomethane of plant B sampled on TA14-CX26 versus on TA14-CpX29 MAT. Compounds marked with a "*" are unequivocally identified.

III.4. Fluctuations of trace compounds in sampled gases

For every gas stream sampled (Table 6.3), total ion current chromatograms (TIC) and charts outlining the per-family relative abundances ($RA_{F,i}$) and global relative abundances ($RA_{G,i}$) of TC identified are presented as a means of 'identity card'. All $RA_{G,i}$ charts are given in the Supplemental Information. Importantly, as already stated, relative abundances only allow to decipher notable trends in TC present in the gases but are nowise proportional to TC concentrations owing to differences in ionization efficiencies between the TC in the mass spectrometer yielding signal intensity-differences in the TIC even at equal concentration.

III.4.1. Plant A

The landfill gas of plant A was sampled in March and November 2021 on TA14-CX26 (Fig.6.7 – 6.8 and Fig.6.SI-7) and on TA14-CpX29 in November 2021 only (Fig.6.4). Fig.6.7 clearly indicates a landfill gas TC-composition difference between March and November with much less TC found in November: On TA14-CX26 tubes, in March, 77 distinct TC (45 distinct molecular formulas) were detected amongst 10 families (Fig.6.8). Sulphur-compounds were numerous with at least 12 distinct species present including H_2S and CS_2 (the most abundant), SO_2 and thiols. Linear alkanes were also numerous (≥ 13 distinct species) with pentane dominating in relative abundance. Multiple aromatics were also found, with *m*- and *p*-Xylene and Toluene dominating. Besides, amongst cyclo-alkanes, light species such as cyclopropane and cyclopentane were dominant. Ethers and ketones were also identified with respectively *n*-methylfuran and *n*-butanone abounding the most. Finally, at least three terpene, two halogenated, one siloxane and one alcohol species were detected (Fig.6.8). Concerning the global relative abundances (Fig.6.SI-7), the vast majority of TC was homogeneously represented (between 0.1 and 2 or 3 % $RA_{G,i}$) although CS_2 was the dominant TC (10.1 % $RA_{G,i}$), testifying the high diversity of TC from various chemical families in the landfill gas, as also found by other authors [6,7,11,12,58]. In contrast, in November on TA14-CX26, only 23 TC (16 molecular formulas) were detected amongst 6 different families (Fig.6.8). No more terpene, alcohol, siloxane nor ketone were found and less TC were found in each remaining family. Amongst Sulphur-compounds, only 4 species were left with SO_2 being dominant. In linear alkanes, 2-methylbutane and butane were dominant. Amongst cyclo-alkanes, cyclopentane was still dominant and in the aromatics, benzene was dominant. Only one halogenated and one ether TC were found. The global $RA_{G,i}$ evidences the lesser diversity of TC in this November sample, where SO_2 and CS_2 become dominant (Fig.6.SI-7). Nonetheless, the TA14-CpX29 sample taken in November has proved more and different TC were present in the gas than actually detected with the TA-CX26 configuration as discussed in section III.3 and Fig.6.4. However no comparison is possible with the March's composition as no TA14-CpX29 samples were taken in March.

The installation of the desulfurization unit upstream the landfill gas sampling point end March 2021 probably explains observed fluctuations in the landfill gas composition between March and November. Although no technical information was available on the nature of the desulfurization process, results (Fig.6.7–6.8 and Fig.6.SI-7) suggest the desulfurization unit efficiently removes the targeted H_2S as well as other Sulphur-compounds yet not SO_2 and CS_2 which remain dominant after installation of the unit. The absence of terpenes, alcohols, siloxanes and ketones as well as the overall lesser number of TC in November are probably mainly due to the

desulfurization, which may remove other species than Sulphur ones, although the evolution of degradation reactions in the landfill is not to exclude. Long-term TC composition variations in landfill gases have been assigned to the age of the landfill and the state of decomposition of dumped wastes as well as to the differences in waste's natures across the years [6,7]. In view of the short time span considered here however (only two sampling days in 8 months), such processes probably have a minor contribution to the landfill gas TC composition fluctuations observed.

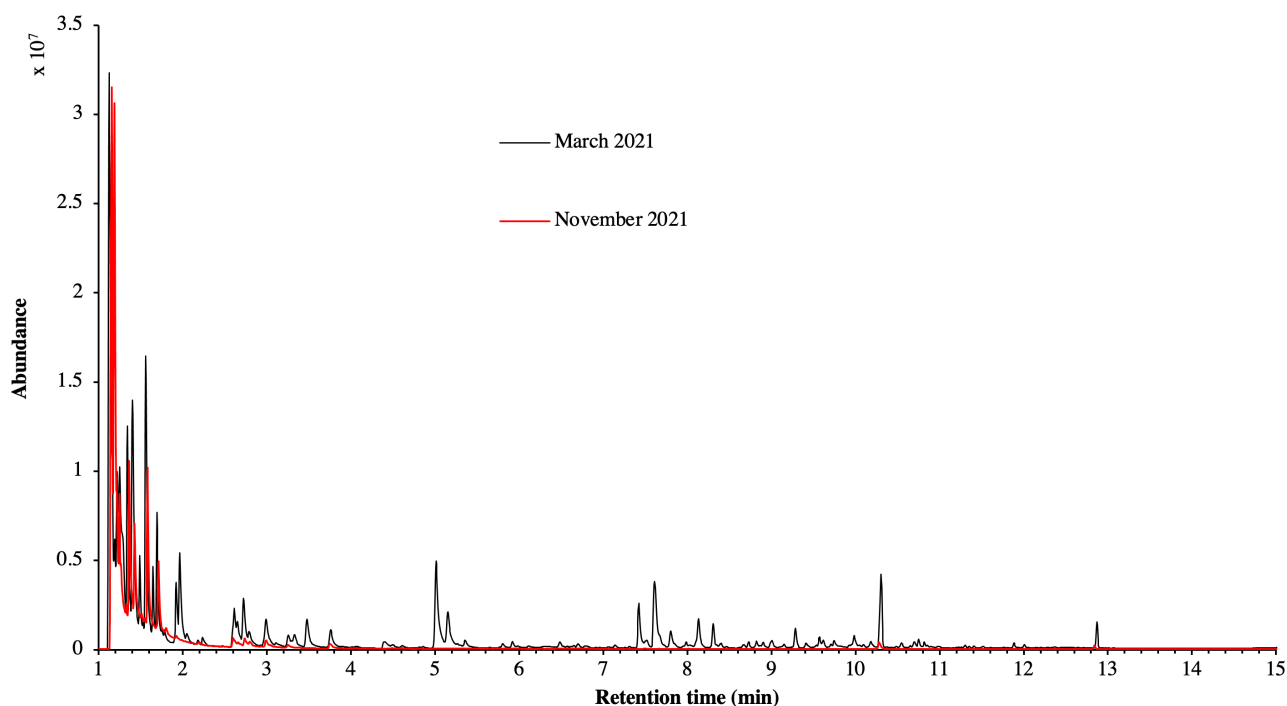


Figure 6.7: TIC of landfill gas (plant A) sampled on TA14-CX26 in March versus in November 2021.

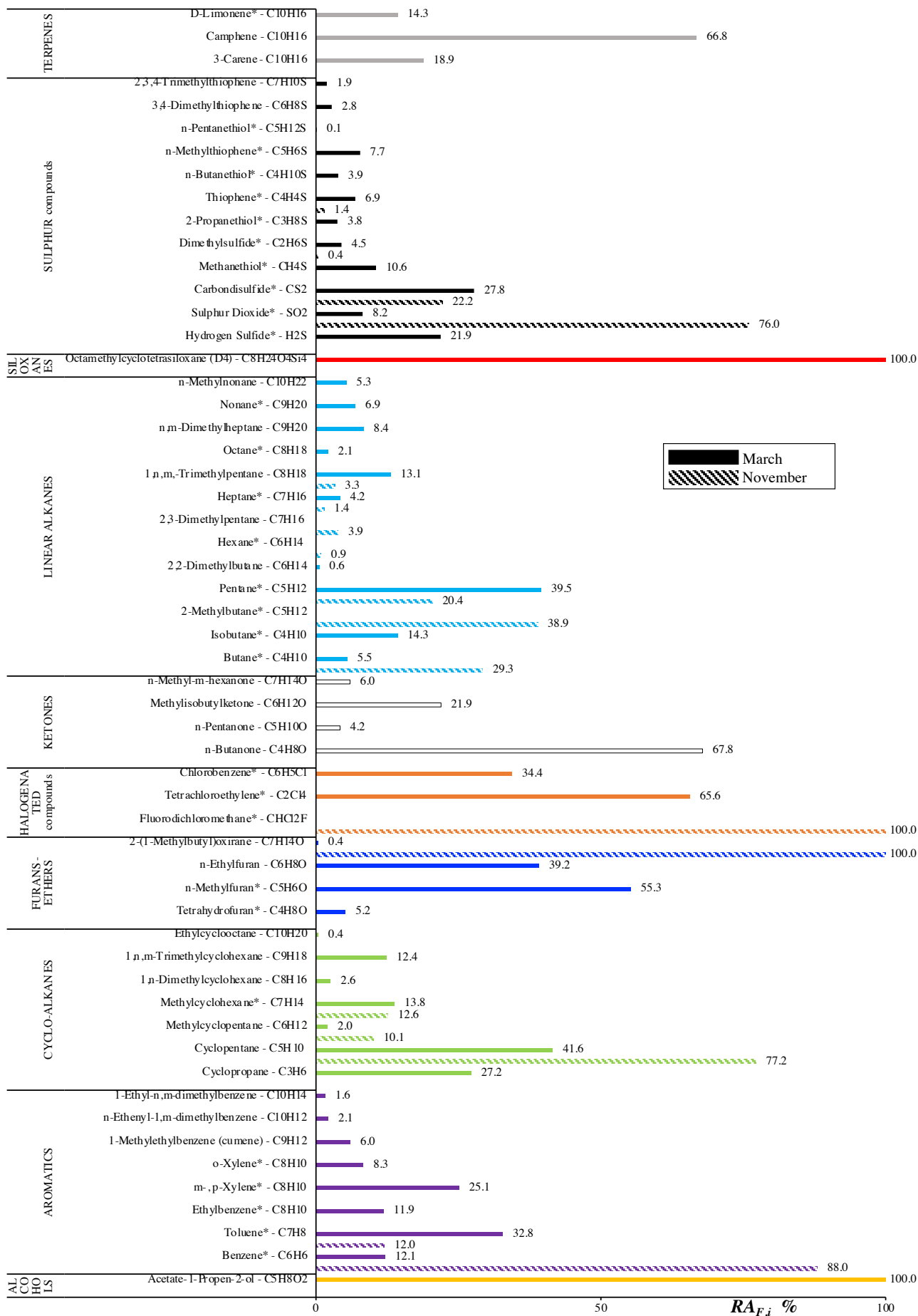


Figure 6.8: Per-family relative abundance (%) of trace compounds identified in the landfill gas (plant A) sampled on TA14-CX26 in March versus in November 2021. Compounds marked with a "*" are unequivocally identified.

III.4.2. Plant B

Fig.6.9–6.10 and Fig.6.SI-8 compare the TC characterized in the raw biogas and dried biomethane sampled on TA14-CpX29 at plant B in March 2021. Fig.6.9 reveals counter-intuitive results, namely the dried biomethane samples gave more chromatographic signals and thus seems to contain more TC than the raw biogas. Indeed, in the dried biomethane, 140 distinct TC represented by 33 molecular formulas in 7 different chemical families were detected against only 93 distinct TC represented by 36 molecular formulas belonging to 11 chemical families in the raw biogas (Fig.6.10, Fig.6.SI-8). In particular, there were more alkenes, linear alkanes and Sulphur-species in the biomethane than in the biogas. However, the diversity in molecular formulas and in chemical families represented was higher in the biogas than in the biomethane, in accordance with expected trends [11,21]. Next to shared families, biogas contained diverse ethers and furans, alcohols and at least one halogenated and one aldehyde species, while biomethane did not. Biogas also contained at least 8 aromatics while biomethane only contained toluene and benzene. D-limonene and α -pinene terpenes, typical in digester-biogas [14,48], were also absent from the biomethane which only contained one terpene (camphene, which has also been found to be a dominant terpenes in by others [14]) (Fig.6.10). Concerning the global $RA_{G,i}$ (Fig.6.SI-8), biogas was especially characterized by a high toluene content (32% $RA_{G,i}$) while octane was dominant in the dried biomethane (24% $RA_{G,i}$). It is unclear why the dried biomethane contained more TC than the raw biogas. Both dried biomethane and raw biogas sampling points were connected to local ball-valves exposed to outdoor grime and dust hence contamination was possible despite preliminary cleaning of the valve thread.

In Fig.6.11–6.12 and Fig.6.SI-9, the TC composition of the grid-biomethane sampled on TA14-CpX29 at plant B in April, May and December 2021 are compared and TC composition fluctuations appear. In April, 41 distinct TC from 22 molecular formulas in 7 families were present, in May there were 110 TC from 27 molecular formulas in 9 families, and in December there were 43 TC from 21 molecular formulas in 7 families (Fig.6.12, Fig.6.SI-9). Although internal digesters temperatures are continuously monitored to keep constant levels, outside temperatures during the April sampling day were $12.6 \pm 1^\circ\text{C}$ against $24.2 \pm 3^\circ\text{C}$ in May and $8.2 \pm 0.1^\circ$ in December (Table 6.3). Several studies have demonstrated the variety of volatile organic TC produced through biological anaerobic digestion are higher in spring and summer when environment temperatures are higher [9,12,14,21], corroborating results found here in May. Chemical families represented in all three grid-biomethane samples were terpenes with camphene always dominating (just as in the dried biomethane sample (Fig.6.10)); polycyclic alkanes with decahydronaphthalene dominating; linear and cyclo-alkanes; aromatics with only benzene, toluene (abounding the most) and xylene isomers; and alkenes. One Sulphur-species (2-Ethyl-1-hexanethiol) was found in May and December. Only the May-sample contained a halogenated species and several alcohol species. Despite the May-sample containing a larger number of total TC and families, there is a relative homogeneity in the per-family $RA_{F,i}$ for TC and families identified throughout the months (Fig.6.12). Some variation is however observed amongst terpenes where camphene always dominated but in April, and December especially, some other terpenes were found. Perhaps the largest variations occurred in the linear alkanes family where heptane and octane dominate in April and December (just as in the dried biomethane in Fig.6.10) but not in May where heavier species such as nonane abound the most. In December, lighter species such as pentane and hexane were additionally substantially

represented (Fig.6.12). More variations appear when regarding the global $RA_{G,i}$ (Fig.6.SI-9): the grid-biomethane in April was characterized by high abundances of cyclobutane, toluene and octane. In May, heavier nonane and other C_9H_{20} linear alkanes as well as C_9H_{18} cycloalkanes were dominant. In December, lighter alkanes (pentane, heptane, octane) and terpenes abounded the most. Next to the higher ambient temperatures in May, potentially enhancing the pre-degradation of organic matter before introduction in the anaerobic digester, causing more high-boiling (heavier) compounds to volatilize during anaerobic digestion, the gas production plant was stopped during the May sampling day due to a too high oxygen level (>7000 ppm) in the biomethane prohibiting its injection in the natural gas grid. This day, biomethane was actually sampled from a buffer tank at 40 bar_a at the injection station. The underlying biogas upgrading hindrances that led to high oxygen levels could have affected the TC's composition of the biomethane previously sent to the buffer tank, with a wider diversity of TC-species and -families detected, among others alcohols, halogenated and Sulphur-compounds (Fig.6.12). Lastly, variations in feedstocks nature and proportions in the anaerobic digester and variations in operational conditions of the upgrading process may also influence the monthly biomethane TC's composition. Note the differences in sampling flowrates through the MAT in April (~ 55 mL \cdot min $^{-1}$), May (~ 500 mL \cdot min $^{-1}$) and December (~ 1 L \cdot min $^{-1}$) (Table 6.3) should not relate to the observed TC composition variations as breakthrough volumes and adsorption efficiencies are not impacted by flowrates in such a small value range (55 – 1000 mL \cdot min $^{-1}$) [59,60].

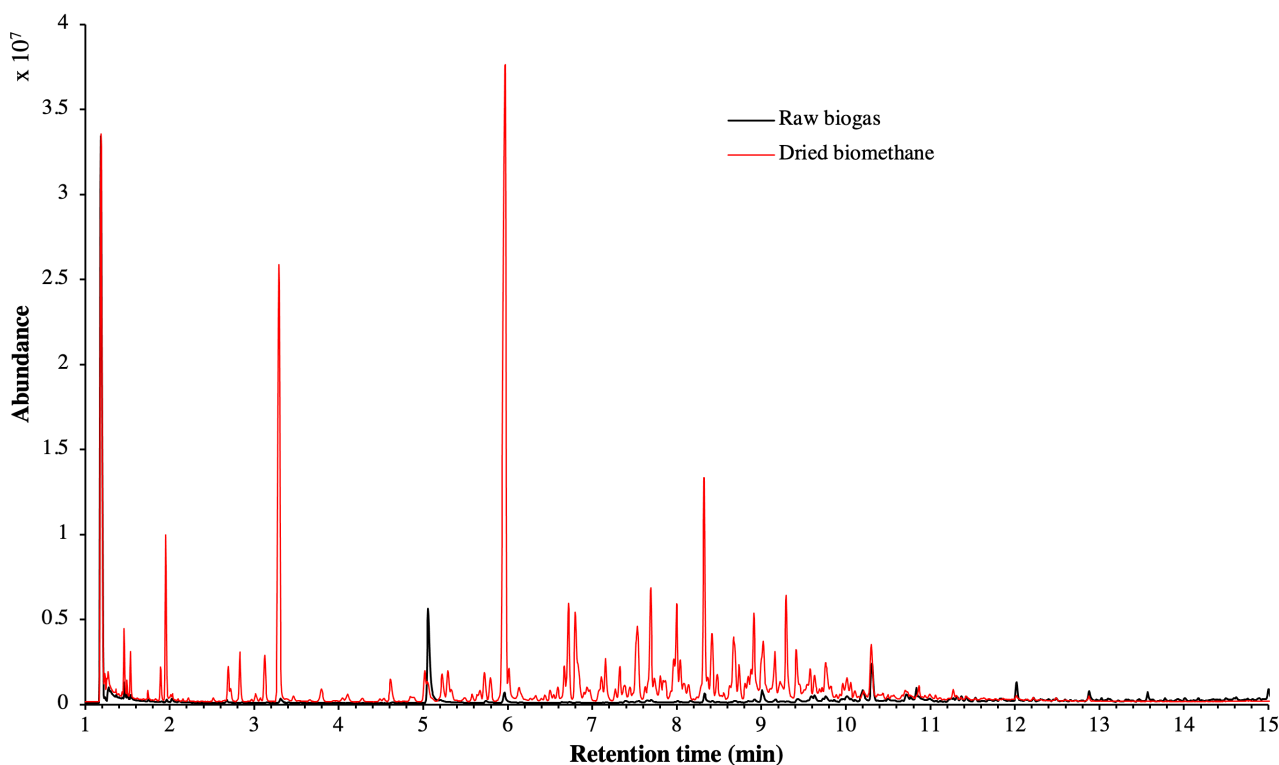


Figure 6.9: TIC of raw biogas and dried biomethane of plant B sampled on TA14-CpX29 in March 2021.

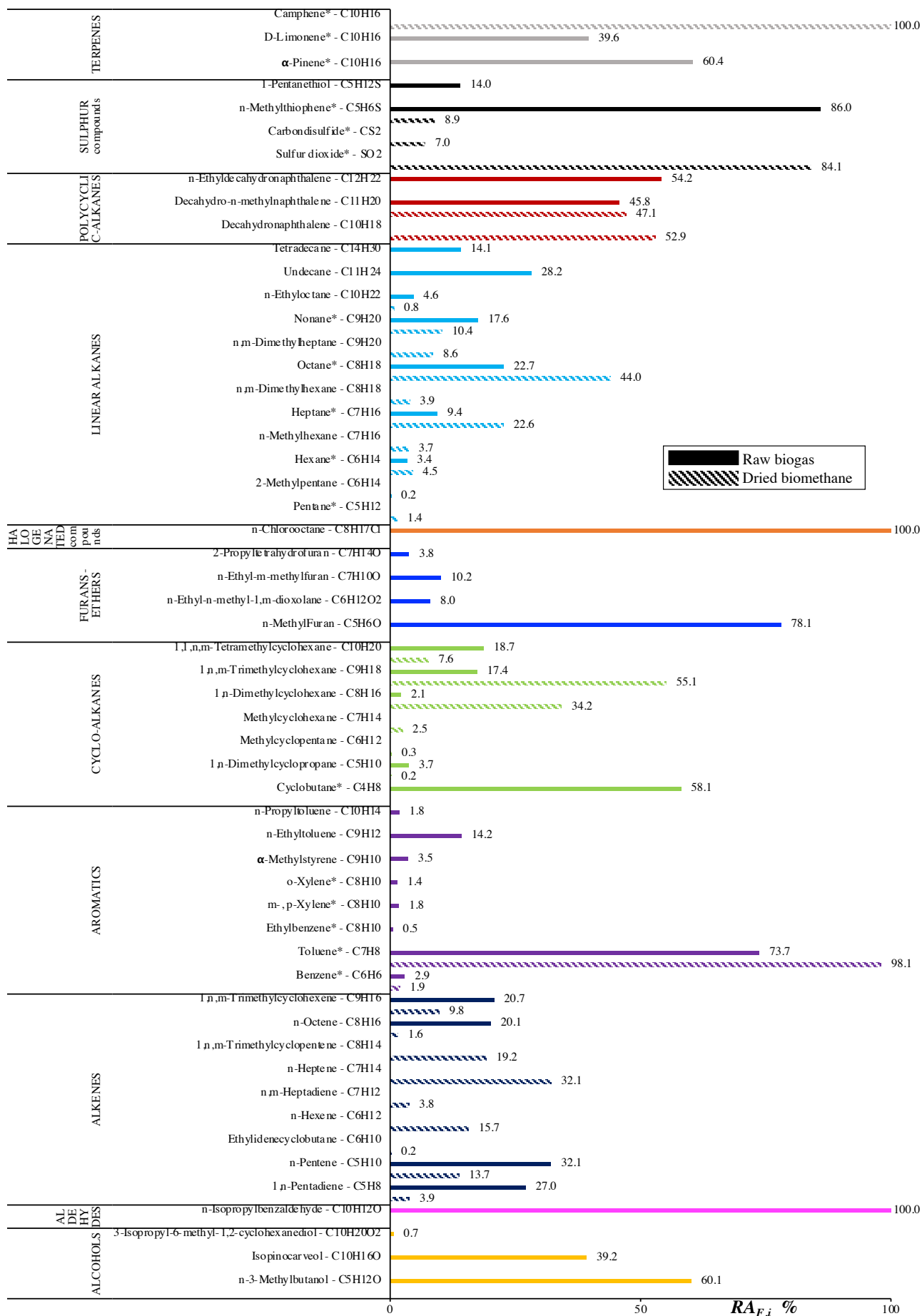


Figure 6.10: Per-family relative abundance (%) of trace compounds identified in the raw biogas and dried biomethane of plant B sampled on TA14-CpX29 in March 2021. Compounds marked with a "*" are unequivocally identified.

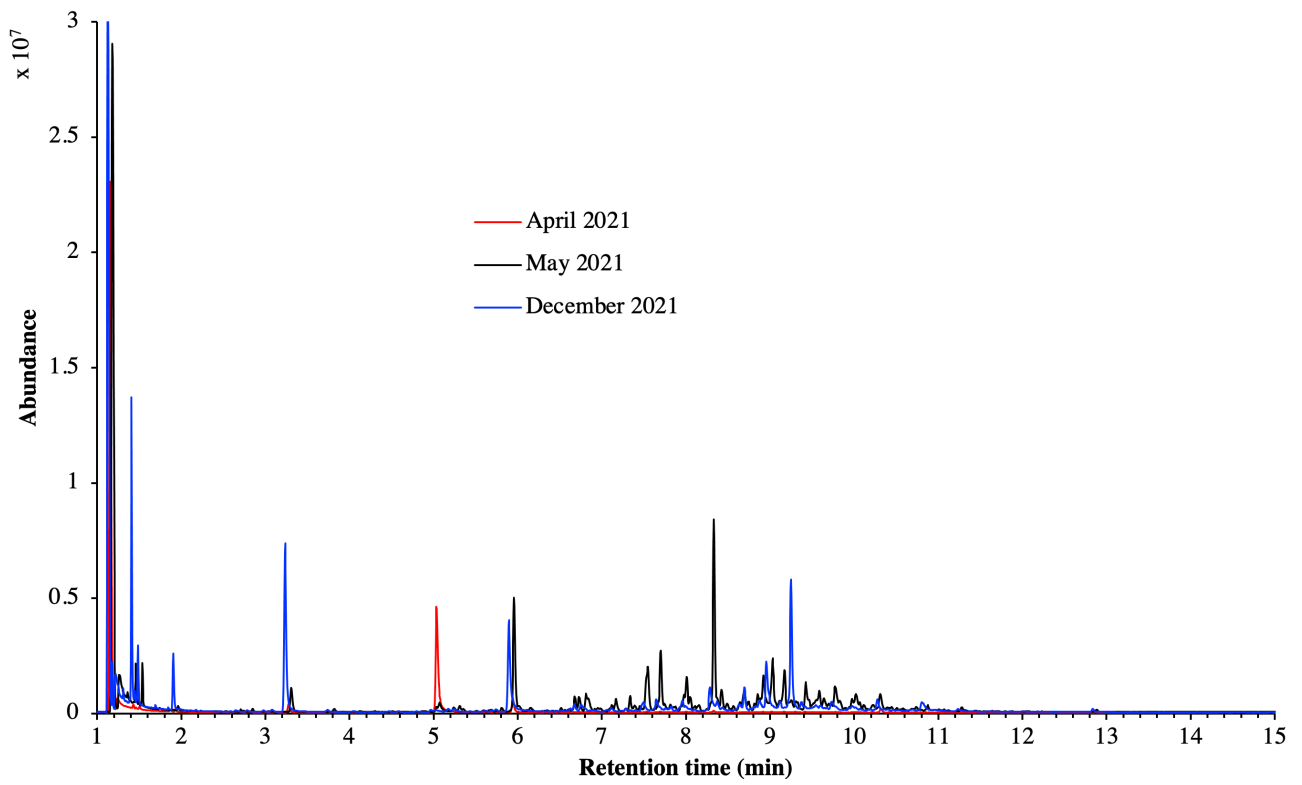


Figure 6.11: TIC of the grid-biomethane of plant B sampled on TA14-CpX29 in April, May and December 2021.

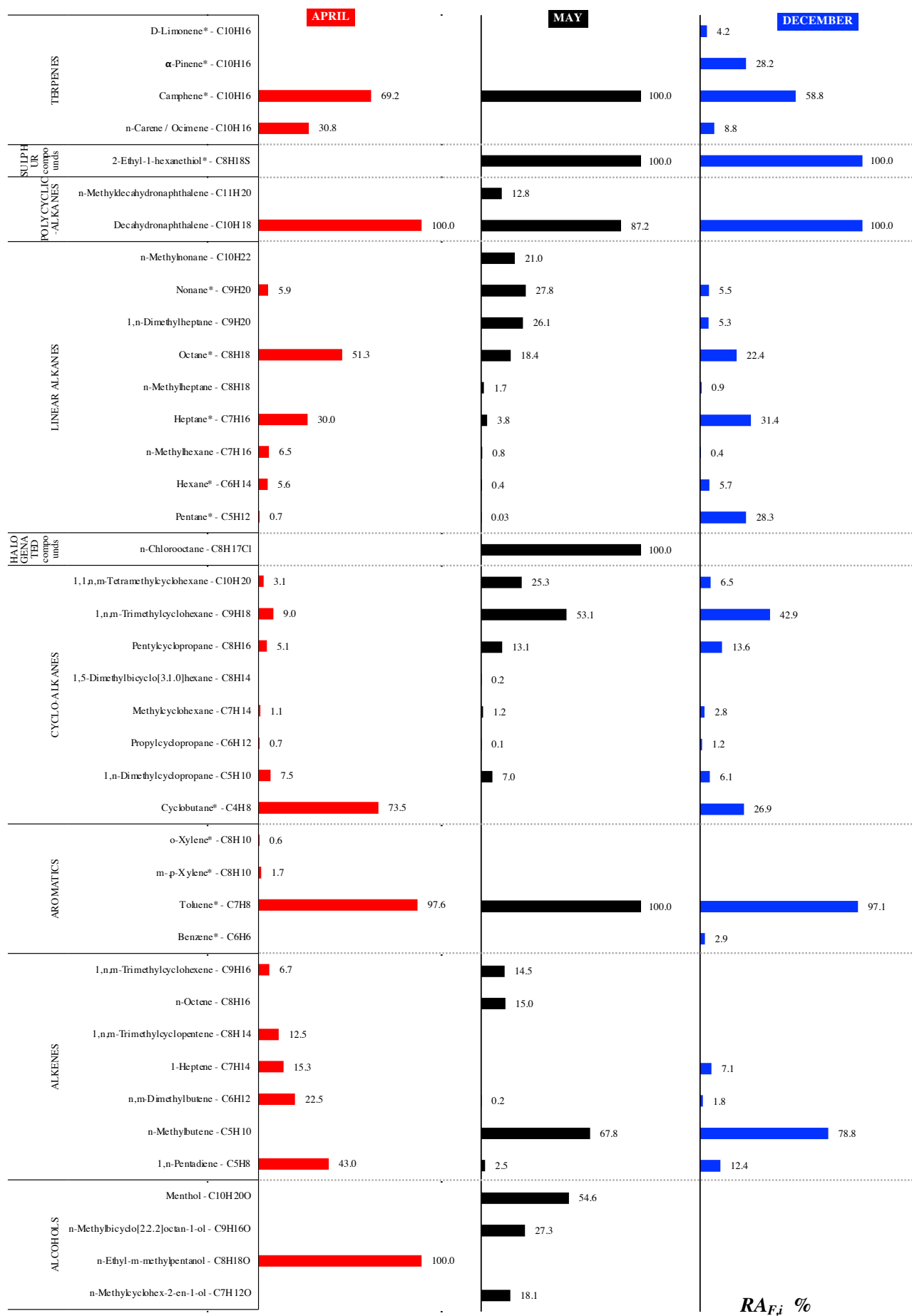


Figure 6.12: Per-family relative abundance (%) of trace compounds identified in the grid-biomethane of plant B sampled on TA14-CpX29 in April, May and December 2021. Compounds marked with a "*" are unequivocally identified.

III.4.3. Plant C

Fig.6.13 – 6.14 and Fig.6.SI-10 present the TC identification results of the 1 L_N samples dried raw biogas and pre-treated biogas in plant C. Fig.6.13 indicates *a priori* a relative similarity between both gas streams. Nonetheless, the dried raw biogas contained 111 distinct TC from 41 molecular formulas belonging to 12 families while, counter-intuitively, the pre-treated biogas presented a higher diversity: 132 TC from 53 molecular formulas in 13 families. Families shared by both gases include terpenes, Sulphur-compounds, alkanes (polycyclic, cyclic and linear), ketones, ethers, esters, aromatics, alkenes, aldehydes and alcohols. A single halogenated species was only detected in the pre-treated biogas (Fig.6.14). At least seven terpenes were identified with α -pinene dominating both before and after pre-treatment of the biogas. Other most abounding terpenes were D-limonene and β -pinene. Regarding Sulphur-compounds, no H₂S was detected in the dried raw biogas on the TA14-CpX29 MAT although plant operators cope with significant H₂S levels upstream the pre-treatment (Table 6.2). H₂S would probably have been detected if the TA14-CX26 MAT had been used. Nonetheless, other Sulphur-species were found: dimethyldisulfide and heavier S-species in the dried raw biogas with dipropyldisulfide dominating. After activated carbon treatment, biogas still contained all S-species detected before the treatment. Three species (dimethyltrisulfide, thiophene and 1-methylthio-1-propene) were only detected in the pre-treated biogas. Amongst polycyclic-alkanes, dimethyldecahydronaphthalene was dominant both before and after pre-treatment. The fate of linear alkanes and aromatics was also not impacted by the pre-treatment. For alkanes, octane was the most abundant. Pentane was not detected in the raw biogas, while it probably lurks there. For aromatics, the mono-terpene *n*-cymene was the most abundant and 1-Isopropenyl-*n*-methylbenzene was the second main aromatic. Alkenes were also poorly impacted by the pre-treatment, and the terpene-like menthene was the most abundant. As for ketones, *n*-butanone was the main species before and after pre-treatment. Pre-treated biogas contained more ketones than raw biogas. Amongst ethers, *n*-methylfuran was dominant before and after pre-treatment and two species were potentially removed during the treatment. Cyclobutane was the most abounding cyclo-alkane in the raw biogas and appeared to be removed after pre-treatment. *n*-butenal was the sole aldehyde species in the raw biogas and after pre-treatment a second minor species (*n*-ethylbutanal) was also present. Finally, more alcohols were detected after pre-treatment with the terpene-like 2,8-*p*-menthadien-1-ol dominating before and after pre-treatment. Thus, for most chemical families including non-H₂S Sulphur-compounds, the activated carbon pre-treatment seems to have no abatement effect since generally as much or even more TC were identified in the pre-treated biogas as in the raw biogas. Extra TC in the pre-treated biogas were either not detected in the raw biogas due to the limited number of sample replicates, or they were generated as pollution from the activated carbon column.

The global $RA_{G,i}$ results (Fig.6.SI-10) corroborate the similarity in TC composition before and after pre-treatment of the biogas at plant C with terpenes and terpene-like TC dominating in both dried raw and pre-treated biogases (*n*-cymene: > 40% $RA_{G,i}$; menthene: ~2 % $RA_{G,i}$).

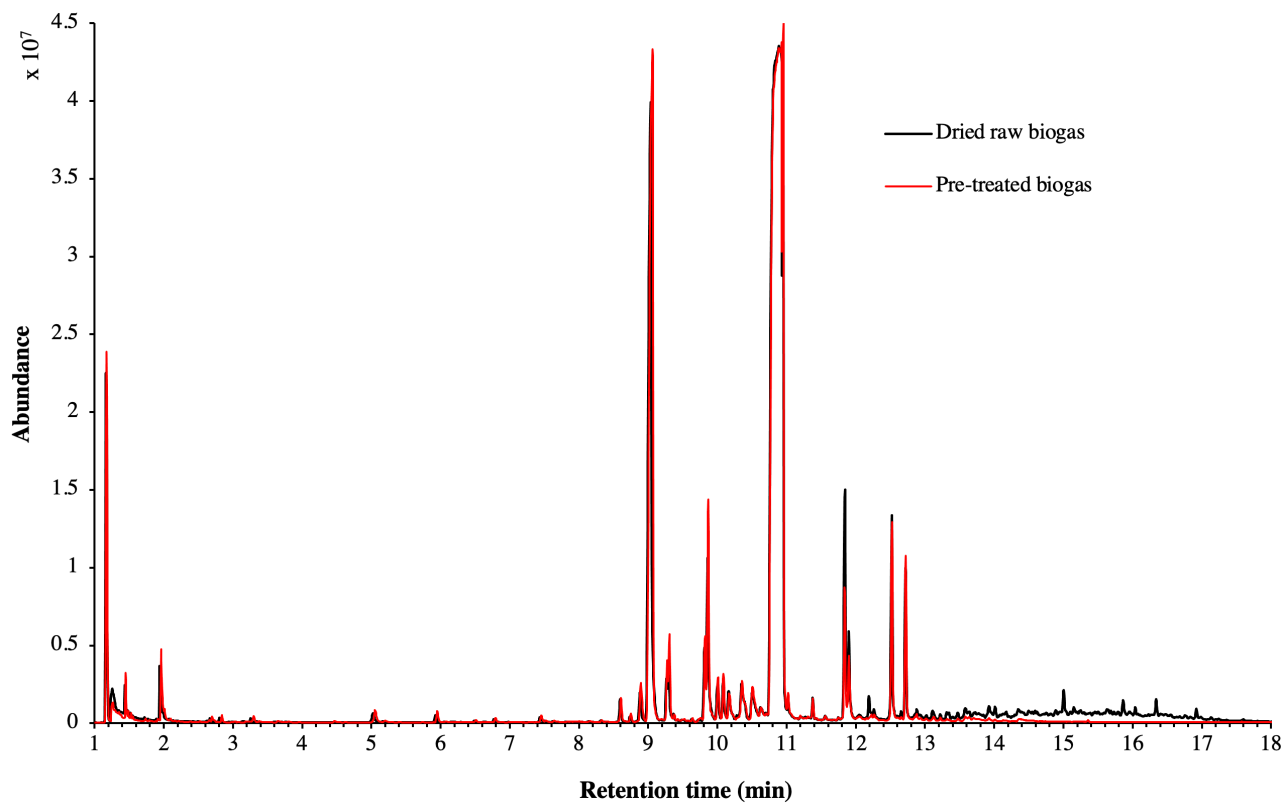


Figure 6.13: TIC of the dried raw biogas and pre-treated biogas of plant C sampled on TA14-CpX29 in March 2021

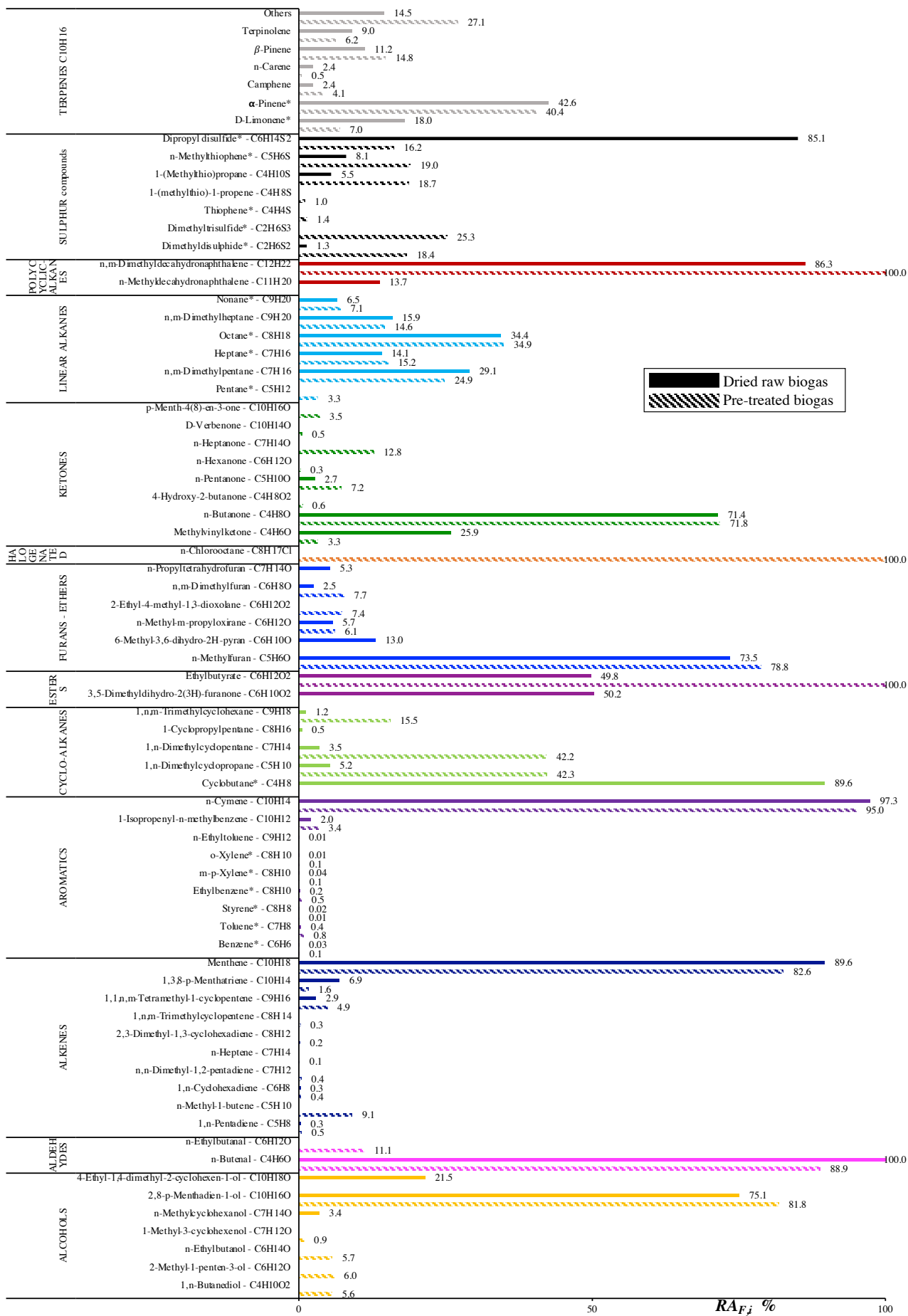


Figure 6.14: Per-family relative abundance (%) of trace compounds identified in the dried raw biogas and pre-treated biogas of plant C sampled on TA14-CpX29 in March 2021. Compounds marked with a "*" are unequivocally identified.

III.5. Potential influences of feedstock's nature on trace compounds in raw biogas and landfill gas

Results in section III.4 enable to outline potential correlations between feedstocks in landfills or digesters and dominant TC found in the generated raw gases. As pre-treatment or upgrading processes implemented affect the TC composition in pre-treated biogas or in biomethane, the nature of feedstocks chiefly impacts the TC composition in the raw gases.

The raw landfill gas of plant A was especially characterized by a relative homogeneous representation of a broad diversity of TC from diverse (ten) chemical families with dominant compounds being CS₂, H₂S, acetate-1-propene-2-ol, toluene and pentane. High abundances of Sulphur-compounds are perhaps the key feature, even after H₂S removal (Fig.6.SI-7). This trend is typical for landfill gas where the large heterogeneity of anthropogenic and synthetic dumped wastes not only directly emits volatile species upon burial [61] but whose degradation also leads to wide ranges of TC at higher concentrations than in digester biogases [6,7,11,12,21,61]. H₂S in landfill gas is mainly assigned to the anaerobic or aerobic reduction of sulfates by sulfate reducing bacteria [62]; sulfates can originate from plasterwork and other dumped gypsum building materials [58]. Plastics, plastic foam, varnished furniture and refrigerators, impregnated wood, flame retardant stuffing and textiles in armchairs or curtains, aerosol propellants, cryogenic and foaming agents, varnish and paint removers, dry cleaning and dyeing solvents, detergents, paints, lacquers, coatings, resins, adhesives, pharmaceuticals, ... are all potential sources of halogenated, aromatic and oxygenated TC in landfill gas while fragrant household detergents and air fresheners are a source of terpenes [6,7,12,58,61]. Besides, residues of hygienic and cosmetic products, lubricants, anti-foaming agents and coatings are all direct siloxane sources generally generating multiple siloxanes in landfill gas [6,10,13,22]. Plant A-landfill gas however only contained one siloxane, namely octamethylcyclotetrasiloxane (Fig.6.8), a very common siloxane in landfill gas [6,10,13,22]. Siloxane-bearing materials were maybe insufficiently dumped or appropriate siloxane-releasing conditions were maybe not reached in plant A-landfill to generate other siloxanes. Further, it has been shown that alkanes and aromatics are predominantly released from older landfill waste-cells while halogenated and alcohols are especially generated at the early decomposition stages with fresh wastes, and that alcohols and esters reach higher levels under high gas production rates [7]. The presence of at least 10 linear alkanes, 7 cyclo-alkanes and 8 aromatics and of only two halogenated and one alcohol species and the absence of esters in plant A-landfill gas (Fig.6.8) corroborates this statement as landfill gas production rate at plant A was very low and as waste-cells wherefrom the gas was extracted were already 7 years old.

In anaerobic digesters, organic feedstocks are less heterogeneous, i.e. have a lesser chemical diversity, than in landfills and digester biogases therefore generally present lower concentrations of TC [11–13] yet still a wide, or wider, diversity of TC amongst numerous chemical families [14] as was the case in biogases of plant B (11 families represented) and plant C (13 families). Biogas of plant B was especially characterized by a high toluene abundance, and other predominant TC were alcohols (*n*-3-methylbutanol, isopinocarveol), *n*-ethyltoluene, cyclobutane, linear alkanes (octane, nonane, undecane) and terpenes (D-limonene, α -pinene) (Fig.6.SI-8). Disregarding the outlying abundance of toluene, maybe due to a singular contamination, other TC were relatively homogeneously abundant. In plant C however, the raw

biogas was exclusively dominated by terpenes (D-limonene, α -pinene, camphene, n-carene, β -pinene, terpinolene and others) and terpenoid TC (*n*-cymene, menthene, 2,8-p-menthadien-1-ol) (Fig.6.SI-10). No Silicon-containing compounds were found in biogases of plants B and C, pursuant to other studies on manure-, agricultural-, green- or food-sourced biogas where Silicon-compounds are generally absent or present at lower concentrations than other TC [12–14,21] insofar as such feedstocks exclude siloxane-bearing anthropogenic and synthetic materials. Regarding terpenes, D-limonene and α -pinene were dominant both in plant B and C (Fig.6.SI-8, 6.SI-10), supporting previous studies demonstrating those species are typical in digester biogas [14,48]. In plant C-biogas, the exclusive predominance of the mono-terpene *n*-cymene and of terpenes, which together accounted for > 90% of all TC identified (Fig.6.SI-10), is explained by the high share of food-sourced feedstocks at this plant (Table 6.2). Arrhenius et al. [48] surveyed 8 biogas plants processing food wastes and found a positive linear relationship between food waste volumes digested and levels of terpenes found. *p*-Cymene and D-limonene systematically reached up to 90% of all volatile organic TC in the biogases, with *p*-cymene prevailing over D-limonene in mesophilic digestion plants, just as in here's plant C. *p*-Cymene naturally occurs in hundreds of food products such as butter, carrots, oranges, raspberries, lemon oil, nutmeg, oregano and nearly all spices. As for D-limonene, it is naturally present in lemon rind, dill, fennel, celery, plants and essential oils and is also synthesized for food flavor additives [48]. The authors postulated D-limonene was prevailing in raw feedstocks and that most of it was converted to *p*-cymene during mesophilic anaerobic digestion. In the same survey, the terpene-removal efficiency of diverse biogas to biomethane upgrading technologies was evaluated and appeared to lie between 83 and 96% for water scrubbers [48]. This relates to results of plant B, upgrading its biogas via a water scrubber, where remnants of especially camphene and occasionally other terpenes were found in the dried- and grid-biomethane (Fig.6.10, 6.12). At plant B, terpenes may originate from agricultural wastes (plants, barks, roots) [14]. Next to terpenes, Gómez et al. [14] found ketones such as acetone and 2-butanone were the predominant TC in several digester biogases. Here, ketones were only detected in the biogas of plant C, with at least 8 distinct species and indeed *n*-butanone abounding the most followed by methylvinylketone (Fig.6.14). Ketones are unlikely present in feedstocks and are rather generated during anaerobic digestion [14]. Pertaining to Sulphur-compounds determined in both biogases of plants B and C, they can originate from the anaerobic degradation of amino acid-rich feedstocks such as a manure and (animal) food-processing residues [12,14,21]. Lastly, aromatics including benzene, toluene, ethylbenzene and xylene isomers (BTEX) were found in both biogases of plants B and C. In such anaerobic digesters, those compounds can originate from the microbially-driven breakdown of large aromatic compounds such as terpenes, phenolic compounds and especially lignin being naturally abundant in organic wastes (agricultural-, food-, green wastes...) [12,63]. Traces of BTEX in biogas can also stem from industrial effluents such as solvents, fats and oils co-digested with other feedstocks [14]. A last possible benzene source in biogas has been found to derive from the microbial conversion of certain pesticides such as hexachlorocyclohexane present in plant biomass into chlorobenzene and benzene via anaerobic reductive dechlorination [64].

III.6. A first step towards semi-quantification

As a first estimate of concentrations of TC identified, Fig.6.15 – 6.18 propose each, merely as a semi-quantitative indication, an overlay of the total ion current chromatogram (TIC) of a sampled gas with the TIC of a certified synthetic gas mixture (SGM) containing 41 halogenated volatile organic compounds each at 1 ppm_{mol} in nitrogen ('TO-14A 41 Component Mix', Scott Airgas Specialty Gases, Plumsteadville, USA, purchased from Restek, France) sampled and analyzed under the same conditions. The 41 compounds of the SGM are listed in Table 6.SI-1: these are mainly chlorinated species and BTEX, some of which were also determined in the gases at plants A, B and C. Disregarding ionization efficiency discrepancies between TC in the real gas samples and in the SGM, the order of magnitude of the concentration threshold at which TC are present in the real gases can be roughly estimated (with 50% error) from Fig.6.15 – 6.18 by contrasting peak signal intensities of real samples to the peaks of the SGM compounds insofar as all compounds in the SGM are certified to be present at 1 ppm_{mol}. The predominant TC are labeled for each sampled gas on Fig.6.15 – 6.18.

In the landfill gas (Fig.6.15), octamethylcyclotetrasiloxane, ethylbenzene, xylene isomers and thiophene seem to reach a ~1 ppm_{mol} concentration threshold. Toluene, *n*-methylfuran, cyclopentane (C₅H₁₀), pentane and carbon disulfide probably lie at concentrations higher than 1 ppm_{mol} and dimethylfuran and other TC at lower concentrations. In the raw biogas of plant B (Fig.6.16), toluene seems to be at ~1 ppm_{mol} while other main TC (octane, nonane, α -pinene, ethyltoluene, D-limonene and others) probably lurk at < 1 ppm_{mol}. In the grid-biomethane of plant B (Fig.6.17), camphene, α -pinene, octane, heptane, hexane, dimethylcyclopropane and pentane seem to lie at \leq 1 ppm_{mol} while other TC probably lurk at lower levels. Finally, in the dried raw biogas of plant C (Fig.6.18), the saturated signal of *n*-cymene and that of D-limonene are respectively ~7 and ~5.5 times larger than the average 1 ppm_{mol} level, indicating up to ~7 ppm_{mol} for *n*-cymene and ~5.5 ppm_{mol} for D-limonene, in line with concentrations reported in [14,48]. Terpinolene and α -pinene also lie at concentrations higher than 1 ppm_{mol} while other terpenes, toluene, *n*-methylfuran and methylvinylketone lurk at lower concentration thresholds.

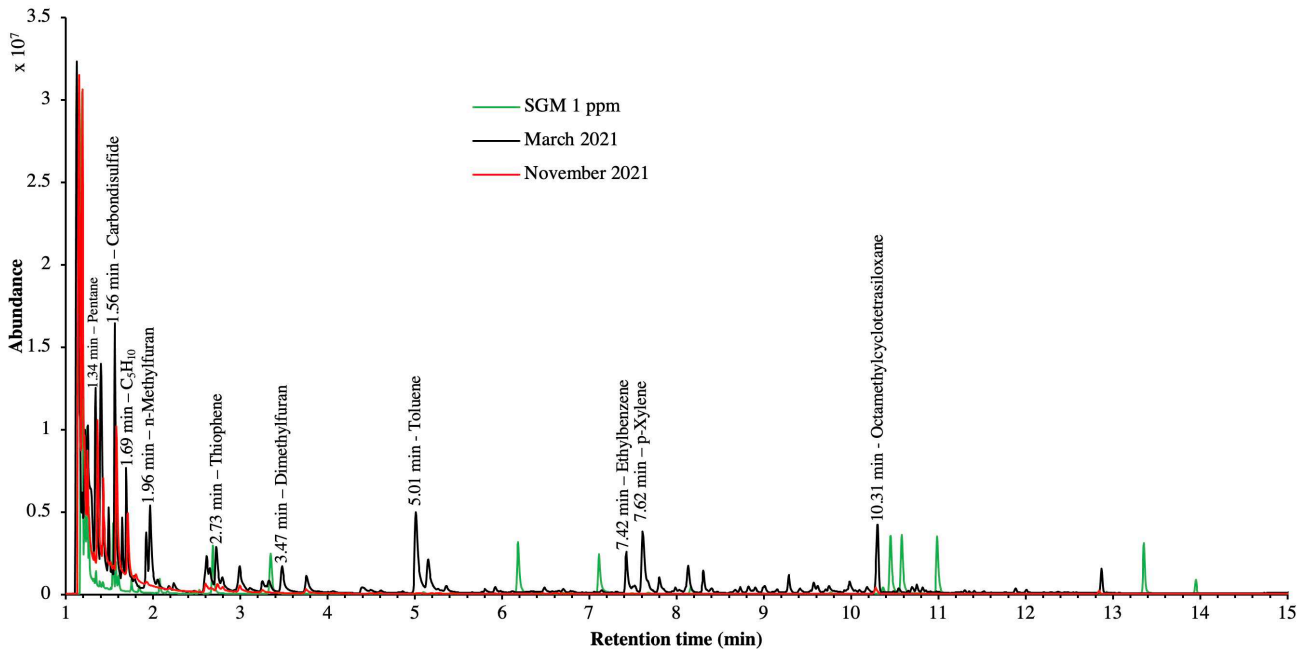


Figure 6.15: TIC of 0.5 L_N landfill gas of plant A sampled in March and November 2021 on TA14-CX26 and of the synthetic gas mixture (SGM) sampled and analyzed identically.

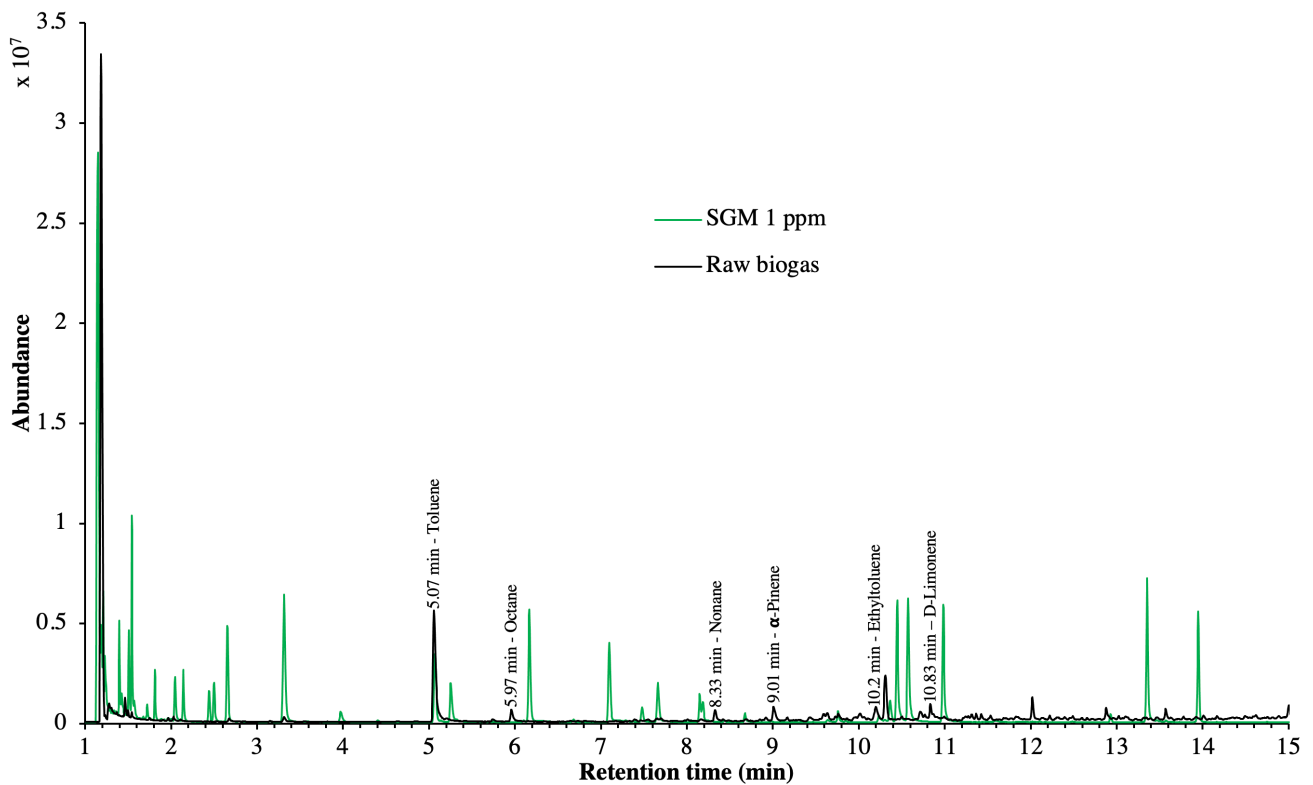


Figure 6.16: TIC of 0.5 L_N raw biogas of plant B sampled in March 2021 on TA14-CpX29 and of the synthetic gas mixture (SGM) sampled and analyzed identically.

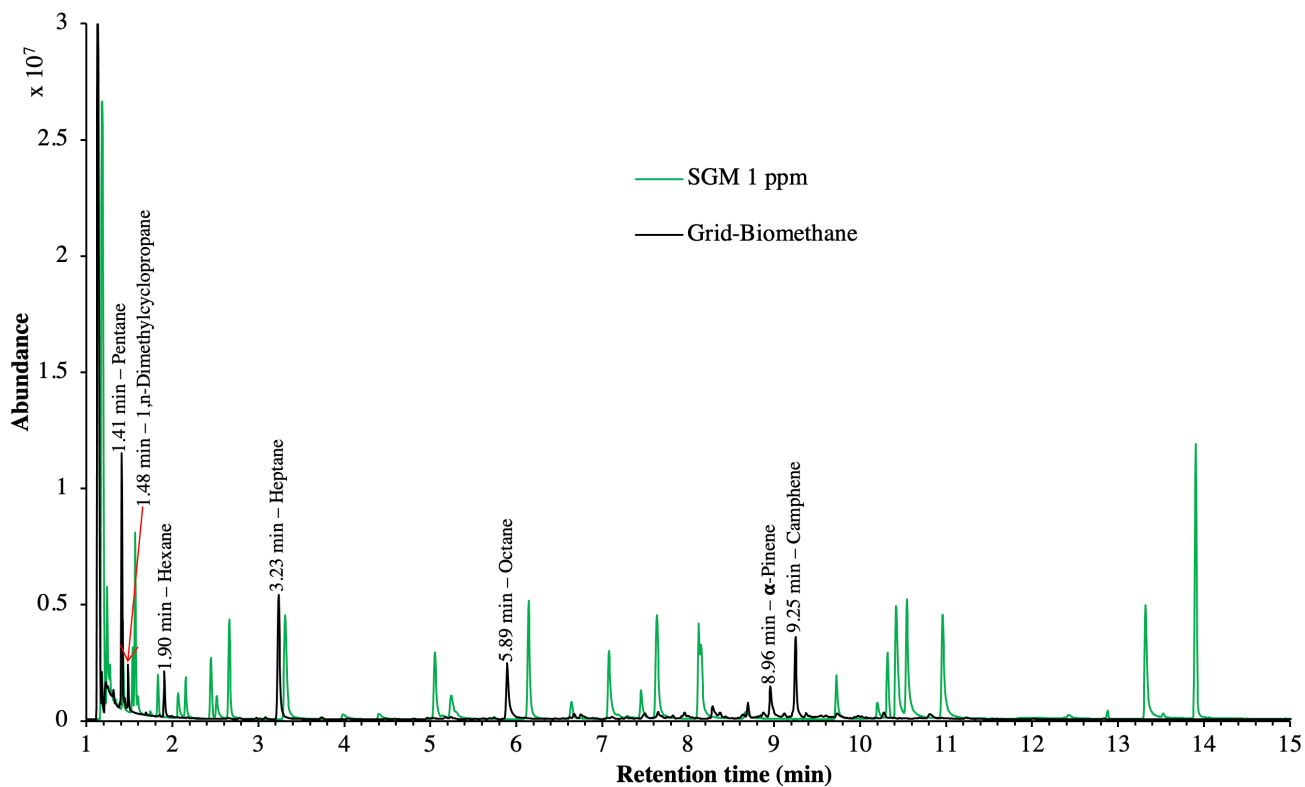


Figure 6.17: TIC of 2.3 L_N grid-biomethane of plant B sampled in December 2021 at 40 bar_a on TA14-CpX29 and of the synthetic gas mixture (SGM) sampled and analyzed identically.

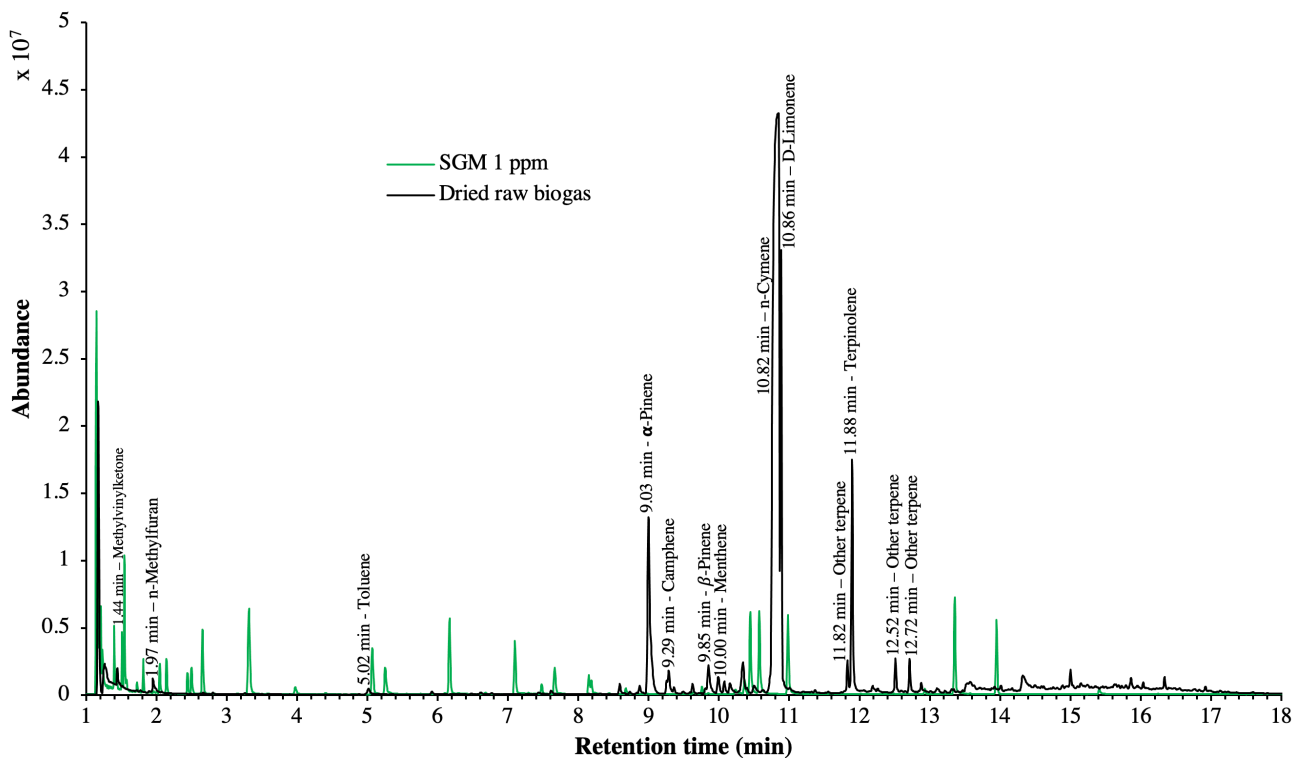


Figure 6.18: TIC of 0.5 L_N dried raw biogas of plant C sampled in March 2021 on TA14-CpX29 and of the synthetic gas mixture (SGM) sampled and analyzed identically.

IV. CONCLUSIONS

This study sought two objectives: (1) improving existing field gas sampling techniques by shortening the sampling chain to minimize contaminations and trace compounds losses by sorption on sampling equipment internal surfaces (tubing, valves, pressure regulators, connectors...), hence guaranteeing a higher sample integrity, and (2) enhancing knowledge on biogas and biomethane's trace compounds to help guarantee their safe and sustainable integration in today's European energy mix. The scientific literature on *biomethane* trace compounds is very limited, on the contrary to that on landfill gas and biogas, hence this paper is an additional contribution for biomethane samples.

When sampling a gas for the first time *in situ*, its composition and concentration ranges are unknown, hence directly choosing the optimal sampling parameters and materials is challenging. Here it was tried to take the best initial hypotheses regarding gas composition based on the knowledge of the feedstocks used and on the gas production process, and to accordingly adapt the sampling method. Although the sampling work was not perfect (flowrates were not constant, tubing material used was not always the same, breakthrough was not accurately determined, insufficient replicates were taken), the direct *in situ* sampling of low volumes (0.5 – 2 L_N) landfill gas, biogas and biomethane streams on TA14-CpX29 multibed adsorbent tubes enabled to decipher a broad range of trace compounds from diverse chemical families in a single sampling run.

Associated Content

Supplemental information

Authors Informations

*Corresponding Author : Isabelle Le Hécho • isabelle.lehecho@univ-pau.fr • Université de Pau et des Pays de l'Adour, E2S UPPA, CNRS, IPREM UMR 5254, Technopôle HélioParc, 2 avenue du Président Angot, 64053 Pau Cedex 09, France

Note

The authors declare no competing financial interests or personal relationships that could have influenced the work reported in this paper.

Acknowledgements

The authors thank *Teréga* (40 Avenue de l'Europe, CS 20 522, 64010 Pau Cedex, France) for the financial support and *nCx Instrumentation* (ZAE Porte du Béarn, 64330 Garlin, France) for the loan of the thermodesorber prototype. Authors are also grateful to the operators of the biogas-biomethane production plants and to the operators of the biomethane grid injection station for their availability and cooperation during sampling operations and for the technical information provided.

V. SUPPLEMENTAL INFORMATION CHAPTER 6

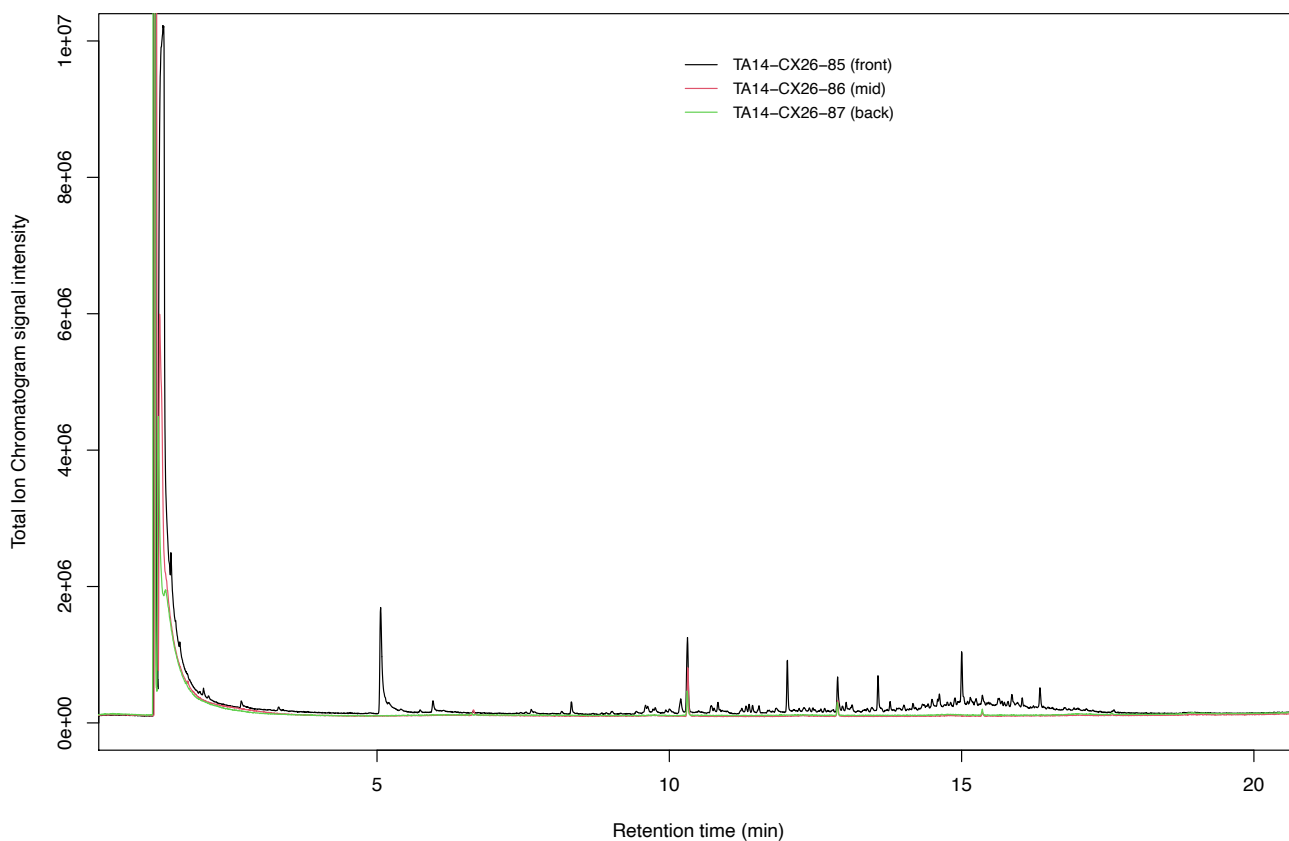


Figure 6.SI-1: 0.5 L_N raw biogas from plant B sampled at $75 \pm 0.5 \text{ mL}_N \cdot \text{min}^{-1}$ on 3 TA14-CX26 MAT in series (front, mid and back MAT): overlay of the TIC of each tube in the series.

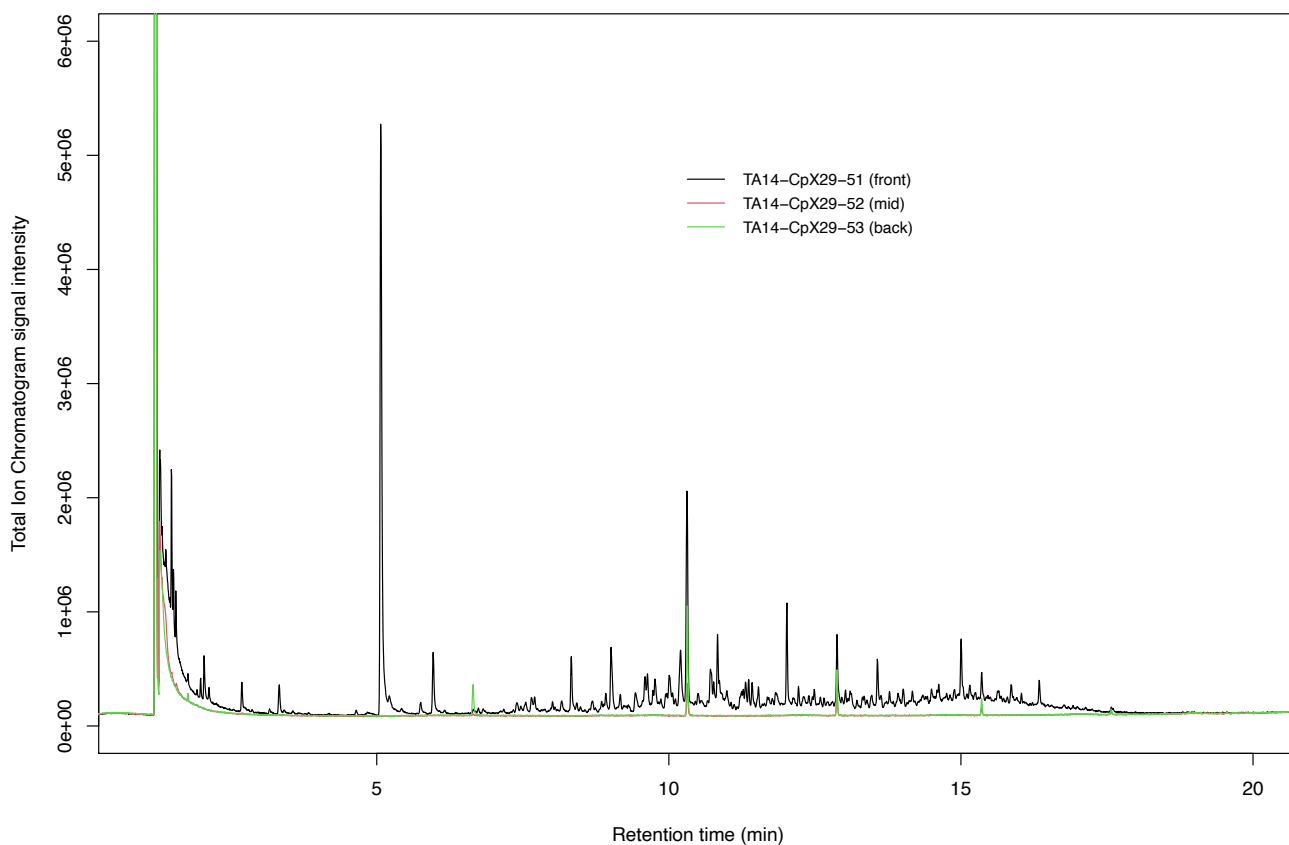


Figure 6.SI-2: 0.5 L_N raw biogas from plant B sampled at $75 \pm 0.5 \text{ mL}_N \cdot \text{min}^{-1}$ on 3 TA14-CpX29 MAT in series (front, mid and back MAT): overlay of the TIC of each tube in the series.

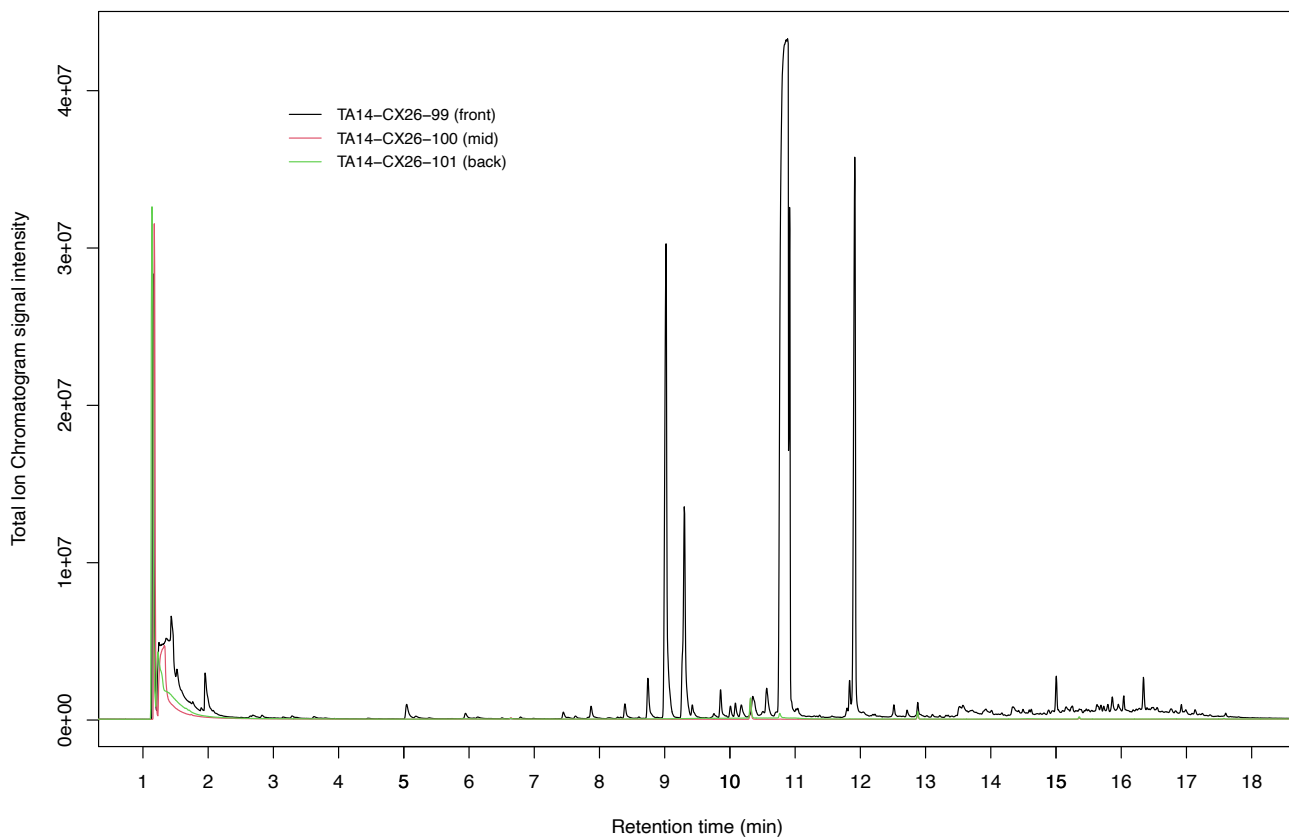


Figure 6.SI-3: $1L_N$ raw biogas from plant C sampled at $60 \pm 0.5 \text{ mL}_N \cdot \text{min}^{-1}$ on 3 TA14-CX26 MAT in series (front, mid and back MAT): overlay of the TIC of each tube in the series.

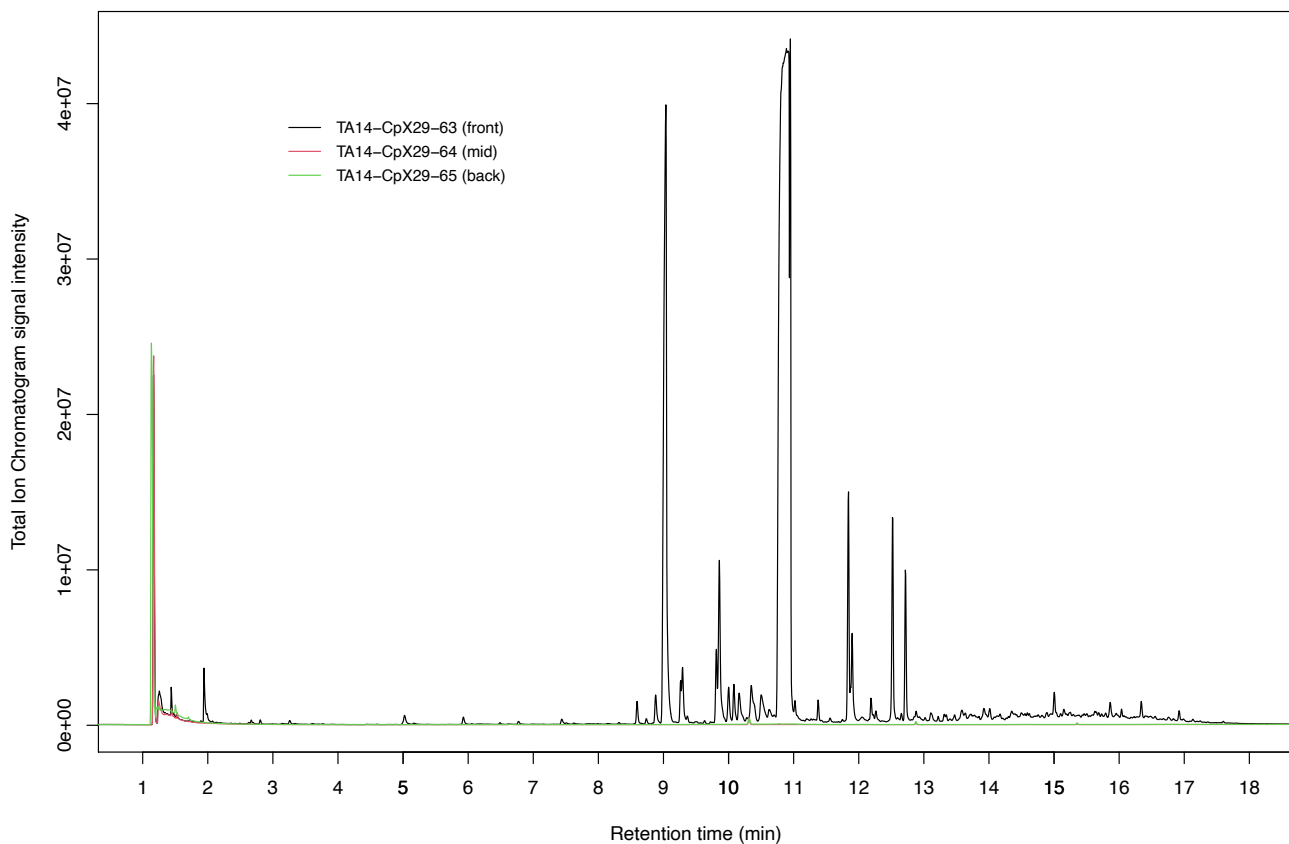


Figure 6.SI-4: $1L_N$ raw biogas from plant C sampled at $60 \pm 0.5 \text{ mL}_N \cdot \text{min}^{-1}$ on 3 TA14-CpX29 MAT in series (front, mid and back MAT): overlay of the TIC of each tube in the series.

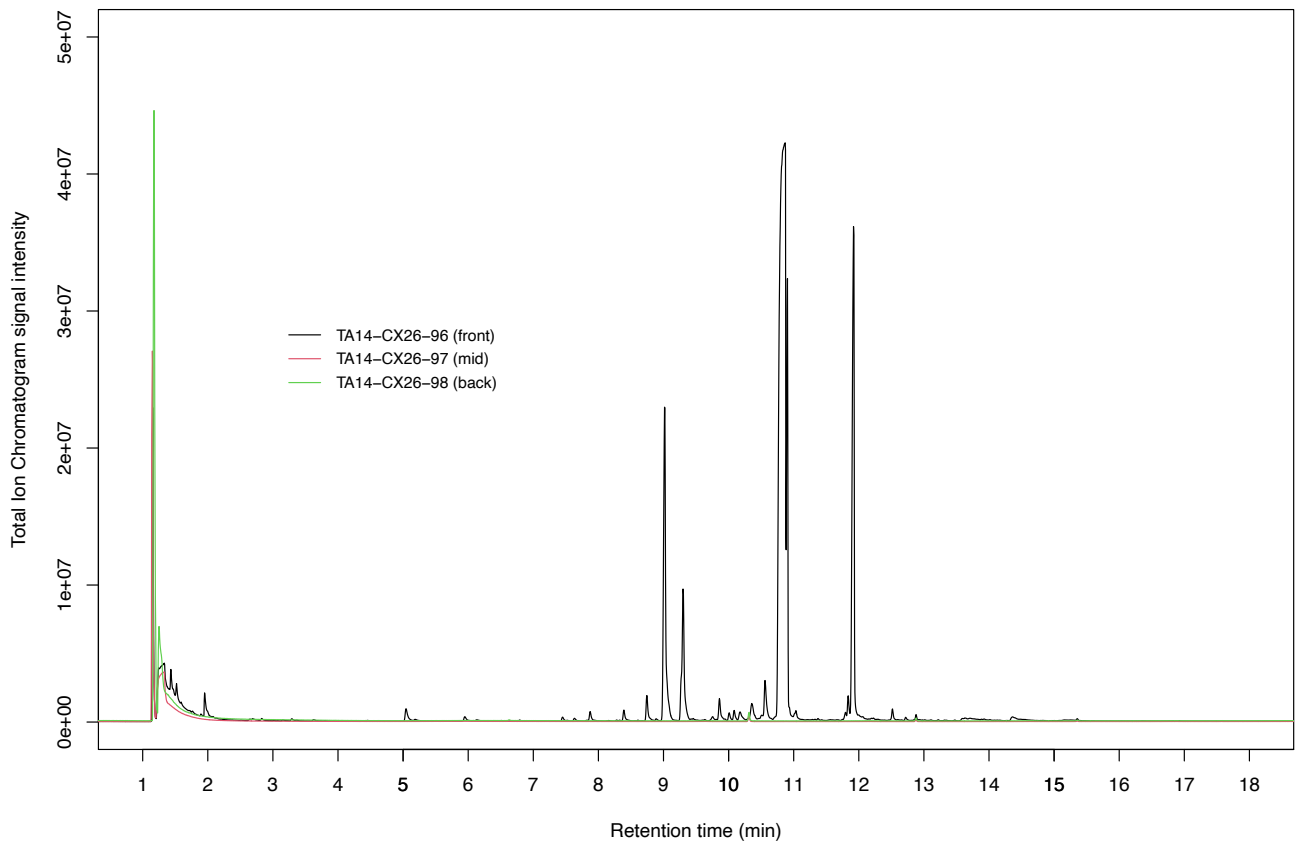


Figure 6.SI-5: $1L_N$ pre-treated biogas from plant C sampled at $65 \pm 0.5 \text{ mL}_N \cdot \text{min}^{-1}$ on 3 TA14-CX26 MAT in series (front, mid and back MAT): overlay of the TIC of each tube in the series.

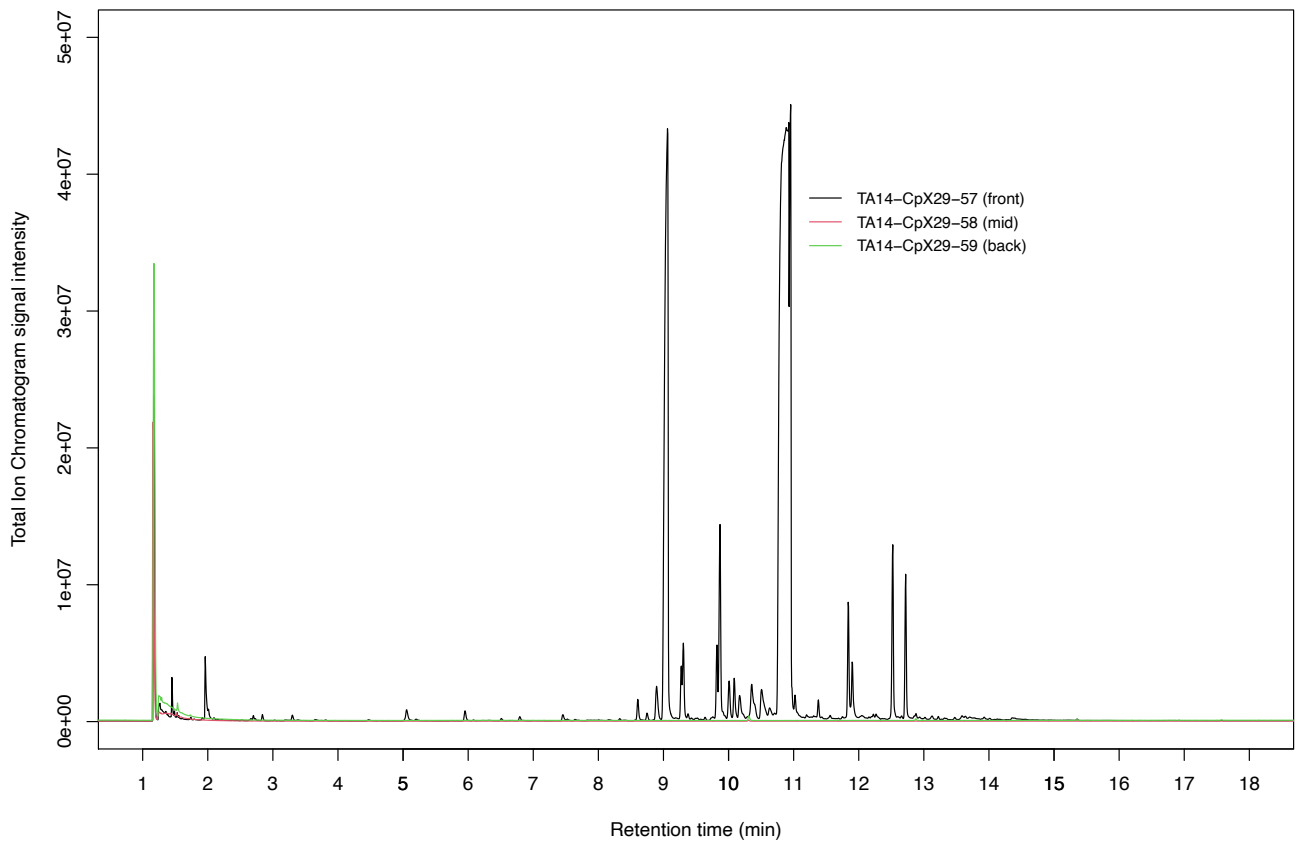


Figure 6.SI-6: $1L_N$ pre-treated biogas from plant C sampled at $65 \pm 0.5 \text{ mL}_N \cdot \text{min}^{-1}$ on 3 TA14-CpX29 MAT in series (front, mid and back MAT): overlay of the TIC of each tube in the series.

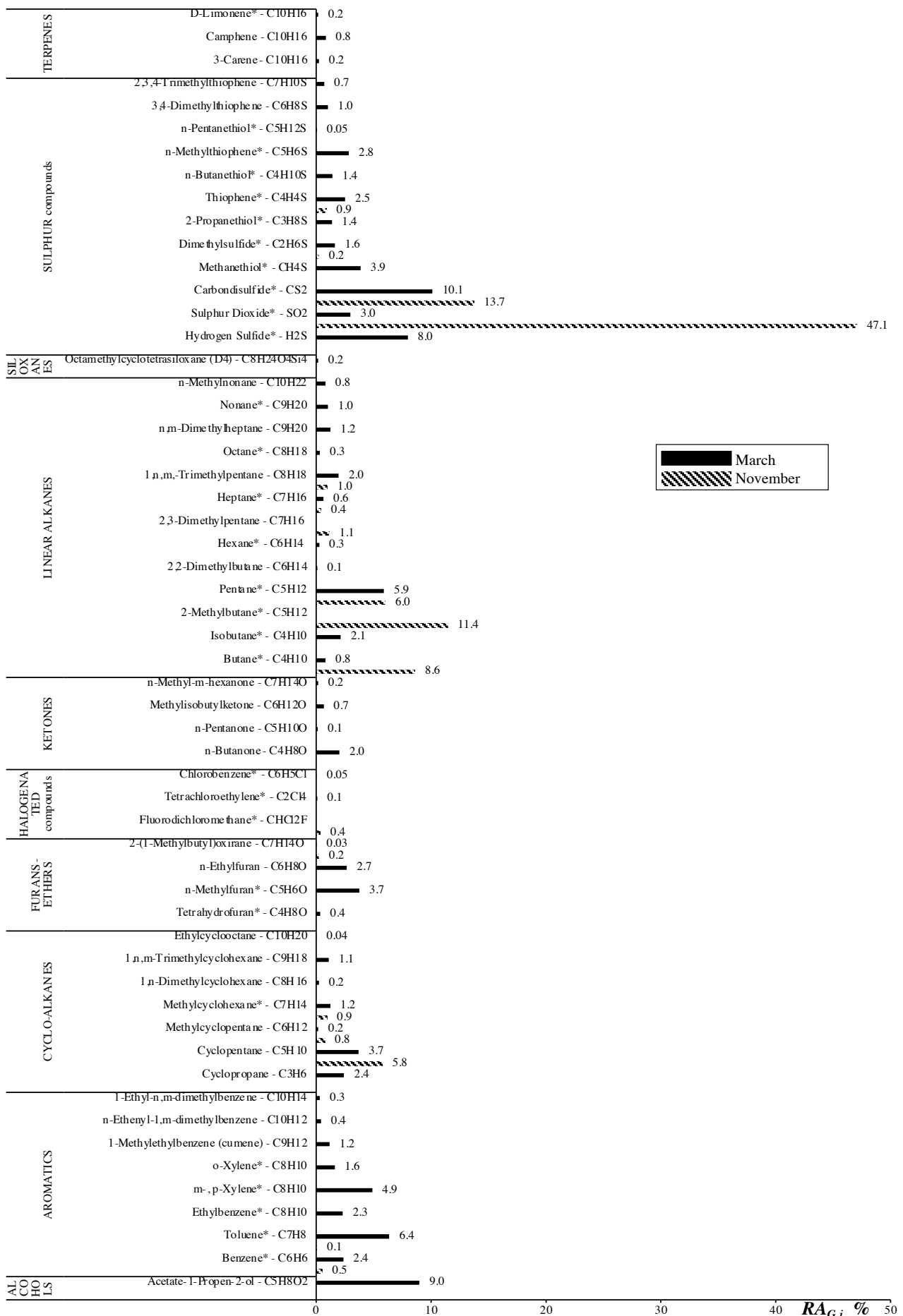


Figure 6.SI-7: Global relative abundance (%) of trace compounds identified in the landfill gas (plant A) sampled on TA14-CX26 in March versus in November 2021. Compounds marked with a "*" are unequivocally identified.

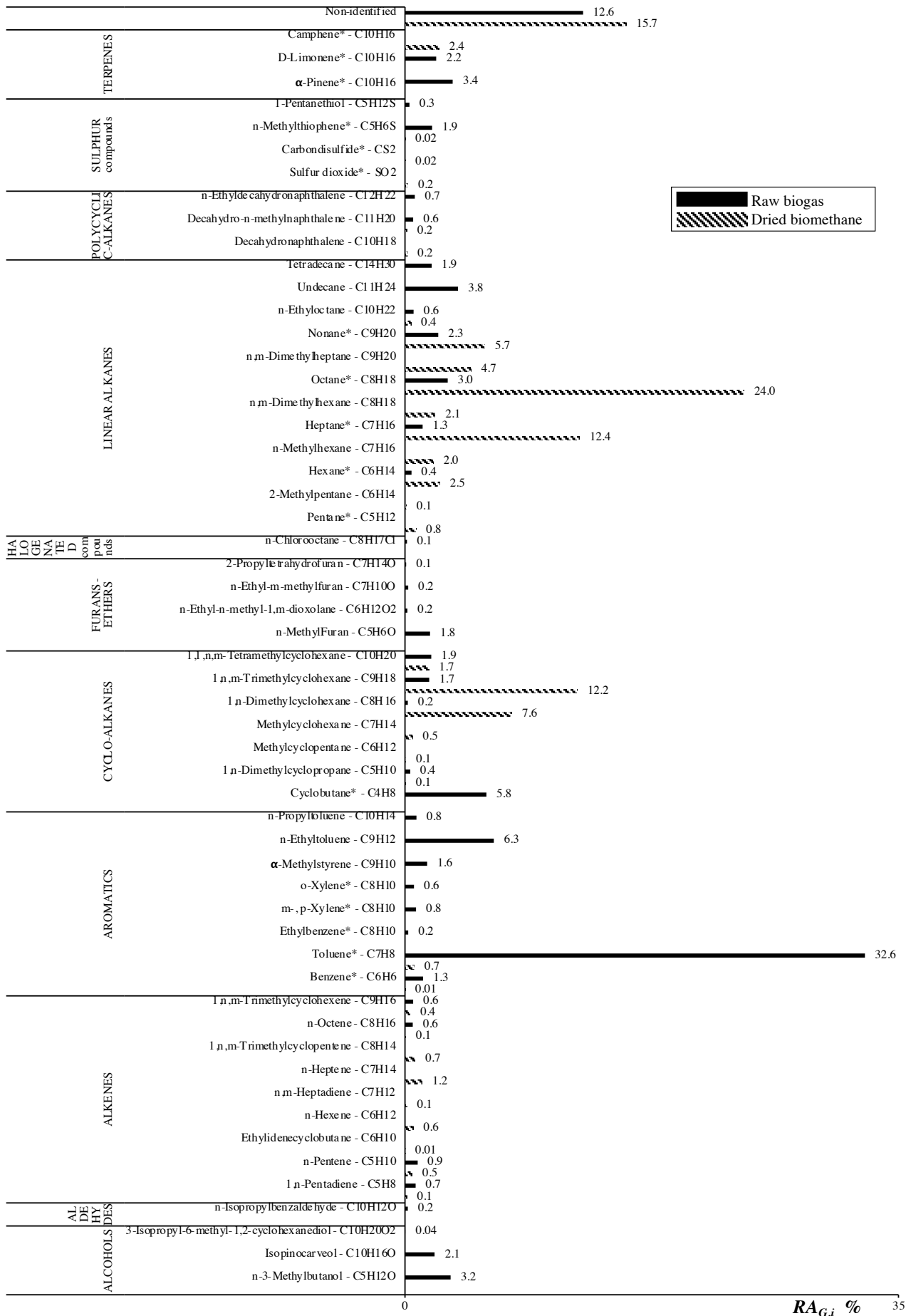


Figure 6.SI-8: Global relative abundance (%) of trace compounds identified in the raw biogas and dried biomethane of plant B sampled on TA14-CpX29 in March 2021. Compounds marked with a "*" are unequivocally identified.

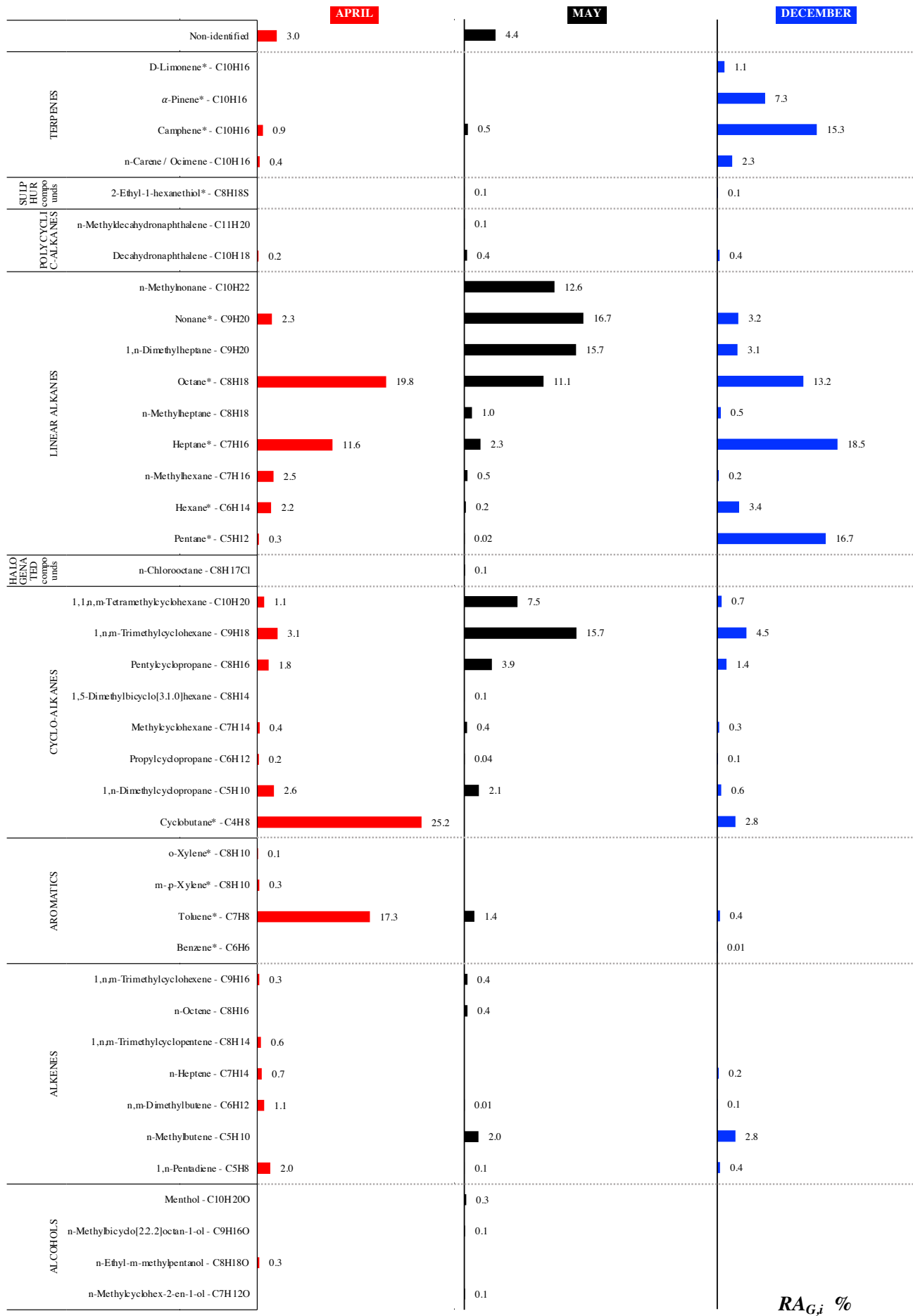


Figure 6.SI-9: Global relative abundance (%) of trace compounds identified in the grid-biomethane of plant B sampled on TA14-CpX29 in April, May and December 2021. Compounds marked with a "*" are unequivocally identified.

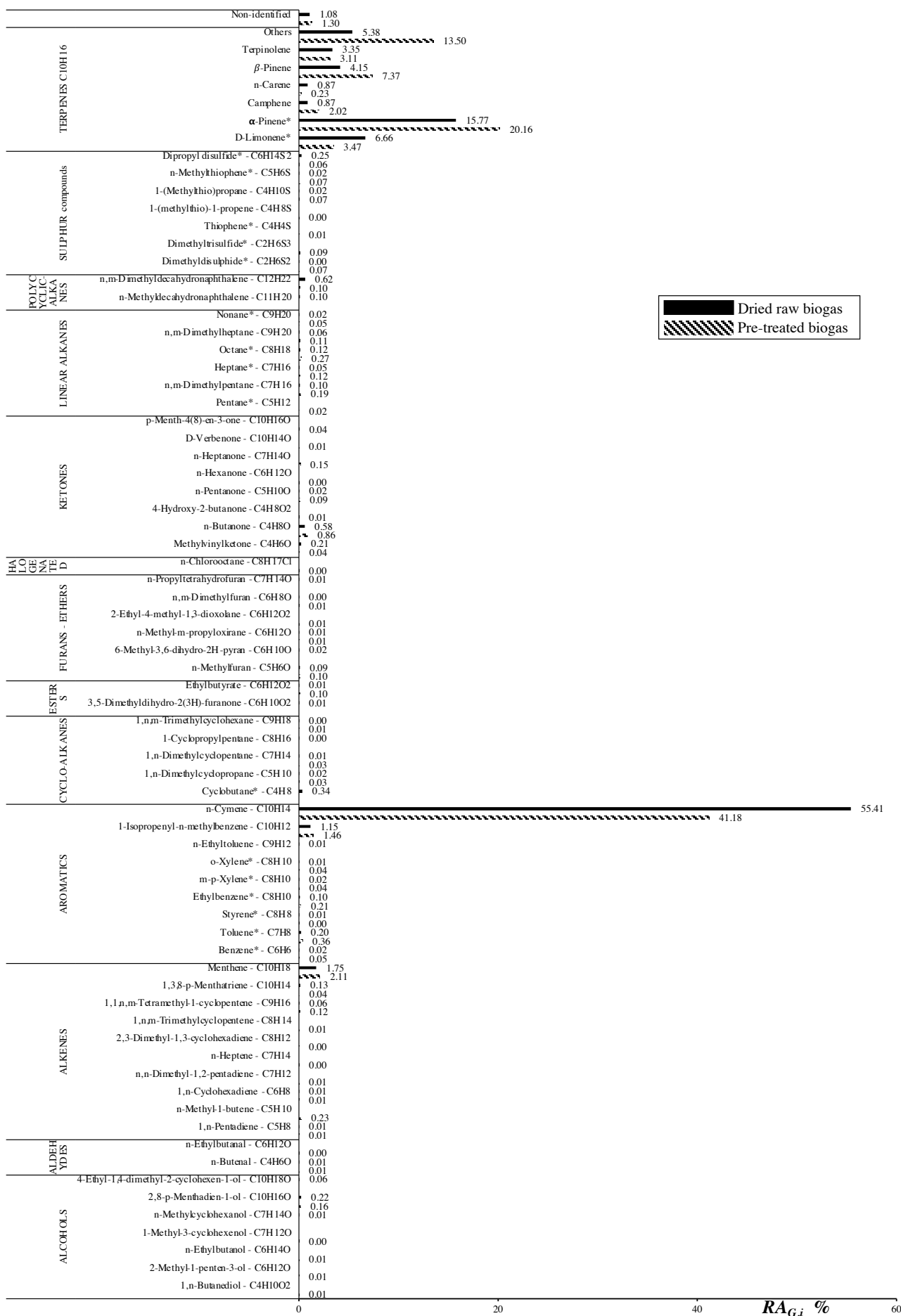


Figure 6.SI-10: Global relative abundance (%) of trace compounds identified in the dried raw biogas and pre-treated biogas of plant C sampled on TA14-CpX29 in March 2021. Compounds marked with a "*" are unequivocally identified.

Table 6.SI-1: The 41 halogenated volatile organic compounds present in the synthetic gas mixture, listed in order of increasing boiling points.

Compound	Boiling point (°C, at P _{atm})	Molecular mass (g·mol ⁻¹)
Dichlorodifluoromethane	-30.0	120.9
Chloromethane	-23.8	50.5
Chloroethene	-13.4	62.5
1,3-Butadiene	-4.4	54.1
1,2-Dichloro-1,1,2,2-tetrafluoroethane	3.6	170.9
Bromomethane	4.0	94.9
Chloroethane	12.5	64.5
Trichlorofluoromethane	23.8	137.4
1,1-Dichloroethene	32.0	96.9
Dichloromethane	39.6	84.9
1,1,2-trichloro-1,2,2-trifluoroethane	48.0	187.4
1,1-Dichloroethane	57.0	99.0
<i>cis</i> -1,2-Dichloroethene	60.2	96.9
Trichloromethane	61.2	119.4
1,1,1-Trichloroethane	74.0	133.4
Tetrachloromethane	76.7	153.8
Acrylonitrile	77.0	53.1
Benzene	80.0	78.1
1,2-Dichloroethane	84.0	99.0
Trichloroethene	87.2	131.4
1,2-Dichloropropane (<i>absent</i>)	96.0	113.0
<i>cis</i> -1,3-Dichloropropene	104.0	111.0
Toluene	111.0	92.1
<i>trans</i> -1,3-Dichloropropene	112.0	111.0
1,1,2-Trichloroethane	112.5	133.4
Tetrachloroethene	121.1	165.8
Chlorobenzene	131.0	112.6
1,2-Dibromoethane	131.5	187.9
Ethylbenzene	136.0	106.2
<i>p</i> -Xylene	138.0	106.2
<i>m</i> -Xylene	139.0	106.2
<i>o</i> -Xylene	144.0	106.2
Styrene	145.0	104.2
1,1,2,2-Tetrachloroethane	146.0	167.8
1,3,5-Trimethylbenzene	164.7	120.2
1,2,4-Trimethylbenzene	170.0	120.2
1,3-Dichlorobenzene	172.0	147.0
1,4-Dichlorobenzene	174.0	147.0
1,2-Dichlorobenzene	180.2	147.0
1,2,4-Trichlorobenzene	213.5	181.4
Hexachloro-1,3-butadiene	215.0	260.8

VI. REFERENCES CHAPTER 6

- [1] International Energy Agency (IEA), Outlook for Biogas and Biomethane. Prospects for Organic Growth. World Energy Outlook Special Report, (2020).
- [2] I. Angelidaki, L. Treu, P. Tsapekos, G. Luo, S. Campanaro, H. Wenzel, P.G. Kougias, Biogas Upgrading and Utilization: Current Status and Perspectives, *Biotechnology Advances*. 36 (2018) 452–466. <https://doi.org/10.1016/j.biotechadv.2018.01.011>.
- [3] V. Nallathambi Gunaseelan, Anaerobic Digestion of Biomass for Methane Production: A Review, *Biomass and Bioenergy*. 13 (1997) 83–114.
- [4] P.Y. Hoo, H. Hashim, W.S. Ho, Opportunities and Challenges: Landfill Gas to Biomethane Injection into Natural Gas Distribution Grid Through Pipeline, *Journal of Cleaner Production*. 175 (2018) 409–419. <https://doi.org/10.1016/j.jclepro.2017.11.193>.
- [5] M.A. Goossens, Landfill Gas Power Plants, *Renewable Energy*. 9 (1996) 1015–1018. [https://doi.org/10.1016/0960-1481\(96\)88452-7](https://doi.org/10.1016/0960-1481(96)88452-7).
- [6] M. Schweigkofler, R. Niessner, Determination of Siloxanes and VOC in Landfill Gas and Sewage Gas by Canister Sampling and GC-MS/AES Analysis, *Environmental Science & Technology*. 33 (1999) 3680–3685. <https://doi.org/10.1021/es9902569>.
- [7] M.R. Allen, A. Braithwaite, C.C. Hills, Trace Organic Compounds in Landfill Gas at Seven U.K. Waste Disposal Sites, *Environmental Science & Technology*. 31 (1997) 1054–1061. <https://doi.org/10.1021/es9605634>.
- [8] A.S. Brown, A.M.H. Van Der Veen, K. Arrhenius, A. Murugan, L.P. Culleton, P.R. Ziel, J. Li, Sampling of Gaseous Sulfur-Containing Compounds at Low Concentrations with a Review of Best-Practice Methods for Biogas and Natural Gas Applications, *TrAC Trends in Analytical Chemistry*. 64 (2015) 42–52. <https://doi.org/10.1016/j.trac.2014.08.012>.
- [9] K.F. Chin, C. Wan, Y. Li, C.P. Alaimo, P.G. Green, T.M. Young, M.J. Kleeman, Statistical Analysis of Trace Contaminants Measured in Biogas, *Science of the Total Environment*. 729 (2020). <https://doi.org/10.1016/j.scitotenv.2020.138702>.
- [10] M. Ghidotti, D. Fabbri, C. Torri, Determination of Linear and Cyclic Volatile Methyl Siloxanes in Biogas and Biomethane by Solid-Phase Microextraction and Gas Chromatography-Mass Spectrometry, *Talanta*. 195 (2019) 258–264. <https://doi.org/10.1016/j.talanta.2018.11.032>.
- [11] F. Hilaire, E. Basset, R. Bayard, M. Gallardo, D. Thiebaut, J. Vial, Comprehensive Two-Dimensional Gas Chromatography for Biogas and Biomethane Analysis, *Journal of Chromatography A*. 1524 (2017) 222–232. <https://doi.org/10.1016/j.chroma.2017.09.071>.
- [12] S. Rasi, A. Veijanen, J. Rintala, Trace Compounds of Biogas from Different Biogas Production Plants, *Energy*. 32 (2007) 1375–1380. <https://doi.org/10.1016/j.energy.2006.10.018>.
- [13] S. Rasi, J. Lehtinen, J. Rintala, Determination of Organic Silicon Compounds in Biogas from Wastewater Treatments Plants, Landfills, and Co-Digestion Plants, *Renewable Energy*. 35 (2010) 2666–2673. <https://doi.org/10.1016/j.renene.2010.04.012>.
- [14] J.I.S. Gómez, H. Lohmann, J. Krassowski, Determination of Volatile Organic Compounds

- from Biowaste and Co-Fermentation Biogas Plants by Single-Sorbent Adsorption, *Chemosphere*. 153 (2016) 48–57. <https://doi.org/10.1016/j.chemosphere.2016.02.128>.
- [15] F.A.T. Andersson, A. Karlsson, B.H. Svensson, J. Ejlertsson, Occurrence and Abatement of Volatile Sulfur Compounds during Biogas Production, *Null*. 54 (2004) 855–861. <https://doi.org/10.1080/10473289.2004.10470953>.
- [16] M. Cachia, B. Bouyssiere, H. Carrier, H. Garraud, G. Caumette, I. Le Hécho, Characterization and Comparison of Trace Metal Compositions in Natural Gas, Biogas, and Biomethane, *Energy & Fuels*. 32 (2018) 6397–6400. <https://doi.org/10.1021/acs.energyfuels.7b03915>.
- [17] J. Feldmann, I. Koch, W.R. Cullen, Complementary Use of Capillary Gas Chromatography–Mass Spectrometry (ion Trap) and Gas Chromatography–Inductively Coupled Plasma Mass Spectrometry for the Speciation of Volatile Antimony, Tin and Bismuth Compounds in Landfill and Fermentation Gases, *The Analyst*. 123 (1998) 815–820. <https://doi.org/10.1039/a707478f>.
- [18] J. Feldmann, Determination of Ni(CO)₄, Fe(CO)₅, Mo(CO)₆, and W(CO)₆ in Sewage Gas by Using Cryotrapping Gas Chromatography Inductively Coupled Plasma Mass Spectrometry, *Journal of Environmental Monitoring*. 1 (1999) 33–37. <https://doi.org/10.1039/A807277I>.
- [19] J. Feldmann, W.R. Cullen, Occurrence of Volatile Transition Metal Compounds in Landfill Gas: Synthesis of Molybdenum and Tungsten Carbonyls in the Environment, *Environmental Science & Technology*. 31 (1997) 2125–2129. <https://doi.org/10.1021/es960952y>.
- [20] J. Feldmann, A.V. Hirner, Occurrence of Volatile Metal and Metalloid Species in Landfill and Sewage Gases, *International Journal of Environmental Analytical Chemistry*. 60 (1995) 339–359. <https://doi.org/10.1080/03067319508042888>.
- [21] S. Rasi, J. Läntelä, J. Rintala, Trace Compounds Affecting Biogas Energy Utilisation – A Review, *Energy Conversion and Management*. 52 (2011) 3369–3375. <https://doi.org/10.1016/j.enconman.2011.07.005>.
- [22] M. Arnold, T. Kajolinna, Development of on-Line Measurement Techniques for Siloxanes and Other Trace Compounds in Biogas, *Waste Management*. 30 (2010) 1011–1017. <https://doi.org/10.1016/j.wasman.2009.11.030>.
- [23] J. Raich-Montiu, C. Ribas-Font, N. [de Arespacochaga, E. Roig-Torres, F. Broto-Puig, M. Crest, L. Bouchy, J.L. Cortina, Analytical Methodology for Sampling and Analysing Eight Siloxanes and Trimethylsilanol in Biogas from Different Wastewater Treatment Plants in Europe, *Analytica Chimica Acta*. 812 (2014) 83–91. <https://doi.org/10.1016/j.aca.2013.12.027>.
- [24] T. Bond, M.R. Templeton, History and Future of Domestic Biogas Plants in the Developing World, *Energy for Sustainable Development*. 15 (2011) 347–354. <https://doi.org/10.1016/j.esd.2011.09.003>.
- [25] P. Jaramillo, H.S. Matthews, Landfill-Gas-to-Energy Projects: Analysis of Net Private and Social Benefits, *Environ. Sci. Technol.* 39 (2005) 7365–7373. <https://doi.org/10.1021/es050633j>.
- [26] L. Pizzuti, C.A. Martins, P.T. Lacava, Laminar Burning Velocity and Flammability Limits in Biogas: A Literature Review, *Renewable and Sustainable Energy Reviews*. 62 (2016) 856–

865. <https://doi.org/10.1016/j.rser.2016.05.011>.

[27] Y. Shiratori, T. Oshima, K. Sasaki, Feasibility of Direct-Biogas SOFC, *International Journal of Hydrogen Energy*. 33 (2008) 6316–6321. <https://doi.org/10.1016/j.ijhydene.2008.07.101>.

[28] N. de Arespacochaga, C. Valderrama, C. Mesa, L. Bouchy, J.L. Cortina, Biogas Deep Clean-up Based on Adsorption Technologies for Solid Oxide Fuel Cell Applications, *Chemical Engineering Journal*. 255 (2014) 593–603. <https://doi.org/10.1016/j.cej.2014.06.072>.

[29] L. Lombardi, E. Carnevale, A. Corti, Greenhouse Effect Reduction and Energy Recovery from Waste Landfill, *Energy*. 31 (2006) 3208–3219. <https://doi.org/10.1016/j.energy.2006.03.034>.

[30] F. Teymoori Hamzehkolaei, N. Amjadi, A Techno-Economic Assessment for Replacement of Conventional Fossil Fuel Based Technologies in Animal Farms with Biogas Fueled Chp Units, *Renewable Energy*. 118 (2018) 602–614. <https://doi.org/10.1016/j.renene.2017.11.054>.

[31] N. Scarlat, J.-F. Dallemand, F. Fahl, Biogas: Developments and perspectives in Europe, *Renewable Energy*. 129 (2018) 457–472. <https://doi.org/10.1016/j.renene.2018.03.006>.

[32] W.M. Budzianowski, D.A. Budzianowska, Economic Analysis of Biomethane and Bioelectricity Generation from Biogas Using Different Support Schemes and Plant Configurations, *Energy*. 88 (2015) 658–666. <https://doi.org/10.1016/j.energy.2015.05.104>.

[33] I. Angelidaki, L. Xie, G. Luo, Y. Zhang, H. Oechsner, A. Lemmer, R. Munoz, P.G. Kougias, Chapter 33 - Biogas Upgrading: Current and Emerging Technologies, in: *Biofuels: Alternative Feedstocks and Conversion Processes for the Production of Liquid and Gaseous Biofuels*, Elsevier, 2019: pp. 817–843. <https://doi.org/10.1016/B978-0-12-816856-1.00033-6>.

[34] R. Augelletti, M. Conti, M.C. Annesini, Pressure Swing Adsorption for Biogas Upgrading. A New Process Configuration for the Separation of Biomethane and Carbon Dioxide, *Journal of Cleaner Production*. 140 (2017) 1390–1398. <https://doi.org/10.1016/j.jclepro.2016.10.013>.

[35] G. Leonzio, Upgrading of Biogas to Bio-Methane with Chemical Absorption Process: Simulation and Environmental Impact, *Journal of Cleaner Production*. 131 (2016) 364–375. <https://doi.org/10.1016/j.jclepro.2016.05.020>.

[36] Z. Bacsik, O. Cheung, P. Vasiliev, N. Hedin, Selective Separation of CO₂ and CH₄ for Biogas Upgrading on Zeolite NaKa and SAPO-56, *Applied Energy*. 162 (2016) 613–621. <https://doi.org/10.1016/j.apenergy.2015.10.109>.

[37] A. Toledo-Cervantes, C. Madrid-Chirinos, S. Cantera, R. Lebrero, R. Muñoz, Influence of the Gas-Liquid Flow Configuration in the Absorption Column on Photosynthetic Biogas Upgrading in Algal-Bacterial Photobioreactors, *Bioresource Technology*. 225 (2017) 336–342. <https://doi.org/10.1016/j.biortech.2016.11.087>.

[38] European Biogas Association, EBA Statistical Report 2020, (2020). https://www.europeanbiogas.eu/wp-content/uploads/2021/01/EBA_StatisticalReport2020_abridged.pdf (accessed January 5, 2022).

[39] International Energy Agency (IEA), IEA World Energy Outlook 2021, (2021). www.iea.org/weo (accessed January 5, 2022).

- [40] Teréga, Prescriptions Techniques Applicables Au Raccordement D'un Ouvrage Tiers Au Réseau De Transport De Gaz Naturel De Teréga, (2017).
- [41] European Committee for Standardization, EN 16723-1 Natural Gas and Biomethane for Use in Transport and Biomethane for Injection in Natural Gas Network - Part 1: Specifications for Biomethane for Injection in the Natural Gas Network, (2016).
- [42] European Committee for Standardization, EN 16723-2 Natural Gas and Biomethane for Use in Transport and Biomethane for Injection in the Natural Gas Network - Part 2: Automotive Fuels Specification, (2017).
- [43] M. Prussi, M. Padella, M. Conton, E.D. Postma, L. Lonza, Review of Technologies for Biomethane Production and Assessment of Eu Transport Share in 2030, *Journal of Cleaner Production*. 222 (2019) 565–572. <https://doi.org/10.1016/j.jclepro.2019.02.271>.
- [44] M. Schweigkofler, R. Niessner, Removal of siloxanes in biogases, *Journal of Hazardous Materials*. 83 (2001) 183–196. [https://doi.org/10.1016/S0304-3894\(00\)00318-6](https://doi.org/10.1016/S0304-3894(00)00318-6).
- [45] D. Papurello, L. Tomasi, S. Silvestri, I. Belcari, M. Santarelli, F. Smeacetto, F. Biasioli, Biogas Trace Compound Removal with Ashes Using Proton Transfer Reaction Time-of-Flight Mass Spectrometry as Innovative Detection Tool, *Fuel Processing Technology*. 145 (2016) 62–75. <https://doi.org/10.1016/j.fuproc.2016.01.028>.
- [46] D. Papurello, A. Lanzini, S. Fiorilli, F. Smeacetto, R. Singh, M. Santarelli, Sulfur Poisoning in Ni-Anode Solid Oxide Fuel Cells (SOFCs): Deactivation in Single Cells and a Stack, *Chemical Engineering Journal*. 283 (2016) 1224–1233. <https://doi.org/10.1016/j.cej.2015.08.091>.
- [47] G. Piechota, B. Igliński, R. Buczkowski, Development of Measurement Techniques for Determination Main and Hazardous Components in Biogas Utilised for Energy Purposes, *Energy Conversion and Management*. 68 (2013) 219–226. <https://doi.org/10.1016/j.enconman.2013.01.011>.
- [48] K. Arrhenius, A. Holmqvist, M. Carlsson, J. Engelbrektsson, A. Jansson, L. Rosell, H. Yaghooby, A. Fischer, Terpenes in Biogas Plants Digesting Food Wastes. Study to Gain Insight into the Role of Terpenes. *Energiforsk AB*. ISBN 978-91-7673-350-9, (2017).
- [49] K. Arrhenius, A.S. Brown, A.M.H. van der Veen, Suitability of Different Containers for the Sampling and Storage of Biogas and Biomethane for the Determination of the Trace-Level Impurities – A Review, *Analytica Chimica Acta*. 902 (2016) 22–32. <https://doi.org/10.1016/j.aca.2015.10.039>.
- [50] K. Arrhenius, H. Yaghooby, L. Rosell, O. Büker, L. Culleton, S. Bartlett, A. Murugan, P. Brewer, J. Li, A.M.H. van der Veen, I. Krom, F. Lestremau, J. Beranek, Suitability of Vessels and Adsorbents for the Short-Term Storage of Biogas/Biomethane for the Determination of Impurities – Siloxanes, Sulfur Compounds, Halogenated Hydrocarbons, BTEX, Biomass and Bioenergy. 105 (2017) 127–135. <https://doi.org/10.1016/j.biombioe.2017.06.025>.
- [51] K. Arrhenius, A. Fischer, O. Büker, Methods for Sampling Biogas and Biomethane on Adsorbent Tubes After Collection in Gas Bags, *Applied Sciences*. 9 (2019) 1171. <https://doi.org/10.3390/app9061171>.
- [52] S. Mariné, M. Pedrouzo, R.M. Marcé, I. Fonseca, F. Borrull, Comparison Between Sampling and Analytical Methods in Characterization of Pollutants in Biogas, *Talanta*. 100

(2012) 145–152. <https://doi.org/10.1016/j.talanta.2012.07.074>.

[53] A. Lecharlier, H. Carrier, B. Bouyssiére, G. Caumette, P. Chiquet, I. Le Hécho, Novel Field-Portable High-Pressure Adsorbent Tube Sampler Prototype for the Direct in Situ Preconcentration of Trace Compounds in Gases at Their Working Pressures: Application to Biomethane, *RSC Advances*. 12 (2022) 10071-10087. <https://doi.org/10.1039/d2ra00601d>.

[54] A. Lecharlier, B. Bouyssiére, H. Carrier, I.L. Hécho, Promises of a New Versatile Field-Deployable Sorbent Tube Thermodesorber by Application to BTEX Analysis in CH₄, *Talanta Open*. 4 (2021) 100066. <https://doi.org/10.1016/j.talo.2021.100066>.

[55] US EPA, Compendium of Methods for the Determination of Toxic Organic Compounds in Ambient Air. Second Edition. Compendium Method TO-17: Determination of Volatile Organic Compounds in Ambient Air Using Active Sampling Onto Sorbent Tubes (EPA/625/R-96/010b), (1999). <https://www3.epa.gov/ttnamti1/files/ambient/airtox/to-17r.pdf> (accessed April 23, 2020).

[56] J. Brown, B. Shirey, A Tool for Selecting an Adsorbent for Thermal Desorption Applications. Technical Report, (2001). https://www.sigmaaldrich.com/content/dam/sigmaaldrich/docs/Supelco/General_Information/t402025.pdf (accessed April 23, 2020).

[57] L. Lamaa, C. Ferronato, L. Fine, F. Jaber, J.M. Chovelon, Evaluation of Adsorbents for Volatile Methyl Siloxanes Sampling Based on the Determination of Their Breakthrough Volume, *Talanta*. 115 (2013) 881–886. <https://doi.org/10.1016/j.talanta.2013.06.045>.

[58] Z. Duan, P. Kjeldsen, C. Scheutz, Trace Gas Composition in Landfill Gas at Danish Landfills Receiving Low-Organic Waste, *Waste Management*. 122 (2021) 113–123. <https://doi.org/10.1016/j.wasman.2021.01.001>.

[59] M. Harper, Review. Sorbent Trapping of Volatile Organic Compounds from Air, *Journal of Chromatography A*. 885 (2000) 129–151. [https://doi.org/10.1016/S0021-9673\(00\)00363-0](https://doi.org/10.1016/S0021-9673(00)00363-0).

[60] UK Health and Safety Executive, Methods for the Determination of Hazardous Substances (MDHS). MDHS 72. Volatile Organic Compounds in Air. Laboratory Method Using Pumped Solid Sorbent Tubes, Thermal Desorption and Gas Chromatography. Her Majesty's Stationary Office: London, Uk, (1992). <https://www.hse.gov.uk/pubns/mdhs/pdfs/mdhs72.pdf> (accessed May 4, 2020).

[61] R. Chiriac, J. Carre, Y. Perrodin, L. Fine, J.-M. Letoffe, Review: Characterisation of VOCs Emitted by Open Cells Receiving Municipal Solid Waste, *Journal of Hazardous Materials*. 149 (2007) 249–263.

[62] Y. Long, Y. Fang, D. Shen, H. Feng, T. Chen, Hydrogen Sulfide (H₂S) Emission Control by Aerobic Sulfate Reduction in Landfill, *Scientific Reports*. 6 (2016) 38103. <https://doi.org/10.1038/srep38103>.

[63] J.E. Hernandez, R.G.J. Edyvean, Inhibition of Biogas Production and Biodegradability by Substituted Phenolic Compounds in Anaerobic Sludge, *Journal of Hazardous Materials*. 160 (2008) 20–28. <https://doi.org/10.1016/j.jhazmat.2008.02.075>.

[64] S. Lian, M. Nikolausz, I. Nijenhuis, A.F. Leite, H.H. Richnow, Biotransformation and Inhibition Effects of Hexachlorocyclohexanes During Biogas Production from Contaminated

Biomass Characterized by Isotope Fractionation Concepts, *Bioresource Technology*. 250 (2018) 683–690. <https://doi.org/10.1016/j.biortech.2017.11.076>.

PART 4 – CONCLUSIONS AND PERSPECTIVES

CONCLUSIONS AND PERSPECTIVES

Worldwide, the valorization of landfill gas, biogas and biomethane is getting momentum as modern societies have placed them at the crossroads of two contemporary challenges, namely developing circular economies and triggering energy transition. The anaerobic digestion of anthropogenic organic wastes in landfills or in controlled digesters concomitantly addresses these two challenges by converting those organic wastes into renewable energy in the form of methane contained in landfill gas, biogas and biomethane. The efficient and sustainable integration of these gases into today's energy mix nevertheless requires their quality to be controlled regarding their major (CH_4), minor and trace constituents to preserve the integrity of engines, boilers, and infrastructures wherein they are burned, transported or stored.

OPERATIONAL ACHIEVEMENTS

This doctoral thesis aimed at developing a new and entire field gas sampling chain enabling to efficiently, easily and reliably preconcentrate trace compounds in landfill gas, biogas and biomethane by directly sampling them *in situ* at their working pressure. All sub-objectives to reach that goal were met. Namely, scientific literature on gas sampling and preconcentration techniques for the determination of trace compounds in methane-like field gas samples was first extensively reviewed. The intricate complexity of sampling trace compounds, of selecting proper sampling units, materials and parameters and of applying suitable sample transport and storage conditions to safeguard the integrity of samples, was emphasized. Moreover, the review pointed out the lack of techniques to directly preconcentrate trace compounds from pressurized gases *in situ* at the pipe working pressure while this would avoid drawbacks diverted from the depressurization of gas samples.

Subsequently, in light of key sampling recommendations highlighted by the review, an efficient and promising direct *in situ* high-pressure preconcentration method and set-up was developed and optimized. To improve this method compared to existing ones, its development focused on two main requests:

1. the conception of a shortened sampling chain minimizing contaminations and trace compounds losses by sorption on sampling equipment internal surfaces; and
2. the ability to sample the gases in a large working pressure range covering pressures used in the transport grids ($\approx 5 - 100 \text{ bar}_a$), especially for biomethane injected in the natural gas grid

For the trace compounds targeted in this work (alkanes (linear, cyclic, polycyclic), aromatics, terpenes, alkenes, halogenated organic species, oxygenated organic species (alcohols, aldehydes, esters, furans and ethers, ketones), siloxanes, organic and inorganic Sulphur-compounds), preconcentration was chosen to be performed by adsorption onto self-assembled multibed adsorbent tubes. Such multibed adsorbent tubes are small ($\sim 5 \text{ cm}$ long, $\sim 5 \text{ mm}$ diameter) and easy to handle, and enable to trap, in a single sampling run, a wide range of trace compounds in a variety of chemical families and in a large volatility range, potentially present in landfill gas, biogas and biomethane. Several multibed adsorbent tube configurations assembling various

combinations of commercial adsorbents (Tenax®TA, Carbopack™B, Carbopack™X and Carboxen®1000) were initially evaluated. Two multibed adsorbent tube configurations were eventually kept, namely one containing Tenax®TA (14 mg) – Carbopack™X (29 mg) and another containing Tenax®TA (14 mg) – Carboxen®1000 (26 mg). Those multibed adsorbent tubes proved suitable, efficient and complementary to preconcentrate (adsorb and release upon analysis) all targeted trace compounds in synthetic gas mixtures used in the laboratory for preliminary validation experiments.

Concomitantly, to remedy the lack of direct *in situ* high-pressure preconcentration methods, a high-pressure adsorbent tube sampling prototype was developed. This device accommodates in its inner central space, a self-assembled multibed adsorbent tube and enables, via an equal-pressure gas flow design principle, to sample pressurized gases (≤ 200 bar_a) directly through the multibed adsorbent tube without any physical damage to the tube and to the adsorbents inside the tube, and where the sampling pressure was shown to have no impact on the efficiency of adsorption and recovery of trace compounds on and from the adsorbents. The main benefit of this prototype is being able to directly plug the adsorbent tubes to the gas pipe to sample pressurized gases over a wide pressure range without preliminary depressurization, implying gas pressure regulators and surplus equipment or high-pressure whole gas sampling cylinders become unnecessary which favorably shortens the field sampling chain and once again limits the risks of contaminations and trace compounds losses by interactions with surfaces of sampling elements and tubing.

Further, the third sub-objective of this thesis was reached, namely validating and optimizing the analytical method where analytes preconcentrated on adsorbent tubes are recovered by thermal desorption followed by gas chromatography – mass spectrometry analysis. The thermal desorption unit used was a prototype. In spite of analytical and mechanical failures encountered using this thermodesorber prototype, it proved yielding much higher resolution of chromatographic peaks than that obtained using techniques involving solid phase microextraction fiber or direct gas injections into the chromatograph. This high resolute power stems from the fast “plug” injection working mode of the thermodesorber prototype where furthermore no re-focusing trap is called for. In collaboration with its manufacturer, the work conducted during this doctoral thesis tremendously contributed to the analytical and mechanical improvement of the thermodesorber prototype.

The last and decisive sub-objective of this work was achieved by applying the developed direct *in situ* high-pressure preconcentration and analysis method to sample and determine trace compounds in real landfill gas, biogas and biomethane samples generated at different production plants from various feedstocks in France. The multibed adsorbent tubes and the performant thermal desorption method enabled to determine a wide range of trace compounds (over 150 distinct compounds) in the landfill gas, biogas and biomethane, belonging to 14 families: aromatics, terpenes, alkenes, alkanes (linear, cyclic and polycyclic), halogenated species, alcohols, aldehydes, esters, furans and ethers, ketones, Sulphur-compounds, siloxanes. Differences in trace compounds composition were evidenced between the different gases and potential correlations between feedstocks nature, treatment processes implemented and trace compounds present were discussed. For compressed biomethane injected in the natural gas grid, the combination of an efficient preconcentration support such as the multibed adsorbent tubes

with the high-pressure sampling prototype enabled to determine its trace compounds with a greater reliability than with conventional approaches like depressurization or whole gas sampling in pressurized cylinders with subsequent transfer to the lab and delayed preconcentration.

STRATEGICAL ACHIEVEMENTS

Overall, the research activities carried out within this work open up opportunities for a more reliable and decisive characterization of trace compounds in complex gas matrices such as landfill gas, biogas and biomethane, even when pressurized. Indeed, the proposed sampling–preconcentration method is freed from as much as possible surplus sampling equipment including pressure regulators, substantially improving the operational ease on field and limiting contaminations and losses of trace compounds. Additionally, the combination of the developed multibed adsorbent tubes, allowing to trap a wide range of various trace compounds, with the high-pressure adsorbent tube sampling prototype **offers a unique and novel sampling tool enabling to** sample gas over a wide pressure range, being especially relevant for biomethane injected in the natural gas grid, while simultaneously efficiently preconcentrating its trace compounds without preliminary knowledge on the nature of these trace compounds and on their presence or not in the gas. The enhanced sample integrity preservation diverted from such a shortened sampling chain where depressurization of pressurized samples is no longer necessary, should free analysts from sample stability incertitude and hence help obtain more reliable results. This could for instance help more reliably understanding and delineating correlations between trace compounds identified in the gases and feedstocks used in landfills or anaerobic digestion plants, gas production conditions and gas treatment processes implemented.

Moreover, the combination of sampling on multibed adsorbent tubes with the analysis via thermal desorption using the new thermal desorption prototype device, leads to outstanding chromatographic resolutions of the large spectrum trace compounds trapped on and recovered from the adsorbent tubes. Together with the narrow dimensions of (~5 cm long, ~5 mm diameter) and the low total mass adsorbents in the self-assembled multibed adsorbent tubes (~40 mg, whereas commercial multibed adsorbent tubes, ~9 cm long, rather handle adsorbent masses of at least ~100–200 mg), the high-resolutive power of the thermal desorption renders the entire sampling – analytical chain able to detect a wide range of trace compounds from a single sampling run where gas volumes as low as 0.5 – 2 L_N suffice. Yet sampling volumes must be optimized for each gas to sample with an eye on breakthrough avoidance, it seems reasonable to declare sampling volumes with the presented sampling method will remain below 2 L_N gas. Bearing in mind the non-negligible number of yearly sampling campaigns gas producers conduct for quality control purposes and the associated vent emissions of CH₄ to the atmosphere during sampling campaigns of e.g. natural gas, biogas or biomethane, proposing an efficient sampling method which furthermore only requires such small gas volumes contributes to lessen the relative atmospheric pollution intrinsically related to such sampling operations.

OPERATIONAL PERSPECTIVES

A primary lead to improve the work conducted during this thesis would consist in the advanced optimization of the operational gas sampling parameters on the self-assembled multibed adsorbent tubes. First, breakthrough curves and safe gas sampling volumes should be precisely determined for an optimal adsorption of the large variety of trace compounds encountered in landfill gas, biogas and biomethane on the different adsorbent multibeds used. Time should then be taken to further investigate the effects of gas pressure and gas sampling flowrate on the adsorption and recovery of the large range of trace compounds on and from the adsorbents over a wider pressure and flowrate range than was handled in this work. In particular, if sampling flowrates higher than $\sim 1 \text{ L}\cdot\text{min}^{-1}$ still yield high adsorption efficiencies without reducing breakthrough volumes, it could shorten the sampling time on field and thus enhance the productivity of sampling campaigns. To deeper study the impact of pressure on breakthrough volumes, 3 high-pressure sampling prototypes, each holding a multibed adsorbent tube, could be placed in series in future sampling campaigns.

The multibed adsorbent tubes themselves could also further be optimized. As their manual assembly is time-consuming, it could be considered to automate the process. The efficiency of additional single adsorbents or combinations of adsorbents in multibeds could be evaluated, and single adsorbent beds or multibeds with selective preconcentration (adsorption and recovery) efficiencies for specifically targeted families of compounds, for instance siloxanes, could be developed. Efficiently monitoring siloxanes in landfill gas, biogas and biomethane is crucial owing to the direct damage they cause to gas combustion infrastructures, thus developing specific preconcentration tools can be essential. Lastly, despite adsorbent tubes analyzed by thermal desorption can theoretically be re-used after quantitative thermal desorption and thermal reconditioning, in this work new tubes were systematically prepared and used for all laboratory- and field-sampling operations to avoid cross-contamination in the case thermal desorption of the initial sample was not quantitative and to avoid build-up of thermal degradation artefacts upon repeated conditioning cycles. However, as the assembly and conditioning procedure of new adsorbent tubes is time-consuming, time could be saved by optimizing the thermal desorption of samples and the subsequent thermal reconditioning of the tubes so as to safely allow reusing the tube without decrease of their analytical quality.

Last but not least, the mechanical and analytical performances of the thermal desorption prototype used in this work must be significantly improved. Owing to analytical repeatability failures of the current version of the thermal desorption prototype, no quantification of trace compounds in the real landfill gas, biogas and biomethane samples could be performed and this was a serious impediment to the doctoral thesis. The work conducted during this thesis already tremendously contributed to the analytical and mechanical improvement of the thermodesorber prototype, and the manufacturer will soon propose a second upgraded version of the prototype.

STRATEGICAL PERSPECTIVES

In order to decisively enhance the knowledge on landfill gas, biogas and biomethane, following considerations can be addressed.

Firstly, the robustness of the post-sampling analytical chain should be strengthened to offer higher levels of resolution between similar trace compounds which typically co-elute when using standard gas chromatography, and to offer reliable quantification. To improve the identification and resolution of non-metallic and non-metalloid trace compounds lurking in the complex mixture of compounds desorbed from the multibed adsorbent tubes, two-dimensional gas chromatography coupled to mass spectrometry (GC×GC-MS) is a promising option¹. Regarding quantification, gas chromatography – mass spectrometry (GC – MS) is already a powerful quantification tool provided a quantitatively repeatable injection of analytes is performed and provided calibration curves are set-up using certified standard synthetic gas mixtures. For complex gas samples such as landfill gas, biogas and biomethane containing a large variety of trace compounds, semi-quantification is often appropriate as no standard gas can be obtained for all trace compounds which moreover are not known until analysis. Other possible quantification techniques include gas chromatography – flame ionization (GC – FID) and gas chromatography – combustion – mass spectrometry with post-column isotope dilution for compound-independent quantification².

Secondly, more sampling campaigns should be conducted at regular intervals on different landfill gas, biogas and biomethane production plants to expand the database of and knowledge on trace compounds found in those gases under given production conditions. Besides, the small size and easy handling of the presented multibed adsorbent tubes not only facilitates direct *in situ* preconcentration, but also offers opportunities for direct *in situ* analysis using the thermal desorption prototype. Indeed, the thermal desorption prototype is mountable on the inlet port of any commercial GC-unit and it can accordingly be deployed *in situ* on field-portable gas chromatographs. Implementing the entire sampling – analytical chain directly *in situ* opens up opportunities for its automation for a continuous monitoring of given species in the gas.

¹ F. Hilaire, E. Basset, R. Bayard, M. Gallardo, D. Thiebaut, J. Vial, Comprehensive Two-Dimensional Gas Chromatography for Biogas and Biomethane Analysis, J. Chromatogr. A. 1524 (2017) 222–232. <https://doi.org/10.1016/j.chroma.2017.09.071>.

² S.C. Díaz, J.R. Encinar, A. Sanz-Medel, J.I. García Alonso, Gas Chromatography-Combustion-Mass Spectrometry with Postcolumn Isotope Dilution for Compound-Independent Quantification: Its Potential to Assess HS-SPME Procedures, Anal. Chem. 82 (2010) 6862–6869. <https://doi.org/10.1021/ac101103n>.



ECOLE DOCTORALE :
Sciences exactes et leurs applications (ED 211 SEA)

LABORATOIRES :

IPREM (Institut des Sciences Analytiques et de Physico-Chimie pour l'Environnement et les Matériaux)

LFCR (Laboratoire des Fluides Complexes et leurs Réservoirs)

Université de Pau et des Pays de l'Adour (UPPA)
Avenue de l'Université
BP 576 - 64012 Pau Cedex
France